7–9 June 2006
Istituti Ortopedici Rizzoli
Bologna, Italy

16th Annual Meeting

EORS

Transactions Vol. 16

Editors: Nicola Baldini, Lucia Savarino

Design: Michela Versari

European Orthopaedic Research Society

Table of contents

EORS 2006 ORGANISING COMMITTEE

Nicola Baldini
Armando Giunti
Heino Kienapfel
Lucia Savarino
Mark Taylor
Nico Verdonschot
Marco Viceconti

REVIEW COMMITTEE

Saverio Affatato
Nicholas A. Athanasou
Sofia Avnet
Massimiliano Baleani
Elisabetta Cenni
Gabriela Ciapetti
Lutz Claes
Luca Cristofolini
Lucy Di Silvio
Davide Donati
Andrea Facchini
Cesare Faldini
Sandro Giannini
Armando Giunti
Enrique Gómez-Barrena
Florian Gottsauner-Wolf
Donatella Granchi
Anita Ignatius
John Jansen
Alberto Leardini
Nadir M. Maraldi
Murilio Marcacci
Thimios Mitsiadis
Michiel Mulier
Luis Munuera
Ugo E. Pazzaglia
Andrea Pellacani
Dominique P. Pioletti
Geoff Richards
Wiltrud Richter
Neil Rushton
Lucia Savarino
Laurent Sedel
Fulvia Taddei
Mark Taylor
Domenico Tigani
Aldo Toni
Andrei Trampuz
Nico Verdonschot
Marco Viceconti

EORS EXECUTIVE COMMITTEE

Heino Kienapfel, President
Florian Gottsauner-Wolf, Vice-President
Nico Verdonschot, Vice-President
Michiel Mulier, Secretary
Dominique P. Pioletti, Treasurer
Wiltrud Richter, Member
Mark Taylor, Member
Neil Rushton, Past-President

Program overview

Wednesday, 7 June 2006

10.00	**SALA DEL VASARI** **IORS MEETING – Session 1**

12.00	**SALA DEL VASARI** **"Photodynamic Therapy of Musculoskeletal Tumors"** Speaker: K. Kusuzaki

14.00	**SALA DEL VASARI** **IORS MEETING – Session 2**

16.30	**SALA DEL VASARI** **"Fracture Healing and Bone Substitutes"** Speaker: Henry J. Mankin

18.30	**CHIOSTRO OTTAGONALE** **EORS OPENING**

Thursday, 8 June 2006

8.30	**AULA MAGNA** **Workshop: "Aseptic Loosening of Prostheses"** Chairman: E. Gómez-Barrena Speakers: N.A. Athanasou, A. Trampuz

	AULA MAGNA **Session 1 - Tissue Engineering 1** Chairmen: S. Giannini, W. Richter	**ANFITEATRO** **Session 2 - Biomechanics 1** Chairmen: A. Leardini, N. Verdonschot
09.30	O1. PLA SCAFFOLDS OBTAINED BY SUPERCRITICAL FLUID FOAMING FOR BONE TISSUE ENGINEERING (Pioletti DP, Montjovent MO, Mathieu L, Schmoekel H, Mark S, Bourban PE, Zambelli PY, Månson JAE, Applegate LL)	O8. COMBINING SUBJECT-SPECIFIC AND COLLECTION DATA TO CREATE PREDICTIVE MODELS TO BE USED IN THE CLINICAL PRACTICE (Viceconti M, Montanari L, Taddei F, Martelli S, Manfrini M, Toni A)
09.40	O2. 3D-BIOACTIVE SCAFFOLDS FOR BONE REGENERATION (Verné E, Vitale-Brovarone C, Robiglio L, Appendino P, Bassi F, Mozzati M, Muzio G, Martinasso G, Canuto R)	O9. FACTORS AFFECTING THE MAXIMUM FLEXION ANGLE IN TKR (Walker PS, Yildirim G, Sussman-Fort J, Roth J, White B, Klein KR)
09.50	O3. TISSUE ENGINEERING FOR MENISCUS REGENERATION IN A SHEEP MODEL (Kon E, Delcogliano M, Filardo G, Chiari-Grisar C, Nehrer S, Ambrosio L, Salter D, Tognana E, Marcacci M)	O10. CAN MUSCULAR STIMULATION INCREASE ARTICULAR STABILITY IN ACL-DEFICIENT KNEES? (Bonsfills N, Núñez A, Gómez-Barrena E)
10.00	O4. EFFECT OF DYNAMIC CULTURING OF HUMAN MESENCHYMAL STEM CELLS ON 3D POROUS PLGA SCAFFOLDS FOR BONE TISSUE ENGINEERING (Stiehler M, Baatrup A, Lind M, Kassem M, Bünger CE, Mygind T)	O11. IN VIVO ANALYSIS OF ANTERO-MEDIAL INSTABILITIES OF THE KNEE, THE ROLE OF ACL (Zaffagnini S, Bignozzi S, Martelli S, Lopomo N, Marcacci M)
10.10	O5. HIGH DOSES OF OP-1 INHIBIT FIBROUS TISSUE ARMORING (Hannink G, Aspenberg P, Schreurs BW, Buma P)	O12. THE INFLUENCE OF SCOLIOSIS ON THE PLANTAR PRESSURE DISTRIBUTION (Pavlačková J, Hlaváček P)
10.20	O6. AC-100, A SYNTHETIC FRAGMENT OF MEPE, PROMOTES BONE FORMATION AND MATURATION IN RODENT AND CANINE BONE REGENERATION MODELS (Rosen DM, Middleton-Hardie CA, Aswani S, Lazarov M)	O13. EXPERIMENTS ON BONE CEMENT POLYMERIZATION: TEMPERATURE AND RESIDUAL STRESSES (Plamondon D, Madrala A, Nuño N)
10.30	O7. *EX VIVO* GENE THERAPY APPROACH USING HUMAN LIM MINERALIZATION PROTEIN-3 TO INDUCE SPINE FUSION IN A RODENT MODEL (Pola E, Logroscino G, Lattanzi W, Logroscino CA)	O14. CHARACTERIZATION OF SHOULDER PATHOLOGY USING 3D KINEMATIC SENSORS (Jolles BM, Aminian K, Bourgeois A, Coley B, Pichonnaz C, Leyvraz PF, Farron A)

10.45 Coffee-break

	AULA MAGNA **Session 3 - Clinical Research 1** Chairmen: A. Giunti, H. Kienapfel	ANFITEATRO **Session 4 - Biomechanics 2** Chairmen: L. Claes, M. Viceconti
11.00	O15. ADAPTIVE BONE REMODELLING OF THE BIRMINGHAM HIP RESURFACING COMPONENT: AN INVESTIGATION ON IMPLANT ORIENTATION INFLUENCE (Kohan L, Gillies RM, Hogg M, Cordingley R)	O22. THE DEPENDENCE OF ESTIMATED FEMORAL CANCELLOUS BONE PERMEABILITY ON TIME USING HIGH AND LOW VISCOSITY CEMENT: PRELIMINARY RESULTS (Abdulghani S, Tidehem J, Wang JS, McCarthy I)
11.10	O16. ION RELEASE FROM METAL-ON-METAL HIP RESURFACING IMPLANTS DOES NOT DIFFER FROM STANDARD METAL-ON-METAL TOTAL HIP REPLACEMENT (Moroni A, Savarino L, Hoang-Kim A, Cadossi M, Greco M, Baldini N, Giannini S)	O23. NUMERICAL SIMULATION OF BONE CEMENT POLYMERIZATION: TEMPERATURE AND RESIDUAL STRESSES (Pérez MA, Nuño N, Plamondon D, Mądrala A, García-Aznar JM, Doblaré M)
11.20	O17. CORROSION AND CORROSION PRODUCTS OF MODULAR-BODY TITANIUM ALLOY FEMORAL STEMS IN CEMENTLESS HIP REPLACEMENT (Urban RM, Gilbert JL, Jacobs JJ)	O24. THE USE OF LOW AND HIGH VISCOSITY CEMENT IN HIP RESURFACING ARTHROPLASTY: AN IN VITRO STUDY (Howald R, Kesteris U, Wittwer M, Zhang K, Yakimicki D, Klabunde R, Krevolin J)
11.30	O18. LONG-TERM FIXATION AND POTENTIAL FAILURE MECHANISMS IN CEMENTLESS ACETABULAR COMPONENTS RETRIEVED POSTMORTEM (Urban RM, Hall DJ, Jacobs JJ, Pourzal R, Wimmer MA, Sumner DR, Galante JO)	O25. BIOTRIBOLOGICAL EVALUATION OF AN ARTIFICIAL DISC ARTHROPLASTY DEVICE. INFLUENCE OF LOADING AND KINEMATIC PATTERNS DURING IN VITRO WEAR SIMULATION (Grupp TM, Yue YY, Garcia R, Schwiesau J, Fritz B, Blömer W)
11.40	O19. HETEROTOPIC OSSIFICATION FALSELY ELEVATES PERIPROSTHETIC BMD (Downing M, Knox D, Ashcroft GP)	O26. INDIRECT DETERMINATION OF TRABECULAR BONE. EFFECTIVE TISSUE PROPERTIES USING MICRO-FINITE ELEMENT SIMULATIONS (Verhulp E, van Rietbergen B, Müller R, Huiskes R)
11.50	O20. ADAPTIVE BONE REMODELING OF AN ACETABULAR CUP: A CLINICAL COMPARISON (Gillies RM, Hogg M, Cordingley R, Kohan L)	O27. VISCOUS AND 'PSEUDO-VISCOUS' EFFECTS OF ELEVATED WATER CONTENT ON LIGAMENT MECHANICS (Zec ML, Thistlethwaite PA, Frank CB)
12.00	O21. EARLY DIAGNOSIS OF CERAMIC LINER FRACTURE: GUIDELINES BASED ON A 12-YEAR CLINICAL EXPERIENCE WITH 3710 MODERN CERAMIC PROSTHESES (Traina F, Stea S, Visentin M, Sudanese A, Giardina F, De Clerico M, Bordini B, Tassinari E, Polmonari M, Cervini A, Di Motta D, Toni A)	O28. INFLUENCE OF FREEZING AND THAWING ON THE BIOMECHANICAL AND STRUCTURAL PROPERTIES OF THE HUMAN POSTERIOR TIBIAL TENDON (Buda R, Di Caprio F, De Pasquale V, Bassi A, Fornasari PM, Giannini S)

12.15	**AULA MAGNA** **Keynote lecture: "Polymorphisms of Genes Associated to Osteoporosis in Caucasian and African Postmenopausal Women"** Speaker: S. Musumeci

12.45	**EORS General Assembly**

13.15 Lunch and Poster Session

	AULA MAGNA **Session 5 - Tumors** Chairmen: N.A. Athanasou, N. Baldini	**ANFITEATRO** **Session 6 - Biomaterials** Chairmen: G. Ciapetti, G. Richards
14.15	O29. CELLULAR AND HUMORAL MECHANISMS OF OSTEOCLAST FORMATION AND RESORPTION IN MELANOMA METASTASIS (Athanasou NA, Lau YS, Sabokbar A, Cerundolo V)	O36. COMBINED GENTAMICIN-HYDROXYAPATITE COATING FOR CEMENTLESS JOINT PROSTHESES SHOWS SIGNIFICANT REDUCTION OF INFECTION RATES AND GOOD BIOCOMPATIBILITY IN A RABBIT MODEL (Alt V, Bitschnau A, Sewing A, Meissner SA, Wenisch S, Domann E, Schnettler R)
14.25	O30. CT-GUIDED PERCUTANEOUS BIOPSY OF MUSCULOSKELETAL LESIONS (Rimondi E, Rossi G, Alberghini M, Bianchi G, Fabbri N, Mercuri M)	O37. BACTERIAL ADHESION ON SURGICAL MATERIALS: EFFECT OF A NEW SURFACE COATING ON ADHERENCE OF *S. AUREUS* (Kinnari TJ, Esteban J, Zamora N, Lappalainen R, Konttinen Y, Gómez-Barrena E)
14.35	O31. NEUROBLASTOMA CELLS SUPPRESS OSTEOBLAST DIFFERENTIATION BY SECRETING WNT INHIBITORS (Amato I, Pagani S, Devescovi V, Carella M, Savino MG, Baldini N, Granchi D)	O38. ANATOMICAL COMPARISON OF PORCINE AND HUMAN THORACOLUMBAR VERTEBRAE (Dath R, Porter KM, Miles AW)
14.45	O32. SSX: A NEW MOLECULAR TARGET REGULATING CELL MOTILITY OF BONE AND SOFT-TISSUE TUMOURS (Itoh K, Naka N, Yoshioka K)	O39. ADHESIVE FORCES SIGNIFICANTLY AFFECT NANOINDENTATION OF SOFT POLYMERIC MATERIALS (Gupta S, Carrillo F, Li C, Pruitt LA, Puttlitz C)
14.55	O33. MECHANISMS UNDERLYING THE ANTICANCER EFFECTS OF ZOLEDRONIC ACID AGAINST HUMAN OSTEOSARCOMA CELLS (Kubista B, Trieb K, Sevelda F, Arrich F, Toma C, Elbling L, Sutterlüty H, Scotlandi K, Kotz R, Micksche M, Berger W)	O40. INCREASING THE CRYSTALLINITY OF CROSSLINKED UHMWPE (Bistolfi A, Turell ME, Thornhill TS, Bellare A)
15.05	O34. PHOTODYNAMIC DETECTION OF MOUSE OSTEOSARCOMA IN THE SOFT TISSUES UTILIZING FLUOROVISUALIZATION EFFECT OF ACRIDINE ORANGE (Satonaka H, Kusuzaki K, Matsubara T, Shintani K, Wakabayashi T, Matsumine A, Uchida A)	O41. OXIDATION IN IRRADIATED UHMWPE WITHOUT ANNEALING (Bellare A, D'Angelo F, Ferretti A, Thornhill TS)
15.15	O35. MUTATIONAL ANALYSIS OF EXT1 AND EXT2 GENES AND CORRELATION WITH CLINICAL EXPRESSION OF DISEASE IN PATIENTS WITH HEREDITARY MULTIPLE EXOSTOSES (Pedrini V, Maini V, Capponcelli S, Mordenti M, Parra A, Picci P, Sangiorgi L)	O42. MATRIX METALLOPROTEINASE-9 IN A SMALL ANIMAL MODEL OF WEAR DEBRIS-INDUCED OSTEOLYSIS (Ibrahim T, Ong SM, Taylor GJS)

15.30-15.45 Coffee-break

	AULA MAGNA **Session 7 - Biomechanics 3** Chairmen: F. Gottsauner-Wolf, U.E. Pazzaglia	**ANFITEATRO** **Session 8 – Clinical Research 2** Chairmen: M. Marcacci, A. Trampuz
15.45	O43. IS HIGHFLEX TKA EFFECTIVE AT HIGHER FLEXION ANGLES AND DOES IT MAINTAIN THE GOOD MECHANICAL PERFORMANCE OF STANDARD TKA AT NORMAL FLEXION ANGLES? (Barink M, De Waal Malefijt M, Van Kampen A, Verdonschot N)	O50. ABSENCE OF LYMPHATICS AT THE BONE-IMPLANT INTERFACE: IMPLICATIONS FOR PERIPROSTHETIC OSTEOLYSIS (Athanasou NA, Edwards J, Schulze E, Sabokbar A, Gordon-Andrews H, Jackson D)
15.55	O44. *IN VITRO* PATELLAR TRACKING DURING NAVIGATED TOTAL KNEE REPLACEMENT (Belvedere C, Leardini A, Ensini A, Moctezuma de la Barrera JL, Catani F, Giannini S)	O51. SHORT-TERM RESULTS OF A NEW DESIGN OF TOTAL ANKLE REPLACEMENT (Giannini S, Leardini A, Romagnoli M, Sarti D, Catani F)
16.05	O45. FUNCTIONAL EVALUATION OF THE PFC AND CKS KNEE SYSTEM (Boonstra M, Eenhuizen C, Schimmel J, De Waal Malefijt M, Verdonschot N)	O52. ALUMINA, ZIRCONIA, AND COMPOSITE CERAMICS IN JOINT PROSTHESES (Macchi F)
16.15	O46. THE INFLUENCE OF CROSS SHEAR ON THE WEAR OF TKE UNDER VARIOUS KINEMATIC CONDITIONS (Knight LA, McEwen HMJ, Jeffers J, Fisher J, Rullkoetter P, Taylor M)	O53. AN *IN VITRO* AND *IN VIVO* EXPERIMENTAL ANALYSIS ON THE ADHESION AND SPREADING OF CELL CULTURES ONTO “TREVIRA” TUBE IN PROSTHETIC RECONSTRUCTION AFTER WIDE RESECTION FOR MALIGNANT BONE TUMOURS (Rosa MA, Maccauro G, Sgambato A, Caminiti R, Alesci M)
16.25	O47. PRIMARY FIXATION IN A REVISION TOTAL KNEE ARTHROPLASTY MAY NOT IMPLY LONG TERM FIXATION: THE EFFECT OF STEM LENGTH (Schmidt J, Henderson A, Ploeg H, Deluzio K, Dunbar M)	O54. RECONSTRUCTION OF MASSIVE ROTATOR CUFF LESIONS WITH A SYNTHETIC INTERPOSITION GRAFT (Audenaert E, Van Nuffel J, Verhelst M, Verdonk R)
16.35	O48. A NEW TECHNIQUE TO MAKE 2D WEAR MEASUREMENTS INSENSITIVE TO RADIOGRAPHIC DIFFERENCES OF CEMENTED TOTAL HIP PROSTHESES. FROM DEVELOPMENT TO VALIDATION (The B, Flivik G, Diercks RL, Verdonschot N)	O55. ANALYSIS OF KEY PARAMETERS IN *IN SITU* CONTOURING SURGERY USING A VALIDATED FINITE ELEMENT MODEL (Lafon-Jalby Y, Steib JP, Lavaste F, Skalli W)
16.45	O49. IMAGE-BASED RSA: A NEW METHOD FOR RSA WITHOUT BONE MARKERS (de Bruin PW, Kaptein BL, Stoel BC, Reiber JHC, Rozing PM, Valstar ER)	O56. EFFECT OF INTRA-ARTICULAR STEROIDS ON DEEP INFECTIONS FOLLOWING TOTAL KNEE ARTHROPLASTY (Joshy S, Thomas B, Gogi N, Singh BK)

Friday, 9 June 2006

08.30	**AULA MAGNA** **Workshop: "Biomimetic Strategies for Bone Tissue Regeneration"** Chairman: N. Rushton Speakers: A.Tampieri; J.A. Jansen; R.G. Richards

	AULA MAGNA **Session 9 - Pathophysiology** Chairmen: N.M. Maraldi, T.A. Mitsiadis	**ANFITEATRO** **Session 10 - Biomechanics 4** Chairmen: J.A. Jansen, A. Toni
09.45	O57.CARTILAGE DERIVED PARACRINE FACTORS INFLUENCE CHONDROGENESIS IN MESENCHYMAL STEM CELLS (Ahmed N, Dreier R, Grifka J, Grässel S)	O64. 68Ga-DOTA-PEPTIDE TARGETING VAP-1 FOR *IN VIVO* EVALUATION OF INFLAMMATORY AND INFECTIOUS BONE CONDITIONS (Lankinen P, Mäkinen TJ, Pöyhönen T, Virsu P, Jalava J, Jalkanen S, Roivainen A, Aro HT)
09.55	O58. EXPERIMENTAL VERTEBRAL GROWTH DISTURBANCES AFTER UNILATERAL MULTISEGMENTARY DAMAGE OF THE EPIPHYSEAL PLATE AND THE NEUROCENTRAL CARTILAGE (Barrios C, Burgos J, Hevia E, Maruenda JI)	O65. PRELIMINARY WEAR RESULTS OF A NEW DESIGN OF ANKLE PROSTHESIS (Leardini A, Affatato S, Leardini W, O'Connor JJ, Viceconti M)
10.05	O59. EFFECTS OF EARLY AND LATE ZOLEDRONATE TREATMENT ON BONE MICROSTRUCTURE IN OVARIECTOMIZED RATS ASSESSED BY IN VIVO MICRO-CT (Brouwers JEM, van Rietbergen B, Huiskes R)	O66. INTER-LABORATORY CONSENSUS ABOUT *IN VITRO* STABILITY TESTING OF CEMENTED AND CEMENTLESS HIP STEMS (Cristofolini L, Duda G, Prendergast PJ)
10.15	O60. BIOMECHANICAL AND HISTOLOGICAL CHANGES IN THE PORCINE DISC AFTER TREATMENT WITH HIFU (Forslund C, Hansson H-A, Ekström L, Holm S)	O67. VIBRATION ANALYSIS ON PARTIALLY CEMENTED CUSTOM HIP STEMS: A PER-OPERATIVE STUDY (Jaecques SVN, Pastrav LC, Mulier M, Van der Perre G)
10.25	O61. NOVEL NONVIRAL GENE TRANSFER SYSTEMS ALLOW FOR AN EFFICIENT GENE DELIVERY INTO CELLS OF MUSCULOSKELETAL ORIGIN (Orth P, Kaul G, Kohn D, Cucchiarini M, Madry H)	O68. THE EFFECT OF IMPLANT DESIGN AND BONE QUALITY ON MICROMOTION OF UNCEMENTED ACETABULAR CUPS (Janssen D, Zwartelé RE, Doets HC, Verdonschot N)
10.35	O62. TOWARDS EARLY DETECTION OF OSTEOARTHRITIS: ASSESSING HUMAN ARTICULAR CARTILAGE BY SCANNING FORCE MICROSCOPY (Raiteri R, Gottardi R, Kilger R, Aeschimann L, Cardinali V, Imer R, König U, Staufer U, Stolz M, Aebi U, Friederich N)	O69. COMPUTATIONAL SIMULATION OF OSSEOINTEGRATION IN TOTAL HIP REPLACEMENTS (Pérez MA, Moreo P, García-Aznar JM, Doblaré M)
10.45	O63. WHICH CELLS ARE PIVOTAL IN ECTOPIC BONE FORMATION? (Toom A, Suutre S, Arend A, Märtson A)	O70. ON THE BONE VOLUME RESECTED AND FIXATION FOR ACETABULAR COMPONENTS OF HIP RESURFACING (Winzenrieth R, Plamondon D, Lavigne M, Vendittoli PA, Nuño N)

11.00 Coffee-break

	AULA MAGNA **Session 11 - Clinical Research 3** Chairmen: N. Rushton, D. Dallari	ANFITEATRO **Session 12 - Tissue Engineering 2** Chairmen: A. Facchini, L. Munuera
11.15	O71. A PROSPECTIVE RANDOMISED TRIAL COMPARING MINIMAL INVASIVE AND STANDARD PARAPATELLAR APPROACHES FOR UNICOMPARTMENTAL KNEE ARTHROPLASTY (Jackson MP, Cottam HL, Apthorp HD, Butler-Manuel PA)	O78. IDENTIFICATION OF CARTILAGE DEDIFFERENTIATION MARKERS THROUGH GENE EXPRESSION ANALYSIS WITH A 30,000 cDNA ARRAY (Boeuf S, Steck E, Buneß A, Witte D, Sültmann H, Poustka A, Richter W)
11.25	O72. MEASUREMENT OF SOFT TISSUE BALANCE DURING TOTAL KNEE REPLACEMENT SURGERY: A TEN YEAR RETROSPECTIVE STUDY (Attfield SF, Wilton TJ, Pinnington LL)	O79. PROTEASE INHIBITOR MEDIATED SUPPRESSION OF LATE STAGE CHONDROGENIC DIFFERENTIATION OF MESENCHYMAL STEM CELLS IN VITRO (Bertram H, Dreyer R, Wachters J, Boehmer S, Richter W)
11.35	O73. A NAVIGATED DRILL GUIDE USING AN INSTRUMENTED LINKAGE FOR THE PLACEMENT OF CUTTING JIGS DURING TOTAL KNEE ARTHROPLASTY (Balicki MA, Forman RE, Walker PS, Wei CS, White B, Roth J, Klein GR)	O80. INFLUENCE OF GEL-LIKE MATRICES ON CHONDROGENIC DIFFERENTIATION OF MSC AND DIFFERENTIATION STABILITY AFTER ECTOPIC IMPLANTATION (Dickhut A, Lorenz H, Bischel O, Richter W)
11.45	O74. ADAPTIVE BONE REMODELLING OF ALL POLYETHYLENE UNICOMPARTMENTAL TIBIAL BEARINGS (Gillies RM, Hogg M, Cordingley R, Kohan L)	O81. A COMPARISON OF THE DIFFERENT GROWTH FACTOR REPERTOIRE AND THE FACTOR REQUIREMENT FOR SUCCESSFUL CHONDROGENESIS OF MSCs FROM BONE MARROW AND ADIPOSE TISSUE (Hennig T, Lorenz H, Götzke K, Richter W)
11.55	O75. DOES LIGAMENT BALANCING TECHNIQUE AFFECT KINEMATICS IN ROTATING PLATFORM KNEE ARTHROPLASTIES? (Jayasekera N, Kashif F, Schmotzer H, Fennema P, Simms M, Gamada K, Banks S)	O82. COMBINED HUMAN IGF-I AND FGF-2 GENE TRANSFER STIMULATES THE REPAIR OF FOCAL CARTILAGE DEFECTS IN VIVO (Madry H, Kaul G, Orth P, Zurakowski D, Kohn D, Cucchiarini M)
12.05	O76. NAVIGATED METHODOLOGY FOR INTRAOPERATIVE KINEMATIC ASSESSMENT OF THE KNEE STABILITY (Martelli S, Zaffagnini S, Bignozzi S, Lopomo N, Marcacci M)	O83. MOLECULAR AND IMMUNOHISTOLOGICAL CHARACTERIZATION OF HUMAN CARTILAGE TWO YEARS FOLLOWING AUTOLOGOUS CELL TRANSPLANTATION (Marconi E, Grigolo B, Roseti L, De Franceschi L, Desando G, Manfredini M, Faccini R, Facchini A)
12.15	O77. NONFIXATED-MOBILE MEDIAL COMPARTMENT KNEE HEMIARTHROPLASTY: OUTCOMES WITH AND WITHOUT ARTHROSCOPIC SYNOVIAL ABLATION (Trotter D, Patari S)	O84. THE DETACHED OSTEOCHONDRAL FRAGMENT AS A SOURCE OF CELLS FOR AUTOLOGOUS CHONDROCYTE IMPLANTATION (ACI) IN THE ANKLE JOINT (Giannini S, Buda R, Grigolo B, Vannini F, De Franceschi L, Facchini A)

12.30	**AULA MAGNA** **Keynote lecture: "Biomechanics of bone repair and regeneration"** Speaker: L. Claes

13.00 Lunch and Poster Session

14.00	**AULA MAGNA** **Keynote lecture: "Future of EORS"** Speaker: EORS President

	AULA MAGNA **Session 13 - Bone Substitutes** Chairmen: A. Tampieri, D. Donati	**ANFITEATRO** **Session 14 - Biomechanics 5** Chairmen: L. Cristofolini, M. Taylor
14.30	O85. EFFECTS OF A NEW BFGF/TCP-COMPOSITE ON PERIIMPLANT BONE (Maus U, Ohnsorge JAK, Andereya S, Siebert CH, Niedhart C)	O92. QUANTIFYING FRACTURE FIXATION USING RADIOSTEREOMETRY (Downing M, Ashcroft B, Ashcroft GP)
14.40	O86. THE BIOLOGICAL PROPERTIES OF CALCIUM PHOSPHATE BONE SUBSTITUTES ARE INFLUENCED BY THE BIOMATERIAL PORE SIZE (Klenke FM, Liu Y, Siebenrock KA, Hofstetter W)	O93. RADIOSTEREOMETRIC ANALYSIS (RSA) OF THREE-DIMENSIONAL MICROMOTION IN A FRACTURE MODEL OF THE DISTAL RADIUS (Madanat R, Moritz N, Mäkinen TJ, Aro HT)
14.50	O87. HEALING OF 1.5 CM ULNA DEFECTS WITH A PORCINE COLLAGEN-DERIVED MATRIX (Smitham PJ, Michaels D, Leong A, Stephens P, Vizesi F, Bruce W, Hill R, Walsh WR)	O94. FEMORAL FRACTURE LOAD AND FAILURE ENERGY IN TWO LOAD CONFIGURATIONS: AN *IN VITRO* STUDY (Duchemin L, Skalli W, Topouchian V, Benissa M, Mitton D)
15.00	O88. 52 WEEK RESULTS OF AN IN VIVO EVALUATION OF BONE GRAFT SUBSTITUTE PARTICULATES IN A RABBIT MODEL (Smitham PJ, Butler A, Vizesi F, Michaels D, Bruce W, Buckland T, Walsh WR)	O95. COMPUTATIONAL SIMULATION OF FRACTURE HEALING UNDER FLEXIBLE AND RIGID FIXATION (Gómez-Benito MJ, García-Aznar JM, Peris JL, Atienza C, Comín M, Doblaré M)
15.10	O89. INCREASED AMOUNT AND STRENGTH OF RESTORED BONE USING A SLOWER-RESORBING TRI-PHASIC CaSO4-BASED CEMENT COMPARED TO CONVENTIONAL CaSO4 PELLETS (Urban RM, Turner TM, Hall DJ, Inoue N, Gitelis S)	O96. THE USE OF TITANIUM FOR OSTEOSYNTHESIS IN RABBITS BY THREADED PINS (Spinelli M, Gabellieri P, Pingitore R, Dini F, Faviana P, Odoguardi F, Carlucci F)
15.20	O90. STRAIN INDUCED RELEASE OF BMP-7 FROM FRESH FROZEN FEMORAL HEAD ALLOGRAFT (Board N, Gowaily K, Rooney P, Kay PR)	O97. MECHANICAL STRENGTH EVOLUTION OF A RECONSTRUCTED FEMUR DURING FOLLOW-UP (Taddei F, Martelli S, Montanari L, Greco V, Leardini A, Viceconti M, Manfrini M)
15.30	O91. ECTOPIC PREFABRICATION OF BONE FLAPS (Scheufler O, Schaefer DJ, Jaquiery C, Braccini A, Wendt D, Pierer G, Heberer M, Martin I)	O98. BIOMECHANICAL ANALYSIS OF SLIPPED CAPITAL FEMORAL EPIPHYSIS (Gómez-Benito MJ, Paseta O, García-Aznar JM, Barrios C, Gascó J, Doblaré M)

15.45 Coffee-break

	AULA MAGNA **Session 15 - Clinical Research 4** Chairmen: E. Gómez-Barrena, M. Mulier	**ANFITEATRO** **Session 16 - Tissue Engineering 3** Chairmen: D.P. Pioletti, W. Richter
16.00	O99. OSTEOCHONDRAL ALLOGRAFT REPLACEMENT IN CONDYLE RESECTION OF THE KNEE (Bianchi G, Donati D, Staals E, Colangeli M, Mercuri M)	O106. EXPERIMENTAL RESURFACING OF ARTICULAR CARTILAGE BY EMBRYONIC STEM CELLS (Manunta A, Manunta ML, Sanna Passino E, Dattena M)
16.10	O100. THE COMBINATION VASCULARISED FIBULA/MASSIVE BONE ALLOGRAFT FOR TIBIA INTERCALARY RECONSTRUCTIONS: IMAGING ANALYSIS AT AN OVER 5-YEAR FOLLOW-UP (Manfrini M, Taddei F, Malaguti C, De Paolis M, Ceruso M, Mercuri M)	O107. MESENCHYMAL STEM CELL AND NUCLEUS PULPOSUS CELL INTERACTIONS: DIFFERENTIATION, STIMULATORY EFFECTS, AND CELL FUSION (Vadalà G, Spiezia F, Denaro E, Kang JD, Gilbertson L)
16.20	O101. REPAIR OF CARTILAGE LESIONS BY PERFORATIONS OF SUBCHONDRAL BONE AND IMPLANT OF A COLLAGEN TYPE I/II MEMBRANE (Gigante A, Guzzanti V, Giordano M, Bevilacqua C, Greco F)	O108. SELF-ASSEMBLED MONOLAYERS AND CARBON NANOTUBES AS NEW TOOLS TO IMPROVE BONE REGENERATION: AN *IN VITRO* APPROACH (Ciapetti G, Pagani S, Dettin M, Gambaretto R, Marletta G, Armentano I, Kenny J, Baldini N, Alava JI)
16.30	O102. VARUS POSTEROMEDIAL ROTATIONAL ELBOW INJURIES (Doornberg JN , Ring D)	O109. NO EFFECT OF LOAD ON CARTILAGE FORMATION IN DEFECTS RECONSTRUCTED WITH POLYESTERURETHANES (van Meel M, Ramrattan NN, Heijkants RGJC, Schouten AJ, Veth RPH, Buma P)
16.40	O103. CORONOID FRACTURE PATTERNS (Doornberg JN, Ring D)	O110. AUTOLOGOUS BONE MARROW DERIVED-CELLS IMPROVE MUSCLE STRENGTH AFTER SKELETAL MUSCLE CRUSH INJURY IN RATS (Winkler T, Matziolis G, Stoltenburg G, Schaser KD, Perka C, Duda GN)
16.50	O104. LONG TERM OUTCOME OF OPERATIVELY TREATED COMPLEX OLECRANON FRACTURES (Lindenhovius ALC, Doornberg JN, Mudgal CS, Ring D, Kloen P)	O111. ELECTROSPUN NANOFIBERS OF DIFFERENT POLYMERS AS SCAFFOLDS FOR TISSUE ENGINEERING (Boudriot U, Dersch R, Wack Ch, Fuchs S, Greiner A, Wendorff JH)
17.00	O105. UPPER EXTREMITY FRACTURES FOLLOWING FRONTAL VEHICLE CRASHES IN A LEVEL ONE TRAUMA CENTRE (Kwong Y, Chong M, Sochor M, Wang S)	O112. GENE EXPRESSION PROFILING OF HUMAN MESENCHYMAL STEM CELLS DURING EXPANSION AND OSTEOBLAST DIFFERENTIATION (Friedl G, Kulterer B, Jandrositz A, Windhager R, Trajanoski Z)

POSTER SESSION

CLINICAL RESEARCH (P1-P49)

P1. COMPARISON OF ELBOW CONTRACTURE RELEASE IN PATIENTS WITH AND WITHOUT HETEROTOPIC OSSIFICATION (Lindenhovius ALC, Doornberg JN, Linzel D, Ring D)

P2. ANALYSIS OF POSTOPERATIVE COMPLICATIONS IN COMPLEX DECOMPRESSION ELDERLY PATIENTS AS A FUNCTION OF COMORBIDITY (Eidelson S, Wilkerson J)

P3. ANALYSIS OF EX VIVO METAL-ON-METAL FIRST METATARSOPHALANGEAL PROSTHESIS AND ASSESSMENT AGAINST THEORETICAL LUBRICATION REGIMES (Joyce TJ)

P4. MODULAR ANKLE-FOOT ORTHOSIS WITH SPRING ELEMENTS (Milusheva S, Karastanev S, Toshev Y)

P5. INTELLIGENT ACTIVE ANKLE-FOOT ORTHOSIS (Veneva I, Toshev Y)

P6. OUTCOME FOLLOWING SCAPHOID BRUISING (Kanagaraj K, Khalid M, Jummani Z, Robinson D, Walker R)

P7. CARTILAGE THICKNESS IN THE HIP JOINT MEASURED BY MRI AND STEREOLOGY (Mechlenburg I, Nyengaard JR, Rømer L, Søballe K)

P8. BONE RESECTION AND MINOR AMPUTATION FOR SURGICAL TREATMENT OF CHRONIC OSTEOMYELITIS IN DIABETIC FOOT (Rosa MA, Galli M, Alesci M, Caminiti R)

P9. THE VALUE OF POSTMENISCECTOMY MRI: “DECEPTION OR DIRECTION?” (D’Hooghe P, Vandekerckhove B, De Rycke J, De Groote W)

P10. CD34+ CELLS IN THE NORMAL AND PATHOLOGICAL HUMAN MENISCUS (Verdonk PCM, Forsyth R, Verdonk R, Almqvist KF, Verbruggen G)

P11. NEW MULTIDIRECTIONAL ORTHOSIS FOR THE TREATMENT OF CONGENITAL CLUBFOOT (Ferrari D, Magnani M, Lampasi M, Donzelli O)

P12. PREDICTION AND PROPHYLACTIC FIXATION OF CONTRALATERAL HIP IN SCFE USING SKELETAL BONE AGE (Gorva AD, Metcalfe J, Jones S, Fernandes JA)

P13. ANATOMICAL AND MORPHOLOGICAL VARIATIONS IN LUMBAR SPINE IN CHILDREN WITH OSTEOGENESIS IMPERFECTA (Gorva AD, Bishop NJ, Cole A)

P14. USE OF STEM CELLS IN SURGICAL TREATMENT OF CONGENITAL PSEUDARTHROSIS IN CHILDREN (Magnani M, Lampasi M, Granchi D, Devescovi V, Donzelli O)

P15. AN ANALYSIS OF BONE STRUCTURAL CHANGES IN PROTEUS SYNDROME AND THEIR RELATIONSHIP WITH GROWTH (Pazzaglia UE, Beluffi G, Bonaspetti G, Ranchetti F, Azzola F)

P16. EPIPHYSEAL DYSPLASIAS. AN OVERVIEW ON CLASSIFICATION AND PATHOLOGY (Pazzaglia UE, Benetti A, Bondioni MP, Bonaspetti G, Beluffi G, Donzelli C)

P17. THE TREATMENT WITH ESWT OF CUFF ROTATOR CALCIFYING TENDONITIS VERSUS SHOULDER IMPINGEMENT SYNDROME (Vitali M, Peretti GM, Mangiavini L, Fraschini GF)

P18. THE TRUE INCIDENCE OF RECURRENT DISC HERNIATION AFTER LUMBAR DISCECTOMY (Nishimura Y)

P19. VERTEBRAL STRENGTH AND STIFFNESS AFTER KYPHOPLASTY OF OSTEOPOROTIC SPINE FRACTURES (Steens J, Verdonschot NJJ, Aalsma AMM, Veldhuizen AG, Hosman AJF)

P20. EXTENSION OF THE INDICATION FOR BALLOON KYPHOPLASTY IN ADVANCED OSTEOPOROTIC VERTEBRAL BODY FRACTURES WITH POSTERIOR WALL INVOLVEMENT (Wagner N, Böhm B, Klonschinski T, Drees P, Heine J)

P21. MID TO LONG-TERM RESULTS OF MODULAR NECKS IN PRIMARY UNCEMENTED TOTAL HIP ARTHROPLASTY (Aldinger PR, Wendt S, Gatermann S, Heisel C, Aldinger G)

P22. CUSTOM MADE UNCEMENTED TITANIUM STEMS IN VERY YOUNG PATIENTS. EXCELLENT 10 YEAR SURVIVAL IN 33 PATIENTS UNDER THE AGE OF 40 (Aldinger PR, Wendt S, Jung A, Gatermann S, Aldinger G)

P23. DEVELOPMENT OF AN OVERNIGHT STAY TOTAL HIP REPLACEMENT PROGRAMME (Apthorp H, Chettiar K, David L, Worth R)

P24. REDUCTION OF OSTEOLYSIS WITH CROSSLINKED POLYETHYLENE: FIVE YEAR IN VIVO RESULTS (Bitsch RG, Heisel C, Ball S, Schmalzried TP)

P25. METAL ION RELEASE IN PATIENTS WITH FAILED TOTAL KNEE ARTHROPLASTY (Bochicchio V, Savarino L, Tigani D, Ferrara T, Maci G, Greco M, Baldini N, Giunti A)

P26. REGISTER OF HIP PROSTHESIS IN THE REGION EMILIA-ROMAGNA: A FIVE YEAR EXPERIENCE (Bordini B, Stea S, De Clerico M, Toni A)

P27. A RANDOMISED PROSPECTIVE TRIAL COMPARING CERAMIC ON CERAMIC VERSUS METAL ON POLYETHYLENE BEARINGS IN THR (Bucher TA, Cottam HL, Apthorp HD, Butler-Manuel PA)

P28. A RANDOMISED PROSPECTIVE TRIAL COMPARING METHODS OF ACETABULAR IMPLANT FIXATION IN PRIMARY TOTAL HIP REPLACEMENT: EARLY RESULTS (Bucher TA, Cottam HL, Apthorp HD, Butler-Manuel PA)

P29. THE USE OF THE ULTRASONIC SCALPEL IN MINIMALLY INVASIVE TOTAL HIP REPLACEMENT (Chettiar K, David L, Worth R, Apthorp H)

P30. OVERNIGHT HOSPITAL STAY FOR MINIMALLY INVASIVE BILATERAL TOTAL HIP REPLACEMENTS (Chettiar K, Findlay I, Apthorp H)

P31. RELATIONSHIP BETWEEN BIOMETRIC CHARACTERISTICS AND STEM SIZE OF CEMENTLESS HIP PROSTHESES (De Clerico M, Bordini B, Stea S, Viceconti M, Toni A)

P32. A TANTALUM MONOBLOCK POROUS CUP AND ACETABULAR REPLACEMENT. A FIVE YEAR FOLLOW-UP STUDY (Fadda M, Zirattu G, Zirattu F, Tranquilli Leali P)

P33. WEAR PARTICLES IN FAILED TOTAL HIP REPLACEMENTS MADE OF Ti ALLOY (Figurska M, Milošev I, Cör A)

P34. PREDICTING THE NEED FOR URINARY CATHETERISATION FOLLOWING LOWER LIMB TOTAL JOINT ARTHROPLASTY. USE OF PATIENT QUESTIONAIRRES (Fox A, Board TN)

P35. BIRMINGHAM HIP RESURFACING IN A PATIENT WITH TAY SYNDROME (Katipalli G, Ganapathi M, Woodnutt D)

P36. FAILURE OF THE UNCOATED TITANIUM PROXILOCK™ FEMORAL HIP PROSTHESIS (Luites J, Spruit M, Hellemondt GV, Horstmann W, Valstar E)

P37. METAL ION RELEASE FROM FRACTURE FIXATION DEVICES (Maci G, Savarino L, Ferrara T, Bochicchio V, Greco M, Baldini N, Giunti A)

P38. SIMPLE TWO-DIMENSIONAL COMPUTER-ASSISTED TECHNIQUE FOR RADIOGRAPHIC ASSESSMENT OF POLYETHYLENE WEAR AFTER TOTAL HIP ARTHROPLASTY (Sandoval MA, Suarez-Vazquez A, Fernandez-Lombardia J, Hernandez-Vaquero D)

P39. SERUM LEVELS OF OSTEOPROTEGERIN (OPG) AND 'RECEPTOR ACTIVATOR OF NUCLEAR FACTOR-K LIGAND' (RANKL) IN PATIENTS WITH TOTAL HIP PROSTHESIS (Spina M, Pellacani A, Amato I, Baldini N, Giunti A, Granchi D)

P40. DIAGNOSTIC PROCEDURES WITH SUSPICION OF PERIPROSTHETIC INFECTION (Wendrich K, Siegel E, Hansen T, Drees P, Schöllner C, Eckardt A)

P41. TREATMENT OF SUPRACONDYLAR FEMORAL FRACTURES AROUND TOTAL KNEE REPLACEMENT WITH RETROGRADE INTRAMEDULLARY NAILING (Chettiar K, Jackson M, Brewin J, Dass D, Miles K, Butler-Manuel PA)

P42. TOTAL MENISCAL KNEE (TMK). CLINICAL EVALUATION OF CEMENTED VERSUS HYDROXYAPATITE COATED PROSTHESES (Cottam HL, James K, Jack C, Miles K, Apthorp HD, Butler-Manuel PA)

P43. THE S-ROM NOILES ROTATING HINGE KNEE-SYSTEM USED IN REVISION ARTHROPLASTY (Frank C, Krämer P, Wentzensen A, Schulte-Bockholt D)

P44. DELAYED ONSET DEEP INFECTION AFTER TOTAL KNEE ARTHROPLASTY: COMPARISON BASED ON THE INFECTING ORGANISM (Joshy S, Thomas B, Gogi N, Mahale N, Singh BK)

P45. ETHNIC DIFFERENCES IN PREOPERATIVE FUNCTION IN PATIENTS UNDERGOING TOTAL KNEE ARTHROPLASTY (Joshy S, Datta A, Gogi N, Singh BK)

P46. A COMPUTER-ASSISTED SURGICAL TECHNIQUE FOR TOTAL KNEE ARTHROPLASTY REVISION (Marcacci M, Nofrini L, Bignozzi S, Iacono F, Zaffagnini S, Lo Presti M, Di Martino A)

P47. IS ARTHRODESIS, IN INFECTED RE-REVISION ARTHROPLASTIES OF THE KNEE, AN UPDATE PROCEDURE? (Rosa MA, Centofanti F, Villari L, Caminiti R, Alesci M)

M, Sgambato A, Piconi C, Caminiti R, Alesci M, Rosa MA)

P141. FGF-2 INHIBITION IN A BONE METASTATIC RENAL CARCINOMA CELL LINE BY ANTISENSE OLIGONUCLEOTIDE AND MONOCLONAL ANTIBODY STRATEGIES (Perut F, Cenni E, Granchi D, Brandi ML, Giunti A, Baldini N)

P142. EXTRACELLULAR MATRIX REMODELLING IN DUPUYTREN'S DISEASE: HISTOPATHOLOGICAL ASPECTS (Tresoldi I, Modesti A, Trono P, Tarantino U)

P143. EFFECTS OF HYPERTHERMIA ON HUMAN OSTEOSARCOMA CELLS (Trieb K, Blahovec H, Kubista B)

P144. RADIOHYPERTHERMOCHEMOTHERAPY ON MALIGNANT FIBROUS HISTIOCYTOMA IN VITRO (Otsuka Y, Takanobu O, Matsushita T, Yamada S, Tsuji H, Fukuoka M, Kobayashi M)

TISSUE ENGINEERING (P145-P171)

P145. FGF-2 EFFECTS ON THE OSTEOGENIC COMMITMENT OF BONE MARROW STROMAL CELLS (Cenni E, Perut F, Cenacchi A, Fornasari PM, Dallari D, Giunti A, Baldini N)

P146. BONE HEALING ENHANCEMENT BY LYOPHILIZED BONE GRAFTS SUPPLEMENTED WITH PLATELET GEL OR PLATELET GEL-BONE MARROW STROMAL CELLS IN PATIENTS WITH TIBIAL OSTEOTOMY FOR GENU VARUS: A RANDOMIZED STUDY (Stagni C, Dallari D, Savarino L, Tarabusi C, Del Piccolo N, Cenacchi A, Dal Vento A, Fornasari PM, Baldini N, Giunti A)

P147. PLATELET RICH PLASMA IMPROVES BONE FORMATION IN A CRITICAL SIZE BONE DEFECT ON A NEW HIGH SURFACE SCAFFOLD CALLED CALCIUM DEFICIENT HYDROXYPATITE (Kasten P, Szalay K, Vogel J, Geiger F, Luginbühl R, Ewerbeck V, Richter W)

P148. TREATMENT OF LARGE BONE DEFECTS WITH AUTOLOGOUS CULTURED BONE MARROW STROMAL CELL LOADED ON A BIOCERAMIC SCAFFOLD (Marcacci M, Kon E, Neri MP, Iacono F, Zaffagnini S, Filardo G, Delcogliano M, Cancedda R)

P149. IMPACT OF A RESORABLE CaP COATING IN A GAP MODEL IN GÖTTINGEN MINIPIGS (Schwarz M, Feuerstack M, Herbig J, Brade J, Becker K, Scheller G)

P150. OPTIMIZATION OF CULTURE CONDITIONS FOR DIFFERENTIATION OF ADULT BONE MARROW DERIVED HUMAN MESENCHYMAL STEM CELLS INTO FUNCTIONAL OSTEOBLASTS (Yrjans JJ, Hentunen TA, Väänänen KH, Aro HT)

P151. CARBON FIBRE REINFORCED POLYMER (CFRP) CAGE INDUCES BETTER CELL ADHESION, SPREADING, AND PROLIFERATION THAN POLYETHER ETHER KETONE (PEEK) CAGE. ANALYSIS BY A NEW CELLULAR MODEL FOR IN VITRO STUDY OF ORTHOPAEDIC BIOMATERIALS (Barbanti-Brodano G, Morelli C, Ciannilli A, Campioni K, Boriani S, Tognon M)

P152. IRRADIATION DOES NOT INFLUENCE INCORPORATION OF IMPACTED MORSELIZED BONE (Hannink G, Schreurs BW, Buma P)

P153. BIOCART™ II, A NOVEL APPROACH FOR 3D RECONSTRUCTION OF ARTICULAR CARTILAGE (Nehrer S, Chiari-Grisar C, Dorotka R, Buchta Ch, Trattnig S, Neria E, Stern B, Barkai H, Zak R, Yaniv Y, Blumenstein S, Yayon A)

P154. A NOVEL ENGINEERED OSTEOCHONDRAL COMPOSITE (Peretti G, Buragas M, Sosio C, Mangiavini L, Scotti C, Di Giancamillo A, Domeneghini C, Fraschini GF)

P155. EFFECT OF BLOOD ON ENGINEERED CARTILAGE (Sosio C, Peretti GM, Boschetti F, Gigante A, Bevilacqua C, Mangiavini L, Scotti C, Gervaso F, Biressi S, Fraschini G)

P156. BMPs PROMOTE THE CHONDROGENIC DIFFERENTIATION OF ADIPOSE TISSUE DERIVED MESENCHYMAL STEM CELLS, BUT INDUCE HYPERTROPHIC MARKERS (Lorenz H, Hennig T, Thiel A, Dickhut A, Richter W)

P157. A TISSUE ENGINEERING APPROACH TO MENISCUS REGENERATION IN A SHEEP MODEL (Chiari-Grisar C, Koller U, Dorotka R, Plasenzotti R, Lang S, Ambrosio L, Tognana E, Kon E, Salter D, Nehrer S)

P158. ATTACHMENT OF MENISCAL FIBROCHONDROCYTES TO A COLLAGEN TYPE I SCAFFOLD INDUCES MMP AND IL-6 EXPRESSION (Hoberg M, Aicher WK, Rudert M)

P159. IN VITRO STUDY OF SHEEP MENISCUS CELLS SEEDED ON TWO SLIGHTLY DIFFERENT BIOMATERIALS MADE FROM HYALURONIC ACID AND POLYCAPROLACTONE (Koller U, Chiari-Grisar C, Kapeller B, Vavken P, Kotz R, Ambrosio L, Tognana E, Nehrer S)

BIOMATERIALS AND BONE SUBSTITUTES (P172-P193)

Keynote presentations

HOW TO DIFFERENTIATE PROSTHETIC JOINT INFECTION FROM ASEPTIC FAILURE?

Andrej Trampuz
University Hospital Basel, Basel, Switzerland
atrampuz@uhbs.ch

The functional implant life. It is well recognized that synthetic materials used to construct implants will not last forever. The functional implant life may be influenced by its material and design (ceramic, stainless steel, Ti, Ti alloy), technical aspects of device implantation (cementing, creation of a porous implant surface or hydroxyapatite cover for stimulating bone apposition), antiadhesive implant coating (antiseptic or bioactive surface properties), quality of host bone, and extent of patient activity. Long-term implant stability depends mainly on good initial fixation (osseointegration) and factors maintaining sufficient local bone density around the prosthesis, which is the net result of bone resorption (osteolysis) and new bone formation. Table 1 shows different mechanisms for implant failure.

Table 1. Septic and Aseptic Causes of Implant Failure

Mechanism	Description
Aseptic biomechanical failure	
A. Wear debris	Loss of material with generation of particles resulting from relative motion between opposed surfaces (adhesive, abrasive or fatigue wear). Inflammatory reaction to particles of orthopaedic wear debris causes bone resorption.
B. Eccentric mechanical loads	Misaligned arthroplasty alters the magnitude and direction of load transmission through the prosthesis and causes implant loosening and mechanical damage to the implant material or the interface between implant and bone.
C. Implant motion	Micromotion of loose prosthesis leads to progressive bone resorption.
D. Hydrodynamic pressure	Synovial fluid is compressed through defects of the prosthesis and host bone. This effect is likely amplified in the presence of excessive wear debris.
Infection	Microorganisms colonize the prosthesis at the time of implantation or postoperatively through hematogenous seeding or spread from a contiguous infectious focus. Bacteria adhere to and grow on an implant surface forming a biofilm protecting them from environmental influences and immune responses.

Aseptic implant failure. Aseptic biomechanical failure often is difficult to distinguish from occult chronic prosthetic joint infection. Osteolysis induced by particulate wear debris from implant materials is recognized as a major cause of long-term prosthesis failure. Wear particles become deposited in the space between the implant and bone (or cement, if present), and are phagocytosed by macrophages, forming a granulomatous tissue layer or membrane. The macrophages in turn release inflammatory mediators, which stimulate osteoclastic bone resorption. Biopsy specimens from osteolytic lesions surrounding tissue often show only acellular, necrotic debris, but biopsy specimens from surrounding tissue may contain granular-appearing macrophages associated with small particles, foreign-body-type giant cells, and osteoclasts, the arthroplasty effect. Migration of macrophages into lymphatic and blood vessels ultimately may result in distant dissemination of orthopaedic wear debris. Other aseptic mechanisms of implant failure include inappropriate mechanical load, fatigue failure at bone-implant interfaces, implant micromotions, and perhaps synovial fluid hydrodynamic pressure.

Prosthetic joint infection. Infections occur in approximately 1% to 5% of all primary arthroplasties. The incidence of prosthetic joint infection is higher after a revision arthroplasty, possibly because of the long operating time, scar formation, or recrudescence of unrecognized infection present at the initial surgery. Microorganisms can colonize the prosthesis at the time of implantation (either through direct inoculation or as a result of airborne contamination of the wound) or colonize the implant postoperatively through hematogenous seeding or spread from a contiguous infectious focus. Once microorganisms attach to and grow on the surface of an orthopaedic implant, they begin to produce a highly hydrated matrix of polysaccharide and protein. This extracellular polymeric substance together with embedded microorganisms is collectively known as a biofilm. Depletion of metabolic substances or waste product accumulation in biofilms causes microbes to enter a slow- or nongrowing (stationary) state, in which they are less susceptible to growth-dependent antimicrobial agents. These characteristics make biofilm microbes not only more resistant to antimicrobial killing as compared to planktonic bacteria, but also more difficult to detect. As a consequence, implant-associated infections are often difficult to diagnose with routine microbiological methods.

Diagnostic methods for differentiation prosthetic joint infection from aseptic failure. Routine diagnostic methods: Increased synovial fluid cell count and presence of acute inflammation in periprosthetic tissue correlate well with infection; however, the causing microorganism cannot be identified with this method. Gram staining has usually a low sensitivity. Periprosthetic tissue and synovial fluid cultures are frequently used as the reference standard for diagnosing infection, however, they do not have an ideal sensitivity and specificity. New diagnostic methods directed to identify microbes in biofilms are needed. Potential new methods: By dispersing adherent bacteria from the surface and disrupting their multicellular structure, the recovery efficiency of diagnostic assays may be increased. Various potential strategies to dislodge microbial biofilms from surfaces have been used in research setting, including mechanical (sonication, vortexing, shock waves), biochemical (enzyme treatment), and electrical approaches. To date, mostly ultrasound has been studied for improvement of recovery of biofilm microbes. In addition, cultures may be false-negative because of prior antimicrobial exposure, a low number of organisms, inappropriate culture media, or fastidious or atypical organisms. Therefore, molecular methods may be used to improve the diagnosis of infection, for example broad-range polymerase chain reaction (PCR).

GENETIC AND ENVIRONMENTAL FACTORS IN HUMAN OSTEOPOROSIS

Salvatore Musumeci

Department of Pharmacology, Gynaecology and Obstetrics, Paediatrics, University of Sassari, Italy and Institute of Population Genetics, National Research Council (CNR), Alghero SS, Italy

smusumeci@tiscalinet.it

Osteoporosis is a reduction in skeletal mass associated with bone micro-architectural deterioration that results in an increased risk of fractures. Often, it is most considered a bone disorder of postmenopausal women. However, younger women can also be affected. With the increase of life expectancy, there is an increase in the proportion of females living beyond menopause, therefore affected by osteoporosis. In general, Caucasian- and Asian Americans are more susceptible to osteoporosis with respect to African and Hispanic Americans. Nevertheless, recently, it has been demonstrated that both are at significant risk as well. There are a lot of genetic and non-genetic risk factors, contributing to the development of osteoporosis, which could interact each other to exacerbate or ameliorate the osteoporosis. To the best of knowledge, the increasing immigration process from undeveloped (Africa, Asia etc) to developed countries suggests that the equilibrium among genetic and non genetic determinants, radically established by selective environmental pressure, may be modified by the change in life style. This can contribute to event sequences that result in overt osteoporosis.

The aim of this study is to determine the prevalence of known gene polymorphisms, associated to osteoporosis in different healthy postmenopausal women from Sub Saharan to Mediterranean areas. Moreover, in a control group of Mediterranean women with documented osteoporosis, the weight of these polymorphisms has been established.

From the analysis of these results and comparing the life habits of these women, it has been possible to identify some characteristics which influence the appearance of this debilitating disease (bone fracture in all districts) with devastating health and economic consequences. The statistical analysis of allele frequencies showed that the Vitamin D receptor (VDR B) polymorphism was significantly lower in healthy African women with respect to healthy Mediterranean ($P < 0.001$) and osteoporotic Mediterranean ($P< 0.01$) women. The estrogens receptor (ER X) allele frequency was significantly lower in both healthy African and healthy Mediterranean than in osteoporotic Mediterranean women ($P< 0.001$). In contrast, the estrogens receptor (ER P) allele frequency was significantly lower only in healthy when compared to osteoporotic Mediterranean women ($P <0.01$). The calcitonin receptor (CTR T) in healthy African and Mediterranean women was significantly lower than in Mediterranean osteoporotic women ($P < 0.001$). The collagen type 1 (Colia 1) polymorphism did not show statistical significant differences among the three studied group women. The genotype analysis showed that the observed percentages of single specific polymorphisms did not differ from those expected with the exception of VDR (B) and ER (X) in healthy African women ($P < 0.001$), and ER (P) in healthy Mediterranean women ($P < 0.001$).

In conclusion, the multivariate analysis, once the social characteristics have been taken into account, demonstrated that both physical activity and healthy diet, associated with a outside work and bone densitometry monitoring are the best prognostic factors for this severe diseases. Finally, the present investigation confirms the opportunity of periodic BMD controls for an early start of estrogens low regimen therapy, in presence of ER XX and ER PP polymorphisms, in addition to appropriate use of bifosfonates in order to prevent severe bone fractures.

BIOACTIVE SIGNALING MOLECULES

John A. Jansen, DDS, PhD

Department of Peridontology and Biomaterials, PO Box 9101, Radboud University Nijmegen Medical Center, Nijmegen, The Netherlands

J.Jansen@dent.umcn.nl

Supported by the prediction of *Time* magazine that tissue engineering will be the number one job by 2010, the main driver for the development of bone tissue equivalents will be the increasing number of older people in the Western population coupled with increasing life expectancy and increasing need for quality of life till a high age.
In case of bone engineering the advance is based on three different pillars: 1. Osteogenesis, 2. Osteoconduction and 3. Osteoinduction.
Considering the problems as faced in the development of cell-based approaches, the clinical future perspective will be the application of biomolecular (growth factors, i.e. defined biomolecules that can lead to new tissue formation) and biomaterial systems that are able to trigger tissue regeneration.
The biomolecules are included in the biomaterial and are placed at the tissue site.
These molecules have the ability to diffuse out the material and are able to direct the function of cells already present at that site and, therefore, to promote the formation of the desired tissue type or structure. A critical component is the development of biomaterials; they have to provide shape to the bone tissue defect that has to be generated. Several materials can be used as carrier material. The ideal carrier material is biocompatible and biodegradable. This means that it is nontoxic and does not elicit a foreign body giant cell reaction.
Further, the carrier material must degrade to biocompatible products, be nonimmunogenic and free of transmittable diseases.
Additionally, other very relevant properties are that carrier materials must have a porous structure with pores that interconnect in order to allow the ingrowth of blood vessels and tissue and that they are easy to handle (moldability and strength). The carrier material also needs to have surface characteristics that support the adhesion of cells and tissue inductive proteins and has to release the included biomolecules in a predictable and standardized way.
Finally, the carrier material has to meet some administrative and regulatory issues, like approval by the Food and Drug Administration (FDA) for human use, cost effective over autografts and verifiable sterilization of the complete device.
Currently used carrier materials for bone tissue engineering are:

- Degradable polymers, like poly (lactic acid), poly (glycolic acid) and collagen
- Calcium phosphate ceramic, like hydroxyapatite and tricalciumphosphate
- Titanium fiber mesh

It has to be emphasized that none of the presently used materials meet all of the required properties.
Besides the development of materials that are indeed able to support tissue regeneration, future investigations have also to focus on the further elucidation of the biomolecule activity as well as optimization of the biomolecule kind, dosage and synergism between various biomolecules.
In the current presentation an overview will be given of various approaches to prepare synthetic bone grafts using morphogens to support the regeneration of bone tissue.

BIOMECHANICS OF BONE REPAIR AND REGENERATION

Lutz Claes

Institute of Orthopedic Research and Biomechanics, Helmholtzstr. 14, 89081 Ulm

lutz.claes@uni-ulm.de

Stability of the fracture fixation and a sufficient blood supply are the two major requirements for obtaining undisturbed fracture healing. Musculoskeletal loading of a stabilized fracture leads to an interfragmentary movement (IFM), which directs the healing process. The IFM causes tissue deformation in the fracture-healing zone, which influences cell proliferation and differentiation. Very small IFM does not stimulate cellular reactions and causes minimal bone formation by osteoblasts and endochondral ossification by chondrocytes, osteoclasts and osteoblasts. Sufficient mechanical stimuli however lead to callus formation around the fracture, which is able to bridge the fracture gap and stabilize the fracture by a „biological osteosynthesis".

This ultimately leads to a limited tissue strain in the remaining fracture, which promotes bony union. Unstable fixations cause large IFM and tissue strains, which do not allow bony healing.

Not only the amplitude but also the main direction of strain relative to the fragments influences the healing process. Whereas moderate axial deformations of the proliferating tissue in the fracture gaps does not hinder the healing process, shear movement in the plane of the fracture line does delay healing. One possible reason for this effect might be that large shear strains and hydrostatic pressures do not allow the revascularization of the healing zone.

Favorable interfragmentary strains and hydrostatic pressures however cannot solve the problem of large fracture gaps or even bone defects. The biological capacity of bone regeneration seems to be limited. Fracture healing is increasingly delayed with greater size of fracture gap and large defects cannot heal at all.

For such clinical problems the reduction of the bony defect and application of a favorable, bone formation stimulating tissue strain can be used. This can be done for bone defects by applying a callus distraction or a temporary shortening and distraction of a fracture with a large fracture gap. The biomechanical favorable conditions for a fast and successful bone regeneration by callus distraction are the same as those for the normal fracture healing process.

The cellular reaction to biomechanical signals can be described as a function of the tissue strain and hydrostatic pressure in the callus zone. This allows for the development of mechano-biological models of the fracture healing process. Such FEM-models can simulate the effects of IFM, blood supply and type of fracture on the fracture healing process. Using these models, it is possible to optimize fracture fixation devices and to reduce the number of animal experiments necessary for the study of various parameters involved in fracture healing.

Oral presentations

PLA SCAFFOLDS OBTAINED BY SUPERCRITICAL FLUID FOAMING FOR BONE TISSUE ENGINEERING

*,***Pioletti DP, *Montjovent MO, ***Mathieu L, ****,*****Schmoekel H, ******Mark S, ***Bourban PE, ** Zambelli PY, *** Månson JAE, *******Applegate LL

*Laboratoire de Biomécanique en Orthopédie (LBO), Ecole Polytechnique Fédérale de Lausanne (EPFL), CH-1015 Lausanne, Switzerland

**Hôpital Orthopédique de la Suisse Romande (HOSR), CH-1005 Lausanne, Switzerland

dominique.pioletti@epfl.ch

INTRODUCTION: Bone is the most commonly replaced tissue of the body, with over 450,000 bone repair procedures performed per year in the United States alone. As part of the bone tissue engineering project developed at Lausanne, a bioresorbable polymer poly(lactic acid) (PLA, Boerhinger Ingelheim) was used to create a structure that could guide bone formation by facilitating cell migration, proliferation and differentiation. The 3-D foam morphology could be modified varying the processing conditions. In addition, the possibility of integrating ceramic materials into the polymer matrix improves its mechanical properties. Hydroxyapatite (HA) and β-tricalciumphosphate (β-TCP) were chosen for this purpose due to their capacity to stimulate natural bone repair. The interesting mechanical properties of such structures and their biocompatibility with primary osteoblasts *in vitro* were recently described [1-3]. The aim of this study was to test these scaffolds *in vivo*. A rat craniotomy critical size defect model was used.

METHODS: Implants were evaluated for local bone formation in a rat critical-size defect (CSD) osteotomy model. Calvarial, 8 mm diameter defects were created in Sprague-Dawley rats. Skulls were harvested 12 days and 18 weeks after surgery. They were analyzed radiographically and histologically.

RESULTS: At the latest time-point, new bone formation was observed within PLA/ceramic porous structures and along the dura mater (Fig. 1).

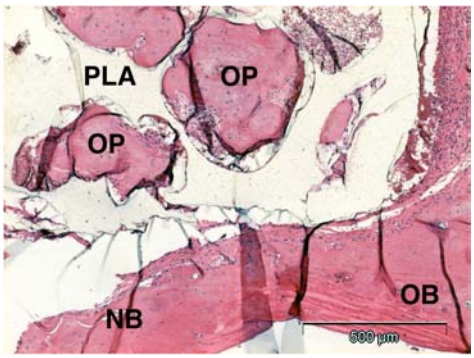

Figure 1: PLA/β-TCP scaffold, 18 weeks after implantation. Note the numerous ossified porous. PLA scaffold (PLA), New bone (NB), Old bone (OB), Ossified porous (OP). Scale bar: 500 µm.

DISCUSSION: PLA composite scaffolds obtained by supercritical fluid foaming showed good acceptance by host tissue. Bone formation was also observed, demonstrating the osteoconductivity of these porous structures.

REFERENCES:

1. Mathieu, L. M., Mueller, T. L., Bourban, P. E., Pioletti, D. P., Müller, R., Månson, J. A. E. Architecture and properties of anisotropic polymer composite scaffolds for bone tissue engineering. Biomaterials 27 (6): 905, 2006.
2. Mathieu, L. M., Montjovent, M. O., Bourban, P. E., Pioletti, D. P., Månson, J. A. E. Bioresorbable composites prepared by supercritical fluid foaming. J Biomed Mater Res A 75 (1): 89, 2005.
3. Montjovent, M. O., Mathieu, L. M., Hinz, B., Applegate, L. L., Bourban, P. E., Zambelli, P. Y., Månson, J. A. E., Pioletti, D. P. Biocompatibility of bioresorbable PLA composite scaffolds obtained by supercritical gas foaming with human fetal bone cells. Tissue Engineering 11 (11/12): 1640, 2005.

ACKNOWLEDGEMENTS: This study was supported by grants from the Swiss National Science Foundation (PNR 46 N°404640-101114/1 and FNRS N°2100-066872.04.01), the Fondation Lémanique pour la Recherche sur le Tissu Osseux, and by the Lausanne Center for Bone Tissue Engineering.

AFFILIATED INSTITUTIONS FOR CO-AUTHORS:

***Laboratoire de Technologie des Composites et Polymères (LTC), Ecole Polytechnique Fédérale de Lausanne (EPFL), CH-1015 Lausanne, Switzerland.
****Laboratoire de Médecine Régénérative et de Pharmacobiologie (LMRP), Ecole Polytechnique Fédérale de Lausanne (EPFL), CH-1015 Lausanne, Switzerland.
*****Poliklinik für Kleine Haustiere der Universität Berlin, D-14163, Germany
******Ludwig Institute for Cancer Research, Lausanne Branch, University of Lausanne, Epalinges, Switzerland.
*******Unité de Thérapie Cellulaire en Orthopédie, Centre Hospitalier Universitaire Vaudois (CHUV), CH-1011 Lausanne, Switzerland.

3D-BIOACTIVE SCAFFOLDS FOR BONE REGENERATION

*Verné E, *Vitale-Brovarone C, *Robiglio L, *Appendino P, **Bassi F,
**Mozzati M, ***Muzio G, ***Martinasso G, ***Canuto R
*Politecnico di Torino, Corso Duca degli Abruzzi 24, 10128 Torino, Italy
enrica.verne@polito.it

INTRODUCTION

Bone replacements are frequently needed due to trauma, bone neoplasia, stabilisation of spinal segments and more generally in many orthopaedic, maxillofacial and craniofacial surgeries. Autograft, allograft and xenograft present some drawbacks such as donor site morbidity, limited availability, immune rejection and risk of viral transmission. For these reasons, artificial grafts (scaffolds) are interesting and challenging candidates for stimulating the bone regeneration and for supporting the newly formed bone. 3D-scaffolds should show a highly porous, open structure to allow a proper vascularisation of the implant, as well as the flow of nutrients and waste products through the scaffold. Specifically, the porous structure should be highly interconnected, with pore size in the range of hundreds of microns (100-500 μm) considering the size of blood vessels and osteoblasts and in amount higher than 50-60 % vol. In this work, a bioactive glass of complex composition was used to synthesise glass-ceramic macroporous scaffolds. It is widely known that certain glasses, when in contact with physiological fluids can stimulate the bone production through a ions exchange phenomena which lead to the precipitation on their surfaces of microcrystals of hydroxylapatite (HAp) which allow a stable bond with the surrounding bone tissue.

METHODS

The glass was prepared through traditional melting and quenching technique. The glass was ball milled and sieved to obtain powders of proper size. The powders where mixed with water and poly-vynil alcohol and the suspension was used to impregnate a polyurethane sponge. The sponge was then dried and thermally treated to remove the organic part and to sinter the inorganic one. The obtained scaffolds were characterised through SEM, EDS and XRD to assess the scaffold morphology, its composition and structure. The porosity was investigated through weight measurements, image analysis and mercury intrusion porosimetry. The *in vitro* bioactivity was tested through soaking in simulated body fluid (SBF) for different time frames.

For the biological test, scaffolds pre-treated in SBF for 1 week were used. The sterilized scaffolds were preconditioned for 24 hours with culture medium in multiwells and used to grow MG-63 osteoblasts. After removing the preconditioning medium, the cells were seeded (10,000 cells/cm^2) in multiwells containing the scaffolds for 10 and 20 days. The scaffolds were used to count the cells grown onto and inside them and to evaluate the presence of calcium nodules and the morphology of the cells on the scaffold. Specifically, to determine the formation of calcium nodules due to mineralization phenomena, cells harvested from scaffolds treated with trypsin were stained with alizarin S red Aiming to study the effect of bone morphogenetic proteins on the scaffold biological behaviour, human BMP-2 were added to the cells immediately after the seeding on the scaffold.

RESULTS

Glass-ceramic macroporous scaffolds were obtained. The total porosity is about 65-70% vol.; the pores are open, highly interconnected and the struts are well sintered and free of cracks. The scaffolds were tested in compression and showed an average strength of 2.5 MPa which is comparable to the data reported in literature. The scaffolds showed a high bioactivity as their surface was completely covered by microcrystals of HAp after only a week of soaking in SBF. The osteoblasts seeded onto the scaffolds proliferated on them showing a good spreading. The histochemical analysis showed several areas positive for calcium both for the control (scaffold pre-treated in SBF) and for the BMP2-treated scaffold.

DISCUSSION

The obtained 3D scaffolds are characterised by a lot of open, highly interconnected macropores within 100 and 500 μm, which is the ideal size reported in literature for a bone substitute. The SEM observations showed that each macropore is surrounded by continuous struts which are free of cracks or other defect, demonstrating the effectiveness of the impregnation and sintering phases. The trabeculae are characterised by a dispersed microporosity in the range of 1-5 μm, which it is known to be useful for protein attachment and cell adhesion. The biological behavior of scaffolds was demonstrated by osteoblast proliferation inside the scaffold and by the synthesis of calcium nodules. The quantity of calcium nodules increased with the time of culture and with the presence of BMP-2. In the latter case, the calcium nodules were larger than in the control even if the cells were in lower number. This fact suggested us the possibility that osteoblasts in the presence of BMP-2 were more differentiated than in the control.

ACKNOWLEDGEMENTS

This work was supported by grants from Regione Piemonte, and by National Research Project PRIN 2003.

AFFILIATED INSTITUTIONS FOR CO-AUTHORS

** Department of Human Oncology and Biomedical Sciences, School Dentistry, Università di Torino, Italy.
***Department of Experimental Medicine and Oncology, Università di Torino, Corso Raffaello 30, 10125 Torino, Italy

TISSUE ENGINEERING FOR MENISCUS REGENERATION IN A SHEEP MODEL

*Kon E[*], *Delcogliano M, *Filardo G, **Chiari-Grisar C, **Nehrer S, ***Ambrosio L, ****Salter D, *****Tognana E, *Marcacci M

[*]Istituto Ortopedico Rizzoli, via di Barbiano 1/10, Bologna 40136, Italy

e.kon@biomec.ior.it

INTRODUCTION

Injuries or complete loss of the meniscus cause cartilage degeneration and osteoarthritis. The healing capacity of the meniscus is limited. Artificial meniscus replacement is a possible alternative to allograft transplantation, which is associated with limited availabilty, logistical difficulties and the risk of disease transmission. Within the framework of the EC-Project GRD1-2001-40401 a pivotal study in sheep was conducted to evaluate surgical technique, critical defect size, implant ingrowth and integration, and postoperative mobilization using a meniscus replacement device.
A new biomaterial consisting of hyaluronic acid and polycaprolactone was used as a meniscus substitute in sheep.

METHODS

Twelwe sheep (right stifle joints) were treated with total meniscus replacements. Six of those received a total meniscus replacement with the implant of the scaffold seeded whit autologous articular chondrocytes while the others six sheep were treated whit the implant of the empty scaffold. The animals received a plaster cast for 5 days. The animals were euthanized after 4 months. The specimens were assessed by macroscopic evaluation focusing on implant aspect and tissue quality, its integration to the capsule, fixation and location using a 'meniscus implant score' (min 9, max 27). A routine histologic processing with paraffin embedding and 3 µm cuts was performed. The specimen were subjected to staining of hematoxilin/eosin for general morphology, Safranin O/Fast Green for glycosaminoglycans (GAG) and Azan for collagen. A mapping system for the implant was created, dividing the implant into a peripheral (zone 1), intermediate (zone 2) and central (zone 3) zone, moreover a superficial (zone s) and a core (zone c) zone were determined. The cartilage underneath the implant was assessed in the periphery (cart – p) and the center (cart – c).
All of the joints were compared with the non-operated ones and evaluated with 'joint changes score' (min 48, max 0).

RESULTS

A mild swelling, due to the thickening of joint capsule, was noted in all animals, there was no joint instability and no infection. The implants remained in position and showed excellent tissue ingrowth and integration to the capsule. However, we observed in some sheep some clefts of the implant and a full substance tear in three of them due to the insufficient mechanical proprieties of the graft. The average meniscus implants score was 22.33 (min 18, max 26) for the scaffold cell seeded and 20.66 (min 17, max 25) for the cell free. The histological investigation revealed tissue formation, cellular infiltration and vascularization.

CONCLUSION

The present study shows promising results concerning the biological qualities of this biomaterial. The mechanical properties of the implant should be improved. The promising results concerning tissue formation and its meniscuslike properties and also the role of the cell will have to be confirmed in future long-term animal studies actually ongoing.

AFFILIATED INSTITUTIONS FOR CO-AUTHORS

[**]Department of Orthopaedics, Medical University of Vienna, Waehringer Guertel 18-20, A-1090 Vienna, Austria
[***]Institute of Composite and Biomedical Materials IMCB-CNR, and Interdisciplinary Research Centre in Biomaterials, Università di Napoli "Federico II", Piazzale Tecchio 80, 80125 Napoli, Italy
[****]Department of Pathology, Edinburgh University Medical School, Teviot Place, Edinburgh EH8 9AG, UK
[*****] Fidia Advanced Biopolymers s.r.l. Via Ponte della Fabbrica 3/B, 35031 Abano Terme (PD), Italy

EFFECT OF DYNAMIC CULTURING OF HUMAN MESENCHYMAL STEM CELLS ON 3D POROUS PLGA SCAFFOLDS FOR BONE TISSUE ENGINEERING

*Stiehler M, *Baatrup A, *Lind M, **Kassem M, *Bünger CE, *Mygind T
*Orthopaedic Research Laboratory, Department of Orthopaedic Surgery E, Aarhus University Hospital, Aarhus, Denmark
maik.stiehler@ki.au.dk

BACKGROUND

The generation of autologous bone tissue for the surgical treatment of musculoskeletal diseases is a major clinical need. Controlled convection of cell culture media around porous scaffolds seeded with rat osteoblasts using spinner flasks has shown to have a positive effect during the early stage of *ex vivo* bone formation.[1,2] The aim of this study was to investigate the effects of dynamic culturing of human mesenchymal stem cells (MSCs) on 3D porous poly(D,L-lactide-co-glycolide) (PLGA) scaffolds in a spinner flask bioreactor with respect to proliferation, distribution, and osteogenic differentiation of the cells.

MATERIALS AND METHODS

Three-dimensional porous scaffolds (dimensions: 8 x 8 x 5 mm, pore size: 100-600 µm) were prepared from 75:25 PLGA by solvent casting and particulate leaching method.[2] Two million immortalized human MSCs[3] were seeded onto each scaffold. The cell/scaffold constructs were either cultured dynamically in the spinner flask bioreactor (**Figure 1**) or maintained in static culture for at 95% air and 5% CO_2 at 37°C. Cellular proliferation was assessed by total DNA determination. Cellular distribution was visualized by fluorescence microscopy using Hoechst 33258-dye labeled cell/scaffold-sections. Osteogenic differentiation was evaluated by spectrophotometrical determination of alkaline phosphatase activity (Sigma-Aldrich) and by Arzenazo III calcium assay (Diagnostic Chemicals Limited). Scanning electron microscopic analysis was performed using a MaXim 2040 EnVac system (CamScan Electron Optics Limited). Real-time quantitative RT-PCR was performed on a 7500 Fast Real-Time PCR system (Applied Biosystems).

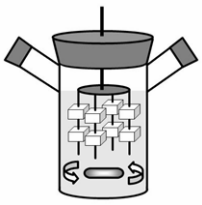

Figure 1
Spinner flask bioreactor generating convective forces by rotation of a magnetic stirrer.

RESULTS

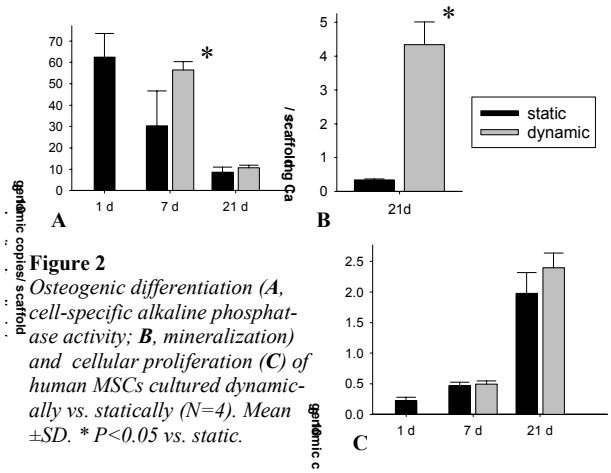

Figure 2
*Osteogenic differentiation (**A**, cell-specific alkaline phosphatase activity; **B**, mineralization) and cellular proliferation (**C**) of human MSCs cultured dynamically vs. statically (N=4). Mean ±SD. * P<0.05 vs. static.*

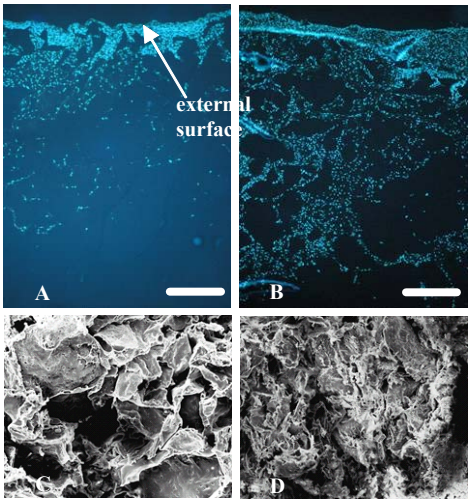

Figure 3
*Improved cellular distribution and extracellular matrix deposition after 21d of dynamic (right) vs. static (left) culturing of cell/scaffold constructs. Fluorescence microscopy (**A**, **B**, scale bars = 100 µm) and scanning electron microscopy (**C**, **D**, X200).*

Osteocalcin, alkaline phosphatase, osteopontin, and bone sialoprotein gene expression were increased for dynamically cultured MSCs.

DISCUSSION

The convection of cell culture media around the cell/scaffold constructs by the spinner flask bioreactor facilitated both nutrient and oxygen transport to and removal of toxic byproducts from the cells at the interior of the scaffold. This explains the accelerated osteogenic differentiation and proliferation of the cells (**Figure 2**, gene expression analysis), the more homogeneous cellular distribution, and the increased extracellular matrix deposition (**Figure 3**) observed under 3D dynamic vs. static culturing condition. Shear stress arising from fluid convection around the cells mimics the physiological dynamic microenvironment in bone tissue thereby providing a further stimulus for osteogenic differentiation of the MSCs. The present study provides evidence for the effectiveness of dynamic culturing of osteoprogenitor cells on porous 3D PLGA scaffolds using the spinner flask bioreactor for *ex vivo* bone tissue engineering.

REFERENCES

1.) Goldstein SA et al., Biomaterials 22(11), 2001.
2.) Sikavitsas VI et al., J Biomed Mater Res 62(1), 2002.
3.) Simonsen JL et al., Nat Biotechnol 20(6), 2002.

AFFILIATED INSTITUTIONS

**Department of Endocrinology, Odense University Hospital, Odense, Denmark

ACKNOWLEDGEMENTS:

Financial support was granted by the Interdisciplinary Research Group "Nanoscience and Biocompatibility" (grant no. 2052-01-0049, Danish Research Agency) and Danish Rheumatism Association (grant no. 233-1192-10.0205).

HIGH DOSES OF OP-1 INHIBIT FIBROUS TISSUE ARMORING

*Hannink G, **Aspenberg P, *Schreurs BW, *Buma P
*Orthopaedic Research Laboratory, Radboud University Nijmegen Medical Center, The Netherlands
**Department of Orthopedics, Linköping University Hospital, Sweden
g.hannink@orthop.umcn.nl

INTRODUCTION: In revision surgery bone defects can be filled with impacted bone grafts. The provision of immediate stability of the implant is the mechanical goal of the operation. The chance of a failure of the reconstruction is the highest immediately after the reconstruction when the bone graft is not yet incorporated. If the incorporation of bone grafts can be facilitated by growth factors, probably the critical period after a reconstruction with impacted bone grafts can be shortened.
Growth factors, such as BMP-2, PDGF and OP-1 are well known stimulators of bone formation. However, BMP-2 stimulates osteoclasts in vitro and PDGF has been associated with aseptic loosening of prostheses. The role of OP-1 in stimulation of osteoclasts has not been studied in vivo but an in vitro study indicates that OP-1 plays an important role in the recruitment of osteoclasts. Furthermore, preliminary results of a trial in humans with a spinal intracorporal application of OP-1 have shown increased bone resorption as a primary event [1].
Impacted morselized allografts around prostheses serve not only as a bone conductor, but also as mechanical support for the prostheses. Uncontrolled bone graft resorption before the formation of bone may cause loss of stability of prostheses, result in micromotions and ultimately in failure. An often suggested solution would be an osteoconductive material providing initial stability after reconstruction. The role of BMPs in hip revision surgery then may be to serve as promoter of bone formation in combination with slow resorbing or unresorbable graft materials, e.g. TCP/HA particles or bone grafts pretreated with bisphosphonates. The aim of the present study is to investigate the early effect of OP-1 on the incorporation process of impacted morsellized allografts and TCP/HA. Three different doses of OP-1 were tested in two bone chamber studies with impacted morsellized allografts and TCP/HA.

METHODS: Cancellous allografts were obtained from the sternum of six donor goats. TCP/HA particles (BoneSave™, Stryker Howmedica Osteonics, Limerick, Ireland) were used as synthetic bone substitute. The particles consisted of a TCP/HA percentage of 80/20, with a size of 2-4mm and 50% porosity.
We used the bone conduction chamber (BCC) which is a model for membranous ossification [2]. The BCC consists of a titanium screw with a cylindrical interior space. It is made up of two threaded half cylinders held together by a hexagonal closed screw cap [Fig. 1].
In two bone chamber studies, ten combinations of the rhOP-1 device, allograft bone, TCP/HA and collagen carrier material were impacted into the BCC [Table 1]. One of the groups was used for testing another drug, which was out of the scope of this study and therefore not mentioned. Impaction was performed by gradually filling the BCC followed by impaction of the material by a constant force of 40N for 2 minutes. The applied pressure was calculated to be 12.5MPa.
A total of twenty-four goats were operated under general anesthesia. Each goat received six implants. The chambers were placed in the tibia of the goat, three chambers per tibia. The implantation position of the six chambers was randomized. After 4 weeks the goats were killed and the content was carefully removed from the chambers. Each specimen was embedded in PMMA and 5µm sections were made. In order to get a tissue and bone penetration distance, the area of the total tissue and the ingrown bone were divided by the width of the specimen, to yield the mean ingrowth distance [3]. The mean of the three sections at 0, 300 and 600µm from the center yields a value for each specimen.
Statistical analysis was performed using One Way Repeated Measurements ANOVA and Tukey post hoc tests.

Treatment group	Dose (µgOP-1/mg collagen)	Description
Allograft	-	allograft
Allograft+0.83µgOP-1	0.83µg/0.24mg	allograft[1]
Allograft+2.5µgOP-1 (recommended)	2.5µg/0.72mg	allograft[2]
Allograft+25µgOP-1	25µg/7.2mg	allograft[3]
Allograft+mg collagen	0µg/0.24mg	carrier[1]
Allograft+mg collagen	0µg/7.2mg	carrier[3]
TCP/HA	-	TCP/HA
TCP/HA+0.83µgOP-1	0.83µg/0.24mg	TCP/HA[1]
TCP/HA+2.5µgOP-1 (recommended)	2.5µg/0.72mg	TCP/HA[2]
TCP/HA+25µgOP-1	25µg/7.2mg	TCP/HA[3]

The OP-1 device consists of 3.5mg rhOP-1 combined with 1g type I bovine-derived collagen

Table 1. Experimental treatment groups

RESULTS: Histologic examination of the specimens revealed cancellous bone in all chambers. Distally, a zone containing vascularized fibrous tissue was observed, followed by a zone with woven-fibered bone more proximally. No difference in amount of bone ingrowth was found. Fibrous tissue ingrowth was significantly lower in the 2.5µg OP-1 groups ($p=0.003$ and $p=0,001$) and the 25µg OP-1 groups ($p<0.001$ and $p<0,001$) compared to the allograft and TCP/HA group, respectively [Fig. 2]. The carrier groups were not significantly different from the equal dose OP-1 groups.

Figure 1. Bone conduction chamber and implanted chambers in the proximal medial tibia of the goat.

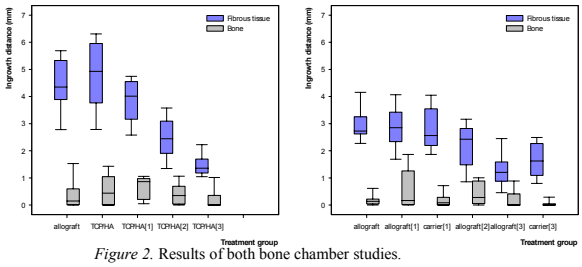

Figure 2. Results of both bone chamber studies.

Discussion: In the present study, a dose-effect relation of OP-1 on total tissue ingrowth was found. Remarkably, an increase in OP-1 dose resulted in a decreasing fibrous tissue ingrowth in both allografts and TCP/HA. It's possible that initially the collagen carrier could have delayed fibrous tissue and bone ingrowth into the bone chambers by its role as a spacer. Since the collagen carrier groups showed similar ingrowth compared with equal dosed OP-1 groups. Another factor may be that the collagen carrier needs extensive exposure to macrophages and other cells to be completely degraded and to release the active substance in a proper way. In an open gap situation an osteoinductive growth factor has immediate access to stem cells and blood supply which are necessary to initiate the osteogenic differentiation process. Within impacted bone chips, the migration of cells into the allograft is compromised and vascularisation is delayed.
During remodeling, e.g. after a hip revision, various parts of the impacted grafts will be at different healing stages, and unremodeled parts are also placed under high stresses. If an increased resistance to graft deformations can be achieved by fibrous tissue ingrowth in parts that have not yet remodeled into new bone, our findings would be clinically relevant. The strength of impacted grafts increased by fibrous tissue armoring may explain, at least partially, why no collapse of morselized impacted grafts occurs with time [4]. Delayed or reduced new bone ingrowth seen in experiments with impaction is therefore of less importance and maybe even beneficial, as long as the graft/fibrous tissue composite remains strong enough to withstand the forces acting on it during remodeling. In our case, using OP-1 device also the fibrous tissue ingrowth is delayed. The observed early failures in impaction grafting could be due to the lack of fibrous tissue armoring using higher doses of OP-1 device, and not necessary due to an increased resorption and remodeling.

ACKNOWLEDGEMENTS: This study was supported by Stryker Howmedica Osteonics, Limerick, Ireland and Stryker Biotech, Hopkinton, MA, USA.

REFERENCES: [1] Laursen et al., Eur Spine J, 8:485-490, 1999
[2] Aspenberg et al., Eur J Exp Musculoskel Res, 2:69-74, 1993
[3] Van der Donk et al., Clin Orthop, 408:302-310, 2003
[4] Tagil et al., Acta Orthop Scand, 72:78-82, 2001

AC-100, A SYNTHETIC FRAGMENT OF MEPE, PROMOTES BONE FORMATION AND MATURATION IN RODENT AND CANINE BONE REGENERATION MODELS

*Rosen DM, *Middleton-Hardie CA, *Aswani S, *Lazarov M
*Acologix, Hayward, CA, USA
david.rosen@acologix.com

INTRODUCTION

Matrix Extracellular Phosphoglycoprotein (MEPE) is a 525 amino acid protein produced primarily by osteoblastic and odontoblastic cells. Its expression has been shown to increase during osteoblastic differentiation and during bone fracture healing. AC-100 (Dentonin®), a central 23-amino acid fragment of MEPE, has previously been reported to have potent anabolic activity on osteoblast and odontoblast precursor cells *in vitro*. *In vivo* studies in rodents indicate that AC-100 stimulates new dentin formation in teeth, and new bone formation at fracture healing sites. Previous data from a rat fracture healing model demonstrated that AC-100 increased the mechanical strength of bone following administration of AC-100. Here we report the effects of AC-100 on bone formation and bone quality in a canine tooth extraction model and a rodent cranial critical defect model.

METHODS

In the canine study, premolars in the mandibles of ten month-old beagle dogs were extracted as a site for evaluation of new bone formation. Sockets were filled with a collagen sponge containing AC-100 at two different doses (1 mg or 10 mg). For controls, sockets were filled with a collagen sponge (CollaPlug) soaked in saline. At days 3 and 28 post-implantation, the mandibles and surrounding soft tissue were removed and fixed in 4% parafomaldehyde, decalcified, and embedded in paraffin. Static histomorphometric analysis was performed on Toluidine blue stained sections using an OsteoMeasure® image analysis system (version 4.00c). For the rodent studies, a critical size defect (8 mm) was created in the parietal bones of 6-7 week old rats as described by Schmitz (Clin Orthop Relat Res 1986). The defects were created using an 8mm dermal biopsy punch and a Dremel (bit#112). The defects were rinsed with saline and filled with a collagen sponge (CollaCote) soaked in saline or AC-100. The rats then received daily injections (100μL) of saline or AC-100 over the surgery site for 6 days. AC-100 was administered at doses from 10 μg to 10 mg per administration. At 28 days, the calvariae were removed, fixed, stained and analyzed as described above. The canine study protocol was reviewed and approved by the IACUC at both SkeleTech and Washington State University and the rodent protocols were approved by the Acologix IACUC.

RESULTS

In the canine study, there was still residual collagen sponge present at 3 days in all groups. Compared to controls, AC-100 treatment groups contained a denser fibroblastic infiltrate along with increased deposition of new collagenous matrix. At 28 days, there was no detectable collagen sponge remaining. In spite of the removal of the septae, presumably due to the young age of the animals, there was still significant new bone formation in the control group. At 28 days, although there was no significant difference between groups with respect to the amount of new bone formed, application of AC-100 resulted in a highly significant and dose dependent improvement in the quality of the newly formed bone. The AC-100 groups had bone quality scores approximately two (1mg; $p=0.077$) and three (10mg; $p<0.005$) times higher than controls. The control group sockets contained new bone with a woven appearance, whereas sockets filled with collagen sponge + AC-100 contained bone that was more lamellar and contained mature osteonic structures. In sockets given the lower dose of AC-100, there was a mix of woven and lamellar bone. In sockets given the higher dose of AC-100, there was very little woven bone remaining.

In the rodent study, there was a biphasic dose-response curve with respect to bone formation with maximal activity being observed at doses of 70-350 μg (cumulative dose). As in the canine study, there was also a dose-dependent increase in the amount of lamellar bone. In this model, there was also a significant increase in the % of defects that were fully bridged.

DISCUSSION

Here we describe the activities of AC-100 relevant to bone repair. These studies demonstrate that AC-100 is capable of forming mature bone in both canine and rodent models. In the rodent critical size defect model, the bone formation was also accelerated compared to control groups. Although a number of bioactive agents have been evaluated pre-clinically in various bone defect models, few products have been approved to date. AC-100 has the advantage that its activities appear to be restricted to cells in the osteoblastic and odontoblastic lineage. This is in contrast to other growth factors that can induce non-specific proliferation and BMPs that can cause ectopic bone formation. Furthermore, since AC-100 is a small synthetic peptide, it also has the advantage of a lower cost of manufacture compared to most recombinant proteins. Most important among its properties is the ability to promote the formation of mature bone. These data in combination with previous data from a rat fracture-healing model, suggest this compound could have utility in a wide variety of orthopedic indications.

EX VIVO GENE THERAPY APPROACH USING HUMAN LIM MINERALIZATION PROTEIN-3 TO INDUCE SPINE FUSION IN A RODENT MODEL

*Pola E, *Logroscino G, **Lattanzi W, *Logroscino CA
*Department of Orthopaedics and Traumatology, ** Department of Anatomy,
Università Cattolica del Sacro Cuore School of Medicine, Rome, Italy

enricopola@hotmail.com

INTRODUCTION

Gene therapy research in the field of orthopaedics and traumatology have evolved during the last decade, leading to possible applications for the treatment of pathological conditions, such as bone fractures and cartilage defects. Regional gene therapy may represent an option to enhance bone formation, since a target gene can be delivered to a specific anatomic site and drive protein production. Many proteins and growth factors are emerging as functional component of the osteogenic cascade. In particular Lim Mineralization Proteins (LMP), coded by three different splice variants (LMP-1, LMP-2, LMP-3) of the same gene, have been identified as regulators of the osteoblast differentiation program. We have previously demonstrated that human LMP-3 (hLMP-3) contributes actively to bone formation. In the present study this transcriptional factor has been tested in a rodent model, to induce spine fusion by an ex vivo approach.

METHODS

C57BL/6J mice have been operated in this experiment. The animals have been divided in 3 groups: mice treated with cells infected with an adenoviral vector expressing human LMP3 and seeded on a scaffold before implantation; mice treated with cells infected with an empty adenoviral vector and seeded on a scaffold; mice treated only with the Hydroxyapatite/Collagen scaffold. All the groups have been evaluated at 2, 4, 8 and 12 months after the operation by radiographic and histological examinations.

RESULTS

All the animals treated with autologous engineered cells transduced *ex vivo* with Ad-LMP-3 developed bone formation already 2 months after the treatment, as confirmed histologically and radiographically. None of the controls showed signs of spine fusion at the different time points.

DISCUSSION

Spine fusion represent an important possible application of gene therapy in orthopaedics. In this study we demonstrate that autologous engineered cells transduced *ex vivo* with Ad-LMP-3 induce efficiently bone formation and spinal fusion in a rodent model, when implanted by the use of a scaffold, validating the *in vivo* osteoinductive properties of the new osteogenic factor human Lim Mineralization Protein-3.

COMBINING SUBJECT-SPECIFIC AND COLLECTION DATA TO CREATE PREDICTIVE MODELS TO BE USED IN THE CLINICAL PRACTICE

*Viceconti M, *Montanari L, *Taddei F, *Martelli S, **Manfrini M, *Toni A
*Laboratorio di Tecnologia Medica, Istituti Ortopedici Rizzoli, Bologna - Italy
viceconti@tecno.ior.it

ABSTRACT
There is an increasing role for computer models in predicting the outcomes of treatment. A common problem is that to be accurate these models need detailed quantitative information on the patient anatomy and physiology, which is only partially retrievable with standard clinical examinations. A possible solution is to merge the few available data on our patient, with the many data available for selected populations subjected to detailed investigations. The scope of this paper is to summarise the state of the art in this emerging domain, with particular reference to the musculoskeletal apparatus.

INTRODUCTION
Computer models are being used to predict treatment outcomes in various medical specialties [1, 2]. In orthopaedics, computer models have been used to analyse long term bone remodelling [3], to investigate the effect of surgical procedures patellar tracking [4], as well as in the surgical planning of skeletal oncology procedures [5, 6]. The methods recently developed to generate subject-specific models are sound [7]; indeed, validation studies confirmed that they can be used in a clinical context [8], and their predictions are accurate [9].
The main problem to a widespread diffusion of these models in the clinical practice is that it usually necessary to have large amount of quantities data on the patient, in order to build them. While these detailed subject-specific data may be collected in a research environment, ethical, logistic and economical constraints make difficult to retrieve the in a clinical setting.
This paper describe a possible alternative approach that combines subject-specific data with generic normality data obtained from large collections such as the Living Human Project [10] or the IUPS Physiome project [11].

MATERIALS AND METHODS
In order to illustrate this approach, we used a complex model that is used to predict the stresses induced by certain rehabilitation programs in the skeletal reconstructions performed to treat skeletal tumours.
The model requires a detailed CT of the reconstructed region, and a complete gait analysis session. In ideal conditions the patient should wear skin markers during both exams, to make possible accurate spatial registration between the anatomical data obtained from the CT and the motion data obtained with the gait analysis. However, this protocol involves a significant complexity and produces a significant logistic impact on the clinical departments.
The complete research protocol was conducted on an 11-years old patient, who had received a distal femur biological reconstruction. Two models were generated, one using all subject-specific data, the second by using average movement data obtained form the literature and properly scaled to the patient body.
The registration between the patient data and the normality data was performed using an advanced environment for data fusion called *Data Manager*, developed by our institution in collaboration with other partners.

RESULTS
The muscle forces predicted with the two models present certain differences that justify the use of the most complex problem for research purposes. However, the differences do not appear to be so important to impose this complexity when the model is being used in a clinical setting simply to assist the surgeon and the physiatrist in the rehabilitation planning.

CONCLUSIONS
The proposed method appears to be adequate for the specified purpose. This approach can be extended to other case, drastically increasing the usefulness of computer modelling in the daily clinical practice.

REFERENCES
1. Hann CE, *et al*. Comput Methods Programs Biomed. 2006 11; [Epub ahead of print]
2. Luboz V, *et al*. Comput Methods Biomech Biomed Engin. 2005 8(4).
3. Lengsfeld M, *et al*. Med Eng Phys. 2005 Oct;27(8).
4. Fernandez JW,*et al*. Bio Mod Mechanobiol. 2005;4(1).
5. Taddei F, *et al*. Chir Organi Mov. 2003;88(2)
6. Taddei F, *et al*. Proc Inst Mech Eng [H]. 2002;216(2)
7. Viceconti M, *et al.* Crit Rev Biomed Eng. 2003;31(1-2)
8. Viceconti M, *et al*. J Biomech. 2004 ;37(10)
9. Taddei F, *et al*. J Biomech. 2005; [Epub ahead of print]
10. http://www.tecno.ior.it/VRLAB/LHP/
11. http://www.physiome.org/

**Skeletal Oncology Department
Istituti Ortopedici Rizzoli
Bologna, Italy

FACTORS AFFECTING THE MAXIMUM FLEXION ANGLE IN TKR

Walker PS, Yildirim G, Sussman-Fort J, Roth J, White B, Klein KR
Department of Orthopaedic Surgery, New York University – Hospital for Joint Diseases, New York, USA
ptrswlkr@aol.com

INTRODUCTION

While the average range of flexion for series of total knees is usually 100-120 deg, there is a large spread within each series (Dennis). An influential predictor of postop range is preop (Ritter) but with improved surgical and rehab techniques, more patients will be able to reach higher angles. Hence it is important that the positioning of the components and the design itself are able to accommodate high flexion before posterior impingement of the femur on the posterior edge of the plastic. Such impingement could cause plastic damage, loosening, and limit flexion. The purpose of this lab study was to determine the effect of surgical and design variables on maximum flexion before impingement.

METHODS

A test rig was constructed for loading the knee and measuring the flexion angle at impingement for a range of positions of the femoral and tibial components on the bones (fig 1), locations of the contact points on the tibial surface, and int-ext rotation angles. The NexGen CR was used, as well as a medial pivot mobile bearing using the NexGen femoral component. Relative to the ideal position of the femoral component on the femur, cuts were also made to seat the component 2mm in either distal, proximal, anterior, or posterior directions (fig 1). Plastic femurs were used for reproducibility. The tibial slope was 2, 5 and 8 degrees. The positions and angles were set with an adjustable slider on the rig. The AP contact positions ranged from the very posterior (zero) to 20 mm anteriorly. Rotation angles were +/- 15 deg. All the ranges were taken from fluoroscopic data (Bellemans; Banks; Bertin; Dennis; Kenekasu). To obtain accurate locations, angles and contact positions, fiducial points were digitized on the bones and components, and were later reconstructed in the computer using Rapidform software.

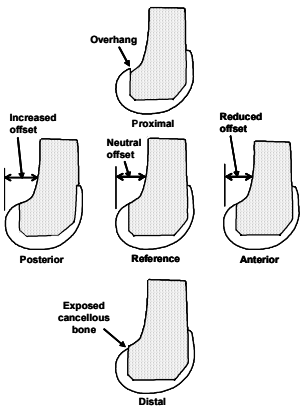

RESULTS

For the reference position, maximum flexion ranged from 156 deg with the contact at the posterior of the tibia, to 142 deg for 20mm anterior (fig 2). Placing the femoral component 2mm posterior on the femur (increasing femoral offset), increased the flexion by up to 5 deg. A more proximal position increased flexion but by a smaller amount. Anterior placement produced the largest reduction by up to 8 deg, with distal placements causing reductions almost as large. Exposed cancellous bone just proximal to the posterior condyles of the component was the main cause of the reductions. The mobile bearing results were very similar except for a 2 deg reduction due to the 1mm higher posterior lip on the plastic. For 10-15 deg rotation in the fixed bearing knee, the reduction in flexion was 2-4 deg. For the mobile bearing there was no reduction so long as the plastic moved with the femur (Dennis). For a change in slope angle of the tibial component, there was a similar change in the flexion angle at impingement.

DISCUSSION

The results are consistent with clinical data from Bellemans for posterior condylar offset, for AP position with Banks, and with Klein for mobile vs fixed bearing. If the target for a TKR is 150 deg with a contact position 10mm from posterior (to avoid deformation and to allow rotation) then proximal and posterior femoral positioning are an advantage with a tibial slope of 5 deg (fig 3). However in addition, it seems an advantage if the posterior condyles of the femoral component are both thicker posteriorly and taller to project above the posterior cut surface of the femur. A mobile bearing can preserve the flexion even in rotation but that only gives a few degrees advantage unless the rotation is beyond 15 deg.

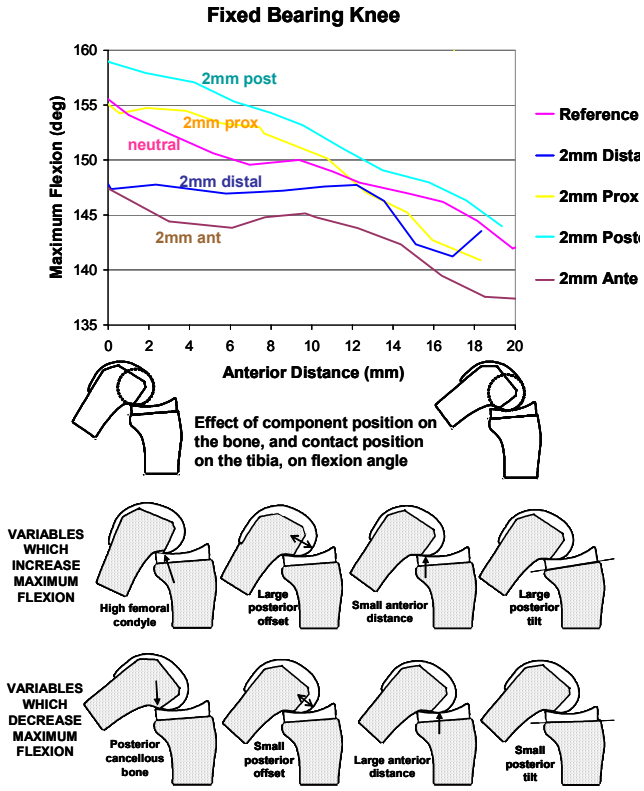

CAN MUSCULAR STIMULATION INCREASE ARTICULAR STABILITY IN ACL-DEFICIENT KNEES?

*Bonsfills N, *Núñez A, **Gómez-Barrena E
Universidad Autónoma de Madrid, Madrid, Spain
nbonsfills@epersonas.net

INTRODUCTION

Muscular stiffness, as well as contraction from precise neuromuscular control, helps to diminish joint laxity. In anterior cruciate ligament (ACL)-deficient knees, neuromuscular control is poor and ineffective, so it may be necessary to compensate it with electrical stimulation. Time-adjusted stimuli can control knee stability without fatigue, and may increase quadriceps and hamstrings stiffness, for a better response to movement. So, our aims are to measure muscular reaction (fibre length and EMG activity) and mechanical response of the knee (anterior tibial displacement ATD and ligament strain) before and after electrical stimulation of periarticular muscles.

METHODS

Seven cat knees were studied under pentobarbital anesthesia to avoid voluntary muscle contraction. Muscle fibre length variations were measured with ultrasonomicrometry of the four main periarticular muscles. EMG was registered with intramuscular electrodes. Ligament strain was obtained from strain gauges attached to the distal insertions of medial collateral ligament and patellar tendon. ATD was calculated from digitized video recordings of the knee on the sagittal plane. The knees were submitted to anterior tibial traction up to 9.8 N before and after ACL transaction at flexion angles of 90 and 30º. In unstable knees, a train of square 0.2 ms pulses was generated both before and after the maximum traction was applied. Protocols of 20 ms, 100 ms, and 500 ms stimulation were applied. Normalized deformation and its slope were calculated from muscles and ligaments, and pre-stimulus EMG activity was measured for each muscle.

ATD, deformation, and electrical activity from muscles, and strain from ligament insertions, were compared in four scenarios: before and after maximum traction, both in stable and unstable knees along each series. Mann-Whitney's test was used for comparisons.

RESULTS

Direct effect of stimulation. Increased anterior laxity with maximal traction was controlled down to the level of stable knees by electrical muscle stimulation in unstable knees. However, external rotation was observed after stimulation with the knee 90º flexed. Stimulation generated a contraction with shortening of both quadriceps and hamstrings that was not different from lengthening due to anterior traction.

Stabilization of unstable knees. Pre-stimulus values of deformation and ligament strain were similar in stable or unstable knees that were stimulated. Deformation slope of muscles was significantly lower in stimulated knees ($p<0.05$). Ligament strain was increased in stimulated knees. Muscular basal electric activity increased after several stimulations, without muscular fatigue comparing the first and last stimulation pulses per series.

Stimulation before the maximum anterior tibial traction produced a controlled tibial displacement that ceased at the end of the stimulation train (Figure 1). When ATD was compared in stable and stimulated unstable knees, the last showed laxity values similar to stable knees (especially with 30º flexion) (Figure 2).

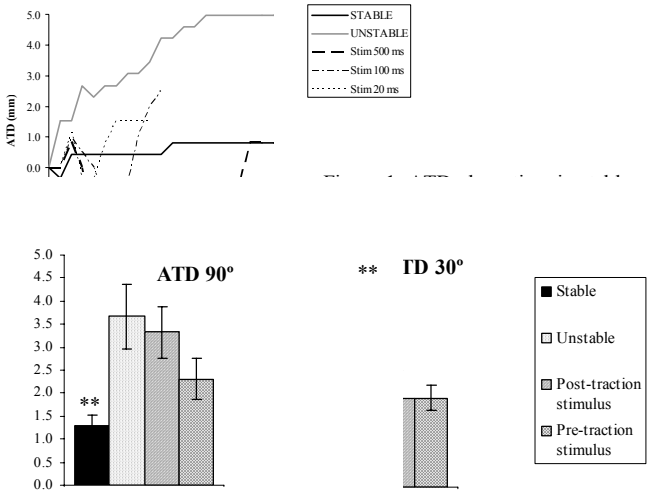

Figure 2. Maximal ATD in stable, unstable, post-traction stimulated and pre-traction stimulated knees (500 ms stimulus). Bars represent mean ± standard error. ** = $p<0.01$.

DISCUSSION

Immediate effect of electrical stimulation can control excessive knee laxity in absence of ACL. The ATD resulting of synchronized stimulus appears to favor that control, at least as long as the stimulus is present, as it is shown in Figure 1. Besides, increased electrical activity and slower lengthening of muscles in stimulated knees suggest an increased resistance of the muscles to be deformed when submitted to anterior tibial traction.

But, stimulated muscles cannot avoid higher strain in periarticular ligaments in unstable knees, values that are not different from the ones in unstable, not stimulated knees. This suggests there is not a fine, precise control of mechanical response of the knee.

ACKNOWLEDGEMENTS

Grant by FIS 01/371, Ministry of Health, Spain.

IN VIVO ANALYSIS OF ANTERO-MEDIAL INSTABILITIES OF THE KNEE. THE ROLE OF ACL

Zaffagnini S, Bignozzi S, Martelli S, Lopomo N, Marcacci M
Laboratorio di Biomeccanica, Istituti Ortopedici Rizzoli, Bologna, Italy

s.zaffagnini@biomec.ior.it

INTRODUCTION

The treatment of ACL lesion combined with torn MCL is a controversial issue []. This residual laxity, in fact, might be responsible for loosening over time of the ACL graft and cause failure of the reconstruction.

Recently, more attention has been given to residual rotational instability and the possibility of addressing ligamentous structures other than ACL in combined ligament injuries. It is clear that further investigation is needed to clarify the correct treatment for combined ACL and MCL injuries. In the literature, in fact, only animal model or clinical follow-up evaluation studies can be found. Few studies have presented *in vivo* results of combined ACL and MCL injuries, focusing mainly on preoperative tibial translation.

The aim of this study was, firstly, to evaluate *in-vivo* if the degree of instability was higher in combined ACL and MCL injury with respect to isolated ACL rupture, and secondly, if a single ACL reconstruction was capable of restoring all the residual knee laxities in isolated ACL or combined ACL and MCL injuries.

METHODS

We studied 18 patients, with a mean age of 30 years. The patients were classified according to the lesions: group "A" included knees with pure ACL lesion (8) and group "AM" included knees with associated MCL lesions (10). Surgery consisted of an arthroscopic double-bundle ACL reconstruction with hamstring tendon technique.

To evaluate the joint laxity we used a custom navigation system consisting of an optical localizer and software developed at our institute for this purpose. During intervention, reference frames were fixed on bones and a brief registration phase was performed through percutaneous digitization of bone reference points, in order to define reference systems of the femur and tibia.

After the registration phase, the operating surgeon performed standard clinical tests, to evaluate joint laxities; these tests included:

- Varus-valgus (VV) stress test at maximum force at 0º and 30º of flexion.
- Internal-external (IE) rotation at maximum force at 30º and 90º of flexion.
- Antero-posterior (AP) stress test at maximum force at 30º and 90º of flexion.

After kinematic tests the graft were inserted and fixed to reconstruct the ACL and the tests were repeated in order to evaluate the residual laxity of the knee.

Statistical analysis, between groups A and AM , in laxity values during the stress tests was performed before and after reconstruction. Comparisons between mean levels of laxity at specific angles of knee flexion were made using Student's test for independent samples. As patients showed a great individual variability in the laxity values a non-parametric statistical analysis, the Mann-Whitney, with Monte Carlo methods for small samples, was performed to verify differences of the values. For both tests the level of significance was set at $P = 0.05$.

RESULTS

Results of test are summarized in table 1

	Pre-op laxity		Post-op laxity	
test	**group A**	**group AM**	**group A**	**group AM**
VV 0º	5.2(1.8)	5.8(1.9)	2.8(1.4)	3.1(0.7)
VV 30º	4.6(1.1)	5.7(2.0)	2.1(0.5)	3.7(1.4) †
AP 30º	9.9(3.5)	11.4(3.9)	3.9(1.7)	5.1(1.8)
AP 90º	6.8(2.8)	10.9(2.9) †	4.1(1.8)	3.9(2.7)
IE 30º	21.3(4.4)	21.3(3.8)	16.0(3.0)	14.4(3.3)
IE 90º	25.5(4.5)	25.0(4.5)	17.6(3.1)	15.4(3.9)

Table 1. Results of kinematic tests. Legenda :†Significantly different from group A ($p < 0.05$). The values are given as the mean, with the standard deviation in parentheses, unit is deg for VV and IE rotations and mm for AP translations.

DISCUSSION

By analyzing the results we have seen that, preoperatively, combined ACL and MCL injuries cause significantly greater AP laxities, at 90º of flexion, with respect to isolated ACL lesions. No significant differences were found for VV and IE rotations.

Postoperative results show that, after the double bundle ACL technique, there is no difference in postoperative AP laxities between isolated ACL and combined injuries. On the contrary, residual laxity remains in the VV test for combined ACL and MCL lesions, with a statistical difference between postoperative laxity values for VV test at 30º of flexion. No difference was fond for IE rotations.

The results obtained in combined injuries confirm the hypothesis that residual laxity remains when isolated ACL reconstruction is performed. This residual laxity might be responsible for loosening over time of the ACL graft and cause failure of the reconstruction. These observations are in line with the cutting studies that have shown that ACL is the primary restraint for AP, while MCL is the primary restraint for VV.

THE INFLUENCE OF SCOLIOSIS ON THE PLANTAR PRESSURE DISTRIBUTION

*Pavlačková J, *Hlaváček P
*Department of Footwear Engineering and Hygiene, Faculty of Technology, Tomas Bata University, Zlín, Czech Republic
pavlackova@ft.utb.cz

INTRODUCTION

Scoliosis is defined as curved spine in the frontal plane. It is one of the most complex afflictions in orthopaedics with diverse causes. The subject of our study was not merely defective posture or scoliosis itself, but primarily to monitor and describe the impact or manifestation of defective posture on children's feet and the total quality of locomotion among school-aged children with such afflicted posture.

METHODS

Measurement of the children – scoliotics was conducted in co-operation with a rehabilitation facility visited by the afflicted children for regular exercises. The monitored group consisted of a total of 22 subjects at the age of 12 ± 3 years, who were monitored over a period of four months. For individual subjects, the following was determined: body height (156.8 ± 19.3 cm), body weight (45.7 ± 12.5 kg) and BMI (18.4 ± 2.3 kg/m^2). Another part of the measurement focused on the anthropometric characteristics of the foot, the heel axis, the status of the foot arches; type of scoliosis; its orientation and localization. The majority of the children suffered from double-major curve scoliosis, of which 50% of the children had scoliosis on the right, another 20% on the left and for the remaining subjects, the orientation could not be determined. The measurement of tread pressure was conducted using a PEDAR® instrument. This equipment serves to measure the pressure between the foot and the insole of footwear when walking. During the measurement of tread pressure, the measured insole was placed inside the footwear in direct contact with the foot. In this way, it is possible to acquire information from a multiple step, when the subject covers an established distance with a loose gait and throughout the entire walking period the pressure between the foot and the insole is recorded. The measured values were entered into a computer. The measurement was repeated four times. With the help of software, values of maximum pressure were determined as well as its occurrence on the foot sole, maximum force and contact surfaces. These values were acquired throughout the entire course of walking, particularly for the right and left foot and also on individual parts of the foot sole, which were divided into masks. Mask M01 describes the area of the heel and extends up to 25% of the length of the sole; mask M02 describes the internal part of the arch, mask MO3 the lateral part of the arch and both of these masks were divided lengthwise along half the splay of the feet. The last mask, M04, describes the front part of the feet and extends up to 75% of the length of the sole through the toes.

RESULTS

For our group, scoliosis of the spine was accompanied by a valgos heel position in 95.5% of the subjects, which contributes negatively to overload on the internal foot arches. A relationship was construed between the maximum force on the heel axis, when this force was targeted to unit weight and fluctuated in a range from 50 to 157% BW, but no physical link was demonstrated between these values (correlation coefficients were up to 0.1). In another phase, the maximum force operating only in mask M01 was assessed and in relation to the axis this already demonstrated a more significant relationship (correlation coefficients 0.2-0.5). Force fluctuated in the range from 2.5 to 96% BW. From the results, the evaluation of maximum pressures in individual masks was observed to shift the load from the medial side of the sole to its lateral side; the greatest load was on the front and rear parts of the sole, i.e. in masks M01 and M04.

DISCUSSION

The manifestations of scoliosis orientation both on the contact surface, the maximum force as well as the maximum pressure did not confirm our hypothesis relating to the unilateral overload of the lower limbs (that is the right or left foot) in the sense of scoliosis orientation, which as we supposed, may be influenced by the posture and locomotion habits to compensate for this orientation. With the rehabilitation period, exercises decreased the size of the contact surface of the foot with the floor, as well as the size of maximum forces and pressures operating on the sole of the foot, which would also correspond to changes in the position of the heel, when the axis in the sense of valgosity, declined and the status of the foot arch also improved.

REFERENCES:

Lomíček M. (1973) *Idiopatická skolióza*. Praha : Avicenum 1973, s. 15.

EXPERIMENTS ON BONE CEMENT POLYMERIZATION: TEMPERATURE AND RESIDUAL STRESSES

Plamondon D, Mądrala A, Nuño N
Département de génie de la production automatisée, École de technologie supérieure,
Laboratoire de recherche en imagerie et orthopédie,
Université du Québec, Montréal, Canada
natalia.nuno@etsmtl.ca

INTRODUCTION

The initial fixation of a cemented hip implant relies on the strength of the interface between the metallic stem, the bone cement and the adjacent bone. During polymerization of bone cement, a polymethyl-methacrylate (PMMA), residual stresses caused by bulk and thermal shrinkage due to the exothermic reaction are generated in the cement mantle. However, the precise magnitude of these stresses is still not well documented and no study can be found in the literature on the direct measurement of these stresses. Until now, very few studies [1, 2, 3] have tried to assess experimentally the residual stresses generated by bone cement curing. Therefore, the main objective of this study is to develop an experimental set-up to measure the residual stresses generated at the stem-cement interface during bone cement polymerization.

METHODS

An experiment has been developed to measure directly the radial residual stresses due to bone cement curing at the stem-cement interface of an unloaded cemented hip prosthesis. The experimental set-up consists of an idealized hip stem (19-mm diameter) placed inside a hollow cylinder (5.5-mm thick) simulating cortical bone, filled with freshly prepared Simplex P PMMA (5-mm thick mantle). A sub-miniature load cell (ELFM-B1-50L, Entran) was inserted inside the idealized stem to measure directly the radial compressive force then converted to stresses, while a thermocouple measured the temperature variation during the polymerization process.

Initial conditions of the cemented hip prosthesis influences the residual stresses generated: i.e. pre-heating the stem [4]; radial adhesion at the cement-bone interface [2]. The initial conditions of the idealized cemented hip specimens were varied. The parameters were the stem and bone temperature, and the adhesion at the cement-bone interface. To simulate adhesion at the cement-bone interface, the surface roughness of the hollow cylinder representing the bone was varied. For no adhesion, an aluminium cylinder was used and for adhesion at the interface a synthetic bone (Sawbones) was used. The experiments were performed inside a thermo center where temperature is controlled at 37°C to simulate the *in-vivo* situation of the implant.

RESULTS AND DISCUSSION

Figure 1 shows the residual stresses and temperature variation recorded during cement curing for the following conditions: no radial adhesion at stem-cement nor at cement-bone interfaces, stem and bone initial temperatures of 37°C and 24°C, respectively. The experimental results showed that a few minutes after the initial mixing of the bone cement, a thermal expansion occurs caused by the rapid increase of temperature (approximately 60°C), corresponding to a small peak in the radial force. Then, the decrease in the temperature corresponds to the increase in the radial residual force recorded. Maximum radial residual stresses at the stem-cement interface of 0.5 MPa in compression during polymerization have been measured during the experiments. The results show that the residual stresses are influenced by the initial conditions of the experiments: adhesion of the cement-bone interface as well as the initial temperature of the stem and the bone.

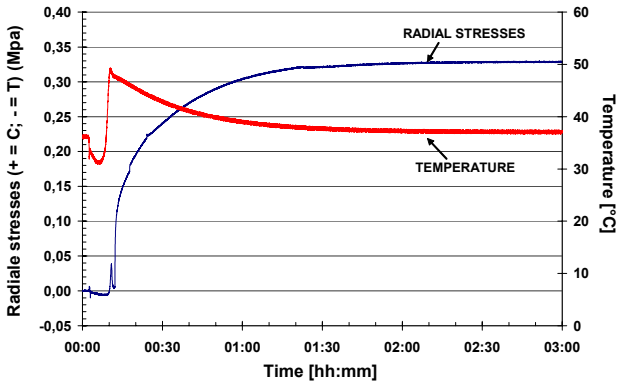

Figure 1. Experimental results: Radial stresses and temperature evolution at the stem-cement interface during the cement curing.

REFERENCES

[1] Nuño and Amabili (2002) Clin Biomech 17, pp.41-48.
[2] Ahmed et al. (1992). J Biomech Eng 104, pp. 21-27.
[3] Roques et al. (2004) Biomaterials 25, pp. 4415-4424.
[4] Li et al. (2004) J Biomed Mater Res 70B, pp.30-36.

ACKNOWLEDGEMENTS

Zimmer, Switzerland; CRSNG, Canada; NATEQ, Québec.

CHARACTERIZATION OF SHOULDER PATHOLOGY USING 3D KINEMATIC SENSORS

*Jolles BM, **Aminian K, *Bourgeois A, **Coley B, *Pichonnaz C, *Leyvraz PF, *Farron A
University Hospital of Lausanne CHUV-HOSR, Lausanne, Switzerland

Brigitte.Jolles@chuv.ch

INTRODUCTION

Variable clinical scores have been used to assess outcome after shoulder treatment. Some of these (such as the Constant score or the American Shoulder and Elbow Surgeons score) are widely used, though none have been accepted as the universal standard. The object of this research was two-fold: finding objective parameters for outcome evaluation after shoulder surgery using kinematics sensors and evaluating the accuracy of these sensors to quantify the difference between healthy and painful shoulder.

METHODS

After ethical approval from our institutional board and written informed consent of each patient, ten healthy subjects (25.1 years old ± 4.1) and 20 patients with unilateral pathological shoulder (rotator cuff disease/ osteoarthritis, 8 women, 12 men: 63.2 years old ± 11.6) were studied. Nine tests, corresponding to daily activity, were carried out for both shoulders. All patients were tested before surgery and 3 months and 6 months after surgery. The Simple Shoulder Test (SST) and Disabilities of the Arm and Shoulder Score (DASH) questionnaires were completed by each subject. The tests were video filmed for studying and validating the movements, and estimating the erroneous movements.

Roll, pitch and yaw movements were measured with 3D accelerometers and 3D gyroscopes attached on the humerus and linked to a light datalogger (Physilog®) carried by the subject. Based on the recorded kinematics, three scores were defined. First, the RAV score: the 3D range of angular velocity (RAV) was calculated during each test in roll, pitch and yaw directions for each subject, and the RAV score was defined as:

$$RAVscore = 100\left(1 - mean\left[\sum_{Test1}^{9} \frac{\mathrm{RAV_{healthy}} - \mathrm{RAV_{painful}}}{\mathrm{RAV_{healthy}}}\right]\right)$$

Second, the P score: the sum of the product of range of acceleration by angular velocity in each axis was calculated during each test.

$$Pscore = 100\left(1 - mean\left[\sum_{Test1}^{9} \frac{\mathrm{P_{healthy}} - \mathrm{P_{painful}}}{\mathrm{P_{healthy}}}\right]\right)$$

Third, the M score was defined as the maximum of the sum of all moments on the humerus (M):

$$Mscore = 100\left(1 - mean\left[\sum_{Test1}^{9} \frac{\mathrm{M_{healthy}} - \mathrm{M_{painful}}}{\mathrm{M_{healthy}}}\right]\right)$$

RESULTS

As illustrated in figure 1, the difference between healthy and painful shoulder was positive for almost all tests, which illustrated the decrease of RAVscore for the painful shoulder. The same results were found for the estimated Pscore and the Mscore for each test, which was always lower for the painful shoulder. However, improvements of these scores were obtained with time after surgery. These results were in correspondence with the clinical evaluations (SST and DASH).

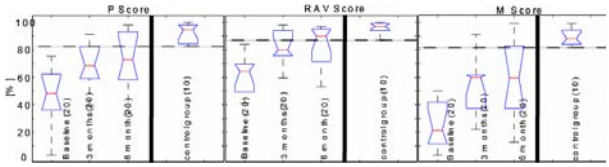

Fig.1: Improvements of the 3 patients' shoulder scores between the preoperative time (1st column) and 3, 6 months after surgery (2nd & 3rd columns) in compari-son with healthy patients(4th column) (- - - : normality limit).

DISCUSSION & CONCLUSIONS

These primary results showed that 3D body fixed sensors could quantify the difference in kinematics between healthy and painful shoulder. We have proposed three objective scores for shoulder outcome evaluation, and showed the improvement of the patient's mobility after surgery based on each score. However, further measurements with more patients are needed to estimate the best score. These results are very encouraging for future evaluation of patients with shoulder injuries. Since the system is ambulatory, it can be used to monitor shoulder kinematics during daily physical activity and provides in this way valuable information about the shoulder function.

ACKNOWLEDGEMENTS:
This work was supported by the Swiss National Foundation (FNS-PNR 53) Grant no 405340-104752/1.

AFFILIATED INSTITUTIONS FOR CO-AUTHORS:
** Swiss Federal Institute of Technology EPFL, Lausanne, Switzerland

ADAPTIVE BONE REMODELLING OF THE BIRMINGHAM HIP RESURFACING COMPONENT: AN INVESTIGATION ON IMPLANT ORIENTATION INFLUENCE

***Kohan L, ***Gillies RM, *Hogg M, ***Cordingley R
*WorleyParsons Advanced Analysis, L1, 95 Nicholson Street, St Leonards, Sydney, NSW 2065, Australia
Mark.Gillies@WorleyParsons.com

INTRODUCTION

The reason for loosening or periprosthetic fracture of an implant is multifactorial, one such factor is loss of supporting bone tissue due to resorption and impaired bone formation. Another can be surgical error, such as notching the bone or positioning of the implant and subjecting it to an abnormal loading environment. The use of a resurfacing component allows the use of a "stem-less" prosthesis prior to the use of a stemmed prosthesis, provided there is adequate bone stock available. Bone remodelling is another predictor of potential outcome in arthroplasties [1-3]. This technique has been shown to be adequate in detecting bony remodelling changes. More studies are required into investigating the use of this predictive technique in orthopaedics to investigate the adaptive bone remodelling response to implant geometry changes. Many studies have been carried out on periprosthetic bone remodeling using the adaptive bone remodelling theory [1, 4-8]. Currently there is no literature on the finite element analysis (FEA) of adaptive bone remodeling of resurfacing components and comparing back to clinical bone mineral density (BMD) data or the influence of implant orientation. This study has used adaptive bone remodeling theory and compared the predictions to clinical bone density data and then investigated the influence of implant orientation on adaptive remodelling of bone.

METHODS

CT scans were used to reconstruct the femur geometry. Two models were generated, a preoperative and a postoperative state model. The post operative model was reconstructed using the Birmingham Hip Replacement (BHR) (Smith & Nephew Inc, Memphis, TN) (Fig 1.) The BHR was oriented according to the surgeon's (LK) templating and in accordance with the manufacturer's surgical technique to allow comparison to the clinical BMD measurements. The cement mantle was also modeled using a mean cement penetration depth. The BMD change at 1 region of interest (ROI) was measured using Global Lab Image/2 and plotted for a period of 36 months. The same method of extracting BMD from images was used to compare the influence of implant orientation on BMD changes to the reference state orientation of the surgeon (LK). Six ROis were used in this case.

Figure 1

RESULTS

The statistical correlation of the clinical and predicted BMD data was found to be 0.72

Figure 2 presents the volume of bone that either increases or decreases in BMD, which has influenced by the change in implant orientation.

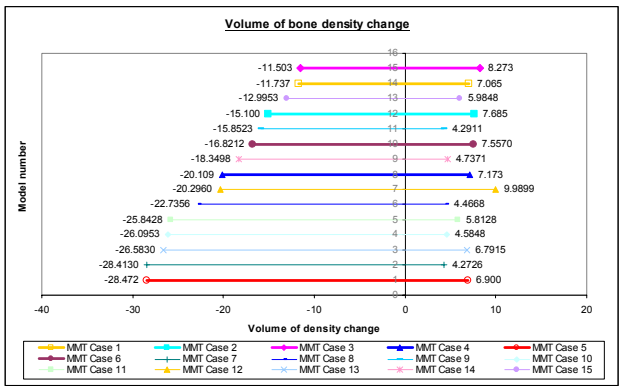

Figure 2

DISCUSSION

The changes in BMD predicted by the adaptive bone remodelling theory correlated strongly with the clinical and published BMD [9] results for BHR implant and across the chosen ROI. The published data of Kishida et al (2004) [9] correlated to the FEA predicted change in density with a correlation coefficient of 0.95 over the 24 month period. Despite some differences, the trends are consistent with the density adaptations found clinically. This study has shown that the theoretical adaptive bone remodeling rule used has predicted the BMD change seen clinically using the BHR. Following the clinical validation; this study has also shown that the implant orientation has a dramatic influence on how the bone adapts to a change in loading environment.

REFERENCES:

1.Kerner, J., *et al.*, J Biomech, 1999. **32**(7): p. 695-703.
2.Arabmotlagh, M., *et al.*, Z Orthop Ihre Grenzgeb, 2003. **141**(5): p. 519-25.
3.Georges, A., *et al.*, Ann Biol Clin (Paris), 2002. **60**(6): p. 683-8.
4.Huiskes, R., *et al.*, J Biomech, 1987. **20**(11-12): p. 1135-50.
5.Weinans, H., *et al.*, J Biomech., 1992. **25**(12): p. 1425-41.
6.Van Rietbergen, B., *et al.*, J Biomech, 1993. **26**(4-5): p. 369-82.
7.Stulpner, M.A., *et al.*, J Biomech, 1997. **30**(10): p. 1063-6.
8.Petersen, M.M., Acta Orthop Scand Suppl, 2000. **293**: p. 1-37.
9.Kishida, Y., *et al.*, J Bone Joint Surg Br, 2004. **86**(2): p. 185-9.

** Orthopaedic & Traumatic Surgery, University of Sydney, Royal North Shore Hospital, Sydney, Australia
*** Joint Orthopaedic Centre, Sydney, Australia

ION RELEASE FROM METAL-ON-METAL HIP RESURFACING IMPLANTS DOES NOT DIFFER FROM STANDARD METAL-ON-METAL TOTAL HIP REPLACEMENT

Moroni A, Savarino L, Hoang-Kim A, Cadossi M, Greco M, Baldini N, Giannini S
Istituti Ortopedici Rizzoli, University of Bologna, Bologna, Italy

giannini@ior.it

INTRODUCTION

Modern metal-on-metal (MOM) hip resurfacing has been introduced as a less invasive method of joint reconstruction for young-active patients (1). Hip resurfacing advantages include: bone stock preservation, wider range of motion, better functional outcomes and lower rate of dislocation. However, considering the large diameter of the coupling components, there are concerns regarding the quantity of metal ion release. The aim of this study was firstly to quantify the production of metal ion release in patients with a MOM hip resurfacing prosthesis and to compare this result with a control group. Secondly, we wanted to compare metal ion release after hip resurfacing with metal ion release after MOM total hip replacement as invetigated in a previous study (2).

MATERIAL AND METHODS

The clinical study was approved by the Institutional Ethics Committee on human research and the subjects signed an informed consent form to participate in the study. We contacted twenty-one subjects (11 female, 10 male) who had undergone either unilateral or bilateral hip resurfacing arthroplasty (16 unilateral and 5 bilateral) with a mean follow-up of 25 months. The prosthesis used in this study was a Birmingham Hip Resurfacing (BHR; Midland Medical Technologies, Birmingham, UK) machined from cast cobalt-chromium-molybdenum (CoCrMo) alloy. Patients completed a questionnaire and provided a sample of blood for serum ion analysis. As we were interested in estimating the systemic release of metal ions from the implanted prostheses, we specifically addressed factors which could have affected the result. These included occupational exposure, the ingestion of prescription or non-prescription medications and the presence of other metal implants within the body. One subject was excluded due to the presence of a metal plate. The reference values were obtained from a population of twenty-four healthy subjects.

Serum Cr and Co content was measured using a graphite furnace atomic absorption spectrometer (GFAAS), equipped with double background correction Deuterium/Zeeman, autosampler and pyrolytic carbon-coated graphite tubes (Unicam Model Solaar 939 QZ, Cambridge, UK). Furnace thermal programs and spectrometer parameters are reported in Table 1.

Calibration was performed by applying the Standard Addition Method and by using certified standard solutions at three concentrations for each element (NIST). All the results were expressed as ng/ml. The sensitivity of the method was established by using detection limits for sample matrix, i.e. 0.06ng/ml for Cr, 0.08 ng/ml for Co and 0.08ng/ml for Ni. All the subjects having ion levels below the detection levels were adjusted to the detection limit values.

Ion values were reported as an arithmetic mean and its standard error, min-max range and median value. Specific differences between groups were evaluated by applying the Mann Whitney U test. The correlation between ion values and other parameters, i.e. coupling size, follow up, age of patients and Harris score, was calculated using Spearman's r coefficient. In all analyses only the p values <0.05 were considered as statistically significant. Data were analyzed with the StatView 5.0.1.0 software (SAS Institute Inc.).

RESULTS

Average serum ion concentrations, expressed as ng/ml, and their standard errors, min-max range and median values are reported in Table 2. Our findings indicate that metal-on-metal bearings produce a significantly higher systemic release of cobalt and chromium (ng/ml) when compared with levels found in the reference group.

A highly-significant positive correlation between Co and Cr values was observed in BHR patients ($r = 0.80$; P value < 0.001), as well as between Cr, Co values and Harris score, by applying the Spearman's test. On the contrary, no correlation was found between acetabular/head diameter and ion concentrations. Likewise, no correlation within patients was found between ion concentrations and age of the patients (years), and between Cr, Co values and follow up, expressed as months from implant surgery.

DISCUSSION

This study shows that patients with hip resurfacing implants had a higher metal ion serum-level compared to the control group. However, regardless of the large head diameter (mean bearing surface diameter 48.1mm), median values for both ions were similar to values measured in patients who underwent MOM total hip replacement with a 28mm bearing surface diameter (Metasul TM, Sulzer Orthopaedics Ltd, CH-8404 Winterthur, Switzerland) and reported in our previous paper (Cr and Co, respectively 1.66 and 0.97ng/ml) (2). This result can be explained according to the classic elastohydrodynamic theory which suggests that fluid-film is more likely in large diameter MOM bearings, and hence it is inferred that wear will be reduced (3), and because of possible differences in the tribology of the two types of prosthesis.

At a median of 16 months, Clarke et al. (4) reported higher median cobalt and chromium serum-levels in patients who underwent resurfacing arthroplasty (Cr and Co, respectively 2.75 and 2.24ng/ml) compared with those who underwent MOM total hip replacement. Conversely, in this study, we found that in BHR patients, after an initial running-in period characterized by high metal ion serum-levels, they tend to decrease at a longer follow-up and become similar to those measured in small diameter MOM total hip arthroplasties.

REFERENCES:

1. Daniel J, Pynsent PB, McMinn DJW. Metal-on-metal resurfacing of the hip in patients under the age of 55 years with osteoarthritis. J Bone Join Surg 86(B), 2: 177-184, 2004.
2. Savarino L, Granchi D, Ciapetti G et al. Ion Release in Patients with Metal-on-Metal Hip Bearings in Total Joint Replacement: A Comparison with Metal-on-Polyethylene Bearings. Mater Res (Appl Biomater) 63: 467-474, 2002.
3. Smith SL, Dowson D, Goldsmith AA. The effect of femoral head diameter upon lubrication and and wear of metal-on-metal total hip replacement. Proc Inst Mech Eng (H) 2001, 215: 161-170.
4. Clarke MT, Lee PTH, Arora A, Villar RN. Levels of metal ions after small and large diameter metal-on-metal hip arthroplasty. J Bone Joint Surg 2003,85(B): 913-917.

CORROSION AND CORROSION PRODUCTS OF MODULAR-BODY TITANIUM ALLOY FEMORAL STEMS IN CEMENTLESS HIP REPLACEMENT

*Urban RM, **Gilbert JL, *Jacobs JJ
Dept. of Orthopedic Surgery, Rush University Medical Center, Chicago, IL USA
robert_urban@rush.edu

INTRODUCTION: Modularity of the body of the femoral stem as well as its head and neck is employed in several systems for revision and complex primary reconstructions of the hip. Concerns regarding fretting and reduced fatigue strength at the proximal stem and sleeve connection have been based largely on laboratory tests [1]. We hypothesized that *in vivo*, severe corrosion could occur at modular-body junctions, in addition to mechanical fretting, even in Ti-alloy components. Retrieved modular-body hip stems were examined to determine the severity of damage at the modular connections, the nature of the degradation processes, the composition of corrosion products generated, and their presence as particulates in the periprosthetic tissues.

MATERIALS AND METHODS: 30 cementless modular-body Ti6Al4V femoral stems (16 S-ROM J&J, 11 ZMR Zimmer, 3 Mallory-Head Biomet) revised after 1-130 months for pain, loosening, infection, dislocation or stem fracture were studied under an IRB protocol. 21 stems had been implanted in a revision and 9 in a primary arthroplasty. The femoral components had a long Morse taper junction between the stem body and a proximal sleeve, and had a modular CoCr head. The devices, degradation debris, and histological sections of the joint pseudocapsules were studied using light and electron microscopy, energy dispersive x-ray analysis, and electron and x-ray diffraction. The degree of damage at the stem taper, proximal sleeve, neck taper, and bore of the head were graded separately as (1) none to minimal; (2) mild: confined to small areas < 5 mm; (3) moderate: markedly larger areas of aggressive corrosion attack; and (4) severe: large regions of severe corrosion damage.

RESULTS: Fretting and corrosion damage was observed at the stem/sleeve junction in 20 of 30 devices. A wide range in the degree of damage, from minimal to severe, was observed in each of the 3 designs examined. Overall, the damage was minimal in 10 stems, mild in 11, moderate in 6 and severe in 3. In two stems, severe corrosion may have contributed to failure of the arthroplasty, including a corrosion-related fatigue fracture of one stem. Metallurgical examination of the moderate and severely corroded stems revealed fretting and extensive corrosion damage including etching, wormholes, and pitting. Severe etching was characterized by dissolution of the ß-phase, exposing the ά grains of the alloy.

Abundant black, brown and white corrosion deposits accompanied the fretting and corrosion damage. Microanalysis identified the deposits as polycrystalline TiO_2 corrosion products at the sites of corrosion attack and as particulates in the joint pseudocapsules. The diffraction studies identified the crystalline component as the rutile form of TiO_2. Particles of TiO_2 appeared in the stained tissue sections as 0.1 to 200 μm amber-colored, refractile inclusions within macrophages and multinucleated giant cells. Many particles were highly birefringent. Examination of the tissues using transmission electron microscopy revealed abundant nanometer-size intracellular needle-like particles of the TiO_2 degradation products.

At the head/neck junction, fretting, corrosion and unique corrosion products were observed in 10 of 30 stems, all of 1 design. Fretting and corrosion was more severe at the head compared to the neck taper. The degree of damage was moderate in 6 heads, mild in 3, and severe in 1, and was characterized by fretting scars and etching of the CoCr alloy. Particles of $CrPO_4$ corrosion product were associated with corrosion at the head/neck junction. These were distinct from the TiO_2 particles and appeared in the joint pseudocapsule as translucent, pale green, and non-birefringent particles ranging from 0.01 to 150 μm within macrophages and multinucleated cells.

DISCUSSION: Crevice corrosion of Ti-alloys has been reported only rarely in certain designs of cemented stems [2]. In the present study of 3 similar designs of explanted cementless devices, corrosion played a major role in degradation at modular-body connections, which had not been predicted in previous *in vitro* tests [1]. The severity of the corrosion damage implies an extraordinarily low pH within the crevice where the protective oxide film becomes unstable and the metallic titanium can be actively attacked, resulting in the severe etching and pitting found with these implants. Stems with severe corrosion damage may be at risk for structural failure as we observed in one stem. The generation and migration of fretting and corrosion products adds to the particulate burden of the tissues and may accelerate bearing surface wear by a third-body mechanism. These features can potentiate the development and progression of osteolysis.

CONCLUSION: Stem modularity can provide great versatility in complex revision hip replacement. However, surgeons should be aware that corrosion of modular-body stems can generate corrosion products and can affect the fatigue life of a device. The risks and benefits of stem modularity should be carefully weighed, particularly in the high-demand patient.

REFERENCES: [1] Bobyn JD. Clin Ortho 1994;298:27-36. [2] Willert HG. Clin Ortho 1996;333:51-75.

ACKNOWLEDGEMENT: NIH AR39310 and Zimmer.

AFFILIATIONS: ** Syracuse Univ., Syracuse, NY.

LONG-TERM FIXATION AND POTENTIAL FAILURE MECHANISMS IN CEMENTLESS ACETABULAR COMPONENTS RETRIEVED POSTMORTEM

Urban RM, Hall DJ, Jacobs JJ, Pourzal R, Wimmer MA, Sumner DR, Galante JO
Department of Orthopedic Surgery, Rush University, Chicago, IL, USA
robert_urban@rush.edu

INTRODUCTION: Porous-coated, hemispherical acetabular cups with UHMWPE (PE) liners are entering the 3rd decade of use with excellent clinical results and very low rates of aseptic loosening. However, the nature of the interface tissues and the long-term durability of bone ingrowth fixation in the majority of patients hosting well-functioning arthroplasties are largely unknown. The purpose of this study was to quantify the extent of various interface tissues, including bone and wear particle induced granulomas in Harris-Galante cups retrieved post mortem after 2-21 years and to relate these findings to bearing surface wear and "back-side" liner damage.

MATERIALS AND METHODS: Thirty-six primary porous-coated Ti acetabular cups implanted with screws (19 HG, 17 HG2, Zimmer) were harvested postmortem after a mean of 8 (range 2-21) yrs under an IRB protocol. Femoral reconstruction consisted of 19 cemented CoCr and 17 cementless TiAlV stems, all with CoCr heads. The Harris hip score at last follow-up was 85 (47-100). Stained sections of each cup with adjoining bone and joint capsule were quantified by point counting for the extent of bone, marrow, fibrous tissue, and particle-induced granuloma surrounding and within the porous coating. SEM images were used to measure the overall area fraction of bone ingrowth. Particles were identified using polarized light or energy dispersive x-ray analysis. Clinical radiographs were reviewed. "Back-side" damage of explanted liners was calculated as the product of severity and area grades. PE bearing surface wear was determined in 22 cups $\geq$ 5 yrs using a touch probe coordinate measuring system. Data were analyzed using the Friedman test and Spearman correlations. Means and standard deviations are reported.

RESULTS: The interface between the porous coating and the surrounding bone was composed of 37.5 $\pm$16.9% bone, 12.4 $\pm$10.2% marrow, 4.4 $\pm$5.3% cartilage, 30.8 $\pm$22.9% fibrous tissue, 0.5 $\pm$1.8% necrotic tissue, 3.0 $\pm$7.1% granuloma, and the balance was screw holes. The extent of bone within the coating was 35.6 $\pm$19.6%. The least extent of bone was at the interface between the porous coating and the metal shell of the cup (12.9 $\pm$12.1%) where a fibrous membrane was often present. Overall, the area fraction of bone ingrowth measured from backscattered electron images was 12.1 $\pm$6.6%.

Particles of PE, Ti and TiAlV alloy were present within holes with or without screws in all of the components. Several cups demonstrated particles of CoCr alloy, barium sulfate or stainless steel from the femoral reconstruction. The particles were found within granulomas composed primarily of histiocytes. Expansion of the granulomas through the screw holes into the periprosthetic bone was observed in 2 of 11 components after< 5 years and in 14 of 25 $\geq$ 5 years. Pelvic granulomas increased from a few millimeters at 5-10 years to ballooning lesions measuring up to 20 millimeters in several specimens with follow up of 15-21 years. The full extent of these granulomas was poorly visualized on plain clinical radiographs. In some of the longest-term specimens, the granulomatous tissue invaded the interface between the porous coating and the metal shell, in effect, undermining bone ingrowth fixation of the components. At the rim of the components, particle-laden granulomas also infiltrated the bone-implant interface tissues, but to a lesser extent. The depth of granuloma penetration at the rim increased with time (r=.502, p=.009).

Damage to the convex side of the PE liners was moderate with a mean damage score of 7.7 $\pm$5.0 out of a possible of 27. Damage scores increased with duration of implantation (r=.388, p=.019). Pitting, scratching, abrasion, and screw hole impressions were common. Burnishing and scratching of the polyethylene surface were the dominant modes of damage in the 9 components with scores of 10 or greater. The damage scores were correlated with the extent of polyethylene particle-induced granuloma at the bone-implant interface (r=.519, p=.007) Liner thickness was not correlated with either "back-side" damage scores, granuloma penetration at the component rim or granuloma at the bone-implant interface overall. The mean polyethylene bearing surface volumetric wear was 44 mm^3/year and was not correlated with the extent of granuloma in the interface tissues.

DISCUSSION: This study documents the durability of bone ingrowth fixation of the acetabular component over 2 decades. Potential failure mechanisms for the very long term are also suggested. Although not fully apparent on plain clinical radiographs, particle-induced granulomas infiltrated the interface tissues, increasing with time, in a highly patterned manner at the rim and screw holes of components with substantial bone ingrowth. In some specimens, the granulomatous tissue invaded the interface between the porous coating and the metal shell, in effect, undermining bone ingrowth fixation. Osteolysis from within the porous coating may prove to be an important mechanism of very late failure. These findings have importance for design of acetabular components. Extensive pelvic osteolysis can present formidable challenges for reconstruction. Therefore, in the very large population hosting these and similar devices, close monitoring of patients with radiographic indications of peri-acetabular osteolysis is warranted.

ACKNOWLEDGEMENT: NIH AR 39310 and Zimmer.

HETEROTOPIC OSSIFICATION FALSELY ELEVATES PERIPROSTHETIC BMD

Downing M, Knox D, Ashcroft GP

Orthopaedic RSA Research Unit, Woodend Hospital,
Grampian Universities NHS Trust, Aberdeen, Scotland

m.downing@abdn.ac.uk

INTRODUCTION

Bone loss is common following primary total hip replacement. Its role in femoral stem loosening is a source of concern. Dual energy x-ray absorptiometery (DXA) has superseded conventional radiographic appraisal in the assessment of periprosthetic bone resorption and is now an established technique used to examine the longitudinal relationship between hip replacement, prosthesis fixation and host bone stock.

The formation of heterotopic ossification (HO) is a common occurrence post hip arthroplasty, and has been recognised to occur in regions liable to affect hip periprosthetic BMD measurements.

As part of a two-year, prospective, randomised, primary cemented total hip replacement trial we investigated the incidence and distribution of HO and the extent to which it affected periprosthetic DXA results.

METHODS

One hundred and sixty-four patients were recruited into a study examining bone remodelling around four designs of replacement. Periprosthetic DXA scans were performed at seven days post-arthroplasty, then at six, twelve, eighteen and twenty-four months. AP hip x-rays of the operated side were taken three days post-op and then at six, twelve and twenty-four months with lateral views at six weeks and twenty-four months. HO was identified from radiographs and localised to the seven femoral Gruen zone regions of interest (ROI). The DXA generated image and a locally developed DXA subtraction programme were used to confirm localisation.

An antero-lateral modified Hardinge approach to the hip was used but in a small sub-group a minimal osteotomy was performed as this approach was also in routine use in our institution. All patients followed the same post-op rehabilitation programme. No patient received HO prophylaxis. All participants gave informed consent and the study protocol was approved by the local ethics review committee.

Chi square and Mann-Whitney tests were used to examine the relationships between different factors and the occurrence of HO.

Mann-Whitney was also used to examine the effect of HO upon percentage BMD change at 2 years.

RESULTS

Results were available for 137 patients (88 females and 49 men) 18 of whom had an osteotomy performed. Factors significantly associated with the formation of HO within the Gruen ROI included male gender, increasing age at the time of operation and the use of an osteotomy approach. Femoral stem type and BMI were not relevant.

HO occurred in 46% of patients and was limited to ROI 1, 2, 6 and 7 (table 1). HO localisation required a lateral x-ray view of the hip in 12% of cases.

ROI	Hardinge	Osteotomy
One	40.3% (48)	72.2% (13)
Two	10.9% (13)	22.2% (4)
Six	1.7% (2)	0
Seven	2.5% (3)	11.1% (2)
Any zone	42% (50)	72.2% (14)

Table 1. Percentage and number of patients affected by HO at 24 months post op

The presence of HO greatly increased measured percentage BMD change.

This reached statistical significance in Hardinge patients for ROI 1 ($p<0.000$). This increase remained significant when analysis investigated the effect of gender (female $p=0.001$ and male $p=0.003$) (figure 1). This was an important finding as sex is known to independently affect post arthroplasty BMD changes.

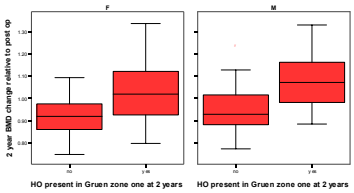

Fig 1. BMD change in ROI 1relative to post op scan. Results compare HO and non-HO affected patients by gender.

DISCUSSION

HO occurs commonly in the regions scanned by DXA. HO significantly increases measured BMD. This can lead to misleading interpretations of results. Two x-ray views, lateral as well as AP, are frequently required to identify it.

ADAPTIVE BONE REMODELING OF AN ACETABULAR CUP: A CLINICAL COMPARISON

* **Gillies RM, *Hogg, M, ***Cordingley R, ***Kohan L
*WorleyParsons Advanced Analysis, L1, 95 Nicholson Street, St Leonards, Sydney, NSW 2065, Australia
Mark.Gillies@WorleyParsons.com

INTRODUCTION

Total hip replacement represents a major surgical achievement for pain relief and restoration of lifestyle due to the debilitating disease of osteoarthritis. Replacement of the diseased hip with a prosthetic femoral and acetabular component has evolved over the past 30 years with a variety of materials, designs and fixation techniques (cemented and uncemented) Peri-prosthetic bone remodeling, following femoral hip replacement has been studied widely over the past several decades. Excessive bone resorption potentially may contribute to the development of prosthesis loosening and failure [1]. In accordance with Wolff's Law, a process of strain adaptive bone remodeling emerges [2].

This study has examined the long-term effects of strain adaptive bone remodeling due to the influence of a titanium cementless acetabular cup replacement and compared it to published clinical data[3] using finite element analysis.

METHODS

CT scans were used to reconstruct the pelvic geometry. A 3D finite element mesh was created using PATRAN (MSC Software, Santa Ana, CA). Two models were generated a preoperative and a postoperative state model. The postoperative model was reconstructed with the T.O.P. acetabular cup (T.O.P., Waldemar Link, Germany). The acetabular cup orientation was in accordance with the manufacturer's surgical technique specifications. Cementless fixation was modeled in 2 stages, sliding for the first 12 weeks followed by ongrowth using tied contact surfaces for the final simulation period. The analysis was carried out using ABAQUS Standard (ABAQUS Inc. Pawtucket, RI). The bone mineral density changes at 3 regions of interest (ROI) were measured using Global Lab Image/2 (Data Translation, Marlboro, MA) and plotted for a period of 36 months.

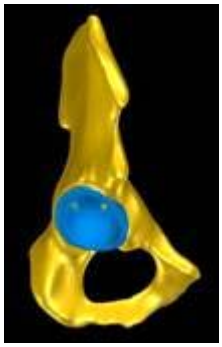

Figure 1.

RESULTS

Figure 2 presents a graph showing the comparison of the clinical data from Sabo et al (1998) and the predictions from the strain adaptive remodeling theory used in this study.

Table 1 presents the correlation coefficients for the comparison of the clinical zones (C*i*; *i* = 1, 2, 3) and finite element analysis predictions (T*i*; *i* = 1, 2, 3).

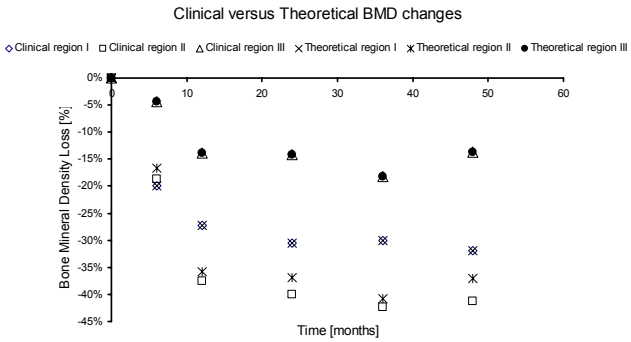

Figure 2

Table 1.

	C1	C11	C111	T1	T11	T111
C1	1					
C11	0.980	1				
C111	0.906	0.967	1			
T1	1	0.980	0.906	1		
T11	0.969	0.998	0.980	0.969	1	
T111	0.906	0.967	1	0.906	0.980	1

DISCUSSION

The current model predicts the clinical behaviour of the bone density in all regions with a good correlation (Table 1). This is similar to what is found clinically [3, 4]. In this study, it is assumed that activity levels are unchanged following surgery. The coated and treated surface of the implant has not been assumed to be fully ingrown or osseointegrated for the length of the simulation, but has a 12 week period for ongrowth to occur [5]followed by an osseointegrated period for the remainder of the simulation. However, the bone remodelling algorithm developed has produced results comparable with average values from the literature as discussed above. This study has concluded that computational bone remodelling theory is a powerful tool and able to produce a clinically relevant result.

REFERENCES:

1.Kroger, H., *et al.*, Clin Orthop, 1998. **352**: p. 66-74.
2.Huiskes, R., Acta Orthop Belg, 1993. **59**(Suppl 1): p. 118-29.
3.Sabo, D., *et al.*, Calcif Tissue Int, 1998. **62**(2): p. 177-82.
4.Engh, C.A., *et al.*, J Arthroplasty, 2004. **19**(7 Suppl 2): p. 54-60.
5.Svehla, M., *et al.*, J Arthroplasty, 2002. **17**(3): p. 304-11.

** Orthopaedic & Traumatic Surgery, University of Sydney, Royal North Shore Hospital, Sydney
*** Joint Orthopaedic Centre, Sydney

EARLY DIAGNOSIS OF CERAMIC LINER FRACTURE: GUIDELINES BASED ON A 12-YEAR CLINICAL EXPERIENCE WITH 3710 MODERN CERAMIC PROSTHESES

Traina F, Stea S, Visentin M, Sudanese A, Giardina F, De Clerico M, Bordini B, Tassinari E, Polmonari M, Cervini A, Di Motta D, Toni A

I Division, Medical Technology Laboratory, Istituti Ortopedici Rizzoli, Bologna, Italy

traina@tecno.ior.it

INTRODUCTION

Ceramic component fractures have been thoroughly investigated, but few studies report on their early clinical diagnosis. When a ceramic fracture involves the head or it is the consequence of a hip trauma or dislocation, the diagnosis is easily done. However, when ceramic fractures are the consequence of repeated micro-trauma, early diagnosis is rarely, except when ceramic fragments are visible on x-ray. The purpose of this exhibit is to present guidelines for early recognition of clinical signs of ceramic liner fractures, based on a 12-year experience

MATERIALS AND METHODS

Reviewing 3710 prostheses implanted between 1993 and 2004, we recorded eight liner fractures (0.21 percent). In four of the latter, the only relevant early clinical sign was a hip noise perceivable during walking. We have then reviewed the last 1000 prostheses implanted in our department since January 2000. all the patients present a Ti alloy prosthesis with ceramic bearing surfaces. The patients were asked if they can perceive a noise at the implanted hip during normal activities. The patients with hip noise were thoroughly clinically investigated to rule out all the cases with noise other than noise from bearing surfaces. The patients with a noisy hip undergo to a CT scan and a needle aspirate was then performed on ten of them. As control the needle aspirate was also performed in stable prosthesis, and synovial fluid samples were taken during revisions performed for aseptic loosening.

RESULTS

At synovial fluid examination, one sample was not appropriate, in 9 the presence of ceramic fragments (range: 10-50 microns) was shown. Fragment dimensions and shapes are not compatible with wear, but with an early stage of liner fracture. Both the revised patients and those presenting hip noise had signs of a minimally instable hip.

DISCUSSION AND CONCLUSIONS

Even though ceramic has very good tribology properties major concerns are related to its brittleness. To achieve very good long term results we have performed an accurate preoperative planning and we have followed a careful surgical protocol. In our experience ceramic failure is not related to preoperative diagnosis, age, cup modularity, revision surgery. Hip instability is probably the major concern for ceramic survival. Improvement of materials as Delta ceramic, new liner designs and big heads could be the solution.

In conclusion, hip noise could be considered an early clinical sign of liner chipping/fracture, clinical signs of hip instability should be sought and a careful examination of the patient is mandatory.

THE DEPENDENCE OF ESTIMATED FEMORAL CANCELLOUS BONE PERMEABILITY ON TIME USING HIGH AND LOW VISCOSITY CEMENT: PRELIMINARY RESULTS

+*Abdulghani S, *Tidehem J; *Wang JS, *McCarthy I
+ Department of Orthopaedics, Lund University Hospital, S-221 85 Lund, Sweden

Saba.abdulghani@med.lu.s

INTRODUCTION

Osteoporotic bone does not always have the strength to hold reconstructive pins or screws in place to retain fracture alignment. Therefore, the failure rate of femoral neck fracture is unacceptably high. Augmenting the fragile bone by injecting the femoral head with cement may be helpful in minimising failure rates. The injectability of cement depends on bone permeability and changing cement viscosity, which is time and shear rate dependent (1). Therefore a better understanding of the bone permeability will help to optimise the injection parameters and consequently cement infiltration in cancellous bone. In this investigation we estimate permeability from two types of cement, high and low viscosity, in femoral cancellous bone.

MATERIALS AND METHODS

Femoral heads from patients receiving a joint arthroplasty after a cervical neck fracture (permission was given by the local ethical council) were collected from Malmö and Landskrona hospitals, Sweden. Cylindrical cores (14 x 14 mm) were cut out and defatted using a chloroform/methanol solution for two hours. The cores were then allowed to dry at room temperature for 48 hours before Bone mineral density (BMD) measurements were carried out on each sample using a Dual Energy X-ray Absorptiometry (DEXA). The cores were then divided into two groups. Group 1 was injected with high viscosity cement: Biomet R (Biomet cementing technology, Sjöbo, Sweden) and the second group was injected with Osteopal (a low viscosity cement). Permeability measurements were carried out in accordance with a method outlined by Baroud et al (2003) (2). The permeability (k) was calculated using Darcy's law:

$$k(t) = vd/\ p'(t)-(2/r)*(h0-vt)\gamma\eta(t,\gamma)$$

Independent rheology measurements were carried out to determine the dynamic viscosity of each cement from the onset of mixing (according to manufacturer's instructions).

RESULTS AND DISCUSSION

Figure 1 shows the strong dependence of estimated permeability on time using high and low viscosity cements. Group 1 showed a more uniform and consistent decrease in permeability with time in accordance with the changes in cement viscosity. On the other hand, such trend was not observed in group 2. It is not clear why there was a difference in the estimated permeability measurement when using the low viscosity cement despite the fact the BMD for those cores was within the same range.

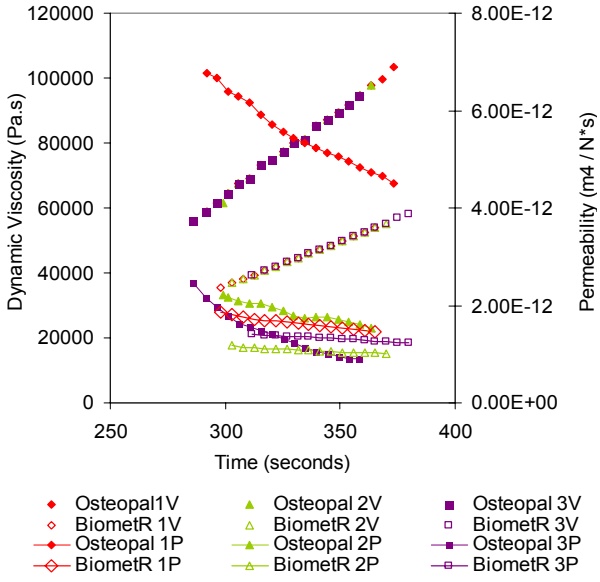

Figure 1 Changes in permeability with time and cement type. (V: viscosity, P: permeability).

Table 1 Average BMD and permeability values

	BMD (g/cm^2)	Permeability (m^4/Ns)
Biomet R	0.29 ± 0.05 Group 1	1.19 ± 0.22 E-12
Osteopal	0.24 ± 0.05 Group 2	2.56 ± 1.62 E-12

No correlation was found between the BMD and the permeability of cancellous bone.

REFERENCES

1. Krause WR et.al. The viscosity of acrylic cements. J Biomed Mater Res 1982; 16 (3): 219-43.
2. Baroud G et.al. How to determine the permeability for cement infiltration of osteoporotic cancellous bone. Medical Eng & Physics 2003; 25: 283-288

ACKNOWLEDGEMENT

This project is supported by a Marie Curie fellowship grant from the European Commission (MEIF-CT-2003-502109) and Medical Faculty of Lund University.

NUMERICAL SIMULATION OF BONE CEMENT POLYMERIZATION: TEMPERATURE AND RESIDUAL STRESSES

*Pérez MA, **Nuño N, **Plamondon D, **Mądrala A, *García-Aznar JM, *Doblaré M
*Group of Structures and Material Modelling Aragón Institute of Engineering Research (I3A)
University of Zaragoza, Zaragoza, Spain
angeles@unizar.es

INTRODUCTION

The use of polymethylmethacrylate (PMMA) as a self-curing cement in the fixation of prosthetic components in total hip arthroplasty (THA) is very common. When bone cement cures, residual stresses due to volumetric and thermal shrinkage will result caused by the exothermic reaction. Present finite element (FE) simulations of THA often do not account for these stresses as an initial condition; this may lead to an overestimation of the fatigue life of the cement, as initial cracks in the cement mantle appear that favors its deterioration [1]. This paper proposes a computational model to predict the polymerization process based on two parameters, temperature and residual stresses. The evolution of these parameters have been measured at the stem-cement interface, during experiments performed at the École de technologie supérieure, Montréal.

METHODS

Experimental Set-up

An experiment has been developed to measure directly radial residual stresses due to bone cement curing at the stem-cement interface of an unloaded cemented hip prosthesis. The experimental set-up consisted of an idealized hip stem placed inside a hollow cylinder made of synthetic bone filled with freshly prepared Simplex P PMMA. A sub-miniature load cell (ELFM-B1-50L, Entran) was inserted inside the idealized stem to measure the radial compressive force generated at the stem-cement interface, while a thermocouple measured the temperature variation during the polymerisation process.

Numerical model

The model presented here is an adaptation of that used by Baliga et al. [2]. The rate of heat generation is proportional to the rate of polymerization of PMMA and the polymerization process is assumed to be a function of the temperature [2]. Other important assumptions are the dependency of the Young modulus evolution on the polymerization degree [3] and the thermal expansion coefficient on the Young modulus [4]. The specific heat is assumed to depend on the temperature, whereas the other model parameters (Poisson's ratio, thermal conductivity, density and total amount of heat generated on completion of polymerization) are considered constant. The model is applied to an axisymmetric FE model of the experiments that recorded the residual stresses and temperature measurements, and an iterative procedure is developed.

RESULTS

Figure 1 shows the radial stresses and temperature evolution of one experiment The computational model developed is able to predict these experimental results during the cement polymerization process. After one hour and a half the residual stresses remain mainly constant.

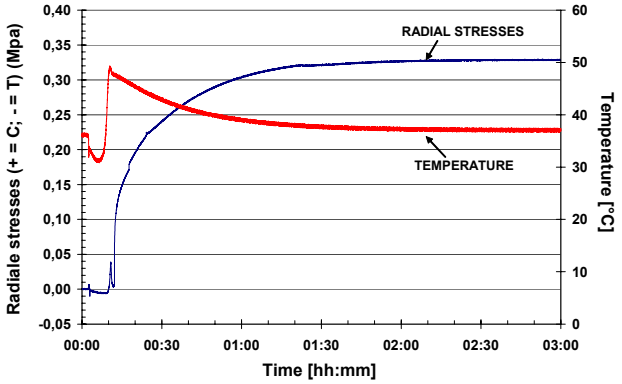

Figure 1. Experimental results: Radial stresses and temperature evolution at the stem-cement interface during the cement curing.

DISCUSSION

The methodology proposed in this study combines both physical and computational models in order to predict the residual stresses (in this case, measured in the radial direction) at the stem-cement interface. During the cement polymerization, shrinkage of cement is reported. This produces residual stresses as predicted in this study that will condition the behavior of the cement (initial cracks within the cement, at the stem-cement interface, fatigue, etc).

REFERENCES

[1] Lennon and Prendergast (2002). J Biomech 35, pp 311-321.
[2] Baliga et al. (1992). J Biomech Eng 114, pp 251-259.
[3] Ahmed et al. (1982). J Biomech Eng 104,pp 28-37.
[4] Ahmed et al. (1982). J Biomech Eng 104,pp 21-27.

ACKNOWLEDGEMENTS

Zimmer, Switzerland; CRSNG, Canada. CICYT FIS2005-05020-C03-03 (2005-2008), Spain.

** Département de génie de la production automatisée, École de technologie supérieure, Laboratoire de recherche en imagerie et orthopédie, Université du Québec, Montréal, Canada

THE USE OF LOW AND HIGH VISCOSITY CEMENT IN HIP RESURFACING ARTHROPLASTY: AN IN VITRO STUDY

* Howald R, **Kesteris U, ***Wittwer M, ****Zhang K, ****Yakimicki D, *Klabunde R, *Krevolin J
*Zimmer Corporate Research, Winterthur, Switzerland
ralph.howald@zimmer.com

INTRODUCTION

Hip resurfacing is increasingly used in orthopedic arthroplasty. It offers a bone conserving option for the young and active patient and more flexibility in case of a revision surgery. An understanding of how the cementing technique and cement type influences cement penetration is important for surgeons to plan and conduct hip resurfacing procedures. In particular it is important to know if high and low viscosity cement can be applied during this procedure. It is argued that high viscosity cement does not penetrate enough into the bone to provide firm fixation. We hypothesize that high viscosity cements can be used with hip resurfacing implants when an appropriate cementing technique is applied.

MATERIALS AND METHODS

Twelve fresh frozen paired whole cadaver femora were used for this study. Mean age of the donors was 50.1 years (SD 12.6 years) and mean weight 78 kg (SD 13 kg). All femora were x-rayed before the experiments. To determine the implant size, pre-operational planning was conducted by the operating surgeon (U. Kesteris). The paired femora were divided into two groups. Group A consisted of the right and group B of the left femora. All bones were defrosted before the experiments.

A Durom Hip Resurfacing (Zimmer GmbH, Switzerland) facsimile made of polyoxymethylene was used in order to provide low x-ray absorption. To compensate for the lower stiffness of the material as compared to the original component the wall thickness was increased. Small grooves were added for positioning purposes. The inner contour of the test components corresponded to the original component. Surgical Simplex (Stryker Orthopaedics, USA) and Palacos R-40 (Biomet Cementing Technologies AB, Sweden) cement were used.

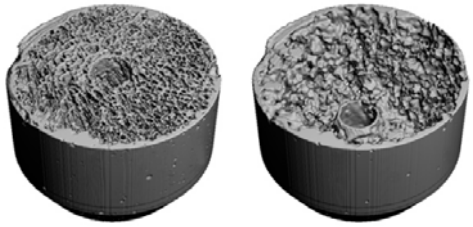

Fig. 1 Three dimensional caudal view on the reference volume (left) and cement penetration volume (right)

In group A low viscosity bone cement (Simplex) at room temperature was applied after a standing period of 3 min. In group B chilled high viscosity bone cement (Palacos) was applied after a standing period of 2 min. Pulse lavage was used in both groups (Pulsavac Plus, Zimmer Inc, USA). The cementing technique in this study corresponded to the clinically applied technique. A standard Durom instrument set was used for the implantations. After the previously defined standing period the implant was placed in its final position on the femora. The grooves marking the center plane of the implant were always aligned in the line of the greater and minor trochanter to provide consistent rotational positioning. The applied force during insertion of the component was controlled using a dynamometer (TEC, USA). 14 kg were applied in group A and 18 kg in group B according to clinical practice. The room and refrigerator temperature were recorded continuously (room mean 22.9°C, SD 0.3°C, refrigerator mean 6.5°C, SD 0.9°C).

The head was resected at the femoral neck and stored in 4 percent buffered formaldehyde solution after the polymerization process of the cement was complete. All samples were digitized using a micro CT-scanner (µCT 80, Scanco Medical, Bassersdorf, Switzerland). Data sets with a resolution of 1042x1024 pixels and a voxel size of 74µm were generated. Using image processing software (IPL 4.30a, Scanco Medical, Switzerland) each sample was segmented in reference volume and cement penetration volume (Fig. 1). The reference volume is the bone that is completely covered by the implant and represents the theoretical maximum bone volume that can be penetrated by the cement. The cement penetration volume is the total bone volume that is penetrated by cement. Based on reference and penetration volume the penetration *ratio* and the penetration *depth* were calculated. For each sample the mean bone density of the non-penetrated bone volume was calculated from the CT-data. A paired T-test was performed between group A and B.

RESULTS

The mean penetration *ratio* in group A (low viscosity cement) was 37% (SD 8%) and in group B (high viscosity cement) 41% (SD 8%). The difference was statistically significant ($p = 0.03$). The mean penetration *depth* in group A was 2.8 mm (SD 0.6 mm) and in group B 3.2 mm (SD 0.7 mm) (Fig. 2). The difference was statistically significant ($p = 0.02$). The mean density of the unpenetrated bone was 194 mg HA/ccm (SD 22.53 mg HA/ccm). There was no statistical significant difference between the right and the left femora in bone

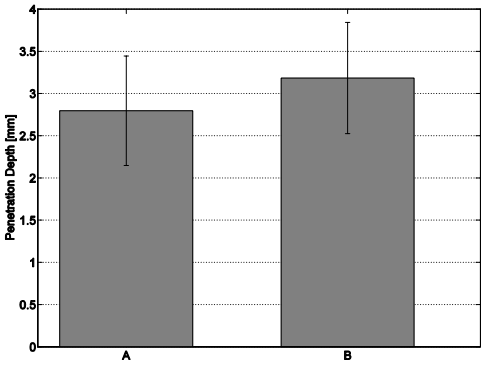

Fig. 2 Cement penetration depth in group A (low viscosity cement) and group B (high viscosity cement).

DISCUSSION

There was a significant increase of 0.4 mm in cement penetration *depth* when a high viscosity cement was used (group B) instead of a low viscosity cement (group A) although intuitively one may tend to think that low viscosity cement would penetrate more easily into the bone. The viscosity of the cement in group B was higher than of group A at the time of implantation, even though it had a shorter standing period. A possible explanation for this behavior could be that a low viscosity cement generates less pressure to penetrate into the bone during insertion of the implant than a high viscosity cement. This behavior is very specific for the investigated type of resurfacing prosthesis that features a predefined pure cement mantle and recesses which allow cement to escape under pressure. These findings may not be transferable to other designs. The study shows that both low and high viscosity cements can be used with the Durom Hip Resurfacing implant.

ACKNOWLEDGEMENT

Biomechanics Group, Technical University of Munich, Germany, Institute for Biomedical Engineering, ETH, Zurich, Switzerland, Scanco Medical, Bassersdorf, Switzerland.

AFFILIATED INSTITUTIONS FOR CO-AUTHORS

** University Hospital, Lund, Sweden
*** Federal Institute of Technology (ETH), Zurich, Switzerland
**** Zimmer Corporate Research, Warsaw IN, USA

BIOTRIBOLOGICAL EVALUATION OF AN ARTIFICIAL DISC ARTHROPLASTY DEVICE – INFLUENCE OF LOADING AND KINEMATIC PATTERNS DURING IN VITRO WEAR SIMULATION

*Grupp TM, **Yue YY, ***Garcia R, *Schwiesau J, *Fritz B, *Blömer W
*Aesculap AG & CO. KG, Tuttlingen, Germany
thomas.grupp@aesculap.de

INTRODUCTION

Degenerative disc desease is one of the most frequently encountered spinal disorders. The intervertebral disc is a complex anatomic and functional structure, which makes the development of an efficient artificial disc a challenge [1]. The idea of artificial total disc replacement is more than 40 years old, but most of the different concepts created remained ideas in patent publications [1]. The outcome of total disc arthroplasty (TDA) depends to a significant extent on the pre-operative degree of painful disintegration of the intervertebral disc and the facet joints and after TDA on the long term properties of the artificial disc device in mostly young and active patients. Based on the complexity of the anatomical structures and the nearly unknown loading and environmental conditions only little knowledge exists about the biotribological behaviour of TDA devices in the human lumbar spine [2,3,4].

The objective of our study was to investigate the influence of loading and kinematic patterns of two different protocols in regard to wear simulation on TDA prostheses.

MATERIALS AND METHODS

In-vitro wear simulation has been performed in a direct comparison of two different test methods according to ISO/CD 18192-1 and ASTM Z9687Z–WK454 Item 5, Draft 8. Testing has been done for 10 Mio cycles (ISO) and 5 Mio cycles (ASTM) on activ L lumbar artificial disc devices (Aesculap, Germany) with a customized 6 station spinal wear simulator (EndoLab, Germany).

The applied kinematic pattern of movement was multi-directional (ISO Fig. 1) and uni-directional (ASTM Fig. 2).

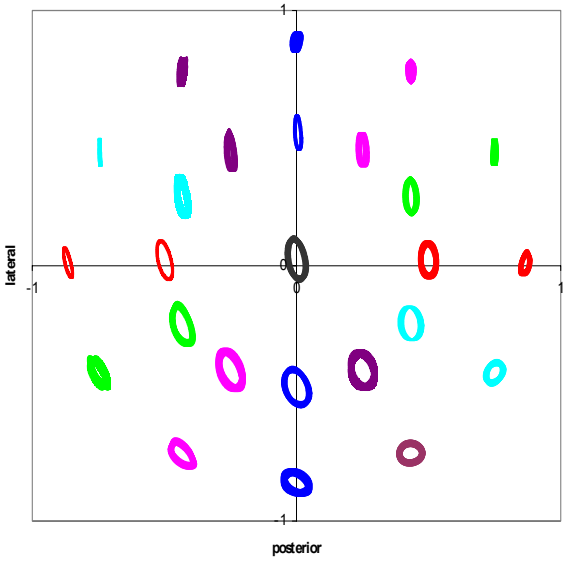

Fig. 1: Pattern of movement of the superior articulation between inlay and cranial disc endplate (ISO/CD 18192-1)

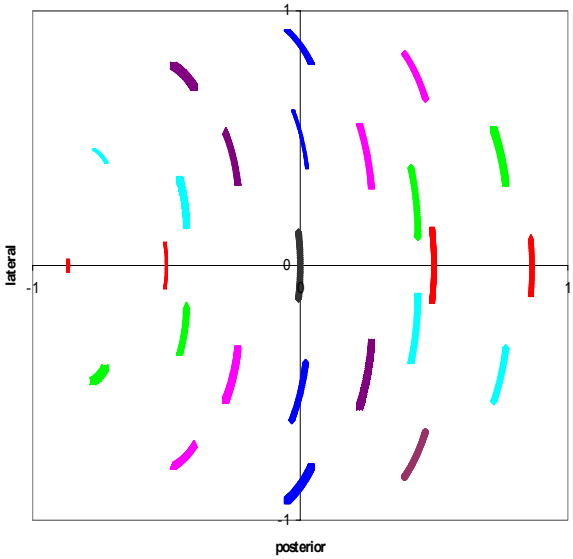

Fig. 2: Pattern of movement of the superior articulation between inlay and cranial disc endplate (ASTM Z9687Z-WK454 Item 5, Draft 8)

unidirectional wear pattern

orientation of polymer chains

RESULTS

The difference in the gravimetric wear amount between the alternative methods ISO and ASTM is more than 20-fold. Therefore a strong influence of load and movement patterns could be determined. The low wear rate during the ASTM load and displacement cycle seems to be related to the strain hardening effect provoked by the linear wear path due to the absence of a phase shift between displacement components. The multi-directional wear path according to ISO prevents a strain hardening of the UHMWPE material due to continously changes of the direction of movement and leads to a significant higher wear rate.

CONCLUSION

Due to previous retrieval observations [4], it seems to be very unlikely, that a lumbar artificial disc is loaded with a linear wear path. Based on these findings it seems to be more reliable to predict the clinical wear behaviour of an artificial disc replacement based on the ISO method.

REFERENCES

1 Szpalski M., Gunzburg R., Mayer M.: Spine arthroplasty: a historical review. EurSpine Journal Vol. 11 Suppl. 2, 2002, pp 65-84

[2] Wilke H.J., Wenger K., Claes L.E.: Testing criteria for spinal implants: recommendations for the standardization of in vitro testing of spinal implants. Eur Spine J 7, 1998, pp.148-154.

[3] Kurtz S., van Ooij A., Peloza J., Villarrag M.: Standardized wear testing for total disc replacements: Perspectives from retrieval analysis. ASTM Symposium on Wear of Articulating Surfaces, Committee F04, Hyatt Regency Dallas, Texas 2005.

[4] Pare P., Chan F., Buchholz P., Kurtz S., McCombe P.: Is unidirectional wear testing clinical relevant for artificial disc implants? ASTM Symposium on Wear of Articulating Surfaces, Committee F04, Hyatt Regency Dallas, Texas 2005.

AFFILIATED INSTITUTIONS FO CO-AUTHORS:

** Dept. of Orthopaedics & Rehabilitation, Yale University School of Medicine, New Haven, CT (USA)
*** Orthopedic Care Center, Aventura, Florida (USA)

INDIRECT DETERMINATION OF TRABECULAR BONE EFFECTIVE TISSUE PROPERTIES USING MICRO-FINITE ELEMENT SIMULATIONS

*Verhulp E, *van Rietbergen B, **Müller R, *Huiskes R
*Dept. of Biomedical Engineering, Eindhoven University of Technology, Eindhoven, The Netherlands

e.verhulp@tue.nl

INTRODUCTION

Trabecular bone can resist considerable forces even when it is loaded in the post-yield range. A better understanding of this behavior is of particular importance for improved predictions of the mechanical integrity of collapsed vertebrae, a condition commonly found in osteoporosis. Understanding this post-yield behavior requires information about bone tissue failure parameters. For trabecular bone, however, these parameters are not well known since these are difficult to obtain from mechanical tests on individual trabeculae.

The objective of this study was to determine trabecular bone tissue failure parameters in an indirect way, by comparing results of nonlinear micro-finite element (µFE) analysis of compression tests on larger bone specimens with those of real mechanical tests of the same specimens.

METHODS

Seven cylindrical trabecular bone specimen (nominal length: 5 mm, ø: 5.35 mm) were extracted from a bovine tibia. Following scanning of the structure with a µCT scanner (µCT-80, Scanco Medical AG) the specimens with attached end-caps were compressed in a micro-compression device (MCD) [1] to a strain of 5 %. After testing, another µCT scan was made of the sample in the deformed state.

The initial scans were converted to µFE models. An isotropic plasticity model based on Hill's yield criterion was chosen to describe to behavior of the tissue. The tissue effective compressive properties of each of the specimens were iteratively adjusted in order to match the simulated load-displacement curves with the measured curves. The deformed meshes were compared with the CT scans of the deformed specimen to study the results on a local level. The geometrically nonlinear analyses were performed using Marc (MSC.Software Corporation, US).

RESULTS

Between 6 and 16 nonlinear analyses were required for the fit procedures per specimen, which resulted in excellent fits (mean (± SD) coefficient of correlation (R^2) of 0.9988 ± 0.0008) (Fig. 1). The resulting effective tissue properties of the seven specimens were averaged to determine to average effective tissue properties (Fig. 2). The applied deformation clearly resulted in heavily strained regions and even cracks in the specimen. Local deformations in the CT scans compared well with deformations and high equivalent strain values in the µFE models (Fig. 3).

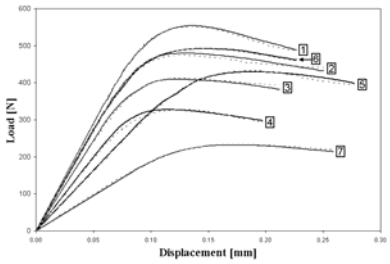

Fig. 1 Measured (solid) and simulated (dotted) apparent behavior of the seven specimens

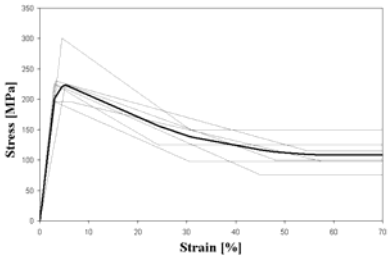

Fig. 2 Effective tissue properties resulting from the fit procedure. The average of the seven curves is shown in black.

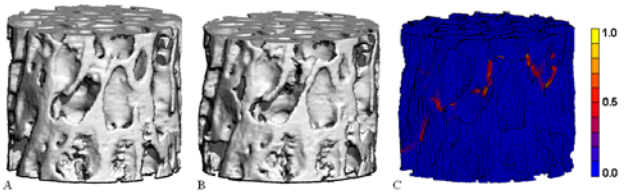

Fig. 3 Rendered CT scans of a sample in its initial (A) and deformed (B) state. The deformed µFE mesh (C) is shown for comparison.

DISCUSSION

Using µFE modeling, trabecular bone tissue properties could be indirectly determined by fitting simulation to experimental results. The effective tissue properties include significant compression softening, and are, therefore, different than those of cortical bone tissue. The results also suggest that there is considerable variation in tissue properties between specimens.

REFERENCES: [1] Müller et al., Technol Health Care 6:433-444

ACKNOWLEDGEMENTS: This work was sponsored by the Dutch NCF and NWO. R.M. was supported by the Swiss SNF.

AFFILIATIONS: **Institute for Biomedical Engineering, University and ETH Zuerich, Switzerland.

VISCOUS AND 'PSEUDO-VISCOUS' EFFECTS OF ELEVATED WATER CONTENT ON LIGAMENT MECHANICS

*Zec ML, ** Thistlethwaite PA, *Frank CB
*McCaig Centre for Joint Injury and Arthritis Research, University of Calgary, Calgary, Canada;
**MEM Research Center for Orthopaedic Surgery. Bern, C
mlzec@ucalgary.ca

INTRODUCTION

Ligament water content varies with age, injury and activity and has been shown to influence the viscoelastic behaviour of ligament tissue. For example, Chimich et al. demonstrated that ligaments with higher water contents experience greater cyclic load relaxation [1]. Similarly, Thornton et al. found that creep strain decreased with decreased tissue hydration and increased with increased hydration [2]. What remains unclear is if the hypotonic solutions used to increase water content alter tissue mechanics by increasing tissue swelling, or if the inherent reduction in viscosity of the hypotonic test solution contributes to these effects. The aim of this study was to observe the effect of altering ligament water content in two ways: by varying the tonicity of the test solution and by altering the amount of slack in the ligaments during the soak prior to loading. We expected that, as shown previously, ligaments cycled in hypotonic solution would lengthen more than those cycled in isotonic solution. Further, we hypothesized that ligaments that were soaked under greater slack (and were therefore more swollen) would lengthen less.

METHODS

Eight medial collateral ligaments from skeletally mature, female NZW rabbits were utilized in this study approved by our animal care committee. Water content was manipulated by testing ligaments in either a hypotonic (0.1%) or an isotonic (10%) sucrose solution and by varying the amount of slack the ligament experienced while soaking. ***In vitro mechanical testing:*** Limbs were mounted and preconditioned at ~70° of flexion in custom-designed clamps in a servohydraulic testing machine (MTS Systems, USA). Prior to soaking in test solution for the first time, ligaments were subjected to 30 load cycles (1 Hz, 10 MPa) in 'air' to establish baseline mechanical behaviour. Ligaments were subsequently subjected to a 1 hour soak (-1mm displacement) followed by 30 load cycles (1 Hz, 10 MPa). Half of the ligaments were tested in isotonic solution while half were tested in hypotonic solution (37°C, with protease inhibitors). This soak-cycle sequence was repeated five times with the amount of slack during soak varied as follows: -2.0 mm, -1.0 mm, -0.1 mm, -1.0 mm and -1.0 mm. Slack states of -1 mm were interposed between 'more slack' (-2.0 mm) and 'less slack' (-0.1mm) states to demonstrate reproducibility of measures obtained at the -1 mm level. All ligaments were loaded repetitively between 0.1N and a load corresponding to 10 MPa. ***Outcome measures:*** In addition to monitoring alterations in peak displacement (l_{max}), *dF/dl* was also determined as a potential means of assessing initial fibre recruitment. Within group comparisons were performed by repeated measures ANOVA with repeated contrasts, while comparisons between groups were performed by paired t-test ($p<0.05$).

RESULTS

Peak cyclic displacements for ligaments cycled in hypotonic solution were significantly greater than for isotonic solution after soaking under -2mm of slack ($p < 0.02$, hypotonic data not shown). In isotonic solution, the l_{max} value for the -2mm condition was less than the first -1 mm condition ($p<0.03$) on the first cycle of loading (Fig 1). Likewise in hypotonic solution, the -2mm condition lengthened less than the first -1mm condition ($p<0.01$). In both isotonic and hypotonic solutions, the value of *dF/dl* was greatest for ligaments soaked under the most slack (i.e. -2mm).

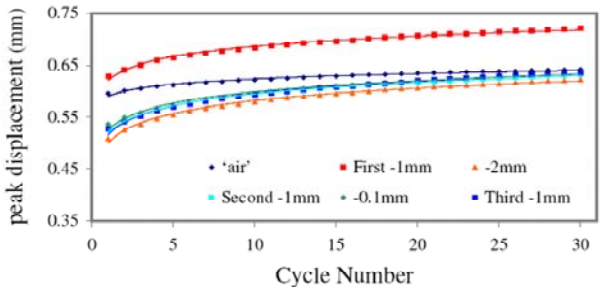

Figure 1. Mean peak cyclic displacement in isotonic solution.

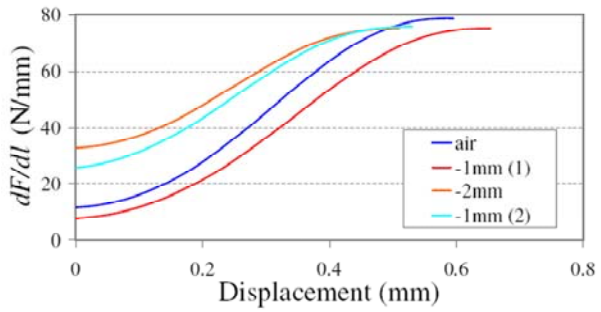

Figure 2. First derivatives of force-displacement data under four loading conditions in isotonic solution – mean data for the first cycle of loading are shown. The final two loading conditions not shown.

DISCUSSION

As predicted, ligaments cycled in hypotonic solution did lengthen more under cyclic load. Consistent with our hypothesis, ligaments lengthened least after being soaked under -2mm of slack irrespective of test solution. The initial elevation of *dF/dl* after soaking at -2mm of slack suggests that, by virtue of swelling, these ligaments may have recruited more collagen fibres thereby becoming stiffer. Hence elevated water content (or swelling) causes decreased displacement. This study illustrates the importance of differentiating the apparent viscosity of the tissue from effects attributable to the viscosity of the test solution.

REFERENCES: 1. Chimich et al. *J Biomech* 25:831. 2. Thornton et al. *J Orthop Res* 19:845.

INFLUENCE OF FREEZING AND THAWING ON THE BIOMECHANICAL AND STRUCTURAL PROPERTIES OF THE HUMAN POSTERIOR TIBIAL TENDON

*Buda R, *Di Caprio F, **De Pasquale V, *Bassi A, *Fornasari PM, *Giannini S
*Rizzoli Orthopaedic Institute, University of Bologna, Bologna, Italy

roberto.buda@ior.it

INTRODUCTION

Allogenic tendons are widely used in orthopaedic reconstructive surgery, and especially in ACL reconstruction. The most common method of storage is fresh freezing at –80°. The literature reports a few studies on the effects of storage on the biomechanical and structural properties of human tendons: most of these studies are carried out on animal ligaments, and their results are contradictory. The aim of this study is to clarify the effects of preservation by fresh-freezing, as to know whether the variability in the effects of fresh-freezing has any influence in the choice of an allograft tissue, analyzing the effects of storage by fresh-freezing at -80°C on the histological, structural and biomechanical properties of the human posterior tibial tendon (PTT).

METHODS

Twenty-two PTTs were harvested from eleven donors. For each donor one tendon was immediately tested without freezing (control), while the controlateral was frozen at -80°C and then thawed in physiologic solution at 37°C before testing. Transmission electron microscopy (TEM) studied the number of collagen fibrils in 1.5 μ^2 sections, the mean diameter of each fibril and the mean interfibrillar gap. Differential scanning calorimetry (DSC) studied denaturation temperature and denaturation enthalpy for each sample. Biomechanical analysis, performed with strain-to-failure tests, studied ultimate load, ultimate deformation and stiffness (calculated from the linear part of the curve), obtained from the Load/Deformation curve; ultimate stress and ultimate strain were obtained from the Strain/Stress curve. Young's modulus was calculated as follows: *Stiffness * Initial Length / Cross-sectional Area*.
Statistical analysis of the results was conducted to detect any structural or biomechanical change in every pair of tendons.

RESULTS

We found the following mean changes in frozen-thawed tendons compared to controls: TEM showed an increase in the mean diameter of collagen fibrils and in fibril non-occupation mean ratio, while the mean number of fibrils per section decreased. DSC showed a decrease in mean denaturation temperature and in denaturation enthalpy in the frozen-thawed tendons; accordingly, frozen-thawed tendons underwent a decrease in triple helix content. Biomechanical analysis showed an increase in the mean cross-sectional area of the frozen-thawed tendons, a decrease in ultimate load and ultimate stress, an increase in stiffness and a decrease in ultimate strain of tendons. No significant variations occured in the Young's modulus.
We also observed a significant variation in the biomechanical properties of tendons among individuals.

DISCUSSION

The histologic study found out a significant decrease in the number of collagen fibrils per section: these results are in agreement with the calorimetric analysis, and in particular with the reduction in denaturation enthalpy, which means decreased triple helix content per mass unit. Tsuchida et al. (1997) reported similar results in *in situ* frozen and stress-shielded rabbit patellar tendon, demonstrating a decrease in the number of fibrils and in the fibril occupation ratio at 3 and 6 weeks after freezing. They observed a decrease in small diameter fibrils and an increase in fibrils with a diameter greater than 360nm. This swelling phenomenon, as well as the splitting and fragmentation of collagen bundles observed by LM, can probably be attributed to ice crystals formation.
The decrease in denaturation temperature is due to the loss in collagen cross-links, which results in a decrease in collagen thermal stability.
These findings are related with the loss in mechanical strength. At variance with the results of previous studies, we did not appreciate any variation in Young's modulus of frozen-thawed tendons most likely because of the decrease in ultimate strain which occurs simultaneously to that in ultimate load.
In conclusion, fresh-freezing brings about significant changes in the biomechanical and structural properties of the human PTT. A high variability exists in the biophysical properties of tendons among individuals and in the effects of storage on tendons. Considering the loss in mechanical strenght which occurs during the remodeling process after implantation, we know we need a tendon graft far stronger than a normal ACL. Therefore, when choosing an allograft tendon for ACL replacement, particular care is needed to choose a biomechanically suitable graft.

AFFILIATED INSTITUTIONS FOR CO-AUTHORS

**Department of Anatomy, University of Bologna, Bologna, Italy

CELLULAR AND HUMORAL MECHANISMS OF OSTEOCLAST FORMATION AND RESORPTION IN MELANOMA METASTASIS

*Athanasou NA, Lau YS, Sabokbar A, CerundoloV
Department of Pathology, Nuffield Department of Orthopaedic Surgery, Nuffield Orthopaedic Centre, Oxford, UK

Nick.athanasou@noc.anglox.nhs.uk

INTRODUCTION

In the past decade there has been a substantial increase in the incidence of cutaneous melanoma among the Caucasian population; in fact the incidence is increasing faster than any other cancer. The number of deaths from melanoma has also increased throughout the world. Osseous metastases from melanoma are common (7%) and occur mainly in the axial skeleton, causing bone pain, neurological symptoms and pathological fractures.

Bone destruction in skeletal metastases of solid tumours is due to stimulation of osteoclast formation and bone resorption. Osteoclasts are formed in the presence of macrophage colony-stimulating factor (M-CSF) by the fusion of marrow-derived mononuclear phagocyte precursors that express RANK (receptor activator of NF-κB) which interacts with its ligand, RANKL, expressed by bone stromal cells. Osteoclast formation by a tumour necrosis factor (TNF-α)-induced mechanism has also been reported.

Tumour-associated macrophages (TAMs) present in both primary and secondary carcinomas are known to be capable of osteoclast differentiation. In this study we determined whether TAM-osteoclast differentiation plays a role in the osteolysis associated with melanoma metastasis and analysed the cellular and humoral mechanisms involved in this process.

METHODS

TAMs were isolated by collagenase digestion from skin and lymph node melanoma metastases and cultured for 21 days in the presence of M-CSF and either RANKL or TNF-α on glass coverslips and dentine slices. Conditioned medium from cultured melanoma-derived fibroblasts or *SK-Mel-29* melanoma cells was also added to cultures of human monocytes +/- inhibitors of RANKL-dependent or independent osteoclast formation.

Cultured monocytes and TAMs were characterized for the expression of the osteoclast markers, TRAP and VNR, the macrophage marker, CD14 and the melanoma markers, HMB-45 and S100. Dentine slices were stained with toluidine blue and examined by light microscopy for lacunar resorption.

mRNA was also extracted from melanoma-derived fibroblasts and gene expression for RANKL and osteoprotegerin (OPG) verified by RT-PCR.

RESULTS

Osteoclast differentiation by TAMs isolated from melanomas was evidenced by the formation of TRAP and VNR – expressing multinucleated cells that were capable of lacunar resorption on dentine slices. Osteoclast formation occurred in the presence of M-CSF and either RANKL or TNF-α.

Osteoclast formation was induced by melanoma fibroblast conditioned medium in the absence of soluble RANKL. This was inhibited by the addition of OPG, a decoy receptor for RANK. On RT-PCR the fibroblasts expressed RANKL mRNA.

SK-Mel-29 conditioned medium also supported monocyte-osteoclast differentiation in the absence of RANKL but this effect was not abolished by OPG or antibodies to TNF-α, TGF-β, IL-8 or IL-6.

DISCUSSION

Our results indicate that melanoma TAMs are able to differentiate into osteoclasts via both RANKL-dependent and RANKL- independent mechanisms.

Melanoma fibroblasts expressed RANKL and induced osteoclast formation by a RANKL-dependent mechanism. Fibroblasts secreted an osteoclastogenic soluble factor, the action of which was inhibited by OPG. Melanoma fibroblasts may promote TAM-osteoclast differentiation via up-regulation of RANKL expression.

Melanoma tumour cells also stimulated osteoclast formation and resorption but this occurred via the production of a soluble factor that induced osteoclast formation by a RANKL-independent mechanism. This was not one of the known stimulators of RANKL-independent osteoclastogenesis. Further analysis showed that the active moiety produced by melanoma cells had a molecular weight exceeding 10,000 Da.

Inhibitors of RANKL-dependent osteoclast formation targeting TAM-osteoclast differentiation and identification of the melanoma-derived osteoclastogenic factor promoting formation RANKL-independent osteoclast formation may have therapeutic potential in controlling osteolysis due to melanoma metastasis.

CT-GUIDED PERCUTANEOUS BIOPSY OF MUSCOLOSKELETAL LESIONS

*Rimondi E, *Rossi G, **Alberghini M, ***Bianchi G, ***Fabbri N, ***Mercuri M
*Radiology, **Surgical Pathology, and ***Orthopaedic Surgery
Istituto Ortopedico Rizzoli, Bologna, Italy

eugenio.rimondi@ior.it

INTRODUCTION

The correct diagnosis of the nature of a bone lesion is mandatory in order to provide an adequate treatment of the lesion and of the underlying desease (infections, inflammation, benign and malignant tumors). Even if recent more sophisticated radiological immaging techniques have a good predictive value in differential diagnosis an histologic or/and cultural examination is often necessary to plan further treatment. Bone biopsies can be performed as open biopsy or percutaneous biopsy (PB). The use of percutaneous biopsy (PB) has increased importance because it is quicker, less expensive, with less complications compared to surgical open biopsy. Percutaneous biopsy can be done through Fine Needle Biopsy (FNB 0.6-1.2 mm gauge,used for soft tissue biopsy), Core Needle Biopsy (CNB,1.7-2.1 mm) and Trephine Needle Biopsy (TNB 3-5 mm). In musculoskeletal diseases, clinical history, objective examination, laboratory tests, and radiological imaging may not be sufficient for diagnosis. Only biopsy can allow diagnosis so that the most suitable treatment may be applied rapidly. The decision to use it is based on clinical, laboratory and radiological imaging tests. Performing the percutaneous biopsy is not difficult in itself, and the success rate in selected cases is excellent. But indications for this technique, the choice of needle, approach to the lesion, harvesting of tissue, and possible need for adjuvant treatment should be assessed beforehand. Needle biopsy is, however, a surgical technique, and therefore it is associated with risks and dangers. Therefore, it should always be performed by a radiologist who is an expert in musculo-skeletal diseases, or by an orthopedic surgeon.
The procedure, any complications, difficulties in performing the technique and possible results should be discussed first with the patient.

METHODS

From January 1990 to January 2006 in the Department of Radiology of the Rizzoli Orthopaedic Institute, we carried out 1010 percutaneous CT-guided bone biopsies.
454 (44.9%) in the spine (10 cervical,138 thoracic, 194 lumbar, 112 sacral) and 556(55.1%) in the appendicular skeleton (73 upper limb, 22 thoracic cage, 225 pelvis, 236 lower limb). 573 patients were males and 437 females, median age 46 years. Needle size was 8/7G in 1001 cases and 14/12G in 9 cases. All biopsies were performed after informed consent obtained and under local anesthesia, except for children under 10 years old, who were treated under general anesthesia. Local anesthesia allows the patient to cooperate and inform the operator if the needle is stimulating a nerve end. All patients had a preliminary anesthesiolgical exam, and those found to be particularly anxious were sedated during local anesthesia.

RESULTS

Diagnosis of nature was possible in 802 cases, tissue was essentially normal bone or sclerofibrotic-bone in 180 cases and non-diagnostic in 28 cases. Follow-up of the 180 cases has shown 61 true negatives and 84 false negatives; no information were available in 35 cases. Diagnostic accuracy has been 85%. There were no complications. In 7 cases of eosinophilic granuloma of the spine, the patient has been managed successfully by frozen section and steroid injection during the same procedure.

DISCUSSION

Our experience in performing CT-guided percutaneous biopsy, resulting from cooperation between the 1st Clinic of Orthopedic Oncology and the Diagnostic Imaging Unit of the Rizzoli Orthopedic Institute shows, as already widely described in the international literature that this radiological technique, despite the risk of harvesting too little material, is:
Reliable. The use of CT improves the approach technique by providing more information before the biopsy and enables larger caliber needles to be used, which increases diagnostic accuracy;
Fast. It takes an average of 30 minutes (ds ±10) to perform with high-speed equipment;
Applicable also to outpatient clinic or day hospital patients, since general anesthesia is not necessary, thus costs are lower than an intraoperative procedure;
Relatively safe, although it requires technical skill and knowledge of potential complications.
The rate of diagnostic accuracy of percutaneous biopsy varies according to the site biopsied, type of disease, operator's experience, and psychological disposition, quantity and quality of tissue harvested, and the cooperation of the patient. The rate is higher in tumoral lesions, especially secondary ones, and lower in inflammatory lesions, especially chronic ones.
CT-guided percutaneous biopsy in selected patients can be performed quickly and effectively in the Diagnostic Imaging Unit. It is always performed, however, under the close collaboration between the radiologist in charge of the procedure, orthopedic surgeon and oncologist in charge of selecting and treating the patient, and anatomo-pathologist responsable for histological diagnosis.
Reliability of the technique and elevated diagnostic accuracy make today CT-guided biopsy cost-effective and the standard procedure for histologic diagnosis of musculoskeletal lesions at most centers worldwide.

NEUROBLASTOMA CELLS SUPPRESS OSTEOBLAST DIFFERENTIATION BY SECRETING WNT INHIBITORS

*Amato I, *Pagani S, *Devescovi V, **Carella M, **Savino MG, *Baldini N, *Granchi D
*Laboratorio di Fisiopatologia, Istituti Ortopedici Rizzoli, Bologna, Italy
ilaria.amato@ior.it

INTRODUCTION

Bone is one of the target organs of metastasis in advanced neuroblastoma (NB). We have previously demonstrated that tumor cells are able to induce osteoclast activation and bone resorption, however, according to recent findings, inhibition of bone formation could also play a role in the pathogenesis of bone metastasis.

Novel insights in skeletal development and osteogenesis ascribe to the canonical Wingless (Wnt) signaling pathway a critical role in the differentiation of pre-osteoblast into bone forming cells. Inhibition of Wnt pathway favors the cell cycle entry of hMSCs and prevents their differentiation. In the presence of Dickkopf 1 (Dkk-1), an inhibitor of Wnt signaling, this cascade is disrupted, in turn blocking osteogenesis. In addition, secreted Frizzled Related Proteins (sFRP) mimic the receptor function of membrane Frizzled proteins for binding to secreted Wnt ligands, and antagonize the Wnt function. In this study, we examined whether NB cells suppress osteoblast differentiation from hMSCs by producing inhibitors which affect the canonical Wnt pathway.

METHODS

Three neuroblastoma cell lines derived from primary tumors (CHP-212, SJ-N-KP, NB-100), and two cell lines derived from bone marrow metastases of neuroblastoma (SH-SY5Y, LAN-1) were used.

Total RNA was extracted and global gene expression through Affymetrix chip technology and quantitative real-time PCR was used to compare sFRP-1 and Dkk-1 expression. The levels of the corresponding proteins in the medium of NB cells were detected by ELISA.

For analyzing the effect of NB on osteoblast differentiation, hMSCs were cultured for up to 14 days with 50% conditioned media (CM) from NB cells. At the endpoint, the soluble and cellular alkaline phosphatase (ALP) activity were evaluated.

RESULTS

Gene expression profiling showed that Dkk-1 was more expressed in SH-SY5Y than in other cells lines, while sFRP-1 was found only in SH-SY5Y. Real-time PCR confirmed the results of microarray analysis. The release of Dkk-1 in the culture medium of NB cells correlated with mRNA levels; on the contrary, sFRP-1 was found in all cell lines, even if the transcript was not detected. When hMSCs were co-cultured with CM-NB cells, SH-SY5Y strongly inhibited osteoblast proliferation and differentiation, as shown by ALP cytochemistry (Figure 1). Moreover, the quantitative analysis of soluble and cellular ALP activity showed that all NB cell lines decreased the enzyme activity (Figure 2).

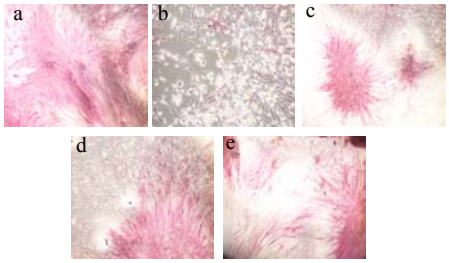

Figure 1. ALP cytochemistry of hMSCs
a) control. b) hMSC + 50% CM-SH-SY5Y. c) hMSC + 50% CM-CHP212. d) hMSC + 50% CM-NB100. e) hMSC + 50% CM-LAN1.

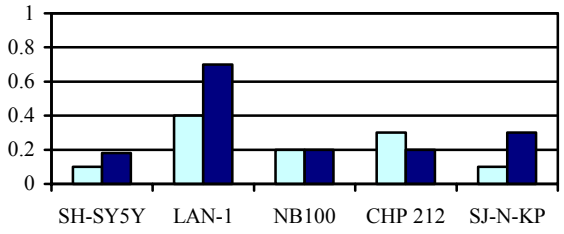

Figure 2. ALP release (light blue bar) and cellular ALP (dark blue bar) in hMSCs cultured with 50% of CM-NB cells. Results are expressed as percentage vs control hMSC (=1).

DISCUSSION

We showed that NB cells secrete soluble factors which are able to inhibit osteoblast differentiation. The presence of Wnt inhibitors in CM-NB is related to the inhibition of osteoblast differentiation in hMSCs, The culture medium of SH-SY5Y impairs the number of committed cells and inhibits osteoblast phenotype and function. As a large amount of Dkk-1 is secreted by SH-SY5Y, it is reasonable to assume that this Wnt inhibitor plays a pivotal role in the pathogenesis of bone metastasis induced by NB cells. Interestingly, the most clear evidence of this activity was observed in SH-SY5Y, a cell line derived from bone microenvironment.

ACKNOWLEDGEMENTS

Grant sponsor: Associazione Italiana per la Ricerca sul Cancro; and Italian Ministry of Health (Ricerca Finalizzata).

** Servizio di Genetica Medica, Ospedale 'Casa Sollievo della Sofferenza', San Giovanni Rotondo, Italy.

SSX-NEW MOLECULAR TARGET REGULATING CELL MOTILITY OF BONE AND SOFT-TISSUE TUMOUR

Itoh K, Naka N, Yoshioka K
Department of Biology, Osaka Medical Center for Cancer and Cardiovascular Diseases, Osaka, Japan
itou-ka@mc.pref.osaka.jp

INTRODUCTION

The SSX (synovial sarcoma X break point) genes were originally identified as fusion partners to the SYT (synovial sarcoma translocation) gene in human synovial sarcomas carrying a recurrent t (X; 18)(p11.2; q11.2) chromosomal translocation. Besides adult human testis, SSX genes were expressed at varying frequencies in a number of malignancies thereby categorized as cancer/testis antigens. Using Nucleic Acid Sequence-Based Amplification, we established the quantitative analysis system for the expression level of SSX transcript in the biopsy specimen. We have already reported that the expression level of SSX in the malignant bone and soft tissue tumors (3.8 ± 1.4 copies/μg of total RNA in log10 order) was significantly higher than that in the benign bone and soft tumors (2.4 ± 0.5, $p<0.0001$). (Ref.1) We also found that the level of expression positively correlated with clinical stage, especially the metastatic case present very high SSX expression. However, the biological function of SSX has not been elucidated. The aim of this study is to investigate the function of SSX in tumor progression, especially invasion and metastasis.

METHODS

Plasmids. cDNAs of the human SSX1 and 2 were amplified from surgically resected osteosarcoma by RCR, and subcloned into the mammalian expression vector pcDNNA3. Small interference RNAs (siRNA) were designed and synthesized to the human SSX1 sequence.

Establishment of stable cell lines. Human osteosarcoma Saos-2 cells were transfected with pcDNA3, pcDNA3-FLAG SSX1 or 2, using Lipofectamine plus transfection reagent. Cells were selected with 800 μg/ml G-418 for 4weeks.

Colony formation assay in soft agar. 2×10^3 cells were plated in 0.3% soft agar and incubated for 3 weeks.

Tumor formation assay in nude mice. 1×10^7 cells in PBS were injected s.c.into BALB/c nude mice. Four weeks after cell inoculation, mice were killed and tumor tissues were examined

***In vitro* motility assay**. 2×10^5 cells suspended in MEM/BSA were added to the upper chamber and human fibrosarcoma HT1080 conditioned medium was added lower chamber. After incubating for 16 h at 37°C, cells migrated to the lower surface of the membrane were fixed, stained, and quantified as described previously (Ref 2).

Rho family activity assays. The amount of active Rho, Rac1 and Cdc42 in the cells were determined using Rho activity assay kit (Upstate Biochemistry) according to the manufacture' s instructions.

RESULTS

We made several clones of SSX 1 and 2 stable transfected Saos-2 cells. The expression of SSX protein was mainly localized in the nucleus with patched pattern. These transfectants increased motility using wound healing assay, chemotaxis (3~4-fold) and invasiveness (3~4-fold) using Boyden chamber assay compare to mock transfectants. Increased expression level of SSX was positively correlated with the enhanced motility. Further, the SSX transfectants showed increased activity of RhoA (2.0-fold) than mock transfectants, but showed no change in Rac1 and Cdc42 activation. The SSX transfectants promoted colony formation (2-fold) compare to mock transfectants in soft agar and tumor formation in nude mice, but showed little change in growth rate in 2D culture. Next, we have used a siRNA strategy to selectively knockdown the expression of SSX1 in HT1080 cells, which highly expressed SSX. The cells transfected with SSX1 specific siRNA markedly decreased the expression of SSX1 protein, membrane ruffling, chemotaxis (52% inhibition) and invasiveness (38% inhibition), but did not affect 2D cell proliferation. Moreover, the SSX1 siRNA cells showed decreased Rac1-activation and myosin light chain phosphorylation.

DISCUSSION

These data suggested that SSX could promote tumor progression and motility, and that these effects of SSX were regulated via Rho-family small GTP binging protein involving actin cytoskeleton dynamics. Since the expression of SSX was restricted in malignant tumour, SSX could be a new molecular target for invasion/metastasis under clinical setting.

REFERENCES

1. Naka, N., Joyama, S., Tsukamoto, Y., Yoshioka, K., Hashimoto, H., Ujiiye T., Hayashi, T., Kawase, M., Mano, M., Ishiguro, S., Myoui, A., Ueda, T., Yoshikawa, H., Araki, N., and Itoh, K.: Quantification of *SSX* mRNA expression in human bone and soft tissue tumors using Nucleic Acid Sequence-Based Amplification (NASBA): J. Mol. Diagn. 7:187-197 (2005)

2. Yoshioka, K., Foletta, V., Bernard, O. and Itoh, K.: A Role for LIM-Kinase in Cancer Invasion: Proc. Natl. Acad. Sci. USA. 100: 7247-7252 (2003)

MECHANISMS UNDERLYING THE ANTICANCER EFFECTS OF ZOLEDRONIC ACID AGAINST HUMAN OSTEOSARCOMA CELLS

*Kubista B, *Trieb K, *Sevelda F, *Arrich F, *Toma C, **Elbling L, **Sutterlüty H, ***Scotlandi K, *Kotz R, **Micksche M, **Berger W
*Department of Orthopaedics, Vienna General Hospital and Medical University of Vienna
bernd.kubista@meduniwien.ac.at

INTRODUCTION:
Due to the use of neoadjuvant chemotherapy the long-term survival of patients with osteosarcoma has improved from 10% - 20% to nearly 80% within the last 25 years.
However, there are still a certain number of non-responders who do not benefit from these improvements and still die early. Thus, there is a great demand for new and more effective therapeutical strategies for these patients. Bisphposphonates are commonly used to prevent bone resorption in a number of metabolic and tumour induced bone diseases, because of their ability to interfere with osteoclast recruitment, differentiation and action, and to induce apoptosis in these cells. However, bisphosphonates have also been shown to have effects on cells other than osteoclasts, including tumour cells. Recent studies have shown that Zoledronate exerts direct cytostatic and proapoptotic effects in a time- and concentration-dependant manner in a variety of human tumor cell lines. Aim of our study was to test the effects of the nitrogen-containing bisphosphonate zoledronic acid (ZOL)-Zometa© on a panel of human osteosarcoma cell lines (N=9) and to investigate possible underlying molecular mechanisms.

METHODS:
Cell culture and reagents: ZOL (Zometa®) a third generation BP, was kindly provided by Novartis Pharma AG (Vienna, Austria). The osteosarcoma cell lines HOS, MG-63, SAOS-2and U2-OS were obtained from the ATCC (Rockville, MD). The osteosarcoma cell lines OS-9, OS-10, MOS, SARG were kindly provided by the Instituti ortopedici Rizzoli, Bologna, Italy and cultured under standard conditions.
Cell growth and viability assays: The proportion of viable cells was determined by MTT assay following the manufacturer's recommendations (EZ4U, Biomedica, Vienna, Austria). Alternatively, ^{3}H-thymidine incorporation measured after drug exposure. For clonogenic assays, 1000cells/well were seeded in six well plates, incubated for 24 hrs and than treated with the respective drugs. Colonies > 50 cells were counted.
Cell cycle analysis: Cell cycle analysis was done after the incubation of cells in the respective drug solutions by flow cytometry (FACS).
The effect of Zoledronate on prenylation of G-proteins and on MAPK pathway activity was determined by Western Blot Analysis.
Cell migration assay: Cells were seeded in 6-well plates and grown until confluence. Than an X-shaped scratch was set with a pipette tip. The closing of the scratch was followed microscopically
Fluorescence staining and apoptosis detection: Cells were seeded in 8-chamber slides grown for 24 hrs, and than incubated with the respective drug concentrations for 48 to 72 hrs. Cells and microfilaments and nuclei were stained by phalloidin-FITC and DAPI.

RESULTS:
Exposure to ZOL at low µM concentrations induced a dose- and time-dependent block of DNA-synthesis and cell cycle progression followed by microfilament breakdown and apoptosis induction. The ZOL-induced cell cycle accumulation in S-phase was accompanied by significant changes in the expression of cyclins and cyclin-dependent kinase inhibitors with a prominent loss of cyclin E and D1. Besides growth, ZOL also inhibited cell migration of osteosarcoma cells. The mevalonate pathway intermediate geranyl-geranol (GGOH) but not farnesol (FOH) significantly inhibited the anticancer effects of ZOL against osteosarcoma cells. Correspondingly, ZOL sensitivity correlated with blockade of protein geranylgeranylation indicated by unprenylated Rap1. Pre-treatment with ZOL led to a down-regulation of serum-induced ERK phosphorylation which could, however, not be rescued by GGOH. These data suggest inhibition of protein geranylgeranylation as predominant molecular mechanism exerted by ZOL against osteosarcoma cells leading to a MAPK pathway-independent breakdown of the microfilament system and deregulation of the cell cycle machinery.

DISCUSSION:
In our study we demonstrate that ZOL exhibits strong cytotoxic and anti-migratory activity against osteosarcoma cells at concentrations clinically achievable in the bone and give evidence for a decisive role of protein geranylgeranylation inhibition as central component of ZOL activity against the tumour cells.
Summarizing, our data suggest that, considering its selective accumulation in the bone, ZOL represents a promising agent to improve osteosarcoma therapy.

AFFILIATED INSTITUTIONS FOR CO-AUTHORS:
**Department of Medicine I, Institute of Cancer Research, Medical University Vienna; Austria;
***Laboratorio di Ricerca Oncologica, Istituti Ortopedici Rizzoli, Bologna, Italy

PHOTODYNAMIC DETECTION OF MOUSE OSTEOSARCOMA IN THE SOFT TISSUES UTILIZING FLUOROVISUALIZATION EFFECT OF ACRIDINE ORANGE

Satonaka H, Kusuzaki K, Matsubara T, Shintani K, Wakabayashi T, Matsumine A, Uchida A
Department of Orthopaedic Surgery, Mie University Faculty of Medicine, Tsu, Japan

stnkhcyk@clin.medic.mie-u.ac.jp

INTRODUCTION

There are various imaging methods to detect malignant tumor in human body. PET is recently becoming so common for this aim in the world. However its accuracy is not perfect, because of some false positive and negative cases and it is also very expensive because of large equipments and valuable radio-isotopes. To improve this issue, we have attempted to develop new imaging technique of photodynamic diagnosis (PDD) with acridine orange (AO). We have already developed photodynamic therapy with AO (AO-PDT) after intralesional tumor excision and have applied to clinical cases with high grade musculoskeletal sarcoma, resulting low risk of local recurrence and excellent limb function. AO also has ability to specifically accumulate into malignant tumor and emit brilliant green fluorescence after blue light excitation (fluorovisualization effect). In this study, we investigate imaging availability of PDD using fluorovisualization effect of AO, in mouse osteosarcoma inoculated in the soft tissues.

MATERIALS AND METHODS

The 1×10^6 mouse osteosarcoma cells of LM8 cell line which has high ability to metastasis to the lung were inoculated into soft tissue of the back of BALB/c nude mice (5-week-old males). After macroscopically detectable tumor formation (6 to 10 mm in diameter), the following studies were performed. Each group with 4 mice is intravenously administrated with 0.1, 0.2, 0.5, 1.0, 2.0 and 5.0 mg/kg AO, respectively. After 2 hours, the tumor and surrounding normal tissue were illuminated by 5000 luminance blue light (450-490nm) for AO excitation using 500W xenon lamp through a single fiber tube. The contrast of fluorescence between the tumor and normal tissue was detected using high resolution digital camera (Canon) equipped with an absorption filter (>520nm). Using 4 mice administrated with 1.0 mg/kg AO, fluorescence contrast between the tumor and normal tissue was also detected sequentially at 0.5, 1, 2, 3, 6 and 12 hours, in order to investigate AO exclusion speed from the tumor and normal tissue. After taking photographs of each view, fluorescence intensity (FI) of the tumor and normal tissue was measured as gray scale (darkness) converted by Scion Image Beta 4.02 software. The ratio (X) of FI which was indicator of contrast was calculated by the average FI of the tumor (B) / that of normal tissue (A).

RESULTS

At 2 hours after intravenous injection of various doses of AO, in the low dose groups (0.1 or 0.2 mg/kg), both of the tumor and normal tissue emitted weak green AO fluorescence, whereas in the high dose group (5.0 mg/kg), both emitted strong fluorescence. X value was almost 1.0 in these dosages. However, the injection of 0.5, 1.0 and 2.0 mg/kg AO provided a clear contrast between both areas, more than 1.5 of X value. In particular, 1.0 mg/kg AO provided most optimum contrast (X=2.5) (Figure 1). After injection of 1.0 mg/kg AO, at 30 minutes or one hour, FI of the tumor was higher than those at late phase, but the X value was the highest at 2 hours (Figure 2).

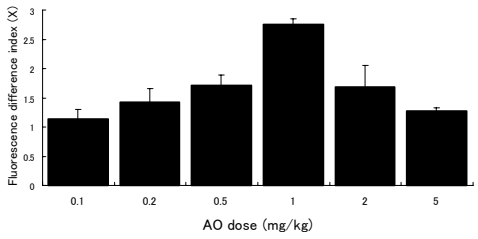

Figure 1. Contrast of fluorescence between the tumor and normal tissue at various doses intravenously AO injected to mice and each fluorescence difference index (X) determined by image analysis (n=4).

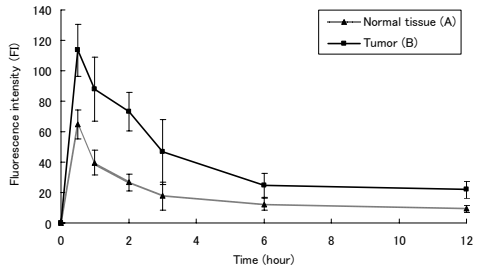

Figure 2. Sequential change in fluorescence intensity and X value after injection of 1.0mg/kg AO by image analysis (n=4).

DISCUSSION

The results of these studies demonstrated that AO-PDD with intravenous administration is available to detect osteosarcoma inoculating into mice soft tissues. Therefore, we believe that AO-PDD might become non-invasive, low-cost, rapid and accurate imaging technique in detecting human musculoskeletal sarcomas, even though it is necessary to use more powerful light source and more high resolution digital camera.

MUTATIONAL ANALYSIS OF EXT1 AND EXT2 GENES AND CORRELATION WITH CLINICAL EXPRESSION OF DISEASE IN PATIENTS WITH HEREDITARY MULTIPLE EXOSTOSES

Pedrini E, Maini V, Capponcelli S, Mordenti M, Parra A, Picci P, Sangiorgi L
Genetics Unit, Lab Oncology Research, Rizzoli Orthopedic Institute, Bologna, Italy

luca.sangiorgi@ior.it

INTRODUCTION: Autosomal dominant Hereditary multiple Exostoses (HME) is one of the most common skeletal disorders. The disease is characterized by the formation of multiple cartilage-capped, benign bone tumours (exostoses) typically located at the meta-epiphyseal areas of the long bones such as distal femur, proximal humerus and proximal tibia. The great variability in size and number of exostoses reflects the clinical heterogeneity and variable severity of HME. In a small percentage of cases (0.5-2%) an exostosis undergoes malignant transformation to a chondrosarcoma.
HME is known to be genetically heterogeneous, with three genes identified by linkage analysis. EXT1 on chromosome 8q24.1 (MIM *608177) and EXT2 on chromosome 11p12 (MIM #608210) have been cloned and represent the major disease genes. Both genes are large, with EXT1 containing 11 exons, and EXT2 containing 14 exons, 13 of which are coding. EXT1 and EXT2 encode ubiquitously expressed, highly homologous glycoproteins of 746 and 718 amino acids implicated in the heparan sulphate polymerisation. Several mutations dispersed throughout the EXT1 and EXT2 genes have been identified in HME patients (Human Gene Mutation Database:
http://archive.uwcm.ac.uk/uwcm/mg/hgmd0.html).
Most of these are responsible of the truncation of EXT1/2 proteins which are likely to become inactive and degrade rapidly, resulting in a nearly complete loss-of-function.
A prospective longitudinal study was undertaken to correlate genotype and phenotype of the disease in families and sporadic cases, with the purpose of defining the disease spectrum of expression.

METHODS: A multidisciplinary clinic, involving geneticists and orthopaedic surgeons, is weekly carried out. In order to evaluate the spectrum and distribution of mutations leading to HME in the Rizzoli cohort of patients a new multi-step DHPLC-based mutation screening method was optimised. For informative families, we adopted a fast pre-screening linkage analysis to selectively focus the DHPLC testing on either EXT1 or EXT2. Patient clinical assessment is carried out using a new classification system substantially based on deformity and functional limitation.

RESULTS: In a small pilot we enrolled 36 unrelated probands, representing 20 families and 14 sporadic cases for the presence of mutations in either EXT1 or EXT2 genes,
Thirty-one out of 36 probands (86%) had mutations either in EXT1 (24/31; 77%) or EXT2 (7/31; 23%), mainly distributed in the amino-terminal region of the proteins and the vast majority of them are responsible of a premature protein truncation. Mutations were found in 10 of 14 sporadic cases (71%) and in 20 of 21 familial cases (95%). No disease-causing mutation has been detected in 5 of 36 patients.
Analysis of the correlation between genotype and phenotype has shown that most of the patients (80%) is not substantially limited by the disease. The condition seems to be clinically more relevant when the underlying mutation is on EXT1 gene.

CONCLUSIONS: our results identified several novel and many private mutations in a large cohort of patients treated at the Rizzoli Institute, confirming the strong allelic heterogeneity of EXT1/2 genes. Our optimised DHPLC-based approach represents a reliable, efficient and highly sensitive diagnostic strategy for rapid detection of germline mutations in HME patients. The genotype-phenotype study is giving indication regarding association of alterations and clinical presentation of the disease.

COMBINED GENTAMICIN-HYDROXYAPATITE-COATING FOR CEMENTLESS JOINT PROSTHESES SHOWS SIGNIFICANT REDUCTION OF INFECTION RATES AND GOOD BIOCOMPATIBLITY IN A RABBIT MODEL

+*Alt V, *Bitschnau A, **Sewing A, *Meissner SA, ***Wenisch S, ****Domann E, *Schnettler, R
+ Department of Trauma Surgery, University Hospital Giessen, Giessen, Germany

volker.alt@chiru.med.uni-giessen.de

INTRODUCTION

Similar infection prophylaxis as in cemented total joint by antibiotic-loaded bone cement cannot be achieved for cementless prostheses. In this study, a gentamicin-coating which can be brought additionally onto standard hydroxyapatite (HA) coatings of cementless prostheses is presented. It was tested whether this gentamicin-coating can reduce infection rates in a rabbit infection model with Staphylococcus aureus compared to compared to standard-HA coating. Furthermore, the biocompatibility of this gentamicin coating was investigated.

MATERIALS AND METHODS

Staphylococcus aureus with a dose of 10^7 CFUs was inoculated into the intramedullary canal of the tibia of 30 rabbits followed by the implantation of standard hydroxyapatite (HA) K-wires, K-wires coated with a HA--gentamicin combination, and K-wires coated with a HA-RGD-gentamicin combination, respectively. The animals were sacrificed after 28 days and clinical, histological and microbiological assessment on the bone and on the removed K-wire itself by agar plating and DNA-pulse field gel electrophoresis were carried out to detect infection. Infection was defined as positive culture growth from the bone and/or cement samples.
In another study with 40 rabbits biocompatibility of the two gentamicin-coating types was assessed after an implantation time of 12 weeks and compared to pure HA-coating and uncoated implants.

RESULTS

Infection rates were 88% (7 of 8 animals) for the standard HA, 0% (0 of 9 animals) for the HA-gentamicin and 0% (0 of 10 animals) for the HA-RGD-gentamicin group. There was a statistically highly significant reduction of infection rates by both gentamicin-coating types compared to standard HA-coating ($p < 0.001$). The animals that were identified to have positive culture growth corresponded to the animals that showed clinical signs of infection. An excellent correlation between agar plating testing results of the K-wires and of the bone samples was found. Detailed histology showed cortical lysis, abcess and sequester formation in the infected animals (Fig. 1). There were no major differences in the biocompatibility between the different groups. There were only a few giant cells and regions of bone marrow necrosis in the gentamicin-groups which was comparable to the control implants. There was a very similar histologic appearance of the gentamicin coatings and the standard HA coating.

CONCLUSION

Both gentamicin-coating types showed significant improvement of infection prophylaxis compared to standard HA coating. Furthermore, both gentamicin coating types revealed good biocompatibility after 12 weeks. Therefore, HA-gentamicin and HA-RGD-gentamicin coatings could help to reduce infection rates in cementless arthroplasty in all day clinical use.

AFFILIATIONS

(+)* Volker Alt, Department of Trauma Surgery, University Hospital Giessen, 35385 Giessen, Germany.
** Biomet Deutschland, Berlin, Germany
*** Laboratory of Experimental Trauma Surgery, University Hospital Giessen, Giessen, Germany
**** Institute of Medical Microbiology, University Hospital Giessen, Giessen, Germany

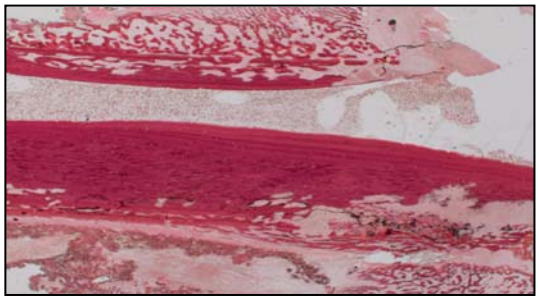

Fig. 1: *All infected animals in the standard HA-coating group showed clear histological signs of infection. Diffuse cortical lysis, reactive subperiostal new bone formation, and beginning sequester formation can be seen.*

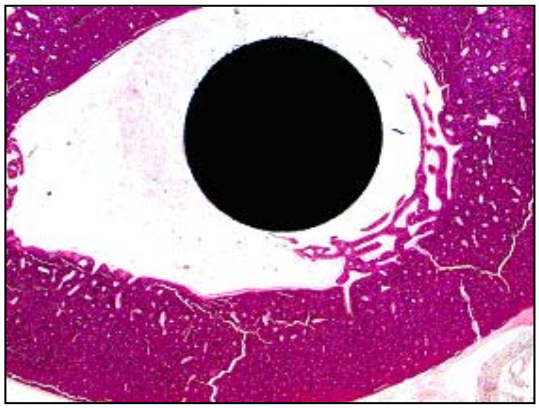

Fig. 2: *New bone formation towards the RGD-gentamicin-HA coated implant with good biocompatibility.*

BACTERIAL ADHESION ON SURGICAL MATERIALS: EFFECT OF NEW SURFACE COATING ON ADHERENCE OF S. AUREUS

*Kinnari TJ, *Esteban J, *Zamora N, **Lappalainen R, ***Konttinen Y, ****Gomez-Barrena E
*Department of Clinical Microbiology, Fundación Jiménez Díaz-UTE. Universidad Autónoma de Madrid, Spain

teemu.j.kinnari@helsinki.fi

INTRODUCTION

Bacterial adhesion on implant surface is a major reason for implant sequelae and can eventually lead to implant removal. Recently some novel non-stick and hard coating materials has been introduced to prevent nosocomial implant infections. In this study we examined the in vitro adherence of *Staphylococcus aureus* on several well established biomaterials such as titanium and silica, as well as a novel biomaterial: high purity diamond like carbon (DLC).

METHODS

A *S. aureus* strain isolated from a prosthetic joint infection was used in the following experiment. The bacteria on plates were collected and suspended in PBS to yield the final concentration of 1 x 10^8 CFU/ml (0.5 McFarland optical density), as confirmed by plate counts. Materials were incubated during 90 min with the previously described solution, washed 3 times with sterile PBS, and stained with Acridine Orange fluorescent stain. Stained materials were subsequently examined with a fluorescence microscope, and 10 oil fields were photographed for each material. Photographs were analyzed using the Image J software, and the percentage of surface covered with bacteria was recorded for each photograph.

RESULTS

The median percentage of surface coated by bacteria was 0.66% (sd 0.4%) for silica, 0.82% (sd 0.5%) for titanium, and 0.96% (sd 0.5%) for diamond (Fig.1). No significant differences appeared between the materials. Although bacteria in the suspension show different adhesion characteristics to the novel DLC material than to the more traditional ones, no significant reduction in bacterial adhesion was found.
Photographs showed bacteria clustered in groups of several units, so each CFU represents in fact a group of more than 3-5 bacterial units.

DISCUSSION

The results show that biomaterial contamination depends not only on the biomaterial, but also on specific bacterial properties. In limited cases use of correct material can lead to inhibition in bacterial contamination and infection of the implants in vivo.

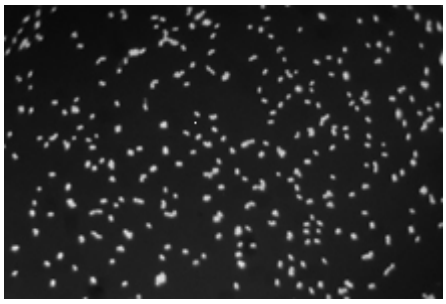

Figure 1: *S. aureus* on diamond-coated surface.

Because bacterial adherence is dependent both on properties of biomaterial and bacterial species, reduction of biomaterial related infections is possible by combining the present knowledge on bacterial adhesion on biomaterials and the knowledge on bacterial species found in the surgical area where the material is supposed to be used.

REFERENCES

Kinnari TJ, Peltonen L, Kuusela P, Kivilahti J, Könönen M, Jero J. Bacterial adherence to titanium surface coated with human serum albumin. *Otol Neurotol*. 2005 May;26(3):380-4.

ACKNOWLEDGEMENTS: T.J. Kinnari was funded by a grant from the Academy of Finland. N. Zamora was funded by a grant from the Fundación Conchita Rábago de Jiménez Díaz (Madrid, Spain). The work was supported by a grant from the Comunidad de Madrid (Spain), PI:

AFFILIATED INSTITUTIONS FOR CO-AUTHORS:
** Department of Applied Physics, University of Kuopio, Finland, ***Biomedicum, University of Helsinki, Finland and ****Department of Traumatology and Orthopedic Surgery, Fundación Jiménez Díaz-UTE, Universidad Autónoma de Madrid, Spain.

ANATOMICAL COMPARISON OF PORCINE AND HUMAN THORACOLUMBAR VERTEBRAE

*Dath R, *Porter KM, **Miles AW
University Hospital Birmigham NHS Trust, Birmingham, UK

roshandath@hotmail.com

INTRODUCTION

With the development of new implants there is an increasing need for biomechanical studies. The problem of obtaining human specimen is well appreciated. Porcine spines are commonly used in Orthopaedic research. A detailed knowledge of the anatomical similarities and differences between porcine and human vertebrae is lacking at this time. The objective of this study is to provide a comprehensive database of measurements for the porcine thoracolumbar vertebrae with a view to help plan future studies contemplating their use.

MATERIALS AND METHODS

6 adult porcine spines from 18-24 month old male pigs weighing 60 to 80 kilograms were obtained and dissected of soft tissue. The lowest thoracic and all the lumbar vertebrae were used in our experiment (n=42). 15 anatomical parameters (Table 1) from each vertebra were measured by 2 independent observers using digital calipers (Draper® PVC150D, accuracy ± 0.03mm). An average of 6 readings per parameter by the 2 observers was used to calculate the statistics. The mean, SD and SEM were calculated using Microsoft Excel. Results were compared with available data on human vertebra (Panjabi et al 1991,1992; Zindrick et al 1987; Kumar et al 2000).

Dimension		Abbreviation
Whole vertebra	Height	WVh
	Width	WVw
Vertebral body	Ventral body	VBv
	Dorsal body	VBd
	Endplate depth upper	EPdu
	Endplate width upper	EPwu
	Endplate depth lower	EPdl
	Endplate width lower	EPwl
Pedicle	Height	PDh
	Width	PDw
Spinal canal	Length	SCl
	Width	SCw
Spinous process	Length	SPl
	Width	SPw
Transverse process	Width	TPw

Table 1 showing the parameters measured

RESULTS AND DISCUSSION

The inter class correlation coefficient for the observers was 0.997. The intra-observer agreement was statistically robust (0.994). The vertebral body height of the porcine vertebra were larger while both the upper and lower endplate depth

and width were smaller than the human specimens. The pedicle width and depth was greater than the human specimen (*Figure 1)*. The spinal canal length and depth of the porcine spine were smaller than humans indicating a narrow spinal canal. The spinous process length showed an increase from T16 to L1. This was in contrast to human spinous process. The results for all the measured parameters and their comparison to human specimen will be presented.

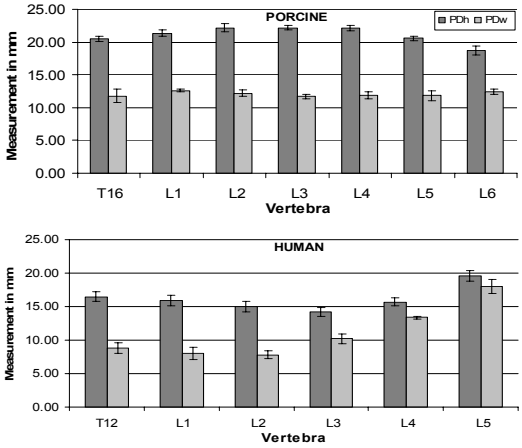

Figure 1 showing pedicle measurements for porcine and human specimen. Error bars show SEM

CONCLUSION

The result from our study provides a database of anatomical measurements for the porcine thoracolumbar vertebrae and highlights their differences with the human specimen. Biomechanical studies involving interbody cages, disc replacements and pedicle screw systems should take into account the differences and match implant size accordingly. The data would beneficial to help design future studies contemplating the use of pig spines. It also provides valuable information for geometric and Finite Element Modelling of the porcine spine. Further results form this study would help in extrapolation of data from experiments which have used the porcine model.

ACKNOWLEDGEMENTS

We would like to thank Mr Julian Cooper, Consultant Orthopaedic Surgeon, University Hospital Birmigham NHS Trust, Birmingham, UK for his help and advise with statistics.

AFFILIATIONS FOR CO AUTHORS

*University Hospital Birmigham NHS Trust, Birmingham, UK**Centre for Orthopaedic Biomechanics, Bath Univeristy, Bath, UK

ADHESIVE FORCES SIGNIFICANTLY AFFECT NANOINDENTATION OF SOFT POLYMERIC MATERIALS

*Gupta S, **Carrillo F, *Li C, *,***Pruitt LA, ***Puttlitz C
*University of California, Berkeley, USA
shikha@berkeley.edu

INTRODUCTION There is a growing interest in nanoindentation of soft biomaterials and tissues. The advantage of nanomechanical testing is its ability to measure localized properties *in–situ*. Thus, the technique can help elucidate the mechanobiology of clinically relevant orthopaedic processes, leading to a better overall biomechanical understanding of the tissues. Though traditionally used to study elastic-plastic materials[1], there have been some preliminary nanoindentation studies on soft, hydrated tissues. However, this technique has not been validated for measuring the properties of soft tissues, and requires further investigation.

Traditional indentation analyses are based on the Hertz contact model. The elastic modulus of the substrate can be obtained from indentation load-displacement curves as follows:

$$E_H = \sqrt{\frac{S^3(1-\nu^2)^2}{6RP}} \qquad \text{(Eq. 1)}$$

where E_H is the elastic modulus of the substrate, ν is the Poisson's ratio of the substrate, R is the nominal radius of curvature, the P is the applied load, and S is the material stiffness ($S=dP/dh$) at P. The classic Hertz's model does not take adhesive interactions into account. The Johnson, Kendall, Roberts (JKR) model, which accounts for interfacial forces outside the Hertz contact , is the most applicable adhesion model for compliant materials. According to the JKR model:

$$E_{JKR}=\sqrt{\frac{S^3(1-\nu_s^2)^2}{6R}}\cdot\left[\left(\frac{2}{3\sqrt{1+\frac{P}{F_{po}}}}+1\right)^3\frac{1}{P+2F_{po}+2F_{po}\sqrt{\left(1+\frac{P}{F_{po}}\right)}}\right] \qquad \text{(Eq.2)}$$

where F_{po} is the adhesive pull-off force at the tip-sample interface. Since adhesive interactions may play a significant role in nanoscale contact mechanics, the following study further elucidates the effects of adhesion forces on the elastic modulus of polydimethylsiloxane (PDMS), a soft elastomeric biomaterial.[7]

METHODS 15 samples were prepared by mixing five different ratios (10-30:1) of a siloxane monomer with a crosslinking agent (Sylgard Elastomer 184, Dow Corning Corporation, Midland, MI, USA). Nanoindentation measurements were performed on 2 mm x 2mm x 5mm squares using a Hysitron TriboIndenter (Hysitron Inc., Minneapolis, MN). 5- 20 µN peak loads were applied to each sample using a 100 µm radius diamond conospherical tip. A trapezoidal loading profile was selected with loading/unloading rate of 1 µN/s and hold time of 20 sec. at the peak load. Multiple indents were performed at each load for all PDMS crosslink concentrations. Material stiffness ($S=dP/dh$) was evaluated at the peak load from the initial unloading portion of the load-displacement (L-D) curve. Pull-off forces (F_{po}) between the diamond conospherical tip and PDMS substrates, as measured by Carrillo et al.,[4] were then used to calculate elastic moduli from L-D using both the Hertz and JKR models. Statistical analyses were performed using Fisher's least significant difference PLSD post hoc test for multiple comparison (Statview, SAS Institute Inc., NC, USA). In all cases, p-values less than 0.05 were considered significant.

RESULTS The L-D curves for all PDMS concentrations are nearly linear for the range of loads tested. Thus, there are no significant differences in the unloading stiffness at different loads for a single PDMS concentration. However, stiffness values between different PDMS concentrations for the same applied load are significantly different. As expected, samples with higher monomer to crosslinker ratios are more compliant.

The Hertz elastic moduli (E_H) (Fig. 1a) exhibit substantial variations with both applied load and PDMS concentration. For all PDMS samples there are significant differences in E_H between all four applied loads for a single PDMS concentration and between concentrations at a given applied load. Previously[2] calculated values for F_{po} varied from 93.1 ± 6.8 µN (for PDMS 10-1) to 43.6 ± 3.6 µN (for PDMS 30-1). Taking these adhesive forces into account, the elastic moduli calculated according to JKR theory (E_{JKR}) are nearly equivalent for different applied loads for each PDMS concentration (Fig. 1b), though the values are lower than the corresponding E_H. The significant differences in modulus with PDMS crosslink concentration are maintained for E_{JKR}.

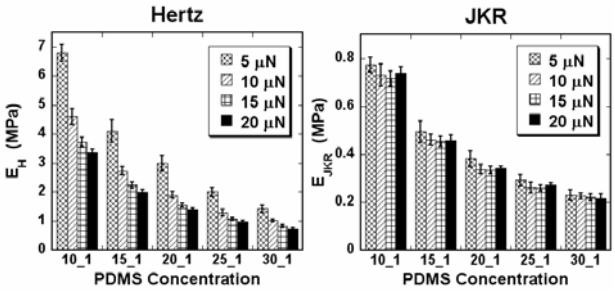

Figure 1. *Elastic modulus calculated from the (a) Hertz model and (b) JKR model*

DISCUSSION For small deformations, the elastic modulus should be constant for a range of nanoindentation loading conditions. According to the Hertz's model, for a linear elastic material, a constant value for E_H is obtained only when the material stiffness is proportional to the applied load: $S \sim P^{1/3}$. In the present experiments, S is independent of P. According to Eq. 1, E_H is then proportional to $P^{-1/2}$, rendering the calculated E_H a stress dependent quantity.

For the JKR model (Eq. 2), a constant stiffness leads to a nonlinear dependence of E_{JKR} upon P. For the PDMS concentrations tested, F_{po} may be anywhere from 2 to 20 times the applied load P. In this case, E_{JKR} is simply a function of F_{po}. Thus, E_{JKR} is also nearly independent of P, with the absolute value determined from S and F_{po}.

The preceding work demonstrates that including adhesive forces in the analysis of the nanoindentation reconciles the differences in E_H observed at the different applied loads and shows that consideration of the adhesion energy at the tip-sample interface is requisite for determining accurate elastic moduli of soft biomaterials from nanoindentation experiments.

**University of California, San Francisco, CA USA
*** Colorado State University, Fort Collins, CO USA

REFERENCES 1. WC Oliver et al. *J Mat Res*, **7**, 1564 (1992). 2. F Carrillo et al. *J. Mat Res* **20**, 2820 (2005)

INCREASING THE CRYSTALLINITY OF CROSSLINKED UHMWPE

*Bistolfi A, *Turell ME, **Thornhill TS, *Bellare A
Department of Orthopaedic Surgery, Brigham & Women's Hospital, Harvard Medical School, Boston, MA

alebistolfi@tiscali.it

INTRODUCTION: Wear of ultra high molecular weight polyethylene (PE) components of joint replacement prostheses has been a major concern for several decades [1]. Laboratory wear tests have shown that radiation crosslinked PE (XPE) have a very high resistance to wear, and they are currently in clinical use in total hip replacements [2, 3]. However, reports that have shown that XPEs have lower mechanical properties compared to uncrosslinked PE [4], especially resistance to fatigue crack propagation [5]. In this study, we used high-pressure processing to increase the crystallinity of PE and XPE and evaluated their wear resistance. We hypothesized that crystallinity, which is known to increase fatigue life, would not affect wear behavior. The results showed that high crystallinity did not change the wear resistance of XPE but that of PE decreased slightly.

MATERIALS AND METHODS: Ram-extruded rod stock of GUR 1050 PE was purchased from PolyHi Solidur (Fort Wayne, IN) and irradiated to a dose of 50 kGy or 100 kGy (Steris Inc, Northboro, MA), melt annealed at 170°C for four hours, and cooled to ambient temperature. The bars was heated to 160°C or 240°C, pressurized to 500 MPa for an hour, slow cooled to room temperature and removed from the high-pressure cell after releasing the pressure. A Perkin Elmer Pyris differential scanning calorimeter (DSC) was used to measure the degree of crystallinity, x, for all groups, using a heat of fusion of 293 J/g. Thereafter, pins of 25mm length and 9.5mm diameter were machined from PE with a crystallinity of 50.2% (PE) and 70.9% (HP-PE) and from 50 kGy XPE with a crystallinity of 46.2% (X-linked-PE) and 67.5% (HP-X-linked-PE) and wear tests were performed using an OrthoPod^{TM} (AMTI Inc, Watertown, MA) multidirectional wear tester operating at a frequency of 1 Hz and a constant applied load of 192 N. The pins articulated along a 5x5mm square path on a smooth, implant grade, smooth (Ra=0.015μm) cobalt-chromium disk for 1-2 million cycles, depending on the wear rate of the materials. The tests were performed in bovine serum (JRH Biosciences); diluted to contain 23 g/l protein, 20 mM EDTA and 0.2% sodium azide, maintained at 37°C.

RESULTS: The high-pressure processes increased the degree of crystallinity of PE and XPE, although for the same process conditions XPEs had a lower crystallinity (Table 1). Crystallinity and melting temperature also increased with crystallization temperature for both PE and XPE. HP-PE wore 1.2 times faster than control PE ($p<0.05$, ANOVA with Fisher's PLSD post-hoc test) are shown in Fig. 1. XPE had a substantially lower wear rate than uncrosslinked, PE. However, no statistically significant difference was observed between the wear rates of XPE and HP-XPE.

DISCUSSION: This study showed that the crystallinity of PE and XPE can be increased using high-pressure crystallization which increased wear rate of PE by 20%, but did not increase the wear rate of XPE. For the same processing conditions, higher irradiation dose resulted in smaller increases in crystallinity. Nevertheless, this study shows that XPEs can have a high crystallinity, which is known increase fatigue crack propagation resistance, without strongly affecting wear resistance.

Tc (°C)	**Tm (°C)**	**Xc (%)**
Rod stock	136.2	57.8
0 kGy ; cont	137.6	53.8
0 kGy ; 160	145.3	76.8
0 kGy ; 240	150.3	81.1
50 kGy ; cont	135.9	52.7
50 kGy ; 160	141.4	63.8
50 kGy ; 240	143.7	67.5
100 kGy ; cont	137.9	52.1
100 kGy ; 160	141.9	63.7
100 kGy ; 240	144.6	66.3

Table 1. Melting temperature (Tm) and crystallinity (Xc) and control PE and 50 and 100 kGy XPEs at crystallization temperature (Tc) of 160°C or 240°C.

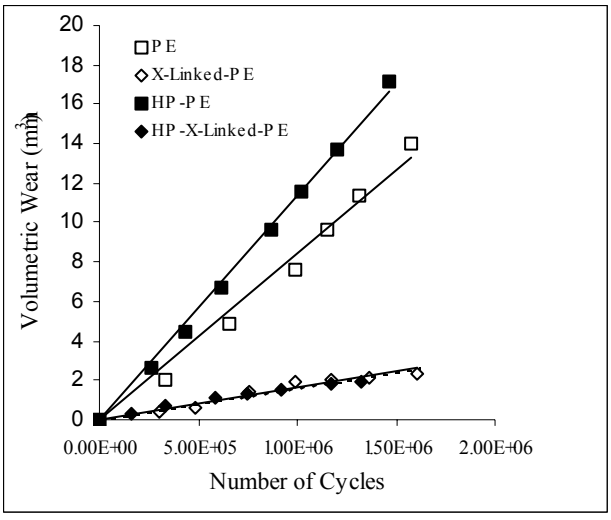

Fig. 1: Volumetric wear of various polyethylenes

REFERENCES: [1]Harris WH, et al. *Clin Orthop Rel Res* 2001;393:66-70 [2] McKellop H, et al. *J Orthop Res*1999;17(2):157-67 [3] Muratoglu O, et al. *Biomat* 1999;29:1463-1470 [4] Gomoll A, et al. *J Orthop Res* 2002; 20:1152-56 [5] Duus LC, et al *Trans ORS* 2000; 25:544

ACKNOWLEDGMENTS: We thank Dr. Aiguo Wang (Stryker Inc) for providing implant grade CoCr disks**.**

OXIDATION IN IRRADIATED UHMWPE WITHOUT ANNEALING

*Bellare A, *D'Angelo F, **Ferretti A, *Thornhill TS
Department of Orthopaedic Surgery, Brigham & Women's Hospital, Harvard Medical School, Boston, MA

anuj@alum.mit.edu

INTRODUCTION: Oxidative degradation of gamma sterilized ultra-high molecular weight polyethylene (PE) in total joint replacement prostheses has been well documented along with its associated detrimental effects on wear, such as delamination in tibial plateaus [1-3] and accelerated particulate wear in acetabular cups [4]. It has been recently shown that the degree of crosslinking and wear resistance decreases with increase in pre-irradiation crystallinity [5]. In this study, we hypothesized that if high dose irradiation is followed by no thermal treatment, there is substantial oxidation, which increases with pre-irradiation crystallinity, i.e. PE can trap more free radicals in the lamellae, which could be slowly released, leading to higher long-term oxidation than low crystallinity PE. A high dose gamma irradiation and accelerated aging was used to verify the hypothesis. The results showed that high crystallinity and crystallization temperature led to high oxidation index (OI) in irradiated PE.

MATERIALS AND METHODS: Ram-extruded rod stock of GUR 1050 PE (Hoechst-Ticona, Bayport, TX) was purchased from PolyHi Solidur (Fort Wayne, IN) and machined into cylinders of 25mm length and 12.5mmm diameter to snugly fit into a custom-built high-pressure cell. A Carver hydraulic press was used to apply a pressure of 500 MPa to PE specimens preheated to 160°C, 180°C, 200°C, 220°C, 240°C and 260°C, slow cooled to room temperature followed by pressure release. The PE cylinders and untreated control PE were subjected to 50kGy gamma radiation (Steris Inc, Northborough, MA), which is a dose sufficient for a high degree of crosslinking in PE. Thermal treatment was not performed so that the free radical population in the PE was preserved. A Parr bomb reactor filled with oxygen gas and operating at 5atm pressure and 70°C temperature was used to oxidize PE for a period of 14 days, according to ASTM standard F2003-02. Fourier Transform Infrared (FTIR) Spectroscopy was performed using a Nicolet Magna 860 spectrometer on thin sections of PE of 100-200μm thickness (n=6), prepared using a Leitz Wetzlar sledge microtome. An IR beam diameter of 100μm was used. The oxidation index, OI, was defined to be the ratio of the area under 1740cm^{-1} carbonyl and 1370 cm^{-1} methylene stretching absorbances. A Q1000 (TA instruments, New Castle, DE) differential scanning calorimeter (DSC) was used to measure the degree of crystallinity (n=3). Percentage crystallinity was obtained as $Xc = 100*\delta H/\delta H_f$, where δH is the area under the endotherm and δH_f is the heat of fusion of PE (293 J/g).

RESULTS: FTIR experiments showed that the bomb aged 50 kGy irradiated PE had a substantially higher OI compared to air aged PE at all subsurface depths, with the maximum OI just below the surface. The bomb aged 50 kGy PE had a maximum OI of 1.68 ± 0.13 compared to 0.29 ± 0.09 for control PE. The DSC experiments showed that there was a substantial increase in crystallinity to approximately 70% for crystallization temperatures in the range of 180-220°C and an applied pressure of 500 MPa with no statistically significant differences in crystallinity among the various PE samples ($p>0.05$, ANOVA). FTIR revealed that the maximum OI, present at the surface, generally increased with increase in crystallization temperature and the differences in maximum OIs were statistically significant for all PEs except for the group of irradiated PEs crystallized at 200, 220 and 240°C (Fig 1).

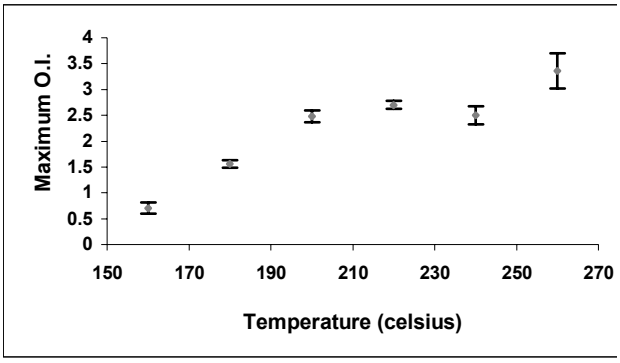

Figure 1. Plot of Maximum oxidation index versus temperature of high-pressure crystallization

DISCUSSION: This study showed, using an aggressive accelerated aging test, that the pre-irradiation crystallinity and temperature of crystallization at 500MPa pressure affect the oxidation resistance of irradiated PE. A comparison of the maximum OI of control PE, 160°C/500MPa PE and 180-260°C/500MPa PEs showed that the maximum OI generally increases with crystallinity. This study is in agreement with a recent study [5], which demonstrated that higher pre-irradiation crystallinity was associated with lower crosslinking and higher wear. A limitation of the study is that the accelerated oxidation protocols do not accurately mimic real time shelf or in vivo aging. It must be specified that all high dose gamma irradiated PEs in clinical use are heat treated to decrease free radical concentration and to improve resistance to oxidation.

REFERENCES: [1] Premnath V et al, Biomat, 1996 17(18):1741-53 [2] Costa L et al. In: UHMWPE for Arthroplasty, Edizioni Minerva Medica 2000 Torino [3] Sutula LC et al Clin Orthop 1995 319: 28-40 [4] Besong AA et al, JBJS-Br 1998. 80(2): 340-4 [5] Greer KW et al, Trans ORS 2004, p243.

**Sant'Andrea Hospital, Università di Roma La Sapienza, Rome, Italy

MATRIX METALLOPROTEINASE-9 IN A SMALL ANIMAL MODEL OF WEAR-DEBRIS INDUCED OSTEOLYSIS

*Ibrahim T, **Ong SM, ***Taylor GJS
University of Leicester, Leicester, United Kingdom

ti11@le.ac.uk

INTRODUCTION

Extracellular matrix degradation and periprosthetic connective tissue remodelling around implants have been regarded as major biologic events in the loosening of total hip prostheses. The contribution of matrix metalloproteinases (MMPs) and their inhibitors is also thought to be important in this process The aim of this study was to demonstrate the presence of MMP-9 in an animal model of wear debris induced osteolysis and whether there was a quantitative change in its presence over time.

MATERIALS AND METHODS

Two sets of animals were used in this study. The first set of animals consisted of 8 mice all from the same litter. The animals were equally randomly allocated to either implantation of ceramic particles into their femora or undergoing sham surgery with injection of hylarounic acid. The other femur was used as control and did not undergo any surgical procedure. The second set of animals consisted of 6 mice all from the same litter. The animals were equally randomly allocated to either implantation of ceramic particles into their femora or undergoing sham surgery with injection of hylarounic acid. The other femur was used as control and did not undergo any surgical procedure. The mice were killed at 4 and 10 weeks respectively.

The immunohistochemistry staining was adapted from Lunsuwanont *et al* (2002) and the same procedure was used for MMP-9. Each set of femora slides were stained with two negative and two positive controls using the breast lobular carcinoma tissue to confirm that the immunohistochemistry staining was working properly.

Several sections from each femora were taken. Tissue sections were analysed using light microscopy to determine the histological staining of MMP-9. Two independent reviewers examined all slides. The femora were quantitatively graded for the amount of MMP-9 staining by examining macrophage and osteoclasts. The cells were identified by looking at cell size and cytoplasmic colour. The amount of staining per slide was calculated by counting the number of macrophages and osteoclasts stained on the slide by the total number of macrophages and osteoclasts on the negative control slide.

All animal procedures undertaken were approved by the Home Office conforming to the laws and regulations of the United Kingdom.

RESULTS

Comparing the staining of MMP-9 between the femora that underwent implantation of particles and those that underwent sham surgery at 4 weeks showed a statistical difference ($p=0.001$). The results show more staining of MMP-9 with the implantation of ceramic particles compared to sham surgery at 4 weeks.

Comparing the staining of MMP-9 between the femora that underwent implantation of particles and those that underwent sham surgery at 10 weeks showed a no statistical difference ($p=0.091$). The results show slightly more staining of MMP-9 with the implantation of ceramic particles compared to sham surgery at 10 weeks.

Despite the unfavourable above results, comparison of all three groups at week 4 and 10 did show statistical significance ($p=0.001$).

To quantify an increase in MMP-9 staining with the implantation of ceramic particles between week 4 and 10, a comparison was made. Results failed to show any statistically difference in the amount of MMP-9 staining ($p=0.188$). We were also unable to show a difference in the staining of MMP-9 between week 4 and 10 even with the sham surgery group ($p=0.5$).

DISCUSSION

We were able to demonstrate positive staining for MMP-9 in the femora that underwent implantation of ceramic particles. There was also a statistically significant difference between the staining of MMP-9 of femora that had implantation of ceramic particles and sham surgery.

To our surprise, we were not able to demonstrate an increase in the staining of MMP-9 at 10 weeks. One possible reason for the decreased staining of MMP-9 is the production of tissue inhibitor metalloproteinase (TIMP). TIMP inhibit the activities of MMP. The activity of MMPs is regulated by the balance between MMPs and their inhibitors. This balance has a key role in normal connective-tissue remodelling, and therefore, MMP release, activation and inhibition are usually tightly regulated. The relative balance between MMP and TIMP must ultimately determine the fate of extracellular matrix.

AFFILIATED INSTITUTIONS FOR CO-AUTHORS:
** Queen's Medical Centre, Nottingham, United Kingdom
***University Hospitals of Leicester, Leicester, United Kingdom

IS HIGHFLEX TKA EFFECTIVE AT HIGHER FLEXION ANGLES AND DOES IT MAINTAIN THE GOOD MECHANICAL PERFORMANCE OF STANDARD TKA AT NORMAL FLEXION ANGLES?

*Barink M, *De Waal Malefijt M, *Van Kampen A, *Verdonschot N
*Radboud University Nijmegen Medical Centre, Orthopaedic Research Lab.,Nijmegen, The Netherlands
m.barink@orthop.umcn.nl

INTRODUCTION

There is a growing demand for high flexion Total Knee Arthroplasty (TKA). Currently, patients experience limitations in activities like squatting, kneeling and gardening because of their knee replacement and there is an increasing demand for high flexion in Asian countries because of cultural and religious reasons. However, it is questionable whether highflex TKA maintains the good mechanical performance of conventional TKA's.
The first question in this study was whether the adapted highflex Sigma RP-F design is effective within the higher flexion range (>120º) as compared to the conventional Sigma RP design. The second question was whether the good mechanical performance of the conventional Sigma RP within the normal flexion range (<120º) is maintained with this highflex Sigma RP-F design.

METHODS

The Sigma RP is a rotating platform knee prosthesis which is designed for flexion angles up to 120º. In this study the posterior stabilized option was used. Two identical dynamic finite element models of the knee joint were created: one for each TKA design. The patella was not resurfaced. The femur and femoral component were modelled as rigid bodies. All other components were modelled as deformable bodies (fig. 1). Elasto-plastic material properties were used to model the polyethylene (Kurtz, 1998). The insert was divided into two areas: the dish and the post. The Von Mises stress and the volume of the dish and the post loaded above the yield stress (yield volume) were calculated during a dynamic simulation of squatting (fig. 2).

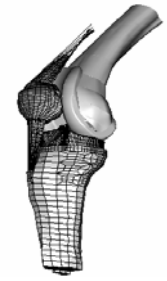

figure 1: FE model

figure 2: squatting range of dynamic simulations

The tibia was loaded at ankle level with a ground reaction force of 350N (simulating a person of about 71 kg). Actuator elements were attached to the proximal side of the quadriceps tendon. During the simulations, the length of these actuator elements was increased with time to obtain a squatting movement. The proximal end of these actuator elements was constrained.

RESULTS

The highflex Sigma RP-F showed an improved performance within the high flexion range as compared to the conventional Sigma RP. The Sigma RP-F produced a smaller yield volume for the dish within the high flexion range (fig. 3). Furthermore, it showed a lower maximum yield volume for the post, which occurred also at a higher flexion angle as compared to the Sigma RP.
Both TKA designs showed a very comparable performance within the normal flexion range. The yield volumes for the dish and the post were very similar for the Sigma RP and Sigma RP-F up to 120º of flexion.
All yield volumes reached the maximum value at the high flexion range, for which highflex TKA is designed.

figure 3 insert yield volumes

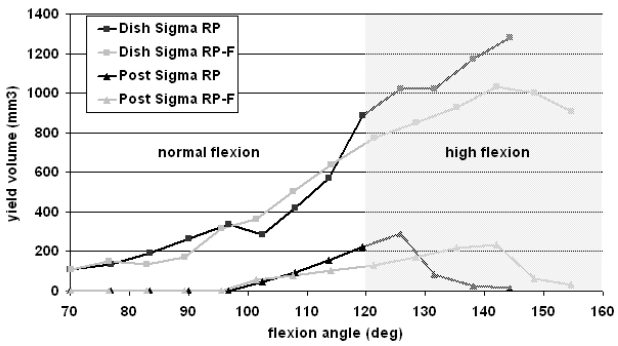

DISCUSSION

Higher yield volumes mean that there is more plastic deformation, which suggests a higher risk of failure.
The yield volumes for the post, for both designs, decrease suddenly after the maximum value. In case of the Sigma RP, the sharp edges of the posterior condyles start to dig into the dish, which releases post-cam contact. In case of the Sigma RP-F, the decrease is caused by a more optimal post-cam contact (high conformity and distal contact location).
The results confirmed that the Sigma RP-F is more suitable for high flexion as compared to the Sigma RP. Furthermore, the highflex design features do not have adverse effects for the performance within the normal flexion range, as compared to the Sigma RP.
However, due to the higher loads involved at high flexion squatting activities, the highflex design features could not prevent that the yield volumes all reached a maximum within the high flexion range; the range where only the Sigma RP-F is intended to function. Hence, the implant safety factor reduces in high flexion.

REFERENCES: Kurtz SM, J. Biomech, 1998 (31), 431
ACKNOWLEDGEMENT: DePuy Orthopaedics

IN VITRO PATELLAR TRACKING DURING NAVIGATED TOTAL KNEE REPLACEMENT

*Belvedere C, *Leardini A, **Ensini A, ***Moctezuma de la Barrera JL, **Catani F, **Giannini S
*Movement Analysis Laboratory, Istituti Ortopedici Rizzoli, Bologna, Italy

belvedere@ior.it

INTRODUCTION:

Patellar maltracking results in patello-femoral (PF) joint disorders and frequently in failure of total knee replacement (TKR) [1]. Prosthesis component misalignments in both tibio-femoral (TF) and PF joint are generally considered the main causes of this maltracking. Several techniques have reported this tracking post-operatively, but to support the surgeon in positioning the prosthesis components according to normal tracks intra-operative systems should be developed. Surgical navigation can be enhanced in this direction, but no standard anatomical and articular conventions are available to track PF joint kinematics. The aim of this study was to test a new technique in-vitro for 3D anatomical-based PF tracking in navigated TKR.

METHODS:

Five fresh frozen amputated legs with the knee free from anatomical defects and with intact joint capsule and quadriceps tendon were analyzed using the Stryker® Knee Navigation System (Kalamazoo, MI-USA). Clusters with active markers were pinned on the femur and tibia. A special prototypal cluster was pined on the patella. The standard pointer was used for system control and landmark digitations. Series of five trials of manually driven knee flexions were performed under condition of 10 kg on the quadriceps, with intact knee and after TKR with patellar resurfacing. Anatomical landmark digitation was used to define anatomical frames for femur and tibia according to recommended definitions [2]. Patellar apex and medial and lateral prominences were used to define a patellar anatomical frame with origin in the prominence mid point, antero-posterior axis as normal to the plane for the landmarks, proximo-distal axis along the vector from the apex to the origin, medio-lateral axis as normal to the previous two axes. TF flex-extension, intra-extra rotation and ad-abduction were calculated according to a standard mechanical convention [3]. PF flex-extension, medial-lateral tilt and rotation were calculated according to a previous proposal [4]. Patellar shift was measured as the translation of patellar origin along medio-lateral femoral axis. Standard deviation and mean values were calculated at each degree of TF flexion for each group of trials.

RESULT:

The light prototypal cluster with a proper design allowed successful digitations and movement registration also for the patella. An intra-specimen repeatable path of motion over repetitions and a coupled path of motion throughout the flex-extension cycle were observed in intact knees, both at TF and at PF joints. PF rotations and shift had a mean standard deviation over TF flexion of respectively less than 1.1° and 1.0 mm over the five knees. In the following figure, PF joint motion is reported before and after TKA in a single well representative knee: restoration of original natural motion was not fully achieved, particularly for the shift.

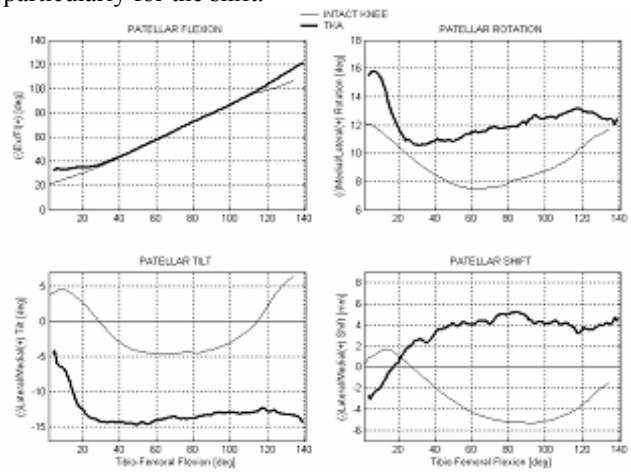

DISCUSSION:

These results revealed the feasibility and relevance of patellar tracking in navigated TKR. PF joint kinematics is fundamental in the overall comprehension of TKR performance since it reflects prosthesis component alignment and soft tissue tensioning. By monitoring intra-operatively also the PF kinematics, the surgeon has a more complete prediction of the kinematics of the final TKR and therefore a valuable support for the most critical surgical decisions. An abnormal patellar shift at the replaced knee can be in the future corrected intra-operatively by more cautious preparation of the femoral and tibial bones, positioning of the relevant components, and also, appropriate arrangements for patellar resurfacing.

REFERENCES:

1. Scuderi GR et al., 1994. J Am Acad Orthop Surg.
2. Cappozzo A et al., 1995. Clin Biomech 10, 171-178.
3. Grood ES, Suntay WJ, 1983. J Biomech Eng.
4. Bull AM et al., 2002. Knee Surg Sports Traum Arth.

AFFILIATED INSTITUTIONS FOR CO-AUTHORS:

**Department of Orthopedic Surgery, Istituti Ortopedici Rizzoli, Bologna, Italy
***Stryker® Leibinger GmbH & Co. KG, Freiburg, Germany

FUNCTIONAL EVALUATION OF THE PFC AND CKS KNEE SYSTEM

*Boonstra M, *Eenhuizen C, *Schimmel J, *De WaalMalefijt M, *Verdonschot N
*Orthopaedic Research Laboratory, Radboud University Nijmegen Medical Centre, Nijmegen, The Netherlands
m.boonstra@orthop.umcn.nl

ABSTRACT
Orthopaedic surgeons can choose between a wide variety of prostheses. In our clinic, the Continuum knee system (CKS, Biomed) total knee arthroplasty (TKA) was replaced by the press-fit condylar sigma knee system (PFC, DePuy) based on intuitive judgments of the surgeons. However, there were no objective data to confirm the functional difference between both TKA types. In this study, we used functional tests to assess the differences in function.

METHODS
A total of 26 subjects were included in this study: 15 with a PFC (age=62.2±10.3 years) and 11 with a CKS-prosthesis (68.6±10.0). A control group of 15 healthy subjects (70.1±5.5) was selected according to matching age. The patients were on average 17.6 ±5.6 (PFC) and 23.0±5.2 (CKS) months post-operative. The implanted TKA prostheses were all of the posterior cruciate retaining type.
All subjects were administered the WOMAC, IKS and SF36 questionnaires. The sit-to-stand (STS) movement was used as functional test. Using bi-axial accelerometers and gyroscopes, upper body and knee angles (a_{upper}, a_{knee}) and velocities (v_{upper}, v_{knee}) were measured [1]. Vertical peak forces (F_{peak}) during rising were measured for each leg, using two force plates and were normalized for body weight. Asymmetry was calculated as the difference in maximum peak force between sound and TKA leg. The time to rise (T_{rise}) was calculated as the time between start and end of STS movement. The subjects had to rise 10 times from a low chair (90º knee flexion), with a short resting period in between (see fig 1).
The two patients groups also performed maximal isometric contraction (MIC) in flexion and extension [2] (fig 1) and the timed up and go test (TUG). The TUG is measured by the time necessary to rise, walk 3 meters, turn, walk back and sit down [3].
For the questionnaires and STS, one-way ANOVA combined with Tukey test was applied to find differences between the control, PFC and CKS groups ($p<0.05$). An independent t-test was used for comparison of PFC and CKS groups for the MIC and TUG ($p<0.05$).

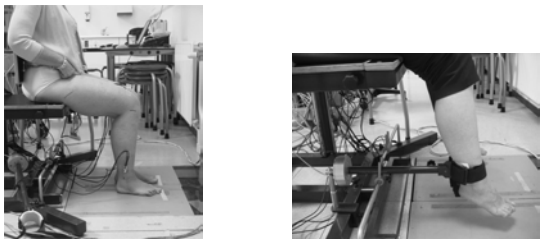

Figure 1: On the left hand side the starting position for STS. On the right hand side the measurement for the MIC.

RESULTS
Questionnaires
The two patient groups differed significantly from the control group for the total SF-36 score. Between the two patient groups only the physical functioning subscale of the SF-36 differed significantly, in favor of the PFC group. For the IKS and WOMAC significant lower scores were found for the CKS group compared to the control group. The CKS group scored significantly lower on the WOMAC physical function subscale and the IKS function subscale compared to the control group.
Sit-to-stand movement
No significant differences were found for maximal knee and upper body angles between the three groups.
The maximal knee angular velocities were 110.0±23.6, 94.65±18.8 and 145.0±14.4 °/sec for PFC, CKS and control respectively. The TKA groups had smaller maximal knee angular velocities than the control group ($p<0.001$) and also the CKS group showed smaller maximal velocities than the PFC group ($p=0.049$), see fig 2a.
The maximal hip angular velocities were 163.6±32.0, 128.9±31.2 and 186.0±36.1 °/sec for PFC, CKS and control respectively. The CKS group had smaller maximal hip angular velocities than the PFC group ($p=0.019$) and control group ($p<0.001$). The maximal hip angular velocity of the PFC group was not different from the control group, see fig 2b.
The average maximal vertical peak forces were 0.623, 0.589 and 0.662 N/kg for PFC, CKS and control groups, respectively. The values for the TKA groups were smaller than for the control group ($p<0.001$). No significant differences were found for the asymmetry in force.
The CKS had a longer T_{rise} compared to control ($p=0.003$) and PFC group ($p=0.005$). The PFC group rose as quickly as the control group. Average rising times were 0.753, 0.906 and 0.750 sec, for PFC, CKS and control group, respectively.
Maximal isometric contractions
For the quadriceps muscles and hamstring muscles no differences were found between the PFC and CKS group for both TKA ($p=0.476$ and $p=0.926$) and sound leg ($p=0.332$ and $p=0.706$). Also, no differences were found between TKA and sound leg (extension: $p=0.077$ for PFC and $p=0.382$ for CKS group, flexion: $p=0.358$ for PFC and $p=0.436$ for CKS group).
Timed up and go
The average time to complete the TUG was 10.82±3.51 sec for the PFC group and 13.06±4.56 sec for the CKS group. No significant differences were found, mainly due to large variations ($p=0.093$).

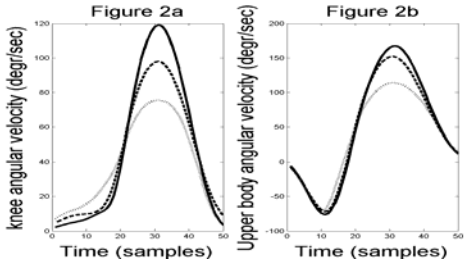

Figure 2: The average knee and upper body angular velocities are shown for PFC (dashed line), CKS (dotted line) and control group (solid line).

DISCUSSION
In this study, we used functional test methods to quantify the functional difference between two patient groups with either a CKS or PFC prosthesis. Of the questionnaires, only the physical functioning subscale of the SF-36 was able to distinguish between the two patient groups, with the CKS patients showing lower scores.
The type of TKA did not affect the muscular strength, as measured with the MIC. However, patients with the CKS rose more slowly than the PFC group and showed smaller maximal knee and upper body angular velocities during the STS. The PFC group rose more similar to the control group, however, their maximal knee angular velocity was still lower. Both patient groups performed the rising movement rather symmetrically according to the measured peak forces.
The TUG appeared not to be sensitive enough to reveal the functional difference between the two TKA types.
In conclusion, the surgeons perception that the PFC outperformed the CKS system was measurable and valid.

REFERENCES
[1] Boonstra et al, J Biomech (39) 2006
[2] Stevens et al, J Orthop Res (21) 2003
[3] Podsialdo et al, J Am Geriatr Sosc (39) 1991

ACKNOWLEDGEMENTS
This study was financially supported by J&J, DePuy

THE INFLUENCE OF CROSS SHEAR ON THE WEAR OF TKE UNDER VARIOUS KINEMATIC CONDITIONS

*Knight LA, **McEwen HMJ, *Jeffers J, **Fisher J, ***Rullkoetter P, *Taylor M
*Bioengineering Sciences Research Group, University of Southampton, Southampton, SO17 1BJ, UK
** Institute of Medical and Biological Engineering, University of Leeds, Leeds, LS2 9JT, UK
*** Department of Engineering, University of Denver, Denver, CO, USA
L.A.Knight@soton.ac.uk

INTRODUCTION: Total Knee Arthroplasties (TKAs) are increasingly implanted into younger and more active patients, placing high kinematic demands on devices that are now expected to last up to and beyond 20 years. It is currently considered that surface wear of the polyethylene-bearing component is a major limiting factor to the longevity of TKAs. The volume of wear generated between two articulating surfaces is proportional to the applied load and the sliding distance. The relative kinematics of the articulating surfaces has also been shown to have a marked effect on the wear volume [1]. This study demonstrates the importance of including cross-shear, a quantification of the relative kinematics, in the computational simulation of TKA wear under various kinematic conditions. Experimental wear simulator results are compared with computational results with and without the inclusion of cross shear.

METHOD: An existing computational model of the PFC Sigma TKA (DePuy) [2] was driven by force/displacement controlled inputs taken from the Leeds simulator [3]. Three analyses for the same knee design were performed for high, intermediate and low kinematics by altering the amount of AP displacement and IE rotation to reflect the variation in patient population [3].

An adaptive remeshing procedure was used to determine the wear volume over 5 million cycles. The computer simulation was run for 1 cycle and then simple wear theory was applied. The wear calculation is taken from work by Maxian et al. [4] and is shown in eqn. 1.

$$H = \sum_{t=0}^{t=n} K_w S p \qquad \textbf{Eqn. 1}$$

where H = wear depth, K_w = wear factor, $3.5\text{x}10^{-6}\text{mm}^3/\text{Nm}$ (dependent on material properties and kinematic conditions), S = sliding distance and p = contact pressure. A sensitivity study was carried out to determine the optimum update interval between wear calculations, which was found to be 1 million cycles.

A measure of the relative kinematics occurring between the articulating surfaces is the cross shear energy. This can be calculated by the eqn. 2 [3]:

$$CS = \left(\sum_{t=0}^{t=n} ML \Big/ \sum_{t=0}^{t=n} AP\right) \qquad \textbf{Eqn. 2}$$

where CS = cross-shear, ML = medial-lateral displacement and AP = anterior-posterior displacement.

A relationship between wear factor and cross shear was derived from simplified wear experiments [5] (eqn. 3) and input into eqn. 1 to include cross shear in the simple wear theory.

$$K_w = 3\times10^{-6}(CS) \qquad \textbf{Eqn. 3}$$

RESULTS: Fig. 1 shows that although the simulation with a constant wear factor predicts a reasonable value for wear volume for the high kinematics model, wear volume for the intermediate and low kinematics models do not correspond with the experimental results. In addition, this computational model does not predict a significant difference between high, intermediate and low kinematics. The computational model that includes cross shear shows good agreement with the experimental results for high, intermediate and low kinematics.

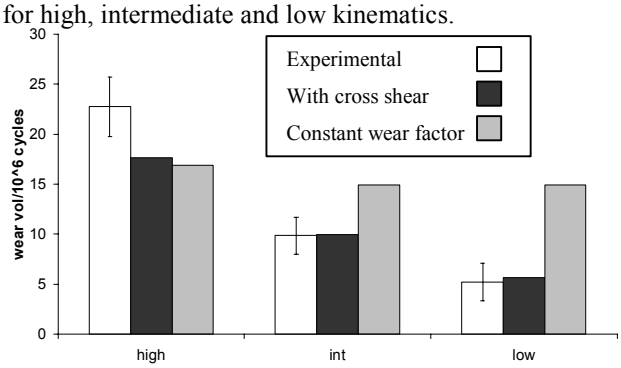

Fig. 1: *Comparison of wear volumes for experiment, and computational simulations with cross shear and with a constant wear factor.*

DISCUSSION: The results have shown that the influence of cross-shear on wear can be simulated using finite element analysis. This study has also outlined the importance of including some factor of cross-shear in computational simulations of wear. If the wear factor is assumed to be constant (i.e. without varying cross-shear), the wear volume is not predicted with changing kinematics. In addition the linear wear distribution on the surface of the tibial component is miscalculated. The computational simulation including cross shear was observed to yield similar wear volumes to the experimental wear simulator for the high, intermediate and low kinematics models. This study suggests that simple wear theory is not sufficient to predict the wear in TKA under various kinematic conditions, and that the cross-shear should be included in simulations for them to be a useful pre-clinical tool.

REFERENCES: **[1]** Fisher, Proc. IMechE, 205(H), p. 73. **[2]** Godest, J. Biomech, 35, p. 267 **[3]** McEwen BORS, 2003 **[4]** Maxian, J. Orthop. Res., 14, p.668. **[5]** Turrell, Wear, 255, p. 1034.

ACKNOWLEDGEMENTS: Funding provided by the ARC.

PRIMARY FIXATION IN A REVISION TOTAL KNEE ARTHROPLASTY MAY NOT IMPLY LONG TERM FIXATION: THE EFFECT OF STEM LENGTH

*Schmidt J, **Henderson A, *Ploeg H, **Deluzio K, ***Dunbar M
*University of Wisconsin-Madison, Madison, USA
jschmidt1@wisc.edu

INTRODUCTION

The Orthopedic Network News reported that 171,335 primary knee and 16,895 revision total knee arthroplasties were performed in 2001 alone [1]. Due to the additional bone loss that accompanies revision surgeries, stemmed implants are used to achieve a well-fixed and stable implant. Yet, evidence-based surgical guidelines for stem selection are not available. Finite element (FE) modeling from computed tomography (CT) data has been previously used to provide a better understanding of bone mechanics when orthopedic implants are inserted [2, 3]. This study combined the results of finite element analysis (FEA) and mechanical testing to investigate the effect stem length has on micromotion between the bone and tibial stem and implant loosening.

METHODS

FE: Models of the left tibia were created from CT data of a composite bone (#3301 Pacific Research Laboratories, Vashon,WA) and the Visible Human Female (United States National Library of Medicine, Bethesda, MD) data sets. Each model was implanted with a 145 and 200 mm revision knee tibial component (Zimmer, Warsaw, IN).

Material	Elastic Modulus (GPa)	Poisson's Ratio
Cortical	7.6	0.3
Cancellous	0.1	0.3
Cement	2.0	0.23
Polyethylene	1.0	0.45
Titanium	110	0.3

Table 1, above
Material properties assigned to FE model of composite and VHF models.

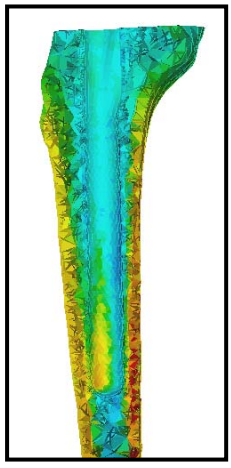

Figure 1, right
Sagittal view of material properties' distribution in bone without implant. Poisson's ratio was 0.3.

The material properties for the composite bone and additional components are shown in **Table 1**. The material properties of the VHF bone were determined from the CT data using previously defined equations [4, 5] and then decimated into 20 distinct groups (**Figure 1**). A total 2 kN load was applied on the two condyle regions with a 60:40 (medial:lateral) distribution. Micromotion was determined as the vector sum of the slip components between the stem and the bone.

Mechanical Testing: Ten composite tibia bones (#3301 Pacific Research Laboratories, Vashon,WA) were implanted with either a 145 mm or 200 mm stem and subjected to a 2 kN sinusodial load with 60:40 (medial:lateral) loading. Displacement of the tibial tray relative to the bone was measured using two LVDTs mounted medially and laterally. Average micromotion (pistoning) was defined as the average of the displacement of the two LVDTs.

RESULTS

The FEA found in both the composite bone and the VHF models, maximum micromotion increased with a longer stem (**Table 2a**). The micromotion in the VHF analysis was significantly lower than the composite bone; however, it was shown that this was dependent on the definition of the material properties. **Table 2b** shows comparable results between the average micromotion 100 mm below the tray (FEA) and pistoning (mechanical testing).

Table 2a FEA results of m*aximum micromotion at bone-stem interface for the composite bone and VHF data sets.*

Bone	Micromotion (145 mm stem)	Micromotion (200 mm stem)
Composite	83 μm	110 μm
VHF	32 μm	42 μm

Table 2b *Average micromotion 100 mm below the tray (FEA) and average displacement of LVDTs (mechanical testing).*

Bone	Micromotion (145 mm stem)	Micromotion (200 mm stem)
Composite (FEA)	73 μm	64 μm
Composite (Mech)	82 μm	74 μm

DISCUSSION

Mechanical testing and FEA in the current study reported decreased pistoning for longer stems, as supported by clinical experience [6]. Yet, FEA results found a higher level of maximum micromotion for a longer stem, which can lead to aseptic loosening [7]. Therefore, a longer stem may increase initial fixation (decrease pistoning), but long term effects due to micromotion may lead to implant loosening.

REFERENCES

1. www.OrthopedicNetworkNews.com. 9/8/03.
2. Cattaneo, PM et al. Proc Inst of Mech Eng, 2001.
3. Keyak, JH, et al in *35th Annual Meeting ORS,* 1989.
4. Hvid, I, et al. J Biomech, 1989.
5. Rho, JY, et al. Med Eng & Phys, 1995.
6. Jazrawi, LM, et al. J. Arthroplasty. 2001.
7. Barker, DS, et al. Proc. IMechE. 2005.

AFFILIATED INSTITUTIONS FOR CO-AUTHORS

** Dalhousie University, Halifax, Canada
*** QEII Health Science Center, Halifax, Canada

A NEW TECHNIQUE TO MAKE 2D WEAR MEASUREMENTS INSENSITIVE TO RADIOGRAPHIC DIFFERENCES OF CEMENTED TOTAL HIP PROSTHESES FROM DEVELOPMENT TO VALIDATION

*The B, **Flivik G, *Diercks RL, ***Verdonschot N
Department of Orthopaedics, University Medical Center Groningen, Groningen, The Netherlands

b.the@orth.umcg.nl

INTRODUCTION

Individual wear curves of patients often show unexplained patterns of irregularity, or even impossible values such as negative wear.
We postulated that the errors of 2D wear measurements are mainly the result of projection differences between the measured radiographs.
The aim of this study was to develop and validate a novel technique to make 2D wear measurements insensitive for differences in radiographic projection of the prosthesis.

MATERIALS AND METHODS

Development of the correction technique
A geometrics-based framework was constructed to model the errors in 2D measurements due to differences in projection of the prosthesis. Based on this model a method was developed to reverse the raw 2D linear wear value into an estimate of 3D linear wear: this is referred to as the corrected linear wear. Theoretically, application of this correction method would make conventional wear measurements robust: identical wear values will be obtained, even when varying the 2D projections of the prosthesis on the radiographs.
The correction method is as follows: the linear wear is decomposed into two vectors. The vector running parallel to the major axis of the elliptical projection of the metal ring of the acetabular cup is kept unaltered. The vector perpendicular to the first vector is altered as follows: vector = v1 x (cos β / cos α) – v2; v1 = vector length on radiograph 1; v2 = vector length on radiograph 2; α = opening angle on radiograph 1; β = opening angle on radiograph 2; opening angle = arcsine [short axis / major axis] (projection of the metal ring). The Pythagorean Theorem is then applied on the two vectors to obtain the corrected linear wear value.
Experimental validation and error analysis
22 radiographs of a cadaver with a THR were made while rotating the pelvis around a horizontal and longitudinal axis. Wear measurements with and without applying the correction method were performed on each of the images using the first radiograph in neutral position as the reference image.
Next, an error analysis was performed by simulating 144 wear measurements with and without application of the correction method under varying conditions: projection differences and degrees of failure to meet the model assumptions were varied from mild to extreme.
Clinical validation by RSA
Rontgen Stereophotogrammetric Analysis (RSA) was performed on 47 patients with a THP to determine the true wear at 1, 2 and 5 years postoperatively. Then, their wear was measured on conventional radiographs with and without application of the correction method.

RESULTS

Experimental validation and error analysis
The error of the raw 2D wear measurements on the cadaveric hip exceeded 0.2 mm if differences in projection of the THP between two radiographs were as small as 5°. When using the correction method, differences were allowed to be greater than 20° before the error exceeded 0.2 mm.
The error analysis revealed a mean absolute error of 1.8 mm (0 - 4.51 mm) when the correction method was not applied, while this was 0.11 mm (0 - 0.27 mm) with application of the correction. Negative wear values were found in 25% of the raw measurements, while none were found in the corrected measurements.
Clinical validation by RSA
An error greater than 0.2 mm was found in 35% of the measurements, while this was reduced to 15% by application of the correction. An r^2 of 0.71 without correction was found, while this was 0.85 when using the correction.

DISCUSSION

Up till now, 3D wear measurements were the only solution to accurately determine individual wear curves of cemented THR. However, these methods are mostly expensive, time-consuming, or demand the use of dedicated software, or implantation of reference objects near the hip joint. We have developed a technique which approaches 3D linear wear values using conventional 2D linear wear measurements: the measurement values are both more valid and less sensitive to differences in 2D projection of the prosthesis; the obtained wear value will be identical with varying projections of the prosthesis on radiographs. The technique is easily implementable in all existing 2D wear measurement applications.
We recommend implementation of the correction method in all orthopedic software packages that use conventional radiographs to enhance accuracy of wear measurements.

AFFILIATIONS:
* Department of Orthopaedics, University Medical Center Groningen, The Netherlands
** Biomaterials and Biomechanics Laboratory, University Hospital Lund, Sweden
*** Orthopedic Biomechanics Laboratory, University Medical Center Radboud, Nijmegen, The Netherlands

IMAGE-BASED RSA: A NEW METHOD FOR RSA WITHOUT BONE MARKERS

*de Bruin PW, *Kaptein BL, **Stoel BC, **Reiber JHC, *Rozing PM, *Valstar ER
*Orthopaedics Department, **Division of Image Processing
Leiden University Medical Center, Leiden, The Netherlands

p.w.de_bruin@lumc.nl

INTRODUCTION

Roentgen Stereophotogrammetric Analysis (RSA) is an accurate method for assessing prosthesis migration. To achieve its high accuracy, the method requires inserting radio-opaque markers in the bone and attaching to the prosthesis. Recent research has led to Model-Based RSA[1], a method that does not need prosthesis markers.
To remove the need for bone markers we have developed Image-based RSA. This method opens new opportunities for performing RSA-related research, for example:

- retrospective studies using standard AP-Xray;
- fluoroscopy on patients without prosthesis;
- validation of computer navigated prosthesis placement.

The goal of this study is to validate the developed Image-based RSA method in a pilot experiment.

METHODS

RSA is performed by taking a stereo image using two synchronised Roentgen tubes that are placed above a calibration box. The projections of the calibration markers provide information to calibrate the images and to calculate the position of the Roentgen foci.

The basis of Image-based RSA is to use a pre-operative 3D CT dataset as reference instead of bone markers. Similar to a standard RSA setup, the CT volume of the patient is virtually placed between the calibrated RSA images and the Roentgen foci. Next, Digitally Reconstructed Radiographs (DRRs) are generated from the CT data. These DRRs are a close approximation of the RSA images that would have been generated with the patient in that pose, see Figure 1. The object is to iteratively adjust the 3D pose of the CT such that each generated DRR matches the corresponding RSA image as closely as possible. Once this pose is found then the RSA images are registered to the CT data and further analysis is possible.

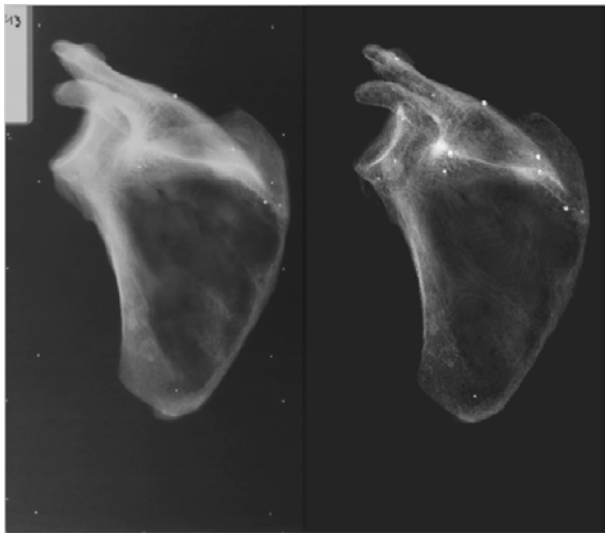

Figure 1: Real RSA Image (left), DRR (right).

The setup of the validation experiment is as follows. For RSA bone markers were inserted in a cadaver scapula. The influence of these marker on Image-based RSA are negligible. A CT dataset of the scapula was made. The scapula was placed in 5 different poses and RSA images were collected. Next, Image-based RSA was applied to each pose. Using RSA as gold standard, the accuracy of Image-based RSA is given by the differences in the calculated poses. The influence of the markers on the registration result is negligible.

RESULTS

Table 1: The differences between the poses calculated using standard RSA and Image-based RSA.

n=5	T_X [mm]	T_Y [mm]	T_Z [mm]	R_X [deg]	R_Y [deg]	R_Z [deg]
mean	-0.046	-0.052	0.050	-0.055	-0.039	0.111
sd	0.270	0.398	0.378	0.313	0.545	0.432

The mean of the error of Image-based RSA, using RSA as gold standard, is 0.06 mm for translations and 0.12 degrees for rotations. The standard deviation of the error is 0.4 mm for translations and 0.55 degrees for rotations.

CONCLUSIONS

The main advantage of the Image-based RSA method is that it does not require prosthesis or bone markers, although one CT of the patient is needed. Image-based RSA is not intented to compete with RSA or Model-based RSA: the lower accuracy of the Image-based RSA method is compensated by its wider research applicability.

[1] B.L. Kaptein, E.R. Valstar, B.C. Stoel, P.M. Rozing, J.H.C. Reiber, A new model-based RSA method validated using CAD models and models from reversed engineering, *Journal of Biomechanics* 36 (2003) 873-882

ABSENCE OF LYMPHATICS AT THE BONE-IMPLANT INTERFACE: IMPLICATIONS FOR PERIPROSTHETIC OSTEOLYSIS

*Athanasou NA, Edwards J, Schulze E, Sabokbar A, Gordon-Andrews H, Jackson D
*Department of Pathology, Nuffield Department of Orthopaedic Surgery, Nuffield Orthopaedic Centre, Oxford, UK

Nick.athanasou@noc.anglox.nhs.uk

INTRODUCTION

Large numbers of implant-derived biomaterial wear particles and wear particle-containing macrophages are found at the bone-implant interface surrounding a loose prosthesis. Particles and particle-containing macrophages are also found in draining regional lymph nodes. It has not been established, whether particles and macrophages are transported via lymphatics from periprosthetic tissues. It is also not known if particles and macrophages found in lymph nodes are derived from the arthroplasty pseudocapsule and/or the pseudomembrane. With regard to aseptic loosening, this consideration is of some importance as accumulation of wear particles at the bone-implant interface has a number of effects including stimulation of cytokine secretion and macrophage-osteoclastic differentiation, both of which would contribute to the osteolysis of aseptic loosening.

METHODS

Expression of LYVE-1 and podoplanin, two highly specific lymphatic endothelial cell markers in the hip arthroplasty pseudocapsule and the pseudomembrane of 20 prosthetic joints removed for aseptic loosening, was determined by an indirect immunoperioxidase technique using monoclonal antibodies to these antigens.

In order to assess the effect of particle accumulation on osteoclast differentiation we also determined whether cultured human monocyte-derived macrophages which had phagocytosed PMMA and titanium particles were capable of differentiating into mature osteoclasts and carrying out lacunar resorption.

RESULTS

LYVE-1 and podoplanin expression in periprosthetic tissues

Lymphatic vessels were commonly found in the arthroplasty pseudocapsule, particularly in the superficial zone of the pseudocapsule. Lymphatic vessels were also seen in underlying fat and connective tissue of the capsule. The fibrous acetabular and femoral pseudomembrane also contained a heavy wear particle-containing macrophage infiltrate, but no lymphatic vessels were identified by LYVE-1 or podoplanin staining of these tissues.

Effect of particle phagocytosis on human macrophage-osteoclast differentiation

Particle phagocytosis by monocytes was seen in 24 hour monocyte cultures. After 14 days incubation with RANKL and M-CSF, numerous multinucleated $TRAP^+$ and VNR^+ osteoclastic giant cells were seen in monocyte cultures to which titanium and PMMA particles had been added. Parallel cultures on dentine slices showed evidence of lacunar resorption with the formation of numerous resorption pits.

DISCUSSION

Our findings indicate that the source of wear particles found in regional lymph nodes around arthroplasties is the pseudocapsule and not the pseudomembrane.

Absence of lymphatics at the bone-implant interface of the pseudomembrane is likely to be significant when there is extensive wear particle generation (e.g. in aggressive granulomatosis). Wear particle accumulation in this location would lead to recruitment of macrophages to phagocytose this foreign material. This would activate macrophages and, as shown in this study, macrophage phagocytosis of metal (titanium) and polymer (PMMA) wear particles does not abrogate macrophage-osteoclast differentiation and resorption. Thus, absence of lymphatic vessels at the bone-implant interface could lead to particle accumulation, macrophage-osteoclast differentiation and periprosthetic osteolysis.

How then is it possible for wear particles to be cleared from the bone-implant interface? It has been proposed that wear particles are dispersed into the "effective joint space" i.e. the sum of all periprosthetic territories accessible to the joint fluid. This effective joint space permits joint fluid and wear debris floating within it to penetrate between the bone and the implant. In this way biomaterial particles may be transported to sites remote from the implant component from which they were originally shed. The effective joint space may provide a route for particles which are shed at the bone-implant interface to be carried to the pseudojoint cavity and pseudocapsule whence they would be transported via lymphatics to draining lymph nodes. Elevated intra-articular pressures, generated during activity, may promote this process, pumping particles and particle-containing cells away from the bone-implant interface towards the pseudocapsule. However, if this clearance mechanism is overwhelmed due to excessive particle accumulation then it is likely that periprosthetic osteolysis would result as a consequence of osteoclast differentiation of macrophages that have phagocytosed wear particles and macrophage stimulation of osteoclast resorption.

SHORT-TERM RESULTS OF A NEW DESIGN OF TOTAL ANKLE REPLACEMENT

*Giannini S, **Leardini A, *Romagnoli M, **Sarti D, ***Catani F
VI Divisione Clinica Ortopedica, ** Laboratorio di Analisi del Movimento, Italy

leardini@ior.it

INTRODUCTION

Total ankle replacement (TAR) is still not as satisfactory as total hip and total knee replacements. For the TAR to be considered a valuable alternative to arthrodesis, an effective range of mobility must be recovered. The disappointing clinical results of the current generation of TAR is mostly related to poor understanding of the structures guiding mobility. A new design has been developed by these authors (Box Ankle, Finsbury Instr. Ltd, UK), able to restore physiologic ankle mobility and a natural relationship between the implanted components and the retained ligaments [1,2].

METHODS

According to prior research, the design features a spherical convex tibial component, a talar component with radius of curvature in the sagittal plane longer than that of the natural talus, and a fully conforming meniscal component. After computer-based modelling and preliminary observations in several trial implantation in specimens, 32 TAR were implanted in 32 patients in our hospital in the period July 2003 – January 2006, mean age was 63 years (range min 41 – 80 max), mean follow-up 13 months (2 – 30). For the meniscal bearing to slide smoothly on both the metal components, these must be implanted in an exact absolute position with respect to the ligament geometry. This was pursued by ensuring that a constant gap is maintained between the tibial and the talar components over the motion arc. Several measurements were taken at operation as for sizing and mobility control. At 3, 6, 12, 18 month follow-up, X-ray radiograms were analyzed, and the AOFAS clinical score system was used to assess patient outcome.

RESULTS

Intra-operatively, osteotomies were successfully performed, and the central antero-posterior length of the tibial mortise at the resection plane was 42.3 mm (32 – 54). The prosthesis components as presently sized fitted and seated properly onto the corresponding osteotomies, difference between antero-posterior length of the tibial mortise and corresponding of the implanted tibial component being 8.6 mm (1 – 16). Under anesthesia, the mean range of flexion at the ankle moved from -1.1° dorsi- to 14.6° plantar-flexion pre-operatively to 10.3° dorsi- to 23.3° plantar-flexion post-operatively, for an overall additional RoM of 20.1° (0 – 40). Complete congruence at the two articulating surfaces of the meniscal bearing was observed throughout the motion arc. No intraoperative complications, no complication in wound healing, and no infections were encountered. Radiographs at maximal dorsiflexion and maximal plantar flexion and fluoroscanning confirmed the meniscal-bearing component moves anteriorly during dorsiflexion and posteriorly during plantarflexion, over an approximate distance of 4-8 mm. Frontal and lateral radiographs in the patients at 6 month follow-up, showed good alignment of the components, and no signs of radiolucency or loosening. The mean AOFAS score was observed to go from 43.7 to 65.6 to 73.1 to 74.4 respectively at pre-op, 3, 8, 15 month follow-up, on a base of 29, 23, 15, 10 patients.

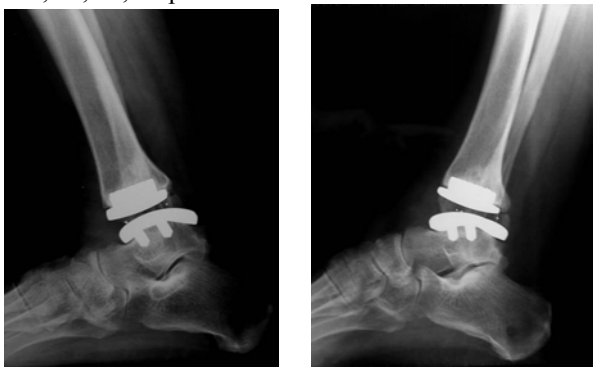

Fig. 1 – Radiographs of an implanted Box Ankle

DISCUSSION

The meniscal-bearing component moves in the direction and approximately for the distance predicted by the computer-based models [1]. The original physiological role of the ligaments must have been restored. Because the function of the ligaments in controlling the passive mobility of the joint is restored, their physiologic contribution to joint stability also should be restored, as predicted by a computer model of the anterior drawer test [3]. As full conformity of the three prosthesis components was observed over the entire motion arc, it is encouraged the prospect of minimizing wear of these components. Slight misplacement of the bone-anchored components does not affect considerably the above observations. The satisfactory though preliminary observations from this novel TAR encourage continuation of the implantation.

REFERENCES

1. Leardini et al. Computer-assisted design of the sagittal shapes for a novel total ankle replacement. Med Biol Eng Comp, 39:168–175, 2001.
2. Leardini et al. Mobility of the Human Ankle and the Design of Total Ankle Replacement, Clin Ortho Rel Res, 424:39–46, 2004.
3. Corazza et al. Ligament fibre recruitment and forces for the anterior drawer test at the human ankle joint, J Biomech 36:363–372, 2003.

ALUMINA, ZIRCONIA, AND COMPOSITE CERAMICS IN JOINT PROSTHESES

Macchi F
CeramTec AG, Medical Division, Roma, Italy

macchif@katamail.com

The bioinert ceramics are mostly used for structural components. Alumina and Zirconia are known for their general chemical inertness and hardness. These properties are exploited for implant purposes, where they are used as an articulating surface in hip and knee joints. Their ability to be polished to a high surface finish make them an ideal candidate for this wear application, where they operate against materials such as ultra high molecular weight polyethylene.

Alumina is aluminium metal in its highest oxidative state. Further oxidation is not possible and the chemical and physical stability of the material is the maximum achievable. In the alpha-alumina lattice, aluminium cations Al^{3+} are surrounded by a layer of oxygen anions O^{2-}. This surface of OH^- anions allows the chemisorptions on the surface of OH^- groups, like bonding of water molecules or protein. In this way the adhesion and stability of lubricating layer at the interface of alumina-on-alumina bearings is enhanced. As with many ceramics, alumina shows very good performance in compression. The tensile strength of alumina improves the higher the density and the smaller the grains size. Optimum results in terms of density and grain size have been achieved using MgO as sintering additives to control discontinuous grain growth. Many laboratory tests and clinical cases have shown that the wear rate of alumina-alumina bearing couple is extremely low (0.001 mm/year). The characteristic molecular structure of alumina guarantee the presence of a fluid film that reduces the coefficient of clutch between the two surfaces involved during the articulation. The colour changes of alumina after gamma sterilization does not induce variation of the mechanical characteristics. The latest generation of alumina has reduced the complications rates to values around 0.01%, maintaining the excellent tribology and wear characteristics. The dimension of grains of the microstructure, currently reduced to inferior values of 2 µm, has allowed to raise a bending strength of about 580 MPa, a fracture toughness (K_{IC}) of around 5 MPa $m^{1/2}$ and an hardness of 2200 HV.
Zirconia is a well known polymorph material that occurs in three phases: monoclinic (M), cubic (C) and tetragonal (T). Garvie showed how to make the best of T-M phase transformation in zirconia to improve mechanical strength and toughness of this material. Using ”stabilising” oxides (CaO, MgO), it was possible to obtain multiphase materials known as Partially Stabilized Zirconia (PSZ). Last development for zirconia (Y-TZP) was introduced by the stabilization with Yttria (Y_2O_3). Thanks to transformation toughening, the mechanical properties of Y-TZP exceed those of alumina. Bending strength up to 1200 MPa and toughness up to 9 MPa $m^{1/2}$ may be achieved, both values being twice those of the best-quality alumina for clinical applications. Today, worldwide more than 500.000 zirconia ball heads have been implanted. Thanks to the high bending strength and toughness of Y-TZP ceramics it is possible to manufacture small diameter Y-TZP ball heads (Ø 22 mm or Ø 26 mm) and long necks.
The introduction of zirconia into an alumina matrix results in a class of ceramic materials with increased toughness, known as zirconia Toughened Alumina (ZTA). This first evolution of the ceramic composite achieved toughness up to 12 MPam$^{1/2}$ and bending strength up to 700MPa. The stabilising oxide and the constraint exerted by the alumina matrix on the metastable tetragonal zirconia particle maintains them in the tetragonal state. The toughening of the material is due to the tetragonal-to-monoclinic transformation of the zirconia particles. Due to the difference in elastic modulus, between the alumina matrix and the zirconia particles, crack will tend to move across the less stiff zirconia particles inducing a phase transformation and then dissipating the crack energy. ZTA has the drawback of the decrease in hardness and it has been balanced with the introduction of small percentage of chromium oxide (Cr_2O_3). To increase the toughness of this material have been used the results of the studies on the toughening of the alumina by addition of whiskers that use the crack energy deflection concept. Elongated grains (platelets) can be enucleated in-situ within the structure of an alumina matrix ceramic composite during the sintering exploiting the solid-state diffusion phenomena that take place during high temperature processing. It lead to a material known as ZPTA (Zirconia Platelet Toughness Alumina). This composite ceramic is nearly as hard (1975 HV) as alumina, has a bending strength of around 1150 MPa and a fracture toughness of about 8,5 MPa $m^{1/2}$. From the stability in wet environment point of view, the ZPTA show a significant increase in hydrothermal stability due to the Yttria coated powders and the diffusion of Al3+ ions at the grain boundaries. ZPTA is opening new and interesting opportunities in the application of ceramics in arthroplasty like ball-heads Ø 22 mm, extra long necks (XL), thin-walled Ø 36 mm ceramic inserts and ceramic-on-ceramic knee and ankle replacement now in development.

AN *IN VITRO* AND *IN VIVO* EXPERIMENTAL ANALYSIS ON THE ADHESION AND SPREADING OF CELL CULTURES ONTO "TREVIRA" TUBE IN PROSTHETIC RECONSTRUCTION AFTER WIDE RESECTION FOR MALIGNANT BONE TUMOURS

*Rosa MA, **Maccauro G, ***Sgambato A, *Caminiti R, *Alesci M
Surgical Specialties Department - Orthopaedic Section - University of Messina – Italy

rosa.ma@tiscali.it

INTRODUCTION

One of the main problems in reconstructive surgery after wide resection for malignant bone tumours is still the soft tissue reconstruction and in particular their anchoring to modular or custom made megaprostheses. This surgical aspect is particularly important if composite prostheses are not utilized.
It is well known that the entity of soft tissue sacrifice induces a functional deficit of the operated limb. "Trevira" tube is currently used in reconstruction after resection for improving soft tissue anchoring to megaprostheses, but few papers are still published concerning the biological mechanisms of this adhesion.
The aim of this study was to analyse soft tissue adhesion to "Trevira" tube using in vitro and in vivo studies.

METHODS

In vitro studies were performed analysing with scanning electron microscopy the adhesion and spreading of fibroblasts onto "Trevira" tube and measuring with MTT test cell viability and proliferation on this material in comparison to Ti-alloy used as a control. We also observed, using SEM, tissue anchoring on prostheses retrieved at the time of revision surgery for aseptic loosening.

RESULTS AND CONCLUSION

Our studies showed the good adhesion and spreading of cells onto "Trevira" tube, demonstrating the good metabolic status of cells. MTT showed that fibroblasts can attach and proliferate on this material. The adhesion was stronger ($p < 0.05$) than the one on Ti-alloy, demonstrating that "Trevira" Tube constitutes an improvement of anchoring soft tissues in comparison to Ti alone.
SEM of specimens retrieved at the time of revision surgery for aseptic loosening showed soft tissue on "Trevira" tube. Through the emission of lamellipodia and filipodia, cells adhered on substrate. This is the basis of cytoskeleton modifications before cell proliferation confirming the good metabolic status of cells.
Our study confirmed that "Trevira" may be considered a useful system for soft tissue anchoring on megaprostheses, because it allows a good adhesion of fibroblasts on the tube.

AFFILIATED ISTITUTIONS:

** Department of Orthopaedic Sciences - Catholic University - Rome -Italy
*** Department of Pathology - Catholic University - Rome - Italy

RECONSTRUCTION OF MASSIVE ROTATOR CUFF LESIONS WITH A SYNTHETIC INTERPOSITION GRAFT

Audenaert E, **Van Nuffel J, **Verhelst M, *Verdonk R
Department of Orthopedic Surgery, Ghent University Hospital, Ghent, Belgium

emmanuel.audenaert@azbrugge.be

INTRODUCTION

Treatment of massive rotator cuff tears still present a major challenge in shoulder surgery. Direct repair of the native rotator cuff tendons to the proximal humerus is impossible because of retraction and inelasticity of the tendons. Conventional techniques for soft tissue release are often insufficient and the remaining tendon edges, altered by chronic degeneration, show inferior tissue quality and are not suited for secure primary repair.

Only a small number of papers are available describing the technique and outcome of synthetic grafting for the treatment of massive rotator cuff lesions. Moreover, only a limited number of patients is described, and there are important differences in patient selection, technique and used synthetic materials. Some of the used synthetic materials have lead to disastrous results, making the use of synthetic grafts in shoulder surgery very controversial.

In the present prospective study, we report about our experience with massive rotator cuff tears treated by means of a nonresorbable transosseously fixated patch combined with subacromial decompression.

MATERIAL AND METHODS

From December 1996 until August 2002, a total of 41 patients were treated with a synthetic interposition graft and subacromial decompression and included in the present study. (Figure 1) All included patients had preoperative ultrasonographic evidence of a primary massive full-thickness tear that was thought to be irreparable by simple suture.

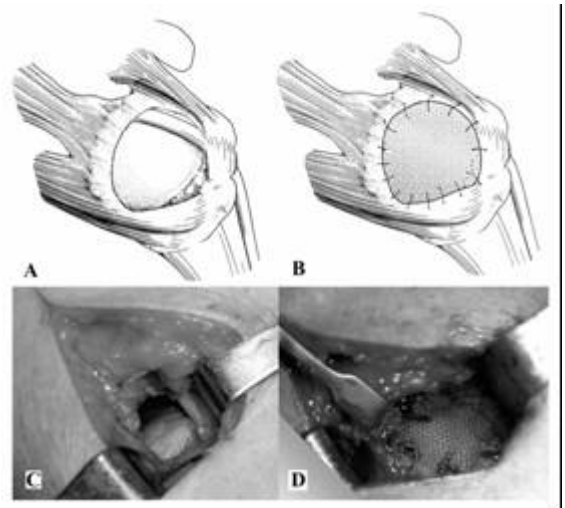

Figure 1 : Surgical technique

Prior to surgery, all patients received maximal conservative treatment. When conservative failed after 3 months, an open surgical approach was scheduled. In all the included patients, it was impossible to conventionally reattach the tendon edges to the greater tuberosity with the arm in less than 30° abduction.

Informed consent was obtained in all patients and they were evaluated preoperatively and postoperatively using the Constant and Murley score, ultrasonography and radiography. All radiographic imaging was fluoroscopic controlled and digital phosphor plates were used, allowing DICOM measurements.

The nonparametric Wilcoxon signed ranks test was used to analyze data. The level of statistical significance was set at an alpha level of $p < 0.05$. All data were analyzed with the SPSS statistical package release 12 (SPSS, Inc., Chicago, IL).

RESULTS

The patients consisted of 23 men and 18 women aged 51–80 years (mean, 67 years). They were followed up for a mean of 43 months (range, 24–86 months). Their mean preoperative Constant and Murley score improved ($P<0.001$) from 25.7 preoperatively to 72.1 postoperatively. Substantial pain relief and improvement in the performance of activities of daily living were obtained. Anatomically, the repair resulted in a mean acromiohumeral interval of 8.6 mm. At the latest follow-up, three patients presented with a new tear between the inserted mesh and the supraspinatus musculotendinous unit. Reoperations were not performed.

DISCUSSION AND CONCLUSION

For short-term periods, restoring a massive rotator cuff tendon defect with a synthetic graft combined with subacromial decompression can give significant pain relief and improvement of range of motion and strength with few complications

REFERENCES

Audenaert E, Van Nuffel J, Schepens A, Verhelst M, Verdonk R. Reconstruction of massive rotator cuff lesions with a synthetic interposition graft: a prospective study of 41 patients. Knee Surg Sports Traumatol Arthrosc. 2005 Oct 27; [Epub ahead of print]

AFFILIATED INSTITUTIONS FOR CO-AUTHORS

** Department of Orthopedic Surgery, St. Andries Hospital, Krommewal 9–11, 8700 Tielt, Belgium

ANALYSIS OF KEY PARAMETERS IN IN SITU CONTOURING SURGERY USING A VALIDATED FINITE ELEMENT MODEL

* Lafon-Jalby Y, ** Steib JP, *Lavaste F, * Skalli W
* Laboratoire de Biomécanique, CNRS UMR 8005, ENSAM, Paris, France.

yoann.lafon@paris.ensam.fr

INTRODUCTION

During the scoliosis surgery, improper force application to the spine trough instrumentation can lead to global imbalance: the biomechanics of surgical correction, depending on surgical maneuvers, could be better understood thanks to finite element simulation. The Cotrel-Dubousset instrumentation surgery has been already simulated [1]. The aim of this numerical study is to investigate key parameters which could influence the surgical outcome of another technique, the In Situ Contouring Technique (SCS).

METHODS

10 patients with thoracic and thoraco-lumbar scoliosis underwent a surgical treatment by In Situ Contouring Technique.

A patient specific validated 3D finite element model was obtained from pre-operative stereo-radiography and X-ray clinical bending tests. Standard procedure simulation of the surgical correction was previously studied [2]: each step of the surgery was simulated according to surgeon experience. The finite element model took into account the rod capacity of cumulative and local plastic deformation with elastic unloading. Sequence of the vertebra levels concerned by multiple surgical contouring maneuvers were driven by an automated procedure, reproducing surgeon's indications.

Resulting virtual spine configuration was first compared to real post-operative one, as assessed from stereo-radiography 3D reconstructions. Then the effects of surgery related parameters were evaluated, particularly the local maneuvers to rotate vertebrae using rotation blocks.

RESULTS AND DISCUSSION

In Situ Contouring surgery simulations regarding ten patients confirmed the coherence of the model for a given standard procedure. Indeed 7 patients presented a very good agreement with in vivo data. Mean difference between model and in vivo configuration was lower than 6mm and 5° when considering respectively 3D position and angulation of vertebrae. A second group of 3 patients presented higher differences, but maxima never exceeded 16mm and 16° respectively. When virtually acting on vertebral rotation, results appeared very close to post-operative findings (mean differences lower than 4mm and 4°. This was a complementary per-operative maneuver that corrected 3D opposite vertebral rotation during the contouring maneuver at a given level. Only for one patient this maneuver did not explain the differences (cf. Figure 1).

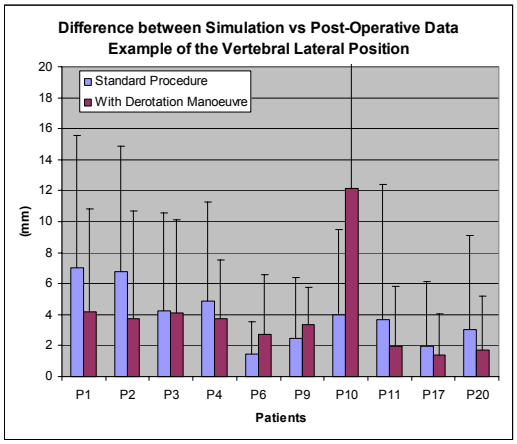

Figure 1.

CONCLUSION

Correction of scoliosis can be achieved in different ways. This study quantified the influence on results regarding to the In Situ Contouring surgery technique, for one main per-operative parameter, the derotation maneuver.

REFERENCES

[1] Lafage V & al (2004): 3D finite element simulation of Cotrel-Dubousset correction. *Comput Aided Surg.* 2004;9(1-2):17-25.

[2] Dumas R & al (2005): Finite element simulation of spinal deformities correction by in situ contouring technique. *Comput Methods Biomech Biomed Engin.* 2005 Oct;8(5):331-7.

AFFILIATED INSTITUTIONS FOR CO-AUTHORS

** Hôpitaux Universitaires de Strasbourg, France

EFFECT OF INTRA-ARTICULAR STEROIDS ON DEEP INFECTIONS FOLLOWING TOTAL KNEE ARTHROPLASTY

Joshy S, Thomas B, Gogi N, Singh BK
Department of Orthopaedics, City Hospital Birmingham, UK

drsurajjoshy@yahoo.com

INTRODUCTION

The aim of our study was to find any relation between deep infections following total knee arthroplasty and intra-articular steroid use prior to the arthroplasty.

Intra-articular steroids have been commonly used for the symptomatic treatment of arthritis.

There are no published studies correlating infections following total knee arthroplasties and previous intra-articular steroid injections.

We hypothesised that intra-articular steroid injection in to the knee could increase the incidence of deep infections following total knee arthroplasty, hence patients with infected knee arthroplasties are more likely to have received intra-articular steroid injections prior to the operation.

MATERIALS AND METHODS

We undertook a retrospective matched cohort study to analyse the effect of intra-articular steroid injections on deep infections following total knee arthroplasty. Study group comprised of patients with confirmed deep infection following total knee arthroplasty.

The control group comprised of patients who underwent total knee arthroplasty but with out any clinical, haematological or radiological evidence of infection in the knee.

The hospital records of all the patients were reviewed. The date of primary operation, secondary procedures, microbiology results, haematology results and radiographs were verified.

Hospital records were verified to find out whether the patients in either group received any intra-articular steroid injections prior to total knee arthroplasty.

Number of injections received and the time gap between the last injection and total knee arthroplasty were also recorded.

In the group with infection the time gap between injection and the diagnosis of infection was recorded.

RESULTS

There was no significant difference between the numbers of patients who received intra-articular steroid injection between the groups(P=1).

DISCUSSION

We believe that infection following total knee replacement is due to multiple factors and the use of intra-articular steroids does not alter the incidence of deep infections following total knee arthroplasty.

CARTILAGE DERIVED PARACRINE FACTORS INFLUENCE CHONDROGENESIS IN MESENCHYMAL STEM CELLS

***Ahmed N, *** Dreier R, **Grifka J, **Grässel S,
*Experimentelle Orthopädie, Zentrum für Medizinische Biotechnologie, BioPark, Regensburg, Germany

nazish.ahmed@stud.uni-r.de

INTRODUCTION

Degenerative diseases as osteoarthritis or cartilage damaging injuries are restrictive and painful for normal mobility. Damaged articular cartilage has limited regeneration capacity mainly due to lack of chondroprogenitor cells. Pluripotent MSCs are the only known adult chondrocytes progenitor cells. Subsequently, as chondrocytes are the only cell type of cartilage it is important to identify the molecular events characterizing chondrogenesis in MSCs. MSCs may also be used for therapeutic purposes e.g. for the repair of focal defects in articular cartilage or diseases like osteogenesis imperfecta. However, information about mutual paracrine effects of surrounding tissue and newly transplanted implant is not sufficient. *In-vitro* studies on chondrogenesis in MSCs cocultured with cartilage may not only give precious information regarding molecular control but it may also be directly relevant to the clinical application. In this study we have set up a coculture system between articular cartilage and MSCs. We hypothesize that the signaling factors secreted by cartilage tissue may compensate for external growth factors required to stimulate chondrogenesis in MSCs.

MATERIALS AND METHODS

Coculture is done in 12 well culture plates and 1µm pore sized inserts. Cartilage chips are kept in the well and rat MSCs suspended in 1.2% alginate are cultured in inserts. Cultures are set up for 21 days maximum in serum free chondrogenic medium with or without TGFß-3. Gene expression is determined by quantitative RT-PCR. SDS-PAGE, immunoblotting and immunofluorescence is used for protein analysis. Soluble signaling factors and enzymes are detected by antibody array from RayBiotech™ and by zymography. Animal experiments are carried out after institutional authorization. One-way ANOVA and student t test are used for statistical analysis. All experiments are done in triplicate.

RESULTS

Our previous data demonstrated elevated gene expression level of *Sox9,* considered as the master transcription factor for chondrogenesis. The immunofluorescence results confirm a progressive expression of Sox9 protein. Both, protein and mRNA levels are higher in the presence of TGFß-3. Additionally, expression and synthesis of extracellular matrix components as collagen I, II, aggrecan and COMP is increased. Monocultured MSCs start expressing and synthesizing collagen X at day 21 while cartilage suppresses collagen X expression in MSCs. Antibody array analysis shows a culture time dependent decrease in VEGF secretion and increase in TIMP-1 secretion. In absence of Tgfß-3 we detect TIMP-2 in coculture supernatants from day 14 onwards. Increasing amounts of pro-MMP-2 are detected in coculture supernatants from day 7 onwards; however, relative activation status remains unchanged compared to day 1. In absence of cartilage active MMP-2 is not detectable after day 7. Neither cartilage nor MSCs secrete pro-inflammatory cytokines with exception of monocyte chemoattractant protein (MCP-1). MCP-1 was detected on day 14 of coculture, monocultured MSCs did not secrete MCP-1.

DISCUSSION AND CONCLUSION

Elevated gene expression level of *Sox9* on day 1 indicates early onset of chondrogenesis in MSCs under influence of cartilage. Profound secretion of VEGF from cartilage at the onset of the culture may have an impact on chondrogenic induction. TIMP-1 and TIMP-2 secretion from cartilage tissue was progressively elevated reciprocated by less active MMP-2 in the culture supernatant. Suppression of collagen X, as an indicator for terminal differentiation of chondrocytes, in the presence of cartilage depicts delayed hypertrophy in our coculture model. High concentration of TIMPs in the late stage of the culture may be the reason of the observed delayed hypertrophy. Interestingly, this effect is more profound in the presence of TGFß-3 which is known to induce dedifferentiation in differentiated chondrocytes and differentiation in MSCs. In TGFß-3 containing cultures, cartilage induces collagen II protein expression along with undesired collagen I expression. While absence of TGFß-3 promotes only low total collagen synthesis, relative amount of collagen II appears to be higher than collagen I. During the study we discovered MCP-1 to be secreted by cartilage tissue, which is reported to be found in initial stage of OA and RA. These data render our coculture model suitable for studying the effect and identity of paracrine signals from differentiated chondrocytes on undifferentiated MSCs.

AFFILIATED INSTITIONS FOR CO-AUTHORS

Orthopädische Universitätsklinik Regensburg, Bad Abbach, Germany; * Institut für Physiologische Chemie und Pathobiochemie, Münster, Germany

EXPERIMENTAL VERTEBRAL GROWTH DISTURBANCES AFTER UNILATERAL MULTISEGMENTARY DAMAGE OF THE EPIPHYSEAL PLATE AND THE NEUROCENTRAL CARTILAGE

*Barrios C, **Burgos J, ***Hevia E, ****Maruenda JI
*Orthopaedics and Trauma Unit, Department of Surgery, Valencia University Medical School, Valencia, Spain

cbarrios@uv.es

INTRODUCTION

Spinal growth modulation has gained credibility as a nonfusion alternative for treatment of idiopathic scoliosis. The effect of isolated or combined unilateral multisegmentary damage of the epiphyseal plate (EP) and the neurocentral cartilage (NCC) on the vertebral growth was experimentally analysed in a pig model.

MATERIAL AND METHODS

Twenty-four 4-weeks-old domestic pigs with a mean weight of 16 kg. were included in the experiment. Through a video-assisted right minithoracotomy, the superior and inferior epiphyseal plates of T5 to T9 vertebra were damaged in 8 animals by hemicircumferential electrocoagulation. In other 8 pigs, right NCC at the same T5-T9 levels were damaged by electrocoagulation. Eight other animals underwent combined lesions of the ipsilateral hemiepiphyseal plates and NCC. Vertebral growth was assessed by conventional X-rays 12 weeks after surgery. After the radiographic study, animals were sacrificed for macroscopic and histological examination. The parameters analysed included the study of vertebral rotational asymmetry, changes in vertebral body height, abnormality of the spinal canal shape, and condrogenic activity of the remaining epiphyseal plate and neurocentral cartilage.

RESULTS

A total of 21 animals could be evaluated after 12 weeks of follow-up. The 7 pigs with hemicircumferential epiphyseal damage developed a very slight scoliotic deformity (mean 12º Cobb), without vertebral rotation.

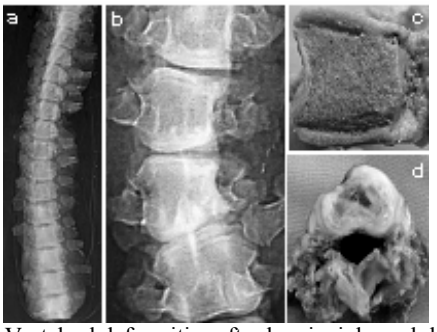

Fig. 1. Vertebral deformities after hemiepiphyseal damage

However, some of the damaged vertebra showed a marked wedgening, with unilateral alteration of the body development including the adjacent discs (Fig. 1). One animal showed a severe kyphotic deformity.

Animals with damage of the NCC developed mild scoliotic curves of 16º-24º Cobb and loss of physiological kyphosis. The macroscopic study revealed an asymmetric growth of the vertebral body with hypoplasia of the pedicle and costovertebral joints at the damaged side (Fig. 2).

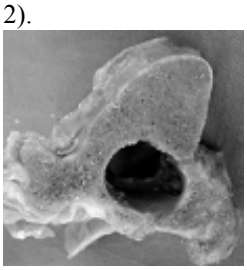

Fig. 2. Vertebral growth modulation after damage of the NCC

Animals with combined epiphyseal and neurocentral lesions developed slight scoliotic curves, average 10-12º Cobb. Macroscopically, there was a lack of development of a vertebral hemibody and disc hypoplasia at the damaged segments (Fig. 3).

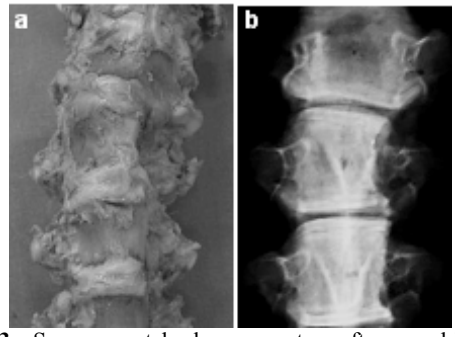

Fig. 3. Severe vertebral asymmetry after combined damage of the NCC and EP

DISCUSSION

Unilateral injury of the epiphyseal growth plate by hemicircumferential electrocoagulation modifies vertebral development, but is not able to experimentally induce scoliosis in the pig. This study questions the efficacy of modern preserving motion techniques for correction of scoliosis, based on vertebral hemiepiphysiodesis. Only animals with damage of the neurocentral cartilage developed mild scoliotic curves of lordotic type. This work rediscovers and emphasizes the decisive role of the neurocentral cartilage in the ethiopatogeny of idiopathic scoliosis.

AFFILIATED INSTITUTIONS FOR CO-AUTHORS
Division of Paediatric Orthopaedics, Hospital Ramón y Cajal, Madrid; * Spine Unit, Hospital La Fraternidad, Madrid; ****Department of Orthopaedic Surgery, University Clinic Hospital, Valencia, Spain

EFFECTS OF EARLY AND LATE ZOLEDRONATE TREATMENT ON BONE MICROSTRUCTURE IN OVARIECTOMIZED RATS ASSESSED BY IN VIVO MICRO-CT

*Brouwers JEM, *van Rietbergen B, *Huiskes R
Eindhoven University of Technology, Eindhoven, The Netherlands
J.E.M.Brouwers@tue.nl

INTRODUCTION

Bisphosphonates have proven to be potent inhibitors of bone loss in osteoporotic patients. It is not well known, however, to what extent they can restore the affected bone microstructure to the pre-osteoporotic state and how this depends on treatment regime. A recent theoretical study predicted that late bisphosphonate treatment would lead to a final microstructure with a more severely affected connectivity than in an early treatment situation, even though the final bone volume fraction was the same[1]. Recently developed animal high-resolution micro-CT scanners, now offer the possibility to accurately monitor individual changes in bone microstructure of small rodents in vivo rather than comparing averages of different groups. In this way it is possible to study the effect of different treatments on the structural changes much more accurately. The goal of this study was to determine the influence of early and late administration of a bisphosphonate on the bone structure in ovariectomized rats, in a longitudinal study using in vivo micro-CT.

METHODS

37 female, retired breeding, 35 weeks-old Wistar rats were divided into four groups: control (9), ovariectomy (OVX) (9), OVX and early zoledronate (ZOL) (10), OVX and late ZOL (9). All rats underwent OVX at week 0, the control group underwent SHAM OVX. The early ZOL group was administered ZOL, kindly donated by Novartis Pharmaceutical (Basel, Switzerland), at a single dose of 20 µg/mg s.c. at OVX. The late ZOL group was administered the same dose 8 weeks after OVX. A 3D micro-CT-scan of 6 mm, with a resolution of 15 microns, was made of the proximal tibia using a Scanco vivaCT 40 scanner at 0, 2, 4, 8 and 12.The metaphyseal area was manually selected and bone structural parameters (bone volume fraction (BV/TV), connectivity density (Conn.D), structure model index (SMI), trabecular number, thickness and spacing (TbNr, TbTh, TbSp) were determined. To compare several scans of the same rat, we developed image registration software to match the position of follow-up scans with the baseline scan (Fig. 1).
The experiments were approved by the Animals Ethics Committee of the University of Maastricht.

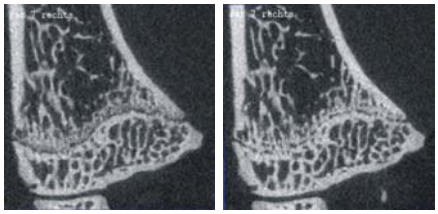

Figure 1: Slice of a baseline (left) and follow-up CT-scan after registration (right) for a sham animal. Results indicate that no changes occur in this group and that the registration procedure works well

RESULTS

Figures 2a-d show the bone volume fractions of the four groups. OVX + early ZOL showed hardly any bone loss, indicating a strong bone-loss inhibiting effect of zoledronate. Two rats in the OVX and two in the OVX + late zoledronate groups that did not show any bone loss were excluded from further statistical analysis.
For every parameter of each animal the ratios between the values of the last and the first measurements were determined. A Kruskal-Wallis test was performed on the data. A Tamhane post-hoc test was performed on all parameters but TbTh. No significant differences ($p>0.05$) between groups were found for SMI and TbSp. For BV/TV and Conn.D, a difference was found between SHAM+OVX, SHAM+late ZOL, OVX+early ZOL and early ZOL+late ZOL. TbNr was different between SHAM+OVX and OVX +eZOL.

DISCUSSION

The use of the in vivo imaging method, image registration and paired statistics enabled us to identify the effects of early and late treatment with zoledronate in much larger detail than was possible before. Significant differences in BV/TV between early and late ZOL groups after 12 weeks were found, unlike the theoretical prediction [1]. The connectivity in the early treated group was better retained than in the late treated group, which agrees with the theoretical predictions.

REFERENCES: 1. Ruimerman R et al, 2004, ESB Proc.

ACKNOWLEDGEMENTS: Netherlands Organisation for Scientific Research

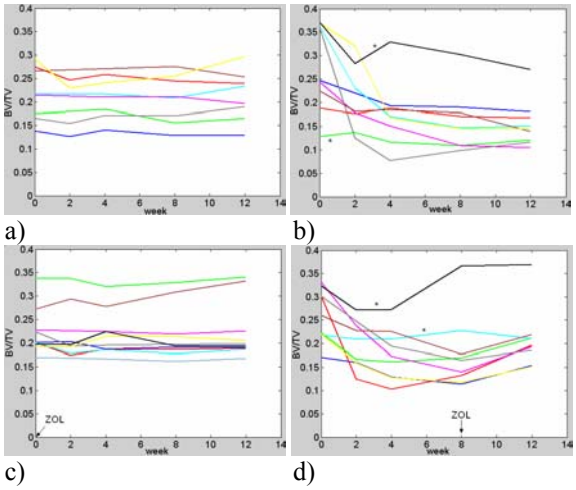

*Figure 2: Bone volume fraction for a) SHAM b) OVX c) OVX + early ZOL d) OVX + late ZOL for each animal. *=excluded from analysis*

BIOMECHANICAL AND HISTOLOGICAL CHANGES IN THE PORCINE DISC AFTER TREATMENT WITH HIFU

*Forslund C, **Hansson H-A, ***Ekström L, ***Holm S
Ultrazonix DNT AB, Malmö, Sweden

cf@ultrazonix.com

INTRODUCTION

Low back pain is one of the leading causes of lost work time and disability. The problems mostly heal by themselves, but a large number of patients remain with chronic pain. We have evaluated High Intensity Focused Ultrasound (HIFU) as an alternative approach for the treatment of herniated discs. HIFU induces high temperatures within a defined volume of tissue. The ultrasound works at a distance from the transducer which can be regulated with the frequency and the degree of focusing due to the design the transducer. Heating a predefined volume of disc tissue to 65ºC or above will result in denaturation of collagen where the hydrogen bonds in the collagen fibrils brake and the collagen structure turn uncoiled resulting in tissue shrinkage. Our aim was to evaluate whether HIFU treatment offers a safe, efficient and easy alternative to currently used surgical procedures.

MATERIALS AND METHODS

*Ultrasound device:*The probe consists of a shaft with a 5 mm diameter pizoceramic transducer at the front; the transducer has a geometric focus of 15 mm, operates at a frequency of 4 MHz and with an acoustic output of 2,5W. Saline irrigation provides cooling of the piezoceramic and acoustic coupling between the probe and tissue via a small hole in the centre of the transducer.

Animal Study: In this study 10 Swedish domestic breed pigs of 12 months (140-180 kg) were used. The probe was under anaesthesia positioned with the aid of x-ray imaging on the lumbar disc. Treatment time was 6 x 60 s. Two lumbar discs were treated per pig, leaving two untreated discs in between. The animals were killed after 0 (n=3), 14 (n=3) or 28 days (n=4).

Biomechanical tests: Spinal segments, comprising two vertebrae with a disc in between, were prepared for biomechanical tests using a materials testing mashine. The vertebrae were mounted in such a way to achieve parallel surfaces perpendicular to the compression axis.

The loading scheme included the application of two sets of cyclic loads, each followed by restitution and thereafter two periods of constant load with restitution in between.

Histology: Histology was performed on discs and vertebral bodies. Slides were prepared for light microscopic investigations.

RESULTS

*Biomechanics:*In the acute group swelling of the disc resulted in increased disc height and stiffness. After 14 days the disc height of treated discs was comparable with that of the controls, while the stiffness as well as load properties were significantly reduced in treated discs as compared to control discs. After 28 days the stiffness was normalized again compared to controls.

Histology: Treated disc specimens in the acute group showed signs of oedema as well as disorganization of the collagen lamella in the annulus fibrosus (AF).

After 14 and 28 days, treated discs showed AF areas, which had been undergoing rebuilding. The AF was characterized by having areas with a considerable reduction in the number of chondrocytes. Vertebral bodies surrounding treated discs showed after 14 and 28 days prevalence of compact bone in the end plates. Blood vessels were recognized to emerge from the bone tissue in the end plate region into the AF. The normally distinct border between the bone, the end plate hyaline cartilage and the AF was less distinct. There were areas of the AF at the end plate with an increased number of fibroblasts along the collagen fibres. Alterations in the nucleus pulposus were observed as well

DISCUSSION

The microscopically analysis of porcine discs exposed to HIFU disclose that AF is significantly affected. The prevalence of repair processes after 2 and 4 weeks further confirmed that the HIFU treatment induced focal damage to the intervertebral discs. Due to spinal movements and muscle contraction, the load properties of treated discs were reduced compared to control discs two weeks after treatment. Already after four weeks the loading properties were normalized again. This was also seen microscopically where rebuilding of the disc was evident. It is reasonable to presume that with a longer follow-up time after treatment, the stiffness of the disc presumably may increase further as a result of the repair and rebuilding of disc tissue.

We believe HIFU is an alternative to current treatments of herniated discs with the advantage of enabling a minimally invasive treatment, as the annulus fibrosus is not penetrated.

AFFILIATED INSTITUTIONS FOR CO-AUTHORS

** Inst of Anatomy and Cell Biology, Göteborg Univ., Göteborg, Sweden. *** Dept. of Othopedics, Sahlgrenska University Hospital, Göteborg, Sweden.

NOVEL NONVIRAL GENE TRANSFER SYSTEMS ALLOW FOR AN EFFICIENT GENE DELIVERY INTO CELLS OF MUSCULOSKELETAL ORIGIN

*Orth P, *Kaul G, *Kohn D, *Cucchiarini M, +*Madry H
+*Lab. Experim. Orthopaedics, Dept. of Orthopaedic Surgery, Saarland University Medical Center, Homburg, Germany

mhmad@hotmail.com

INTRODUCTION

Nonviral gene transfer is a valuable tool for orthopaedic research [1]. The aim of this study was to evaluate novel nonviral gene delivery systems, including lipid- and nanoparticle-based compounds in primary cells and established cell lines of musculoskeletal origin. We tested the hypothesis that, under optimized conditions, nonviral gene transfer systems are capable of yielding high transfection efficiencies.

METHODS

Primary cultures of lapine articular chondrocytes and muscle cells and of human cells from fibrous dysplasia, the human cell lines SAOS-2 (osteosarcoma), CS-1 (chondrosarcoma) [2] and NIH 3T3 fibroblasts were used. Cells were transfected in monolayer in 24-well plates with plasmid expression vectors carrying the *Photinus pyralis* luciferase gene, the *E. coli lacZ* gene or the human IGF-I gene under the control of the CMV-IE promoter/enhancer. Plasmid DNA was complexed with the nanoparticle-based systems Nanofectin 1 and 2 (PAA), the activated-dendrimer transfection reagent Superfect (Qiagen), the linear polyethylenimine reagent JetPEI (PolyPlus Transfection), the lipid-based compounds GeneJammer (Stratagene), Effectene (Qiagen), TransPass D2 (NEB), FuGENE 6 (Roche), the cationic liposomes Lipofectamine 2000 (Invitrogen), Dreamfect (Oz Bioscience), Metafectene (Biontex), Escort III (Sigma) and the Calcium-Phosphate co-precipitation method. Transgene expression was determined 48 hours after transfection by chemiluminescence (luciferase) and ELISA (IGF-I; R&D Systems). Transfection efficiency was calculated using X-gal staining. Data are from at least three independent experiments with each test condition in triplicate and are given as mean ± standard deviation (s.d.). Statistical significance was assessed by ANOVA.

RESULTS

Lapine muscle cells. Of the thirteen transfection systems tested, Dreamfect produced the highest transfection efficiency of 13,013 ± 593 RLU, corresponding to 60.8 ± 21.2% as visualized by X-Gal staining (**Fig. 1**). In contrast, Escort III exhibited a minimal efficiency (435 ± 21 RLU), 30-fold lower than Dreamfect. Maximal transgene expression was seen at a (v/w) lipid/DNA ratio of 4:1. IGF-I expression levels in IGF-I-transfected cells were of 142.3 ± 7.0 ng/10^6 cells/24h, significantly higher than in all other cell lines tested ($P < 0.02$), except for NIH 3T3 cells ($P > 0.05$).

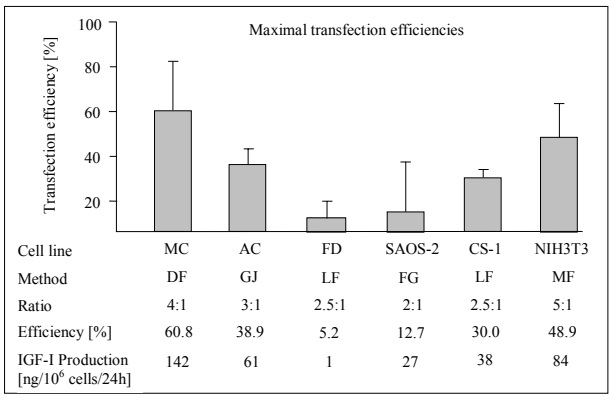

Figure 1. *Maximal transfection efficiencies. SAOS-2: human osteosarcoma cell line, CS-1: human chondrosarcoma cell line, FD: primary human cells from fibrous dysplasia, NIH 3T3: murine fibroblast cell line, MC: primary lapine muscle cells, AC: primary lapine articular chondrocytes. FG: FuGENE 6, LF: Lipofectamine 2000, MF: Metafectene, DF: Dreamfect, GJ: Gene Jammer.*

Lapine articular chondrocytes. GeneJammer mediated the highest efficiencies (22,806 ± 8,373 RLU), Nanofectin 2 mediated the lowest efficiencies (1,296 ± 1,214 RLU). Under optimized conditions, transfection efficiency was of 38.9 ± 5.9% (**Fig. 1**), obtained at a (v/w) lipid/DNA ratio of 3:1. IGF-I secretion in transfected cells was 61.3 ± 12.0 ng/10^6 cells/24h, significantly lower than in lapine muscle cells ($P < 0.02$).

Fibrous dysplasia. Lipofectamine 2000 achieved the highest transfection efficiency of 5.2 ± 8.0% (**Fig. 1**) with a (v/w) lipid/DNA ratio of 2.5:1. IGF-I secretion levels (0.9 ± 0.2 ng/10^6 cells/24h) were 2.5-fold higher than those of non-transfected cells (0.4 ± 0.0 ng/10^6 cells/24h) without reaching statistical significance ($P = 0.65$).

Osteosarcoma cells. Maximal gene expression was seen with FuGENE 6 (11,430 ± 9,480 RLU) at a (v/w) lipid/DNA ratio of 2:1, corresponding to an efficiency of 12.7 ± 16.2% (**Fig. 1**). In contrast, Escort III exhibited a minimal transfection efficiency (415 ± 275 RLU), 28-fold lower than FuGENE 6. IGF-I expression levels were of 27.3 ± 7.1 ng/10^6 cells/24h, compared with 1.2 ± 0.0 ng/10^6 cells/24h in non-transfected cells.

Chondrosarcoma cells. Lipofectamine 2000 produced the highest efficiency (8,470 ± 6,204 RLU) (**Fig. 2**), corresponding to a mean transfection efficiency of 30.0 ± 3.5% (**Fig. 1**). Efficiency was minimal with TransPass D2 (375 ± 205 RLU), 26-fold lower than Lipofectamine 2000. Maximal gene expression was seen at a (v/w) lipid/DNA ratio of 2.5:1. IGF-I expression levels in IGF-I-transfected cells were of 37.9 ± 8.8 ng/10^6 cells/24h, compared with 1.3 ± 0.0 ng/10^6 cells/24h in non-transfected cells.

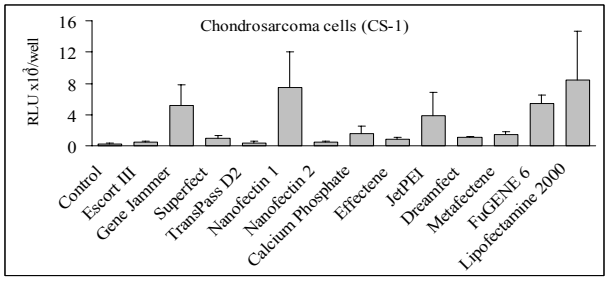

Figure 2. *Comparative analysis of transfection efficiencies for the chondrosarcoma cell line CS-1. Data are given as mean luciferase activity (relative light units, RLU) per well ± s.d..*

NIH 3T3. Efficiency was highest with Metafectene (45,370 ± 25,958 RLU), 40-fold higher than with TransPass D2. Maximal transgene expression was 48.9 ± 13.0%, obtained with a (v/w) lipid/DNA ratio of 5:1 (**Fig. 1**). IGF-I expression levels were 84.2 ± 16.9 ng/10^6 cells/24h, compared with 0.7 ± 0.7 ng/10^6 cells/24h in non-transfected cells.

DISCUSSION

Nonviral gene transfer methods can be optimized to achieve relatively high transfection efficiencies in primary cells and cell lines of musculoskeletal origin Our data further indicate that significant amounts of recombinant human IGF-I, a potential therapeutic candidate, can be secreted following nonviral gene transfer. These data may be useful for gene delivery approaches relevant in orthopaedic research using cell transplantation and in orthopaedic oncology.

REFERENCES

[1] Evans CH *JBJS Am.* **1995**, [2] Shao L *Biochem Pharmacol.* **2003**

ACKNOWLEDGMENTS

Supported by the Deutsche Forschungsgemeinschaft (DFG MA 2363/1-2 of HM). We thank L. Weissbach and F. Hornicek for providing the CS-1 cell line.

TOWARDS EARLY DETECTION OF OSTEOARTHRITIS: ASSESSING HUMAN ARTICULAR CARTILAGE BY SCANNING FORCE MICROSCOPY

‡Raiteri R, +‡Gottardi R, *Kilger R, †Aeschimann L, +Cardinali V, †Imer R, •König U, †Staufer U, +Stolz M, +Aebi U, *Friederich N
*Department of Orthopaedic Surgery & Traumatology, Kantonsspital, Bruderholz/Basel, Switzerland; +M.E. Müller Institute for Structural Biology, Biozentrum University of Basel, Switzerland, •Ortho Clinic Rhein-Main, Center of Shoulder and Knee Surgery, Offenbach am Main, Germany;
‡Department of Biophysical and Electronic Engineering, University of Genova, Italy; †Institute of Microtechnology, University of Neuchâtel, Switzerland
rr@unige.it

INTRODUCTION: Osteoarthritis (OA) is a painful and disabling progressive joint disease that is characterized by degradation of the articular cartilage and affects millions of people. OA poses a dilemma: it usually begins attacking different joints long before middle age, but cannot be diagnosed until it becomes symptomatic decades later, at which point the structure and biomechanical properties of the affected cartilage are usually irreversibly altered. Currently available devices for testing cartilage typically work at the millimeter scale or above [1-3, 6], therefore cannot resolve the cellular and molecular features of cartilage, i.e. the scale at which biomechanical processes occur and pathological lesions start. In contrast, the scanning force microscope (SFM) - the prototype of a nanotool – can readily image cartilage morphology and measure its biomechanical properties at the micrometer scale and beyond. Thus, the SFM opens the exciting possibility to detect pathological features of articular cartilage long before they become symptomatic and cause a functional impairment of the affected joint. Detection of OA at a presymptomatic stage might be key to develop effective therapies to slow down or stop its progression.
Hence, our objective was to evaluate the morphological and functional changes from healthy to osteoarthritic human cartilage by SFM.

METHODS: Cartilage was harvested from human donors suffering from osteoarthritis and therefore undergoing knee or hip arthroplasty, and from subjects undergoing knee arthroscopy using biopsy needles (~7 mm x 2 mm). The location of cartilage harvest was determined in a standardized manner and the chondrosis graded by three independent orthopaedic surgeons according to the Outerbridge classification (OA grade 0-IVº).
According to a previously described procedure [5], the specimen were stored at 4°C in phosphate buffered saline (PBS) at pH 7.2 supplemented with a protease inhibitor cocktail (Boehringer, Mannheim, Germany). For imaging, fresh cartilage samples were embedded and sectioned with a cryostatic microtome (SLEE, Mainz, Germany) at -15°C and adhered to glass coverslips. For stiffness measurements, the cartilage samples were glued onto a Teflon disc using histoacryl tissue glue.
All SFM experiments were performed using a Multimode® SFM (Veeco, Santa Barbara, CA). Images of articular cartilage topography were obtained in SFM contact mode at a scanning rate of ~2 Hz, in air on dehydrated thin-sectioned samples.
For testing the dynamic elastic modulus (E*) automated protocols were employed in combination with precision instruments that may enable the surgeon to perform a much more quantitative and objective inspection of the patient [5]. Spherical indenter tips for micrometer-scale measurements (radius = 7.5 µm, k = 8 N/m) and sharp pyramidal tips (radius = 20 nm, k = 0.06 N/m) were employed for probing micrometer-scale and nanometer-scale responses, respectively. E*-values were obtained at 3 Hz from 1024 unloading response curves recorded at a given location on cartilage.

RESULTS: Figure A and B show the difference of collagen alignment of healthy (grade 0º) and OA cartilage (grade IIIº). In Figure A the 67-nm axial repeat distance of individual collagen fibers was clearly resolved by SFM. In contrast to the normal cartilage that exhibited a random orientation of the collagen fiber network, in the diseased cartilage (Figure B) the collagen fibers coalesced and exhibited a preferred orientation (white arrows). This might follow the directed movement within the joint once the glycosominoglycans (GAGs) are digested in the course of the disease progression.
Indentation testing at the micrometer scale exhibited only small changes in stiffness with increasing OA grades (~2.6 MPa). At the nanometer scale instead a clear softening was observed, i.e. from 0.137 MPa to 0.009 MPa. As shown in Figure C, the comparison of the slopes of the force displacement curves indicated softening of articular cartilage for more severe ostheoarthritis.

DISCUSSION: The SFM not only provides us with the 'eyes' for imaging biological matter from the millimeter to the nanometer scale, but it also gives us the 'fingers' to measure the mechanical properties of cartilage. Imaging with micrometer-scale spherical tips cannot resolve fine-structural details [5], but the nanometer-scale pyramidal tips are resolving the individual collagen fibers, in imaging ('seeing') and indentation ('feeling') mode, and allow to directly probe the state of the soft gel-like GAGs moiety in between the collagen fibers. This finding, in turn, opens the prospect of early diagnosis, hopefully at a stage when disease progression can still be slowed down. To this end, an arthroscopic SFM is now being developed to measure articular cartilage stiffness directly *in situ* by a minimally invasive intervention.

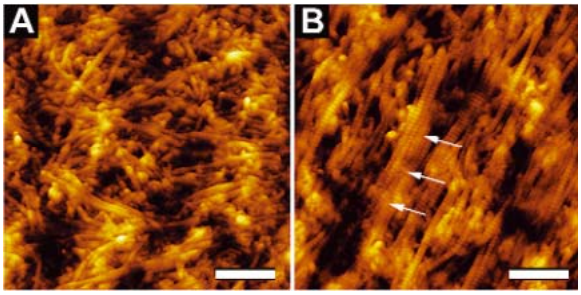

C **Indentation testing of human knee articular cartilage at different degrees of OA progression**

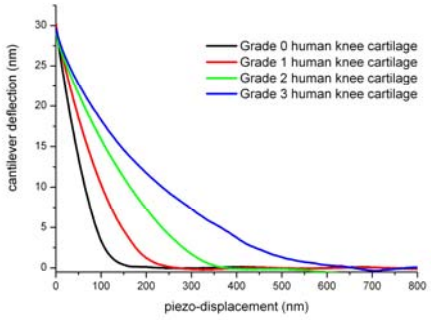

Figure 1: Surface topography of (A) normal articular cartilage (grade 0º), (B) osteoarthritic articular cartilage (grade IIIº), and (C) the corresponding elasticity measurements at the nanometer scale performed with a sharp pyramidal tip. Scale bars, 1 µm (A and B).

REFERENCES:
1. Appleyard *et al.*, 2001. Phys. Med. Biol. 46. **2.** Lyyra *et al.*, 1995. Med. Eng. Phys. 17. **3.** Shepherd and Seedhom, 1997. Proc. Inst. Mech. Eng. H. (J. Eng. Med.). 211. **4.** Stolz *et al.*, 2003. Bioworld (www.bioworld.ch). **5.** Stolz *et al.*, 2004. Biophys J 86. **6.** Tkaczuk *et al.*, 1982. J. Med. Eng. Technol. 6.

ACKNOWLEDGEMENTS:
This work was supported by a National Center of Competence in Research program grant on “Nanoscale Science” awarded by the Swiss National Science Foundation, the M. E. Müller Foundation of Switzerland, and the Canton Basel-Stadt.

WHICH CELLS ARE PIVOTAL IN ECTOPIC BONE FORMATION?

*Toom A, **Suutre S, **Arend A, *Märtson A
*Tartu University, Clinic of Traumatology and Orthopaedics, Tartu, Estonia
**Tartu University, Department of Anatomy, Tartu, Estonia
alar.toom@ut.ee

INTRODUCTION

Ectopic bone formation is a common phenomenon after total hip arthroplasty. It has been suggested that bone marrow stromal cells together with scattered microscopic bone debris may play a crucial role in ectopic bone formation after total hip arthroplasty. However, it was also demonstrated, that the perivascular multipotent cells, i.e. pericytes, can under controlled conditions be easily converted into osteochondral development [Diaz-Flores 1992]. Hence, a considerable source of cells with the osteogenic potential should be assumed everywhere where the vasculature can be found. Recently, using the rabbit-model, was shown that irradiation of the femoral canal resulted in a lower degree of ossification compared with irradiation of the surrounding musculature [Rumi 2005].

Aim: We intended to verify the hypothesis of the basic role of the cells originating from the femoral canal in ectopic bone formation.

MATERIALS AND METHODS

In order to verify this hypothesis, we designed a model of ectopic ossification, using the osteoconductive matrix and/or osteoinductive protein, in which case it was possible to allow or to completely restrict access for the femoral canal cells to the site of ectopic bone formation.

20 adult male Wistar rats were operated under general anesthesia using transgluteal approach. Gluteus medius muscle was pinched for 2 minutes with a standard clamp to produce muscular damage. Bilateral femoral capsulotomy was performed and an implant of beta-tricalcium phosphate was placed into capsulotomy wound. In a half of the animals, the implants were immersed in a solution of 12.5 μg rhBMP-2 per implant. Control implants were immersed in phosphate-buffered isotonic saline. On the right side femoral canal was opened exposing implant to the femoral canal cells. Animals were euthanized after 3 and after 21 days. Removed implants were dissected following principles of stereology. Sections were intended for histological investigation using azan and metachromatic staining as well as for immunohistochemical staining for osteocalcin, osteonectin and collagen-1.

Cell counting was performed and relative and absolute volumes of different types of tissues were estimated applying Cavalieri's principle and stereologic techniques.

Statistical calculations were performed using t-test for paired and unpaired data and, z-test. The Animal Ethics Committee at the University of Tartu has approved this study.

RESULTS

3 days. In all implants the pores were mostly filled with few inflammatory cells. There was no significant difference between the implants in the degree of cellular penetration. Also, some colonies of connective tissue cells with the low differentiation were presented, mostly in outer pores of implants. Their number was statistically different between the rhBMP-2 and saline treated implants: 5.22±1.67% and 1.31±0.35%, respectively, ($p=0.042$). There was no obvious difference between the implants where the femoral canal cells were present or absent in respect of their later cellular consistence. In the connective tissues surrounding the rhBMP-2 treated implants we detected numerous low differentiated connective tissue cells localized close to vessels in, but there was no difference between the legs with opened or unopened femoral canals.

21 days. In the implants immersed in saline there was detectable minimal formation of osteoid and cartilage on the surface of the outer pores, but there was no significant difference between the implants.

In all the implants immersed in rhBMP-2 there was presented significant bone formation. The ratio of bone volume to the total volume (BV/TV) in the implants with present or absent femoral canal cells was 33.1% and 30.0%, respectively ($p>0.05$). Also, the absolute volume of ectopic bone was similar. Moreover, comparison of those implants revealed, that bone mineralization has been faster in the group with unexposed implants, where the mineralized volume (Md.V/TV) was higher: 18.2% vs 12.7% ($p=0.019$).

DISCUSSION AND CONCLUSIONS

When the surrounding muscular tissues and the joint capsule were injured in similar way, there were no differences in the cellular function or intensity of bone formation between the implants with the presence or absence of femoral canal cells.

This, and also more advanced bone formation in the implants with absence of femoral canal cells indicates, that the main cause of ectopic bone formation can be damage of the surrounding tissue.

For clinical practice our suggestion would be focus on careful handling of the surrounding highly vascularized tissues rather than to attempt absolutely remove the bone debris generated by femoral canal reaming.

REFERENCES:

Diaz-Flores L et al. *Clin Orthop*. 1992;275:280–6.
Rumi MN et al J Bone Joint Surg Am. 2005; 87:366-73.

^{68}Ga-DOTA-PEPTIDE TARGETING VAP-1 FOR *IN VIVO* EVALUATION OF INFLAMMATORY AND INFECTIOUS BONE CONDITIONS

*Lankinen P, *Mäkinen TJ, **Pöyhönen T, **Virsu P, ***Jalava J, ****Jalkanen S, **Roivainen A, *Aro HT
*Orthopaedic Research Unit, Department of Orthopaedic Surgery and Traumatology, University of Turku, Turku, Finland.
Petteri.Lankinen@utu.fi

INTRODUCTION

Positron emission tomography (PET) using 2-[^{18}F]fluoro-2-deoxy-D-glucose (^{18}F-FDG) has been introduced as a promising imaging modality for the evaluation of various infectious conditions of the skeleton, but the diagnosis of infection in the postoperative states remains a diagnostic challenge. The problem is that early bone healing involves an inflammatory phase that represents a highly activated state of cell metabolism and glucose consumption, mimicking infection on ^{18}F-FDG PET imaging.

Vascular adhesion protein 1 (VAP-1) is a human endothelial protein. Its cell surface expression is induced under inflammatory conditions, making it a highly promising target molecule to study inflammatory processes *in vivo* by PET. This study evaluated the feasibility of a new ^{68}Ga-DOTA-peptide binding to VAP-1 for PET imaging of early inflammatory and infectious processes in healing bones.

METHODS

Sixty-eight adult male Sprague-Dawley rats (Harlan) weighing a mean of 434 g (SD 61 g) were used. The local Animal Welfare Committee and the Provincial State Office of Western Finland approved the study protocol. In each animal, the left tibia was operated and the right contralateral tibia served as the intact control. A standardized diffuse rat osteomyelitis model (Stage IVA in Cierny-Mader classification) was applied. A 1 mm cortical defect was drilled in the proximal tibial metaphysis, followed by an injection of sodium morrhuate and *Staphylococcus aureus* inoculum ($3x10^8$ CFU/ml) into the medullar cavity. The cortical defect was sealed with bone wax. In control animals, neither sodium morrhuate nor bacterial suspension was applied.

An explanatory time series analysis of PET-uptake in infected and control healing bones was performed at 12 hours, 24 hours, 36 hours, 7 days, 14 days or 28 days (n=2/group/time point). Based on the results of the time-series analysis, two time points (24 hours and 7 days) were chosen for the statistical comparison of PET-uptake (n=10/group/time point). Quantitative analysis of peptide uptake was performed on standardized circular regions of interest (d=3.0 mm) in the operated and intact tibias followed by the calculation of standardized uptake value (SUV). Peripheral quantitative computed tomography and plain radiography were performed immediately after PET imaging. Bone samples for quantitative bacteriology were taken. Specimens were also processed for histomorphometry of inflammatory and infectious reactions. All the results are expressed as the mean ± SD. The significance of differences between the study groups were estimated using linear models. The intra-animal comparison between the operated and non-operated sides was estimated using repeated measures ANOVA. In non-parametric analyses, the Fisher´s exact test was used. A *P* value of 0.05 was considered significant.

RESULTS

In the time series analysis, PET imaging showed uptake of ^{68}Ga-DOTA-peptide in both osteomyelitic (bacterial infection) and control (healing bone defect i.e. sterile inflammation) tibias during the first 36 hours after surgery. Thereafter, only the osteomyelitic tibias were delineated by PET.

In the pivotal experiment, the osteomyelitic and control animals showed a similar uptake of the ^{68}Ga-DOTA-peptide at 24 hours, but a significant difference at 7 days (P<0.001). In the osteomyelitic animals, a significant increase (P=0.002) in the SUV ratios was seen between the two time points (1.50 ± 0.16 and 1.87 ± 0.41 at 24 hours and 7 days, respectively). In the control animals, the measured SUV ratios showed a significant decrease (P<0.001) between the time points (1.48 ± 0.18 and 1.09 ± 0.08 at 24 hours and 7 days, respectively).

The inoculated pathogen was cultured from the pulverized bone specimens in all animals with induced osteomyelitis. The CFU/g of bone was $2.8 \pm 3.0 \times 10^7$ and $1.3 \pm 3.8 \times 10^9$ at 24 hours and 7 days after surgery, respectively. No bacteria could be cultured from specimens retrieved from the control animals.

DISCUSSION

The current study showed that PET imaging with this new ^{68}Ga-DOTA-peptide could accurately demonstrate the phase of inflammation in healing bones and the development of bacterial infection in osteomyelitic bones. The animals with healing bone defect showed a transient tracer uptake at 24 hours after surgery, which normalized by 7 days. In contrast, osteomyelitis resulted in increasing, locally intense uptake of the peptide analogously to the progress of infection.

The imaging technique could be applied to delineate the effects of anti-inflammatory agents on bone healing as well as in the evaluation of treatment response in antimicrobial studies of bone infection. From the clinical point of view, this new PET tracer could be valuable for the detection of infection at its early stages.

**Turku PET Centre, Turku University Hospital, Turku, Finland. ***Department of Human Microbial Ecology and Inflammation, National Public Health Institute, Turku, Finland. ****MediCity Research Laboratory; Turku, Finland.

PRELIMINARY WEAR RESULTS OF A NEW DESIGN OF ANKLE PROSTHESIS

*Leardini A, **Affatato S, **Leardini W, ***O'Connor JJ, **Viceconti M
Laboratorio *Analisi del Movimento, ** Tecnologia Medica, Istituti Ortopedici Rizzoli, Bologna, Italy

leardini@ior.it

INTRODUCTION

There has been renewed interest in total ankle replacement (TAR) following the introduction of more robust designs with more encouraging early clinical outcome. Research has been published on the mobility and stability of the natural and replaced ankle, and advanced modeling studies, including finite element analysis (1). However, in our knowledge no literature is available regarding wear tests of TAR specimens. The aim of this work was to evaluate the wear behaviour of a new three-part TAR design (2).

METHODS

Four full 'small' size Box prostheses (Finsbury Instr. Ltd, UK), made of metallic tibial and talar parts and a UHMWPE meniscus, were tested in a four station knee joint simulator (Shore Western, U.S.A.). The prosthesis features full conformity together with articular surface shapes in the sagittal plane compatible with isometric rotation of certain ligament fibers.

Before the components were tested, all specimens were pre-soaked for four weeks as recommended by international standards. In each station of the simulator, the implants were mounted in a neutral anatomical position, assumed as the zero position. The motion of flexion/extension was imposed on the tibial component, antero-posterior translations and axial rotation were imposed on the talar component and the meniscal bearing was left free to find its own position.

Curves of the relative kinematics and loading of the components were taken from a recent mechanical model of the ankle when replaced with the design under analysis (1). Range of motion, axial and A/P force, as well as an Int/External torque, had been taken from the literature for the simulation of the stance phase of walking, whereas the overall kinematics was predicted by the model. Plantar-/dorsi-flexion ranged between –10° and +20°, Int/External rotation ranged between -2.6° and 7.7°, the A/P displacement ranged between 0 and 8.45mm, the axial load had a maximum of 1600N. The A/P force and Int/Ext torque were also monitored during the test. A frequency of 1 Hz was used and deionized water was used as lubricant during the test under controlled temperature.

At intervals of about 0.05 million cycles, the specimens were removed from the simulator for weight measurements. Weight loss was calculated using a microbalance (SARTORIUS AG, Germany) with an uncertainty of about ±0.03 mg. The wear trend was assessed in terms of weight loss, as recommended by the international standard (ISO, 2000).

RESULTS

After $500x10^3$ cycles the weight loss for the three inserts were 5.18 mg, 4.02 mg, and 7.31 mg, respectively. The variation of the weight loss over the number of cycles performed for the three inserts is plotted in Figure 1.

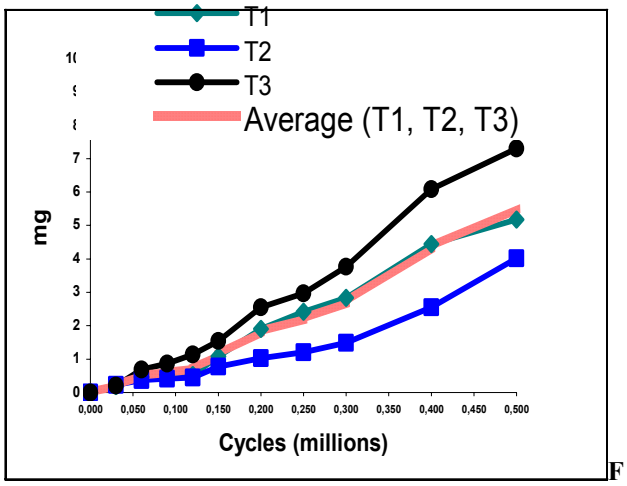

Fig. 1 – Wear trend of the ankle UHMWPE inserts.

The extrapolated average linear penetration after 500.000 cycles in the worst case is 0.0159 mm/Year.

DISCUSSION

Corresponding results from other TAR designs are not available. However, the extrapolated linear penetration of these test data compares very well with corresponding values reported for some knee and hip joints. In particular, it is well within the range obtained for the Oxford Unicompartmental Meniscal Knee from both retrieval, simulator and in vivo RSA (3) studies. This prosthesis which was designed according to criteria very similar to the presently analyzed TAR, i.e. fully congruous unconstrained meniscal bearing with articular surfaces designed to be compatible with ligament natural function. The wear risk might be even smaller considering the steady-state might have not achieved yet. Simulator tests on Oxford Knees demonstrated a reducing wear rate during the first one million cycles of testing before a steady state was achieved (4).

REFERENCES

1. Reggiani B. et al. J Biomech. 2006, in press
2. Leardini A et al. Clin Orth Rel Res 2004, 424
3. Price AJ et al. J Bone Joint Surg Br. 2005, 87(11)
4. Schroeder D, Scott RD Trans Orth Res Soc 2000, 446

AFFILIATED INSTITUTIONS FOR CO-AUTHORS

*** OOEC, University of Oxford, UK

INTER-LABORATORY CONSENSUS ABOUT *IN VITRO* STABILITY TESTING OF CEMENTED AND CEMENTLESS HIP STEMS

[a,b]Cristofolini L, [c]Duda G, [d]Prendergast PJ
[a]Medical Technology Lab, Rizzoli Orthopaedic Institutes, Bologna; and [b]Engineering Faculty, University of Bologna, Italy
cristofolini@tecno.ior.it

Loosening is the main cause of failure of cemented and cementless hip stems. The research groups in Bologna, Berlin and Dublin developed three *in-vitro* test protocols. The setup in Bologna[1] replicates different motor tasks, and includes interface micromotion measurement and cement damage assessment (Fig. 1). The setup in Berlin[2] simulates stair-climbing, actively simulating four muscles, while micromotions are assessed (Fig. 2). Dublin implemented a system[3] for tracking stem-bone 3D motion and for applying abductors, tensor-fasciae-late and vastus-lateralis through a linked-lever (Fig. 3). While we developed independent procedures, we came to common conclusions:

- Simulations should allow comparative *in-vitro* ranking, based on stems for which the clinical outcome is known
- Stair-climbing is more critical than walking. Baseline load history should simulate patient negotiating stairs. As failure is a rare event, demanding load profile should include other motor tasks, eventually stumbling.
- A sufficient amount of information exists about load and frequency in daily activities[4].
- Primary stability of cementless stems can be quantified with 1000cycles, by measuring bone-stem micromotion
- Long-term stability of cemented hips cannot be predicted by measuring migration alone, as some stems (eg: Exeter) migrate more than others without failing
- Trends of inducible and permanent micromotions are the best indicators of the tendency to stabilize/loosen.
- Composite femurs are advantageous test-bench, as they provide high consistency, and withstand long-term tests
- It should be mandatory to assess pre-clinically the short and long-term stability of hip stems with *in-vitro* tests.

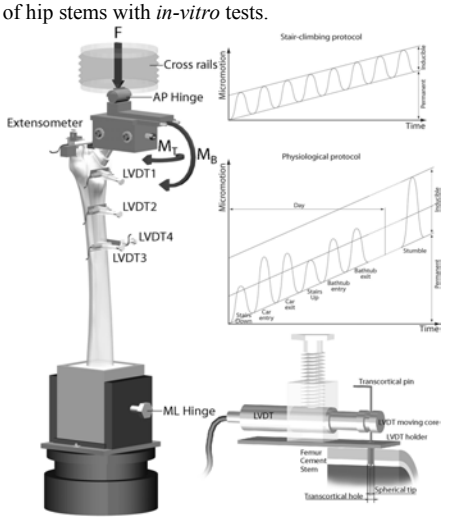

Fig. 1 – The setup used in Bologna, replicating different motor tasks (stair climb&descend, bathtub entry&exit, car entry&exit, stumbling), and measuring stem-cement interface micromotion

This work has shown that reliable protocols exist to test hip stem stability preclinically. A consensus exists among some major research groups about the best approach. It is hoped that in the future new designs will undergo thorough pre-clinical testing prior to clinical use.

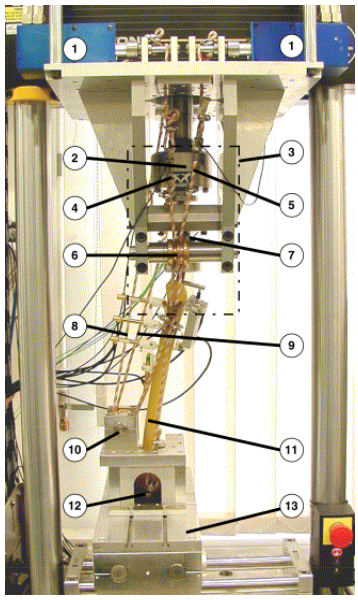

Fig. 2 –Setup used in Berlin: (1) muscle force actuators; (2) actuator with load cell; (3) loading ropes representing: (3) tensor fascia latae, (5) abductors, (8) vastus lateralis; (9) vastus medialis; (6) pulleys to adjust the direction of the muscle forces; (7) 3D load cell to record the joint force; (10) pulleys to adjust the direction of the distal muscles; (11) implanted composite femur, with movement transducers to record the load-induced interface movements; (12) distal ball bearing of the femur; (13) x–y table to adjust the adduction and flexion angles of the femur.

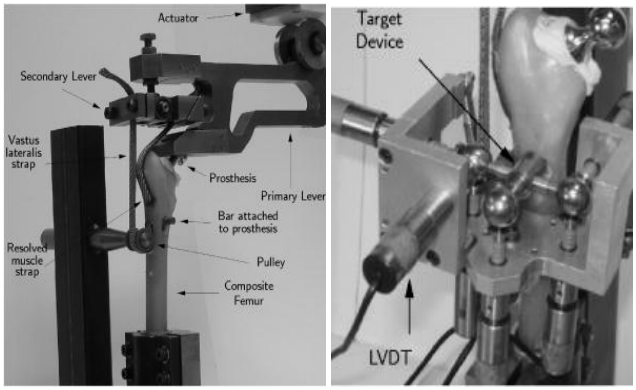

Fig. 3 – Linked lever (top) and stem-position tracking device developed in Dublin

REFERENCES

1. Cristofolini *et al.* (2003) JBiomech.36:1603-15
2. Kassi JP *et al.* (2005) J. Biomech. 38:1143-54
3. Britton, Prendergast (2005) J.Biomech.Eng. 127, 872-80.
4. Bergmann (2001) "Hip98 - Loading of the hip joint" CD

AFFILIATED INSTITUTIONS FOR CO-AUTHORS

[c] Charité – Univ. Medicine, Center for Musculoskeletal Surgery, Berlin, Germany. georg.duda@charite.de
[d] Trinity Centre for Bioengineering, School of Engineering, Dublin, Ireland. pprender@mail.tcd.ie

VIBRATION ANALYSIS ON PARTIALLY CEMENTED CUSTOM HIP STEMS: A PER-OPERATIVE STUDY

*Jaecques SVN, *Pastrav LC, **Mulier M, *Van der Perre G.
*K.U.Leuven, Division of Biomechanics and Engineering Design, Leuven, Belgium
Siegfried.Jaecques@mech.kuleuven.be

INTRODUCTION

A change in the stability of an implant can be indicated by an alteration of the vibrational behaviour of the implant-bone structure [1, 2, 3].
This experimental study presents the frequency response function (FRF) change between two different fixation stages of total hip replacement (THR) stems in per-operative conditions.

MATERIALS AND METHODS

The experiments were performed on custom made hybrid hip stems (Advanced Custom Made Implants, Leuven, Belgium) that were partially cemented distally [4]. In a first stage, the surgeon inserts the stem completely in the femur without cement, for a trial reduction of the artificial joint. In a later stage, the stem is removed, cement is introduced in the distal part of the cavity, the stem is re-introduced and after the cement has fully cured, the implant should be well fixed. In both stages the FRF of the stem-femur structure is measured in the range 0-10000 Hz using a Pimento vibration analyser (LMS International). The neck of the prosthesis is excited by a shaker with white noise. The input force and the response acceleration are measured in the same point using an impedance head. In some cases, an auxiliary accelerometer was used. Nine volunteering patients in the orthopaedic hospital Pellenberg were included in this study after informed consent and approval by the institutional review board.

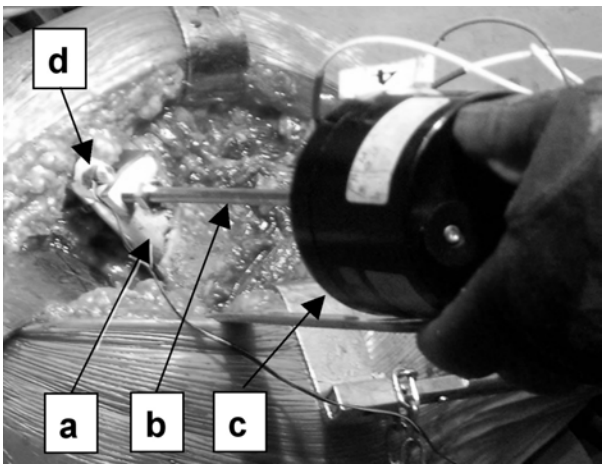

Fig. 1 *Shaker excitation on prosthesis: (a) hip stem; (b) stinger & clamping system; (c) shaker; (d) auxiliary accelerometer.*

RESULTS

In seven cases (77.8%) an important difference was observed between the two FRF graphs, in frequency and amplitude; a typical example is shown in fig. 2. In the other two cases, although an amplitude alteration could be noticed, the resonance frequencies did not substantially change; fig. 3 shows a typical example.
In all cases the highest FRF peaks were found above 4000-5000 Hz.

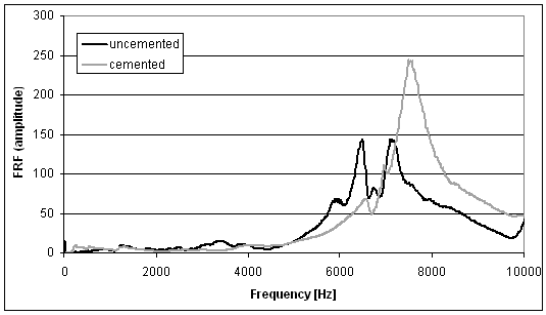

Fig. 2 *FRF of uncemented first stage (black line) and after cement curing (grey line). One of seven similar cases where the resonance frequencies increased.*

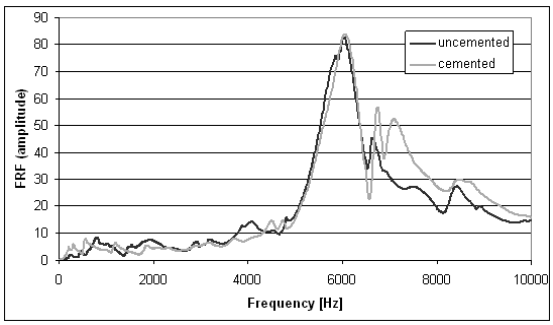

Fig. 3 *FRF of uncemented first stage (black line) and after cement curing (grey line). One of two similar cases where the resonance frequencies did not increase noticeably.*

DISCUSSION

In the first stage, the uncemented stems are well fixed only in the proximal part because the distal part is thinner than the corresponding femoral cavity. The stability of the same implants should increase in the second stage because the distal part is fixed in cement. In seven cases the FRFs shifted to the right indicating an increased stiffness, i.e. an increased stability. In two cases the resonance frequencies corresponding to the highest FRF peaks did not increase. The interpretation could be that in these cases the implant stability did not considerably change after cementation.

CONCLUSION

In a per-operative pilot study, it was shown that the primary stability of a partially cemented hip stem can be evaluated by resonance frequency analysis.

REFERENCES

[1] N.Meredith et al, Clin Oral Impl Res, 1997; **8**(3):234-243.
[2] S.V.N. Jaecques et al, Proc. ESDA 2004, 19-22 July 2004, Manchester, UK, Paper ID 58581, 10 pp.
[3] Georgiou A.P., Cunningham J.L., Clin Biomech, 2001; **16:**315-323.
[4] Mulier JC et al Clin Orthop Rel Res 1989;249:97-112.

ACKNOWLEDGEMENT

Funded in part by K.U.Leuven grant OT/03/31.

AFFILIATED INSTITUTIONS CO-AUTHORS

**Dept. Orthopaedic Surgery, Univ. Hospitals Leuven.

THE EFFECT OF IMPLANT DESIGN AND BONE QUALITY ON MICROMOTION OF UNCEMENTED ACETABULAR CUPS

*Janssen D, **Zwartelé RE, **Doets HC, *Verdonschot N
*Orthopaedic Research Laboratory, Radboud University Nijmegen Medical Centre, Nijmegen, The Netherlands
n.verdonschot@orthop.umcn.nl

INTRODUCTION

It is sometimes suggested that cementless acetabular cups designed with a polar clearance provide a beneficial stress distribution in terms of bone remodelling. The initial implant stability of such a design may, however, be reduced when compared to conventional hemispherical cups. Especially in case of poor bone stock such an implant may become unstable, thereby affecting bone ingrowth. In the current FEA study the stability of a cup with a polar clearance design was analysed in combination with various implant-bone interface conditions, and compared with a hemispherical cup.

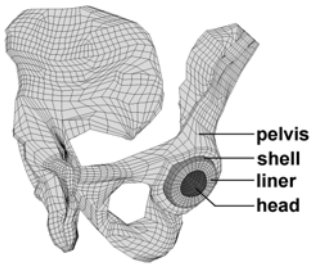

Figure 1. FE model of the pelvis with a cementless acetabular implant

METHODS

A cementless acetabular cup with a polar clearance (flat cup) and a conventional hemispherical cup (sphere cup) were introduced into an existing FEA model of the human pelvis [1]. Elastic-plastic material properties were assigned to the subchondral and cortical bone. In the models the quality of subchondral bone, the level of underreaming and friction coefficient were varied. During a walking cycle, muscle forces and the hip joint contact force were applied in eight phases. During each simulation, first, one walking cycle was simulated for pre-conditioning of the model, after which the steady state cyclic micromotions were monitored during a second walking cycle. Additionally, bone-implant normal contact stresses were monitored.

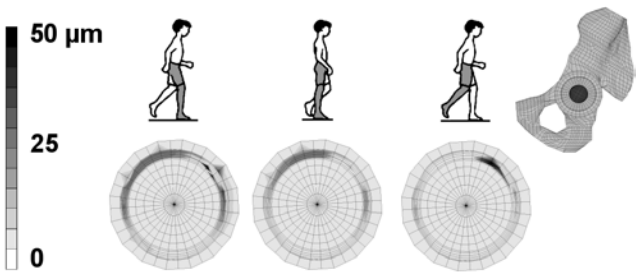

Figure 2. Interface micromotion patterns during the phases in which the highest micromotions occurred. The position of the pelvis is indicated in the upper right corner.

RESULTS

The highest interface micromotions occurred during the beginning of and halfway the single support phase and at the beginning of the swing phase (Figure 2). In case of good bone stock, the maximum interface micromotion for the flat cup was lower than that of the hemispherical cup (21 µm vs. 25 µm, see Figure 3). The maximum micromotion was increased in case of poor bone stock (74 µm for the flat cup vs. 33 µm for the hemispherical cup). Increasing the press-fit reduced these micromotions (60 µm for the flat cup). In case of a lower friction coefficient or no underreaming, micromotions increased dramatically (178 and 309 µm, respectively). The compressive contact normal stresses were highest at the beginning of the single support phase (phase 2, see Figure 3). The maximal normal contact stresses were the highest for the flat cup with a low friction coefficient (148 MPa) and the lowest for the flat cup without underreaming.

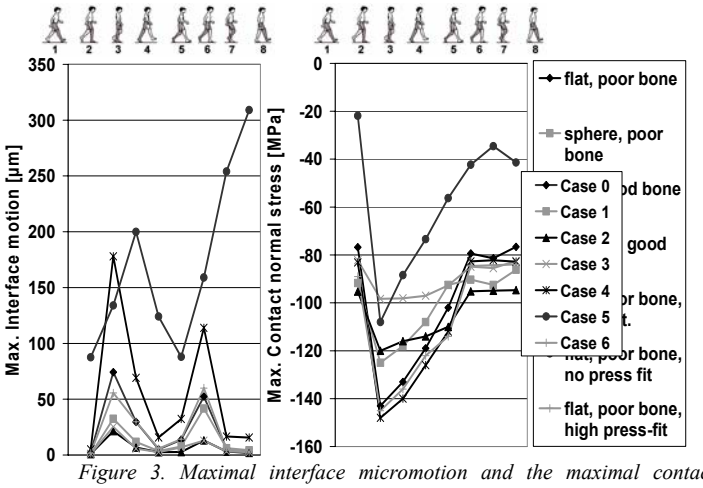

Figure 3. Maximal interface micromotion and the maximal contact normal stresses during one walking cycle for the various models.

DISCUSSION

Optimal interface conditions are essential in order to minimize micromotions of cup designs with a polar clearance. This study indicates that in case of such a design good bone stock improves the chances for adequate fixation. In case of poor bone stock, implant fixation can be improved by increasing the level of underreaming.

REFERENCES

[1] Dalstra and Huiskes, J Biomech 28, 1995

ACKNOWLEDGEMENTS

This work was supported by Plus Orthopedics AG, Switzerland

AFFILIATED INSTITUTIONS

**Slotervaartziekenhuis Amsterdam, The Netherlands.

COMPUTATIONAL SIMULATION OF OSSEOINTEGRATION IN TOTAL HIP REPLACEMENTS

Pérez MA, Moreo P, García-Aznar JM, Doblaré M
Group of Structures and Material Modelling Aragón Institute of Engineering Research (I3A)
University of Zaragoza, Zaragoza, Spain
angeles@unizar.es

INTRODUCTION

Aseptic loosening is one of the major and challenging problems in cementless hip implants [1]. Radiolucent lines, which may be an indication of long-term loosening, have been observed at the bone-implant interface of total hip replacements. The principal cause of aseptic loosening is the lack of primary stability. A stable immediate (primary) fixation is a requirement for a successful secondary fixation by bone ingrowth. Several computational studies have simulated bone ingrowth, but they do not consider the full evolutive process of this kind of interfaces. This paper proposes a computational model able to simulate the evolutive behaviour (deterioration and osseointegration) of living interfaces.

METHODS

Mechanical interface model

The interface model proposed is based on a combined theory of damage-repair, grounded in the theory of Continuum Damage Mechanics. The formulation of the interface model is established in terms of the normal and tangential components of the tractions and relative displacements, depending on four mechanical properties of the bone-implant interface in each direction: initial linear stiffness, maximum relative displacement, critical failure energy and apparent strength. We assume that failure of the interface only takes place under shear or tensile loading, not under compression. To avoid penetration under compression a Coulomb frictional model is added. The state variable that describes the bonding degree of the bone-implant interface (α) defined as the relation between the initial linear stiffness in a completely osseointegrated interface and the current one. An explicit evolution for α is proposed based on experimental data, and also fatigue failure of the bone-implant interface is considered.

Finite element (FE) modeling

The model proposed has been applied to simulate bone ingrowth at the bone-implant interface in a Zweymüller non-cemented prosthesis (Allo Pro, Baar, Switzerland). A 3D FE model was developed. Initially, the bone-implant interface is completely debonded (α=0), a period of one week with null loading conditions is simulated, and then 300 days of healthy activity are simulated, combining four different load cases: walking, standing, stair climbing and resting.

RESULTS

The evolution of the bonding degree (α) for a stainless steel stem has been represented in Figure 1. Initially the bone-implant interface is completely debonded (α=0). After the period of one week with null loading condition a partial osseointegration is achieved: values of the bonding degree vary from 0.6 at the proximal and distal regions to 0.8 in the rest of the interface. Bone ingrowth continues and after 20 days of loading most of the bone-implant interface is fully osseointegrated (α>0.9), except the distal and proximal regions (α<0.2).

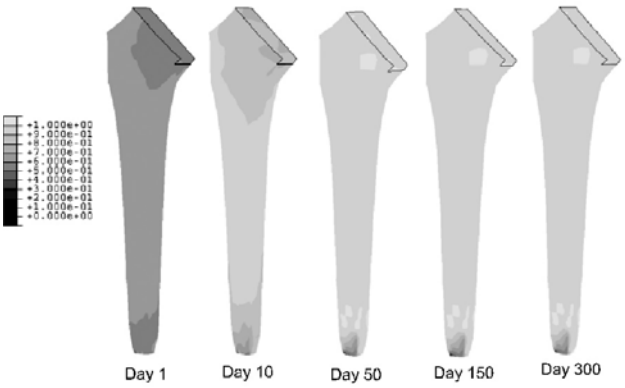

Figure 1. Evolution of the bond parameter (α) with the stainless steel stem (E=210 GPa) since the week with null loading state.

Several analyses were also performed in order to analyze the influence of important factors such as: the stem stiffness, the patient activity, the surface finishing of the stem or the mechanical properties of the stem-bone interface.

DISCUSSION

The model here presented is able to reproduce progressive deterioration and bone ingrowth at the same time. Although, the model currently exhibits several limitations mainly due to the lack of experimental tests, this methodology offers a systematic technique to determine the influence of several mechanical factors on the bonding degree of the bone-implant interface and the performance of cementless implants.

REFERENCES

[1] Malchau et al. (2000). 67th Meeting of the American Academy of Orthopaedic Surgeons, Orlando, Fl. USA.
[2] Bücher et al. (2003). Biomechan Model Mechanobiol, 1(4), pp 239-249.

ACKNOWLEDGMENTS

This research was performed within project CICYT FIS2005-05020-C03-03 (2005-2008), whose help is highly appreciated.

ON THE BONE VOLUME RESECTED AND FIXATION FOR ACETABULAR COMPONENTS OF HIP RESURFACING

*Winzenrieth R, *Plamondon D, **Lavigne M, **Vendittoli PA, *Nuño N
*Département de génie de la production automatisée, École de technologie supérieure, Université du Québec Montréal, Canada

natalia.nuno@etsmtl.ca

INTRODUCTION

A clear advantage of surface arthroplasty of the hip (SRA) over total hip arthroplasty (THA) is femoral bone stock preservation [1]. Modern metal-metal SRA component present different geometric characteristics generating different volumes of acetabular bone resection when placing the prosthesis inside the pelvis [2]. A good fixation of the prosthesis is crucial for the long-term survivorship of the arthroplasty. It is necessary for the surgeon to reach a compromise between minimal bone loss, for a future revision necessary approximately 15 years later, and the optimum contact area between the prosthesis and the surrounding bone to achieve good fixation. The aim of this study is to determine the volume of bone resected and their corresponding contact area for different acetabular components of hip resurfacing.

METHODS

A 3D pelvis is reconstructed from CT scans of Vakhum project (www.vakhum.com). The acetabular component of Durom hip resurfacing and the hemispherical reamer used by the surgeon to perform the arthroplasty are modeled using the commercial software *Catia v5*.

The acetabular cup component implantation in the model mimics the clinician when performing the surgery. The hemispherical reamer, a surgical tool, is used to prepare the inside of the acetabular fossa of the pelvis. Then, the acetabular component is placed into the reamed acetabular fossa. The amount of volume resected to fix the acetabular component into the pelvis is computed as the interference between the pelvis and the component (nominal outside cup diameter). The percentage of the contact area is computed as the ratio between the reamed bone surface area of the acetabular fossa and the external surface area of the acetabular cup. A good fixation can be obtained with 70-80% of contact area. All analyses are solved using the software *Catia v5*.

In this study, the effect of the geometric characteristics of SRA acetabular cup on the volume of bone resected and percentage of contact area is studied. The edges of the acetabular cavity are used to define the anatomical reference plane. The cup is placed in the orthopaedic position (45° abduction and 20° anteversion). The cup component has a covering angle set as 165°, 170° (not complete hemispheres) and 180°. In addition, the implantation depth, below the anatomical reference plane, are set as 0, 1, and 2 mm.

RESULTS AND DISCUSSION

For the pelvis considered in this study, the surgeon will choose between different femoral head components available commercially (i.e. diameter of 48, 50 and 52 mm) and the corresponding acetabular component (i.e. nominal external diameters of 54, 56 and 58 mm). Figure 1 shows the contact area between the acetabular component and the pelvis. Intuitively, as the implantation depth increases, the contact area percentage also increases, consequently leading to a greater amount of resected bone. For example, the results show that for an acetabular cup of 56 mm in diameter, changing the implantation depth from 0 to 1 mm increases the contact area by 10%, but the bone volume resected increases by 30%. Further increasing the depth to 2 mm increases the contact area by another 6% and increases the bone volume by more than 30%. For the same implantation depth (i.e. 0 mm), selecting a larger acetabular cup (58 mm diameter instead of 56 mm) increases the contact area by only 7% while increasing by almost 70% the bone volume removed.

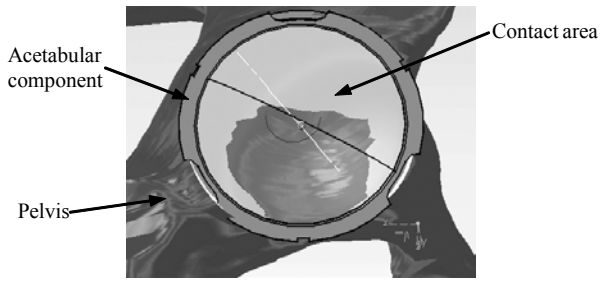

Figure 1. Acetabular component positioned inside the reamed acetabular fossa.

The choice of the acetabular component and its implantation inside the pelvis has a significant influence on bone resection and component fixation. A compromise needs to be reached between size of the component, depth and contact area.

REFERENCES

[1] Amstutz et al. (2004) J Bone Jt Surg Am. 86-A: pp.28-39.
[2] Grigoris et al. (2005) Orthop Clin North Am 36, pp.125-134.

ACKNOWLEDGEMENTS

Zimmer, Warsaw
**Département d'Orthopédie, Hôpital Maisonneuve-Rosemont, Montréal, Canada.

A PROSPECTIVE RANDOMISED TRIAL COMPARING MINIMAL INVASIVE AND STANDARD PARAPATELLAR APPROACHES FOR UNICOMPARTMENTAL KNEE ARTHROPLASTY

*Jackson MP, Cottam HL, Apthorp HD, Butler-Manuel PA
*The Conquest Orthopaedic Research Unit, Hastings, UK

howie@doctors.org.uk

INTRODUCTION

We investigated the advantages of the minimal invasive approach in the early post-operative stage, comparing outcome measures in a randomised group of patients undergoing unicompartmental knee arthroplasty.

METHODS

100 patients on the waiting list for UKA were recruited into the trial for which local ethical approval was obtained. Patients were randomised into 2 groups:
Group 1 - longitudinal skin incision with dislocation of the patella
Group 2 - the minimal invasive approach.
Standard milestones were recorded post-operatively: time to achieve IRQ, independent stair climbing and to discharge. Additionally, patients were scored with the American Knee Society Score and Oxford Knee Questionnaire pre-operatively, at 6 weeks, 6 months and 1 year.

RESULTS

No significant differences were found between the two groups in the measured parameters.

CONCLUSION

To our knowledge, there has been no previous randomised trial to investigate the results of less invasive surgery for UKA. We have been unable to demonstrate a significant advantage of this approach. With the continued drive for early return to function, some centres incorporate a 24hr accelerated discharge protocol. The less invasive approach may make this more achievable. We recommend however that the surgical procedure and implant position must not be compromised for the benefit of rapid discharge to the deficit of long term results.

MEASUREMENT OF SOFT TISSUE BALANCE DURING TOTAL KNEE REPLACEMENT SURGERY: A TEN YEAR RETROSPECTIVE STUDY

*Attfield SF, *Wilton TJ, ** Pinnington LL
Derby Hospitals NHS Foundation Trust, England
steve.attfield@derbyhospitals.nhs.uk

INTRODUCTION

The importance of soft tissue balance (STB) for the long term outcome of total knee replacement (TKR) surgery has been the subject of debate for several years. Whilst it is commonly accepted that gross soft tissue contracture should be corrected during surgery, it is not clear how much residual soft tissue imbalance can be tolerated. Many authors claim that if a knee is 'correctable', by passive varus/valgus force, this is satisfactory[1], whereas others attempt to reduce imbalance to an absolute minimum[2]. The procedures for soft tissue release are well established and are carried out partly to reduce the asymmetric passive forces exerted on the implant. By taking precise measurements of STB, it is hoped that the number of prostheses that fail due to biomechanical factors will be reduced. Survival of TKR prostheses is often measured after a ten year interval[3] and both surgical revision and/or the presence of pain[4] have been used as the main outcome variables.

METHOD

The health records of 137 patients, (182 knees) who underwent total knee replacement surgery between 1990 and 1994 for osteoarthritis of the knee were studied. All operations carried out between 1990 and 1992 followed standard surgical procedures and included an examination of soft tissue tensions and balances by manual palpation. All patients treated between 1993 and 1994 underwent comparable operations, however soft tissue tensions were measured objectively using a Soft Tissue Balancer[5], at zero and 90 degrees of knee flexion. Soft tissue releases were performed on the basis of clinical judgment at either the prosthesis trial stage or following measurements of STB. The health records were reviewed to establish the incidence of TKR failure during the ten year follow-up period. Prostheses were judged to have failed, if one of the following events was reported: a) component failure/loosening due to biomechanical factors b) presence of symptoms sufficiently severe to warrant a clinical intervention e.g. provision of an injection c) Moderate / severe pain[6].

RESULTS

Ninty one knees were followed up in each of the two groups (75 males, 107 females). The mean age of the patients was 70.2yrs (Comparison) and 69.7 yrs (Measured) 28.6% of the cases were reported as failures in the comparison group (5.5 % Clinical and 23.1% Biomechanical) compared to 15.4% in the measured group (7.8% Clinical and 7.8% Biomechanical). Although a difference was noted between the thickness of the tibial inserts used during the four year period studied, only a marginal difference was present between the thickness of inserts within each cohort. (Comparison 10.1mm full group, 10.5mm failed subsection. Measured 12.8mm full group, 12.7mm failed sub group). The mean years to failure was also longer in the measured group (4.1 compared to 3.7yrs). The percentage of cases that required significant soft tissue balancing was 66.0% for the Measured group compared to 38.5% in the Comparison group. The ten year Kaplan-Meier survival curves can be seen below.

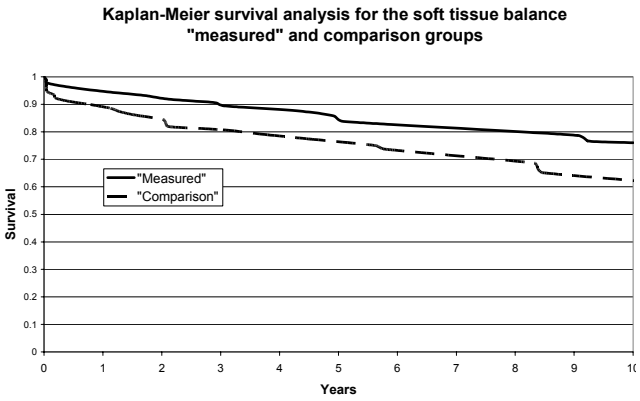

DISCUSSION

This study evaluated the outcome of 182 prosthetic knees fitted over a four year period by three orthopaedic surgeons using one type of TKR prosthesis and has shown that there are considerable differences in the outcome of prostheses fitted under measured and standard conditions. This project documents the clinical significance of measuring soft tissue imbalance for the first time and indicates that the failure rate of TKR components arising from biomechanical factors can be reduced. Further research is now required to investigate the effects of STB measurement prospectively.

REFERENCES

1. Moreland JR. Mechanisms of failure in total knee arthroplasty. Clinical Orthopaedics & Related Research 1988-226:49-64.

2. Wilton T, Sambatakakis A, Attfield SF. Soft tissue balancing at the time of knee replacement: rationale and method. The Knee 1994;(1):111-6.

3. Ansari S, Ackroyd CE, Newman JH. Kinematic posterior cruciate ligament-retaining total knee replacements. A 10-year survivorship study of 445 arthroplasties. American Journal of Knee Surgery 1998;11-1:9-14.

4. Murray DW, Frost SJ. Pain in the assessment of total knee replacement. Journal of Bone & Joint Surgery - British Volume 1998;80-3:426-31.

5. Sambatakakis A, Attfield SF, Newton G. Quantification of soft-tissue imbalance in condylar knee arthroplasty. Journal of Biomedical Engineering 1993;15-4:339-43.

6. Murray DW, Carr AJ, Bulstrode C. Survival analysis of joint replacements. Journal of Bone & Joint Surgery - British Volume 1993;75-5:697-704.

** Division of Rehabilitation & Ageing, University of Nottingham, England.

A NAVIGATED DRILL GUIDE USING AN INSTRUMENTED LINKAGE FOR THE PLACEMENT OF CUTTING JIGS DURING TOTAL KNEE ARTHROPLASTY

*Balicki MA, *Forman RE, +*Walker PS, **Wei CS, *White B, *Roth J, *Klein GR
+*New York University-Hospital for Joint Diseases Orthopaedic Program, New York, NY

ptrswlkr@aol.com

INTRODUCTION

Computer-assisted surgery using optical navigation for the placement of slotted cutting jigs has reduced the number of outliers and has provided other advantages (Victor & Hoste, 2004; Sparmann et al, 2003). However, such navigation systems are expensive and still retain much of the original instrumentation. The purpose of our study was to determine the accuracy of navigating pin placement for slotted cutting guides using an instrumented linkage. We tested the simplicity of the system and whether the results would be independent of operator experience.

MATERIALS & METHODS

The experimental plan was to navigate the placement of a slotted cutting guide onto a simulated tibia using the navigated drill guide, to perform a tibial resection using an oscillating saw, and to measure the cut accuracy. A six degree-of-freedom MicroScribe G2LX (Immersion Corp) instrumented linkage with a point accuracy of 0.23 mm at the tip was used. This was rigidly anchored next to the foam plastic tibia (Sawbone) which has comparable mechanical properties to an actual tibia (Fig. 1). Points on the tibia holder and on the upper tibia were used to define the target resection plane 10mm below the tibial surface. A dual drill-guide with holes corresponding to those of the slotted saw guide was attached on the end of the linkage. PC-based software was written to determine the location of the tibia, to track the drill guide and to navigate the placement of the drill guide against the anterior tibia (Fig. 2). The surgeon positioned the guide by aligning a set of circles on the computer screen, one for target hole position on the bone and the other set for orientation. Pins of 3.2 mm diameter were then tapped into the holes. The slotted saw guide was placed over the pins and the upper tibial resection made. The MicroScribe was used to measure the accuracy of the mean depth and the angle in frontal and sagittal planes. The system was tested by a medical student, a resident trainee, and a senior total knee surgeon, each cutting 10 tibias.

RESULTS

The mean results of all three operators were within 0.5 mm of the target depth and 1.2 degrees in both frontal and sagital planes (Fig. 3). The overall mean errors and standard deviation were as follows: the level of the cut surfaces was 0.19 ± 0.48 mm, the frontal plane angle was 0.66 ± 1.14 degrees and the sagittal plane angle was 0.88 ± 0.72 degrees.

DISCUSSION

The mean errors in the depth of cut and in the angles were small in the context of knee replacement. The error in the sagittal plane was due to motion of the cutting guide during cutting and the bending of the saw blade. Small proximal-distal inaccuracies in pin insertion were a source of error for the frontal as well as sagittal planes. Even further improvement in accuracy has subsequently been achieved by directly drilling the pins into the bone, and using a third pin to further anchor the cutting guide. The simplicity of the system was demonstrated by the fact that each operator was comfortable after only one trial, because each step was easy to perform and the computer graphics intuitive. There was also no 'risk' involved with the drilling process even while glancing at the computer screen. No one operator was more accurate than any other, overall. This may have been because of the small inherent errors in the system, and the absence of errors of any significant magnitude.

Our current step is the incorporation of an instrumented linkage into a complete surgical procedure. Other applications using an instrumented linkage are also possible, including freehand navigation with a saw attachment (Walker et al, 2002, 2003). The common factors are speed, accuracy, and simplicity.

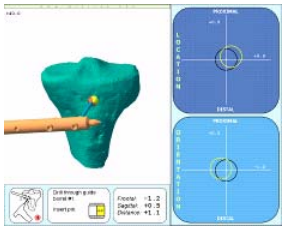

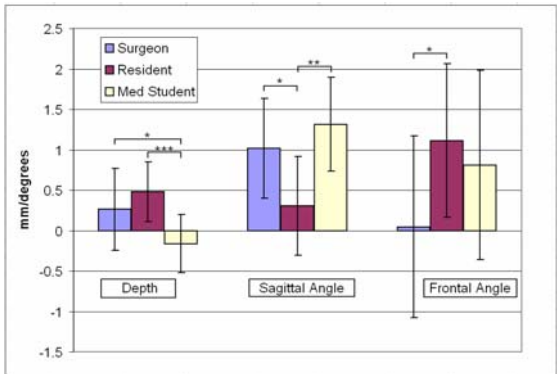

ADAPTIVE BONE REMODELLING OF ALL POLYETHYLENE UNICOMPARTMENTAL TIBIAL BEARINGS

***Gillies RM, *Hogg M, ***Cordingley R, ***Kohan L
*WorleyParsons Advanced Analysis, L1, 95 Nicholson Street, St Leonards, Sydney, NSW 2065, Australia
Mark.Gillies@WorleyParsons.com

INTRODUCTION

Bone is a dynamic tissue known to respond to imposed loads and remodel [1, 2]. Unicompartmental knee replacement (UKR) clinical results are equivalent to total knee replacement (TKR) results [3]. The reasons for failure of UKR and TKR are similar and are normally due to the reduction in bone mineral density [4]. This has been hypothesised to occur due to a reduction in the stress distribution [2, 5]. UKR has the additional risk of progressive osteoarthritis in the retained compartments [6]. Khan et al. (2004) investigated 30 patients three times by blind and randomized assessment to measure the progression of osteoarthritis within the remaining compartments. They concluded that progression of arthritis in the unreplaced compartments is not a significant problem after fixed bearing UKR. We have modeled all polyethylene tibial components and investigated the periprosthetic adaptive remodelling of the bone.

METHODS

CT scans were used to reconstruct the tibial geometry. A 3D finite element mesh was created using PATRAN (MSC Software, Santa Ana, CA). Two models were generated for each design (Fig 1.) (Eius, Stryker Orthopaedics, Mahwah, NJ and St Georg Sled, Waldemar Link, Germany), a preoperative and a postoperative state model. UKR implants were modeled as inlay designs. Cement mantles were modeled also. The bone mineral density changes at 3 ROI were measured using Global Lab Image/2 (Data Translation, Marlboro, MA) and plotted for a period of 36 months.

Figure 1: All polyethylene unicompartmental designs. St Georg Sled (L) and Eius (R)

RESULTS

Figure 2 presents the change in bone mineral density for both all polyethylene components. All ROI became stable at the 12 month time-point. Predictive bone mineral changes where minimal in both resorption and deposition. These findings are consistent with the clinical experience of UKR [6, 7].

DISCUSSION

There is no literature on the BMD changes following UKR. There is, however, a large amount of literature [6, 8-10]on radiographic and quality of life follow-up studies

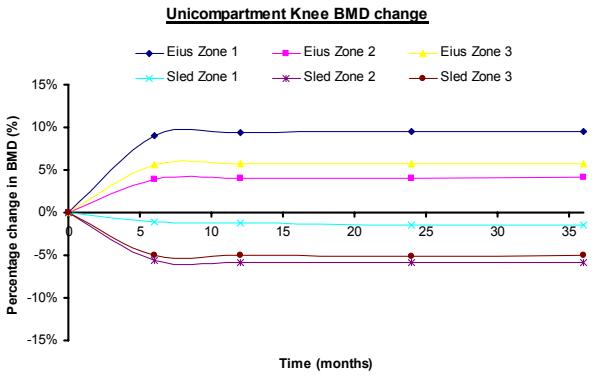

Figure 2

of UKRs. These studies investigate the expected life of the implants and it is clear that in approximately 95% of the cases, with a 95 to 98% survival, they are revised due to osteoarthritic changes in the lateral compartment[6, 8]. In this study, it is assumed that activity levels of the patient are unchanged following surgery. The finite element predictions illustrate that the Eius component tends to cause the bone to increase in density, whereas the there is a very small amount of resorption for the St Georg Sled. The decrease in BMD for the St Georg Sled would due to the stress shielding induced by the keel, which has increased the flexural rigidity of the implant. The survival of each implant would not be affected by the increase or decrease in BMD and the changes would not be clinically relevant. As mentioned in the introduction, the literature has the revision of the UKR due to arthrosis in the contralateral compartment. This study has shown, by investigating the change in BMD that the Eius and St Georg Sled UKR loads the proximal tibia and maintains the supporting subchondral bone density and structure and that a change in geometry will influence the loading environment and as a consequence the adaptive response of the bone is also influenced.

REFERENCES

1.Whiteside, L.A., *et al.*, Clin Orthop, 1989(239): p. 168-77.
2.van Loon, C.J., *et al.*, Acta Orthop Belg, 1999. **65**(2): p. 154-63.
3.Newman, J.H., *et al.*, J Bone Joint Surg Br, 1998. **80**(5): p. 862-5.
4.Weale, A.E., *et al.*, J Bone Joint Surg Br, 1999. **81**(5): p. 783-9.
5.Parry, B.R., *et al.*, Orthopedics, 2000. **23**(10): p. 1051-6.
6.Khan, O.H., *et al.*, Knee, 2004. **11**(5): p. 403-7.
7.Weale, A.E., *et al.*, J Bone Joint Surg Br, 2000. **82**(7): p. 996-1000.
8.Ashraf, T., *et al.*, Knee, 2004. **11**(3): p. 177-81.
9.Gleeson, R.E., *et al.*, Knee, 2004. **11**(5): p. 379-84.
10.Yang, K.Y., *et al.*, Singapore Med J, 2003. **44**(11): p. 559-62.

** Graduate School of Biomedical Engineering, UNSW, Sydney
*** Joint Orthopaedic Centre, Sydney

DOES LIGAMENT BALANCING TECHNIQUE AFFECT KINEMATICS IN ROTATING PLATFORM KNEE ARTHROPLASTIES?

*Jayasekera N, *Kashif F, **Schmotzer H, **Fennema P, ***Simms M, ***Gamada K, ***Banks S
*Mayday Hospital, Croydon, U.K

Naja01@doctors.org.uk

INTRODUCTION: Ligament balance is thought to play a particularly important role in the function of rotating-platform knee arthroplasties, and numerous balancing techniques have been reported. However, no well designed studies of ligament balance and knee kinematics have been reported. The goal of this study was to perform a prospective, randomized, blinded trial of two ligament balancing techniques for rotating platform TKA and determine if these affect postoperative knee kinematics. We hypothesized that ligament balancing with a calibrated spreader/balancer would provide more reproducible physiologic knee kinematics than ligament balancing with fixed thickness spacer blocks.

METHODS: Sixteen patients with unilateral rotating platform TKA (TC-SB, Plus Orthopedics, Switzerland) consented to participate in this prospective, randomized, blinded, and IRB approved study. All patients were operated by a single senior surgeon (FK). Eight knees received the prosthesis using a ligament balancing technique employing fixed thickness spacer blocks (control group). Eight knees received the same prosthesis design employing a calibrated spreader/balancer device to equalize the joint gaps and ligament balance in flexion and extension (spreader group). A standard sequential soft-tissue releasing technique was utilized in both control and spreader groups. There were no differences between the control and spreader groups for height, weight, age, sex distribution, preoperative deformity or preoperative clinical scores.

Patients performed weight-bearing a maximum flexion lunge activity, kneeling on a padded bench and stepping up and down on a 25cm step. A lateral view of the knee was recorded using fluoroscopy for each activity. Computer assisted shape matching techniques were used to determine the three-dimensional position/ orientation of the knee components using implant surface models (CAD) for each knee. Joint angles were computed using standard methods. Anteroposterior translations of the condyles were computed with respect to the anteroposterior midpoint of the tibial base-plate. Researchers were unblinded to subject group membership only after all data had been produced. Statistical comparisons were performed using two-way repeated measures ANOVA with post-hoc pair-wise comparisons at a 0.05 level of significance.

RESULTS: No significant differences were found in knee flexion angle, tibial abduction or external rotation, medial or lateral condyle AP position for the lunge or kneeling activities. The ratio of lateral to medial posterior translation was 20% and 50% greater for the spreader group for the lunge and kneel activities, respectively.

Tibiofemoral kinematics during the step activity were compared using average Centers of Rotation (COR) for femoral motion with respect to the tibial baseplate. For the entire step-up/down cycle, the COR's were at 0% (central) and 13% (medial) for the control and spreader groups respectively ($p=0.058$). Both groups of knees showed tibial internal rotation with knee flexion, 8.5° and 7.6° for the control and spreader groups, respectively. These differences were not statistically significant.

DISCUSSION: The goal of TKA is to reproduce normal knee kinematics. Ligament and soft-tissue balance are thought to play critical roles in obtaining optimal kinematic behavior. The merits of many balancing techniques and instruments have been advanced. This prospective randomized study evaluated two ligament balancing techniques to determine if different kinematics would result. Balancing technique did not have a demonstrable effect on knee kinematics in maximally flexed postures. The dynamic step activity revealed an almost significant difference in average center of rotation, suggesting the spreader group tended to have greater posterolateral translation with flexion than the control group. The lack of significant findings suggests two possibilities: First, the spreader technique provides more physiologic kinematics, but the sample size was too small to demonstrate significant findings. Alternatively, the simpler surgical technique provides results just as good results as the instrumented technique. The first choice seems likely given almost significant findings in this small study group.

In conclusion, our prospective randomized study revealed no statistically significant clinical differences between the two study groups for deeply flexed and dynamic stepping knee kinematics. Knees treated with an instrumented balancing device tended to show patterns of motion more closely resembling those observed in the normal knee, but this was not statistically significant.

AFFILIATED INSTITUTIONS FOR CO-AUTHORS:
** Plus Orthopaedics, Rotkreuz, Switzerland
***University of Florida, Gainesville, Florida, USA
This research was funded by Plus Orthopaedics, Switzerland

NAVIGATED METHODOLOGY FOR INTRAOPERATIVE KINEMATIC ASSESSMENT OF THE KNEE STABILITY

Martelli S, Zaffagnini S, Bignozzi S, Lopomo N, Marcacci M
Laboratorio di Biomeccanica, Istituti Ortopedici Rizzoli, Bologna, Italy
s.martelli@biomec.ior.it

INTRODUCTION

This paper describes a protocol for an accurate and extensive computer–assisted in vivo evaluation of joint laxities during reconstructions of anterior cruciate ligament (ACL). The paper reports the acquisition procedure to be performed by the surgeon, the evaluation protocol which permit to estimate quantitatively and qualitatively the performance of the intervention and the original intra-operative interface for displaying the results. The new methodology has been used during 70 ACL reconstruction.

MATERIALS AND METHODS

The method consists of a new application of a navigated procedure. Polaris optical localizer (NDI, Canada) is used intra-operatively setting two reference arrays on femur and tibia, in the surgical incision. During ACL reconstruction the surgeon acquires percutaneous anatomical landmarks by a digitized and then the system is able to record and elaborate standard kinematic tests such as valgus/varus (VV) rotation, internal/external (IE) rotation, the drawer or Lachman.
Laxities are computed in real-time and displayed in a simple and effective interface able to provide the surgeon the estimation of the current knee state and eventually compare it with a previously recorded evaluation, e.g. before and after the reconstruction (FIG. 1).
The system has been used during 67 ACL reconstructions 10 females and 57males, to estimate its precision, its reliability and its clinical efficacy. Mean age of patients was 32 (17-49). 39 patients underwent to a Single bundle technique, and 28 to a double bundle technique. Tests of inter-operator repeatability were performed by a senior surgeon repeating the tests 4 times in 30 cases; inter-operator repeatability was estimated comparing 2 expert surgeons and a non-expert one during 40 cases; algorithms and interface were estimated and optimized every 20 cases. The laxities estimated with our method were compare with IKDC score and Rollimeter (***)

RESULTS

The proposed method is fast (10 minutes of additional surgical time), has a short learning time (5 cases), is scarcely invasive (both for patients and for surgical technique). The computation of laxity-stability showed a intra-surgeon repeatability of 1.5° for varus-valgus rotation, 3° for internal-external rotation, and 2 mm for antero-posterior displacement: the inter-operator repeatability is 1.6° for varus-valgus rotation, 2.3° for internal-external rotation, and 1.5mm for antero-posterior displacement both when comparing experts surgeons or expert and non-expert ones.
Difference between Rolimeter measurements and AP translation were 2mm for test at 30º of flexion and 1 mm for test at 90º of flexion.

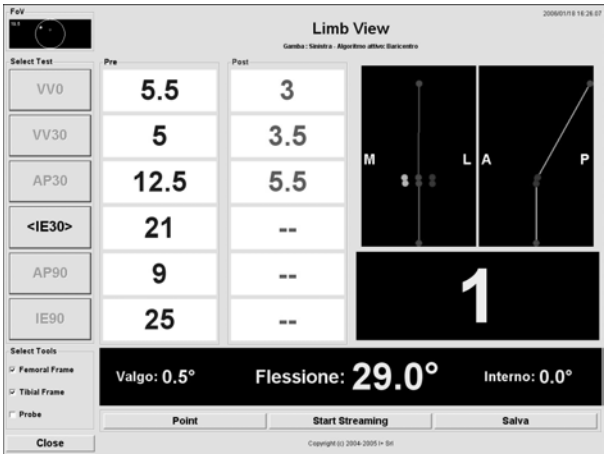

Fig 1 Software interface.

DISCUSSION

The proposed protocol, designed to optimize surgical times and minimize invasiveness, resulted easy to use and reliable for quantitative intra-operative evaluation of knee kinematic behaviour. This methodology provides the surgeon with a repeatable tool to measure knee state during different steps of surgery and to have an immediate assessment of the graft performance. The method improved the capability to evaluate the efficacy of ACL reconstructions in our clinical experimentation and could be used for routine estimation and documentation of this surgical procedure, to better decide the need of further treatment or optimize the result of the reconstruction.

NONFIXATED-MOBILE MEDIAL COMPARTMENT KNEE HEMIARTHROPLASTY: OUTCOMES WITH AND WITHOUT ARTHROSCOPIC SYNOVIAL ABLATION

*Trotter D, Patari S
*Center for Sports Orthopaedics, S.C., Hoffman Estates, IL USA 60194
davedoc911@aol.com

INTRODUCTION

Unicompartmental knee arthroplasty has become increasingly popular; providing pain relief and improved function, with decreased perioperative morbidity over total knee arthroplasty. The reported results of mobile unicompartmental knee hemiarthroplasty have been relatively limited and mixed. This study evaluates the utilization of a nonfixated (condylar-oriented) unicompartmental hemiarthroplasty with and without concomitant arthroscopic synovial ablation, in the treatment of medial compartment arthritis.

METHODS

In a (institutional review board approved/ informed consented) retrospective study, a nonfixated-mobile unicompartmental knee hemiarthroplasty was performed in 2 series for a total of 115 knees (108 patients, avg. age 59 yrs). Knees with a minimum1 year follow up are reported.

The **first** series consisted of 40 knees that underwent arthroscopic evaluation and then (limited arthrotomy) implantation of the UniSpacer device (Zimmer, Warsaw, IN, USA).

The **second** series consisted of 42 knees that underwent arthroscopic synovial ablation in addition to UniSpacer implantation. The combined series average age was 58.1 yrs (36 – 85 yrs of age). The 2 series were combined for statistical evaluation. Pre- and postoperative evaluation of each knee consisted of the Knee Society clinical rating system and Lysholm scoring, along with visual analog pain scale. Radiographic limb alignment was evaluated. Patients were evaluated postoperatively at 3 and 6 months, and yearly intervals. The results at 1 and 2 years are presented, respectively.

RESULTS

Eighty-two knees were evaluated at 1-year post arthroplasty. Knee Society scores improved 227% at 1 year. The functional component improved 51%. Lysholm scores improved 80%. Patients had an 80% improvement in pain levels (preoperative= 7-10, postoperative= 1-3). Concomitant arthroscopic synovial ablation improved overall pain and functional scores and decreased the rate of postoperative events. This was statistically significant in the subgroup of patients >60 years of age.

Forty-four knees were evaluated at 2 years post arthroplasty. Knee Society scores improved 245%. Lysholm scores improved 80%. Patients who underwent concomitant synovial ablation had a significantly greater improvement in Knee Society scores (492% improvement vs 245%).

Thirteen knees have been followed for 3 years. Knee Society scores improved 284%. The functional component and Lysholm scores improved 71% and 100%, respectively.

Postoperative effusion (requiring aspiration etc.) was the most common adverse event. 15 knees required post-op arthroscopic debridement. 5 knees required manipulation. 1 knee was revised to another size implant. 4 knees were revised to total knee arthroplasty; 2 for dislocation and 2 for persistent pain (4.3% overall). The implant dislocation rate was 1.7% (2 of 115).

DISCUSSION

Nonfixated-mobile medial compartment hemiarthroplasty of the knee is an acceptable alternative to fixated medial compartment and total knee arthroplasty, when utilized in the appropriate clinical setting. It is best suited for the younger patient population, providing a less invasive alternative to fixed knee arthroplasty. It also provides an excellent option to the active elderly population, potentially decreasing perioperative morbidity and serious complications.

Concomitant arthroscopic synovial ablation appears to reduce morbidity and improve post-operative clinical rating scores when performed with this nonfixated-mobile metallic medial compartment implant. Most recently, a technique modification towards enhanced anatomical contouring/symmetrization of the joint surfaces appears to trend towards an additional enhancement to this hemiarthroplasty procedure.

IDENTIFICATION OF CARTILAGE DEDIFFERENTIATION MARKERS THROUGH GENE EXPRESSION ANALYSIS WITH A 30,000 cDNA ARRAY

*Boeuf S, *Steck E, **Buneß A, *Witte D, **Sültmann H, **Poustka A, *Richter W
*Division of Experimental Orthopaedics, Orthopaedic Clinic, University of Heidelberg, Germany

Stephane.Boeuf@ok.uni-heidelberg.de

INTRODUCTION

A cell population that is broadly discussed to support cartilage regeneration in several fields from traumatic lesions to osteoarthritic degeneration is mesenchymal stem cells (MSC). Differentiation of MSC into articular chondrocytes, spontaneous regeneration of injured cartilage and enhanced repair after surgical treatments like microfracture, cell therapy (ACT) and tissue engineering approaches are, however, still poorly understood on the molecular level. For molecular analysis of cartilage regenerates the knowledge of cartilage relevant marker molecules is demanded. Most studies aiming to identify cartilage relevant genes focused either on disease related genes or on the identification of gene fragments expressed in cartilage without discrimination to other mesenchymal tissues or undifferentiated mesenchymal stem cells.

The aim of this study was to identify cartilage and MSC expressed genes out of a large, nearly genome wide, number of transcripts (30.000 gene fragments) and to extract possible marker genes by subtraction.

METHODS

MSC were isolated from bone marrow of patients undergoing total hip replacements of iliac bone graft harvest (n=5) or from adipose tissue from lipoaspirates generated during elective liposuction procedures (n=5). Cartilage tissue was obtained from tibia plateaus and condyles of patients undergoing total knee replacement surgery (n=10). The studies were approved by the local ethics committee and informed consent was obtained from all individuals.

RNA and mRNA were isolated from the samples. For hybridization mRNA was directly reverse transcribed to labelled cDNA using ^{33}P-labelled dATP and hybridized to Human Unigene Set (RZPD1) cDNA arrays. The arrays were exposed to imaging plates and images were captured on a phosphor imager. Normalization of data was performed using a variance stabilizing normalization method and significant differences between cartilage and MSC were identified using the significance analysis of microarrays software (SAM, http://wwwstat.stanford.edu/~tibs/SAM/).

Quantitative RT-PCR was used as a second independent method to confirm the results of the array analysis using cartilage and bone marrow MSC samples. RT-PCR was used to assess expression profiles of genes of interest in cartilage samples and in dedifferentiating chondrocytes.

RESULTS

Using SAM for data analysis of the entire arrays we selected 105 differentially expressed clones with a more than 3-fold difference in expression intensity. After sequence analysis of these clones, 67 cartilage and 20 MSC relevant genes were identified.

From 67 cartilage relevant genes, 26 genes have already been published to be expressed in cartilage tissue. These genes include extracellular matrix molecules like collagen type 2, aggrecan or decorin, integrins like integrin alpha 10, matrix metalloproteinases like MMP3, growth factors like CTGF, receptor molecules like FGFR3, or others like CHI3L2. Identifying a large number of known cartilage relevant genes within the cartilage tissue but not within the MSC group is an evidence for the high quality of our data analysis. Another 31 genes belonged to already known genes not published to be expressed in cartilage so far. Within this group we detected membrane proteins, proteins involved in intracellular signalling, nuclear proteins and several genes whose biological function is unclear. The remaining 10 fragments belonged to previously unknown genes.

For a selection of genes with higher expression in cartilage, the differential expression was confirmed by quantitative RT-PCR. Two protease inhibitors were found with a down-regulation of expression during dedifferentiation parallel to collagen type II.

DISCUSSION

Through a genome-wide gene expression analysis of cartilage and MSC we identified 31 previously not described cartilage genes and 10 unknown transcripts expressed in cartilage. Through the detailed analysis of the expression profiles of some of these genes two potential dedifferentiatiom markers were identified. Correlation of the expression of these markers to ectopic cartilage formation capacity in immuno-incompetent mice is currently established.

ACKNOWLEDGMENT

This work was supported by a grant of the Land Baden-Württemberg.

AFFILIATED INSTITUTIONS FOR CO-AUTHORS

** Molecular Genome Analysis, DKFZ-Heidelberg, Germany

PROTEASE INHIBITOR MEDIATED SUPPRESSION OF LATE STAGE CHONDROGENIC DIFFERENTIATION OF MESENCHYMAL STEM CELLS IN VITRO

Bertram H, Dreyer R, Wachters J, Boehmer S, Richter W
Division of Experimental Orthopaedics, Orthopaedic University Clinic Heidelberg, Germany

wiltrud.richter@ok.uni-heidelberg.de

INTRODUCTION

Chondrogenically differentiated mesenchymal stem cells derived from bone marrow (BMSC) or adipose tissue (ATSC) appear to be attractive sources for cell therapeutic applications like the treatment of articular cartilage lesions. Unfortunately, hypertrophic markers like collagen type X are induced by common in vitro protocols for chondrogenic differentiation of mesenchymal stem cells (MSC) and also ALP activity as well as calcification of microossicles related to endochondral ossification can be observed in MSCs once implanted subcutaneously in vivo. For clinical application of MSC-derived chondrocyte-like cells a stable phenotype of permanent articular chondrocytes is however desired.

OBJECTIVE

The aim of this study was to evaluate whether known inhibitors of hypertrophic differentiation like inhibitors of proteases or matrixmetalloproteinases are able to delay or suppress hypertrophic differentiation of MSCs in vitro.

METHODS

Chondrogenic differentiation of BMSC and ATSC was induced in high density culture in the presence of TGF-beta, or TGF-beta/BMP6, or the inhibitors leupeptin, pepstatin, aprotinin and hydroxamate were added for 28 days. Gene expression was analysed by RT-PCR and differentiation of the spheroids was evaluated by alcian blue staining for acid proteoglycans and by immunohistology for collagen type I and II.

RESULTS

After leupeptin-, pepstatin- and aprotinin treatment deposition of collagen type II protein and proteoglycans was reduced in ATSC but not BMSC derived spheroids. Transcripts for COL2A1, besides transcripts for COL10A1, MMP3, MMP13 and AGC1 were detectable. However, a complete suppression of chondrogenic differentiation by hydroxamate on protein level was evident since proteoglycan and collagen type II staining was absent both in spheroids from ATSCs and BMSCs.

CONCLUSION

The evaluated inhibitors of proteases resulted in a minor downregulation of chondrogenic differentiation on protein level without downregulation of hypertrophic transcripts like COL10A1 and MMP13 whereas the MMP3-Inhibitor hydroxamate effectively blocked TGF-beta induced chondrogenesis of MSCs.

INFLUENCE OF GEL-LIKE MATRICES ON CHONDROGENIC DIFFERENTIATION OF MSC AND DIFFERENTIATION STABILITY AFTER ECTOPIC IMPLANTATION

*Dickhut A, *Lorenz H, *Bischel O, *Richter W,
Division of Experimental Orthopaedics, Orthopaedic Clinic, University of Heidelberg, Germany

Andrea.Dickhut@ok.uni-heidelberg.de

INTRODUCTION

Due to their multilineage capacity mesenchymal stem cells (MSC) are attractive candidates for the cell-based reconstruction of different tissues including cartilage. The aim of this study was to compare different gel-like carrier materials for their capacity to support the chondrogenic differentiation of MSC in vitro and to stabilize ectopic cartilage formation after subcutaneous implantation into SCID mice.

METHODS

MSC from human bone marrow (BMSC) and adipose tissue (ATSC) were expanded, and embedded in different gel matrices consisting of collagen type I, fibrin, peptides (PuraMatrix) or basement membrane (Matrigel). Cell differentiation, viability, collagen synthesis, and proteoglycan deposition were analyzed over time in vitro. After culture under chondrogenic conditions for five weeks, part of the constructs were implanted subcutaneously into SCID mice. Four weeks after implantation ectopic transplants were evaluated based on Alcian blue staining, collagen type II immunohistology, and Alizarin red staining.

RESULTS

Cell viability was sustained in all carrier materials and the volume was enhanced compared to the carrier-free pellet, especially with Matrigel and PuraMatrix. Matrigel and fibrin improved collagen synthesis, whereas PuraMatrix constructs showed better proteoglyan deposition. Matrigel was superior to PuraMatrix regarding mechanical stability and handling characteristics.

Matrix culture especially improved chondrogenesis of ATSC and allowed differentiation at reduced growth factor concentrations, which were ineffective in carrier-free pellets.

Ectopic transplants were positive for collagen type II and rich in proteoglycans. Calcification was abundant in pellet cultures, fibrin and collagen constructs. Compared to the other materials Matrigel and PuraMatrix constructs were larger and showed clearly reduced calcification in vivo, when seeded with ATSC. Calcification of BMSC biocomposites was only slightly influenced by the carrier materials.

DISCUSSION

Matrix materials can be used to optimize cell density and enhance and stabilize chondrogenic differentiation. Remarkably there was no correlation between in vivo calcification and proteoglycan deposition or collagen synthesis of biocomposites in vitro. ATSC were superior to BMSC not only in regard to isolation procedures and growth characteristics, they can also be influenced by carrier materials like Matrigel to prevent or delay matrix calcification of ectopic transplants.

In summary, our study supports the use of carrier materials to facilitate transplantation and to improve and stabilize chondrogenesis of MSC.

ACKNOWLEDGEMENTS

We thank K. Goetzke and R. Foehr for technical assistance and S. Schneider and C. Weidmann for statistical analysis. This work was supported by a grant of the research fund of the Stiftung Orthopädische Universitätsklinik Heidelberg.

A COMPARISON OF THE DIFFERENT GROWTH FACTOR REPERTOIRE AND THE FACTOR REQUIREMENT FOR SUCCESSFUL CHONDROGENESIS OF MSCs FROM BONE MARROW AND ADIPOSE TISSUE

Hennig T, Lorenz H, Götzke K, Richter W
Department of Orthopaedic Surgery, University of Heidelberg
Schlierbacher Landstr. 200A, 69118 Heidelberg, Germany

thea.hennig@ok.uni-heidelberg.de

INTRODUCTION

Mesenchymal stem cells (MSCs) can differentiate into various cell types including chondrocytes and they may represent an alternative cell source for the treatment of cartilage defects. Under standard chondrogenic *in vitro* differentiation protocols MSCs derived from adipose tissue (ATSCs) have a lower chondrogenic differentiation potential compared to MSCs from bone marrow (BMSCs). The aim of this study was to analyze limiting factors in chondrogenic differentiation of ATSCs with respect to endogenous production of growth factors and the requirement of exogenous factors for successful chondrogenesis.

MATERIALS AND METHODS

BMSCs and ATSCs were expanded *in vitro* and differentiated under standard chondrogenic conditions (dexamethasone, ascorbic acid) for 6 weeks in micromass culture in the presence of TGF-beta3 and/or other growth factors. Differentiation was assessed by alcian-blue and collagen type II-staining and gene expression was quantified by Real Time-PCR.

RESULTS

Undifferentiated BMSCs differed from ATSCs by expression of mRNA for BMP2, BMP4, BMP6, osterix, osteocalcin, PDGF-BB and Alk-5 while no differences were obvious for BMP2 and 7, TGF-beta 1,3, FGF1, FGF2, IGF, CTGF, MATN1, Cbfa1, Sox9, MMP3, MMP13, Alk-2, ACVR2A, BMPRIA, BMPRIB and BMPRII. In contrast to BMSCs, ATSCs required BMP6 besides TGF-beta for successful differentiation during which Col2A1, Col10A1, BMP4 and Indian hedgehog mRNA and alkaline phosphatase enzyme activity were up-regulated.

DISCUSSION

Discrepant expression of BMP4 between ATSCs and BMSCs indicates that this factor may be crucial for chondrogenic differentiation of MSCs. It is tempting to speculate that in BMSC cultures BMP4, osterix and osteocalcin may derive from contaminating osteogenic progenitor cells from bone marrow which are not found in ATSC cultures derived from liposuction material. We demonstrate that addition of BMP2, 4 and BMP6 enhance chondrogenic differentiation of ATSCs but only BMP6 eliminates the reduced chondrogenic capacity of ATSCs in comparison to BMSCs.

REFERENCES

[1] M.F. Pittenger, A.M. Mackay, S.C. Beck, et al. *Science:* Multilineage Potential of Adult Human Mesenchymal Stem Cells 284 (1999), pp.143-147.
[2] P.A. Zuk, M. Zhu, H. Mizuno, et al. *Tissue Eng:* Multilineage Cells from Human Adipose Tissue: Implications for Cell – Based Therapies 7 (2001), 211-228.
[3] A. Winter, S. Breit, D. Parsch, K. Benz, E. Steck, H. Hauner, R. M. Weber, V. Ewerbeck and W. Richter, *Arthritis Rheumatism:* Cartilage – Like Gene Expression in Differentiated Human Stem Cell Spheroids 48 (2003), pp. 418-429.
[4] E. Steck, H. Bertram, R. Abel, B. Chen, A.Winter, W. Richter, *Stem Cells:* Induction of Invertebral Disc – Like Cells from Adult Mesenchymal Stem Cells 23 (2005), pp. 403-411.

ACKNOWLEDGEMENTS

We thank K. Götzke and R. Föhr for technical assistance.
This work was supported by a grant of the research fund of the Division of Experimental Orthopaedics of Heidelberg.

COMBINED HUMAN IGF-I AND FGF-2 GENE TRANSFER STIMULATES THE REPAIR OF FOCAL CARTILAGE DEFECTS *IN VIVO*

*Madry H, *Kaul G, *Orth P, **Zurakowski D, *Kohn D, *Cucchiarini M
*Laboratory for Experimental Orthopaedics, Department of Orthopaedic Surgery, Saarland University Medical Center, Homburg, Germany

hmad@hotmail.com

INTRODUCTION

Transplantation into cartilage defects of genetically modified articular chondrocytes overexpressing therapeutic genes may improve cartilage repair. Overexpression of human insulin-like growth factor I (IGF-I) and fibroblast growth factor 2 (FGF-2) has been previously demonstrated to enhance cartilage repair *in vivo* [1, 2]. Here, we tested the hypothesis that the combined gene transfer of IGF-I and FGF-2 enhances the repair of full-thickness (osteochondral) cartilage defects *in vivo*.

METHODS

NIH 3T3 cells were transfected with expression plasmid vectors carrying either the E. coli *lacZ* gene (pCMV*lacZ*), a human IGF-I cDNA (pCMVhIGF-I) or a combination of human IGF-I and FGF-2 cDNA (pCMVhFGF-2) using the lipid-based reagent FuGENE 6 (v/w ratio 1:2). Transfected cells were encapsulated in 1.2% alginate and the resulting *lacZ,* IGF-I and IGF-I/FGF-2 spheres were cultured for 21 days *in vitro*. At the indicated time points, IGF-I and FGF-2 concentrations in the cell culture supernatants were measured by ELISA (R&D Systems). Animal experiments were conducted under an Institution Animal Studies Committee approved protocol. One cylindrical osteochondral defect (3.2-mm in diameter) was created in each patellar groove of 12 female rabbits (n = 28 defects). One day after transfection, alginate-NIH 3T3 spheres were press-fit into the defects. The right and left knees alternatively received *lacZ* or IGF-I spheres (n = 6) or *lacZ* or IGF-I/FGF-2 spheres (n = 6). At 3 weeks post operation, cartilage repair was assessed based on safranin-O-stained sections that were taken at 100 µm intervals from the center of the defect using a histological grading system [3]. This grading system ranges from 0 points (normal articular cartilage) to 31 points (no repair tissue). Grading was performed independently by two individuals who were blinded with respect to the treatment. A total of 272 sections were scored. Data are expressed as mean ± standard deviation. Comparisons were made by repeated-measures ANOVA (knees within the same animals).

RESULTS

At day 2 *in vitro*, IGF-I expression levels in IGF-I and IGF-I/FGF-2 spheres were of 229.1 ± 82.8 and 281.4 ± 44.0 ng/10^7 cells/24 h, respectively ($P > 0.05$, n = 3; *lacZ* spheres: 0.1 ± 0.0 ng/10^7 cells/24 h). By day 7 after transfection, IGF-I levels in IGF-I and IGF-I/FGF-2 spheres declined to 8.1 ± 4.2 and 11.7 ± 4.1 ng/10^7 cells/24 h, respectively, but were still 11- and 17-fold higher than in *lacZ* spheres (0.7 ± 0.1 ng/10^7 cells/24 h; $P < 0.05$, n = 3). IGF-I returned to baseline levels by day 14 both in IGF-I and IGF-I/FGF-2 spheres. FGF-2 expression levels in IGF-I/FGF-2 spheres at day 2 were of 28.7 ± 5.0 ng/10^7 cells/24 h (*lacZ*: 0 ng/10^7 cells/24 h) and were of 23.4 ± 7.6 ng/10^7 cells/24 h at day 4. FGF-2 expression returned to baseline levels by day 7. The total cell numbers remained unchanged over the course of the *in vitro* cultivation in all groups. In contrast, cell viability, which was above 90% at the time of encapsulation in all groups, declined by day 21 to 41.6 ± 12.4%, 37.6 ± 4.4%, and 43.1 ± 3.5% in *lacZ*, IGF-I and IGF-I/FGF-2 spheres, respectively ($P > 0.05$, n = 6).

At 3 weeks after *in vivo* transplantation, there were no signs of adverse reactions of the grafts in any treatment group. Combined gene transfer of IGF-I and FGF-2 significantly improved average individual scores for integration, cell morphology, subchondral bone formation and tidemark formation (Fig. 1, Table 1). Values for all other individual categories were also improved, although they did not reach statistical significance. The average total score after 3 weeks *in vivo* was significantly improved for defects receiving IGF-I/FGF-2 spheres compared with defects receiving *lacZ* spheres and IGF-I spheres alone (both $P < 0.05$, n = 6). In contrast, gene transfer of IGF-I alone improved all individual categories and the average total score without reaching statistical significance when compared with defects receiving *lacZ* spheres ($P > 0.05$, n = 6).

Fig. 1 *Cartilage repair 3 weeks following trans-plantation of* (**A**) lacZ, (**B**) *IGF-I or* (**C**) *IGF-I/FGF-2 spheres. Magnification x 40.*

Table 1*. Effects of transplanted IGF-I and IGF-I/FGF-2 spheres on the histological grading of the repair tissue after 3 weeks* in vivo.

Category	*lacZ* Mean (95% CI)	IGF-I/FGF-2 Mean (95% CI)
Filling of defect	0.26 (0.02 – 0.60)	0.01 (0.00 – 0.35)
Integration	1.58 (1.11 – 1.94)	0.97 (0.61 – 1.34)*‡
Matrix staining	2.41 (1.67 – 3.14)	1.68 (0.94 – 2.41)
Cell morphology	3.78 (2.87 – 4.70)	2.41 (1.49 – 3.32)*
Architecture: defect	1.25 (0.79 – 1.71)	0.93 (0.47 – 1.39)
Architecture: surface	1.36 (0.71 – 2.00)	1.08 (0.43 – 1.72)
Subchondral bone	2.83 (1.98 – 3.69)	1.25 (0.40 – 2.12)*
Tidemark	3.91 (3.15 – 4.65)	2.69 (1.94 – 3.45)*‡
Average total score	**17.1 (14.4 – 19.9)**	**11.2 (8.3 – 13.8)*‡**

Category	*lacZ* Mean (95% CI)	IGF-I Mean (95% CI)
Filling of defect	0.46 (0.12 – 0.81)	0.32 (0.01 – 0.66)
Integration	2.03 (1.66 – 2.39)	1.72 (1.35 – 2.08)
Matrix staining	2.65 (1.92 – 3.38)	2.43 (1.69 – 3.16)
Cell morphology	3.80 (2.88 – 4.71)	3.42 (2.50 – 4.33)
Architecture: defect	1.50 (1.04 – 1.96)	1.04 (0.58 – 1.50)
Architecture: surface	1.23 (0.59 – 1.87)	0.87 (0.23 – 1.52)
Subchondral bone	2.42 (1.56 – 3.27)	1.99 (1.14 – 2.84)
Tidemark	3.80 (3.05 – 4.55)	3.68 (2.92 – 4.43)
Average total score	**17.9 (15.1 – 20.7)**	**15.5 (12.7 – 18.2)**

*Means indicate the estimated scores in points for each category (lower score: better healing). CI = confidence interval. Statistically significant: * $P < 0.05$ vs. respective control; ‡ $P < 0.05$, IFG-I vs. IGF-I/FGF-2.*

DISCUSSION

IGF-I/FGF-2-transfected NIH 3T3 cells embedded in alginate secrete human IGF-I for at least 7 and human FGF-2 for at least 4 days *in vitro*. Combined IGF-I/FGF-2 overexpression within cartilage defects via alginate-embedded NIH 3T3 cells significantly enhances the repair of full-thickness osteochondral cartilage defects after 3 weeks *in vivo* in a magnitude that is larger than with IGF-I alone. These results suggest that gene delivery of combinations of therapeutic growth factors to cartilage defects may be superior than the application of single factors alone. Future studies need to evaluate the long-term properties of this repair tissue.

REFERENCES

[1] Madry *et al. Gene Ther* **2005**, [2] Kaul *et al. J Gene Med* **2005**, [3] Sellers *et al. J Bone Joint Surg Am* **1997**.

ACKNOWLEDGMENTS

Supported by the Deutsche Forschungsgemeinschaft (DFG MA 2363/1-2 of HM).

**Department of Biostatistics, Harvard University, Boston, MA, USA

MOLECULAR AND IMMUNOHISTOLOGICAL CHARACTERIZATION OF HUMAN CARTILAGE TWO YEARS FOLLOWING AUTOLOGOUS CELL TRANSPLANTATION

*Marconi E, *Grigolo B, *Roseti L, *De Franceschi L, *Desando G, **Manfredini M, **Faccini R, *Facchini A.
*Laboratorio di Immunologia e Genetica, Istituto di Ricerca Codivilla Putti, Istituti Ortopedici Rizzoli, Bologna, Italy

labimge@alma.unibo.it

INTRODUCTION

Autologous chondrocyte transplantation (ACT) is a relatively widely used technique for the treatment of cartilage lesions.
The reported good clinical results at 2-10 year follow-up have encouraged further use of this method.
Moreover, this therapeutic strategy seems to have been improved recently by the use of biocompatible scaffolds, that allow better fixation of the cells inside the defect while retaining the original cellular phenotype.
Conflicting results in the literature reflect, in part, different methods of evaluating the repair tissues and recently common criteria have been established since objective evaluations of the characteristics of the transplanted tissues are needed.
To our knowledge, there are no in-depth investigations, at the molecular level, on the tissue in the newly reconstructed cartilage.
The aim of our research was to evaluate biopsies of tissue from patients who had undergone ACT 24 months previously using molecular biology and immuno-histochemistry techniques.

METHODS

The cartilage biopsies from each patients who had been treated by autologous chondrocyte transplantation and from two healthy patients were used. Real-Time Reverse Transcriptase Polymerase Chain Reaction (RT-PCR) analysis was performed to evaluate the expression of types I, II and X collagen, aggrecan, cathepsin B, early growth response protein-1 (Egr-1) and Sry-type high-mobility-group box transcription factor-9 (Sox-9) mRNAs. Immunohistochemical analysis for matrix proteins and regulatory proteins was carried out on paraffin embedded sections.

RESULTS

Type I collagen mRNA was expressed in all the samples evaluated. Type II collagen was present in autologous chondrocyte transplantation samples, but at lower levels compared with controls.
Aggrecan mRNA was present in all the samples at lower levels than in the controls while cathepsin B messenger levels were higher, and Egr-1 and Sox-9 mRNAs were expressed at lower levels.
The immunohistochemical analysis showed slight positivity for type I collagen. Type II collagen was found in all the samples with positivity confined inside the cells. Cathepsin B was slightly positive in all the samples. Egr-1 protein was particularly evident in the areas negative for type II collagen. Sox-9 was evident in the superficial layer.
In biopsies of autologous chondrocyte transplantation tissue at two years, there is evidence of the formation of a new tissue which displays varying degrees of organization with some fibrous and fibrocartilaginous features.

DISCUSSION

In biopsies of autologous chondrocyte transplantation tissue at two years, there is evidence of the formation of a new tissue which displays varying degrees of organization with some fibrous and fibrocartilaginous features.
Long-term follow-up investigations are needed to verify if, once all the remodelling processes are completed, the new-formed tissue will acquire the more typical features of articular cartilage.
Our data provide important further information about the nature of the new cartilage tissue formed two years after autologous chondrocyte transplantation allowing a better interpretation of the clinical and histological findings.

AFFILIATED INSTITUTIONS FOR CO-AUTHORS:

**Divisione di Ortopedia e Traumatologia, Ospedale Del Delta, Lagosanto, Ferrara, Italy.

THE DETACHED OSTEOCHONDRAL FRAGMENT AS A SOURCE OF CELLS FOR AUTOLOGOUS CHONDROCYTE IMPLANTATION (ACI) IN THE ANKLE JOINT

[†*]Giannini S, [†]Buda R, [‡]Grigolo B, [†]Vannini F, [‡]De Franceschi L, [‡]Facchini A
[†]Orthopaedic Department, Rizzoli Orthopaedic Institute, Bologna, Italy
[‡]Immunology and Genetics Laboratory, Rizzoli Orthopaedic Institute, Bologna, Italy

giannini@ior.it

INTRODUCTION

Autologous chondrocyte implantation (ACI) has been successfully used for the treatment of osteochondral lesions of the talus. One of the main problems of this surgical strategy is related to the harvesting of the cartilage slice from a healthy knee. The aim of this study was to examine the capacity of chondrocytes harvested from a detached osteochondral fragment to proliferate and to serve as a source of viable cells for ACI in the repair of ankle cartilage defects.

METHODS

Detached osteochondral fragments harvested from the ankle joint of 20 patients with osteochondral lesions of the talus served as the source of human articular cartilage specimens. All of the osteochondral lesions were chronic and of traumatic origin. In all cases, the fragments were utilized to evaluate the viability and proliferation of the cells, the histological appearance of the cartilage tissue and the expression of specific cartilage markers by real-time PCR.

In the 16 patients scheduled for ACI, the expanded chondrocytes were used for chondrocyte implantation. In the other 4 patients, with lesion size <1.5 cm^2, microfractures were created during the initial arthroscopic step. As a control group, 7 patients with comparable osteochondral lesions underwent the same surgery, but received chondrocytes harvested from the ipsilateral knee.

RESULTS

According to the AOFAS system, patients in the experimental group had a preoperative score of 54.2±16 points and a postoperative one of 89±9.6 points after a minimum follow-up time of 12 months ($p<0.0005$). The control group of patients had a preoperative score of 54.6±11.7 points and a postoperative one of 90.2±9.7 points at a minimum follow-up time of 12 months ($p<0.0005$). The clinical results of the two groups did not differ significantly from each other.

Chondrocytes isolated from the detached fragments were highly viable, phenotypically stable, proliferated in culture and redifferentiated when grown within the three-dimensional scaffold used for ACI.

The morphological and molecular characteristics of the cartilage samples obtained from the detached osteochondral fragments were similar to those of healthy hyaline articular cartilage.

CONCLUSIONS

The good results achieved with this strategy indicate that cells derived from the lesioned area may be useful in the treatment of osteochondral defects of the talus.

EFFECTS OF A NEW BFGF/TCP-COMPOSITE ON PERIIMPLANT BONE

Maus U, Ohnsorge JAK, Andereya S, Siebert CH, Niedhart C
Department of Orthopaedic Surgery, University of Aachen, Pauwelsstr. 30, 52074 Aachen, Germany

umaus@ukaachen.de

INTRODUCTION

Basic fibroblast growth factor (bFGF) is a well known osteoanabolic protein, which effects have been studied with different bone substitutes. But the study results are inconsistent. Aim of our study was to determine the bone-regenerative effects of a new composite, consisting of an in situ setting, resorbable tricalcium phosphate cement (TCP) and bFGF in the periimplant area, and to compare it with autologous bone graft.

METHODS

A trepanation defect of 9,4 mm diameter and 10 mm depth in distal femur epiphyses of 10 adult sheep was filled with the bFGF/TCP-composite (200µg bFGF/cm³ TCP), pure TCP, autologous bone graft or left empty. After 12 weeks animals were euthanized and the defect and the periimplant area were examined by radiography, computertomography, histology, histomorphometry and microradiography.

RESULTS

CT-scans showed bony ingrowth up to the middle of the defect and resorption of the TCP. The histological examination of the empty control defects showed no bony ingrowth after 12 weeks, while the autologous bone graft was completely incorporated. In defects treated with pure TCP or the TCP/bFGF-composite trabecular bony ingrowth could be shown. In the periimplant area were no significant differences detectable in radiography, histology or microradiography. Histomorphometry showed an ingrowth of bone in the empty defect of 5,1 % in relation to the whole defect. Defects treated with autologous bone graft were filled with 19,9 % bone, treated with TCP with 25 % newly formed bone and 11,3 % cement. The TCP/bFGF composite showed significantly less bony ingrowth with 15,7 % newly formed bone ($p<0.05$) and 14,4 % cement. In the periimplant area the bone content in relation to the measured area was 22,75% around defects treated with pure TCP, 20,09% around defects treated with autologous bone graft and 16,85% around defects treated with the TCP/bFGF-composite. These results were not significant.

DISCUSSION

In this study, bFGF showed a negative effect on bone ingrowth into the TCP/bFGF-composite compared with TCP alone and autologous bone graft. Furthermore, bFGF seems to have negative effects on resorption of the TCP cement. Addition of bFGF to the TCP showed negative effects on periimplant bone. In conclusion, the addition of bFGF to this newly developed TCP showed negative effects on bone ingrowth and the periimplant bone. In contrast to the pure TCP it is not useful for clinical application.

THE BIOLOGICAL PROPERTIES OF CALCIUM PHOSPHATE BONE SUBSTITUTES ARE INFLUENCED BY THE BIOMATERIAL PORE SIZES

*Klenke FM, ***Liu Y, *Siebenrock KA, **Hofstetter W
*Clinic of Orthopedic Surgery, Inselspital, University of Bern, Switzerland

frank.klenke@dkf.unibe.ch

INTRODUCTION: The limited availability of autologous bone grafts, the standard material for the reconstruction of bone defects, has enforced the demand for biomaterials that can be used as bone substitutes. The successful osseointegration and the subsequent substitutions of these biomaterials by newly formed bone are largely dependent on angiogenesis and vascularization. We hypothesize that angiogenesis and vascularization can be influenced by varying the pore size of bone substitute materials.
The aim of this study was to investigate angiogenesis and microvascularization during osseointegration of bone substitutes *in vivo*. The effects of pore sizes of biphasic calcium phosphate (BCP) bone substitutes on angiogenesis and osseointegration were analyzed.

METHODS: 36 Balb/c mice were provided with a cranial window preparation where the calvaria served as the site for orthotopic implantation of biphasic calcium phosphate (BCP) bone substitute ceramics. Approval for the experiments was given by the local animal review board. Dense BCP ceramic (n=6) and porous BCP ceramics with a total porosity of 75% and pore sizes of 40-70µm, 70-140 µm, 140-210 µm, and 210-280 µm (n=6 each) were implanted into a 4 mm critical size defect in mice calvariae. For Controls, the defects were left empty in 6 animals. Angiogenesis, microvascularization and leukocyte-endothelium interaction during osseo-integration of the bone substitutes were analyzed by means of intravital microscopy. As a parameter of vascularization, functional vessel density (*FVD*) was determined as the length of all perfused vessels within the implantation site in relation to its two-dimensional surface [mm/mm²]. Intravital fluorescence video microscopy was performed on days 7, 14, 21 and 28 after implantation of the biomaterials, using a vertical illumination fluorescence microscope unit. After 28 days the *in vivo* experiments were terminated and representative tissue samples were excised for subsequent histological investigations. To assess the formation of new bone, quantitative histomorphometry was performed on serial ground sections. The percentage of the outer and inner surface of the ceramics covered by newly formed bone served as an indicator for the osteoconductivity of the biomaterials. Data were statistically analysed with ANOVA. Student-Newman-Keuls method was applied for multiple-comparison procedures. Differences were considered significant at $p<0.05$.

RESULTS: Empty defects did not show spontaneous healing within the investigation period of 28 days, proving the defect of 4 mm in diameter to be of critical size. Intravital microscopy demonstrated that vessel formation and the onset of perfusion in newly formed vessels occurred significantly earlier in BCP ceramics with pore sizes greater than 140 µm compared to ceramics with pore sizes smaller than 140 µm and dense materials. The time course experiments demonstrated that the functional vessel density (FVD) was initially greater in ceramics with pore sizes of 210-280 µm than in dense ceramics and materials with pore sizes between 40 µm and 140 µm. FVD increased in all groups within the investigation period, and, except for the ceramics with 40-70 µm pore sizes, finally reached similar levels.
The leukocyte-endothelium interaction (*LEI*), a sensitive indicator for immune reactions elicited by the biomaterials, was not elevated in the BCP groups compared to Controls. Among the BCP groups there were no differences found in LEI.
After 28 days, the amount of new bone formation determined histologically was greatest in ceramics with pore sizes of 210-280 µm and was significantly higher compared to ceramics with pore sizes of 40-70 µm and dense BCPs. There also was a higher extent of new bone formation found in ceramics with the largest pore sizes compared to ceramics with pore sizes of 140-210 µm and 70-140 µm. This difference however did not reach the level of statistical significance.

DISCUSSION: The dynamics of angiogenesis and vascularization of bone substitute materials seem to be influenced by the biomaterials' pore sizes. The similar leukocyte-endothelium interactions of BCP groups and Controls demonstrate that the differences in angiogenesis and microvascularization were not modulated by an immune reaction to the biomaterials. In addition to the influence on angiogenesis, the pore sizes of bone substitute materials seem to have impact on the osteoconductivity and the dynamics of new bone formation. The present study demonstrates that the pore size of calcium phosphate bone substitutes is a critical structural parameter. Varying the pore size represents a possibility to influence the biological properties of bone substitutes. Since the mechanical stability of calcium phosphate ceramics is in a reverse relation to pore diameter, a pore size representing the most suitable compromise between biological and mechanical properties should be chosen for clinical applications.

AFFILIATED INSTITUTIONS FOR CO-AUTHORS:
**Department Clinical Research, University of Bern, Switzerland
***ITI Research Institute for Dental and Skeletal Biology, University of Bern, Switzerland

HEALING OF 1.5 CM ULNA DEFECTS WITH A PORCINE COLLAGEN-DERIVED MATRIX

*Smitham P, *Michaels D, *Leong A, *Stephens P, *Vizesi F, *Bruce W, **Hill R, *Walsh WR
Surgical & Orthopaedic Research Laboratories, University of New South Wales, Sydney, Australia
W.Walsh@unsw.edu.au

INTRODUCTION

The treatment of bony defects due to trauma, tumors or osteolysis presents a surgical as well as biological challenge based on size and anatomical location. Associated morbidity with the use of autograft, potential disease transmission or limited source using allograft and the large number of bone graft substitute materials can complicates surgical treatment even further. EMatrix, a novel material composed of gelatin and dextran biopolymer designed to mimic the extracellular matrix found in early fetal development. This study examined the radiographic, bone mineral density, mechanical properties and histology of the ulna defects filled with either test material compared to an empty defect at 4 and 12-week time points.

METHODS

A unilateral ulna defect was created in thirty-six (3.0 kg) New Zealand white rabbits following ethical approval. Ulna diaphyseal defects 1.5 cm in length were created using a mini-sagittal saw referenced 2 mm distal from the ulna collateral ligament. The ulna segment along with its attached periosteum was removed with a pair of forceps. The ulna defects were either filled with EMatrix Lyophilized or EMatrix Lyophilized + Cross Linked formulations suspended in a gel form of EMatrix or left empty as controls (Figure 1).The animals were allowed unrestricted activity until sacrifice.

Animals were killed at 4 and 12 weeks (n=6 per group). End points included magnified radiographs graded in a blinded fashion, bone mineral density (BMD) compared to the contralateral side, torsion testing following the method of Kukobo et al. [1] using a biaxial MTS machine and H & E histology. Data was analysed using an analysis of variance (ANOVA) followed by a post-hoc multiple comparison using SPSS for Windows. The histology examination included at the bony margins and centre of the defect. Time 0 histology and radiographs of the EMatrix material was also performed.

RESULTS

Surgery was uneventful with no intraoperative or postoperative complications. All animals mobilized well by day 2-3 and wounds were well healed at 4 and 12 weeks. No adverse reactions to the implanted materials were noted. No radiographic evidence of the material was noted at time 0, 4 or 12 weeks. Some non-unions occurred in all groups proximally as well as distally. New bone was observed at the proximal and distal margins in all groups. The treated defects performed superior to the empty defects but was not statistically significant. BMD increased with time in the treated defects but did not increase in the empty defects between 4 and 12 weeks. Torsional properties increased with time for all 3 groups while no significant differences were found between groups.

Histology at time 0 revealed the open cell structure of E-Matrix (Figure 2a.b). Residual EMatrix in either form was undetectable at 4 or 12 weeks based on histology. 4-week histology revealed abundant new woven bone formation in the defect site in the Lyophilized, Cross-linked and the Empty defect groups. The bone was very cellular and normal in appearance. The defects were not filled with fibrous tissue. The osteotomy margins were well defined at 4 weeks and did not show evidence of massive thermal damage or acellularity. Healing to the margins at the site of the osteotomy was well progressed by 4 weeks. 12-week histology revealed an improvement in healing from 4 weeks. Resorption of the woven bone in the centre of the defect and the establishment of a marrow cavity was noted in all 3 groups. A new cortex was established in the Lyophilized and Cross-linked group that qualitatively was more advanced compared to the Empty defects. The cortex in the treated groups was similar to that of the normal intact ulna compared to the control that still had yet to remodel back to this level.

Figure 2a-b: LYO EMatrix, polarized light, H&E;
2c: XL; H &E

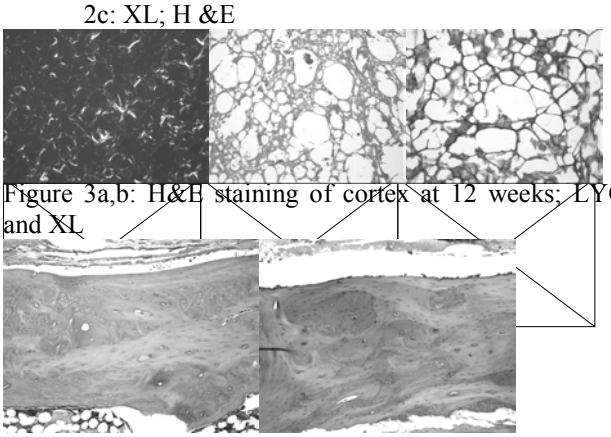

Figure 3a,b: H&E staining of cortex at 12 weeks; LYO and XL

DISCUSSION

Surgical handling of EMatrix was excellent. Mechanical data was similar to that reported by Kokubo using BMP 2. Both formulations of EMatrix had abundant new bone and a mature cortex by 12 weeks. A surprising finding of this study was that the 1.5 cm ulna empty defects in the cortical bone heal to some extent at 4 and 12 weeks. This is contrast in to the literature, which has generally assumed a 1.5 cm defect in the ulna to be critical. This may reflect differences in surgical technique in terms of minimal tissue trauma and good muscle coverage of the more proximal defect.

REFERENCES

[1] *Biomaterials* 24(9): 1643-1651, 2003

52 WEEK RESULTS OF AN IN VIVO EVALUATION OF BONE GRAFT SUBSTITUTE PARTICULATES IN A RABBIT MODEL

* Smitham PJ, *Butler A, *Vizesi F, *Michael D, *Bruce W, *Buckland T, *Walsh WR
Surgical & Orthopaedic Research Laboratories, University of New South Wales, Sydney, Australia

W.Walsh@unsw.edu.au

INTRODUCTION

Chemistry, size, shape, porosity and time can all potentially influence the in vivo response. This study evaluated the influence of the porosity of particulate calcium phosphate bone graft substitutes in a bilateral tibial defect model in NZ white rabbits based on radiographic, mechanical, histomorphometry and histology to 52 weeks following surgery.

METHODS

A bilateral metaphyseal - diaphyseal tibial defect in adult rabbits [1] was used to examine implant resorption and bony response of 4 bone graft substitutes in particulate form (table 1) at 2, 4, 12 and 52 weeks. The defects were flushed with sterile saline prior to being filled with the 4 different calcium phosphate bone graft substitutes (table 1) to the height of the original cortex. End points included; AP and lateral Faxitrons, mechanical testing in torsion in load and angle control to failure, SEM for histomorphometric analysis and routine paraffin histology. Samples at 0 wks were examined with radiographs and PMMA – SEM histomorphometry only.

Table 1: Study design

Implant	Material	Porosity	Particle size	Time points
Apapore-60	Synthetic HA	60%	2-5 mm	2, 4, 12, 52 wks
Actifuse	HA, 0.8% Silicon substituted	80%	2-5 mm	2, 4, 12, 52 wks
Apapore-80	Synthetic HA	80%	2-5 mm	2, 4, 12, 52 wks
OsSatura	80% HA, 20% Beta-TCP	75%	1-2 mm	2, 4, 12, 52 wks

RESULTS

Faxitron radiographs versus time revealed a progression in new bone formation and healing of the defect. New bone formation was observed by 4 weeks in all groups and appeared well healed by 12 weeks with new bone formation in the defect site in concert with the implanted materials. By 52 weeks new bone was integrated well within the remaining materials. All samples failed in a spiral fashion initiated at the distal margin of the defect in torsion testing. The properties increased as the defects healed and new bone formed within the defect and cortex reconstituted with time. No differences were noted between materials.

SEMS revealed a progression of new bone formation with time for all materials. New bone ingrowth into the porous domains and ongrowth to the surface of the materials was evident at 2 weeks and progressed with time. The synthetic HA materials did not show any resorption based on histomorphometry versus time. New bone ingrowth improved with time and stabilised at 52 weeks (figure 1).

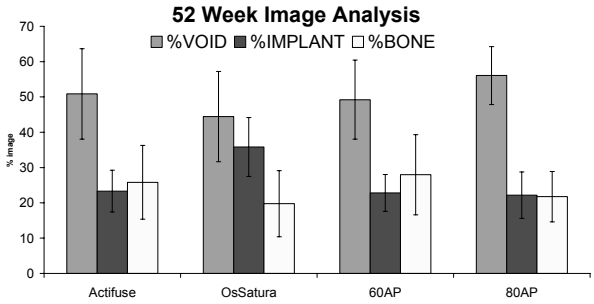

DISCUSSION

The empty defects do not heal in this model, supporting the critical nature of this defect [1]. New bone formed at the margins of the defect, posterior endosteal cortex and within the defect itself, confirming the osteoconductive of the materials examined. The performance of all 4 materials was similar in this model while they were all superior to ProOsteon 200R based on data using the identical experimental conditions [1].

The macroscopic, microscopic and chemical differences in the materials did not result in any major differences in in-vivo bone response in terms of mechanical properties or histomorphometry data apart from implant resorption as expected for the HA/TCP material. The lack of any differences may reflect the use of these materials in particulate form as opposed to solid blocks. Hing et al., [2] recently reported that microporosity enhances bioactivity of synthetic bone graft substitutes. The packing of the defect may override the differences in material microporosity when in particulate form. Interestingly, the OsSatura material is reported to have particle size of 1-5 mm whilst the other materials studied were 2-5 mm in size. This difference in particle size may influence the overall void in the defect and packing as well as available surface area. The slow degradation profile of the synthetic materials may also contribute to an overall slower new bone formation due to the presence of the material itself. These materials do demonstrate overall excellent biocompatibility and osteoconductive properties and remain present even at 52 weeks.

REFERENCES

[1] Walsh et al., *J Orthop Res* 21(4): 655-661, 2003.
[2] J Mat Sci Mat Med, 16: 467-475, 2005

AFFILIATED INSTITUTIONS

* ApaTech Ltd, Queen Mary, University of London, London, E1 4N

INCREASED AMOUNT AND STRENGTH OF RESTORED BONE USING A SLOWER-RESORBING TRI-PHASIC $CaSO_4$-BASED CEMENT COMPARED TO CONVENTIONAL $CaSO_4$ PELLETS

Urban RM, Turner TM, Hall DJ, Inoue N, Gitelis S
Dept. of Orthopedic Surgery, Rush University, Chicago, Illinois, USA
robert_urban@rush.edu

INTRODUCTION: $CaSO_4$ pellets have been used successfully as a synthetic bone graft, and their equivalency to autologous bone has been demonstrated for treatment of contained defects [1]. In some applications, notably subchondral and vertebral, an injectable, slower-resorbing $CaSO_4$ is needed. A tri-phasic $CaSO_4$-based cement, incorporating a matrix of $CaSO_4$ and dicalcium phosphate dihydrate with a distributed phase of ß-tricalcium phosphate (TCP) granules, was engineered. We hypothesized that the amount and compressive strength of restored bone would be significantly greater and the material resorption profile slower when defects were treated with the new cement compared to conventional $CaSO_4$ pellets in a canine bilateral defect model after 13 and 26 weeks.

MATERIALS AND METHODS: Under an IACUC-approved protocol, 10 skeletally mature, male dogs (25-32 kgs) had a critical-size, axial medullary defect (13mm dia X 50mm) created bilaterally in the proximal humerus [1] and were studied for 13 (N=5) and 26 (N=5) weeks. The defect in one humerus was injected with 6 cc of the test material (SR cement, Wright Medical). An identical defect in the contralateral humerus received an equal volume of $CaSO_4$ pellets (OSEOSET® pellets, Wright Medical). Radiographs were obtained at 0, 2, 6, 13 and 26 weeks. Transverse, undecalcified stained sections of the bones were prepared. The area fractions of new bone and implanted residual materials in the defects were quantified using standard point-counting techniques. The sections were also examined using high-resolution contact radiographs. The yield strength and modulus of an 8mm dia. X 20mm test cylinder cored from the midlevel of each defect was determined in unconfined, uniaxial compression tests at a crosshead speed of 0.5 mm/min. The histomorphometric and biomechanical data were analyzed using the Friedman and Mann-Whitney tests. Data are presented as the mean and standard deviation.

RESULTS: The clinical and postmortem radiographs revealed markedly different rates of resorption of the bone graft substitutes and replacement with bone in the defects. Resorption of the $CaSO_4$ pellets was apparent beginning at 2 weeks and substantially complete by 6 weeks. There was slower resorption of the SR cement, also beginning at 2 weeks, but some cement persisted at 26 weeks.

In all of the stained histological sections, there was restoration of the defects by bone and marrow with only focal areas of fibrous tissue and relatively low volumes of residual implanted material. The area fraction of new mineralized bone at 13 weeks was 2-fold greater in defects treated with SR cement (39.4±4.7%) compared to defects treated with conventional $CaSO_4$ pellets (17.3±4.3%) (p=0.025). At 26 weeks, the bone had remodeled to a more normal architecture, but there was still more bone in defects treated with cement (18.0±3.4%) compared to pellets (11.2±2.6%) (p=0.025).

Residual matrix and ß-TCP granules were incorporated into bone trabeculae. Surfaces of the materials not covered by bone appeared to be undergoing remodeling by osteoclast-like cells, some of which contained minute particles. The area fraction of residual matrix was greater in the cement-treated defects at 13 weeks (2.9±2.8%) and at 26 weeks (0.6±0.8%) compared to pellet-treated defects (0.0% at 13 and 26 weeks) (p=.025 and .083, respectively). Residual matrix decreased with time in the cement-treated defects (p=.047). The area fraction of residual ß-TCP granules also decreased from 13 weeks (3.6±1.0%) to 26 weeks (0.8±1.4%) (p=.016). The maximum dimension of the ß-TCP granules decreased from 348±13 µm at 13 weeks to 296±29µm at 26 weeks (p=.008).

Cored bone samples from defects treated with the cement were considerably stronger and stiffer than those treated with $CaSO_4$ pellets at both 13 and 26 weeks (Table). For comparison, similar cored trabecular bone specimens from 8 normal proximal humeri had a yield strength of 1.4±0.66 MPa and a modulus of 117±72 MPa.

Strength and Stiffness of Restored Bone (MPa)

	Time (wks)	SR Cement	$CaSO_4$ Pellets
Yield Strength	13	5.3 (2.6)*	.90 (.44)
Yield Strength	26	2.2 (.41)**	.47 (.46)
Modulus	13	283 (217)	40.8 (35.6)
Modulus	26	150 (73)*	15.8 (23.6)

*p = 0.025, **p=.046, different from pellets

DISCUSSION: Several Ca-based materials with different resorption rates were successfully combined to produce a cement with a tailored, slower resorption profile. In this cement, the majority of the calcium sulfate and dicalcium phosphate dihydrate matrix resorbs early, promoting bone formation deep into the bolus of cement, while the distributed ß-TCP granules provide a scaffold, incorporate into new bone, and are then more slowly resorbed. The engineered cement increased the amount, strength and stiffness of restored bone when compared to conventional $CaSO_4$ pellets after 13 and 26 weeks. This cement holds promise for clinical applications where a strong, injectable and highly biocompatible bone graft substitute would be advantageous.

REFERENCES: [1] Turner TM. JBJS 2001;83A:8-18.

ACKNOWLEDGEMENT: Wright Medical Technology

STRAIN INDUCED RELEASE OF BMP-7 FROM FRESH FROZEN FEMORAL HEAD ALLOGRAFT

*Board TN, *Gowaily K, *Rooney P, **Kay PR
*Tissue Service R&D, National Blood Service, Liverpool, UK and **Wrightington Hospital, Wigan, UK.

boardtim@hotmail.com

INTRODUCTION

The success of impaction-grafting for revision hip arthroplasty depends on mechanical stability and adequate bony incorporation of the graft.

Full incorporation of this type of graft has been demonstrated histologically and depends on many factors including the biological activity of the graft. Bone morphogenic proteins (BMPs) are known to play a central role in bone formation and their presence reflects the biological activity of a graft material.

The aim of this study was to determine the activity of fresh frozen femoral head (FFH) allograft by analysing BMP-7 release during strain imposed by the impaction process.

METHODS

Forty, 10mm cancellous bone cubes were cut from 7 FFH specimens.

The marrow content was removed. The cubes were then washed and the fluid assayed for BMP-7 activity using a commercially available ELISA kit.

The cubes were then divided into 4 groups and each group was subjected to strain of either 20%, 40%, 60% or 80% using a material testing machine. The cubes were washed again and the wash fluid analysed for BMP-7 activity. Results were analysed and statistical tests performed using Microsoft Excel.

RESULTS

BMP-7 activity was found to be present in all groups. Release of BMP-7 was found to increase with increasing strain. At 80% strain the mean concentration of BMP-7 released (830 pg/g) was 58% greater than that released at 60% strain (527 pg/g), 150% greater than the concentration at 40% strain (333 pg/g) and 476% greater than at 20% strain (144 pg/g).

The differences between release at 80% and 40% strain and between 80% and 20% strain were statistically significant ($p=0.036$, $p=0.002$).

CONCLUSIONS

Activity of BMP-7 in FFH has not previously been demonstrated.

This study shows that the freezing and storage of femoral heads allows some maintainance of biological activity.

Furthermore we have shown that BMP-7 may be released from FFH cancellous bone in proportion to the strain applied to the bone.

This confirms that large bone morsels should be used during the grafting process to allow release of BMPs during impaction.

ECTOPIC PREFABRICATON OF BONE FLAPS

*Scheufler O, *Schaefer DJ, *Jaquiery C, **Braccini A, **Wendt D, *Pierer G, **Heberer M, **Martin I
*Clinic for Reconstructive Surgery
*Institute for Surgical Research and Hospital Management
University Hospital Basel

oscheufler@uhbs.ch

INTRODUCTION

The use of bone flaps is the gold standard to repair large bone defects associated with severe soft tissue damage and poor vascularity, but is limited by the availability of donor tissue and by donor site morbidity. A bone tissue engineering approach consisting in the loading of bone marrow stromal cells (BMSC) into porous ceramic scaffolds has the potential to generate autologous osteoinductive grafts of virtually unlimited size, but is limited by the lack of graft vascularization at the time of implantation. In this work, we combined the concepts of flap prefabrication and bone tissue engineering to generate large ectopic bone flaps in a rabbit model. We then aimed at determining possible limitations in the extent of bone formation within the prefabricated flaps.

METHODS

Porous hydroxyapatite scaffolds (80 ± 3% porosity, Fin-Ceramica, Faenza, IT) were fabricated in the shape (i) of small disks (4mm height, 8mm diameter), used to validate the osteogenic capacity of rabbit BMSC in vivo, and (ii) of tapered cylinders (30mm height, 20mm upper base diameter, 10mm lower base diameter), used to determine if the extent of bone tissue formation depends on the diameter of the construct. BMSC were expanded in monolayer from bone marrow aspirates of 12 young adult New Zealand White rabbits. Expanded BMSC were loaded onto disks and tapered cylinders at a density of 10 x 10^6 cells per cm^3 of scaffold by continuous perfusion in alternate directions through the scaffold pores at a velocity of 1.2 ml/min for 24 hours (Wendt et al., Biotech Bioeng, 2003). Cell seeding efficiency and uniformity were assessed by DNA quantification and MTT staining, respectively. In each animal, a disk loaded with autologous BMSC (group 1) and a cell-free disk (group 2) were implanted subcutaneously. In addition, tapered cylinders loaded with BMSC, wrapped in a panniculus carnosus flap and covered by a semipermeable membrane (group 3) or covered by a semipermeable membrane and inserted under the panniculus carnosus (group 4) were implanted on opposite sides of the back to test bone formation under respectively vascularized and non-vascularized conditions. Constructs were explanted after 12 weeks and assessed histologically and by MRI.

RESULTS

Cell loading by perfusion was highly efficient (over 90%) and uniform both in disks and tapered cylinders. Uniform bone formation was observed in all cell-seeded disks (group 1), whereas no bone formed in cell-free disks (group 2). Tapered cylinders wrapped in the flap (group 3) were uniformly vascularized, but bone formation was found only in the outer 2.5 ± 0.3 mm and not in the central core. No bone tissue was formed in constructs where vascularization was prevented by the membrane (group 4). MRI reproducibly detected a sharp signal transition between the periphery and central core in all vascularized tapered cylinders (group 3), but a uniform signal in all non-vascularized constructs (group 4).

CONCLUSIONS

A panniculus carnosus flap supported ectopic prefabrication of large engineered bone flaps in rabbits. The finding that at 12 weeks bone tissue was restricted to the outer region of the flaps could be explained by insufficient vascularization of the central core of the constructs upon implantation and prompts for the development of strategies to improve vessel ingrowth from the flap.

QUANTIFYING FRACTURE FIXATION USING RADIOSTEREOMETRY

*Downing M, *Ashcroft B, **Ascroft G
Orthopaedic RSA Research Unit, Woodend Hospital,
Grampian University Hospitals Trust, Aberdeen, Scotland

m.downing@abdn.ac.uk

INTRODUCTION

Fracture healing is influenced by intermittent micro-motion between the fractured bone segments, induced by the forces to which the bone is subjected. Excessive or inadequate amounts of motion may delay fracture union. This study assesses a new application of RSA (Radiostereometric Analysis) to measure fracture micro-motion in-vivo.

METHODS:

Nine patients, with unilateral distal radial fractures were recruited and underwent primary fixation with AO titanium locking plates. There were 7 females with a mean (range) age of 50 (30-65) and 2 males (47,57 years). An anterior approach to the distal radius was used under tourniquet control. Prior to final reduction of fracture and fixation with plate, approximately 4-7 tantalum beads of diameter 1mm were inserted into both the distal and proximal bony fragment. Standard fracture fixation and wound closure was carried out.

RSA examinations were performed at 2 days, then at 2, 6, 26 and 52 weeks. The patient's forearm was placed in mid pronation on a rest inside a bi-planar reference cage. Exams were taken with the wrist relaxed, and then with an induced load on the fracture by the patient gripping a Jamar dynamometer with maximal voluntary compression Both exams were repeated at each occasion with repositioning to assess repeatability.

Migration, relative movement of the distal segment with respect to the proximal fragment, was assessed over time by comparison of the unloaded exam with the unloaded post-op exam. Induced displacement was assessed by comparing the loaded to the resting exam within one occasion. Films were examined using locally developed software and the UmRSA system.

RESULTS

One patient was lost to follow-up after 6 weeks and two more after 26 weeks. Precision (95%) was similar for both whole body migration and induced movement, ranging from 0.05mm axially to 0.1mm volar, and rotation from 0.3 degrees abduction to 0.8 degrees pronation.

All patients experienced proximal migration of the distal fragment (figure 1). Typically this was 0.5mm in the first 6 weeks and a similar amount in the next 20 weeks. No cases had significant movement after 6 months.

Induced proximal motion (figure 2) increased up to 2-6 weeks, which this coincided with increased applied load. Thereafter it decreased, becoming less than 0.05mm between 6 and 12 months. A similar pattern was observed for the other translation and rotations.

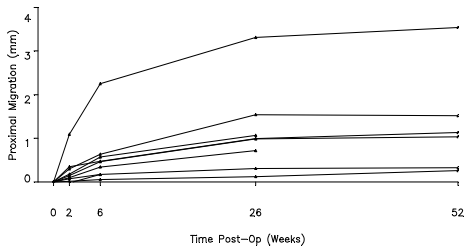

Figure 1. Axial migration for each patient.

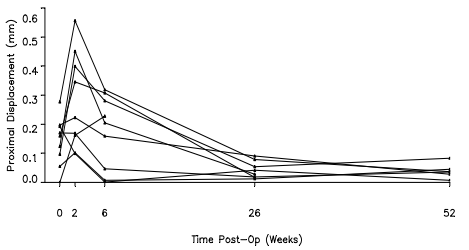

Figure 2. Axial induced displacement for each patient.

DISCUSSION

Induced movement was reproducibly measured in this study. It reduced to a small residual between 6 weeks and 6 months, giving evidence of full union within this period.

Although there are no previous reports assessing induced fracture motion with RSA, the precision was poorer than a reported in-vitro study for migration (Madanat 2005). In-vivo precision is limited by markers occluded by metal work, and marker movement within the bone which appears to be higher in the vicinity of fractures compared to joint replacements. We recommend a bead pattern with high redundancy and wide spread for the reference segment. This study demonstrates that the small dynamic movement of fracture fragments may be measured during fracture healing which will lead to improved understanding of different treatments and the potential for defining normal union rates.

AFFILIATED INSTITUTIONS FOR CO-AUTHORS

**Orthopaedic Dept, University of Aberdeen, Scotland.

REFERENCES

Madanat R. et al, J Orthop Res, 2005, 23: 481–8.

RADIOSTEREOMETRIC ANALYSIS (RSA) OF THREE-DIMENSIONAL MICROMOTION IN A FRACTURE MODELOF THE DISTAL RADIUS

Madanat R, Moritz N, Mäkinen TJ, Aro HT
Orthopaedic Research Unit, Department of Orthopaedic Surgery and Traumatology
University of Turku, Turku, Finland

rami.madanat@utu.fi

INTRODUCTION

Functional disability after a fracture of the distal radius is closely related to the residual anatomical deformity. Awareness of the factors that predict instability in fractures of the distal radius is important in anticipating the final outcome and in selection of the appropriate treatment modality. Conventional radiography has its limitations in estimation of the inherent fracture stability and the risk for the loss of reduction.

Radiostereometric analysis (RSA), is a powerful research tool, which has revolutionized the possibilities of measuring small relative three dimensional displacements of body parts or implants in vivo. The method is based on implantation of metallic landmarks (tantalum beads). Stereoradiographs are then used to determine the location of the markers three-dimensionally, and this allows the calculation of relative displacements between different segments. The RSA method enables measurement of translation and rotation in three dimensions.

The main purpose of the current study was to verify the feasibility of radiostereometric analysis (RSA) in monitoring of three-dimensional fracture micromotion in fractures of the distal radius. The second goal of this study was to create a realistic accurate computer model for preoperative planning of RSA studies.

METHODS

For the first part of the study the experimental set-up consisted of a physical simulated model of an extra-articular Colles' fracture marked with a total of ten tantalum RSA beads. The fracture model was rigidly fixed to high precision micrometer stages allowing controlled translation in three axes and rotation about the longitudinal and transverse axes. The whole construct was placed inside a RSA calibration cage with two perpendicular radiographic film cassettes. In order to determine the accuracy and precision of RSA in measuring translational and rotational displacements of the distal fracture fragment, altogether 80 radiostereometric examinations were performed. Accuracy was calculated as the 95% prediction intervals from the regression analyses between the micromotion measured by RSA and actual displacements measured by micrometers. Precision was determined as the standard deviation of five repeated measurements of a 200 µm displacement or a 0.5° rotation along a specific axis.

In the second part of the study a realistic 3-D computer model of the radius was created from a set of tomographic scans. Two fracture types were created and both simple and comlex micromotion was simulated. The simulation of the radiographic imaging was performed using ray-tracing software (POV-Ray). RSA measurements were performed according to standard protocol.

RESULTS

The results showed that translations from 25 µm to 5 mm were measured with an accuracy of ± 6 µm and translations of 200 µm were measured with a precision of 2-6 µm. Rotations ranging from 1/6º to 2º were measured with an accuracy of ± 0.073º and rotations of 1/2 º were measured with a precision of 0.025º - 0.096º.

In the computer simulation study using a two-part fracture model (AO/ASIF type A2), it was found that for simple movements in one axis, translations in the range of 25 µm to 2 mm could be measured with an accuracy of ± 2 µm. Rotations ranging from 1/6º to 2º could be measured with an accuracy of ± 0.015º. Using a three-part fracture model (AO/ASIF type C1) the corresponding values of accuracy were found to be ± 4 µm and ± 0.031º for translation and rotation respectively. For complex 3-D motion in a three part fracture model the accuracy was ± 6 µm for translation and ± 0.120º for rotation.

DISCUSSION

These results show that RSA is both a highly accurate and precise method for measuring micromotion in a fracture model of the distal radius. The results suggest a strong rationale for the use of RSA as an objective tool for comparing different treatment modalities and novel bone graft substitutes aimed at stabilization of fractures of the distal radius. The use of 3-D computer modelling can provide a method for preoperative planning of RSA studies in complex fractures of the distal radius and in other clinical situations in which the RSA method is applicable.

FEMORAL FRACTURE LOAD AND FAILURE ENERGY IN TWO LOAD CONFIGURATIONS: AN IN VITRO STUDY

*Duchemin L, *Skalli W, *Topouchian V, *Benissa M, *Mitton D
* Laboratoire de Biomécanique, ENSAM-CNRS UMR 8005, Paris, France

Laure.Duchemin@paris.ensam.fr

INTRODUCTION

Large efforts have been carried out to reduce the medical and social cost of osteoporosis. Relevant investigations on femoral strength have been performed through in-vitro studies, providing a better knowledge of fracture process and mechanical data. But most of them have been performed in only one load configuration.

The aim of the present study was to evaluate bone strength in stance and lateral loading conditions and to investigate the influence of the configuration on the specimen behaviour.

METHODS

A total of 80 human femora (40 matched pairs) were collected from 24 female and 16 male donors (47 to 100 years, mean 82 years).

One randomly selected femur of each pair was tested to failure in stance configuration (Fig.1a) [1], while the contralateral femur was loaded in lateral configuration (Fig.1b) [2]. Biomechanical tests were performed on a universal testing machine (INSTRON® 5500-R) at 12.7 mm/min. Fracture load was defined as the first peak load, and absorption energy to failure was calculated as the area under the load-displacement curves until fracture load.

A non-parametric Wilcoxon test was performed to evaluate statistical differences between load configurations, and a Pearson correlation test was achieved to assess the relationships between fracture load and absorption energy to failure.

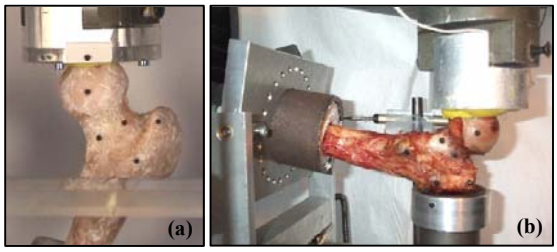

Fig. 1: Experimental testing in (a) stance and (b) lateral configuration

RESULTS

Both loading conditions demonstrate their capacity to reproduce fractures consistent with clinical observations. Fracture load (F) and absorption energy to failure (W) for both configurations are presented in Table 1. For stance as well as for lateral loading, energy to failure was highly correlated with fracture load (r = 0.94 and r = 0.98 respectively). Strong linear correlations were also found between data obtained in lateral and stance configurations (r = 0.87 for fracture load, r = 0.88 for absorption energy, $p<0.05$) (Fig.2).

Table 1: Mechanical results for stance and lateral loading

	Age (year)	**Stance** (n=40)		**Lateral** (n=40)	
		F (N)	W (J)	F (N)	W (J)
Mean	82	9032	12	2586	15
SD	12	3412	6	1146	9
Min.	47	3994	3	890	4
Max.	100	15886	26	5126	35

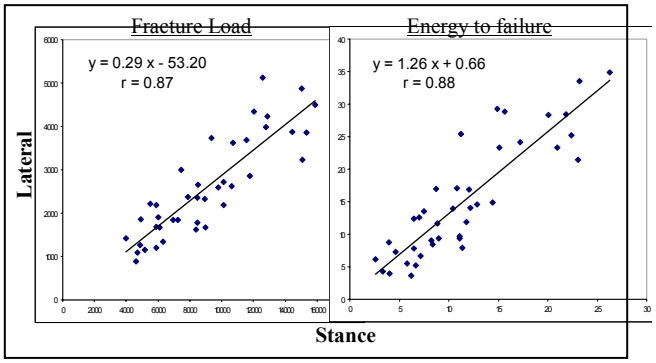

Fig. 2: Correlations between data for stance and lateral configurations

DISCUSSION

Significant correlations were obtained for a large amount of matched specimens (N=2x40), in accordance with previous results on smaller sets [3,4]. The strong relationship between mechanical parameters in stance and lateral configurations may be useful for hip fracture prediction from one position to the other.

ACKNOWLEDGEMENTS

The authors thank S.Persohn for his technical help. This work was partly supported by the European Research Grant EU QCK6-CT-2002-02440.

REFERENCES

[1] Le Bras A *et al.* 25th Annual Meeting ASBMR, Mineapolis, USA, 2003.
[2] Le Bras A *et al.* 29ème congrès SB, Créteil, France, 2004.
[3] Esses SI *et al.* J Bone Miner Res. 1989;4:715-22.
[4] Keyak JH *et al.* J Biomech. 2000;33:499-502.

COMPUTATIONAL SIMULATION OF FRACTURE HEALING UNDER FLEXIBLE AND RIGID FIXATION

*Gómez-Benito MJ, *García-Aznar JM, **Peris JL, **Atienza C, **Comín M, *Doblaré M
GEMM (I3A), Campus Río Ebro. Ed. Agustín de Betancourt,
University of Zaragoza, c/ María de Luna s/n, 50018-Zaragoza, Spain

gomezmj@unizar.es

INTRODUCTION

Fracture healing is a process highly influenced by the mechanical environment. Much attention has been paid to study this influence experimentally and computationally[1]. In this work, we combine finite element simulation and a set of experiments performed in rabbits to study this process and how mechanical factors influence on it.

The main aim of this work is to explore the potential of a previous computational model[2] to predict mechanical properties of callus evolution under two external fixators with different stiffness (high and low).

METHODS

A finite element model of a rabbit tibia is obtained from a set of CT scans. This tibia is attached to both rigid and flexible external fixators (Fig. 2). A 1-mm ostetomy gap is simulated.

Using a previous developed computational model[2], bone healing simulation is performed on this tibia. This model simulates cellular events and callus growth by means of a combination of different analyses: biphasic poroelastic, diffusion and thermoelastic one.

RESULTS

Bone healing process under high and low fixation stiffness are simulated and compared to experimental results. Differences are expected between fractures healed under flexible and rigid fixation not only in tissue distribution and callus size but also in callus healing speed.

The model proposed in previous work[2] is going to be validated on a real geometry (rabbit tibia). Experimental and computational results are compared.

Model validation is going to be performed comparing predicted torsional and bending stiffness with the ones obtained in "in vitro" experiments in osteotomised rabbit tibia treated with these fixation devices[3].

Static analyses are performed each week of simulation to reproduce four-point bending and torsion tests in fracture callus. This "virtual" test provides us the evolution of bending and torsion stiffness.

CONCLUSION

In this work we simulate changes in callus size and evolution of tissue types in a realistic geometry of a rabbit tibia. As far as authors know, this is the first work in which computational simulation is performed on a real geometry and compared to experimental results.

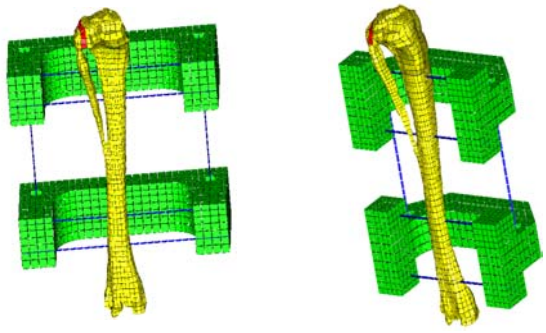

(a) (b)

Fig. 2: Finite element model of the low (a), and high (b) fixator stiffnesss including osteotomised rabbit tibia.

If the model is able to simulate callus size and shape progression (such as tissue differentiation, and torsional and flexion stiffness evolution obtaining similar results to experimental observations) it will be a useful tool to predict bone healing process and it will help to the design of new fixation devices and fracture treatments.

REFERENCES

[1]Claes L.E., Heigele C.A., Neidlinger-Wilke C., Kaspar D., Seidl W., Margevicius K.J., Augat P., Effects of mechanical factors on the fracture healing process. Clin. Orthop. Relat. Res. 2998, 355S, S232-247.

[2]Gómez-Benito MJ, García-Aznar JM, Kuiper JH, Doblaré M, Influence of fracture gap size on the pattern of long bone healing: a computational study, J. Theor. Biol. 2005; 235(2); pp. 205-229.

[3]Peris JL, García-Roselló M, Cuenca MD, Atienza C, Gómez A, López A, Prat J, Soler C. Effect of rhBMP-2 and fixation stiffness on fracture healing: Biomechanical study. 5th World Congress of Biomechanics 2006 (sent for revision).

AFFILIATED INSTITUTIONS FOR CO-AUTHORS

**Instituto Biomecánica de Valencia (IBV). Universidad Politécnica de Valencia (Edificio 9C) Camino de Vera s/n. 46022 Valencia. España. Tel.: +34 96 387 91 60, Fax:+34 96 387 91 69

THE USE OF TITANIUM FOR OSTEOSYNTHESIS IN RABBITS BY THREADED PINS

*Spinelli M, *Gabellieri P, **Pingitore R, ***Dini F, **Faviana P, °Odoguardi F, ***Carlucci F
*Orthopaedics and Traumatology Unit - ASL 6 Livorno

pullega@citieffe.com

INTRODUCTION

Screws and plates by titanium and its alloys are currently being employed in orthopaedics and traumatology, dentistry, and maxillo-facial surgery. Titanium has an elevated degree of biocompatibility, is malleable and radiopaque, and has a low specific weight, a low thermal conductibility, and an elevated index of resistance to the corrosion. This metal presents a good ability to osteointegration, determining an elevated resistance of the interface between bone and metal. However, an extreme osteointegration may also be responsible for difficulties in removal.

METHODS

The purpose of our research was to evaluate the influence of galvanization on the osteointegration of titanium.
Eighteen rabbits were operated to put a transcortical titanium screw without galvanization in the distal part of the right femur, and a galvanized one in the left femur. The animals were sacrificed after 60, 120, 180 days (six for each time set); the femurs were framed and fixed in formaline just before taking an xray.
For each femur, the segment close to the screw was isolated keeping a border from the screw of 4-5 mm each side.
The samples were dripped in acrylic resin and cut in slices of 350 μm with a wheeling diamont blade. The samples were rubbed down to 130 μm of thickness and coloured with toluidine blue and acid fucsin.
The slides were examined by optical microscopy and the bone-metal interfaces were photographed with a digital camera.
The images obtained were enhanced and combined using Adobe photoshop, and analysed by means of Autocad software to carry out precise measurements.
The interfaces were studied by measuring the lengh of the sections where the osteointegration was not present.

RESULTS

The postoperative management was regular. X-ray examinations showed a periostal reaction near the screws without galvanization. Histology did not show any acute, chronic or granulomatous flogistic process.
The morphometric analysis showed that the metal surfaces (bone-screw interface) of the bone was greater in the galvanized screws (22.3% versus 19.5%). This difference was less evident in the cases observed after six months.

DISCUSSION

Galvanization seems to reduce (15%) the osteointegration in the contact surface, but does not interfere with the healing process, maintains optimal titanium biocompatibility, and does not modify the stability of the implant.

AKNOWLEDGEMENTS

Citieffe srl - 40012 Calderara di Reno (BO)

AFFILIATED INSTITUTIONS FOR CO-AUTHORS:

** University of Pisa – Surgery Department
*** University of Pisa – Veterinary Clinic Department
° University of Pisa - Oncology Department

MECHANICAL STRENGTH EVOLUTION OF A RECONSTRUCTED FEMUR DURING FOLLOW-UP

*Taddei F, *Martelli S, *Montanari L, *Greco V, **Leardini A, *Viceconti M, ***Manfrini M
*Laboratorio di Tecnologia Medica, Istituti Ortopedici Rizzoli, Bologna, Italy

taddei@tecno.ior.it

INTRODUCTION

In the past twenty years, limb-salvage surgery has been increasingly adopted in the treatment of primary bone sarcomas, but still the optimal reconstruction is debated. The finite element (FE) method is a powerful tool to investigate the risk of fracture during various activities of the reconstructed segments[1], and to optimize the surgical technique and the rehabilitation protocol. The methods recently developed to generate subject-specific FE models of bones from Computed Tomography (CT) data are reliable[2]; relevant validation studies having confirmed that these can be used in a clinical context[3], and their predictions are accurate[4].

Aim of the present work is to present a subject-specific FE study performed to estimate the evolution of the mechanical strength of a complex distal femoral reconstruction during the first three years of follow-up.

MATERIALS AND METHODS

In 2001 a 10 years-old boy underwent a distal femoral reconstruction for a primary bone sarcoma, by means of a massive bone allograft in conjunction with a vascularised fibula autograft. A metal internal fixator plate was used for stabilizing the reconstructed bone (Fig. 1). The vascularised fibula remained alive and the bone kept growing regularly as both femoral growth plates were spared. During the first three years of follow-up the patient was CT scanned at nearly regular time intervals within routine control exams. One pre-operative and five post-operative CT exams were analysed. At the time of the fourth exam, the patient underwent gait analysis at the Movement Analysis laboratory of our institute. An recently developed protocol was used, which requires application of several markers on the patient skin prior to CT scanning, to allow for the spatial registration of patient's kinematics to the skeletal model.

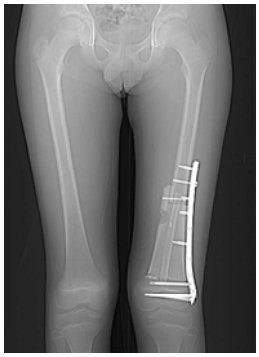

Fig.1 A RX of the reconstructed femur

A complete subject-specific muscle-skeletal model of the patient's lower limbs was build integrating CT with kinematics data using the DataManager©[5]. Muscles were represented with linear segments starting from the muscles' origin to their insertion. Muscles with broad origin or insertion areas were represented with more than one segment.

FE models of the operated femur and of the intact contralateral one, at each control exam, were built from the CT data by using a validated procedure that can accurately represent the bone morphology and the inhomogenous material property distribution[4]. The muscles' forces acting on the femurs, at the instant of maximum hip joint reaction, were estimated and used as boundary conditions for the FE models.

The evolution of the femoral strength was then put into relation with the changes in the bone density and morphology occurred over the follow-up.

RESULTS AND DISCUSSION

The preliminary results on the intact contralateral femur showed that the stresses induced during gait are always far below the ultimate stress of the bone tissue. In the reconstructed femur, more irregular stress and strain patterns were found, due to the altered and more complicate morphology of the bone segment. The highest stresses were predicted on the metal plate and screws. The altered biomechanical conditions seem to affect the risk of fracture in the reconstructed bone and this may be related to the alteration observed in the bone mineral content together with the presence of the metal fixation device. Although still in progress, this study has shown that, using the potentialities offered by the DataManager software that allows the fusion of different medical data, it is possible to go a step forward in the generation of fully subject-specific FE models of bones that take into account the patient's muscle-skeletal morphology, the bones' mechanical characteristics and the muscle forces that act on the bones during the a specific motor task.

REFERENCES

1. Taddei F, *et al*. Proc Inst Mech Eng [H]. 2003;**217**(2).
2. Viceconti M, et al. Crit Rev Biomed Eng. 2003;**31**(1-2).
3. Viceconti M, et al. J Biomech. 2004; **37**(10).
4. Taddei F, et al. J Biomech. 2005 [Epub ahead of print]
5. www.tecno.ior.it/multimod/

ACKNOWLEDGMENT

This study has been partially funded by AIRC (Associazione Italiana per la Ricerca sul Cancro)

AFFILIATED INSTITUTIONS FOR CO-AUTHORS

**Movement Analysis Laboratory
***Musculoskeletal Oncology Department
Istituti Ortopedici Rizzoli
Bologna, Italy

BIOMECHANICAL ANALYSIS OF SLIPPED CAPITAL FEMORAL EPIPHYSIS

*Gómez-Benito MJ, *Paseta O, *García-Aznar JM, **Barrios C, **Gascó J, *Doblaré M
*GEMM, Campus Río Ebro. Ed. Agustín de Betancourt,
University of Zaragoza, c/ María de Luna s/n, 50005-Zaragoza, Spain.

gomezmj@unizar.es

INTRODUCTION

Different anatomical and mechanical factors inducing growth plate overloading [1, 2] have been implicated in the etiology of Slipped Capital Femoral Epiphysis (SCFE). So far, loading at the epiphyseal growth plate of the femoral head has been poorly investigated.

In this work, a Finite Element Analysis (FEA) was performed in order to study the influence on the growth plate of mechanical factors, such as geometry and loads in different positions and physical activities.

METHODS

The geometry of both proximal femora of a 14-years-old boy with SCFE in his left leg were reconstructed from a set of computer tomographies (CT).

Later we develop a complete FE model considering three different (linear elastic isotropic behavior) materials: cartilage for the growth plate, trabecular and cortical bone.

Loads applied were the corresponding to the patient´s weight (92 kg) acting at the following activities: walking, sitting and going up stairs. Von Misses stresses at both the healthy and slipped growth plate were analysed.

RESULTS

In all load cases von Misses stresses at the SCFE plate were higher than at the healthy plate (Figure 1).

The critical regions corresponded to the site where usually the growth plate failure starts. Von Misses stresses in the SCFE plate were up to four times as compared with the healthy plate in the going up stairs case; these stresses reached a maximum of 12MPa. In the sitting case maximum stresses were 1.2MPa also in the medial area of the slipped hip.

CONCLUSION

The epiphyseal plate failure mechanism seems to be a combination of two effects:

i) Stresses produced by the loads corresponding to walking and going up stairs, which are mainly cyclical. They can influence on fatigue failure of growth plate. This fact could explain the lateral slipping of femoral head (Figure 1a).

ii) Stresses corresponding to sitting (mainly shear stresses), which are static stresses. They could cause the posterior slipping of femoral head (Figure 1b).

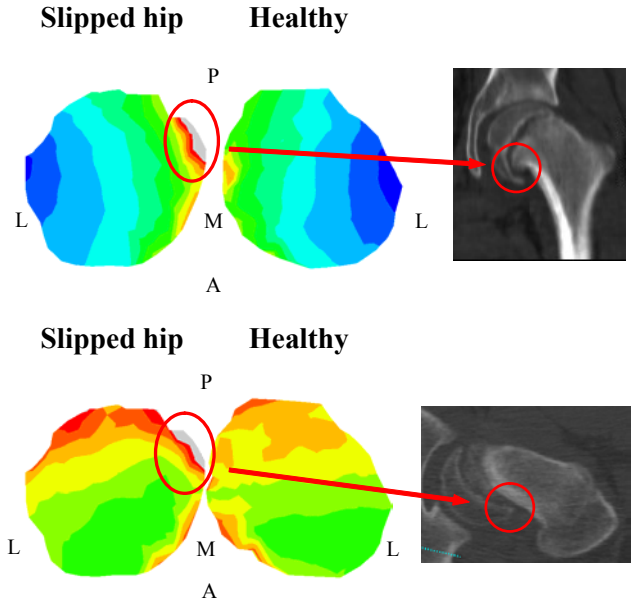

Figure 1. Von Mises stresses (MPa) in: (a) the highest load case of the gait cycle; (b) the sitting load case.
A: Anterior, P: Posterior, M: Medial, L: Lateral

REFERENCES

[1] Barrios, C., Blasco, M., Blasco, M. & Gascó, J. (2005). Posterior Sloping Angle of the Capital Femoral Physis. A Predictor of Bilatery in Slipped Capital Femoral Epiphysis. *Journal of Pediatric Orthopaedics,* 25(4), 1067–1078.

[2] Pritchett, J. & Perdue, K. (1989). Mechanical Factors in Slipped Capital Femoral Epiphysis . *Journal of Pediatric Orthopaedics,* 3, 385–388.

AFFILIATED INSTITUTIONS FOR CO-AUTHORS

**Orthopaedics and Trauma Unit, Department of Surgery, Valencia University Medical School, Valencia, Spain.

OSTEOCHONDRAL ALLOGRAFT REPLACEMENT IN CONDYLE RESECTION OF THE KNEE

Bianchi G, Donati D, Staals E, Colangeli M, Mercuri M
Musculoskeletal Tumour Department, Istituti Ortopedici Rizzoli, Bologna, Italy

giuseppe.bianchi@ior.it

INTRODUCTION

Osteochondral allograft replacement in condyle resection of the knee is a rarely used reconstructive technique and is required whenever the articular surface of the joint cannot be spared because of tumor invasion. Aim of this study is to assess the reliability of osteochondral allografts after complete medial or lateral condyle resection of the distal femur or proximal tibia.

METHODS

From January 1989 to September 2005, 13 condylar resection of the proximal tibia or distal femur were performed in our hospital. The patients (9 females and 4 males) had a mean age of 31.8 yrs (range 16-63). In 9 cases the left knee was affected and the right in 4. In 10 cases the resected condyle was of the distal femur (6 medial and 4 lateral) and in 3 of the proximal tibia (2 medial and 1 lateral). The osteochondral graft was fixed with screws in 9 cases and with a plate in 4. The mean follow up was 77.6 months (range 1-196).

RESULTS

Three grafts reported mechanical complication (subchondral fractures) but only a medial distal femoral graft failed after 29 months and was replaced. Two (15.3%) patients with mild knee pain underwent arthroscopy, 1 (7.6%) had a surgical debridment because of knee stiffness and 1 (7.6%) had a screw removal because of painful borsistis. 6 (46.1%) patients had considerable knee instability (5 valgus and 1 varus). The mean knee flexion was 99.2° (range 60°-120°). No graft infection were reported.
At follow-up, one patient with an osteosarcoma of the proximal tibia died because of pulmonary metastases at 148 months. No local recurrences were reported.

DISCUSSION

Our results showed a very low incidence of graft complications after osteochondral allograft replacement in condyle resection of the knee. Only one patient required graft replacement because of fracture after 29 months. All patient were able to walk free of crutches even if 6 complained considerable knee instability, but no restriction of daily activities was reported. An excellent range of motion (mean 0°-99°) was achieved in all patients. In conclusion, the use of a osteochondral allograft replacement represent our standard reconstructive techniques in condyle resection of the knee because of low major complication rate and good functional results.

THE COMBINATION VASCULARISED FIBULA/MASSIVE BONE ALLOGRAFT FOR TIBIA INTERCALARY RECONSTRUCTIONS: IMAGING ANALYSIS AT AN OVER 5-YEAR FOLLOW-UP

Manfrini M, Taddei F, Malaguti C, De Paolis M, *Ceruso M, Mercuri M
Istituti Ortopedici Rizzoli, Bologna , Italy

marco.manfrini@ior.it

INTRODUCTION

From February 1994 to October 2004, a vascularised fibula autograft (VFA) was inserted into a massive bone allograft (MBA), to reconstruct the tibia diaphysis in a homogeneous group of 30 young patients affected by bone sarcomas.
Implant biological behaviour was investigated on the basis of serial radiological examinations obtained in all patients, regularly followed for an average time of 75 mos (range 14-142). Mean age was 14 years (range 4-31) and 26 patients received neoadjuvant chemotherapy

METHODS

All patients were studied by standard X-ray every 6 months in the first 5 years and then every year; in all cases an average of 3 CT postoperative evaluations (2-6) at over-one-year intervals were performed. Computer assisted analysis was performed at 3 constant levels within the reconstruction, so that the subsequent CT exams could be compared. The following measurements were recorded: VFA Maximal Sagittal and Transverse Diameter, Total and Medullary Area, Maximum Cortical Thickness and Cortical Density; MBA Cortical Thickness and cortical density.

RESULTS

In the first postoperative year, two patients had the implant removed because of deep sepsis and one other died for drug toxicity. In 2 cases no changes in fibula parameters were seen along the years, while in all other patients radiographic analysis reveals two patterns, variably mixed in each case: A) When MBA cracks, load over VFA rapidly increases. Living fibula produces a fast, dense cortical hypertrophy. B) MBA preserves its original strength and absorbs the majority of load. Living VFA presents a progressive but slower enlargement of both external and medullary diameter with a low-density cortex.
Serial CT analysis demonstrated statistically significant changes in both VFA diameters ($p<0.001$)and areas ($p=0.0001$). These increments increased when patients abandoned braces. From the second p.o. year, a layer of ossification appeared on the endosteal surface of the allograft; tissue between VFA and inner MBA showed a slow maturation with axial bridges between the two bones. After 5 years the inner fibula completely fused to the allograft that, if mechanically intact, appeared almost completely substituted by new reactive bone.

DISCUSSION

VFA can rapidly adapt to new mechanical situations: cortical changes are directly correlated to load. Serial radiological analysis shows complete remodelling of MBA with inlaid VFA and demonstrates bone-inductive activity of VFA on the endostal surface of MBA.

REFERENCES

Manfrini M, et al: Imaging of vascularized fibula autograft placed inside a massive allograft in reconstruction of lower limb bone tumors. Am J Roentgenol. 2004;182:963-70.

ACKNOWLEDGEMENTS

This work has been partially funded by AIRC (Associazione Italiana per la Ricerca sul Cancro)

Affiliated Institutions for co-authors
*Centro Traumatologico Ortopedico (CTO), Firenze, Italy

REPAIR OF CARTILAGE LESIONS BY PERFORATIONS OF SUBCHONDRAL BONE AND IMPLANT OF A COLLAGEN TYPE I/II MEMBRANE

*Gigante A, Guzzanti V, Giordano M, *Bevilacqua C, *Greco F
*Dept. Orthopaedics, Politechnic Univ. Marche, Ancona, Italy

agigante@iol.it

INTRODUCTION

Lesions of the articular cartilage constitute an unsolved therapeutic problem. The aim of this study was to evaluate the development of articular lesions treated with perforations of the subchondral bone and implant of a collagen type I/II membrane.

METHODS

In the knees of 10 adult sheeps we induced bilateral osteochondral lesions (8mm large x 5mm deep): two lesions in the throclea and two lesions in the femoral condyle of each knee were created. One lesion in the throclea and one in the condyle were treated with perforations of the subchondral bone and implant of a collagen type I/II membrane (Group A) (Fig. 1). The other untreated lesions served as controls (Group B) (Fig. 2).
After 6 (5 sheeps) and 12 months (5 sheeps), the filling of the defects, tissue types, and visual semiquantitative histological scores were determined by histological, immunohisto-chemical and ultrastructural methods.

RESULTS

The untreated defects revealed the least amount of defect fill. The largest quantity of reparative tissue was found in the lesions treated with perforations of subchondral bone and implant of the membrane. Semiquantitative scores were best in group A.
At 6 and 12 months the lesions of group A were almost completely filled by reparative tissue, which showed a great number of differentiated chondrocytes. This tissue was almost totally vital, showed some of the characteristics of mature hyaline cartilage and restored the articular surfaces both in condylar (Fig. 3) and in throclear lesions (Fig. 4).
In group B the reparative tissue showed gross alterations of the matrix, necrotic chondrocytes, absence of a clear tide-mark and clean separation from the surrounding cartilage.
In none of the knees there was histological evidence of cell-mediated immune reaction.

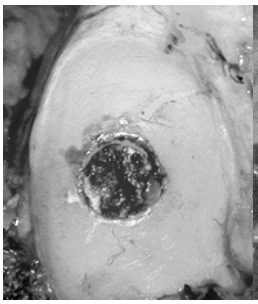

Fig. 1

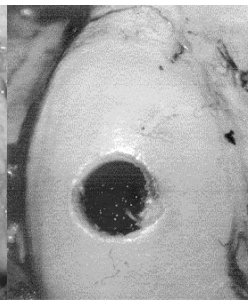

Fig. 2

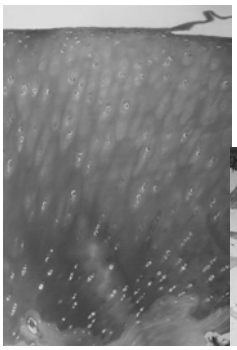

Fig. 3

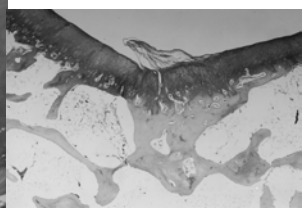

Fig. 4

DISCUSSION

Perforations of subchondral bone alone did not enhance the healing response. The implantation of a collagen membrane clearly improved the outcome.
This experimental study open the way to utilise this method in the treatment of the articular cartilage lesions in humans, because it permits to achieve good histological results, it is a not expensive procedure and avoids the problems of cell therapy (two surgical procedures, GMP, costs) such as in autologous chondrocytes implantation both in suspension (ACI) or seeded on membrane (MACI).

AFFILIATED INSTITUTIONS FOR CO-AUTHORS

*** University of Cassino and Dept. of Orthopaedics “Ospedale Pediatrico “Bambino Gesù”, Rome, Italy

VARUS POSTEROMEDIAL ROTATIONAL ELBOW INJURIES

*Doornberg JN, *Ring D

*Orthopaedic Hand and Upper Extremity Service, Massachusetts General Hospital, Harvard Medical School, Boston MA, USA

jdoornberg@partners.org

INTRODUCTION

Varus posteromedial rotational elbow injury is a recently described and incompletely characterized pattern of traumatic elbow instability.

METHODS

A single surgeon participated in the treatment of sixteen patients with a varus posteromedial rotational injury pattern.

All of the injuries were characterized by varus angulation of the elbow without dislocation and fracture of the anteromedial facet of the coronoid process.

All but three patients had avulsion of the origin of lateral collateral ligament complex from the lateral epicondyle (two patients with olecranon fractures and one with a concomitant fracture of the base of the coronoid process did not have LCL injury).

Associated fractures included 3 olecranon fractures, 3 radial head fractures, 1 fracture of the medial trochlear lip, and one fracture at the base of the coronoid process.

There were 14 men and 2 women with an average age of 49 years (range 18 to 85).

Twelve patients were treated for the acute fracture and four were managed after initial treatment elsewhere. The initial treatment was operative in 14 patients and non-operative in 2 patients.

In twelve patients the coronoid was repaired with a plate applied to the medial surface of the coronoid, in one it was repaired with a screw, and in three it was not repaired (subsequently reconstructed with a fragment of radial head in one patient).

RESULTS

Four patients had malalignment of the anteromedial facet of the coronoid with varus subluxation of the elbow—two because the fracture was not specifically treated, and two due to loss of fixation (one screw and one plate treated patient).

One of these patients and one additional patient had a deep infection.

All four patients with coronoid malalignment and residual subluxation had arthrosis and a fair or poor result according to the Mayo Elbow Performance Index. The remaining twelve patients regained an average of 120 degrees of elbow flexion and had good or excellent elbow function.

DISCUSSION

Varus posteromedial rotational elbow injuries are a distinct type of elbow fracture-dislocation that must be recognized and adequately treated to restore good elbow function.

In particular, inadequate fixation of the anteromedial facet of the coronoid—best treated with a plate on the medial surface of the coronoid—is associated with subluxation, arthrosis and a poor result.

CORONOID FRACTURE PATTERNS

*Doornberg JN, *Ring D
*Orthopaedic Hand and Upper Extremity Service, Massachusetts General Hospital,
Harvard Medical School, Boston MA, USA

jdoornberg@partners.org

INTRODUCTION

It has been suggested that specific types of coronoid fractures are strongly associated with specific patterns of traumatic elbow instability. This hypothesis was tested in a review of a large consecutive series of patients with fracture of the coronoid as part of a fracture-dislocation of the elbow.

METHODS

One surgeon repaired 67 coronoid fractures as part of a fracture-dislocation of the elbow over a 7-year period. Each coronoid fracture was characterized on the basis of operative exposure. Pearson Chi-squared analysis was used to evaluate the association of coronoid fracture type--as characterized using the systems of Regan and Morrey (RM) and O'Driscoll (OD)—with one of four common patterns of elbow fracture-dislocation.

RESULTS

The coronoid fracture was associated with an anterior (6 patients) or posterior (18 patients) olecranon fracture-dislocation in 24 patients; an elbow dislocation and radial head fracture in 32 patients; and a varus posteromedial rotational instability pattern injury in 11 patients. Among the twenty-four patients with olecranon fracture-dislocation, 22 had large coronoid fractures and 2 had small (less than 50%) coronoid fractures (22 RM and OD Type 3 and 2 RM Type 2 or OD Type 1 fractures).

All 32 patients with terrible triad injuries had small (less than 50%) coronoid fractures (RM Type 2) with one of these being a fracture of the anteromedial facet of the coronoid (31 Type 1 and 1 Type 2 according to O'Driscoll). Among patients with varus posteromedial rotational pattern injuries, nine had fractures small fractures of the anteromedial facet (Type 2 in both systems) and two had larger fractures (Type 3 using both classification systems). The association of coronoid fracture type with injury pattern was strongly statistically significant ($p < 0.001$) for both classification systems.

DISCUSSION

The following associations were confirmed by this study: large fractures of the coronoid process (Type 3) are strongly associated with anterior and posterior olecranon fracture-dislocations (C); small transverse fractures (Type 1) with terrible triad injuries (A), and anteromedial facet fractures (Type 2) with varus posteromedial rotational instability pattern injuries (B). Awareness of these associations and their exceptions may help guide optimal management of these injuries.

LONG TERM OUTCOME OF OPERATIVELY TREATED COMPLEX OLECRANON FRACTURES

*Lindenhovius ALC, *Doornberg JN, *Mudgal CS, *Ring D, **Kloen P
*Orthopaedic Hand and Upper Extremity Service, Massachusetts General Hospital, Harvard Medical School, Boston MA, USA

alindenhovius@partners.org

INTRODUCTION

The study of complex fractures of the olecranon has been limited by the infrequency of the injury resulting in only a small number of retrospective case series with relatively short-term follow-up. We analyzed the long-term (10 to 30 years) functional and radiographic outcomes of complex olecranon fractures and fracture-dislocations after operative treatment. Comparisons with their early follow-up were made to evaluate deterioration over time.

METHODS

Seventeen patients with complex olecranon fractures treated operatively between 1974 and 1994 were identified from a comprehensive database. From this group, six patients with posterior olecranon fracture-dislocations had passed away (average age at the time of injury: 67 years; average time from injury to death: 15 years). One patient could not be located. Ten patients were evaluated an average of 16 years (range, 11 to 20 years) after injury. The mean age at the time of injury was 32 years (range, 14 to 53 years). Six patients had a posterior olecranon (Monteggia) fracture-dislocation, two had an anterior olecranon fracture-dislocation and two had a comminuted olecranon fracture with no apparent subluxation of the ulnohumeral joint.

One patient required revision of internal fixation 2 months after the initial surgery—this patient had several subsequent surgeries for implant removal, refracture and infection. Two other patients had additional surgery: one had ulnar nerve transposition, and one had an elbow capsular release.

RESULTS

The final average arc of flexion was 131 degrees (range, 115 to 145 degrees), compared to 104 degrees (range, 60 to 135 degrees) at early follow-up (average, 12 months). The average arc of forearm rotation was 144 degrees (range, 0 to 180 degrees). Three patients complained of symptoms suggestive of ulnar nerve compression at the elbow. Eight patients had radiographic signs of arthrosis; 2 severe, 2 moderate and 4 mild according to the system of Broberg and Morrey. According to the Mayo Elbow Performing Index the functional result was excellent in 7 patients, good in 1 patient, and fair or poor in 2 patients. The average ASES score was 83 points (range, 41 to 100 points); ASES satisfaction score 8.5 points (range, 0 to 10 points); and Disability of Arm Shoulder and Hand score 14.2 points out of 100 (range, 0 to 52 points).

DISCUSSION

Good initial results after operative treatment of a complex olecranon fracture are durable over time. When a good trochlear notch is restored, arthrosis progresses slowly and good function is maintained. Even patients with advanced arthrosis did not request reconstructive surgery. Ulnar neuropathy was encountered in four of ten patients.

AFFILIATED INSTITUTIONS

**Department of Orthopaedic Traumatology, Academic Medical Center, University of Amsterdam, Amsterdam, The Netherlands

UPPER EXTREMITY FRACTURES FOLLOWING FRONTAL VEHICLE CRASHES IN A LEVEL ONE TRAUMA CENTRE

*Kwong Y, **Chong M, ***Sochor M, ***Wang S
*University of Warwick, Warwick, UK

myune8@yahoo.com

INTRODUCTION

There have been many improvements in vehicle safety design and legislation in the last several decades, with the aim of reducing passenger injuries. As a result of these regulations and increased seat belt usage, there has been a decrease in fatalities and severe injuries. However, it is unclear what the impact of these regulations has been on extremity injuries. Several studies have evaluated the incidence and distribution of lower limb injuries but there is a paucity of equivalent information for upper extremity injuries. The aim of this study is to analyse the pattern of upper extremity injuries sustained in motor vehicle crashes in a single level one trauma unit based in Michigan, USA. The outcome of this study may have implications for primary prevention by creating a basis for vehicular safety devices.

METHODS

The patients in this study were identified through research being conducted by the Crash Injury Research and Engineering Network (CIREN), in the US. CIREN is a trauma-center-based crash reconstruction study, investigating the causes and outcomes of automotive crashes involving vehicles with modern restraint systems. The CIREN team is made up of a multidisciplinary collaboration of physicians, surgeons, engineers, crash analysts, and epidemiologists. To be eligible for inclusion in CIREN, study subjects must be occupants of late model year passenger vehicles (less than 6 years old at the time of the crash) and be involved in frontal or side impact motor vehicle crashes. Also, subjects must have sustained significant injuries (Abbreviated Injury Scale (AIS) ≥3 or two injuries with AIS ≥2).

All cases of upper extremity fractures from the CIREN centre based at the University of Michigan, between 1997 and 2004, were extracted. We limited our study to front seat passengers involved in frontal impacts only. All statistical analyses were performed using SPSS 12.0 for Windows (SPSS Inc., Chicago, IL).

RESULTS

From 1997 to 2004, 257 cases with upper extremity injuries were analysed by the CIREN team. After applying the inclusion criteria, there were 159 cases, which formed the basis for this study. The most commonly injured region was the forearm (29.7%) and the hand region (29.7%). Clavicle and shoulder injuries (21.3%) were the next most common followed by humeral fractures (19.3%). Forearm fractures accounted for the largest group (47.1%) of severe AIS 3 injuries.

The elderly (> 60 years old) were the age group most likely to sustain multiple injuries (defined as ≥3 injuries). 34.7% of those over 60 years old sustained 3 or more fractures. The odds ratio for the elderly sustaining multiple injuries, compared to the < 60 age group, was 2.7 ($p = 0.03$).

There was no significant difference in injury severity between car occupants who were restrained by a seat belt and those who were not ($p=0.06$). A similar result was found for airbags ($p=0.04$).

DISCUSSION

Forearm injuries were the most common injuries and were also the most severe. The forearm seems to be the most vulnerable region of the upper limb, and should be the focus of further work on injury prevention. The elderly are especially vulnerable to upper limb fractures in MVCs, This group of elderly trauma victims will increase in importance in coming years with an ageing population in Western Countries.

The improvements in passive safety systems in modern vehicles, which are effective in reducing head and trunk injuries, and overall mortality, did not seem to have a similar influence in the reduction of upper extremity fractures. There was no difference in injury frequency among occupants whether they were wearing a seat belt or not, or whether an airbag was deployed or not.

ACKNOWLEDGEMENTS

This article has been partly supported by the U.S. Department of Transportation/National Highway Traffic Safety Administration (DOT/NHTSA) and is based on research conducted under the Crash Injury Research and Engineering Network (CIREN) project funded by DOT/NHTSA. This material represents the position of the authors and not necessarily that of DOT/NHTSA.

AFFILIATED INSTITUTIONS

**Birmingham Automotive Safety Centre, Birmingham, UK

***University Hospital Michigan CIREN centre, Ann Arbor, USA

EXPERIMENTAL RESURFACING OF ARTICULAR CARTILAGE BY EMBRYONIC STEMS CELLS

* Manunta A, **Manunta ML, **Sanna Passino E, ***Dattena M
* Orthopaedic Department, University of Sassari, Sassari, Italy

a.manunta@uniss.it

INTRODUCTION

Articular cartilage has a limited capacity to repair, and the defects may eventually progress to clinically defined degenerative joint disease. Orthopaedic surgeons currently use various methods to repair articular surface, but there is no know treatment that result in long term functional restoration of articular cartilage. Because of escalating cost, new therapies to preserve joint structure are being developed. Recently, tissue engineering based on stem cells has emerged as a new discipline that amalgamates aspects from biology, engineering, material science and surgery and that has as goal the fabrication of functional new tissue to replace damage tissue. The possibility of biologic repair by embryonic stem cells (ES) that posses a nearly unlimited self-renewal capacity and developmental potential to differentiate into virtually any cell type of an organism, offers major opportunities in the treatment of joint disease. The aim of our study was to verify if the pluripotent cells derived from inner mass cell (ICM, Inner Cell, MA) of embryos at the first stages of development (blastocysts), seeded on Tissucol, maintain their properties, grow, and form cartilage in chondral defects when used for repair the lesion.

METHODS

In our study, the animal model is represented by sheep. The experiment was organized with lab phase to cultivate the ES cells and surgical procedures to transplant the cells into the sheep's knee. An osteochondral full thickness lesion was produced in the medial femoral condyles of twelve sheeps. The ICMs arising from day 6-7 blastocysts were isolated by immunosurgery, disaggregated, seeded and cultured onto mitomycin-C inactivated mouse STO fibroblasts (feeder layer) for at least 2 passages (15 days of culture). The pluripotent cells were then isolated from feeder layer and seeded on fibrin glue before the transfer. We proceded with aspiration of ES cells in fibrinogen and successively addition of thrombin at time to transplantation. In 12 sheeps, in correspondence of medial femoral condyle on both knees, we performed a 5 mm diameter hole, 3 mm deep, being careful to avoid bleeding, so as to obtain a chondral full thickness lesion. The creation of full-thickness defects was performed in such a manner as to render it impermeable to blood-borne cells and signaling substances emanating from the subchondral bone-tissue spaces. After this, into the left knee 170 µl of Tissucol were inserted whether on right knee 170 µl of Tissucol with 120,000 ES cells into the hole. The number of stem cells obtained initially correspond to the maximum quantity avalaible before the last differentiation of them.
The new tissue obtained was tested using the ICRS classification, and analysed biomechanically by the Artscan 200 series. We also performed immunohistochemical evaluation of cartilage to check collagen type I.

RESULTS

The compressive stiffness of the reparative tissue was higher in the treated group (ES cells + Tissucol) mean = 1.02 N than in the control group (Tissucol) mean = 0.68 N).
Four weeks after transplantation immunohistological analysis show cartilaginous tissue in the treatment group. The cells in the repair cartilage were round and arranged in numerous small clumps; the matrix showed strong metacromasia, indicating that this was hyaline cartilage. Eight weeks after transplantation, the cells were largely distributed on the area and the repair tissue still resembled hyaline cartilage. In the extracellular matrix it was possible to distinguish specific tissue types like Type I, Type II and proteoglycan. In the control group four weeks after implantation fibrous tissue filling the defect with spindle-shape mesenchymal cells were observed. After eight weeks the repair tissue implanted was fibrous with prevalence in extracellular matrix of Type II collagen.

CONCLUSION

Pluripotent cells obtained from sheep embryos produced in vitro have the capacity to differentiate into various tissue types. Passage in fibrinogen and the addition of thrombin doesn't alter the properties of the cells. Tissucol mimics embryonic environment and appears to be quite suitable and appropriately flexible delivery vehicle. This repair tissue manifests neither a arcade-like organization of its fibers nor a well-define zonal stratification of its chondrocytes but detection of Type I collagen rendering the pluripotent-cells-fibrin glue complex a possible candidate for the repair of cartilage lesions.

INSTITUTIONS OF CO-AUTHORS

** Dept. of Veterinary Surgery, University of Sassari, Sassari, Italy
*** Zootechnic Institute of Bonassai (Sassari, Italy)

MESENCHYMAL STEM CELL AND NUCLEUS PULPOSUS CELL INTERACTIONS: DIFFERENTIATION, STIMULATORY EFFECTS, AND CELL FUSION

*╪Vadalà G, ╪Spiezia F, ╪Denaro E, *Kang JD, *Gilbertson L
*Ferguson Lab for Orthopaedic Research, Dept. of Orthopaedic Surgery, University of Pittsburgh, Pittsburgh, PA, USA

GilbertsonL@upmc.edu

INTRODUCTION

Intervertebral disc (IVD) degeneration is a chronic process characterized by progressive loss of cells, proteoglycans, and water content in the nucleus pulposus. Current therapies are aimed at treating the pathologic and disabling conditions arising from IVD degeneration rather than directly treating the disc itself. Our group and others are actively exploring the potential of Stem Cell Therapy to repopulate the disc and prevent loss of proteoglycans in disc degeneration [1,2]. The combination of mesenchymal stem cells (MSC) and nucleus pulposus cells (NPC) has been shown to increase extracellular matrix synthesis—in-vitro as well as in-vivo—though the precise mechanisms remain to be determined.

The present study tested MSC differentiation towards a chondrogenic phenotype, stimulatory effects exerted by MSCs upon NPCs, and cell fusion after co-culture.

METHODS

Human female NPCs and male MSCs were labeled by transduction with Ad/GFP (Green Fluorescent Protein) and Ad/RFP (Red Fluorescent Protein), respectively, and co-cultured at 50:50 ratio in alginate beads and pellets. Alginate beads were dissolved after 1 day (control) and 14 days of co-culture. Cells were then sorted by fluorescence activated cell sorting (FACS), mRNA extracted separately from NPCs and MSCs, and collagen-II expression assessed by real-time RT-PCR. Pellets were fixed after 2 weeks of co-culture and fluorescence in situ hybridization (FISH) was performed visualizing X and Y chromosomes.

RESULTS

The gene expression of collagen-II was increased in both NPCs (4 fold) and MSCs (10.5 fold) after 2 weeks of co-culture, as compared with control (Figure 1).

FACS analysis after 14 days of co-culture, showed that 0.5% of cells were double fluorescent for GFP and RFP. However, both male and female cells were independently identified by FISH (Figure 2).

DISCUSSION

These data demonstrate that the interaction between MSC and NPC may derive from a combination of MSC differentiation towards a more chondrogenic phenotype as well as stimulatory paracrine effects exerted by MSCs upon NPCs.

The presence of few two-color positive cells by FACS, without any qualitative observation of cells with tetraploid DNA by FISH, leads us to consider cell fusion a rare phenomenon for MSCs and NPCs in this culture system.

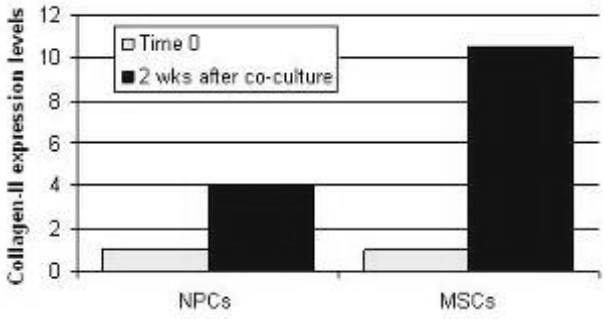

Figure 1. *Collagen-II expression levels of isolated NPCs and MSCs after 2 weeks of co-culture.*

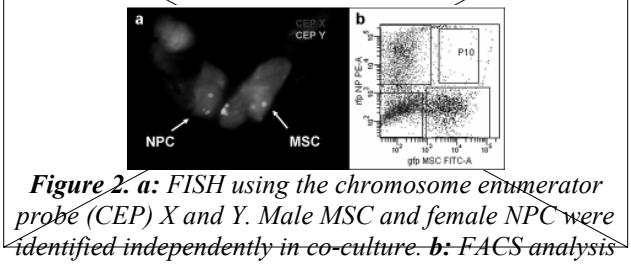

Figure 2. a: *FISH using the chromosome enumerator probe (CEP) X and Y. Male MSC and female NPC were identified independently in co-culture.* ***b:*** *FACS analysis after co-culture show the double fluorescent cells fraction (P10).*

Ongoing studies of mRNA expression of other genes will further clarify the interaction between MSC and NPC

This study further clarifies the mechanism of the interaction between MSCs and NPCs, and improves the understanding of the potential of MSCs to alter the course of intervertebral disc degeneration.

REFERENCES:

1. Sobajima, S., et al. Feasibility of Stem Cell Therapy for the Treatment of Intervertebral Disc Degeneration. Spine (In Press), 2006.
2. Sakai, D., et al. Differentiation of mesenchynal stem cells transplanted to a rabbit degenerative disc model. Spine, 30, 2379, 2005.

ACKNOWLEDGMENTS

This study was supported by the North American Spine Society Grant and The Pittsburgh Foundation.

AFFILIATED INSTITUTIONS FOR CO-AUTHORS

╪ Department of Orthopaedic Surgery, University Campus Bio-Medico, Rome, Italy,

SELF-ASSEMBLED MONOLAYERS AND CARBON NANOTUBES AS NEW TOOLS TO IMPROVE BONE REGENERATION: AN *IN VITRO* APPROACH

Ciapetti G, Pagani S, [1]Dettin M, [1]Gambaretto R, [2]Marletta G, [3]Armentano I, [3]Kenny J, Baldini N, [4]Alava JI
Istituti Ortopedici Rizzoli, Bologna; [1]Dip. Processi Chimici dell'Ingegneria, Università di Padova; [2]Dip. Scienze Chimiche, Università di Catania; [3]INSTM, Università di Perugia, Italy; [4]INASMET-Tecnalia, San Sebastian, Spain.

gabriela.ciapetti@ior.it

INTRODUCTION

Material scaffolds intended as engineered matrices for orthopaedics should support cell functions toward bone regeneration. To address this issue, several implant modifications, including ion beams, coatings, and chemical surface changes, have been attempted to increase the tissue compatibility of prosthetic surfaces. Biomimetics, i.e. extracellular matrix simulation at the material surface, has been recently explored as a strategy for attracting cells and stimulating tissue regeneration. Self-assembled monolayers (SAMs) and carbon nanotubes (CNTs) are among the most promising synthetic 'nano-structures' which could be integrated to materials and interact with cells. Using *in vitro* procedures, compatibility and efficiency of such structures have to be ascertained during their development. In this study, human bone-derived cells were seeded on experimental surfaces and tested.

METHODS

Cells. After local ethics committee approval, bone fragments and bone marrow are obtained from patients during hip surgery. Osteoblasts (HOB) and marrow stromal cells (MSC) are cultured with α-MEM/10% FCS/ascorbic acid-2 phosphate, plus 10^{-8} dexamethasone for MSC differentiation to osteoblasts; at confluence, cells were detached, seeded on the surfaces and cultured for fixed time periods. Cell adhesion/morphology was assessed by fluorescence microscopy.

Materials. Starting from a 'basic' sequence named *pept1* (Ala-Glu-Ala-Glu-Ala-Lys-Ala-Lys)2, that is able to spontaneously form a membrane after addition of different salts, new sequences have been developed at the University of Padova. *Pept7* contains a fragment for osteoblast adhesion, while *pept8* is a 'scrambled' derivative of *pept1* with RGD. The sequences were layered onto cell-culture substrate and tested for HOB adhesion.

Single walled carbon nanotubes with COOH functionalization (SWNT-COOH, Sigma) were deposited as a film onto glass surfaces by drop casting using DMF solution and solvent evaporation at the INSTM (University of Perugia). MSC were used to test their toxicity. Both SAMs and SWNTs were treated with antibiotic/antimycotic solution prior to cell seeding.

RESULTS

Despite a scarce attachment of cells at 4 hr both on SWNT surface and glass used as control surface, at 96-120 hr from seeding a discrete layer of MSC was detected on SWNT surface. Pre-wetting of the sample with FCS-added medium, and the deposition of cells on the surface strongly affected the final result. Pre-wetted surfaces allowed cell spreading with cytoskeleton organization, and cell deposited as a droplet reached early confluence which in turn influenced the proliferation rate.

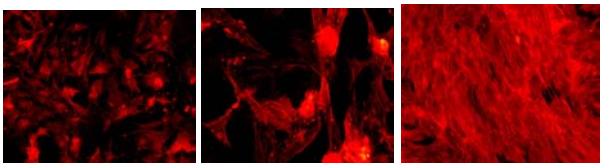

Fig. 1. MSC at 96 hr on SWNT (a, 20X) glass (b, 20X) and polystyrene (c, 10X) (rhodamine-TRITC)

At 48 hr, HOB adhered to experimental SAMs as follows: *pept1*< *pept7* < *pept8* ≅ RGD (Fig. 2). The observed differences were not only in terms of number of attached cells, but also as cytoskeleton organization and spreading.

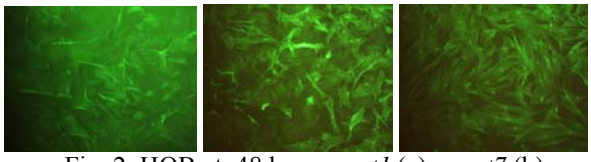

Fig. 2. HOB at 48 hr on *pept1* (a), *pept7* (b), and *pept8* (c) (rhodamine-FITC, 10X).

DISCUSSION

After functionalization, SWNTs are intended to improve the bioactivity of a polymer-based composite and to increase the mechanical properties of the matrix. Our preliminary investigation using human marrow stromal cells showed that these cells are allowed to attach and grow onto pure layers of SWNT, but their viability and functions have to be measured at longer times. SAMs modulate protein adsorption and cell adhesion. Experimental peptides show differences as far as human osteoblasts attach and proliferate: the contribution of sequences and/or RGD in improving cell attachment can be derived from *in vitro* results. This in turn will aid in refining the structure of novel surfaces through molecular self-assembly.

CONCLUSION

Biomimetics and nanotechnology provide attracting tools to improve standard surfaces, but interactions with cells have to be checked. Human primary cells involved in bone regeneration offer a reliable *in vitro* model.

ACKNOWLEDGEMENT

NANOBIOCOM project under EU FP6.

NO EFFECT OF LOAD ON CARTILAGE FORMATION IN DEFECTS RECONSTRUCTED WITH POLYESTERURETHANES

*Meel M van, *Ramrattan NN, **Heijkants RGJC, **Schouten AJ, *Veth RPH, *Buma P
*Laboratory of Orthopedic Research, Dept Orthopedics, University Hospital Nijmegen, Nijmegen, the Netherlands.

mM.vanMeel@orthop.umcn.nl

INTRODUCTION: A meniscus made from polyesterurethanes (PCLPU) was implanted in dogs after meniscectomy [1]. After three months the implant is fully infiltrated with fibrous tissue, while after six months the implant is partially filled with cartilage-like tissue. The cartilage-like tissue is located in the inner part of the implant at the same location as where fibro-cartilaginous tissue is found in the native meniscus. Our hypothesis is that load is the main factor involved in the differentiation of the tissues into cartilage. To test this hypothesis we implanted punches of PCLPU into the trochlea of rabbits. Punches were implanted flush (Normal Load, NL), or they were elevated 1 mm above the surface to generate extra loading (HL).

METHODS: The PCLPU has pores that are all interconnected to allow tissue ingrowth. Porosity was 78%[2]. The compression modulus was 300 kPa at 20% compression. Punches of PCLPU with a diameter of 4 mm and a height of 3 mm (NL) or a height of 4 mm (HL) were implanted in the trochlea of 7 New Zealand rabbits (age 12 weeks). In all knee joints two implants were placed, one for NL and one for HL. The location within the joint was alternated. Operations were performed bilaterally, which indicated 14 implants of each group for the analysis. After 8 weeks the rabbits were killed and sections through the implant were stained with HE and with saffranin O. The surface area of cartilage-like tissue was quantitated in all implants within the border of the original defect and expressed as a percentage of the total area of the defect.

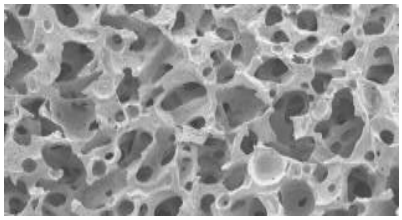

Fig. 1. The PCLPU foam. Note interconnective porosity

RESULTS: None of the knees showed any significant degenerative changes, nor did the synovium show signs of irritation. The implant was integrated with the surrounding host cartilage and the surface of both NL and HL implants was smooth and not elevated above the level of the host cartilage. All implants were completely filled with cellular tissue. In the center of the scaffold the tissue was relatively cell-poor compared to the deeper layers. Areas with a cartilage-like tissue were easily recognized by the matrix staining (Fig. 2A-C). The cells in these areas were rounded and strongly resembled chondrocytes (Fig. 2B,C). Safranin O positive areas were mainly located in the deeper regions of the scaffold (Fig. 2A).

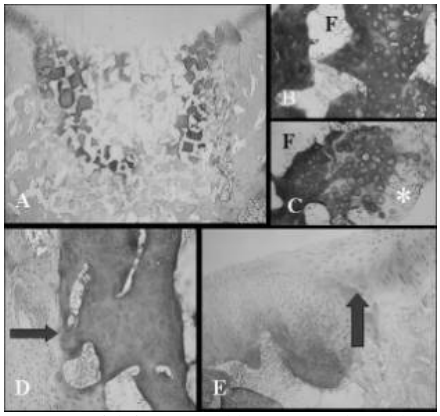

Fig. 2. A. Overview of defect in trochlea. B. Cartilage-like phenotype of cells. C. Hypertrophic cartilage cells (*). D. Interface of implant with host bone (arrow). E. Interface of implant with host cartilage (arrow).

In some areas, in between the cartilage in the scaffold and the host bone, the cartilage was hypertrophying and was replaced by bone, which was in direct contact with the PCLPU. Quantification showed no difference in the surface area of cartilage in NL implants, 14.09% ± 12.2, versus 10.08 ± 9.17 in the HL implants.

DISCUSSION: The lack of difference between NL and HL implants in cartilage formation indicates that load is probably not that important for tissue differentiation, or that the effect of load was only temporary directly after the surgery and lost by non-elastic compression of the HL PCLPU scaffolds by the load. After the relatively short follow-up period, the cartilage formation is considerable and the PCLPU foam has an excellent biocompatibility, for both cartilage and bone. No foreign body cells were found and a direct connection with the host cartilage and bone was formed. It might be expected that in the deeper parts of the defect the cartilage will further remodel into bone in longer follow-up periods. Also, based on the good tear strength and the compression modulus that can be further adapted to cartilage, we think that this material has a potential for cartilage repair in larger defects. In this experiment the variation between individuals was considerable, and therefore it might be necessary to stimulate a more predictable transformation of ingrowth tissue into cartilage with growth factors.

REFERENCES [1] van Tienen et al. Proceedings ORS 2003: poster 1257. [2] Heijkants et al. J Mat Science, Mat in Med, 15; 423, 2004.

AFFILIATED INSTITUTIONS FOR CO-AUTHORS
**Department of Polymer Chemistry, State University of Groningen, Groningen, the Netherlands.

AUTOLOGOUS BONE MARROW-DERIVED CELLS IMPROVE MUSCLE STRENGTH AFTER SKELETAL MUSCLE CRUSH INJURY IN RATS

*Winkler T, *Matziolis G, **Stoltenburg G, *Schaser KD, *Perka C, *Duda GN
*Center for Musculoskeletal Surgery, Charité - Universitätsmedizin Berlin, Free and Humboldt -University, Germany

mtobias.winkler@charite.de

INTRODUCTION

Incomplete regeneration after traumatic muscle injury with residual functional deficiencies is a common problem in orthopaedics and traumatology. Muscle-derived stem cells and satellite cells have previously been identified as sources of muscle recovery.

Based on these reports tissue engineering may possibly have the potential to reduce functional deficits and to stimulate muscle regeneration following muscle trauma with the ultimate goals to reduce the impairment of function, to effectively shorten rehabilitation periods and enhance resulting skeletal muscle performance. Therefore, transplantation of autologous pluripotent cells capable to differentiate into contractile cells seems predestinated to address this request.

The present study evaluates the hypothesis that local injection of autologous bone marrow-derived (BMD) cells leads to improved functional muscle regeneration following blunt skeletal muscle injury.

MATERIALS AND METHODS

Sixteen male Sprague Dawley rats (250 to 300 g) were used for this study (n=8 per group). The study was approved by the local legal representative (Landesamt für Arbeitsschutz, Gesundheitsschutz und technische Sicherheit, Berlin: Reg 0234/03).

Autologous BMD cells were harvested by aspiration from both tibiae of each animal and cultured under standard conditions in monolayer. Hematopoetic cells were removed by medium change every second day. Seven days after BMD-cell harvest the left soleus muscle was bluntly crushed. 14 days after BMD-cell harvest, i.e. seven days after injury one million BMD cells were injected into the traumatized muscle (n=8) while in the control group medium was applied in an identical manner (n=8). Contraction forces of both soleus muscles of each animal were determined three weeks after BMD-cell transplantation after fast-twitch (0.1 s) and tetanic (3 s) stimulation of the sciatic nerve (9 mA / 75 Hz).

The animals were sacrificed after biomechanical testing and muscles were harvested and prepared for histological evaluation.

All data are given as arithmetic mean and standard deviations. Statistical significance analysis was performed using the non-parametric Wilcoxon test for dependent samples when comparing measurements intra-individually. The non-parametric Mann-Whitney-U test for independent samples was used for comparisons between the treatment and the control group. The level of significance p was set to ≤ 0.05.

RESULTS

Control and injured muscles showed similar contraction force patterns. Control muscles without trauma had a mean fast-twitch contraction force of 0.69 ± 0.13 N and a maximum contraction force following tetanic stimulation of 1.32 ± 0.37 N.

Intraindividual normalization of the contraction force of the injured left soleus muscle versus the right control muscle (set to 100%) revealed a recovery of tetanic contraction force to $39 \pm 10\%$ ($p<0.001$) in control animals. In contrast to this, animals transplanted with autologous BMD cells displayed a $54 \pm 9\%$ ($p<0.001$) recovery of tetanic contraction force. The difference to untreated animals was found statistically significant ($p=0.014$) .

Comparable results were obtained under fast-twitch stimulation. Control animals had $59 \pm 12\%$ ($p<0.001$) contraction force of the uninjured muscle, whereas BMD cell treated animals showed a significant increase of functional recovery to $72 \pm 13\%$ ($p<0.001$), indicating effective restoration of muscle forces in BMD-treated animals ($p\leq0.05$).

Independent from the form of muscle stimulation autologous BMD injection lead to a comparable increase of both contraction forces (15% tetanic vs. 13% fast-twitch), demonstrating a marked improvement of functional muscle recovery.

DISCUSSION

In the presented rat model BMD cells were capable of improving muscle function already 3 weeks after controlled trauma.

The use of cells derived from the stem cell pool within the bone marrow has the advantage of nearly negligible donor site morbidity compared to the harvest of muscle cells for cellular regeneration of muscle trauma. Whole muscle trauma as mimicked in our trauma model seems to be a possible field for future clinical applications of autologous BMD cells since distribution of the cells can be easily reached by local injections. A limiting factor for a clinical application of this approach may be the little window of opportunity between cell harvest and application before the development of fibrosis.

AFFILIATED INSTITUTIONS FOR CO-AUTHORS:
**Institute for Neuropathology, Charité – Universitätsmedizin Berlin, Free and Humboldt-University, Germany

ELECTROSPUN NANOFIBERS OF DIFFERENT POLYMERS AS SCAFFOLDS FOR TISSUE ENGINEERING

*Boudriot U, **Dersch R, *Wack Ch, *Fuchs S, **Greiner A, **Wendorff JH

mboudriot@post.med.uni-marburg.de

INTRODUCTION

Treatment of structural defects in human organs and tissues nowadays includes stem cell techniques and methods of tissue engineering. However, those techniques depends on the use of appropriate scaffolds to allow three-dimensional growth of cell-constructs. Most scaffolds for tissue engineering consist of either natural or synthetic polymers. Depending on the method of processing, a variety of different three-dimensional structures can be produced. During the last decade, a promising new technology to process polymeric materials has evolved. The electrospinning of polymeric nanofibers is a promising new tool to generate "tailor made" scaffolds for biomedical applications. The aim of the study was to investigate the osteogenic differentiation of human mesenchymal stem cells (hMSC) growing on matrices of non-woven electrospun nanofibers of different polymers.

METHODS AND MATERIALS:

Using an electrospinning method we fabricated membranes of non-woven nanofibers of: polylactide; polycaprolacton; poly(dl-lactid-co-caprolacton); poly-dl-lactide; poly(l-lactide-co-glycolide) and poly(3-hydroxybutyrate-co-3-hydroxyvalerate). The membranes were spunned on glas slides, sterilized and placed into 12-well plates. Membranes were seeded with hMSC ($3x10^4$ cells/cm^3) and left proliferating for 10 days. Then, osteogenic differentiation was induced by changing media to osteogenic differentiation media. After 3 weeks of osteogenic differentiation probes has been harvested and analyzed. Scanning electron microscopy, fluorescence staining for osteogenic markers and media analysis for OPG-concentration were performed.

RESULTS

Cells demonstrated no evidence of cell death. Fluorescence staining for osteogenic markers (Collagen I, osteopontin, osteocalcin, and bone specific alkaline phosphatase) demonstrated osteogenic differentiation. SEM showed three-dimensional cell-growth in all matrices. Remarkable differences were observed in fiber degradation. OPG-concentrations were significantly lower in all media probes of polymeric nanofiber meshes in comparison to the reference probes without fibers.

CONCLUSIONS

Due to its fine structure, electrospun nanofibers promise to be an ideal scaffold for tissue engineering. They can be combined with additives and are equally biocompatible and biodegradable. Further investigations concerning the appropriate polymer, optimal fiber size, porosity, and pore size are necessary.

ACKNOWLODGEMENT

We thank Deutsche Arthrose-Hilfe e.v. for the financial support.

REFERENCES:

1. Boudriot U, Dersch R, Götz B, Griss P, Greiner A, Wendorff J H, Elektrogesponnene Poly-L-Laktid-Nanofasern als resorbierbare Matrix für Tissue Engineering. Biomedizinische Technik, 49 (2004), 241-246
2. Boudriot U, Dersch R, Götz B, Greiner A, Wendorff J H, Role of Electrospun Nanofibers in Stem Cell Technologies and Tissue Engineering. Macromolecular Symposia, 225 (2005), 9-16
3. Dersch R, Steinhart M, Boudriot U, Greiner A. Wendorff J. H, Nanoprocessing of polymers: Application in medicin, sensors, catalysis, photonics. Polym Adv Technol, 16 (2005), 276-282

AFFILIATIONS:

* Department of Orthopaedics and Rheumatology, Medical Center, Philipps-University, Marburg, Germany Department, Marburg, Germany

**Department of Chemistry, Center of Material Science, Philipps-University, Marburg, Germany

GENE EXPRESSION PROFILING OF HUMAN MESENCHYMAL STEM CELLS DURING EXPANSION AND OSTEOBLAST DIFFERENTIATION

*Friedl G, **Kulterer B, ***Jandrositz A, *Windhager R, **Trajanoski Z
*Department of Orthopaedic Surgery, Medical University, Graz, AT

mgerald.friedl@meduni-graz.at

INTRODUCTION

Human mesenchymal stem cells (hMSC) with the capacity to differentiate into osteoblasts provide potential for the development of different approaches for human treatment, such as improved healing of large bone defects. Their low frequency in bone marrow necessitate ex vivo expansion for further clinical application.
Additionally, ex vivo manipulation, by treatment with distinct media supplements, is needed, to direct hMSC towards the osteogenic lineage.
However, the underlying mechanisms governing expansion and targeted differentiation of hMSC are not completely understood. In this study, we asked if hMSC are developing in an aberrant or unwanted way during in vitro long-term cultivation and if artificial cultivation conditions exert any influence on their stem cell maintenance.

METHODS

We developed human oligonucleotide microarray slides with 30,000 elements and performed large-scale expression analysis of long-term expanded hMSC and hMSC differentiating into osteoblasts.

RESULTS

The results showed that the expression profiles of hMSC are not altered during expansion.
They do not alter their osteogenic differentiation capacity, surface marker profile and also keep their multidifferentiation capacity. Microarray analysis of hMSC during osteogenic differentiation identified candidate genes for further examination and functional analysis.
Additionally, we were able to reconstruct the main development phases during osteoblast differentiation for the first time in a human model and due to mapping of expression data on pathways, the non-parallel activation of the SMAD signaling pathways by TGF-β2 and BMPs could be illustrated.

CONCLUSION

In conclusion, with a variety of assays we could show that hMSC represent a cell population which can be expanded for therapeutical application

AFFILIATED INSTITUTIONS

**Institute for Genomics and Bioinformatics and Christian Doppler Laboratory for Genomic and Bioinformatics, Graz, Austria
***Eccocell Biotechnology Inc., Graz, Austria

Poster presentations

COMPARISON OF ELBOW CONTRACTURE RELEASE IN PATIENTS WITH AND WITHOUT HETEROTOPIC OSSIFICATION

*Lindenhovius Alc, *Doornberg Jn, *Linzel D, *Ring D
*Orthopaedic Hand And Upper Extremity Service, Massachusetts General Hospital, Harvard Medical School, Boston Ma

alindenhovius@partners.org

INTRODUCTION

Heterotopic ossification has been regarded with trepidation and considered a poor prognostic factor for operative restoration of elbow motion. We compared the results of elbow contracture release in patients with and without heterotopic ossification blocking elbow motion to test the hypothesis that heterotopic bone is associated with diminished elbow motion after release.

METHODS

Nineteen patients with heterotopic bone restricting elbow motion (but not complete bony ankylosis) were compared with twenty-two patients with capsular contracture alone. The sex, age, initial injuries, percentage of dominant limbs, number of prior procedures, mechanisms of injury, open injuries, polytrauma patients were comparable between groups. The average pre-operative arc of flexion and extension in the patients with heterotopic bone was 52 degrees (range, 5 to 90 degrees) and 52 degrees (range, 10 to 90 degrees) in patients with capsular contracture alone.

RESULTS

After the index procedure, the flexion-extension arc in patients with heterotopic ossification averaged 105 (range, 45 to 105 degrees) and the arc in the capsular release group averaged 86 degrees (range, 0 to 135 degrees). The average improvement in F-E arc was 53 degrees (range, -20 to 107 degrees) for the HO patients and 34 degrees in the capsular release group (range, -20 to 75 degrees). The difference in improvement after the first release was significant ($p = 0.034$).

Six of 22 patients (26%) in the capsular release group and two of eighteen patients (12%) in the HO group had a second procedure for capsular release. At an average of 24 months follow-up (range, 6 to 63 months), the final arc of flexion and extension averaged 105 degrees in the patients with heterotopic bone (range 40 to 145 degrees) and 96 degrees (range, 45 to 135 degrees) in patients without HO. The average improvement in flexion-extension arc was 53 degrees (range, -20 to 107 degrees) in the HO group and 43 degrees (range, -15 to 80 degrees) in the capsular contracture group. The greater improvement in final range of motion in patients with heterotopic ossification compared to patients with capsular contracture alone was not significant with the numbers available ($p = 0.122$).

DISCUSSION

Heterotopic bone restricting motion, but not causing total ankylosis, is associated with more predictable and slightly better restoration of motion after elbow contracture release.

ANALYSIS OF POSTOPERATIVE COMPLICATIONS IN COMPLEX DECOMPRESSION ELDERLY PATIENTS AS A FUNCTION OF COMORBIDITY

*Eidelson S, *Wilkerson J
*SYA Press and Research Institute, Boca Raton, FL

s.g.eidelson@spineuniverse.com

INTRODUCTION

Surgery poses a health risk to every patient and the risk is exacerbated when patients are elderly with comorbidities. Comorbidities currently considered to increase surgical risk include heart disorders, diabetes, asthma, obesity, and chronic obstructive pulmonary disease (COPD). Further characterization of postoperative complications in relation to comorbidities is needed for lumbar decompression with fusion and instrumentation surgery and this study seeks to provide clinical results.

METHODS

A chart review was conducted on the hospital and office records of 92 patients, ages 65 years and older, who underwent this procedure between the years of 2000 and 2003. A statistical analysis was performed to find trends within comorbidities and complications. Comorbidities were evaluated based on their frequency to cause associated complications.

RESULTS: The age range was 66 to 88 years. Of 92 patients, 74 had comorbid conditions and 11 of these had postoperative complications in the following breakdown: various critical heart complications=4, wound infection=3, onset of confusion=2, and sepsis=1. 1 patient was healthy and 10 had comorbidities in the following breakdown: heart disorders=10, diabetes=3, asthma=2, obesity=1, COPD=1 and patients with a combination of comorbidities=5. The 4 critical heart complication patients had heart disorders.

CONCLUSION

The comorbidity that presented with the highest frequency was heart disorder and showed a greater tendency for related critical complications. The low rate of comorbid elderly patients who experienced postoperative complications gives statistical indication of safety for patients who need lumbar decompression with fusion and instrumentation surgery. In conclusion, this study indicates safety for comorbid elderly patients to pursue complex lumbar surgery with a slightly higher risk to those patients with heart conditions.

ANALYSIS OF EX VIVO METAL-ON-METAL FIRST METATARSOPHALANGEAL PROSTHESIS AND ASSESSMENT AGAINST THEORETICAL LUBRICATION REGIMES

Joyce T J
Centre for Rehabilitation and Engineering Studies, School of Mechanical and Systems Engineering,
University of Newcastle upon Tyne, Newcastle upon Tyne, UK
t.j.joyce@ncl.ac.uk

INTRODUCTION

Replacement of the first metatarsophalangeal (MTP) joint is a relatively uncommon procedure compared with hip and knee arthroplasty. A range of different designs of first MTP prosthesis have been proposed [1]. A cobalt chrome-on-cobalt chrome prosthesis, which had a diamond like carbon (DLC) coating applied to its articulating faces, was implanted. However, due to poor clinical results the cohort of implants were removed and one was obtained for ex vivo analysis. The aim of this paper was to evaluate the explant and calculate the predicted lubrication regimes applicable to it.

MATERIALS AND METHODS

The articulating faces of the ex vivo MTP implant were examined using standard microscopy, an environmental scanning electron microscope and a non-contacting profilometer, while the radii of the articulating faces were measured using a co-ordinate measuring machine. Modeling the ball and socket implant as an equivalent ball-on-plane model and employing elastohydrodynamic theory [2] allowed the minimum film thickness to be calculated and in turn the lambda ratio (λ) to indicate the lubrication regime [3]. Boundary lubrication is indicated for λ less than 1, mixed lubrication for λ between 1 and 3, and fluid film lubrication for λ greater than 3. Roughness measurements of worn and unworn regions of the articulating faces were taken. These values allowed the lambda ratio to be calculated for the prosthesis when new and at the time of retrieval. The calculations were undertaken for a 0 to 30mm/s range of entraining velocities and a 0 to 800N range of loading values.

RESULTS

The implant was measured to have a nominal radius of 10mm and a radial clearance of 0.1mm. The DLC coating had been removed from the entire face of the phalangeal component and from most of the face of the metatarsal component. From the latter it appeared as if the coating had been scratched and then flaked away parallel to the scratches. In turn this suggested a corrosion based failure of the interface between the DLC coating and the cobalt chrome subsurface, a result noted recently elsewhere [4]. Even within the apparently undamaged DLC coating, closer investigation revealed relatively deep pits which again were felt to indicate damage due to corrosion. The DLC coating had a typical roughness value of 0.020µm Ra, while that of the surface without the DLC coating was 0.030µm Ra on the metatarsal component and 0.063µm Ra on the phalangeal component. The presence of scratches on the articulating faces of the ex vivo sample (fig 1) implied boundary or mixed lubrication.

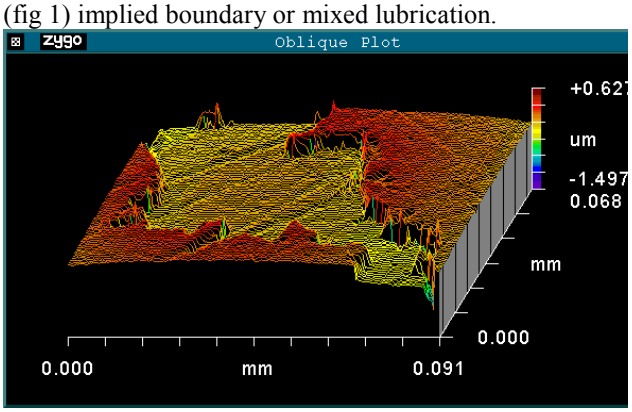

Fig 1: Damage to DLC coating on metatarsal component

Calculations showed that, for the range of loads and entraining velocities considered, the worn implant would operate in the boundary lubrication regime (fig 2) thus supporting the results of the visual examination. Therefore surface to surface contact would most frequently take place, with little separation due to lubrication between the articulating surfaces. However, it was also noted that when new, it was possible that the implant could have operated under the somewhat more favorable condition of mixed lubrication, especially at lower loads and under higher entraining velocities.

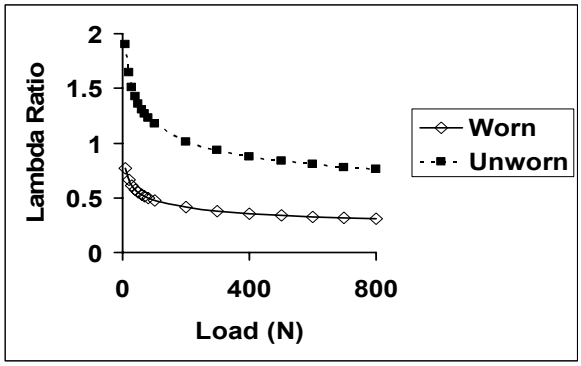

Fig 2: Variation of lambda ratio with load

DISCUSSION

It should also be recognized that when the joint is not moving, for example when a person is at rest, there is likely to be surface to surface contact of the implant as there will be zero entraining velocity. Therefore other factors should be considered if choosing an MTP implant.

REFERENCES

[1] Joyce TJ. Expert Rev Med Devs, 2005; 2:453-464. [2] Hamrock BJ, Dowson D. Trans ASME J Lubn Tech, 1978; 100:236-245. [3] Johnson KL. Greenwood JA,

MODULAR ANKLE-FOOT ORTHOSIS WITH SPRING ELEMENTS

Milusheva S, Karastanev S, Toshev Y
Institute of Mechanics and Biomechanics, Sofia, Bulgaria

slavyana@imbm.bas.bg; stefan@info.imbm.bas.bg; ytoshev@imbm.bas.bg

INTRODUCTION

Ankle-foot orthosis (AFO) is commonly used to help subjects with weakness of ankle dorsiflexor muscles due to peripheral or central nervous system disorders. Both these disorders are due to the weakness of the tibialis anterior muscle which results in lack of dorsiflexion assist moment. The deformity and muscle weakness of one joint in the lower extremity influences the stability of the adjacent joints, thereby requiring compensatory adaptation.

During level plane ambulation the ankle should be close to a neutral position (right angle) each time the foot strikes the floor. Insufficient dorsiflexion may be the result of hyperactive plantarflexors that produce very high plantarflexion moment at the ankle, or weakness of the dorsiflexion muscles. This affects the ability of the ankle to dorsiflex. As result the patient make a forefoot contact instead of normal "heel-strike". If there is a weak push-off, the stride length reduces, and the gait velocity decreases. Similarly, during the gait swing phase, the ankle is dorsiflexed to allow the foot to clear the ground while the extremity is advanced. Hyperactive or weak dorsiflexors may result in insufficient dorsiflexion, which must be compensated by alterations in the gait patterns so that the toes do not drag. This insufficient dorsiflexion during the gait swing phase is termed as "foot-drop". In addition to the toes dragging, the foot may become abnormally supinated, which may result in an ankle sprain or fracture, when the weight is applied to the limb. Foot-drop is commonly observed in subjects after a stroke or personal nerve injury.

There are several possible treatments for foot-drop - medicinal, orthotic, or surgical. It is to note that the most common is the orthotic treatment.. Orthotic devices are intended to support the ankle, to correct deformities, and to prevent further occurrences. A key goal of orthotic treatment is to assist the patient achieving normal gait patterns.

Different orthoses are used to enhance the ankle-foot position and mobility. The most common types are hingeless and hinge orthoses. Using springs, the hinge orthoses could assist ankle flexion/extension during gait, i.e. they are pseudo-active orthotic devices. The standard ankle foot orthoses (AFO) is a rigid polypropylene structure which prevents any ankle motion.

METHODS

The study is oriented to develop modular ankle foot orthosis (MAFO) with two units (shank brace and foot brace) connected with lateral and medial adjustable hinged joints.

Which are to assist the quite popular gait abnormalities inherent to a spring-controlled human ankle-foot complex. Previous studies have shown the DACS (dorsiflexion assist controlled by spring) AFO to have the following desirable characteristics: 1) the magnitude of the dorsiflexion assist moment and the initial ankle angle of the AFO can be changed easily, and 2) no plantarflexion assist moment is generated.

RESULTS

A modular ankle-foot orthosis (MAFO) with one degree-of-freedom (dorsiflexion-plantarflexion motion) has been developed. The flexion/extension is controlled by a spring. Dorsiflexion correction is achieved via the compression force of a spring within the assistive device. During controlled plantar flexion, a torsional spring control is applied where orthotic joint stiffness is actively adjusted to minimize forefoot collisions with the ground.

DISCUSSION

The magnitude of the MAFO dorsiflexion assist moment and the initial ankle angle can be modified by variation of the spring parameters (spring constant, spring rest angle). Regardless the simplicity of MAFO, the results in improvement of plantarflexion during swing phase are similar to the results obtaing using commercial AFOs.. The proposed modular ankle-foot orthosis is currently under additional mechanical durability tests. Continuous plantarflexion was applied to MAFO to check the durability of each part. At present, more than two million repetitions of plantar flexion have been applied and no serious problems have arisen. The results of the durability test will be use to improve the design of MAFO. Our MAFO can be used by the patients daily, and is also useful for gait training, since various characteristics can be easily modified. Moderately large dorsiflexion assist moment and small dorsiflexion initial ankle angle facilitates the increase of knee extension muscle forces, thus preventing forward foot slap during the initial stance phase.

REFERENCES:

Milusheva S., Tochev D., Karastanev S. (2005) Ankle-foot orthosis with spring elements. Proceedings of the 10th Congress on Theoretical and Applied Mechanics, Varna, pp. 145-149

ACKNOWLEGEMENTS:

The study was supported by grant TN 1407/04 - Bulgarian National Reasearch Fund.

INTELLIGENT ACTIVE ANKLE-FOOT ORTHOSIS

*Veneva I, *Toshev Y

Institute of Mechanics and Biomechanics, Bulgarian Academy of Sciences, Sofia, Bulgaria

veneva@imbm.bas.bg

INTRODUCTION

The aim of the work is to present an approach to control active ankle-foot orthoses /AAFOs/. AAFOs are orthotic devices intended to assist or to restore the motions of the ankle-foot complex and are based on force-controlled actuator and biologically inspired micro-control schemes. The presented AAFO is particularly oriented to assist the ankle flexion-extension in case of "Drop Foot", i.e. the inability to point the toes toward the body (dorsiflexion) or move the foot at the ankle inward or outward.

It is to note that the leading Orthotics&Prosthetics companies Otto Bock Health Care, Becker Orthopaedic, Maramed Orthopaedics Systems etc. doesn't propose to the market multifunctional intelligent active ankle-foot orthoses.

The key goal of the proposed AAFO is to assist the patient achieving normal gait patterns and to reduce the pain, the weakness, and the numbness accompanying in many cases the loss of function.

METHODS

The proposed intelligent control is oriented to modify different models of personalized ankle-foot orthoses (AFO) designed using reverse engineering and rapid prototyping by the joint team Bulgarian Academy of Sciences/Cardiff University [3, 4, 5]. A direct drive actuator is attached laterally to an AFO in order to assure automatic adaptation of the joint torque. The actuator and the hinge joint "replace" the damaged muscle complex like a tendon in series with a muscle. Realizing flexion/extension the actuator applies a torque proportional to the joint position of a normal human ankle during level ground walking. The control signals are received from two sensor arrays incorporated in the foot part of AFO and in the insole of the healthy leg. The sensors signals are computed by a programmable microcontroller, which controls the direct drive actuator.

RESULTS

The proposed control system was designed and tested. The joint torque of the actuator was automatically modulated to match patient specific gait requirements to permit smooth and natural heel strike to forefoot transition in drop-foot patients. Seven AAFO external sensors and a rotary potentiometer measure ankle joint position in real-time and send signals to the microcontroller (ATMega128). These sensors data are then used in every step of the control algorithm in order to optimize the heel to forefoot transition during the stance phase or swing phase of walking. During each gait cycle, by measuring the total time when the foot remains in contact with the ground, the microcontroller estimates the forward speed and modulates the swing phase flexion and extension in order to achieve quite normal lower limb dynamics.

DISCUSSION:

The proposed possibilities to integrate active systems into AFOs hinge joint provide gait control during real-use situations, enhance the functional performance and improve the patient comfort. The adaptation schemes presented here automatically modulate joint torque throughout the stance and the swing phases of walking. The described device enables patients to walk in a safe, comfortable and smooth manner using only local sensing and computation.

REFERENCES

1. Blaya J, Herr H. Adaptive Control of a Variable-Impedance Ankle-Foot Orthosis to Assist Drop-foot Gait. IEEE Transactions on Neural Systems & Rehabilitation engineering. Vol. 12(1), 24-31, 2004.
2. Kastner J., Nimmervoll R., and Wagner I. What are the benefits of the Otto Bock C-leg? A comparative gait analysis of C-leg, 3R45 and 3R80, Med. Orthop. Tech., vol. 119, pp.131-137, 1999.
3. Milusheva S., Toshev Y., Taiar R. Development of Active Ankle-Foot Orthosis. Acta of Bioengineering and Biomechanics, vol. 5, 335-339, 2003.
4. Y.E. Toshev, L.C.Hieu, L.P. Stefanova, E.Y. Tosheva, N.B. Zlatov, St. Dimov, Reverse engineering and rapid prototyping for new orthotic devices. In: Pham, D.T., Eldukhri, E.E., Soroka, A.J. (Eds.) "Intelligent Production Machines and Systems", Elsevier, pp. 567-571, 2005.
5. Stefanova L., Milusheva S., Zlatov N., Taiar, R., Toshev Y. Computer modelling of ankle-foot orthoses using CAD model of human body. Proceedings of the International Conference on Bionics, Biomechanics and Mechatronics, Varna, pp. 285-289, 2004.

ACKNOWLEDGEMENTS:

The study was supported by the Bulgarian National Research Fund (Grant TN 1407/2004).

OUTCOME FOLLOWING SCAPHOID BRUISING

Kanagaraj K, Khalid M, Jummani Z, Robinson D, Walker R
Nevill Hall Hospital, Abergavenny, United Kingdom NP7 7EG

mitrakraj@hotmail.com

INTRODUCTION

Diagnosis of occult scaphoid fracture is increasingly being done using MRI scanning. Consequently, scaphoid bruising is being reported increasingly. We studied the significance of this finding.

MATERIALS AND METHODS

Out of a total of 611 patients who underwent MRI scanning for occult scaphoid fractures over a 3 year period, 55 wrist MRIs in 52 patients (3 bilateral) were found to have bruising of scaphoid. There were 35 males and 17 females. Average age was 17.68 years (range 7-62 years). Our protocol for clinically suspected scaphoid fractures with negative initial radiographs was to apply a futora splint and re-examine in 4-5 days and in presence of persistent pain/tenderness over the anatomical snuff box to request an MRI scan. A majority of the scans were done within 2 weeks. The imaging was carried out using a Siemens 1 tiesla scanner with a dedicated extremity coil. Coronal T1 and STIR images were obtained. The average scanning time was 7 minutes.

RESULTS AND CONCLUSIONS

All patients with scaphoid bruising were treated symptomatically with scaphoid casts or futora splint with thumb extension for up to 6 weeks period. Immobilization was continued until the patients were asymptomatic. All patients had complete resolution of symptoms and returned to full functional activities. Radiographs at final follow up (average 6 weeks) did not show any fracture. We therefore conclude that scaphoid brusing predominantly occurs in younger age group. It is not associated with any complications in the short term and that it could be adequately treated symptomatically. Long term follow up however, is needed to determine the true natural history of this condition. This is important because concerns have been raised on the basis of experimental studies that bone bruising alters the mechanical properties of the subchondral bone and may predispose to arthritis

CARTILAGE THICKNESS IN THE HIP JOINT MEASURED BY MRI AND STEREOLOGY

* Mechlenburg I, ** Nyengaard JR, ***Rømer L, *Søballe K
*Department of Orthopaedics, University Hospital of Aarhus, Denmark
**Stereology and Electron Microscopy Laboratory, University of Aarhus, Denmark
***Department of Radiology, University Hospital of Aarhus, Denmark

inger.mechlenburg@ki.au.dk

INTRODUCTION

Periacetabular osteotomy is performed in dysplastic hips and the result of surgery is largely dependent on the degree of preoperative osteoarthritic involvement. As periacetabular osteotomy is performed on dysplastic hips to prevent osteoarthritic progression, changes in the thickness of the articular cartilage is a central variable to evaluate. For this purpose we developed a method by which the thickness of the articular cartilage in the hip joint can be quantified based on Magnetic Resonance Imaging (MRI) and 3D design-based sampling principles (stereology).

MATERIAL AND METHODS

Twenty six dysplastic hips on twenty two females and four males were MR scanned preoperatively. The first 13 patients were examined twice, with complete repositioning of the patient and set-up in order to obtain an estimate of precision of the method used. To show the acetabular and femoral cartilages separately, an ankle traction device was used during MRI. This device pulled the leg distally with a load of 10 kg.

RESULTS

The mean thickness of the acetabular cartilage was 1.26 mm, SD 0.04 mm and CV 0.03. The mean thickness for the femoral cartilage was 1.18 mm, SD 0.06 mm and CV 0.05. The precision calculated as the coefficient of error of the mean was estimated for the thickness of the acetabular cartilage 0.01 and femoral cartilage 0.02. The measurements took 15-20 minutes per hip to carry out.

CONCLUSION

The described method is an unbiased and precise method for quantifying the thickness of the articular cartilage in the hip joint. We suggest that the method can be advantageous for assessing the progression of osteoarthritis in dysplastic hips after periacetabular osteotomy.

BONE RESECTIONS AND MINOR AMPUTATION FOR SURGICAL TREATMENT OF CHRONIC OSTEOMYELITIS IN DIABETIC FOOT

*Rosa MA, **Galli M, *Alesci M, *Caminiti R
*Surgical Specialties Department-Orthopaedic Section, University of Messina, Italy

rosa.ma@tiscali.it

INTRODUCTION AND METHODS

Foot bones infection is common in the diabetic patient and represent a rapidly evolving condition in the presence of ischemia. 63 patients were operated on and followed for at least one year after surgery. 33 single ray amputation, 21 metatarsal resection and 9 partial calcanectomy gave an high rate of favourable results. Early recognition and prompt treatment is mandatory in order to avoid the loss of the limb or the patient itself.

DISCUSSION AND CONCLUSION

Surgical removal of all necrotic and infected tissue and drainage of pus should be performed immediately without waiting for revascularization. Adjunctive surgery will follow revascularization which is needed to save the limb. In the absence of significative ischemia or after an effective revascularization, management of osteomyelitis traditionally involves surgical removal of infected bone, combined with antibiotic therapy.

Foot deformities resulting from surgery may cause reulceration and a high morbility that may eventually fail to save the leg. Thus, the aim of surgery should be to control the infection, but also, to preserve a functional limb.

Various demolitive interventions with limited loss of bone segments of the forefoot or hind foot have demonstrated to be well tolerated.

Results are better if the patients is inserted in a post-operative protocol of surveillance with appropriate prescription of orthosis. The best results are achieved within a multidisciplinary setting.

AFFILIATED ISTITUTION:

**Department of Orthopaedic Sciences, Catholic University, Rome, Italy.

THE VALUE OF POSTMENISCECTOMY MRI: "DECEPTION OR DIRECTION?"

D'Hooghe P, Vandekerckhove B, De Rycke J, De Groote W
Department of Orthopaedics, AZ Sint Jan , Brugge, Belgium

pieter.dhooghe@azbrugge.be

INTRODUCTION

The purpose of this study is to evaluate a postmeniscectomy MRI protocol by an independent radiologist and an orthopaedic surgeon, without them knowing that they are evaluating a meniscus that was operated on. We conducted a prospective controlled trial considering the value of a knee MRI protocol after partial meniscectomy.

In clinical practice, we encounter patients with the so-called post-meniscectomy knee syndrome. They often present with the images and protocol of an MRI documented new tear in the meniscus of a knee that was recently operated on. In some cases, the surgeon can feel tempted if not obliged to perform a revision arthroscopy – guided by the MRI data – that intra-operatively appears normal. The value of a postmeniscectomy MRI protocol remains unclear. Therefore, we wanted to quantify the value of the MRI protocol in this study setup. Does it offer a surplus or does it blur our postoperative guidelines in meniscal surgery?

METHODS

50 meniscal tears were integrated in to this prospective study group. The age of the patients was between 20 and 55 years old. The duration period of the related trauma was not longer than 3 months. They all had a control – MRI taken, 3 weeks after arthroscopic meniscal surgery. The partial meniscectomy procedure was performed mechanically, without the use of a shaver nor laser or vapor. All patients were treated by the same orthopaedic surgeon. An independent MRI radiologist and an independent orthopaedic knee surgeon were asked to make a protocol out of the given MRI pictures. They were unaware of the fact that the meniscus has been operated on and is considered stable. Their MRI protocol offers us the necessary data to see if our hypothesis is correct and if any conclusions can be drawn furthermore.

RESULTS

The collected data show a clear discrepancy between the postmeniscectomy arthroscopic protocol and the MRI protocol ($p<0,01$). Furthermore, they show that there is no clear difference between the results from a partial medial or lateral meniscectomy.

There is however a clear difference between the location of the presenting pre-operative tear. There is more discrepancy between the MRI and the intra-operative protocol when the tear is located in the midcorpus of the meniscus, compared to the posterior and the anterior horn ($p<0,01$). The same reports were collected for the medial and the lateral meniscus. There is a clear difference in data between a longitudinally directed tear compared to the other tear types. The longitudinal tear is most frequently and faultly considered as a re-tear after arthroscopic meniscal surgery.

DISCUSSION - CONCLUSION

There is a clear tendency that a postmeniscectomy MRI protocol cannot be used as an absolute guideline in revision meniscal surgery. This deception is due to the healing process of the scarred meniscal and its surrounding tissue. There is no significant difference between lateral compared to medial meniscal surgery. There is however a clear difference between the location of the presenting pre-operative tear.

CD34+ CELLS IN THE NORMAL AND PATHOLOGICAL HUMAN MENISCUS

Verdonk PCM, §Forsyth R, Verdonk R, Almqvist KF, *Verbruggen G

§Department of Orthopaedic Surgery, Ghent University Hospital, Belgium
Goormagtigh Institute, Ghent University Hospital, Belgium
*Department of Rheumatology, Ghent University Hospital, Belgium

INTRODUCTION

We recently characterized different cell types in the normal human meniscus based on the synthesis of extracellular matrix compounds and the expression of specific cell membrane markers (*Osteoarthritis Cartilage. 2005 Jul;13(7):548-60)*. To further explore the biology of the meniscus, an immunohistochemical analysis was performed on both normal and pathological specimen.

MATERIAL AND METHODS

Human knee menisci were harvested from pathological joints at the time of total joint arthroplasty or partial meniscectomy. Specimen were obtained from joints diagnosed with rheumatoid arthritis (N=3), osteoarthritis (N=8), traumatic tear of the meniscus (N=12). The normal meniscus (N=3) specimen were obtained from the University Tissue Bank through the general organ donor program. A semi-quantitative immunohistochemical scoring (0=absent, 1= weak staining, 2= intermediate staining, 3= strong staining) was performed on paraffin embedded section: H&E, PAS, Saffranine-O, CD34, CD31 and smooth muscle actin (SMA).

RESULTS

The normal meniscus was characterized by a CD34+ superficial cell layer. This cell type was not observed in pathological menisci. In the case of a chronic meniscus tear, the superficial cell layer was characterized by cell proliferation, expression of SMA and myofibroblast-like morphology, while the osteoarthritic meniscus is characterized by a general decrease of cell number and more chondrocyte-like morphology. In both cases, CD34+ cells could not be observed. Acute meniscus tears showed the presence of CD34+ cells, no proliferation of the superficial layer and the absence of SMA expression. The RA specimen were covered by synovial pannus tissue characterized by the presence of vascular elements and CD34+ fibroblasts.

CONCLUSION

To our knowledge, this is the first study to illustrated the in vivo biological response of the human meniscus in different pathological conditions. Trauma induced a proliferative repair response of the superficial cell layer in contrast to degenerative disease which was characterized by a general hypocellularity. CD34+ superficial cells were not observed in these conditions. We hypothesize that the recently described CD34+ superficial meniscus cell plays a role in the homeostasis of the human meniscus.

NEW MULTIDIRECTIONAL ORTHOSIS FOR THE TREATMENT OF CONGENITAL CLUBFOOT

Ferrari D, Magnani M, Lampasi M, Donzelli O
8^ Divisione, Istituti Ortopedici Rizzoli, Bologna, Italy

onofrio.donzelli@ior.it

INTRODUCTION

The authors describe an innovative orthosis for the treatment of congenital clubfoot. The orthosis is composed by four different structures, which are connected and articulated to each other by means of mechanical elements. These elements allow the different components of the limb and of the deformity to be adjusted and positioned as needed on the three dimensions of the space, thus making the orthosis appropriate for the anatomical features of the patient.
This peculiarity enables the orthosis to be easily reprogrammed, based on the growth of the limb and on the corrections obtained.
Indicated for the non-operative treatment of grade I clubfoot and for the post-operative period (after 21 days of casting) in the grade II clubfoot.
Light and aesthetically pleasant, easy to wear and to remove in order to practice regular manipulations and physiokinesitherapy, it allows to limit hypotonia and hypotrophy of affected tissues.

MATERIALS AND METHODS

We reviewed 18 patients treated for congenital clubfeet (7 cases grade I, 11 cases grade II). In grade I clubfeet, daily manipulations were performed, and between physical therapy sessions the orthosis was applied, progressively increasing the degree of correction, based on the clinical improvements obtained. In grade II clubfeet, after the surgical correction, achieved by means of the modified Codivilla technique, an above-the-knee cast was applied (with 90-degree flexion at the knee and a mild overcorrection of valgus and dorsiflexion at the foot). After 21 days, the cast was removed and the orthosis, modified based on the corrections achieved, was applied. The orthosis had to be removed by parents 2-3 times a day to practice manipulations. At the age of 8 months, the orthosis was stopped and children began wearing symmetrical straight shoes (with an anterior-external 3-4 mm wedge correction in the shoe) during the day and utilizing a below-the-knee brace with a mild overcorrection (dorsiflexion, valgus and pronation) at night for the next 8-10 months.

RESULTS

Clinical examinations were performed in all the cases 8-10 months after orthosis removal. All the feet showed a good correction of the deformity with no signs of relapse.
Relapses are possibile even several years after surgical correction. For this reason, a periodical follow-up has to be planned also after the above-mentioned time of treatment.

DISCUSSION

Equinus-varus-adductus clubfoot is the most frequent type of congenital clubfoot. We use a 3-grades classification of increasing severity. Treatment has to be started soon, during the first weeks of life, by means of manipulations and casting. In more severe cases, a surgical procedure has to be performed at the age of 3 months, followed by a 3-4 months period of casting. After cast removal, manipulations, custom shoes and nighttime braces are used for further 8-10 months.
The orthosis we propose enables to minimize the time of casting as it provides the proper correction of the deformity by adapting itself to the progressive clinical improvement achieved, thus reducing hypotrophy and hypotonia of affected tissues.

PREDICTION AND PROPHYLACTIC FIXATION OF CONTRALATERAL HIP IN SCFE USING SKELETAL BONE AGE

*Gorva AD, *Metcalfe J, *Jones S, *Fernandes JA
*Department of Paediatric Orthopaedics,Sheffield Children's Hospital,
Western Bank, Sheffield S10 2TH

dranandortho@yahoo.com

INTRODUCTION

Prophylactic pinning of an asymptomatic hip in SCFE is controversial. Bone age has been used as evidence of future contralateral slip risk and used as an indication for such intervention. The efficacy of bone age assessment at predicting contralateral slip was tested in this study.

PATIENTS AND METHODS

18 Caucasian children prospectively had bone age assessment using wrist and hand x-rays when presenting with a unilateral SCFE. Patients and parents were informed about the chance of contralateral slip and risks of prophylactic fixation, and advised to attend hospital immediately on development of symptoms in contralateral hip. After in-situ fixation of the affected side prospective monitoring in outpatient department was performed. Surgical intervention was undertaken if the contralateral hip was symptomatic.

RESULTS

Three children (2 boys) went on to develop to a contralateral slip at a mean of 20 months from initial presentation. 6 children (5 boys) were deemed at risk of contralateral slip due to a bone age below 12.5 years for boys and 10.5 for girls. Only one from this group developed a contralateral slip. The relative risk of proceeding to contralateral slip when the bone age is below the designated values was 1 (95% confidence interval of 0.1118 to 8.95). The sensitivity and specificity were 33% and 66% respectively. With positive predictive value of 15% and diagnostic efficiency of 61%.

CONCLUSION

Delayed bone age by itself is not a good predictor of future contralateral slip at initial presentation. Routine prophylactic pinning is not justified based on bone age alone, with the risks of surgical fixation it carries. Prospective long term longitudinal study is required.

ANATOMICAL AND MORPHOLOGICAL VARIATIONS IN LUMBAR SPINE IN CHILDREN WITH OSTEOGENESIS IMPERFECTA

*Gorva AD, *Bishop NJ, *Cole A
*Department of Paediatric Orthopaedics, Sheffield Children's Hospital,
Western Bank, Sheffield S10 2TH

dranandortho@yahoo.com

INTRODUCTION

Lumbar spine morphology is well described in healthy children but has not been described in children with Osteogenesis Imperfecta (OI).

AIMS

To look at lumbar bony morphometry in OI children and to consider the importance of these factors in spinal surgery in these children

METHODS

21 lumbar vertebrae (from L3-5) of 7 OI (6 OI type 3 and 1 OI type 4) children with scoliosis were analysed using Reformatted Computer Tomographic scans. The following measurements obtained: Spinal canal diameters, Transverse pedicle width, Total pedicle length, Pedicle root length, Transverse pedicle angle and Sagittal pedicle angle. Results are compared with previously published data of normal age-matched lumbar spine measurements

RESULTS

The mean age was 12 years (range 7-18 years). 6 females and 1 male. All had spondylolisthesis at L5-S1.Results were analysed by Wilcoxon Signed Rank test (nonparametric test). The transverse pedicle width was significantly narrower at all 3 levels ($p<0.01$). Transverse pedicle angle was significantly less angled at all 3 levels (L3 $p=0.04$, L4 & L5 $p<0.01$) whilst the sagittal pedicle angle was significantly more angled at all 3 levels ($p<0.01$). Spinal canal diameter (AP) was significantly increased at all 3 levels (L3 & L5 $p<0.01$, L4 $p=0.02$). And no significant differences in spinal canal transverse diameter and total pedicle length. Pedicle root length Significantly longer at all 3 levels (L3 & L4 $p<0.05$, L5 $p<0.01$). All children had grade-I spondylolisthesis at L5/S1.

CONCLUSIONS

A longer pedicle root with a narrower transverse diameter (and thinner cortices) and a reduced transverse angle is essential knowledge when passing pedicle screws in the lumbar spine in children with OI. This is a difficult technique and its safety requires further evaluation

USE OF STEM CELLS IN SURGICAL TREATMENT OF CONGENITAL PSEUDARTHROSIS IN CHILDREN

*Magnani M, *Lampasi M, **Granchi D, **Devescovi V, *Donzelli O
*8^ Divisione and **Laboratorio di Fisiopatologia Ortopedica, Istituti Ortopedici Rizzoli, Bologna, Italy

onofrio.donzelli@ior.it

INTRODUCTION

The authors describe a new multidisciplinary technique for surgical treatment of congenital pseudarthrosis in children affected (or not) by Neurofibromatosis.

The procedure requires the use of stem cells added to traditional techniques of treatment, intramedullary nailing and external fixation, with or without autogenous or homologous bone grafting.

The first cases still under study are reported in this abstract.

MATERIALS AND METHODS

The authors analyze 5 children affected by neurofibromatosis presenting with pseudarthrosis of the tibia and treated by intramedullary nailing or external fixation (Ilizarov circular external fixator) and contemporary application of stem cells.

The number of patients recruited is still to be defined and long-term results are still missing.

The success of regenerative medical strategies is linked to the advancing knowledge on the potential of stem cells and to the progressive development of techniques stimulating cells to differentiate and successively guiding specific cellular activities.

DISCUSSION

Neurofibromatosis is a genetic disorder, affecting tissues of ecto-, meso-, and endodermal origin with varying degrees of expressivity. Hereditary forms show an autosomic dominant transmission with almost complete penetrance.

The most frequent form of the disease (1/3000-4000 births) is the type 1 (NF1 or von Recklinghausen disease).

The clinical features of NF1 include cutaneous alterations of melanogenic origin, café-au-lait spots, multiple peripheral neurofibromas and several other clinical manifestations (neurological, hematological, dermatological, orthopedic, cerebral and extracerebral tumors, mental retardation, hypertension, scoliosis, etc).

The main orthopedic manifestation is congenital pseudarthrosis of the leg, affecting the tibia and/or the fibula.

In most cases the pseudarthrosis presents spontaneous fractures which do not consolidate. At the site of the pseudarthrosis, dysplastic tissue with areas of fibrosis and obliteration of the medullary canal can be found.

Therapeutic options include different possibilities according to the severity and location of the lesions.

Surgical treatment can be performed by internal or external fixation and use of bone grafting in order to obtain the definitive consolidation, that generally occurs at the age of 15 years.

Surgical treatment of pseudarthrotic lesions could benefit of regenerative medicine, which provides a biological approach to consolidation, based on the use of cells and growth factors. These elements could lead to tissular healing and consolidation, in cases where traditional techniques fail.

This work describes an innovative technique, resulting from a multidisciplinary collaboration, and the clinical and radiographic features of the different types of pseudarthrosis, either at presentation or at the time of the definitive surgical treatment.

AN ANALYSIS OF BONE STRUCTURAL CHANGES IN PROTEUS SYNDROME AND THEIR RELATIONSHIP WITH GROWTH

Pazzaglia UE, **Beluffi G, *Bonaspetti G, *Ranchetti F, *Azzola F
*Clinica Ortopedica e Traumatologica Spedali Civili di Brescia, Università degli Studi di Brescia, 25123 Brescia, Italy

g.bonaspetti@libero.it

INTRODUCTION

Proteus Syndrome is a rare disease, so named for its highly variable manifestations: it causes tissue overgrowth in a mosaic pattern and may affect tissues derived from any germinal layer. Skeletal manifestations include asymmetrical limb overgrowth and length discrepancy, macrodactyly of individual bones of hands and foot, vertebral abnormalitites and hyperostosis.

METHODS

Radiogrphic follow-up of 13 years and 8 months, with evaluation of rate of growth of hand bones to compare overgrown bones with normal.

RESULTS

The analytical x-rays study in the period of long follow-up showed that bone growth did not differ significantly in overgrown bones.

DISCUSSION

Most of the typical bone malformations are secondary to the altered mechanical conditions of the deformed bones. The primary lesion seems to have occurred in the early embryonic period when in the limb buds mesenchymal cells condensate and cartilage differentiates.

** Radiologia, Ospedale S. Matteo, Pavia, Italy

EPIPHYSEAL DYSPLASIAS.
AN OVERVIEW ON CLASSIFICATION AND PATHOLOGY

*Pazzaglia UE, **Benetti A, ***Bondioni MP, *Bonaspetti G, ****Beluffi G, **Donzelli C
*Clinica Ortopedica e Traumatologica Spedali Civili di Brescia, Università degli Studi di Brescia, 25123 Brescia, Italy

g.bonaspetti@libero.it

INTRODUCTION
The classification of osteochondral dysplasias is founded for a well established tradition on the radiographic study of the skeleton and specific types disorder in individual cases are referred in broad terms to the anatomic division of growing bones into epiphysis, metaphysis and diaphysis. Different combinations of shape deformities, growth defects and abnormalities of the calcification/ossification process have contributed to identification of specific disorders. Epiphyseal dysplasias are the most evident example of a complex and diversified spectrum of cartilagineous disorders, whose diagnostic criteria still rest on clinical and imaging assessment.

METHODS
A case of chondrodysplasia punctata with x-rays and histology of bones and two cases of atypical epiphyseal dysplasia both with long radiographic follow-up (one of them with bioptic study) were available.

RESULTS
Radiographic aspects were correlated to histopathological findings, with particular interest to growth of epiphyseal cartilage and its pattern of ossification.

DISCUSSION
This findings offered a deeper insight into the development and structural organization of the epiphyses of long bones and the morphological deviations in epiphyseal dysplasias.

** Cattedra di Anatomia Patologica, Università degli Studi di Brescia, 25123 Brescia, Italy
*** 2^ Radiologia, Spedali Civili di Brescia, 25123 Brescia, Italy
**** Radiologia, Ospedale S. Matteo, Pavia, Italy

THE TREATMENT WITH ESWT OF CUFF ROTATOR CALCIFYING TENDONITIS VERSUS SHOULDER IMPINGEMENT SYNDROME

*Vitali M, **Peretti GM, **Mangiavini L, **Fraschini GF
Scuola di Specializzazione Ortopedia e Traumatologia I°, Università degli Studi di Milano, Milano, Italy

matteovitali@yahoo.it

INTRODUCTION

Shock waves therapy was introduced in the medicine field in the eighties and it was used for kidney calculosis treatment. Then, new studies in such a specific field have been carried out and the use of ESWT (extracorporeal shock wave therapy) as high/medium-energy shock waves was identified as potential tool for the treatment of specific musculoskeletal disorders [1]. As a matter of facts, it was observed how ESWT produced important effects on soft tissues of the body such as anti-inflammatory, analgesic and revascularization action.
At the beginning, the ESWT was most used for patients having problems on their shoulders, although with different results.
The aim of our study was to study the shock waves therapy efficacy in the treatment of patients suffering for calcification of the rotator cuff versus those with the "impingement syndrome" in the shoulder.

METHODS

From July 2004 to November 2005 a number of 233 patients were treated with ESWT; it was counted that 130 patients suffered from calcification of the cuff rotator and 103 patients had pain in shoulder with "impingement syndrome".
Each patients was treated with 1700 pulses having a medium energy of 0,28 mJ/mm^2 with Wolf Piezoson 300 Dornier Medtech 7,5 MHz with ultrasounds for three times in a month. No patient needed a local anaesthesia. The only people excluded from this therapy were because of pregnancy, people having pacemakers or coagulation disorders or cancer.
A clinical check was done right before the beginning of the ESWT and after the first and fourth months at the end of the therapy, by using three scales (NRS, McGill Pain Questionnaire e Chronic Pain Grade Questionnaire) to test pain and joint functions.
The evaluation was done by using X-ray, Ultrasound and MRI.

RESULTS

The treatment for patients suffering from the "impingement syndrome" was positive in 55% of cases with pain reduction and joint-function recovery. Lately, a MRI check showed that no changes occurred in the rotator cuff.
As for the treatment in the calcification of the rotator cuff it was observed that the pain was reduced or totally disappeared in 83% of patients, with also a joint-function recovery.
Also X-rays after 4 months from the end of the therapy have showed, as highlighted by other researchers, a decrease or even the disappearing of the calcification process on the rotator cuff.

DISCUSSION

It is interesting to consider the different results obtained in the two different pathologies with ESWT.
As a matter of fact, the difference of positive results after the shock wave therapy is a 28% in favour of people suffering from the calcification of the rotator cuff compared to the patients suffering from the" impingement syndrome".
Considering the different results on these two pathologies, we assume that, as already explained in literature, there is a different physiopathological mechanism.
As a matter of facts, the most important cause of the "impingement syndrome" is a mechanical phenomenon that cannot be eliminated with shock waves therapy. It can only be relieved through a rehabilitation therapy.
The shoulder with calcification is the expression of a chronic inflammatory at the rotator cuff [2]. Therefore, shock waves therapy has an analgesic and anti-inflammatory effect on the shoulder and it reduces the calcification with the reduction/removal of the painful symptoms. In this case, a surgery can be postponed or even not required.
However, in both painful pathologies, it is necessary to note that ESWT cannot and must not be replaced by surgery.
In conclusion, according to our clinical experience, we believe that in order to obtain the best results from shock waves therapy, it is necessary to join it with a long period of rehabilitation therapy.

REFERENCES:

1. J. Ogden. Shock waves therapy in musculoskeletal disorders. Clin Orth Rel Res, n° 387 2001.
2. Unthoff et al.: "Calcifying tendonitis. A new concept of its pathogenesis." Clin Orthop, 1976.

AFFILIATED INSTITUTIONS FOR CO-AUTHORS:

** Divisione Ortopedia e Traumatologia Università Vita-Salute San Raffaele, via Olgettina 60 Milano.

THE TRUE INCIDENCE OF RECURRENT DISC HERNIATION AFTER LUMBAR DISCECTOMY

Nishimura Y
Shimabara Orthopaedic Nishimura Clinic, Shimabara-shi, Nagasaki, Japan

kisoukai@celery.ocn.ne.jp

INTRODUCTION

In past investigations, the incidence of recurrent disc herniation after posterior lumbar discectomy ranges from 5 to 15%. However, these are not the true recurrence rate , but the re-operation rate. The purpose of this study is to clarify the true recurrence rate at one year after operation prospectively.

METHODS

From 2000/4/1 to 2004/8/30, I operated 102 cases by single level posterior discectomy without fusion for lumbar disc herniation. The patients that were lateral lumbar disc herniation were excluded from this study. In all cases, preoperative, 4-weeks and 1-year postoperative Magnetic Resonance Imaging (MRI) examination were planned. However, 13 cases were not checked 1-year postoperative MRI, so the remaining 89 cases were investigated in this study. There were 57 males and 32 females. The average age at operation was 51 years (18-85 years). The operated level were L2/3 in 2 cases, L3/4 in 4 cases, L4/5 in 48 cases, L5/S1 in 35 cases. In all cases, herniated mass were good removed at 4-weeks postoperative MRI. The MRI findings at 4-weeks and that at 1-year were compared in detail. The definition of recurrent disc herniation was the presence of herniated disc and the enlarged compression for the neural tissues at 1-year MRI more than 4-weeks MRI at the previously operated site and side. The patient's occupations were classified into three grade, the house work, the desk work, the hard work, and were studied whether the occupation related to the recurrence or not. I investigated whether there were difference about age at operation, sex, operated disc level, range of motion and posterior slippage of operated disc between the recurrent cases and non-recurrent cases. Clinically I examined whether there were difference between the recurrent cases and non-recurrent cases with JOA (Japanese Orthopaedic Association) score at 1 year after operation. In JOA score, 29 points was full score. I used the Mann-Whitney U test or Fisher's exact test for statistical analysis. A p value of less than 0.05 was considered significant.

RESULTS

Of the 89 patients who had posterior discectomy for lumbar disc herniation, 19 patients (21.3%) showed recurrent disc herniation at the same level, same side at 1 year after operation. But only two of these complained radicular pain. One was treated by reoperation, and the other was treated conservatively. There was no significant difference about the JOA score between the recurrent cases (26.6 points) and non-recurrent cases (27.9 points) at 1 year after operation. There were no significant difference about the age at operation (recurrent cases 54.4 years, non-recurrent cases 42.4 years) and the hardness of occupations. 8 cases (16.7%) out of 48 patients in L5/S1 and 10 cases (28.6%) out of 35 patients in L4/5 revealed recurrence. But there was no significant difference. 3 cases (9.4%) of the 32 females and 16 cases (28.1%) of the 57 males revealed a recurrence. There was significant difference between the sex. The range of motion and posterior slippage of the operated disc level were 8.9 degrees and 2.4mm in the recurrent cases, and 8.2 degrees and 1.6mm in the non-recurrent cases. There were no significant differences.

DISCUSSION

The true recurrence rate at 1 year after posterior discectomy for lumbar disc herniation was 21.3% unexpectedly. However, many of the recurrent cases were clinically asymptomatic, and there were no difference of JOA score between the recurrent cases and the non-recurrent cases. About the factors which affected to the recurrence, there was difference only in sex, but there were no significant differences in occupational hardness, operated level, age at operation, range of motion and posterior slippage of the operated level. From this study, more another factors influence the recurrence of disc herniation

VERTEBRAL STRENGTH AND STIFFNESS AFTER KYPHOPLASTY OF OSTEOPOROTIC SPINE FRACTURES

+Steens J, #Verdonschot NJJ, *Aalsma AMM , ¶Veldhuizen AG, +Hosman AJF
+ Dept Orthop Surg & #Orthop Res Lab, Radboud University Medical Center, Nijmegen. * Baat, The Netherlands
¶Department of Orthopaedic Surgery, Groningen University Medical Center, Groningen, The Netherlands
A.Hosman@orthop.umcn.nl

INTRODUCTION

Osteoporotic vertebral fractures represent an enormous public health burden. They cause significant pain and may lead to disability and a decrease in quality of life. Vertebroplasty, in which the fracture is stabilized by injecting bone cement into the vertebral body, has gained acceptance over the past years as treatment of these fractures. Feasibility and safety of the procedure has been well established, however, major complications do occur, often related to cement leakage. Kyphoplasty is a variation on this technique, in which a void is created in the fractured vertebral body, reducing the pressure needed to inject cement into the vertebral body. This technique may also restore some height of the collapsed vertebral body. The rate of complications may be lower in this technique compared to conventional vertebroplasty. In this study we describe vertebral strength and stiffness in kyphoplasty after height restoration in cadaver fractured vertebra. An **ex**perimental **t**ool (**ExT**) was used, creating a void and expanding the vertebra. The influence of amount of vertebral height loss and amount of vertebral height restoration was also determined.

MATERIALS AND METHODS

From four human cadaver vertebral columns, 25 intact vertebra were obtained (10 lumbar vertebra, 15 thoracic vertebra). Age of the subjects was between 78 and 93. All four vertebral columns were strongly osteoporotic at inspection. This was confirmed by a DEXA scan.

Preoperative crush sequence: In 21 vertebra anterior wedge fractures (Denis type 1B, AO type A1.2) were created by displacement controlled eccentric external force. The preset amount of height reduction was 35%. Force (N) necessary to achieve height reduction was recorded during the entire crush sequence, and visualized in a force/displacement diagram. The vertebra was loaded at low speed (5 mm/min) to avoid dynamic effects. In addition, to verify crush methods from literature and to draw comparisons between the results of known literature with our trials, four vertebra were compressed to only 25% height reduction. Our hypothesis is that when the vertebra is crushed with a height reduction of 25%, the cortical walls remain intact and will still contribute significantly to the post-crush strength and stiffness. Therefore the reconstruction with PMMA will have less influence on the post crush strength and stiffness. ***Height restoration and cementing technique***: A spine surgeon trained in the kyphoplasty technique undertook all the **ExT** insertion and height restoration trials. A bilateral transpedicular approach was used. Height was restored within 0.5 mm of the original height (confirmed by X-ray and anterior height measurements) under a load of 50-100 N. After height restoration the loadsimulator was unloaded and bone cement was inserted immediately. Of the four vertebrae that were crushed to only 25% vertebral height, two vertebrae were reconstructed as described above. Another two vertebrae were not reconstructed after 25% height reduction to test the post fracture strength of an untreated vertebra. The cement selected for the trials was the Parallax cementing system. ***Postoperative crush sequence***: The strength and stiffness of the VB after height restoration and curing of the cement was determined by fracturing the vertebra again in a postoperative crush sequence identical to the preoperative crush sequence. Strength and stiffness were compared with there original pre-operative values. In the two vertebra in which height restoration was not attempted, "post-fracture strength and stiffness" of the VB was determined after unloading the vertebra and letting it recoil for 15 minutes. ***Statistical analysis***: Results are presented as mean and standard deviation of the mean (SD).

RESULTS

All vertebrae in the 35% height reduction group were restored to at least 100% of their original height (102 ± 2%) and filled with cement. Figs. 1 and 2 show the force/displacement graph as obtained in two vertebrae. The fracture of the cortex is clearly visible in the force/displacement graph as a sudden drop in the force. Mean maximal compression force during the initial crushing sequence was 1200 ± 496N. After reconstruction mean maximal compression force was 935 ± 340 N, a decrease of 16 ± 30%. Vertebral body stiffness is derived from the force/displacement graph just before reaching the first failure (max. force) of the vertebra. Mean stiffness during the initial crushing sequence was 233 ± 126 N/mm. After reconstruction mean stiffness was 93 ± 45 N/mm, a decrease of 52 ± 28%. As shown in the figures, endplate-to-endplate PMMA filling seems to result in a better reproduction of pre clinical results. Two vertebrae were deformed with 25% of their original height but not restored. A lower maximal force at the initial crushing sequence was observed: 715 ± 233N; maximal force at the second crushing sequence was 680 ± 141N. Results in the other two vertebra, that were deformed with 25% of their original height, but were restored to their original height were remarkably similar. In these vertebrae, maximal force at the initial crushing sequence was 865 ± 190N; maximal force at the second crushing sequence was 690 ± 14N.

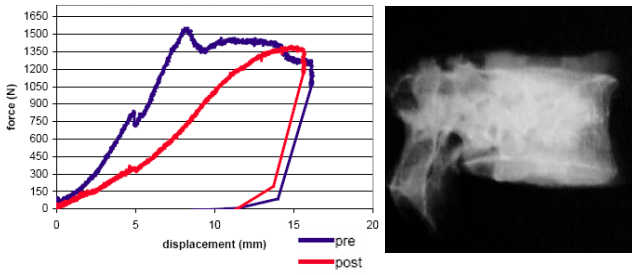

Fig.1: Force/displacement graph in endplate-to-endplate PMMA filling

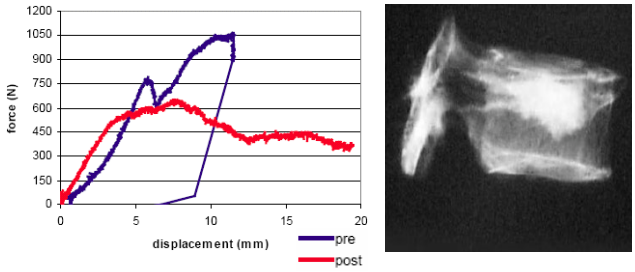

Fig.2: Force/displacement graph in partial VB height PMMA filling

DISCUSSION

Based on literature data, post-operative strength and stiffness were expected to be similar or higher compared to preoperatively. However, in our study postoperative strength and stiffness were lower than expected. After fracturing, height restoration and cementing, post-operative vertebral body strength was 80-90% compared to preoperatively. Average postoperative stiffness was 40-50% compared too preoperatively. Several differences in study design may account for the differences in results. First, in our study only clinically relevant osteoporotic anterior wedge fractures were created (AO 1.2). In most other studies the fracture types are not clearly defined and vary from non-wedge VB endplate impaction (AO 1.1) to complete burst fractures (AO 3.3). The strength and stiffness of a wedge fracture before reconstruction may be higher, resulting in a relatively larger decrease in postoperative strength and stiffness. Second, in other studies vertebral height was decreased only by 25%. If no fracture but only plastic deformation had occurred, this will probably influence the postoperative results strongly, as shown in this study. Third, the reconstruction technique: In our study a void was created in the sagittal plane before cementation. However, endplate-to-endplate cementation was not an objective in our study protocol. Although other studies suggested that the inserted amount of PMMA has minor influence on postoperative strength and stiffness, preliminary X-ray data suggest that endplate-to-endplate filling may profoundly enhance postoperative vertebral strength and stiffness. These data will be further analyzed.

EXTENSION OF THE INDICATION FOR BALLOON KYPHOPLASTY IN ADVANCED OSTEOPOROTIC VERTEBRAL BODY FRACTURES WITH POSTERIOR WALL INVOLVEMENT

Wagner N, Böhm B, Klonschinski T, Drees P, Heine J
Orthopaedic Department, University of Mainz, Germany

nataliewagner@gmx.de

INTRODUCTION

The management of osteoporotic vertebral body fractures (VBF) with posterior wall involvement is problematic. Besides open surgery, new procedures as minimally invasive balloon kyphoplasty can be considered.

MATERIALS AND METHODS

Between 01/2003 and 07/2005, 184 patients with symptomatic osteoporotic fractures were admitted for surgical treatment via the emergency of the orthopaedic University Clinic Mainz. 166 patients were managed with a minimally invasive procedure. In 10 patients with an advanced osteoporotic VBF with posterior wall involvement we performed balloon kyphoplasty. The mean patient age was 71.1 years; the median follow-up period was 11.6 months (3.5-16.5). In 8 of the 10 patients the fracture occurred after a trauma. Preoperatively 6 of the 10 patients reported leg pain, neurological deficit was present in 2 of these cases. In two cases a spinal decompression was done during the same operation session.

RESULTS

With a dislocated fracture (n=2/8). In patients with an increased surgical risk, the outcome of balloon kyphoplasty treatment is good, even in VBF with posterior wall involvement.

Two of the 10 patients were lost for follow-up, 1 woman died and 1 patient was not available for follow-up control. The back pain improved from 8.1 preoperatively to 2.3 immediately post intervention (n=10, VAS). Leg pain resolved completely in 1/3 patients and was reduced in 2/3. During the follow-up period the leg pain was reduced from 3.9 to 2.2 (n=8, VAS). Quadriceps weakness KG 4 remained unchanged in one case. X-ray and CT control showed in the 8 patients available for follow-up a reconstruction in vertebral body height from 26 % (15.0-30.8%) to 71 % (56.6-72.4%) of the initial vertebral body height. The kyphotic angle was corrected from 17° kyphosis to 2° lordosis.

CONCLUSIONS

When critically analyzed, the pain reduction obtained in patients with VBF with posterior wall involvement is lower than in patients with uncomplicated VBF. In this patient group we noted 75 % (6/8) of the patients with ostoporotic VBF with posterior wall involvement indicate a reduction of back and leg pain. They returned to their normal domestic environment. Clinically unsatisfactory results were only seen in the patie

MID TO LONG-TERM RESULTS OF MODULAR NECKS IN PRIMARY UNCEMENTED TOTAL HIP ARTHROPLASTY

Aldinger PR, Wendt S, Gatermann S, Heisel C, Aldinger G
Orthopädische Klinik Paulinenhilfe im Diakonieklinikum Stuttgart, Germany
Stiftung Orthopädische Universitätsklinik, Heidelberg, Germany

peter.aldinger@ok.uni-heidelberg.de

INTRODUCTION

Improved biomechanics facilitated by modularity in THA has the potential to make the surgery easier and thereby decrease the complication rate. Increased fretting wear at the connecting interfaces may be a drawback. 10 year survival exceeding 90% is required to endorse modular necks.

MATERIALS AND METHODS

We followed the first 190 consecutive implantations of an uncemented, straight femoral stem with a modular neck available in 12 different geometries with combinations of two lengths, two offset versions, three anteversions (European Hip System (EHS) / Profemur E, Wright Medical Technology Inc., Arlington, TN, USA) and a grit blasted titanium acetabular cup with a ceramic on polyethylene bearing in 178 patients from 1992 to 1997. Mean time of follow-up evaluation was 10 (8–13) years.

RESULTS

At follow-up, 21 patients (22 hips, 11,6%) had died, and 13 (14 hips, 7,4%) were lost to follow-up. One hip underwent femoral revision for a periprosthetic fracture. Overall stem survival was 99 (98–100) % at 10 years, survival with femoral revision for aseptic loosening as an end point was 100 (99–100) % at 10 years. Three acetabular components were revised, one for infection and two for aseptic loosening of the titanium shell. There was one fracture of an high offset modular neck at the laser labeling without trauma. The laser mark was identified as a stress riser and the neck design was changed subsequently. The mean Harris-Hip-Score at follow-up was 88 points. 153 hips were available for radiolographic evaluation. None of the femoral components showed signs of loosening. Radiolucent lines (< 2mm) in Gruen zones 1 and 7 were present in 4,1% (8 hips) and 5,0% (9 hips), respectively. Radiolucencies in zones 2 – 6 were not found. No case of femoral or acetabular osteolysis was found. Accelerated wear was not detected on radiographs. Patients with 116 hips gave informed consent for a metal ion analysis in the serum samples. The results showed no increased serum ion levels compared to an age matched control group.

CONCLUSIONS

The long-term results for this uncemented hip system are encouraging. The complication rate was extremely low with a high patient (and surgeon) satisfaction. The modular neck system proved to be reliable and enabled the surgeon to accurately reconstruct hip mechanics. The metal ion analysis revealed no elevated serum ion levels compared to an age matched control group. Modular necks of this type are a reliable and durable option in primary total hip arthroplasty.

CUSTOM MADE UNCEMENTED TITANIUM STEMS IN VERY YOUNG PATIENTS EXCELLENT 10 YEAR SURVIVAL IN 33 PATIENTS UNDER THE AGE OF 40

Aldinger PR, Wendt S, Jung A, Gatermann S, Aldinger G
Orthopädische Klinik Paulinenhilfe im Diakonieklinikum Stuttgart, Germany
Stiftung Orthopädische Universitätsklinik, Heidelberg, Germany

peter.aldinger@ok.uni-heidelberg.de

AIM
Custom made uncemented femoral components have been developed to overcome the limitations of intra- and extramedullary femoral deformities in THA and to improve postoperative implant fit and joint geometry. The implants were manufactured according to a set of CT images of the proximal femur with a fit and fill concept and reconstruction of the joint geometry for correct anteversion, offset and leg length.

METHODS
We evaluated the clinical and radiographic results of a consecutive series of 41 implantations of a custom made tapered titanium uncemented femoral stem (CT3D-A, Orthopaedic Services, Mainhausen, Germany) implanted from 1992-1994 in 33 patients under the age of 40 (mean 35, 24-40) years.

RESULTS
After a mean follow-up of 11 (10–13) years, 1 patient (1 hip) had died and 2 (2 hips) were lost to follow-up. No patient underwent femoral revision; there were two revisions of the uncemented cup, one for excessive PE wear and one for aseptic loosening. Overall survival for the femoral component was 100% at 11 years (95%-confidence limits, 93% - 100%), survival with a worst case scenario with lost patients as failures was 92% (95%-confidence limits, 88% - 100%). The median Harris-Hip-Score at follow-up was 92 points. No thigh pain was found. No femoral osteolysis was found.

CONCLUSIONS
The mid- to long-term survival with this type of femoral component is excellent and compares favorably with cemented stems and uncemented of the shelf implants in this young age group.

DEVELOPMENT OF AN OVERNIGHT STAY TOTAL HIP REPLACEMENT PROGRAMME

*Apthorp H, *Chettiar K, *David L, *Worth R
The Conquest Hospital, Hastings, United Kingdom

HApthorp@aol.com

INTRODUCTION

Recently there has been much interest in minimally invasive hip surgery, with less attention being directed to maximising the potential benefits of this type of surgery. We have developed a new multidisciplinary program for patients undergoing total hip replacement in order to facilitate an overnight hip replacement service.

METHODS

The program involves a pre-operative regimen of education and physiotherapy, a modified anaesthetic technique, a minimally invasive surgical approach and a portable local anaesthetic pump infusion for post operative pain control. Strict inclusion and exclusion criteria were developed based on age, medical status and social circumstances. Patients were mobilised on the day of their operation and discharged home with an 'outreach team' support network. No patient complained that their discharge was early. Independent evaluation was performed using the Oxford Hip Questionnaire, the Merle d'Aubigne clinical rating system and Visual Analogue Pain Scores.

RESULTS

Forty one (41) patients underwent total hip replacement using the new protocol.
The average length of stay was 1.4 days. The mean pain score on discharge was 1.3/10. The Oxford Hip Questionnaire and Merle d'Aubigne scores were comparable to patients who underwent surgery prior to the introduction of the new protocol. Minimising in-patient stay for total hip replacement benefits the patient by reducing exposure to nosocomial infection and expediting the return to a normal environment for faster rehabilitation. This new programme allows patients undergoing total hip replacement to be discharged after 1 night post operatively without compromising safety or quality of care**.**

CONCLUSION

Minimally invasive surgery with a suitable infrastructure can be used to dramatically reduce the length of stay in suitable patients. This can be achieved reliably, safely and with high patient satisfaction. In order to gain the benefit of minimally invasive total hip replacement surgery we recommend introducing this type of comprehensive programme.

REDUCTION OF OSTEOLYSIS WITH CROSSLINKED POLYETHYLENE: FIVE YEAR IN VIVO RESULTS

*Bitsch RG, *Heisel C, **Ball S, **Schmalzried TP
*University of Heidelberg, Germany

rbitsch@ix.urz.uni-heidelberg.de

INTRODUCTION

Marathon crosslinked polyethylene (PE) has shown reduced wear in short-term studies that approached the wear reduction predicted by wear simulators. With a 5 year follow-up, the true wear rate can be better determined as well as an assessment of osteolysis.

METHODS

32 patients received a crosslinked PE liner (Marathon™, DePuy, Warsaw, IN) and 24 hips a conventional PE insert (Enduron™, DePuy, Warsaw, IN). True wear rates were measured on radiographs using a linear regression analysis of data generated with a validated computer-assisted technique. Patient activity was assessed by a computerized two-dimensional accelerometer worn on the ankle (Stepwatch, Cyma, Seattle, WA). Five year radiographs were assessed for osteolysis by three different Orthopaedic surgeons.

RESULTS

The mean follow up time was 5.3 years (range: 3.9-7.0 years). The group with Enduron™ PE showed a mean linear wear rate of 0.108 mm/year (range: 0.019-0.409 mm/year) and 0.054 mm/million cycles (range: 0.014-0.207 mm/million cycles). Patients with Marathon™ PE showed a mean linear wear rate of 0.038 mm/year (range: 0.004-0.233 mm/year) and 0.020 mm/million cycles (range: 0.003-0.126 mm/ million cycles). Linear wear rate in the Marathon™ group was 65% lower than in the Enduron™ group ($p<0.0001$). 8 of 24 hips with Enduron™ liners showed osteolysis. Osteolysis was radiographically not apparent in any of the 32 patients with Marathon.

DISCUSSION

After five years *in vivo*, Marathon crosslinked polyethylene demonstrates a 65% relative reduction in wear, which is less reduction than in the two-year results and in the predictions of wear simulator studies. More importantly is the absence of osteolysis in this cohort. Concerns of an increased risk of osteolysis due to smaller particles from crosslinked polyethylene are assuaged by this medium-term experience.

Radiograph of a 46 year old female patient, 64 month after the implantation of an artificial hip joint with a conventional PE insert: visible wear and osteolysis.

AFFILIATED INSTITUTIONS FOR CO-AUTHORS:
**Joint Replacement Institute, Los Angeles, USA

METAL ION RELEASE IN PATIENTS WITH FAILED TOTAL KNEE ARTHROPLASTY

*Bochicchio V, *Savarino L, *Tigani D, *Ferrara T, *Maci G, *Greco M, *Baldini N, *Giunti A
*Laboratorio di Fisiopatologia Ortopedica & 7^ Divisione, Istituti Ortopedici Rizzoli, Bologna, Italy
valerio.bochicchio@gmail.com

INTRODUCTION

Excessive release of metal wear particles from orthopaedic implants represents a continuous exposure to bioactive, potentially hazardous substances.
Tissue damage, cytotoxicity, toxic/sensitizing effects of corrosion products on the immune system, as well as an involvement of metal ions in the pathogenesis of prosthesis loosening, are the main involved effects.
Little is known about the corrosion process in the presence of knee prostheses. Aim of our study was to analyze the serum levels of chromium (Cr), cobalt (Co), molybdenum (Mo), nickel (Ni), aluminum (Al), titanium (Ti) and vanadium (V), in a group of patients with failed total knee arthroplasty (TKA).

METHODS

A consecutive series of 33 individuals (7 M; 26 F) who underwent total knee arthroplasty (TKA) and showed clinical-radiological signs of loosening was enrolled in the study**.** Implants with at least a CoCrMo component and a TiAlV one were studied.
Results were compared with serum ions levels of 41 healthy donors (34 M; 7 F)
Serum samples were analyzed by grafite furnace atomic absorption spectrometry (GFAAS) to detect Ti, Al, V, Co, Cr and Mo concentrations in relation to their presence in the implant alloy. Each sample was analyzed in triplicate and the resulting levels of metal ions (ng/ml) were expressed as mean±SE, and min-max range.

Table 1. GFAAS parameters.

Step	*Chromium*			*Cobalt*			*Molybdenum*		
	Temp (°C)	Time (s)	Ramp (°C/s)	Temp. (°C)	Time (s)	Ramp (°C/s)	Temp (°C)	Time (s)	Ramp (°C/s)
1	90	60.0	10	90	55	10	90	20.0	10
2	110	20.0	1	150	20	1	110	30.0	1
3	480	20.0	50	480	10	50	480	20.0	50
4	1200	20.0	50	1800	25	50	1200	20.0	250
5	2500	3.0	0	2750	3	0	2100	3.0	0
6	2700	3.0	0	2800	5	0	2700	3.0	0
	λ=357.9 nm BC:Zeeman			λ=240.7 BC: deuterium			λ= 313.3 nm BC: Zeeman		
Step	*Titanium*			*Aluminium*			*Vanadium*		
	Temp (°C)	Time (s)	Ramp (°C/s)	Temp. (°C)	Time (s)	Ramp (°C/s)	Temp (°C)	Time (s)	Ramp (°C/s)
1	90	40.0	10	90	60.0	10	90	50.0	10
2	150	30.0	5	150	15.0	5	140	20.0	3
3	480	20.0	50	480	15.0	10	480	10.0	50
4	700	10.0	100	1500	15.0	100	1200	20.0	50
5	1600	5.0	100	2400	3.0	0	2750	3.0	0
6	2800	3.0	0	2800	5.0	0	2800	3.0	0
7	2900	5.0	0	2800	2.0	0			
	λ= 365.4 nm BC: Zeeman			λ=396.2 nm BC: Zeeman			λ= 318.5 nm BC: Zeeman		

BC=Background Correction

Osteoarthritis was the most frequent disease that led to joint replacement (81%).
Specific differences between groups were evaluated by the Student's *t* test.
The correlation between ion values, and between ion values and follow-up/age was calculated using the Fisher's correlation test.
The Bonferroni–Dunn's multiple comparison test was applied to detect specific gender differences.
In all analyses only the P values less than 0.05 were considered as statistically significant.
Data were analyzed with the StatView 5.0.1.0 software (SAS Institute Inc.).

RESULTS

Results are reported in Table 2.
Loosened implants showed a significant increase in the serum levels of Cr and Co; on the contrary, Mo, Ti, Al and V concentrations did not show a significant variation.
A significant correlation was found between Cr and Co values ($P<0.0001$), whereas follow up and age of the patients were not correlated with the release.
Neither gender or the presence of a controlateral implant did induce any significant difference.

Table 2. Ion values expressed as ng/ml (m±SE, and min-max range)

	Cr	*Co*	*Mo*	*Ti*	*Al*	*V*
TKA	0.42±0.05* 0.06-1.44	1.18±0.44* 0.08-8.80	1.06±0.08 0.83-2.25	3.12±0.17 2.91-6.43	2.83±0.40 1.36-8.99	2.28±0.03 2.22-2.87
Ctls	0.24±0.03 0.06-0.50	0.26±0.02 0.08-0.58	0.83±0.00 0.83-0.83	3.45±0.28 2.91-8.80	3.51±0.38 1.36-7.39	2.22±0.00 2.22-2.22

**p<0.05 vs controls*

DISCUSSION

In the presence of loosened knee implants, a corrosion process leading to increased cobalt and chromium release was observed.
Such process is probably due to mechanical dysfunctions of the device and joint micromovements, which induce an accelerated component wear. A concurrent sub-clinical infection could accelerate the corrosion process.
For this reason, ion serum level analysis could be proposed as a marker of failure in total knee replacements.
Moreover, limited data are available about the long-time 'endogenous' metal exposure resulting from stable knee prostheses: such exposure could give rise to adverse health effects related to various organs or tissues, as well as mutagenic and carcinogenic effects.

CONCLUSION

Ion profile would be carefully monitored in a significant number of patients with failed and stable implants, and the epidemiological survey implemented, in order to evaluate any potential risk due to Cr and Co release, and to establish the tolerance values, especially in younger subjects, where a long-term 'endogenous' exposure has to be faced.

REGISTER OF HIP PROSTHESIS IN THE REGION EMILIA-ROMAGNA: A FIVE YEAR EXPERIENCE.

*Bordini B, *Stea S, *De Clerico M, *°Toni A
*Laboratory for Medical Technology, Istituti Ortopedici Rizzoli, Bologna, Italy

bordini@tecno.ior.it

INTRODUCTION

On the basis of the benefits obtained by the Scandinavian arthroplasty registers, a similar local register was set up in the Emilia-Romagna region, in the north of Italy. It was started up on 1st January 2000, first regional register in our country; it collects data on primary total hip replacements, hemiarthroplasties and revisions, performed both in public and in private hospitals. All previous attempts to establish voluntary registers failed due to very low adhesion of surgeons, that is the reason why local health authorities decided to force the adhesion by linking the reimbursement of the DRG (Diagnosis Related Groups) to the participation in the Register.

METHODS

The recording of data is done for each operation by the surgeon. A form is completed in with identification of the patient (name, surname, date and place of birth, region of residence), information about diagnosis or reason for re-operation, weight and height, side, surgical approach, antibiotic and anti-thromboembolic prophylaxis, blood transfusions, use of bone grafts, perioperative complications. Cup, stem, head and liners are separately registered, using stickers with catalogue numbers provided by the manufacturers. Batches are also recorded.
Revision of at least one component is used as an end-point in all the analyses. Lifetime of primary prosthesis ends at time of prosthesis removal. Lifetime of revision prosthesis starts from the date of implant. Survival analysis is done following Kaplan Maier method.
The Oracle database is set at CINECA (Inter-University Calculation Centre in Bologna). The transmission of data via web is encrypted to ensure privacy (http://ripo.cineca.it).

REULTS

Adhesion rate to R.I.P.O. reached 93% of all surgeries.
Cumulative survival rate at five years is 97.4% for THA, 98.0% for hemiarthroplasties and 93.4% for total revision.

DISCUSSION

Survival rate at five years in Emilia-romagna region for THA is comparable to the Swedish one (98.5%) and the Danish (97.2). No comparison can be done for hemiartroplasties and total revision because no other register collects this data. Revision is a too crude endpoint, but we do agree with the decision of the Scandinavian registers as it would be practically impossible to choose other parameters, such as clinical data or X-ray findings and make all surgeon report with the same score.
The major problems in managing of the R.I.P.O. are quality of data and costs, which are partially connected to each other. Maintaining a detailed and accurate database is a costly proposition. Up to now cost of the R.I.P.O. has been covered by funds of the Institute Rizzoli and public grants; each registered operation roughly costs 18 € compared to 19 € in the Norwegian register.
Main targets of a register have already been reached and others will be got as soon as follow-up will increase. At present time the register is providing feedback to surgeons and to the local health authorities on the early performance of implants and it has already facilitated identification of individual patients who have received an implant in case of urgent clinical review (zirconia balls and Hylamer components).

ACKNOWLEDGEMENTS:

The Emilia-Romagna Department of Health has partially funded the regional register.

AFFILIATED INSTITUTIONS FOR CO-AUTHORS:

°1st Orthopaedic Department, Istituti Ortopedici Rizzoli,

A RANDOMISED PROSPECTIVE TRIAL COMPARING CERAMIC ON CERAMIC VERSUS METAL ON POLYETHYLENE BEARINGS IN THR

*Bucher TA, Cottam HL, Apthorp HD, Butler-Manuel PA
*The Conquest Orthopaedic Research Unit, Hastings, UK

howie@doctors.org.uk

INTRODUCTION

Polyethylene wear is the major cause of long term failure in total hip replacement. Recent improvements in polyethylene manufacture and cup design will hopefully result in increased longevity of metal on polyethylene bearings. Ceramic bearings with low frictional properties have been available for many years but brittleness and unacceptable fracture rates have prevented widespread use. Modern ceramic bearings have hopefully addressed this problem. This randomized prospective study compares the outcome of metal on polyethylene versus ceramic on ceramic bearings using the most up-to-date materials.

METHODS

Patients under the age of 72 undergoing primary total hip replacement received an uncemented proximally coated HA stem and an HA coated press fit cup. The patients were prospectively randomized to receive either a metal head with a polyethylene liner or an Alumina ceramic head with an Alumina ceramic liner. The patients were assessed pre-operatively and reviewed at 6 weeks, 6 months and yearly in a research clinic. Outcome measures were the Merle D'Aubignon Postel, Oxford Hip and Visual analogue pain scores. The implants were assessed radiographically and all complications were recorded.

RESULTS

To date 200 patients have been recruited. 110 patients have reached two year follow up. There were no differences in the mean satisfaction, pain or hip scores between the two groups. There were two revisions (aseptic loosening of the femoral components) and two dislocations in the ceramic group. There were two wound infections and one intra-operative metaphyseal fracture in the metal on polyethylene group.

DISCUSSION

We would not have expected any failures due to wear of the polyethylene bearing at this stage but our early results show no ceramic fractures which is encouraging. The dislocation rate within the ceramic group is not statistically significant but may be explained by the lack of hooded ceramic bearings.

A RANDOMISED PROSPECTIVE TRIAL COMPARING METHODS OF ACETABULAR IMPLANT FIXATION IN PRIMARY TOTAL HIP REPLACEMENT: EARLY RESULTS

*Bucher TA, Cottam HL, Apthorp HD, Butler-Manuel PA
*The Conquest Orthopaedic Research Unit, Hastings, UK

howie@doctors.org.uk

INTRODUCTION

Acetabular loosening can limit long-term success of total hip replacement. There are at least 62 different prosthesis designs available in the UK, many of which have no long term results. Revision surgery is expensive, challenging and potentially dangerous. There is still currently debate about the best method of acetabular fixation, in particular, regarding the use of press fit devices in elderly osteoporotic bone. Our study aims to test the null hypothesis that there is no significant difference in outcome between cemented and non-cemented acetabular fixation in this group of patients.

METHODS

Patients over 72 years of age were prospectively randomised to receive either a cemented Exeter cup or a HA coated press fit cementless cup. Both groups received a cemented Exeter stem. The patients were assessed pre-operatively and reviewed at 6 weeks, 6 months and yearly in a research clinic, by an independent observer. Outcome measures were the Merle D'Aubignon Postel, Oxford Hip and Visual analogue pain scores. The implants were also assessed radiographically and all complications were recorded.

RESULTS

To date 151 patients have been recruited into the trial. 2 year data is available for 69 patients. There were no differences in satisfaction, pain or hip scores between the groups.

There have been no major surgical complications. In particular, there have been no failures of acetabular fixation, dislocations or deep infections.

DISCUSSION

There have been no failures in either group. Although there is insufficient data at this stage to reject our null hypothesis, there is no early evidence for concern in using cementless cups in elderly patients.

THE USE OF THE ULTRASONIC SCALPEL IN MINIMALLY INVASIVE TOTAL HIP REPLACEMENT

*Chettiar K, *David L, *Worth R, Apthorp H
Conquest Hospital, Hastings, United Kingdom

Krissenchettiar@hotmail.com

INTRODUCTION

High-frequency ultrasound is an effective mechanism for coagulating and cutting tissue. We report the first use of the ultrasonic scalpel in orthopaedic surgery, with the aim of minimising blood loss and tissue trauma in minimally invasive total hip replacement.

METHODS

This is a prospective, single-blind, case-matched study to compare blood loss in minimally invasive total hip replacement using an ultrasonic scalpel versus electrodiathermy. Twenty cases have been performed via a minimally invasive posterior approach. The treatment was otherwise no different between the two groups. The groups were compared with regard to blood loss, post-operative pain and wound healing.

RESULTS

The mean intraoperative blood loss in the ultrasonic scalpel group was 242mls compared with 319mls in the electrodiathermy group. This is statistically significant ($p < 0.05$). The percentage drop in Haemoglobin was also reduced in the ultrasonic scalpel group (18.9% compared with 26.4%), which is also statistically significant ($P< 0.01$). There was no significant difference in the operating time or post-operative pain scores and there were no wound complications in either group.

DISCUSSION

The **ultrasonic scalpel** works by converting electrical energy into mechanical energy resulting in longitudinal oscillation of the blade
at 55,500Hz. This achieves coagulation and tissue dissection at lower temperatures than standard diathermy. The potential advantages include less lateral tissue damage, minimal smoke and no electrical energy passed to or through the patient. With the development of minimally invasive hip replacement surgery this technique can be used to reduce tissue trauma. The initial results from this study suggest that the ultrasonic scalpel has a useful role in minimally invasive hip replacement surgery in terms of reducing blood loss and tissue trauma. This may help to facilitate early mobilisation and reduced hospital stay.

OVERNIGHT HOSPITAL STAY FOR MINIMALLY INVASIVE BILATERAL TOTAL HIP REPLACEMENTS

*Chettiar K, *Findlay I, *Apthorp H
Conquest Hospital, Hastings, United Kingdom

Krissenchettiar@hotmail.com

INTRODUCTION

We describe the first report of a patient being discharged directly home 23 hours after bilateral total hip replacements (THRs). A 58 year old gentleman had suffered from progressively severe pain in both hips for several years, with a diagnosis of osteoarthritis.

METHOD

A direct anterior, minimally-invasive approach was used which avoided detachment of hip musculature. Pre-operative assessment was carried out, with early multi-disciplinary team input. Modified anaesthetic techniques with an ambulatory pain pump were employed. Follow-up in the community was carried out by an outreach team. All these factors were important in a successful early supported discharge. We believe this to be the first such case reported.

All his other joints were pain-free. Clinically both hips were stiff and irritable. Internal and external rotation were extremely limited, with flexion of only 70° bilaterally. He was enrolled onto the Short Stay Hip Replacement Programme, consisting of extensive pre-operative education and physiotherapy, including the use of crutches. The principles of the programme were discussed with the patient at this point.

The THRs were performed using minimally-invasive surgical techniques. A direct anterior approach was used on both sides with the patient in the lateral position. Tissue dissection was performed with a harmonic scalpel (Ethicon Endosurgery). Hydroxyapatite-coated ABG II prostheses were inserted (Stryker Howmedica) with ceramic-on-ceramic bearing surfaces. Appropriate minimally- invasive equipment was used, including an offset acetabular reamer and introducer. An ambulatory pain pump infiltrating the wounds with bupivicaine was left

in situ for 48 hours (Stryker Howmedica). Incision length was 9cm on both legs. Operative time was 2 hrs 45 mins in total. Peri-operative blood loss was 240mls, with an overnight haemoglobin drop of 2.0 g/dl.

Post-operatively he was mobilised 4 hours after surgery, weight-bearing as tolerated. By the following morning he was comfortable on below elbow crutches. Implant position was assessed radiographically (Figure 1). Pain scores were no greater than 1 out of 10 throughout. 23 hours post surgery, he had fulfilled all of our discharge criteria and was allowed home.

He was reviewed in the community on days 2 and 4 by a senior orthopaedic nurse and at one week by a physiotherapist as part of the short stay programme team. After 2 days he was walking unaided for short distances.

At his six week review clinic review his Merle D'Aubigne Postel score was 18, his Oxford Hip score was 12 and Visual Analogue pain scores were 0/10.

DISCUSSION

Currently, minimally-invasive hip surgery has been met with both enthusiasm and concern amongst the orthopaedic community (2). Previous studies have shown a reduced length of hospital stay using this minimally-invasive technique for unilateral THRs (3,4). The direct anterior approach used minimises tissue trauma. Deep dissection to the joint utilises the plane between sartorius and tensor fascia lata, followed by an anterior capsulectomy. No muscle fibres are detached. It is noted that incision length is decreased compared to conventional THRs (5). However, we believe that the emphasis preservation of the musculature is the principle surgical factor leading to early mobilisation. The short-stay programme has been successfully used in our hospital to achieve overnight stay for over 40 unilateral THRs.

RELATIONSHIP BETWEEN BIOMETRIC CHARACTERISTICS AND STEM SIZE OF CEMENTLESS HIP PROSTHESES

*De Clerico M, *B. Bordini, *S. Stea, *Viceconti M*°, Toni A
*Laboratory for Medical Technology, Istituti Ortopedici Rizzoli, Bologna, Italy

declerico@tecno.ior.it

INTRODUCTION

Total hip prosthesis is composed of an acetabular and a femoral component. Both components are fixed to the bone by means of bone cement or by direct press-fit into reamed bone. The design of the stem is crucial for the outcome of the uncemented fixation, because primary stabilization is obtained only through congruity of the endosteal and prosthesis surfaces. This can be achieved only when critical dimensions of the stem match the corresponding size of the femoral canal.

METHODS

The authors examined 2329 uncemented hip prosthesis stems, ANCA fit (Wright Medical Technology, Arlington, TN, USA) implanted between 1996 and 2004 due to primary coxarthrosis. This is the most commonly used stem in the Emilia-Romagna region, in northern Italy, according to data of RIPO (Register of orthopedic prostheses). It is produced in 8 sizes for each side. Measures of the different sizes are illustrated in Fig 1.

Fig. 1 The different sizes of the AncaFit stem

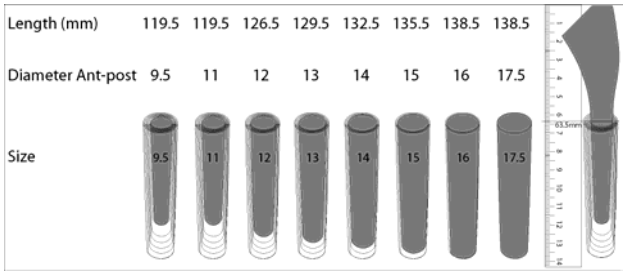

We analyzed the relationship between stem size and anthropometric data. 49.5% of the patients were men and 50.5% were women; mean age at surgery was 64.1 years (SD 9.1), mean height was 167 cm (SD 8.4), and mean weight was 75.7 kg (SD 12.7).

RESULTS

Multifactorial analysis demonstrated that stem size is influenced by sex, age, and height, but not by weight. Besides this, there was an interaction between sex and age: in women, but not in men, the stem size increased with ageing.

To understand the interaction between age and sex the mean stem size implanted in men and women according to class of age and height was calculated. It resulted that only in women, for each height class, there was an increase in size with the increase in age.

DISCUSSION

This study might influence the design of cementless prostheses used on old patients. In fact, it is likely that the increased size of the endosteal canal, indicated by the choice of larger implants in elderly women, corresponds to an overall different femur morphology, which might benefit from prostheses with customized stems.

ACKNOWLEDGEMENTS:
The Orthopedic Units of RIPO (Register of orthopedic prostheses).

AFFILIATED INSTITUTIONS FOR CO-AUTHORS:
°1st Orthopaedic Department , Istituti Ortopedici Rizzoli, Bologna, Italy

A TANTALUM MONOBLOCK POROUS CUP AND ACETABULAR REPLACEMENT A FIVE YEAR FOLLOW-UP STUDY

Fadda M, Zirattu G, Zirattu F, Tranquilli Leali P
Orthopaedic Dpt., University of Sassari, Italy

mfadda@uniss.it

INTRODUCTION

Trabecular metal associated with monoblock elliptical design represent a valid surgical solution for orthopaedic acetabular reconstructive procedures and second surgery. We report our clinical results to determine the way of fixation of the trabecular metal (porous tantalum). .

MATERIAL AND METHODS

From 1999 to 2005, 67 patients between 45 and 81 years cementless trabecular metal elliptical cup implantation were performed. The following pre-po diagnosis was oteoarthritis (60), osteonecrosis (7). Clinical evaluation through Harris Hip Scoretest. Bone-implant interface was studied through radiography with reference to three Charnley's areas. Follow-up (ranging 2 to 5 years) were performed preoperatively, at six months and yearly thereafter.

RESULTS

Clinical results showed high improvement of H.H.S (average score before surgery 46, after surgery 90) .Radiography revealeed bone apposition to the porous tantalum toward all the perifhery of the interface withaut radioluncencies. No local (osteolysis) or general (DVT) complications was seen.

CONCLUSIONS

Tantalum monoblock elliptical cup with high volumetric porosity,flexibility and high biocompatibility associated with particular microstructure permits direct apposition of bone more extensive osseointegration with the maximum bone contact. The trabecular metal cup increases the initial stability helping in the prevention of osteolysis and loosening.

WEAR PARTICLES IN FAILED TOTAL HIP REPLACEMENTS MADE OF Ti ALLOY

*, **Figurska M, ***Milošev I, ****Cör A
Polish Academy of Science, Warsaw, Poland

mfigur@ippt.gov.pl

INTRODUCTION

Wear particles produced during the articulation of artificial joints contribute to aseptic loosening. The biomaterials used to manufacture the artificial joints have different wear rate and liberate particles of different size, which have different biological reactivity. The aim of this study was to compare the histological response and types of wear particles prevalent in fibrous periprosthetic tissues from two groups of total hip replacements. The femoral component in both groups was cemented self-locking (SL) stem made of Ti_6Al_4V alloy, and the acetabular component was polyethylene cup. The two groups differ in the material of femoral head, which was either metal (stainless steel, AISI 316L) or ceramic (Al_2O_3).

METHODS

Periprosthetic tissue specimes were collected at revision surgery. Some specimens were frozen and some were fixed in buffered formalin and embedded in paraffin. 5 µm thick paraffin sections were stained with hematoxylin and eosin. Oil-o-red staining was used for polyethylene particles visualization in cytoplasm of macrophages and in giant cells.

The tissues slides were examined under standard and polarized light microscope (E80i, Nikon).

The modified version of the Mirra classification[1] was used to estimate number of metal and PMMA particles, number of giant cells and also acute and chronic inflammatory cells, as well as areas of necrosis and necrobiosis.

Frozen tissues samples were used for isolation of wear particles. Tissue was shaken overnight on the shaker in the mixture of chloroform and methanol (2:1) to extract lipids and then digested in 5M sodium hydroxide for 4 h in 65°C. The digest was than centrifuged (1 h 6 000 rpm) with 5 % sucrose. Metal, cement and ceramics particles which are present in the bottom layer are washed with distilled water and collected.

The upper dense layer which contains polyethylene particles was collected and hydrolyzed for 1 h in 80°C and than centrifuged with isopropanol (1 h 6 000 rpm). Polyethylene particles form thin white band on the top.

RESULTS

No significant difference in cellular reaction between the two groups was found. However, there was a major difference in size and composition of particles isolated from tissues.

In the group with metal femoral heads we isolated all possible particles in the periprosthetic tissue – stainless steel, titanium, bone cement (PMMA) and polyethylene particles. Whereas metal particles were usually agglomerated micron-sized flakes, polyethylene particles appeared in different sizes and shapes: (i) large, several tens of micrometer, elongated particles, (ii) small, micrometer-sized, elongated particles and (iii) sub micrometer-sized round particles. In contrast, in the group with ceramic femoral head only PMMA particles and sub micrometer-sized round particles of polyethylene were isolated. We could not identify ceramic particles, although the presence of the related elements, Al and O, was evidenced in EDS spectra. Ceramic particles are presumably too small to be detected by the method used in the present work.

DISCUSSION

Variety in shape and composition of different wear debris particles present in the periprosthetic tissue of the group with metal heads would suggest a more complex inflammatory response and maybe even accelerated process of aseptic loosening. Our study shows, however, that tissues retrieved from titanium alloy stem combined with ceramic head exhibit similar histological response as the former group. This observation may imply that a diversity of particles involved in the wear process does not necessarily mean a more intense inflammatory response, and that large number of smaller, less diverse, particles, evoke similar reaction.

REFERENCES

1. P.F. Doorn, J.M., Mirra, P.A. Campbell and H.C. Amstutz. Tissue reaction to metal on metal total hip prostheses. Clin. Orthop. Relat. Research. 329S: S187 – S205, 1996.

AFFILIATED INSTITUTIONS FOR CO-AUTHORS:

**Jožef Stefan Institute, Ljubljana, Slovenia
ingrid.milosev@ijs.si
*** Orthopaedic Hospital Valdoltra, Ankaran, Slovenia
**** University of Ljubljana, Faculty of Medicine, Institute of Histology and Embriology, Ljubljana, Slovenia
andrej.coer@MF.UNI-LJ.SI

PREDICTING THE NEED FOR URINARY CATHETERISATION FOLLOWING LOWER LIMB TOTAL JOINT ARTHROPLASTY. USE OF PATIENT QUESTIONAIRRES

*Fox A, Board TN
Blackburn Royal Infirmary, Balckburn, UK

boardtim@hotmail.com

INTRODUCTION

Acute urinary retention requiring catheterisation following lower limb arthroplasty is associated with an increased risk of deep sepsis in the arthroplasty. It is also unpleasant for patients and can lead to permanent bladder dysfunction. In order to identify factors that may be predictive of retention we performed a prospective study of 180 consecutive patients undergoing hip or knee arthroplasty.

METHODS

Patients completed a preoperative urinary symptom score (International Prostate Symptom Severity score for males and a modified King's Health Questionnaire for females). Data regarding all aspects of the surgery and post-operative care was recorded. Statistical analysis was performed using SPSS.

RESULTS

Ninety one patients (60%) consented to complete preoperative urinary symptom scoring. In our study population there were 83 male and 68 female patients with mean age 67. The overall rate of retention was 28.5% (95% CI 22-36%). The factors significantly associated with an increased likelihood of urinary retention were increasing age, BMI closer to the normal range, a previous history of post-operative retention and the use of spinal anaesthesia. The incidence of retention in patients receiving spinal anaesthesia was 33% and 17% in those receiving general anaesthesia ($p=0.04$). Although single dose bupivacaine and diamorphine spinal anaesthesia increased the risk of retention, the quantities of these drugs given did not appear to influence its development. Preoperative urinary symptom scores in both male and female patients showed a trend towards higher values in catheterised patient but this was not statistically significant (median scores for catheterised males:4.5 uncatheterised males 3, median scores for catheterised females:3 uncatheterised females 2).

DISCUSSION

It was not possible to develop a useful preoperative predictive scoring system for postoperative retention indicating that the development of urinary retention in this setting is multifactorial. In conclusion, the development of urinary retention following arthroplasty is a complex event that can not be predicted on the basis of urinary symptom scoring.

BIRMINGHAM HIP RESURFACING IN A PATIENT WITH TAY SYNDROME

Katipalli G, Ganapathi M, Woodnutt D
Morriston Hospital, Swansea, UK

katipalligopi@aol.com

INTRODUCTION

Tay syndrome is a hereditary disorder characterised by trichothiodystrophy (sulphur-deficient brittle hair) with photosensitivity, ichthyosiform erythroderma, progeria-like facies, growth and mental retardation and occasional infertility. Other associated features include osteosclerosis, muscular spasticity, and hip dysplasia. The use of hip replacement to rehabilitate such particularly small patients has not been previously described in the literature.

MATERIALS AND METHODS

We present the use of a custom made prosthesis (Birmingham Hip Resurfacing) in a 19-year old woman with Tay syndrome with a painful arthritic hip. She was 4ft 2inch in height and weighed 3stone 7lb. Radiologically, she had subluxed, degenerate hip with a very narrow medullary canal and noticeable thickening of cortices.

RESULTS

The preoperative Harris Hip Score was 33.6 which improved to 91.8 postoperatively Conventional endo-femoral hip replacement would have been difficult due to her small skeleton and would not have addressed the problem of her inevitable revision. This was overcome by using a custom made prosthesis (Birmingham Hip Resurfacing, 38mm Femoral component with a shorter stem and 44mm Acetabular cup).

FAILURE OF THE UNCOATED TITANIUM PROXILOCK™ FEMORAL HIP PROSTHESIS

*Luites J, **Spruit M, **Hellemondt GV, **Horstmann W, ***Valstar E
Sint Maartenskliniek Research, Development & Education, OrthoResearch Unit, Nijmegen, The Netherlands

j.luites@maartenskliniek.nl

INTRODUCTION

The 10-year survival of uncemented femoral prostheses in total hip arthroplasty (THA) increased from 56.9% in 1989 to 87.7% in 2000.[1] Still, uncemented prostheses have worse results relative to modern cemented techniques (94.8%). New stem designs ostensibly improve the clinical outcome. However, failures occur [2]. Therefore fast and adequate judgment of new designed prostheses is necessary.

Aseptic loosening of the femoral component is one of the main reasons for revision. [1] Early migration predicts future aseptic loosening. With radiostereometric analysis (RSA) the three-dimensional migration of prostheses can be assessed accurately. The relation between short-term results of RSA and future loosening [3] illustrates that it is an ideal method to ascertain early stability of new implants within a short followup period.

The ProxiLock™ (STRATEC Medical, Oberdorf, Switzerland) femoral component is claimed to achieve better proximal fixation through a double wedge design and retention of a large medial segment of the femoral neck. Special coatings contribute to better fixation of the prosthesis. The ProxiLock™ stem is a grid-blasted titanium alloy and available with hydroxyapatite (HA) coating. Generally, HA seems to have a positive effect on stability of uncemented femoral components, although reported results are varying.

The questions adressed in this study are: (1) What is the migration pattern of the ProxiLock™ stem during the first 24 months? (2) Has the HA-coating an additional effect to the fixation process? (3) Is the design sufficient to guarantee stability and good clinical performance?

METHODS

In a prospective randomized clinical trial 22 titanium (Ti) and 20 hydroxyapatite coated (HA) ProxiLock™ femoral hip prostheses were implanted during THA after primary (36 patients) or secondary (6 patients, 5 dysplasia and 1 femoral head necrosis) osteoarthritis. One patient (Ti stem) was lost to follow up. An immediate postoperative full weight bearing protocol was applied. The patients (35–77 years) were followed for 24 months with clinical, radiological and radiostereometric analysis. The RSA precision, determined by the 99% confidence interval of double examinations in all patients, was 0.3 mm (x), 0.2 mm (y), 0.4 mm (z) and 0.8° (x), 0.9° (y) and 0.3° (z).

Statistic analyses were performed using the Wilcoxon signed rank sum test and the Mann–Whitney U test (two sided, $P<0.05$), to detect differences within and between the groups. Approval of the medical ethics committee and patient's consent were obtained.

RESULTS

During the first two months 16/21 Ti and 18/20 HA stems subsided (max 3.9 mm) and/or rotated towards retroversion (max 9.2°) more than the detection limit. No difference ($P>0.05$) was seen between the coated and uncoated stems.

After 24 months 4 Ti stems were revised. The patients had clinical complaints and large migrations with maximums of 4.9 mm translation and 11.0° retroversion. Two Ti stems showed continuous retroversion (13.5° and 5.9°). The patients had no clinical complaints, but will be closely followed. Four Ti stems showed continuous migration with maximums of 0.5 mm subsidence and 1.1° retroversion in the second year. Eleven Ti stems were well fixed, as were 16 of the 20 HA stems. Four HA stems showed continuous migration in the second year with maximums of 0.4 mm dorsal translation and 0.7° retroversion.

Harris Hip scores (from 60 to 98) and VAS-pain scores (from 58 to 2) were significantly improved ($P<0.05$) at the 24-month follow up in both groups.

DISCUSSION

It appears to be difficult to achieve primary fixation of the ProxiLock™ femoral hip prosthesis during surgery. The initial press-fit position is not sufficient to allow immediate full weight bearing, which is demonstrated by the migration pattern after two months.

However, stems become stable and hydroxyapatite seems to be a contributing factor to achieve earlier fixation after the initial settling period.

Although most uncoated stems stabilize, 4 revisions and 2 continuous migrating stems demonstrate an unacceptable failure rate. Therefore we conclude that the design is not sufficient for good clinical performance.

REFERENCES:

1. Malchau et al. (2002) JBJS [AM] 84-A: 2-20.
2. Snorrason et al. (1989) AOS 60 : 81-85.
3. Kärrholm and Snorrason (1993) CORR 287: 50-60.

ACKNOWLEDGEMENTS:

We thank dr. P.W. Pavlov and dr. B.A. Swierstra for their contributions to the study.

AFFILIATED INSTITUTIONS FOR CO-AUTHORS:

**Sint Maartenskliniek, Department of Orthopaedics, Nijmegen, The Netherlands.
***Leiden University Medical Centre, Department of Orthopaedics and Delft University of Technology, Department of Biomechanics, The Netherlands.

METAL ION RELEASE FROM FRACTURE FIXATION DEVICES

*Maci G, *Savarino L, *Ferrara T, *Bochicchio V, *Greco M, *Baldini N, *Giunti A
*Laboratorio di Fisiopatologia Ortopedica & 7^ Divisione, Istituti Ortopedici Rizzoli, Bologna, Italy

gaetanomaci@yahoo.it

INTRODUCTION

Stainless steel is the most frequently used material in internal fixation because of its mechanical strength, low costs, and the possibility of bending and shaping the implant to create a custom fit in the operating room.
However, major disadvantages of stainless steel are well-documented: surface corrosion phenomena and the high rate of locally and systemically released corrosion products.
Ion serum levels reflect the systemic distribution, so the aim of this study was to analyze the release of nickel (Ni) and chromium (Cr) in patients with stainless steel fracture fixation devices.

METHODS

Thirty-seven patients treated with stainless steel osteosyntheses (19 intramedullary nails and 18 plates) with a median 15-month followup were recruited for this study. Patients with smaller size implants, with external fixation and patient with others metal implants were excluded from the study. Serum samples were analyzed for Cr and Ni content using a graphite furnace atomic absorption spectrometer (GFAAS), equipped with double background correction Deuterium/Zeeman (Unicam Solaar 939 QZ, Cambridge, UK). Furnace thermal programs and spectrometer parameters are reported in Table 1. Results were compared with levels of 50 healthy donors. Serum ion concentrations (ng/ml) were reported as mean±standard error (m±SE), min-max range and median value. Specific differences between groups were evaluated by the Mann-Whitney U test.
The correlation between Cr and Ni and between ion values and follow-up, as well as between ion values and age of patients, was calculated (Spearman's correlation test). Only the *P* values less than 0.05 were considered as statistically significant. Data were analyzed by using the StatView 5.0.1.0 (SAS Institute Inc.).

Table 1. GFAAS parameters.

	Chromium			*Nickel*		
Step	Temp °C	Time (s)	Ramp °C/s	Temp °C	Time (s)	Ramp °C/s
1	90	60.0	10	90	20.0	10
2	110	20.0	1	110	30.0	1
3	480	20.0	50	480	20.0	50
4	1200	20.0	50	1200	20.0	250
5 RD	2500	3.0	0	2100	3.0	0
6	2700	3.0	0	2700	3.0	0
	λ=357.9 nm BC=Zeeman			λ=232.0 nm BC=Deuterium		

RD= read BC= background correction

RESULTS

As reported in Table 2, a significant increase of Cr values was observed in patients in comparison with control subjects, whereas Ni concentration did not show any statistical difference between the groups.
Nevertheless, a significant positive correlation between Cr and Ni values was observed in patients, by applying the Spearman's r coefficient (r= 0.55; p=0.001).
No correlation was found between ion concentrations and age of the patients, expressed as years, as well as between ion values and followup, expressed as months.

Table 2: Cr and Ni concentrations, expressed as ng/ml.

	Controls	Patients	P value
Chromium			
m±se	0.19±0.03	0.47±0.09	
(median value)	(0.09)	(0.30)	*0.01*
min-max range	0.06-0.56	0.06-2.80	
Nickel			
m±se	0.73±0.07	0.84±0.17	
(median value)	(0.74)	(0.54)	n.s.
min-max range	0.10-1.69	0.10-5.40	

DISCUSSION

In this study, an irrilevant increase of Ni serum concentration was observed, probably because it is rapidly transported to the urine and eliminated from the body; consequently, it was not considered to be a concern in the biological response to fracture fixation devices.
On the contrary, substantially higher concentrations of chromium were found, as compared with controls.
Corrosion in implants may originate from different processes such as electrochemical dissolution, wear, or a combination of both. Controversial data are reported about chromium effects; however, in excessive amounts, Cr ions are potentially toxic through: 1) metabolic alterations; 2) immunologic interactions of metal moieties by virtue of their ability to act as haptens (specific immunologic activation) or antichemotactic agents (nonspecific immunologic suppression). Moreover, hexavalent Cr is a recognized class-I human carcinogen (International Agency for Research on Cancer).

CONCLUSION

In conclusion, a corrosion process, leading to Cr release in stainless steel fracture fixation devices, is present. For this reason, ion profile would be carefully monitored in the medium- and long-term, as well as other biochemical markers, in order to establish if a correlation exists between serum metal concentrations and adverse health effects, even if no radiographic and clinical alteration is observed. In any case, it could be appropriate to remove the implants which undergo preferential release of metal ions, as early as their function is accomplished.

SIMPLE TWO-DIMENSIONAL COMPUTER-ASSISTED TECHNIQUE FOR RADIOGRAPHIC ASSESSMENT OF POLYETHYLENE WEAR AFTER TOTAL HIP ARTHROPLASTY

*Sandoval MA, *Suarez-Vazquez A, *Fernandez-Lombardia J, ** Hernandez-Vaquero D
*Hospital St Agustin, Aviles & ** Faculty of Medicine, University of Oviedo, Spain

sandovalmag@yahoo.es

INTRODUCTION

In order to use a simple computer-assisted technique for clinical measurements of polyethylene wear in a specific Total Hip Arthroplasty (THA), we analysed the accuracy and precision in an experimental model.

METHODS

A modular polyethylene acetabular component of the Bihapro THA (Biomet Orthopaedics), retrieved in a revision surgery for accelerated wear, was coupled with its corresponding metal-backed and it was analysed in a coordinate measuring machine (CMM) for finding the standard measurement. Radiographs of the component placed in an acrylic model in a simulated pelvis AP projection were achieving and digitising (Epson GT-12000 A3 scanner) for making the computer model of the femoral head and the acetabular component for four times. With the circle drawing, radius obtained and distance tools of a computed-assisted drawn program (autoCAD) we could obtain radiographic wear vector. For each one of the five radiographs, the measurement was thirty times achieved.

RESULTS

Wear measurement in the CMM was 2,46 mm. Accuracy on the basis of the 95% confidence interval of the standard error was: A) -0.07 mm, B) -0.08 mm, C) -0.1 mm, D) +0.18 mm for each one of the four radiographs and the corresponding precision was: A) +/- 0,04 mm, B) +/- 0,04 mm, C) +/- 0,04 mm, D) +/- 0,06 mm. The worst results in the D group were agree with a bad definition as a circunference of the border of metal-backed acetabular component.

DISCUSSION

The accuracy and precision of this simple computer-assisted technique is on line with others computer-assisted techniques, but it is dependent of the radiographs quality. This concern is relevant in the clinical setting although utilizing sophisticated methods of measurement.

SERUM LEVELS OF OSTEOPROTEGERIN (OPG) AND 'RECEPTOR ACTIVATOR OF NUCLEAR FACTOR-K LIGAND' (RANKL) IN PATIENTS WITH TOTAL HIP PROSTHESES

Spina M, Pellacani A, Amato I, Baldini N, Giunti A, Granchi D
7^ Divisione & Laboratorio di Fisiopatologia Ortopedica, Istituti Ortopedici Rizzoli, Bologna, Italy

donatella.granchi@ior.it

INTRODUCTION

The pathogenesis of aseptic loosening of total hip arthroplasty (THA) appears to be strictly connected to bone loss around the implant. Two proteins play a pivotal role in the bone remodelling process: OPG has a powerful osteoclastogenesis-inhibiting action and acts as a decoy-receptor by binding to RANKL, which is an essential protein for differentiating and activating osteoclasts. According to their role in regulating formation and resorption of bony tissue, RANKL and OPG serum levels have been proposed as markers of bone remodeling in a variety of clinical conditions, however no studies have been performed to evaluate their clinical significance in patients undergoing THA. The purpose of this study was to investigate the association between the circulating levels of these molecules and periprosthetic osteolysis. In addition, we also evaluated the diagnostic performance and clinical usefulness of these markers.

METHODS

Serum levels of OPG and RANKL were determined by immunoenzymatic method. Blood samples from 128 subjects were collected: 39 had a severe osteoarthritis and were candidates for THA (Group A), 33 patients had a stable THA (Group B), and 36 patients showed clinical and radiographic evidence of aseptic loosening (Group C). The remaining 20 individuals were normal volunteers (healthy donors). THA were deemed stable when neither symptoms nor radiographic findings of osteolysis were evident, and were considered loosened when at least one component had to be replaced. The severity of osteolysis was evaluated following Gruen's criteria for femoral osteolysis[1], and 'DeLee and Charnley' criteria for periacetabular bone resorption.[2] The study design was approved by the institutional ethical committee on human research.

RESULTS

OPG was significantly higher in Group A and Group C than in healthy donors or in Group B. Serum levels of RANKL increased significantly in Group B, while the OPG-to-RANKL showed a significant decrease. The abnormal levels of OPG which were found in failed THA were unrelated to the type of bearing. A significant increase in RANKL serum level and a significant decrease in OPG-to-RANKL ratio were found in patients who had a stable ceramic-on-ceramic THA. OPG and RANKL levels were significantly increased in Group C patients with cemented implants. Since the alteration concerned both cytokines, no difference was found with regard to the OPG-to-RANKL ratio. The OPG serum level was significantly higher when both femoral stem and acetabulum were loosened (5692 ± 1999 pg/ml), in comparison with single component failure (3959 ± 1199 pg/ml, $P=0.03$), or the absence of osteolysis (2397 ± 1632 pg/ml, $P< 0.0001$). The total number of regions showing a radiographic bone loss was considered as an indicator of the extent of osteolysis. The sum of osteolytic areas detected in the femoral stem correlated with the RANKL serum level (R= 0.38, $P= 0.02$), and OPG-to-RANKL ratio (R= -0.29, P= 0.04), while no relationship between markers and periacetabular osteolysis emerged. The ROC analysis was performed to determine a cut-off value discriminating the presence of osteolysis. OPG showed a good performance (cut-off value 2296 pg/ml, sensitivity 91.7%, specificity 75%). Moreover the diagnostic accuracy was confirmed by the positive and negative likelihood ratios, which were 7.1 (95% CI 2.5-20.8) and 0.2 (95% CI 0.1-0.4), respectively, which means that in THA osteolysis is seven-fold more likely if OPG serum levels are higher than the threshold value.

DISCUSSION

Our results support the hypothesis that increased OPG serum level in patients with loosened THA represents an attempt to protect bone from excessive resorption. As an additional evidence regarding the association between OPG and periprosthetic osteolysis, the highest serum levels were found in patients who had radiological signs of loosening around both femoral stem and acetabulum. We calculated a threshold value of OPG that might distinguish stable or loosened THA.

REFERENCES:

1. Gruen TA, McNeice GM, Amstutz HC. Clin Orthop. 1979;141:17–27.
2. Delee JG, Charnley J.. Clin Orthop. 1976;121:20–32.

DIAGNOSTIC PROCEDURES WITH SUSPICION OF PERIPROSTHETIC INFECTION

Wendrich K, [2]Siegel E, [3]Hansen T, Drees P, Schöllner C, Eckardt A
[2] Department of Microbiology, University of Mainz
[3] Department of Histopathology, University of Mainz

kwendrich@gmx.de

INTRODUCTION

Loosening of hip and knee prostheses which must be operatively revised is a serious complication. The preoperative differentiation between septic and aseptic loosening is essential for an effective therapeutic process. Despite clinical, radiological suspicion of an infectious happening is often no microbiological bacterial evidence to be found. Gradual loosening of the prosthesis can be caused by very slow growing bacteria namely nutrition deficient streptococci (Abiotrophia species). They are found in Biofilm directly upon the prosthesis and can only by means of very extensive and long brooding methods proven to be present. The attached study should clarify the worth of this method as a complement to the usual diagnostic procedures.

PATIENTS AND METHODS

76 patients (median age 70 years old) who received either hip or knee prosthesis revisions between 04/2002 and 06/2004 were subjects of this study. Preoperatively the occurring clinical and laboratory inflammatory parameters were examined, a bone scan and joint puncture were also performed. The intraoperative taken tissue samples were analysed with the common microbiological procedures. The tissue biopsies were histologically prepared with respect to an inflammatory reaction.

RESULTS

In none of the cases were Abiotrophia proven to be evident. Bacterial evidence was found via puncture, via biopsy and upon the prosthesis in 16 of the 24 patients. The most commonly occurring bacteria were staphylococcus aureus. Of the 41 patients who had no clinical signs of infection 26 cases were found to be contaminated. Of these 26 cases 23 of the prosthesis were infected with coagulase negative streptococci (CNS). These findings were only evident by means of brooding the prosthesis and not via puncture, bacterial probe or biopsy. 24 of the 76 patients had neither clinical signs of infection or bacterial evidence. Such patients were then diagnosed with an aseptic prosthetic loosening.

CONCLUSION

The brooding of the prostheses of patients with clinical signs of infection demonstrated no additional bacterial evidence. Abiotrophia could in none of the cases be evidenced. The increased numbers of CNS, which were only evidenced upon the prostheses makes the suspicion of contamination strong. Because of these reasons in our opinion is an additional extensive analysis of the prosthesis not indicated.

TREATMENT OF SUPRACONDYLAR FEMORAL FRACTURES AROUND TOTAL KNEE REPLACEMENT WITH RETROGRADE INTRAMEDULLARY NAILING

*Chettiar K, *Jackson M, *Brewin J, *Dass D, *Miles K, *Butler-Manuel PA
Conquest Hospital, Hastings, UK

Krissenchettiar@hotmail.com

INTRODUCTION

Periprosthetic fractures are an infrequent but increasingly prevalent problem and can be technically difficult to manage. Various techniques have been described to manage periprosthetic supracondylar fractures around a Total Knee Replacement (TKR) including, immobilisation, plate fixation, rush rods, LISS (less invasive stabilisation system) and retrograde nailing. The aim of this retrospective study was to evaluate the effectiveness of the retrograde intramedullary nail.

METHODS

We identified all patients who underwent retrograde intramedullary nail for the treatment of periprosthetic femoral fractures between January 1999 and October 2005. Notes, x-rays and operation data were examined retrospectively. Outcomes were measured by radiological union, limb alignment, return to function, pain and complications.

RESULTS:

Of the 16 patients (17 knee replacements) 2 died of coexisting medical problems during the follow-up period, but both with good fracture alignment. 14 patients united between 12 – 24 weeks (mean 15 weeks), 13 regained pre-injury function with alignment good in 14. 13 were pain free at follow-up, 4 patients required non-steroidal analgesia intermittently. There was one delayed union (53 weeks). There was one post operative complication where a patient with bilateral fractures required one night stay on ITU.

CONCLUSION

Intramedullary nailing of periprosthetic fractures around a TKR gave excellent functional results and 100% union in this series.

TOTAL MENISCAL KNEE (TMK) - CLINICAL EVALUATION OF CEMENTED VERSUS HYDROXYAPATITE COATED PROSTHESES

* Cottam HL, James K, Jack C, Miles K, Apthorp HD, Butler-Manuel PA
*The Conquest Orthopaedic Research Unit, Hastings, UK

howie@doctors.org.uk

INTRODUCTION

To assess the clinical and radiological outcome of the Total Meniscal Knee (TMK Biomet) knee arthroplasty, using two different fixation techniques (a) cemented and (b) uncemented hydroxyapatite coated (HA).

METHODS

Since April 2001, patients under the age of seventy five years who required total knee arthroplasty for osteoarthritis or post-traumatic arthritis, under the care of the senior authors, were prospectively randomized to receive either a cemented or uncemented HA coated implant. Patients were scored pre-operatively and post-operatively at six weeks, six months, and yearly thereafter, using the Hospital for Special Surgery, the Oxford and the American Knee Society knee scoring systems, together with regular radiological assessment using the American Knee Society Radiological Score.

RESULTS

We present our early data at one year (127 patients), two year (79 patients) and three year (44 patients). There were no significant differences in clinical outcome between the cemented and HA groups. There was one bearing-exchange for instability, one deep infection (cemented) requiring revision, one case of tibial loosening (HA), which is pending revision.

DISCUSSION

Our study shows that there is no disadvantage using HA over cemented fixation, using the Total Meniscal Knee arthroplasty at a maximum follow-up of 3 years.

THE S-ROM NOILES ROTATING HINGE KNEE-SYSTEM USED IN REVISION ARTHROPLASTY

Frank C, Krämer P, Wentzensen A, Schulte-Bockholt D
BG-Unfallklinik Ludwigshafen,
Department of Trauma and Reconstructive Surgery, Ludwigshafen, Germany

christian.b.frank@t-online.de

INTRODUCTION

We wanted to know if function and stability could be restored with the S-Rom Noiles Rotating Hinge Knee-System in cases of major bone defects after Knee-Arthroplasty. We analyzed the early results including reinfections, early loosening, fractures and the handling of the prothesis.

METHODS

Since April 2004 16 patients were followed prospectively concerning arthroplasty as a salvage-procedure due to major bone defects and ligament instability. In 10 cases the procedure was performed to resolve infection-situations after osteosynthesis or knee-arthroplasty. 6 patients had either aseptic loosening or highly unstable situations. Follow-up period was up to 20 month.

RESULTS

There were no deep vein thromboses clinically, no major bleeding complications, no dislocations or early loosening. Adverse events included one intraoperative fracture and 2 reinfections. Reinfections were controlled by revision surgery consisting of one change of inlay and one second step prosthesis replacement. Mean duration of operation was 189 min. The functional outcome was good even in obese patients with multiple comorbidities. The mean BMI was over 31.

Range of motion increased by roughly 35°. 2 patients had a loss of ROM but a restored joint function. Radiologically all showed correct fit of the prosthesis with regular bone-cement interface. Mean ICU-time was 2.1 days. Average time of hospitalisation was 29 days.

Scores concerning functional outcome, Activity of daily living and depression evaluation were determined.

CONCLUSION

The S-rom Noiles Rotating Hinge Knee-System is a safe and feasible prothesis especially in high risk cases. It provides good functional outcome along with high patient satisfaction. Because of high costs for the prosthesis and hospitalisation including ICU the treatment is hardly profitable in the German health care system.

DELAYED ONSET DEEP INFECTION AFTER TOTAL KNEE ARTHROPLASTY: COMPARISON BASED ON THE INFECTING ORGANISM

Joshy S, Thomas B, Gogi N, Mahale N, Singh BK
Department of Orthopaedics, City Hospital Birmingham, UK

drsurajjoshy@yahoo.com

Infection following total knee arthroplasty is a serious complication. Recently there has been increasing incidence of isolation of multi-drug resistant bacteria from peri-prosthetic infections. The aim of our study is to identify the organisms causing delayed deep infections following primary total knee arthroplasty in the current situation. We also compared the differences in outcome based on the infecting organism. We undertook a retrospective study of all the patients who presented with delayed deep infection following primary total knee replacement during a six year period between April 1998 and March 2004. Organisms were isolated in 27 of the 31 patients who presented with delayed deep infection. Forty-four % of the organisms isolated were multi-drug resistant with increasing incidence of Methicillin resistant Staphylococcus aureus and multi-drug resistant Staphylococcus epidermidis infections. Statistical analysis was done using Fisher's Exact test for categorical data and Mann-Whitney U test for the non-parametric numeric data.

Successful outcome following an infected total knee arthroplasty was lower compared to the previous studies where there were fewer multi-drug resistant organisms. The average number of surgical procedures carried out was significantly higher when the organism isolated was multi-drug resistant. The number of patients with satisfactory outcome is significantly lower when the organism isolated is multi-drug resistant.

ETHNIC DIFFERENCES IN PREOPERATIVE FUNCTION IN PATIENTS UNDERGOING TOTAL KNEE ARTHROPLASTY

Joshy S, Datta A, Gogi N, Singh BK
Department of Orthopaedics, City Hospital Birmingham, UK

drsurajjoshy@yahoo.com

AIMS
To compare the preoperative knee function in patients of Asian origin and Caucasians living in the same community.

BACKGROUND
The prevalence of osteoarthritis is high in all ethnic and demographic groups. The timing of surgery is important as poor preoperative functional status is related to poor postoperative function.

METHODS
Prospective study of 63 Asian patients age and sex matched with Caucasian patients undergoing total knee arthroplasty. Pre operative Knee Society Clinical Rating System scores were recorded as a separate Knee Score and Knee Function.

RESULTS
The mean preoperative Knee Score in Asian patients was 37.6 in comparison to 41.5 in Caucasians ($p<0.10$) this difference was not statistically significant. The mean preoperative Knee Function in Asian patients was 32.5 in comparison to 45.0 in Caucasians ($p<0.001$) this difference was highly statistically significant.

CONCLUSIONS
Patients of Asian origin undergoing total knee arthroplasty have lower preoperative knee function to Caucasians. Cultural beliefs and social support explain part of this discrepancy but health care providers must also attempt to educate patients and close family members about the importance of timing the surgery to obtain the optimum benefits of pain relief and function.

A COMPUTER ASSISTED SURGICAL TECHNIQUE FOR TOTAL KNEE ARTHROPLASTY REVISION

Marcacci M, Nofrini L, Bignozzi S, Iacono F, Zaffagnini S, Lo Presti M, Di Martino A
Biomechanics Lab -Istituti Ortopedici Rizzoli -Bologna- Italy
m.marcacci@biomec.ior.it

INTRODUCTION

Total Knee Arthroplasty Revision (TKA Revision) is a skill-demanding intervention due to the complexities that exists after the removal of the failed prosthesis: bone deficiencies and lack of anatomical references make it difficult to understand the normal knee kinematic and adequately plan the intervention. Since main landmarks are not available, the surgeon use some secondary parameters that if contemporarily considered provide precise indications for implant positioning. Most of existing navigated techniques for TKA Revision use navigation systems developed for primary TKA, that requires some anatomical landmarks that don't exists anymore due to the previous procedure. Therefore, the operation is planned according to rough anatomical landmarks that do not reflect patient's original anatomy, disregarding those useful indications provided by secondary parameters. A computer assisted technique for TKA Revision is presented. Early results obtained using this navigated technique on five patients by an expert surgeon are reported.

METHODS

The surgery starts performing surgical incision and fixing navigation markers to the distal femur and distal tibia. After prosthesis removal, data acquisition starts: using the sensorized instruments, the surgeon detects several anatomical landmarks (12 points) for the computer system to construct the 3-dimensional representation of the patient's lower limb. After reaming the medullary canal of both tibia and femur, two dedicated navigated tools developed to acquire the canals directions and to provide the surgeon with information on the tibial cut and femoral distal cut orientation, called TibialMod and FemoralMod, are positioned on the bones. Once the appropriate cutting level is determined by the surgeon considering the bone quality, the two cuts are performed using the navigated instruments. With the FemoralMod and the TibialMod inserted into the bones, navigated joint space assessment in extension and in flexion is performed using a custom made balancer and the symmetry of each gap is evaluated. The two planes are graphically shown on the system interface together with numerical information about their distance and the angle between them, updated in real time. Moreover, during flexion space acquisition the relationship between the actual FemoralMod median line and the transepicondylar line is highlighted (Fig1). Gathered data are used by the system to automatically plan the intervention. Even if during acquisition phase some specific points (e.g one or both the epicondyles) can not be identified, since for each prosthetic component several criteria to set each degree of freedom are considered and compared, the system is able suggest an intervention plan.

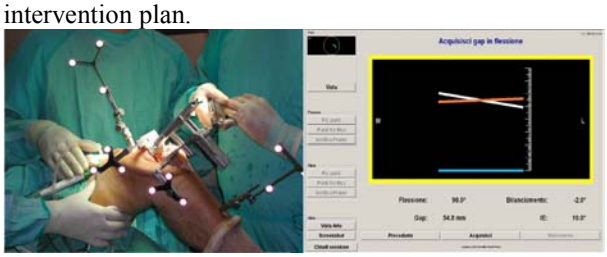

Fig1 Intraoperative setup during flexion space estimation

A range of acceptability for the joint line level is determined related to the medial and lateral epicondyle height, the patella pole and the fibular head and together with the measured extension space it allow to provide also indications about the tibial polyethylene insert size and need of femoral augmentation. The IE rotation of the femoral component is set considering the transepicondylar line or the femoral neck axis and the flexion space. The femoral components size is determined considering the prosthesis properties, the distance between the navigated stem and the anterior femoral shaft and the flexion space. On tibial side, the component size is set considering the estimation of the tibial plateau done through points acquisition; IE rotation is determined related to the tibial tuberosity position.
The system provides the surgeon with tools to analize and modify the proposed plan monitoring the behaviour of the residual joint gap in flexion and in extension. Once refined the intervention plan, the system provide the surgeon with tools to reproduce the plan on the patient.

RESULTS

Till now the presented technique was used on five patients by an expert surgeon. Qualitative results, collected after the intervention through a questionnaire on surgeon feelings, in order to assess the functionality, user friendliness and the data visualization criteria implemented were very satisfying.System reliability was assessed intraoperatively analyzing joint line height, limb alignment and knee stability using trial components: based on his experience, the surgeon checked some acceptable components combination and compared the corresponding outcome with the one provided by the implant planned by the system. In three out five cases the suggested implant was considered the best by the surgeon, while in one case he decided to change the tibial insert of one size because of knee instability and in another case he changed the tibial component of one size because the planned one was too small.Final limb alignment evaluated with postoperative x-rays, was satisfactory in all cases.

IS ARTHRODESIS, IN INFECTED RE-REVISION ARTHROPLASTIES OF THE KNEE, AN UPDATE PROCEDURE"

*Rosa MA, **Centofanti F, *Villari L, *Caminiti R, *Alesci M
*Surgical Specialties Department - Orthopaedic Section - University of Messina – Italy

rosa.ma@tiscali.it

INTRODUCTION AND METHODS

Authors have made a retrospective study of the last 4 years (from 2000 to 2004) on 20 patients, mean age 71, the gender was female in 12 and male in 8, in 14 cases the left knee and in 6 the right one was involved.
All patients underwent to total knee arthroplasties (TKA) and all of them were complicated by a "late" infection.
Re-revision with a "two step surgery" could not stop the infection and arthrodesis with different techniques was finally performed.
Follow-up ranged between 6 and 48 months and good results were obtained in all cases. No particular complications were observed except in 1 case where dehiscence of the surgical wound verified at the removal of stitches, healing resulted after few cycles of medications.
Arthrodesis was performed employing :

- An axial external fixation in 1 case
- Axial external fixation associated with two crossed Steinmann nails in 4 cases
- Femur-tibial long locked nail in 1 case
- Ilizarov method external fixation in 2 cases
- In the great majority of our series, 12 cases, arthrodesis was performed with a modular prosthesis and in 2 cases of them the prosthesis was "silver" coated.

Antibiotic therapy has been administered for a long term period, of at least three months, in association with arthrodesis following to the individuation of responsible pathogen.

RESULTS AND CONCLUSIONS

In all cases arthrodesis resulted for all patient the end of suffering also if it meant the loss of the articular function. This technique was chosen by the patient to avoid amputation.
In Authors opinion arthrodesis in infected re-revision arthroplasties must be considered as a long lasting surgery.

AFFILIATED ISTITUTIONS:
** Codivilla-Putti Institute - Cortina (BL) - Italy

COMPUTER-ASSISTED IN TKA WITH DEFORMITIES: A PROSPECTIVE STUDY

*Sandoval MA, ** Hernandez-Vaquero D, *Suarez-Vazquez A, *Gava R
Hospital St Agustin, Aviles, Spain

sandovalmag@yahoo.es

INTRODUCTION

It has been known for some years that a key issue for a long survival of total knee arthroplasty is to achieve a good alignment in limb axes. An error in component alignment can be responsible for femoro-patellar complications, instability, periprosthetic fractures, subsidence and loosening. To get the correct position of the total arhroplasty in knee deformities is more difficult than in normal axes.

METHODS

The aim of this work was to compare the final alignment obtained in two arthroplasty groups: in one of them using the standard manual instruments and in the other the same instruments but with a wireless surgical navigation system (Stryker system). It is a prospective study for 40 knee arthroplasties, 20 in each group, performed by the same surgeons, using the same knee implant and following the same post-op protocol. All the patients underwent surgery because of degenerative arthritis, with deformities greater than ten degrees varus-valgus. Sex, age and weight were similar. Femoral angle (formed by the mechanical axis of the femur and femoral component), tibial angle (between the tibial mechanical axis and the tibial platform), and femoro-tibial angle (between the femoral and tibial mechanical axes) were measured on a computed tomography of the limb obtained in the immediate postoperative period.

RESULTS

In the computer-assisted surgery group the average femoral angle was 90.3º, the tibial angle was 89.9º and the femoro-tibial one was 179.8º; in the standard group the average femoral angle was 91.9º, the tibial angle 90.4º and the femoral-tibial angle 177.1º The differences were statistically significant for the femoro-tibial angle. Ninety percent of the computer-assisted surgery patients reached a correct femoro-tibial angle (180±3º) but only the 60% of the standard group patients. We have not seen any complications related to the use of computer assisted system.

DISCUSSION

The computer-assisted surgery is useful in total knee arthroplasty with preoperative deformities. The alignment obtained is better that with standard mechanical instrumentation.

** Faculty of Medicine, University of Oviedo, Spain

MICROENDOSCOPIC POSTERIOR DECOMPRESSTION FOR LUMBAR SPINAL STENOSIS

*Ikuta K, *Tono O, *Tanaka T, *Arima J, *Nakano S, *Sasaki K, *Fukagawa S, *Oga M
*Dept Orthopedic Surgery, Hiroshima Red Cross and Atomic-bomb Survivors Hospital, Hiroshima, Japan
koikuta@mac.com

INTRODUCTION: Minimally invasive procedures have led to remarkable changes in spinal surgery. The authors applied the technique of microendoscpoic discectomy (MED), which is an endoscopic technique in which the tubular retractor is used to treat lumbar disc herniation, to posterior decompression procedures for lumbar spinal stenosis. The purpose of this study was to evaluate the clinical and radiographic results of microendoscopic posterior decompression (MEPD).

METHODS: MEPD procedure, which involves a unilateral endoscopic approach for bilateral decompression (Fig. 1), was performed in 118 patients to date. The patient population comprised 75 men and 43 women whose mean age at surgery was 68 years (range 31-91 years). Spondylotic spinal stenosis was observed in 69 patients, degenerative spondylolisthesis was documented in 36, degenerative scoliosis was presented in 6, sponlylolysis was revealed in 3, and a facet joint cyst was presented in four patients. The clinical outcomes and radiographic studies were evaluated in 79 patients, who could be followed minimum 1 year after surgery. The mean follow-up duration was 24 months. The clinical evaluation was conducted using the Japanese Orthopedic Association Lumbar Score (JOA score), visual analog scale (VAS) score, and Prolo's functional economic outcome rating scale. The effectiveness of decompression was evaluated on a cross-sectional area of the dural sac at the disc level, which was demonstrated on axial T2-weighted magnetic resonance imaging (MRI) obtained before and after MEPD.

RESULTS: Access-related complications occurred in 9 patients (7.6%): six dural violations and three fractures of the inferior facet. The presence of nerve injury during surgery and wound infection was not investigated. The JOA score was 14.3 ± 4.0 before surgery and increased up to 24 ± 3.6 at the final follow-up. The VAS score was 70 ± 12.9 before surgery and decreased to 31 ± 22.5 at the final follow-up. The clinical outcome was regarded as excellent in 21 patients, good in 31, satisfactory in 15, and poor in 12, based on the Prolo's scale. There were two patients who underwent a revision surgery during the follow-up periods. On radiographic studies, the progression of disc degeneration after surgery was revealed in two patients, including one with postoperative instability. On MRI evaluations, the cross-sectional area of the dural sac was 60 ± 31 mm^2 before MEPD, and this increased up to 145±41 mm^2 after MEPD. There was a significant difference in the cross-sectional area of the dural sac when comparing pre- and post-MEPD images. The sufficient decompression of the spinal canal was observed in almost all the patients.

DISCUSSION: The endoscopic procedure offers several advantages such as a reduced tissue trauma, and a wide and excellent visualization. Those are far superior to those of the conventional procedures. We found that good results were presented in 80-85% of the patients at a mean 24 months after MEPD, based on the JOA score and Prolo's scale, and these results were on par with those of the conventional procedures. The MEPD procedure, in addition, could be undertaken to preserve the posterior structures of the lumbar spine and prevent the developing postoperative instability in almost all the patients. In conclusions, the MEPD is a minimally invasive procedure and as useful as other conventional procedures in treating lumbar spinal stenosis. The follow-up duration in the present study, however, was not sufficient to allow for evaluation of the effectiveness of MEPD for treatment of lumbar spinal stenosis. We consider that further follow-up studies should be performed to evaluate the long-term outcomes.

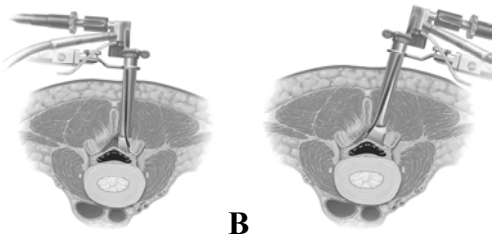

Figure 1. MEPD procedure is a unilateral endoscopic approach for bilateral decompression (**A**: approach side, **B**: contralateral side)

CALCULATION OF LUBRICATION REGIMES IN TWO-PIECE FIRST METATARSOPHALANGEAL IMPLANTS

Joyce T J
Centre for Rehabilitation and Engineering Studies, School of Mechanical and Systems Engineering, University of Newcastle upon Tyne, Newcastle upon Tyne, United Kingdom
t.j.joyce@ncl.ac.uk

INTRODUCTION

A range of concepts for first metatarsophalangeal (MTP) arthroplasty have been proposed over the years, including various two-piece designs which have spherical bearing surfaces in a ball and socket arrangement. These designs have used a range of biomaterial couples including ceramic-on-ceramic (CoC), metal-on-metal (MoM) and metal-on-polymer (MoP) [1]. The aim of this paper was to compare the predicted lubrication regimes in the application of a first MTP prosthesis for these various biomaterial couples.

MATERIAL AND METHODS

Modeling the ball and socket implant as an equivalent ball-on-plane model and employing elastohydrodynamic theory [2] allowed the minimum effective film thickness to be calculated. In turn, the lambda ratios were calculated which allowed the lubrication regime to be identified, as lambda < 1 indicates boundary lubrication, lambda > 3 signifies fluid film lubrication, and between these values mixed lubrication is indicated [3]. Based on pertinent biomechanical data for the first MTP joint, calculations were undertaken for: a range of entraining velocities of 0 to 30mm/s; a prosthesis radius of 3 to 15mm; and a range of loads from 50 to 1500N. Other relevant values were taken from the literature [4] [5].

RESULTS

By varying the entraining velocity from 0 to 30mm/s, the resultant changes in lambda ratio are given in figure 1.

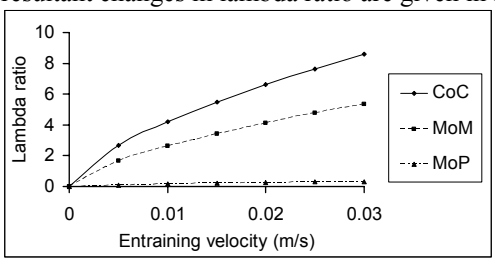

Fig 1: Variation of lambda ratio with entraining velocity

As can be seen, under the chosen test conditions, for most of these velocities a CoC implant would operate in the fluid film lubrication mode (lambda > 3). A MoM implant would function in the fluid film lubrication regime above approximately 12mm/s entraining velocity, while a MoP implant would operate in the boundary lubrication regime (lambda < 1). When the prosthesis radius was varied between 3mm and 15mm the greatest values of lambda ratio were seen with CoC, followed by MoM and finally MoP, as shown by figure 2. Figure 3 offers the lubrication regime results when the various load calculations were undertaken. Again, the order from enhanced lubrication to more difficult operating conditions is CoC, MoM and MoP.

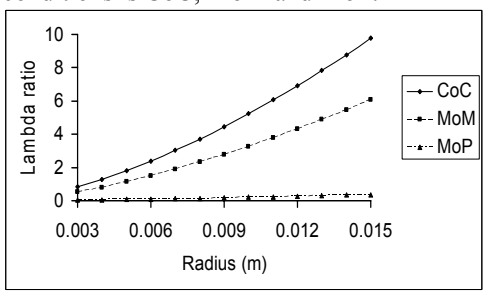

Fig 2: Variation of lambda ratio with prosthesis radius

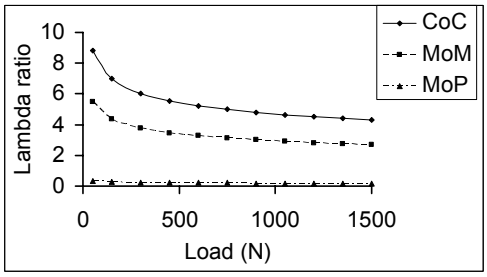

Fig 3: Variation of lambda ratio with load

DISCUSSION

Ceramics provide a hard, scratch resistant surface whic likely to retain its low roughness values during opera However catastrophic in vivo fracture of a CoC first M prosthesis has recently been reported [6]. The M combination often achieved fluid film lubrication (lambda but this situation is reliant on maintaining excellent valu surface finish. It has been shown that the MoP combina will operate in the boundary lubrication regime (lambda < However, it is recognized that most MoP hip prosth operate in the boundary lubrication regime [7] and while does occur and is a concern, the majority of patients provided with a functional and successful prosthesis [8] addition the positive results for CoC and MoM need to b against recognition that, when the toe is not moving, entraining velocity is zero and so surface contact will o with a concomitant potential for wear.

REFERENCES

[1] Joyce TJ. Exp Rev Med Devs, 2005; 2:453-464. [2] Hamrock BJ, Dowson D. Trans ASME J Lubn Tech, 1978; 100:236-245. [3] Johnson KL, Greenwood JA, Poon SY. Wear, 1972; 19:91-108. [4] Pylios T, Shepherd DET. J Biomechanics, 2004; 37:405-411. [5] Smith SL, Dowson D, Goldsmith AAJ. J Engng Tribology, 2001; 215:483-493. [6] Pavier J. The Foot, 2005; 15:47-49. [7] Jalali-Vahid D, Jagatia M, Jin ZM, Dowson D. J Biomechanics, 2001; 34:261-266. [8] Nercessian OA,

INTRA-OPERATIVE STABILITY OF CEMENTLESS HIP IMPLANTS BASED ON VIBRATIONAL TECHNIQUE

[1,2]Bialoblocka E, [1,2]Varini E, [2]Lannocca M, [2]Cappello A, [1,2]Cristofolini L
[1]Istituti Ortopedici Rizzoli, Laboratorio di Tecnologia Medica, Bologna, Italy
[2]University of Bologna, Engineering Faculty, Bologna, Italy
bialoblocka@tecno.ior.it

INTRODUCTION

Long-term stability of cementless hip prostheses depends strongly on the achievement of a good initial press-fitting of the stem into the femur.

Two different approaches have been explored aiming to evaluate hip implant primary stability. The first one is based on direct measurement of stem-bone micromotion, which is compared to a threshold[1,2]. The second method is based on vibrational testing[3]. In this direction, based on recent results, it seems that it is possible to discriminate a stable implant from a grossly unstable one by studying the harmonic content of the implant-bone system, when subjected to an excitation[3]. But, with the aim of helping the surgeon evaluating the degree of fixation of an implant, it is necessary to detect also the cases of moderate instability.

The purpose of this study was to develop and test a prototype device able to discriminate stable from quasi-stable implants during surgery.

METHOD

Both stable and quasi-stable implants behave linearly. Unstable ones behave as non-linear systems. Thus, the frequency response function (FRF) of the stem-bone system was measured with a controlled excitation.

The designed device consisted of:

i) Hardware (piezoelectric vibrator to apply a controlled tangential excitation, accelerometer to detect the output vibrations)

ii) Software (parameters setting, signals generation and acquisition, data processing and results visualization).

Validation tests were performed on an implanted composite femur to optimize the protocol. An in-vitro trial was then performed on four more composite specimens in order to explore the potentiality of the device. To simulate the most critical loading condition for primary stability, a torque (15Nm) was applied during each test. The FRF of the system was measured before, during and after the torque application. Frequency, amplitude and phase at the principal resonance frequency (PRF) were considered for the elaborations. The results obtained were correlated with the linear micromotion measured with an additional displacement transducer, placed at the femur-implant interface.

RESULTS

The device was successfully developed (Fig.1). The optimal frequency range was defined as 1.2-2kHz, with a resolution of 5Hz.

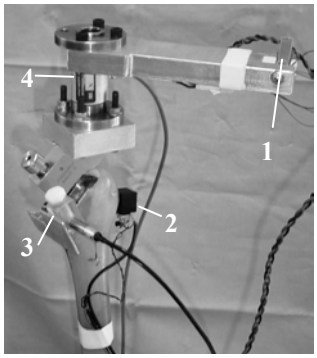

Fig.1 The prototype device:
1. piezoelectric vibrator;
2. accelerometer;
3. displacement transduce
4. torsional load cell

In case of stable and quasi-stable implants the PRF ranged 1550-1700Hz. The error in the estimation of the PRF was less than 0.1%. Fluctuations of each spectral component of the acceleration signal were less than 1% of the amplitude at the PRF.

Between all the parameter considered, the one that correlated best with the implant stability was the shift of the PRF considering the system before and after the torque application (R^2>0.91) (Fig.2).

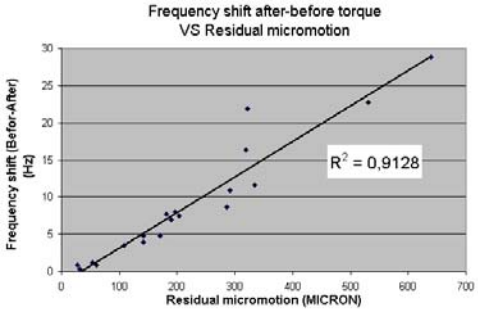

Fig.2 Typical correlation graph.

DISCUSSION

The goal of the study was to develop and test a device based on vibrational technique for the intra-operative evaluation of stem stability. In particular, the presented device was designed to diagnose different degrees of instability.

The device developed showed good repeatability in the generation of the excitation signal and high accuracy in acquisition of the accelerometer signal. From the experimental results, it seems that the shift of the PRF is a reliable indicator of stem stability. More tests on both composite and cadaver femurs are needed to confirm the presented results.

REFERENCES

1. Søballe K, 1993, Acta Orthop Scand.
2. Cristofolini L., et al.,2005,Med Eng Phys,3;in press.
3. Jaecques SVN et al., 2004, Proc. Int. Conference on Noise and Vibration Engineering, pp.443-456.

THE DISTRIBUTION OF BONE DENSITY OF THE PROXIMAL TIBIA AS DETERMINED BY MULTISLICE CT SCANNING

*Cottam HL, Shepperd JAN, Taylor M
*The Conquest Hospital, Hastings, UK

howie@doctors.org.uk

INTRODUCTION

To assess the ability of high resolution multislice CT scanning techniques to measure bone density of the tibial plateau and assist in the creation of accurate finite element analysis models.

METHODS

Redundant CT data of the proximal tibia were collected from seven non-arthritic patients who had undergone a CT angiogram for vascular pathology, using the Toshiba Aquilion 64 Multislice CT scanner, which acquires 3D images with a resolution of up to 0.5mm. These images were analysed with Mimics 9.0 software allowing calculation of the average density of a $50mm^3$ area on the axial slices. These areas were measured at increasing depths on the anterior, mid- and posterior regions of both the medial and lateral tibial plateau condyles.

RESULTS:

Our data confirm greater densities within the medial condyle, and show greater densities in the posterior regions of each condyle.

CONCLUSION

This use of redundant CT data provided a non-invasive method to analyse bone characteristics. The higher resolution offered by multislice CT scanners improves 3D data collection, allowing the creation of increasingly accurate finite element analysis models. These models will further the understanding of knee biomechanics and be a useful tool in future prosthesis design.

OSTEOLYSIS IS INDUCED BY FLUID PRESSURE BUT NOT BY TRAUMA TO THE MEMBRANE

*Fahlgren A, *Aspenberg P
Department of Orthopaedics and Sports Medicine, Faculty of Health Sciences, Linköping University, Linköping
Anna Fahlgren@inr.liu.se

INTRODUCTION

Fluid pressure, instability and particles have been proposed as mechanisms leading to periprosthetic bone resorption. We have an experimental model for periprosthetic bone resorption [1]. A fibrous membrane is created and the model compresses this tissue between bone and implant to generate a hydrostatic pressure. This result in a resorptive bone lesion within 5 days, which shares many histological characteristics with the osteolysis observed at implant loosening. There might be several mechanisms behind this osteolysis. Except from the hydrostatic pressure or fluid flow, as possible direct stimuli, tissue damage within the squeezed fibrous membrane might be another stimulus. Tissue damage leads to an inflammatory reaction which could lead to bone resorption [2]. The current study investigates the effect of tissue damage for osteolysis in comparison with fluid pressure.

MATERIAL AND METHODS

Thirty SD rats received a titanium plate at the proximal tibia. A central plug was inserted. After 4 weeks of osseointegration, the central plug was changed to a piston. Soft tissue was allowed to form between the piston and the bone for 5 days. 2 types of pistons were used: The pressure piston pressurizes the soft tissue under the piston, and the trauma piston traumatizes the tissue without pressure via small pegs that tears the tissue apart when it is rotated. The pressure piston was subjected to a transcutanous force of 5N. Each episode of pressure comprised 20 pressure cycles at 0.17 Hz, which was done twice a day. The trauma piston was rotated 20 half-turns (180°) with the same frequency as the pressure piston.
The rats were randomized to 3 groups. 10 rats were killed after 5 days (before the first pressure or trauma episode) as controls. 10 rats had pressure pistons and 10 had trauma pistons. These rats were killed after 10 days, (ie after 5 days of pressure or trauma). The tissue under the piston was prepared for histology. Occurence of bone resorption underneath the piston was first evaluated blindedly. Thereafter, qualitative histology was performed. Institutional guidelines for care and treatment of experimental animals were followed.

RESULTS

There were 2 exclusions, due to technical problems.
7 of 9 pressure specimens showed bone resorption, but none of the others (Fisher´s exact test, p=0.0001).
The soft tissue in the controls showed an organized fibrous callus with osteoid formation. The trauma group showed intact original bone and ongoing new bone formation adjacent to it. The soft tissue was richly vascularized with abundant macrophage-like cells and polymorhonuclear leukocytes. Some macrophages contained metal debris. The pressure group showed bone resorption at the interface to the soft tissue, which appeared similar to the trauma group, but with fewer blood vessels and with areas of necrosis (and no debris).

DISCUSSION

Fluid pressure within the adjacent soft tissue (membrane) induced osteolysis, in contrast to tissue trauma without pressure. This suggests that the bone resorption induced by pressure is mediated via other pathways than those activated by inflammation alone. Also when inflammation is induced by wear particles the resorptive response is weak in this model. Other models have demonstrated synergy between mechanical instability and particles. This again suggests an effect of fluid pressure, which is independent of inflammation. The pathways by which pressure induces resorption are unknown, but it is likely related to local fluid flow velocity.

REFERENCES

1. Skripitz, R. and P. Aspenberg, J Orthop Res, 2000. 18(3): p. 481-4.
2. Ferrier, G.M., et al., J Bone Joint Surg Br, 2000. 82(5): p. 755-9.
3. McEvoy, A., et al., Bone, 2002. 30(1): p. 171-7.
4. Skoglund, B. and P. Aspenberg, J Orthop Res, 2003. 21(2): p. 196-201.

ACKNOWLEDGEMENTS

We thank Bibbi Mård for technical assistance. This investigation was supported by the Swedish Research Council (project 2031), Materials in Medicine and Tore Nilssons Foundations.

RELIABILITY OF DIGITAL TEMPLATING IN TOTAL HIP ARTHROPLASTY

*Franken M , *Schönhuth C , **,***Grimm, B , **van Asten W **,***Heyligers, IC;
*University of Technology, Eindhoven, NL ; **Atrium MC, Heerlen, NL ; *** AHORSE, Heerlen, NL
mfn04@atriummc.nl

INTRODUCTION

Manual templating is a common technique in total hip arthroplasty (THA) for preoperative planning and implant sizing[1]. Transparencies with printed anteroposterior (AP) and mediolateral (ML) implant projections are superimposed onto conventional radiographs and visually checked for implant size, position and orientation. Templates are provided by the implant manufacturers for each device and are typically available in two magnification levels (115% and 120%).

As hospitals replace analog with digital radiography the demand arises for digital templating tools such as Endomap, Orthoviewer, iPlan, OT3000 or Medicad II. Such software relies on a calibration object of known dimensions to be placed in the image. Clinical studies comparing digital versus manual templating have shown that the surgical planning was less frequently correct with digital than with analog templating[2]. In another study, incorrect positioning of the calibration object by insufficiently trained staff or as a result of patient obesity has been identified as a major cause for such templating errors[3].This study evaluates the accuracy and reliability of digital preoperative templating.

METHODS

Postoperative AP radiographs from 19 patients with a Stryker ABG-II THA (14 women, 5 men, 71 years [57-76]) were analyzed for stem size (n = 22) and cup size (n= 22) using one of the most popular orthopaedic templating software (Endomap V2.01; Hectec GmbH, Germany) and a 30mm calibration ball (recommended). The two observers were blinded to the actual implant size to which their measurements were compared and categorized as correct, over- or undersized. ("Retrospective templating"). The measurements were repeated twice within one month by one observer for an intra-observer reliability test. Reliability was calculated using the kappa coefficient (κ).

RESULTS

During the first observation 9/22 stems (41%) were sized correctly while 8/22 stems (36%) was either one size underestimated or one size overestimated 5/22 (23%, Table 1).

	Stem					
	Observer I-1		Observer II		Observer I-2	
Sizing error	**n**	*%*	**n**	*%*	**n**	*%*
-2	0	*0%*	0	*0%*	2	*9%*
-1	8	*36%*	6	*27%*	8	*36%*
0	**9**	***41%***	**9**	***41%***	**10**	***46%***
+1	5	*23%*	5	*23%*	2	*9%*
+2	0	*0%*	2	*9%*	0	*0*

Table 1: Results stem templating.

Cup templating showed same results with only 41% (9 cups) sized correctly during the first observation. Templating error by only one size was observed for 8 cups (36%) but for 5 cups (23 %) the error was two cup sizes or more. Most cups were underestimated (41%) than overestimated (18%, Table 2).

Intra-observer: On second observation the number and ratio of correctly and incorrectly sized components was very consistent for all implants overall but it was seen that only 55% (12/22) of the individual stems (κ = 0.35) and 68 % (15/22) of the individual cups (κ=0.44) were sized the same between both observations.

	Cup					
	Observer I-1		Observer II		Observer I-2	
Sizing error	**n**	*%*	**n**	*%*	**n**	*%*
-3	1	*5%*	0	*0%*	1	*5%*
-2	2	*9%*	0	*0%*	2	*9%*
-1	6	*27%*	4	*18%*	6	*27%*
0	**9**	***41%***	**5**	***23%***	**9**	***41%***
+1	2	*9%*	8	*36%*	3	*14%*
+2	2	*9%*	3	*14%*	1	*5%*
+3	0	*0%*	2	*9%*	0	*0%*

Table 2: Results cup templating.

Inter-observer: Regarding the stem size both observers scored similar overall results (41% correct). However, inter-observer reliability was low (κ = 0.25) as both observers agreed on stem size in only 11/22 cases (50%). Templating the cup observer two had a success rate of only 23% versus 41% for observer 1. However, both observers had a higher agreement sizing the cup than the stem (59 %) resulting in κ = 0.6. The highest errors and differences between observations were seen when the stem was rotated or the cup inclination was high.

DISCUSSION

This study using "retrospective templating" confirmed that digital templating can lead to significant errors in implant sizing as reported in clinical studies. In clinical practice the incorrect positioning of the calibration ball with reference to the implant is the major reason for this problem. The overall results between both observers were relatively consistent but intra- and inter-observer reliability was low suggesting uncertainties and ambiguities in the method. The fact that sizing errors occurred more frequent with rotated stems or highly inclined cups highlights a principal weakness of 3D to 2D imagery and suggests that reliable templating should be done on both AP and ML x-rays. However, most importantly staff must be trained well to place the calibration object. We are currently testing positioning aids and alternative calibration methods.

REFERENCES

[1] Della Valle et al., J Arthroplasty 2005, 20(1):51-8
[2] The B et al. Acta Orthopaedica 2005 76(1): 78-84
[3] Franken M, et al., Proc. ORS 2006

X-RAY CALIBRATION IN DIGITAL TEMPLATING: A SOURCE OF ERROR IN TOTAL HIP ARTHROPLASTY

*,**Grimm B, **Franken M, *Schönhuth C, *,**Tonino AJ, *,**Heyligers, IC
*Dept Orthopaedics, Atrium MC, Heerlen, NL; ** AHORSE, Heerlen, NL; *** University of Technology, Eindhoven, NL
mfn04@atriummc.nl

INTRODUCTION

Preoperative templating is of paramount importance for obtaining quality in modern total hip arthroplasty (THA)[1]. In manual templating, transparencies with printed anteroposterior (AP) and mediolateral (ML) implant projections are superimposed onto conventional radiographs and visually checked for implant size, position and orientation. Templates are provided by the implant manufacturers for each device and are typically available in two magnification levels (115% and 120%).

Hospitals are changing increasingly from analog to digital radiography[2] driving the need for digital templating software such as Endomap, Orthoviewer, iPlan, , OT3000 or Medicad II. Clinical studies comparing digital versus manual templating have shown that the surgical outcome of THR was less frequently correct with digital than with analog planning[3].

Digital templating tools use a calibration object of known dimensions such as a ball or ruler in the image for scaling instead of a fixed magnification. This study evaluates 1.) the accuracy of digital templating using the recommended calibration object and 2.) whether a fixed magnification may be superior to object calibration.

METHODS

Postoperative AP radiographs from 19 patients with 22 Stryker ABG-II THA (14 women, 5 men, avg. age: 72 years [44-78]) were measured for stem size (n = 22) and cup size (n = 22) using one of the most popular templating software (Endomap V2.01; Hectec GmbH, Germany). The two independent observers were blinded to the actual implant size to which their measurements were compared and categorized as correct or over- or undersized ("retrospective templating"). Image calibration was done either using a 30mm ball as recommended by Endomap or by assuming a fixed magnification of 115% for all images such as with manual templates.

RESULTS

Using the calibration ball, templating accuracy was low for both observers with only 9/22 (41%) of the stems and 5/22 (23%) of the cups sized correctly (Table 1). For observer 1 14/22 stems (59%) were measured either one size too large or too small while observer 2 scored 2/22 stems (9%) even two sizes too large. With the cup having smaller dimensional steps between sizes 5/22 implants (23%) were wrongly templated by two sizes or more.

Using the fixed magnification templating accuracy increased. The ratio of correctly sized stems improved to 13/22 (59%) for observer 1 and 14/22 (64%) for observer 2 (Table 1). The ratio of incorrectly sized stems went down accordingly. No implant was sized incorrectly by two sizes anymore. For both observers combined the stem sizing accuracy between ball calibration (18/44) and fixed magnification (27/44) improved significantly (p=0.04, Fisher exact test). The ratio of correctly sized cups improved from 23% (5/22) to 32% (7/22, n.s.) and the number of cups wrongly templated by two sizes or more dropped significantly from 5/22 (ball) to 0/22 (fixed magnification, p= 0.01). The cups still wrongly sized by one number were mainly oversized (14/22) and not undersized (1/22). This trend was also true for the stems (oversized: undersized = 16:1). Using the calibration ball, the number of wrongly sized implants was higher but the ratio of oversized to undersized stems and cups was more balanced (12:14 and 4:13 respectively).

	Calibration ball						**Fixed magnification**					
	Stem				**Cup**		**Stem**				**Cup**	
Sizing	Obs. 1		Obs. 2		Obs. 2		Obs. 1		Obs. 2		Obs. 2	
error	*n*	*%*	*n*	*%*	*n*	*%*	***n***	*%*	***n***	*%*	***n***	*%*
-2	**0**	*0%*	**0**	*0%*	**0**	*0%*	**0**	*0%*	**0**	*0%*	**0**	*0%*
-1	**8**	*36%*	**6**	*27%*	**4**	*18%*	**0**	*0%*	**1**	*4%*	**1**	*4%*
0	**9**	*41%*	**9**	*41%*	**5**	*23%*	**13**	*59%*	**14**	*64%*	**7**	*32%*
+1	**5**	*23%*	**5**	*23%*	**8**	*36%*	**9**	*41%*	**7**	*32%*	**14**	*64%*
+2	**0**	*0%*	**2**	*9%*	**3**	*14%*	**0**	*0%*	**0**	*0%*	**0**	*0%*
+3	**0**	*0%*	**0**	*0%*	**2**	*9%*	**0**	*0%*	**0**	*0%*	**0**	*0%*

Table 1: Correct sizing, over- and underestimation per calibration method, observer and implant.

DISCUSSION

Using a calibration object as recommended by the templating software makers can produce critically low planning accuracy in clinical practice. While a calibration object may allow the calculation of the exact magnification factor and facilitate precise templating in theory it was shown that the accuracy of ball positioning required to distinguish between implant sizes can be less than ± 20mm in the AP direction[4]. This is difficult to achieve in radiological practice particularly on obese patients or with staff insufficiently trained on the new method. Thus the fixed magnification factor of analog templates (115%) gives better templating accuracy and can be used until clinically more reliable digital calibration methods are available. Furthermore, this way x-rays can be digitally templated which previously had to be rejected due to a missing or obviously misplaced calibration object. The higher proportion of oversized implants suggests that a higher magnification factor of 116-118% may even be more appropriate. If the x-ray shows another implant with a known dimension (e.g. ball of contra-lateral hip) we recommend it for calibration.

REFERENCES

[1] Della Valle et al., J Arthroplasty 2005, 20(1):51-8; [2] www.orthoview.com; [3] The et al. Acta Orthopaedica 2005 76(1): 78-84; [4] Franken et al., Proc. ORS 2006

PERIPROSTHETIC FRACTURES IN ELDERLY PATIENTS: AN EXPERIMENTAL STUDY CEMENTLESS VS CEMENTED SYSTEM

Jakubowitz E, Seeger J, Clarius M, Thomsen M
Orthopeadic Surgery Hospital, University of Heidelberg, Germany

Eike.Jakubowitz@ok.uni-heidelberg

INTRODUCTION

Postoperative periprosthetic fractures after total hip arthroplasty are an uncommon (0.1% to 4.0%) but severe complication that can be difficult to treat.
Although cementless components may be a risk, there is a trend to implant these components also in elderly patients and start with full weight bearing.
Aim of the study was to compare two established stem designs (cemented/ cementless) in defined experimental conditions.

METHODS

After bone density measurement (DEXA) 10 matched pairs of fresh frozen femurs have been implanted by an experienced surgeon. One side got a cementless Spotorno CLS®-stem (Zimmer, Warsaw, Indiana, USA) and the other side a cemented MS30®-stem (Zimmer, Warsaw, Indiana, USA). The cement itself was Palacos® (Heraeus Medical, Hanau, Germany) with third generation cementing technique.
Donor data: f/m = 3/7, age: Ø = 75.4 years, BMI: Ø = 28.8kg/m².
Then maximum loads up to 10.000N, simulating normal walking (13.1° adduction and 31.8° internal rotation) were performed to induce a periprosthetic fracture. Load versus displacement curves for crack propagation were analysed.

RESULTS

The average load to induce a periprosthetic fracture was F_{max} = 7544 N (3.000 - >10.000N) in the cemented group, whereas 3.502 N (1.800- 7.647 N) was needed to have a fracture in the cementless group. This corresponds to 961 % bodyweight (361 -1.550 %BW) for cemented and 448 % BW (194 – 1.033 %BW) in the cementless group. In four specimens with CLS-stems the force to cause a periprosthetic fracture is less than the hip load during normal walking (F_{max} = 233%BW).
Whereas the CLS showed subsidence with a medial proximal fracture, all cemented stems induced a subprosthetic fracture. There was significant correlation between F_{max} and the bone density only in the CLS group.

DISCUSSION

There is a significant high protective effect of a cemented hip arthroplasty in the initial phase in elderly patients. An initial full weight bearing for a patient with a low bone density in an uncemented hip may cause a periprosthetic fracture.

PRE-CLINICAL TESTING OF A NOVEL CEMENTLESS HIP IMPLANT

*Janssen, D, **Thümler P, *Verdonschot N
*Orthopaedic Research Laboratory, Radboud University Nijmegen Medical Centre, Nijmegen, The Netherlands
n.verdonschot@orthop.umcn.nl

INTRODUCTION

The Eurometric stem is a novel hip implant based on the experience of the Euroform implant. The Eurometric stem has been designed with the objective to promote proximal loading and to increase implant stability. In order to investigate whether the design goals of the implant have been met, the initial stability of the cementless Eurometric implant was tested experimentally and compared with that of the cementless Euroform implant. Furthermore, it was tested whether leg length discrepancy was minimized by the designs. For this purpose, the mismatch between trial reduction and final implant position was measured.

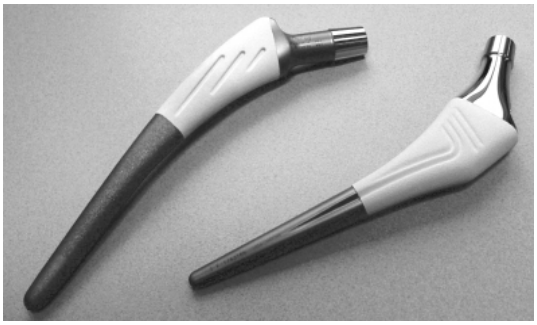

Figure 1 *The Euroform (left) and the Eurometric (right) cementless hip implants.*

METHODS

Pairs of cadaveric human femurs were used to create five matched reconstructions with the Eurometric and the Euroform implant. Preplanning and implantation were performed by Dr. Thümler. During the procedure the position of the final rasp, used for the trial reduction, was measured using RSA and compared to the final position of the implant. Subsequently, in the first experiment the reconstructions were cyclically loaded with an increasing load amplitude for four hours at a frequency of 1 Hz. In a second experiment the reconstructions were subjected to a cyclic torque load. The migration of the implants was measured at various moments in the loading history using RSA. The locations were the load was transferred to the surrounding bone was monitored through strain gauge measurements. The strain gauges were attached to the femurs at different levels, measuring the bone hoop stresses. Significant differences between the two designs were tested using a Paired T-test (p=0.05).

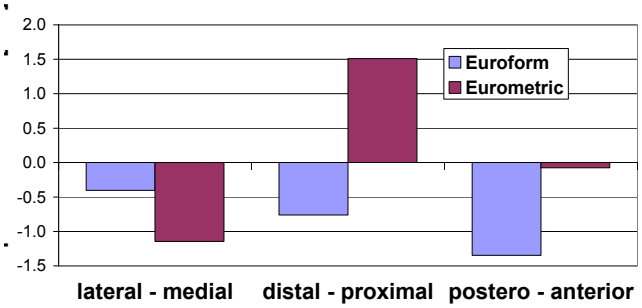

Figure 2 *Rasp-stem mismatch for the two implant designs.*

RESULTS

The rasp-stem mismatch was very low for both implant designs (Figure 2). A significant difference from zero was found only in the proximal direction with the Eurometric implants. The results of the first experiment indicated that in the reconstructions with the Eurometric stems the loads were mainly transferred in the proximal region, while in the reconstructions with the Euroform stems the loads were transferred more distally, although this difference was not statistically significant (Figure 3, right). Furthermore, the subsidence of the Eurometric stems tended to be lower than in the reconstructions with the Euroform stems. The RSA-results of the torque-load experiment showed that the Eurometric stems migrated more, although again the difference with the Euroform stem was not statistically significant.

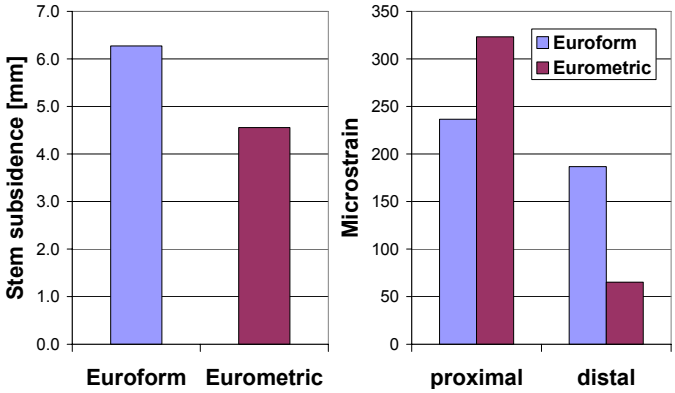

Figure 3 *Stem subsidence (left) and location of load transfer (right) for the Euroform and Eurometric implant.*

DISCUSSION

The results of the experiments indicate that the design objectives of the Eurometric implant concerning the proximal load transfer and increased stability were met. This mechanism of proximal load transfer is only effective if the bone is of good quality. Implantation in bone with poor proximal bone stock may compromise the (rotational) stability. The new design will function optimally with very good proximal bone quality and creates slightly less stress shielding than the old design, thereby providing a sound basis for long-term fixation.

ACKNOWLEDGEMENTS

This study was supported by DePuy France SAS

AFFILIATED INSTITUTIONS
**Orthopädische Klinik, St. Vinzenz Krankenhaus, Düsseldorf, Germany.

MODEL-BASED RSA OF A HIP STEM USING GEOMETRICAL SHAPE MODELS

*Kaptein BL, *,**Valstar ER, *Spoor CW, ***Stoel BC, ***Reiber JHC, *Rozing PM
*Biomechanics and Imaging Group, Dept. of Orthopaedics, Leiden University Medical Center, Leiden, The Netherlands
**Dept. of Biomechanical Engineering, Faculty of Mechanical, Marine, and Materials Engineering, Delft University of Technology, Delft, The Netherlands
***Dept. of Radiology, Division of Image Processing, Leiden University Medical Center, Leiden, The Netherlands
B.L. Kaptein@lumc.nl

INTRODUCTION

Roentgen stereophotogrammetry (RSA) is a highly accurate three-dimensional (3-D) measuring technique for assessing micromotion of orthopaedic implants. To facilitate accurate measurements, at least three noncollinear spherical tantalum markers must be inserted in the host bone and attached to the implant. Because of regulatory issues, attaching markers to implants is a difficult and tedious task. One alternative that does not rely on attached implant markers involves creating a surface model of the implant. Another alternative to attached markers is the use of elementary geometrical shapes (EGS) (eg, straight lines, spheres, circles, and cones) to create a representation of the implant. The EGS model-based RSA technique might not be used for implants that have more complex shapes, such as femoral components in total knee arthroplasty.

GOAL

The aim of our study was to validate and compare two different model-based RSA techniques (model-based RSA using surface models, and model-based RSA using elementary geometrical shape (EGS) models) to determine micromotion of a commercially available hip stem. We assessed if model-based RSA techniques were an accurate alternative for marker-based RSA.

EXPERIMENTS

The two model-based RSA methods were validated by an in vitro phantom experiment and compared in an in vivo experiment. Laser scanning was used to produce reverse engineered models for each implant size.

We tested two stems simultaneously during an in vitro validation experiment. One stem was marked with three spherical tantalum markers. Each stem had a 28 mm head attached and was rigidly fixed in a sawbone with eight tantalum markers attached at clinically representative locations. Twelve RSA radiographs were obtained in random, clinically relevant orientations. Migration was measured between the component and the bone using standard marker-based RSA (as a reference) and both model-based RSA techniques. There was no change in relative pose between the component and the markers in the sawbone, so for successive RSA radiographs, the mean of the calculated migrations measured the systematic algorithm errors. The standard deviation (SD) of the calculated migrations measured the accuracy of zero motion, or precision of the RSA algorithm.

The in vivo experiment was done with 19 RSA examinations of seven patients from a historical cohort. We calculated the migration between the model of the hip stem and the three markers attached to the hip stem. Because the motion between the implant and its attached markers was zero, the mean and standard deviation provide information about the accuracy and precision of the RSA algorithm.

TABLE 1: Mean and Standard deviation of migration between implant and bone in phantom experiment

	X (mm)	Y (mm)	Z (mm)	Rx (deg)	Ry (deg	Rz (deg)
Implant markers	-0.00 (0.05)	-0.03 (0.04)	0.02 (0.12)	0.00 (0.10)	0.04 (0.28)	0.02 (0.07)
Surface model	-0.03 (0.15)	-0.01 (0.13)	0.02 (0.21)	-0.03 (0.35)	-0.01 (1.76)	000 (0.24)
EGS model	0.02 (0.07)	0.01 (0.08)	-0.01 (0.14)	-0.01 (0.16)	0.05 (0.61)	-0.00 (0.10)

TABLE 2: Mean and Standard deviation of migration between implant and implant markers in clinical data

	X (mm)	Y (mm)	Z (mm)	Rx (deg)	Ry (deg	Rz (deg)
Surface model	0.00 (0.05)	0.01 (0.17)	-0.01 (0.20)	-0.02 (0.12)	-0.06 (0.59)	001 (0.06)
EGS model	-0.00 (0.07)	-0.01 (0.15)	0.02 (0.17)	0.03 (0.11)	0.06 (0.70)	-0.01 (0.07)

RESULTS

The phantom experiment showed that the accuracy of model-based RSA using surface models is the same as the accuracy of marker-based RSA, however, the precision is lower than the precision of marker-based RSA. No significant differences in accuracy and precision were found between the EGS model-based RSA algorithm and marker-based RSA (Table 1). In contrast to the results from the phantom experiment, the clinical data did not show large differences between the two model-based RSA algorithms (Table 2).

DISCUSSION

Main advantage of EGS model-based RSA compared with model-based RSA using surface models is that in EGS model-based RSA there is no difference in shape between the model and component.

We are convinced that both model-based RSA algorithms are a possible replacement for marker-based RSA. However, because of its higher precision, for this hip stem, EGS model-based RSA provides the best alternative for marker-based RSA.

ISO TESTING OF EXPLANTED HIP STEM PROTHESES

*Kretzer JP, *Lee C, *Heisel C, *Thomsen M
*Laboratory of Biomechanics and Implant Research,
Orthopedic surgery hospital, University of Heidelberg, Germany

kretzer@arthroplasty-research.com

INTRODUCTION

Failures of implanted hip stems are rarely but may end up in severe complications for the patient in case of fracture.
The ISO requirements for testing the endurance properties of stemmed femoral components (ISO 7206) specified a load magnitude of 2300N and a number of $5*10^6$ applied load cycles to confirm the endurance properties.
The number of steps per year is about $2*10^6$ and the hip load reaches about 5000N during fast walking.
For two designs it was seen that laser gravures at the neck or the welding seams at head/neck level led to stem fracture.
Aim of the study was to investigate if the ISO requirements are sufficient for testing the in-vivo fracture resistance of these two failure mechanism.
The focus was to determine if an increased number of applied load cycles or an increased magnitude of load cause failure of the implants.

METHODS

Five explanted stems (Alloclassic and Mueller straight design) which were at least five years in vivo (representing about $10*10^6$ load cycles) were exposed to a dynamic fatigue test by using an axial-load testing machine (Mini Bionix, MTS). First, the number of load cycles was increased to $30*10^6$ cycles. Second the magnitude of load was raised stepwise up to 4800N.
Additionally three implants were tested with an increasing load until the prosthesis or the embedding medium fractured. The implant fatigue strength was determined using the Locati technique. The tests were done by a frequency of 25 Hz.
The fractured components were inspected using SEM.

RESULTS

All five explanted hip stems survived the increased number of load cycles (in total $40*10^6$ cycles) and the stepwise load raising to 4800N without any visible signs of fracture.
With increasing load two prostheses fractured.
One fractured in the distal part of the stem at a load of about 8800N. The second prosthesis fractured at the neck region at a load of 12200N. This fracture started at the lateral part of the neck and grew to the medial part. Thus the laser gravure (which was located anterior) doesn't seem to be responsible for the fracture.

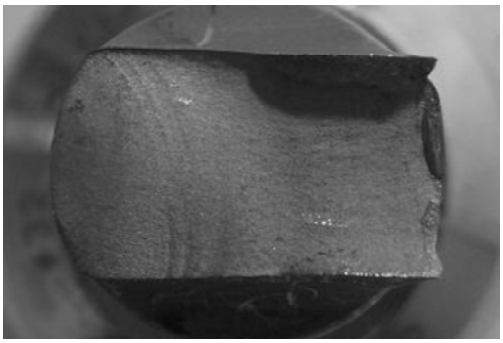

Fig. 1: Area of fracture

DISCUSSION

By increasing the number of applied load cycles six times and increasing the load magnitude two times above the ISO requirement no specific prostheses failure could be induced.
Fracture and failure of prostheses may occur in extreme stress situations.
Limitations which need to be considered are the unphysiological unidirectional load and the test frequency during the tests.
The ISO requirements seem to be sufficient for testing the endurance properties of prostheses. Nevertheless applying a higher amount of load cycles and a higher magnitude of load is recommendable to ensure the endurance properties of prostheses.

INITIAL STABILITY OF CEMENTLESS CUSTOM-MADE HIP PROSTHESES: GEOMETRICAL CONSIDERATIONS

*Labey L, *Jaecques SVN, *Gelaude F, **Mulier M, *Van der Perre G
*K.U.Leuven, Division of Biomechanics and Engineering Design, Leuven, Belgium
Luc.Labey@mech.kuleuven.be

INTRODUCTION

The stability of cementless hip prostheses is one of the determining factors for their long-term performance. We used the principle of virtual work and a straightforward mechanical model to obtain algebraic formulas to estimate the role of the geometry of custom-made hip stems in their initial stability. The initial stability of a set of ten custom-made hip stems was estimated and compared with the stability of the Charnley and 3M Capital hip stems.

METHODS

The geometry of the stem surface was described by a set of triangles (a so-called STL-description). In our simplified mechanical model, the resistive forces from the supporting bone are assumed to act at the centre of gravity of these triangles and to be perpendicular to their surface. Furthermore, frictional forces are neglected (although friction could be straightforwardly implemented in a later stage). The supporting bone is considered as a linear elastic material and the thickness of bone is supposed equal for all triangles.

According to the principle of virtual work:

$$R \cdot \delta r_O + M \cdot \delta\theta + \sum_i F_i \cdot \delta r_{Ci} = 0 \qquad (1)$$

with R and M the force and moment acting on the prosthesis and F_i the resistive force of the bone on triangle i. The prosthesis stem has six degrees of freedom, so (1) gives rise to six scalar equations. Here, we consider only the cases of subsidence, axial rotation and varus-valgus tilting.

RESULTS

From the mechanical model the resistance against subsidence, axial rotation and varus-valgus tilting can be easily derived. The resulting formulas are:

$$\frac{E}{\ell_0} \cdot \sum_i A_i \cdot n_{iz}^2 \qquad (2)$$

$$\frac{E}{\ell_0} \cdot \sum_i A_i \cdot \left(-y_{Ci} n_{ix} + x_{Ci} n_{iy}\right)^2 \qquad (3)$$

$$\frac{E}{\ell_0} \cdot \sum_i A_i \cdot \left(z_{Ci} n_{ix} - x_{Ci} n_{iz}\right)^2 \qquad (4)$$

where E is the Young's modulus of bone, A_i is the area of triangle i, ℓ_0 is the thickness of the supporting bone when it is undeformed, (x_{Ci} y_{Ci} z_{Ci}) are the coordinates of the centre of gravity of triangle i and (n_{ix} n_{iy} n_{iz}) are the components of the normal vector of triangle i.

The resistance against subsidence, axial rotation and varus-valgus tilting was derived for a set of ten custom-made hip stems that were previously implanted in patients. The results were compared with the results for a standard Charnley hip stem and a Capital hip stem (both of which are cemented prostheses).

a b c

Fig. 1: (a) Charnley, (b) Capital and (c) custom made hip stems.

Resistance values are shown in Table 1. For the ten custom-made designs only the average, standard deviation and range are given.

Table 1: Resistance against a) subsidence b) rotation c) tilt

	(a) [10^8 N/m]	**(b)** [10^{10} Nm/rad]	**(c)** [10^{13} Nm/rad]
Average	**6.66**	**14.38**	**2.95**
StdDev	2.17	6.95	2.04
Min	3.14	2.42	0.66
Max	10.80	23.80	7.50
Charnley	**1.83**	**2.47**	**0.62**
Capital	**1.85**	**1.67**	**0.41**

DISCUSSION

Average geometric resistance values for the uncemented custom stems are significantly higher than for the cemented reference stems ($p<0.01$). This was expected, as the custom stems cannot rely on cement for primary stability. Regarding resistance against rotation and tilting, the Capital has the lowest values of all considered designs and the highest failure rate [1].

These findings support the relevance of the derived geometric parameters for the stability of hip prosthetic stems, although the comparison between cemented and non-cemented designs requires further analysis.

CONCLUSION

Based on a simple mechanical model, a relation was established between the geometry of a hip stem and its stability. Future work will include validation of this relation with clinical data from custom hip stems.

ACKNOWLEDGMENT: K.U.Leuven grant OT/03/31.

REFERENCES

[1] Roy N et al Acta Orthop Scand 2002;73(4):400-402.

AFFILIATED INSTITUTIONS FOR CO-AUTHORS:
**Dept. Orthopaedic Surgery, Univ. Hospital Leuven.

WHICH LENGTH DO WE NEED FOR GOOD PRIMARY STABILITY IN THA

*Lee C, *Jakubowitz E, *Bitsch R, *Thomsen M,
Orthopeadic Surgery Hospital, University of Heidelberg, Germany

Christoph.Lee@ok.uni-heidelberg

INTRODUCTION

Primary stability is a most important parameter for the successful osseointegration of a cementless hip prosthesis and many standard stems do very well. With the new generation of short or neck preserving stem designs the length needed for good primary fixation is a matter of discussion.

The aim of the study has been the determination the optimal length for the shortening of a standard stem until it looses stability regarding rotation and tilting.

METHODS

The primary stability of five successful prostheses (AGB®/ Size 6, Proxilock®/ Size 10, G2®/ Size 7, CLS®/ Size 10 and BiContact®/ Size 13) was characterized using a well established experimental model for the measurement of spatial micromovement with six degrees of freedom.

All prostheses were prepared by an experienced surgeon and pressed into a synthetic femur (Composite Bone # 3106, Pacific Research Lab) in two steps of 25 cycles, first with 2000 N followed by 4000N.

Torsional as well as tilting loads were applied and the complex response was recorded under standard length conditions. Since recordings are taken regularly at several measuring points, behavior like twisting or bending of stem and bone can be seen reliably as well.

Then the prostheses were shortened consecutively and the measurements were repeated to find the “critical” length.

RESULTS

With consecutive shortening the primary rotational stability did not change for proximal locking designs (At the level of the lesser trochanter: ABG® 5.4 mdeg/Nm, G2® 5.9 mdeg/Nm) or little (CLS® 5.7 mdeg/Nm, Proxilock® 7.8 mdeg/Nm). With the shortening steps the remaining length at which the prostheses tilted like a rigid body were determined (ABG® 9 cm, G2® 8.5 cm, CLS® 8.8 cm, Proxilock® 9.5 cm).

For further distally locking systems the anchoring quality partly changed from distal to proximal. The primary stability decreased which each shortening step (BiContact® 8.1 mdeg/Nm up to 16.2 mdeg/Nm). The tilting properties were determined as well (BiContact® 11.4 cm).

DISCUSSION

Shortening of proximally locking regular length prostheses may be an ideal step in the development of short stem prosthesis. Shortening of more distally locking designs may be interesting as well if the remaining primary stability is sufficient.

Determining the length at which the prostheses started tilting like rigid bodies is important because stress peaks at the lateral cortex may occur and they are a plausible reason for occasional clinical problems. They occur much earlier than more fatal consequences such as perforation of the cortical bone.

We consider a certain elastic deformation (counter swing) of the implant important and that depends on the length of the design.

PRE-CLINICAL VALIDATION OF A NEW CONSERVATIVE PROXIMAL EPIPHYSEAL REPLACEMENT

*Martelli S, **Moindreau M, °Rushton N, °°Field R, *Viceconti M
*Istituti Ortopedici Rizzoli, Bologna, Italy
martelli@tecno.ior.it

INTRODUCTION

Aim of this study is to investigate the mechanical behavior of a new implant design under different conditions using a subject-specific finite element modeling (FEM) method. The subject-specific FEM model of a human femur implanted with a new prosthetic design was developed and validated against experimental measurements. The model was then modified to simulate an osteoporotic femur, different levels of cement interdigitation and uncertainties in prosthesis position during surgery. Results were used to assess the risk associated to a number of failure scenarios, including increased risk of spontaneous femoral neck fracture, accumulation of cement damage, stem-cement fretting, and adverse bone remodeling. The new stem presents negligible risk for all these scenarios.

METHODS

A human femur without any evident pathological condition was scanned with a Computed Tomography (CT). The geometry of the bone was extracted from the CT scan. An experienced surgeon defined the position of the prosthesis inside the femur using a CT-based pre-operative planning environment (HipOp v1.4, B3C, Italy). The subject-specific FEM model was generated following a well-established procedure [1]. The model was loaded with conditions that simulated joint and muscular loads acting on the proximal femur during level walking, stair climbing and single leg stance [3]; these activities were found to be the most critical among those commonly performed by THR patients with respect to the failure scenarios to be investigated. For each activity the instantaneous loading condition that produced the peak hip joint force was simulated.

To simulate the presence of osteoporosis, the tissue density was decreased to typical values found in mildly and severely osteporotic patients [2].

The surgeons reported a typical range of values for the thickness of the fully interdigitated bone, based on radiographic observations made on similar implants. The extreme values of this range were modeled in the present study.

From trial surgical session on cadavers, we estimated a typical uncertainty of 3 mm for the position of the stem with respect to the bone, compared to the ideal position defined during the CT-based preoperative planning. Positions mismatch of the prosthesis was simulated changing the prosthesis position on the frontal plane medially, laterally, distally and proximally of this extent.

We run large number of simulations, due to the combination of loading conditions, degree of simulated osteoporosis and surgery-related parameters (interdigitation and stem position).

Results were collected in terms of bone strains, cement stresses, bone-implant micromotion, and changes in strain energy density from the intact femur.

RESULTS

In all simulations the peak bone strains were induced in the superior-lateral aspect of the femoral neck, in agreement with the experimental results obtained *in vitro*. In all cases, the presence of the stem did not increase the femoral neck strains with respect to the intact femur, suggesting that the risk of femoral neck fracture is not increased by the presence of the stem.

The stress in the cement was found to be in all cases lower than 10 MPa, e.g. well below the fatigue limits of the bone cement. Thus, the risk of cement cracking due the cyclic loading seems very unlikely.

The bone-implant micromotion, as predicted at the frictional large sliding interface, was always below 35 microns. This amplitude is small enough to be accommodated by elastic deformation of the cement crests, preventing any fretting damage to be produced.

Last, but not least, the changes in strain energy density due to the insertion the stem were below the threshold commonly considered for the activation of adverse bone remodeling processes.

DISCUSSION

The new stem design presents minimal risk associated to the investigated failure scenario, within a broad range of conditions relative to the patient and to the surgical procedure. If these results are confirmed by controlled experiments *in vitro*, we can recommend the use of the device in clinical experimentation.

REFERENCES

1.Taddei, F., et al., J Biomech, 2005. **5**: p. 5.
2.Polikeit, A.. J Biomech, 2004. **37**(7): p. 1061-9.
3.Bergmann, G., et al. J Biomech, 2001. **34**(7): p. 859-71.
4.Huiskes R, et al. J Biomech. 1987;20(11-12):1135-50),

ACKNOWLEDGMENTS

The present work was carried out thanks to the financial support of Stryker Corp.

** Stryker Orthopaedics, Benoist Girard, Caen, France; ° The Orthopaedic Research Unit, University of Cambridge, UK; °° The Orthopaedic Research Unit, St Helier Hospital, London, UK

BIOMECHANICAL CHARACTERIZATION OF THE PROXIMAL INTACT FEMUR

*Pallini F, *#Juszczyk M, *°Schileo E, *Taddei F, *#Cristofolini L
*Istituti Ortopedici Rizzoli, Laboratorio di Tecnologia Medica, 40136 Bologna, Italy
cristofolini@tecno.ior.it

INTRODUCTION

There is renewed interest in resurfacing hip prostheses. While stemmed prostheses have been extensively studied in the past, little is known about the biomechanics of proximal epiphysis. Our aim was to develop a combined experimental-numerical tool to study the intact proximal epiphysis. Experimental procedures and tools were adopted to this scope. Bone stress and failure mode in the intact femur were investigated.

METHODS

Twelve human cadaver femurs were studied intact, to fully characterize the proximal epiphysis. They were tested in the elastic range, while strains were measured with 15 rosettes.

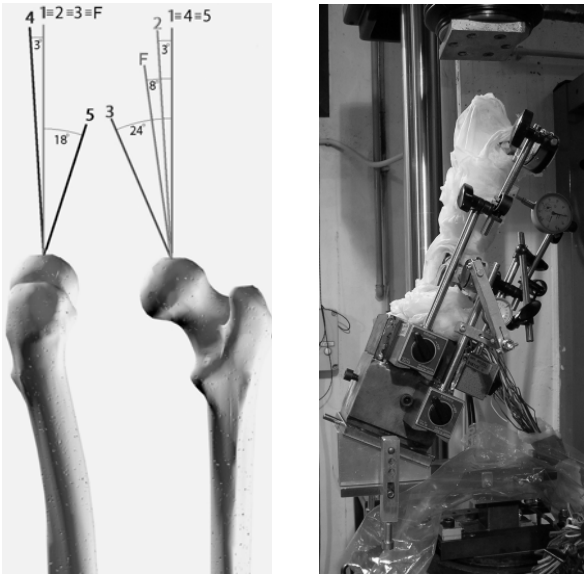

Fig. 1 – *Left:* right femur (lateral & posterior views) with the direction of the hip joint force in simplified loading scenarios 1-5 (non-destructive tests) and F (test to failure). *Right:* Schematic anterior view of the femur tilted in the frontal plane. The load cell for detecting the position of the resultant force is visible below the specimen (covered by a plastic sheet). Also visible are the 4 dial gauges for measuring deflection in the two directions

A total of 5 load scenarios were simulated to cover the range of typical motor tasks[1]. The actual position of the resultant force is extremely critical in achieving good agreement between FE and experimental simulation. A strain-gauge based transducer was designed that allowed measuring the position of the vertical force by measuring the bending moment in two directions. To allow extensive validation of the FE model, additional measurements were taken *in vitro*: bone deflection in various points; digitizing of bone surface and gauge locations[2].

The FE model was also used to identify the relevant load scenario to recreate *in vitro* spontaneous head-neck fractures, typical of elderly, osteoporotic subjects (F in Fig.1).

RESULTS

Strain measurements were successfully obtained in the intact femurs, providing the natural strain pattern. Inter-specimen unpaired variability was 18-50% in the head-neck region and 15-45% in the diaphysis. Variability within pairs was 2-3 times lower. The transducer was able to measure the position of the resultant force with an intrinsic accuracy of 1.4mm.

In vitro failure tests were successful: all specimens fractured, with a variety of failures ranging from sub-capital to trans-trochanteric (Fig.2).

Fig. 2 – Failed intact femurs, showing a variety of fractures ranging from sub-capital (left) and neck base (right).

DISCUSSION

These results confirm the suitability of this test model to investigate physiological stress and to replicate spontaneous fractures in elderly subjects. This method successfully predicts the stress distribution and failure mode in the proximal femur.

REFERENCE:

1. Taddei et al., J Biomech. 2005;[Epub ahead of print].
2. Schileo E. (2006) EORS.

AFFILIATED INSTITUTIONS FOR COAUTHORS:

#University of Bologna, Engineering Faculty, V. Risorgimento 2, 40136 Bologna, Italy. Tel: +39 051 2093266, Fax +39 051 2093412. E-mail: luca.cristofolini@unibo.it
°University of Padua, Engineering Faculty, Via Gradenigo 6A, 35139 Padua, Italy Email: enrico.schileo@unipd.it

SAMPLE SIZING MULTI-FEMUR FINITE ELEMENT ANALYSIS OF IMPLANT DESIGNS

*Radcliffe I, **Prescott P, ***Man HS, *Taylor M
*Bioengineering Research Group, University of Southampton, Southampton, UK
iajr@soton.ac.uk

INTRODUCTION

Finite element analysis (FEA) has been used extensively in the analysis of the skeleton, tissue growth, remodeling and most frequently in the analysis and design of orthopaedic devices[1]. The use of patient specific Computer Tomography (CT) based FE models has become commonplace over the last decade; and has been shown to be an effective analysis tool[2]. It was however noted by Pancanti et al.[3] that implant performance varies as much between patients as it does between tasks. The aim of this work is to investigate the levels of inter-patient variation within a group of femurs: to deduce whether or not a multi-femur analysis is necessary to assess an implant design, and determine a suitable sample size. The analysis will be undertaken on a group of 16 femurs, comparing the strain levels in the intact femurs and after the femoral head resurfacing arthroplasty.

METHOD

CT scans of a group of 16 femurs were used to create 3D FE models of the intact and resurfaced states. The patients in this study varied in weight from 54-136kg (mean value 95.3kg). Models were solid meshed using I-DEAS and analysed in ANSYS. Material properties were assigned based on the CT Data using the freeware program BONEMAT[4]. Physiological loads, proportional to the patient's body weight, representing contact force and abductor muscles were applied in accordance with Bergmann et al.[5].

RESULTS

The femurs were divided into 20 zones for comparative analysis of the mean "Von Mises" strains. The results for the whole group were compiled to give mean values and standard distribution for each section of the femur.

Plots of the equivalent strain levels show the stress shielding induced by the resurfacing implant as reported by Shybut et al.[6]. Strains ranged from 1000-6000με with a significant correlation to the patient's weight noted in every section of the femur. Statistical methods[7] were employed, using these results as part of an estimation study, to determine the sample size required to estimate the effect of the resurfacing implant to a given accuracy.

$$n > \frac{8\sigma^2}{w^2} \qquad \text{Equation 1}$$

The sample size calculation (Equation 1) determines the minimum number of samples {n} to provide results to a given accuracy {w}; also known as the maximum sampling error, chosen as 10%. The calculation is based on the within-subject standard deviation {σ} calculated as the standard deviation of the percentage change in strain.

DISCUSSION

The results of comparison between intact and resurfaced femurs agree with the findings of previous studies[6].

The sample size calculations used in this study determined that a sample size of 10 femurs would be required for the analysis to produce result with 90% a confidence levels. The necessity of this sample size was shown by randomly selecting groups of 3 femurs from the full 16 and comparing the percentage change in strain between the intact and resurfaced femurs for these groups. Figure 1 shows how in one particular section of the femoral neck the group selection can vary an analyst's interpretation of the strains. Reviewing group 1 confidently shows the implant to increase strain (with a narrow confidence interval); group 2 would show load shielding within the section, but with a wider confidence interval. Group three shows a larger increase in strain with a wide confidence interval casting doubt on its accuracy. A random selection of 10 femurs shows an increase slightly greater than the full group but with a similar confidence interval.

This analysis concurs with the findings of Pancanti et el.[3], showing the large effects of inter-patient variation. It concludes that for a confident FE analysis of this implant design, a minimum of 10 femurs is required.

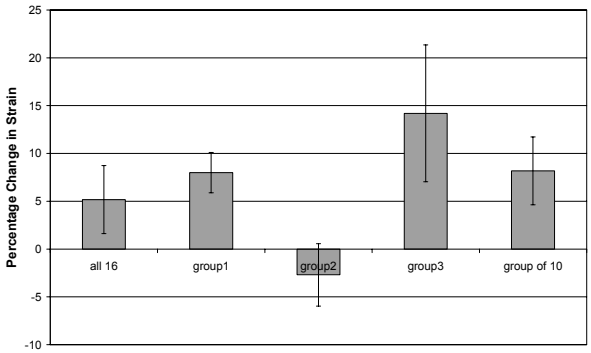

Figure 1: Comparison of the Percentage change in Strains of randomly selected groups of femurs within the selection of 16 in a section of the femoral neck

REFERENCES:

1. Prendergast, P. Clinical Biomechanics, 1997. **12**(6): p. 343-366.
2. Keyak, J.H. et al. MED ENG & PHYS, 2003. **25**: p. 781-787.
3. Pancanti, A., et al. Journal of Biomechanics, 2003. **36**(6): p. 777-85.
4. Taddei, F., et al. Med Eng & Phys, 2004. **26**: p. 61-69.
5. Bergmann, G., et al. Journal of Biomechanics, 2001. **34**: p. 859-871.
6. Shybut, G., et al. Trans Am Soc Art Intern Organs, 1979. **25**: p. 24-26.
7. Julious, S.A., Statistics in Medicine, 2004(23): p. 1921-86.

ACKNOWLEDGEMENTS:

DePuy is gratefully acknowledged for the supply of CT Data and for supporting this research.

AFFILIATED INSTITUTIONS FOR CO-AUTHORS:

** School of Mathematics, University of Southampton, Southampton, UK
*** Hartington Statistics and Data Management, London, UK

STRAIN PREDICTIONS ACCURACY IN FINITE ELEMENT MODELS OF LONG BONES FROM CT DATA

*Schileo E, *Taddei F, **Helgason B, *Pallini F, *,***Cristofolini L, *Viceconti M
*Laboratorio di Tecnologia Medica, Istituti Ortopedici Rizzoli, Bologna, Italy

schileo@tecno.ior.it

INTRODUCTION

The determination of the mechanical stresses induced in human bones is of great importance in both research and clinical practice. Since the stresses in bones cannot be measured non-invasively *in-vivo*, this can be done through subject specific finite element models. Subject-specific finite element models of bones from Computed Tomography (CT) data could bring to an accurate prediction of stresses and strains because of their ability to include local information about geometric and material properties. However, thorough finite element method (FEM) validation against in vitro experimental measurements is required before this method can be used in the clinical practice. At present time only few studies report extensively on stresses and strains prediction validation. In a previous study [1] a method was proposed for the automatic generation of finite element models from CT data and its accuracy in the prediction of superficial bone stresses was checked against experimental tests. However, focusing the attention on strain comparison makes the validation possible with direct experimental measurements (coming from strain gages). Moreover, assessing the accuracy on strain predictions meets the growing consensus on the importance of strain-based criteria for the failure of bone. The aim of this study is thus to improve the proposed modelling technique to enhance the strain prediction ability on long bones.

METHODS

Eight osteoporotic cadaver femurs were used in this study. All the femurs were CT scanned. Subject-specific finite element models of all the femurs were built starting from CT-data using an automatic procedure which has already been validated [1]. Bone mechanical properties were assumed as isotropic but inhomogeneous. In order to improve the accuracy in the definition of the finite element material properties derived from CT-data, a new mapping algorithm was applied. Moreover, three different density-modulus relationships were identified from the literature [2-4] and tested. All the femurs were tested in vitro under six different loading scenarios, which represent the maximum and minimum physiological angles of hip-reaction recorded in hip patients [5] during a wide range of activities. Strain were measured in 15 locations by triaxial strain gages, mostly placed in the structurally critical metaphysis-neck region. The boundary conditions and gage locations were replicated in the finite element models following a strict spatial registration procedure. The results of the experimental tests were then used to validate the FE models by means of descriptive and regression statistics on the comparison of experimentally measured and FEM calculated strains.

RESULTS

Results are reported for the material mapping law which led to the most accurate FEM calculation of strains in comparison with the experimental ones. The mean findings on calculations on the first 5 femurs studied are shown in the table below.

Experimental vs FEM strain comparisons Mean values on 5 femurs	
R^2	0.91
Slope	1.01
Intercept (□□)	6.66
RMSE%	11 %

DISCUSSION

An excellent agreement was reached between experimental measurements and FEM calculations. The choice of the density modulus relationship showed to be one of the most critical parameters to achieve a good overall accuracy in predicting the mechanical behaviour of a bone segment.

REFERENCES

1. Taddei et al., Subject-specific finite element models of long bones: An in vitro evaluation of the overall accuracy. J Biomech, in press.
2. Carter and Hayes, The compressive behavior of bone as a two-phase porous structure. J Bone Joint Surg Am, 1977. 59(7): p. 954-62.
3. Keller, Predicting the compressive mechanical behavior of bone. J Biomech, 1994. 27(9): p. 1159-68.
4. Morgan and Keaveny, Dependence of yield strain of human trabecular bone on anatomic site. J Biomech, 2001. 34(5): p. 569-77.
5. Bergmann et al., Hip contact forces and gait patterns from routine activities. J Biomech, 2001. 34(7): p. 859-71.

** Faculty of Mechanical and Industrial Engineering, University of Iceland, Iceland
***D.I.E.M., Engineering Faculty, University of Bologna

DEXA ANALYSIS TO COMPARE BONE REMODELLING BETWEEN IMPLANT TYPES: THE INFLUENCE OF MATCHING PATIENTS FOR PREOPERATIVE BONE QUALITY

*van der Wal BCH , **Rahmy A , *Grimm B , ***Blake GM , ***, *Heyligers IC , *Tonino AJ
*Dept Orthopaedics, Atrium MC, Heerlen, NL; **Dept Nuclear Medicine, Atrium MC, Heerlen, NL,
*** Dept Nuclear Medicine, Guy's Hospital, London, UK
bchvanderwal@yahoo.com

INTRODUCTION

The ABG-I and ABG-II femoral stems are both proximally HA-coated, cementless anatomic stems, which differ only slightly in design (shorter and thinner distal stem, polished distal stem, increased HA-coating on the shoulder, increased lateralization). Recently it was shown that the design changes from the ABG-I to ABG-II stem resulted in a better proximal bone preservation[1]. However, differences failed to become significant. Our hypothesis was that by retrospectively matching patients for preoperative bone quality, an important determinant for post-op bone remodeling[2], statistical power would increase and that the trend of better proximal bone preservation in ABG-II might become significant.

METHODS

24 ABG-II patients were compared to different ABG-I groups: a.) 24 patients from a prospectively randomized comparison previously published[1], b.) a large group of "combined" ABG-I patients (n=49) including those of a.) and c.) a group of 24 patients selected from the combined group to perfectly match the ABG-II group for gender, age and preoperative bone quality.

Preoperative dual-energy x-ray absorptiometry (DEXA) scans were acquired of the posteroanterior and lateral lumbar spine, the contralateral hip and the non-dominant forearm to classify pre-op bone quality according to the WHO definitions[3] (normal, osteopenic or osteoporotic). Postoperative DEXA scans were performed to measure periprosthetic bone mineral density (BMD) at 10 days (treated as baseline) and at various time points thereafter using a standard Gruen zone analysis. Results were expressed as the percentage change from baseline and the differences in BMD loss between both implants analyzed at 2 years follow-up (unpaired, double-sided student t-test). Clinical Merle d'Aubigne (MdA) hip scores were evaluated at the same moment of BMD measurements.

RESULTS

Bone preservation (less BMD loss) was better for the ABG-II than the ABG-I (all three groups) in the proximal zones 1 & 7 but also in the mid-stem zones 2 & 6 (Table 1) where even an average BMD increase was noted for the ABG-II (R6). In zone 7 BMD loss at 2 years for the ABG-II was only -4.1% but between -11.9 to -14.5% for the ABG-I depending on the group. In the distal zones 3-5 the BMD loss was less for the ABG-I than the ABG-II (except R4 for the matched and combined groups).

All these distinct differences between both ABG stems became more pronounced when the ABG-II was compared to the matched or the combined ABG-I group than the unmatched group (Table 2). In zone 7 the positive difference in BMD preservation increased from +7.9% (unmatched ABG-I) to 10.4% (matched and combined ABG-I). These difference became also statistically significant at p=0.03 and p=0.02 respectively. In zone 1 the difference (ABG-II-I) increased from +1.4% to 3.3% (matched) and 4.9% (combined). The p-value went down but the comparison remained statistically non significant. The same applied to R2 and R6.

	Relative BMD loss 2 years post-op [%]							
	----------ABG-I ----------						**-- ABG-II --**	
Gruen zone	**Unmatched[1]**		**matched**		**combined**		**Reference**	
	Mean	**SEM**	**Mean**	**SEM**	**Mean**	**SEM**	**Mean**	**SEM**
R1	**-9.3**	*2.6*	**-11.3**	*3.2*	**-12.9**	*2.1*	**-7.9**	*2.5*
R2	**-4.1**	*2.6*	**-7.8**	*3.3*	**-7.5**	*1.9*	**-3.5**	*2.0*
R3	**-2.9**	*1.7*	**-4.0**	*2.0*	**-4.6**	*1.2*	**-5.9**	*2.5*
R4	**-1.5**	*1.3*	**-3.8**	*1.6*	**-4.0**	*1.1*	**-2.8**	*1.2*
R5	**-1.7**	*2.4*	**-3.6**	*1.9*	**-2.9**	*1.5*	**-4.5**	*1.5*
R6	**-1.4**	*2.2*	**-2.6**	*2.2*	**-2.9**	*1.5*	**+2.8**	*2.8*
R7	**-11.9**	*3.3*	**-14.5**	*3.0*	**-14.4**	*2.1*	**-4.1**	*3.7*

Table 1: Relative BMD loss from baseline 2-years post-op [mean ± SEM] per ABG-I/II group.

	Difference BMD loss (ABG-II minus I) [%]					
	----------ABG-I ----------					
Gruen zone	**Unmatched[1]**		**matched**		**combined**	
	II - I	***p***	**II - I**	***p***	**II - I**	***p***
R1	**+1.4**	*0.70*	**+3.3**	*0.42*	**+4.9**	*0.13*
R2	**+0.7**	*0.84*	**+4.3**	*0.28*	**+4.0**	*0.16*
R3	-2.9	*0.34*	-1.9	*0.56*	-1.3	*0.65*
R4	-1.2	*0.49*	**+1.0**	*0.62*	**+1.2**	*0.48*
R5	-2.8	*0.33*	-0.8	*0.72*	-1.6	*0.46*
R6	**+4.2**	*0.24*	**+5.4**	*0.14*	**+5.7**	*0.08*
R7	**+7.9**	*0.12*	**+10.4**	*0.03*	**+10.4**	*0.02*

Table 2: Difference in BMD loss between ABG-II and ABG-I groups (grey = p<0.05).

DISCUSSION

There is a lot of evidence that the ABG-II stem leads to less bone loss and thus better bone preservations than the ABG-I particularly in the in the proximal zones 1 & 7. Both by matching the patients for preoperative bone quality or by increasing the group size of the ABG-I group, statistical power could be improved and a statistically significant difference could be validated for zone 7 in favor of ABG-II. This confirms that the philosophy behind the design changes from the ABG-I to ABG-II works in clinical application and the shorter, thinner stem, a polished distal tip and additional proximal HA coating enhances load transfer and bone growth stimulation in the proximal region which is critical for long-term fixation.

In future studies using DEXA, patients should be matched for preoperative bone quality to limit the number of patients which are needed to show differencesbetween implants which are only slightly different in design

REFERENCES

[1] van der Wal et al. Acta Orthopaedica, *in press*
[2] Rahmy et al. Osteoporos Int. 2004 Apr;15(4):281-9
[3] The WHO Study Group. Geneva, 1994

COMPONENT ALIGNMENTS IN NAVIGATED TKA

*Ensini A, *Bianchi L, **Leardini A, *Catani F
Istituti Ortopedici Rizzoli, Bologna, Italy
* VI Divisione Clinica Ortopedica, ** Laboratorio di Analisi del Movimento
andrea.ensini@ior.it

INTRODUCTION

Navigation-assisted surgery in total knee arthroplasty (TKA) is aimed at improving the accuracy with which prosthesis components are implanted in the bones, according to anatomical plane orientations. Traditional surgical techniques based on the identification of transepicondylar and intramedullary axes are replaced with those based on segmental anatomical frame definitions following anatomical landmark identification. These frames are offered on the screen to the surgeon to target in real time the alignment goal by adjusting position and orientation of the bone saw guides. However, immediately after sawing, final bone, and in case cement, preparation and component implantation is necessarily a series of operations performed manually by the surgeon. In the current study, we wanted to compare intra-operatively the final component alignments with the corresponding at the original resection planes.

METHODS

In this series, 25 Scorpio and 25 Optetrak TKAs were analyzed, assuming no major differences exist between the two designs for the purpose of the present study. The operation technique followed was that recommended by the Stryker Knee Navigation System (Stryker-Navigation, Kalamazoo, USA), which implies trackers attached through bone screws to the distal femur and proximal tibia and to the bone saw guides. An 'anatomical survey' defined anatomical frames for the femur and tibia, based on relevant anatomical landmark identification, and provided target orientations for all the relevant bone cuts. These references were targeted in all three anatomical planes, and bone cuts were made accordingly. Corresponding alignments of the bone resection planes in the frontal, sagittal and transverse planes for the femur and in the frontal and sagittal planes for the tibia were recorded, with a 0.5° resolution. Then, component implantation was performed and alignments were measured again by means of an instrumented probe. Because of the shape of the prosthesis components, only the alignments in the frontal plane for the femur and in the frontal and sagittal planes for the tibia were recorded.

For these three alignments, the differences between pre- and post-implantation were calculated.

RESULTS

The differences in alignment are reported in the Table. The values are the number of patients who showed the indicated (±1, ±2, ..) integer angular difference plus those with a 0.5° additional difference toward the relevant extreme (i.e. '+2' includes +2.0° and +2.5° difference, etc.), '0' including those within ±0.5° difference.

	-3°	**-2°**	**-1°**	**0°**	**+1°**	**+2°**	**+3°**
Femur frontal	0	0	6	29	8	7	0
Tibia frontal	0	2	5	36	5	1	1
Tibia sagittal	1	3	11	19	11	3	2

DISCUSSION

Surgical navigation is nowadays performed in many TKAs, and several studies in the literature have reported recently comparisons of final component alignment between those operated with the conventional or with the modern navigation techniques. Unfortunately, comparison is based on standard lateral and frontal radiograms, by looking manually at the different performance in femoral and tibial component alignments, together with overall lower limb mechanical axis. These measurements are affected by the manual measurements but mainly by the nature of the comparison, not really at the original characteristic results of the two techniques, i.e. at the resection planes immediately after bone preparation. The present study offers a figure for the different alignment between resection planes and final implanted components, necessarily the effect of the manual procedures implied in TKA for the final implantation of the components.

In the frontal plane of the femur, and in the frontal and sagittal planes of the tibia the difference in alignment before and after component implantation was larger than 1° respectively in 42%, 28%, 62% of the patients. Considering that 1° is the claimed achievable accuracy of the navigation systems, and that the correct alignment goal was achieved at the resection planes, these figures reveal that in a considerable number of patients the benefit obtained by navigation are then lost by the manual procedures implied in component implantation. Even more concerning is the observation that these procedures can result in 3° malalignment in several cases. These differences in alignment put also concerns in the post-operative statistical comparison between conventional and navigated TKAs.

THE EFFECT OF A MOBILE BEARING TOTAL KNEE PROSTHESIS ON CO-CONTRACTION DURING A STEP-UP TASK

*Garling E, **Wolterbeek N, **Velzeboer S, *Nelissen R *, *·***Valstar E, **Doorenbosch , **Harlaar J
Department of Orthopaedics Leiden University Medical Center, The Netherlands

e.h.garling@lumc.nl

INTRODUCTION

It was hypothesized that patients with a total knee prosthesis that allows axial rotation of the bearing (MB) will have more co-contraction to stabilize the knee joint during a step-up task than subjects with a fixed bearing total knee prosthesis (FB) where this rotational freedom is absent while having the same articular geometry.

METHODS

Surface EMG, kinematics and kinetics were recorded during a step-up task of a MB group (n=5), a FB group (n=4) and a control group (N=8). Surface EMG levels of thigh muscles were calibrated to either knee flexion or extension moments by means of isokinetic contractions on a dynamometer. During the step up task co-contraction indices were determined using this EMG-force model.

RESULTS

Controls showed a higher active ROM during the step-up task then the patient group, 96 vs. 88 degrees (p = 0.009). In the control group higher average muscle extension, flexion and net moments during single limb support phase were observed than in the patient group. During the 20-60% interval of the single limb support, MB patients showed a significant higher level of flexor activity, resulting in a lower net joint moment; however co-contraction levels were not different. Compared to the control group arthroplasty patients showed a 40 % higher level of co-contraction during this interval (p= 0.009). Control subjects used higher extension moments, resulting in a higher net joint moment.

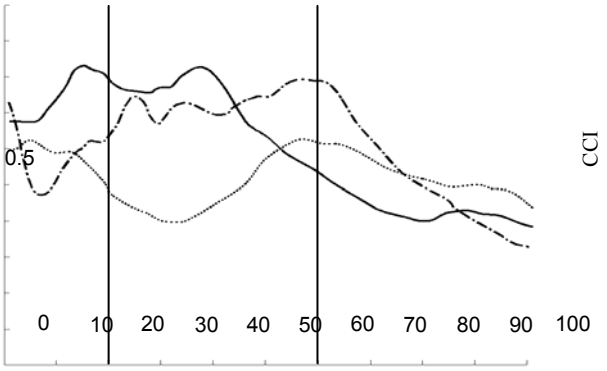

Figure 1. CCI values for the MB group (line), the FB group (dash-dotted) and the control group (dotted) during the single limb support phase. The 20%-60% interval is also indicated.

DISCUSSION

After total knee arthroplasty patients have a lower net knee joint moment and a higher co-contraction than controls, indicating avoidance of net joint load and an active stabilization of the knee joint. MB and FB patients showed no difference in co-contraction levels, although coordination in FB patients is closer to controls than MB subjects.

AFFILIATED INSTITUTIONS:
** Department of Rehabilitation Medicine, VU University Medical Center, Amsterdam, The Netherlands

*** Department of Biomechanics, Faculty of Mechanical Engineering, Delft University of Technology, The Netherlands

CAN A THICKER ALL-POLYETHYLENE UNICONDYLAR COMPONENT PROTECT THE TIBIAL BONE?

*Jeffers JRT, **Aram L, †Fitzpatrick D, *Barrett DS, *Taylor M
*University of Southampton, UK
j.jeffers@soton.ac.uk

INTRODUCTION: Unicondylar knee replacement is used to treat arthritis in patients where the condition is limited to either the medial or lateral tibio-femoral compartment. The all-poly tibial component allows for easier alignment and removes the metal/poly interface in the tibial component, but at the expense of component stiffness. One possible means to increase the stiffness of the all-poly tibial component (and therefore protect distal cancellous bone) is to increase the thickness of the component. A drawback of using a thicker component is that a deeper resection depth is necessary to maintain the same joint line. This may be undesirable as the cancellous bone strength deteriorates distally through the tibial condyles [1]. The aim of the current study is to determine whether the advantages of the thicker (stiffer) component are offset by the deeper resection depth and loading of weaker cancellous bone. A patient specific computational approach is taken, with both bone geometry and bone material properties taken from patient CT data.

METHODS: Finite element models of six tibiae were generated from CT data, and medial unicondylar replacements (of thickness 7mm and 9.5mm) were virtually implanted by an experienced surgeon (DSB). Material properties for bone were assigned using BONEMAT v2.1 (Laboratorio di Tecnologia Medica, Istituti Ortopedici Rizzoli, Bologna, Italy), which related the CT data to apparent bone density and subsequently Young's modulus. Elements were assigned material properties based on their coordinates and an integral of the CT data over the element volume (see [2] for details). Cement and polyethylene were assigned Young's modulus and Poisson's ratio of 2.8GPa and 0.3 and 0.5GPa and 0.3 respectively. Loading considered was two-point static rock, applied at the dwell point and an anterior point on the bearing surface.

RESULTS: Taking five layers of bone distal to the resection plane, the average Young's modulus was compared for each layer (Figure 1). Figure 2 shows the difference in average bone strains in the bone distal to the resection plane when the thicker 9.5mm component was used. Strains were generally increased by using the thicker component, but for the worst case scenario (Tibia C), the average strain was reduced. Figure 3 shows the volume of bone at a strain level greater than the yield strain value for bone (0.7%). Only Tibiae B and C had bone above this threshold value for either thickness component.

DISCUSSION AND CONSLUSIONS: Using the thicker component made no great difference in four out of the six tibiae (A, D, E, F), as bone quality was good (Fig 1). Tibiae B had significantly increased strains with the thicker component, as the good quality bone (Layer1) was removed to facilitate the deeper resection depth required to preserve the joint line. Because the bone in Layer1 for Tibia C was not stiffer than that further distally, using the thicker component was beneficial. Standard CT scans are capable of determining whether the patient has either a layer of stiffer bone that would benefit from a thinner component, or bone that would be suited to a thicker component. Out of curiosity, we modified the finite element models to simulate metal backed components in Tibiae B and C. The volume of bone above yield strain dropped to virtually zero for all thickness components/loadcases. We therefore propose that CT scans could prove useful in choosing the all poly component thickness (although the increased cost and radiological exposure should be considered), and in scenarios where bone quality is suspect, metal backed components are used.

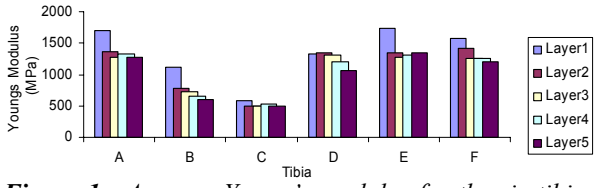

Figure 1: *Average Young's modulus for the six tibiae at layers distal to the resection plane. Layer 1 represents the most proximal layer.*

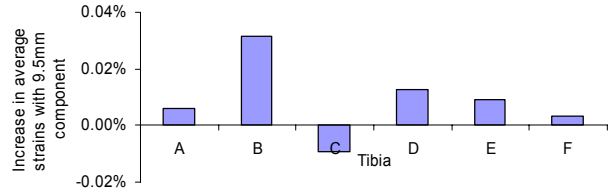

Figure 2: *Increase in average strain for the six tibiae in bone distal to the resection plane when the thicker component was used.*

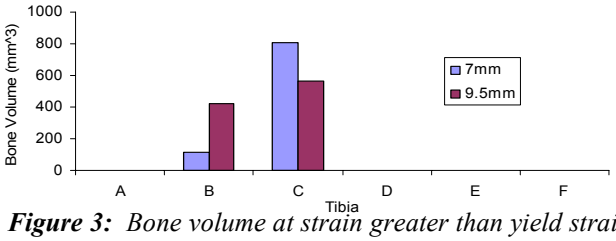

Figure 3: *Bone volume at strain greater than yield strain (0.7%) for the different thickness components.*

ACKNOWLEDGEMENTS: Niall Rooney (†) and Ian Radcliffe (*). Study funded by DePuy.

REFERENCES:

[1] Hvid (1988), CORR 227:210-21
[2] Taddei (2004), Med Eng & Phys 26:61-9

**DePuy, Warsaw, IN
†University College Dublin, Ireland

SURFACE GUIDED TOTAL KNEE USING KINEMATIC CRITERIA

Walker PS
Department of Orthopaedic Surgery, New York University – Hospital for Joint Diseases, New York, NY
ptrswlkr@aol.com

INTRODUCTION

Goals of knee replacement are to maximize function and restore the 'feeling of the normal knee' (Pritchett), which can be translated into achieving normal knee kinematics. For design and pre-clinical purposes, the criterion can be stated as 'after implantation, the neutral path of motion and the constraint, are the same as the intact knee'. The neutral path can be described as flexion of the femur about a transverse axis coupled with axial rotation of the tibia about a medial axis (Freeman, Churchill). The latter produces posterior displacement of the center of the femur with flexion. At each flexion angle there is rotational and AP laxity. Various test machines have been used for cadaveric testing, including derivatives of the Oxford rig and a special robot (Li & Rubash), while computer models have also been developed (Taylor). While retention of both cruciates in a total knee may be the ideal, resection is surgically preferred in about half of the cases. Cruciate function is then substituted by cam-post mechanisms and dished surfaces, but the kinematics is still not normal. This paper describes a method where normal kinematics can be provided by the contours of the bearing surfaces. The method can also be used to design cams and other features for further motion augmentation.

METHODS

The starting point was to to define a curve for the sagittal contour, and a set of tranverse profiles (fig 1). The patella groove profile was preserved up to the distal femur, but beyond that, the depth of the groove steadily diminished. The bearing spacing was reduced with flexion, while the side height was increased. This generating femoral component (GFC) was then placed on to a tibial block at zero flexion and a Boolean subtraction performed. The GFC was then placed at successive flexion angles with the required posterior displacement and rotation, and subtractions performed. Tibial surfaces were produced with rollback only (figs 2,3 left), and with rollback plus rotation (fig 3 right). The tibial surface was then smoothed. The GFC was larger than the actual femoral component so that there would be laxity in the resulting tibial surfaces. For more definitive posterior displacement with flexion, a central cam was designed in the same way, by defining a cavity in the intercondylar region. To prevent anterior femoral sliding with flexion, a further feature was added on the anterior lateral and medial sides. Finally, the outer profiles of the femoral and tibial components were designed around the surfaces.

RESULTS

The basic design of the femoral component had similar overall shapes and interior cuts to standard condylar knees (figs 2, 3) but the bearing surfaces were not standard, as described above. The tibial surface consisted of an anterior platform which contacted in extension, and a ramp which sloped from anterior to posterior. The interaction of this ramp with the diminishing height of the patella groove of the femur, caused a rollback of the femur with flexion. Premature rollback was prevented by the interaction of the sides of the femoral condyles and the ramps at the posterior corners of the tibia. Conversely, these latter features caused rollforward of the femur when the knee was extended from a flexed position. At all angles of flexion, rotational laxity was evident. For combined rollback and rotation (fig 3), the medial side of the tibia was more dished and it would act as a 'medial pivot' but with the rollback-rollforward motion of the lateral side guided by the interaction of the femoral and tibial surfaces. The motions were confirmed in a simple test machine, details beyond the scope of this paper.

DISCUSSION

The method enabled surfaces to be designed for defined kinematics. Guiding the motion by the interaction of femoral and tibial surfaces can replace the function of the cruciates and allow for rotational and AP laxity, which should result in more natural knee motion.

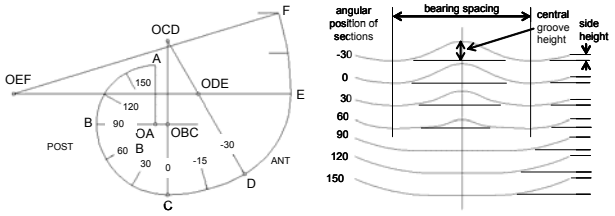

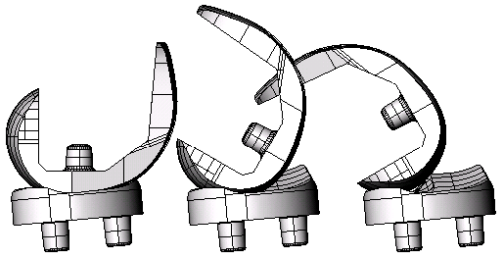

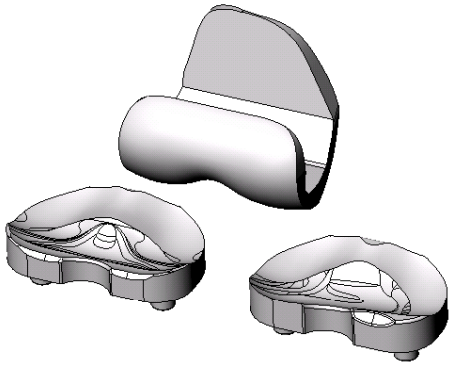

SUPRACONDYLAR HUMERUS FRACTURES IN CHILDREN: A BIOMECHANICAL ANALYSIS OF FOUR METHODS FOR OSTEOSYNTHESIS

*Castellani C, *Weinberg AM, **Arzdorf M, **Schneider E, ***Gasser B, **Linke B
Dept. For Paediatric Surgery, University Medical School Graz, Austria

c.castellani@gmx.at

INTRODUCTION

Supracondylar humerus fractures are among the most common lesions in children. Conservative treatment is suggested for undisplaced fractures, whereas displaced lesions have to be stabilized by osteosynthesis. Instable fixation may lead to torsion and thus to a loss of contact area. If the loss of contact area is big enough this may result in tilting of the distal fragment in the horizontal plane resulting in a cubitus varus deformation. Crossed K-wire osteosynthesis (CKO) has been suggested as standard procedure for surgical treatment of displaced supracondylar humerus fractures in children. Especially for the CKO a high rate of secondary displacements, resulting in such a deformity is reported in the literature. Therefore many authors suggest additional application of a cast to increase stability. However, a cast is also associated with disadvantages: functional after-treatment and clinical examination of the elbow axis are not possible and radiological diagnostics are difficult. These disadvantages of CKO led to the introduction of alternative methods as Elastic Stable Intramedullary Nailing (ESIN) and external fixation. Although clinically more and more established, there is no biomechanical data available comparing these methods. Therefore the aim of this study was first to obtain basic biomechanical data and second to analyze the performance of the aforementioned implants during a loading condition simulating functional after-treatment.

METHODS

32 adult cadaver humeri were randomized into four groups of 8 bones each by their bone mineral density obtained by quantitative computed tomography. For stabilization CKO, ESIN, a fixateur extern with k-wires as proposed by von Laer (FEL) and one with Schanz screws (FES) were chosen. In quasi static loading the stiffness values in flexion, extension and torsion were obtained. In cyclic loading the proximal fragment was subjected to a torsional moment causing external rotation and thus loss of contact area. A simultaneously applied compression was used to cause flexion of the distal fragment - or tilting, if the loss of contact area was big enough. These movements were chosen analogue to the mechanism reported as cause for a cubitus varus clinically. Data was managed using MATLAB ® and SPSS 11.0 ®. For statistical analysis non-parametric tests were applied due to the low number of specimen per group. First a Kruskal-Wallis-Test was applied to search for significant global differences between the implant groups. If a global significance was detected a Mann-Whitney-U-Test was performed to calculate the p-value.

RESULTS

Quasi static loading could reveal no significant global differences in flexion ($p=0.46$) and extension ($p=0.23$). In torsion a trend towards a higher stiffness of CKO was observed ($p=0.076$). In cyclic loading we could verify an irreversible torsional deformation below 20° for all methods ($p=0.22$) resulting in a low loss of contact area. Compared to the literature this implies the conclusion that all methods could prevent coronal tilting. Additionally we could ascertain a lower reversible torsional deformation for CKO and ESIN compared to the external fixators. 5 ESINs and one FEL failed during cyclic loading, in contrast to CKO and FES, where all bones passed the test. 1 CKO had to be excluded due to a technical problem of the testing machine.

DISCUSSION

The high drop-out-rate of ESIN in cyclic loading was probably due to the cadaver model using adult bones. Our biomechanical data reveal that the CKO has the highest stiffness in cyclic and lowest loss of reduction under cyclic loading. The external fixators proved to be good alternatives to CKO. Regarding the differences between any biomechanical test and the clinical situation it is difficult to draw direct conclusions to a functional after-treatment. Regarding our results we can only encourage a functional after-treatment with CKO - similar to the other methods where it is already clinically established - if a correct positioning of the wires can be assured intra-operatively.

ACKNOWLEDGEMENTS:

This study was financed by an AO Research Fund. Surgical implants were provided by the Dr. hc. Robert Mathys Foundation.

AFFILIATED INSTITUTIONS FOR CO-AUTHORS:

* Dept. For Paediatric Surgery, Medical University of Graz, Austria.
** AO Research Institute, Davos, Switzerland.
*** Dr. hc. Robert Mathys Foundation, Bettlach, Switzerland.

MAINTAINING ANATOMICAL REDUCTION WITH EXTERNAL FIXATION IN COMMINUTED INTR-ARTICULAR DISTAL RADIAL FRACTURES: A RADIOLOGICAL EVALUATION

*Clifton R, **Chowdhury A, **Soni RK,
*Bedford Hospital, Bedford, England

Rupert@doctors.net.uk

INTRODUCTION

Does external fixation alone maintain anatomical reduction of unstable distal radial fractures? Patients treated at Bedford Hospital with a Hoffman external fixator had five radiographic parameters measured preoperatively, postoperatively and at 12 week follow-up.

METHODS

Retrospective study of patients treated at Bedford District General Hospital between January 2001 and January 2004. All patients sustaining an unstable distal radius fracture were treated with a Hoffman external fixator alone. Standard anteroposterior and lateral radiographs were taken preoperatively, postoperatively and at 12 week follow-up. Measurements for dorsal angle, dorsal shift, radial angle, radial shift and radial shortening were recorded using the method of Van der Linden and Ericson.

RESULTS

There was no significant difference between the numbers of males and females, handedness of the patient or side of injury. Mean age was 46. 87% of patients sustained a fall causing the fracture. External fixation significantly improved dorsal angulation, dorsal shift, radial angle and shortening ($P<0.005$) when compared to pre-operative values. This improvement was maintained at 12 week followup.

DISCUSSION

Our findings are in agreement with other studies that have examined the efficacy of external fixation to maintain reduction. The correction of dorsal angulation has been shown to be particularly important in achieving better functional outcomes. In our study the mean dorsal angulation preoperatively was 23.8 degrees which improved to a mean at follow-up of 3.65 degrees. Severe radial shortening is thought to cause disruption of the distal radioulnar joint leading to impaired pronation and supination. Our data demonstrate external fixation is effective at maintaining radial length once corrected by manipulation.

Our study could be critised for not accounting for ulnar variance in measuring radial shortening. However due to ethical issues we could not irradiate an uninjured wrist. Our paper does no explore clinical function or patient satisfaction but this has been extensively reported on by other authors. Patients may lose anatomical reduction later than 12 weeks.

In conclusion external fixation is effective in maintaining anatomical reduction, as assessed by validated radiological parameters in the management of comminuted displaced intraarticular fractures of the distal radius.

**Bedford Hosptial, Bedford, England

THE GEOGRAPHY OF FEMUR FRATURES IN PORTUGAL

*de Fátima de Pina M, *Alves S, *Barbosa MA
*Instituto de Engenharia Biomédica, Laboratório de Biomateriais, Porto University, Porto, Portugal

fpina@ibmc.up.pt

INTRODUCTION

The hip fractures are the most serious consequence of osteoporosis and affects million of people around the world. The knowledge of the spatial distribution of hip fractures can help health decision-makers to plan intervention and prevention actions to reduce fractures and improve quality of life. The objective of this paper is to map, describe, quantify, and evaluate the spatial distribution of hip fractures incidence in Portugal, using Geographical Information Systems and Spatial Statistical tools.

METHODS

From the National Hospital Inpatients Data Registers, all admissions from 2000-2002 of individuals over 50 years age old with a hip fracture caused by low or moderate impact were selected. The population census of 2001 was used to calculate the direct age adjusted cumulative rates in municipality level. Due the Small Number Problem, the rates were smoothed by the Empirical Bayesian (EB) method. Exploratory Spatial Data Analysis (ESDA) techniques were used to measure spatial dependency and identify spatial clusters.

RESULTS

From the total admissions selected (n = 25 634), about 77% were women, with a mean age of 80.6 (standard deviation SD 8.6) years old while men have a mean age of 77.7 (SD 10.0) years old. The cumulative incidence rates rank from 463.3 to 1716.7 in women and 232.0 to 694.4 (per 100 000) in men. The Index of Spatial
Autocorrelation, Moran's I, for women and men rates were, respectively, 0.56 and 0.45. The incidence of hip fractures increases with age and it is greater in women in all Portuguese regions (female-to-male ratios varying from 1.5 to 5.1). There is a strong geographic pattern with clusters of high incidence in Northeast, South and part of Center and clusters of low incidence in Center-south and Northwest.

DISCUSSION

The health-disease process is not only a result of biological and genetic factors but also a result of territorial occupation and socio-economical and environmental conditions that together form the totality of external elements that influence the health and the welfare of populations. The use of Geographical Information Systems allowed the description of the femur fracture occurrence in Portugal and, together with spatial statistics, the identification of significant geographical clusters, which were found to have different patterns for men and women. Osteoporosis is considered an important problem in public health. However, its prevention can only be obtained if its real intensity nationwide is known. The fact that the standardized rates for hip fractures have different expression within regions of the country, varying about 2.9 times in men and 3.7 times in women, indicates that this event cannot be viewed only as a result of ageing, and suggests the influence of external factors, such as environmental, social, economical, behavioral.

CORONOID FRACTURE SIZE IN TERRIBLE TRIAD INJURIES

*Doornberg JN, van Duijn PJ, *Ring D
*Orthopaedic Hand and Upper Extremity Service, Massachusetts General Hospital,
Harvard Medical School, Boston MA

jdoornberg@partners.org

INTRODUCTION

The coronoid fractures that occur in the terrible triad pattern of traumatic elbow instability (posterior dislocation with fractures of the radial head and coronoid (C&D)) are usually small transverse fragments. Attempts to classify these fragments according to size as suggested by Regan and Morrey have been inconsistent and contentious. The purpose of this study is to quantify coronoid fracture size in terrible triad injuries.

METHODS

The height of the coronoid process of the ulna and the coronoid fracture fragment were measured on computed tomography scans of 13 patients with terrible triad pattern elbow injuries. Two observers performed the measurements with excellent intra- and interobserver reliability (Pearson correlations all 0.94 or greater).

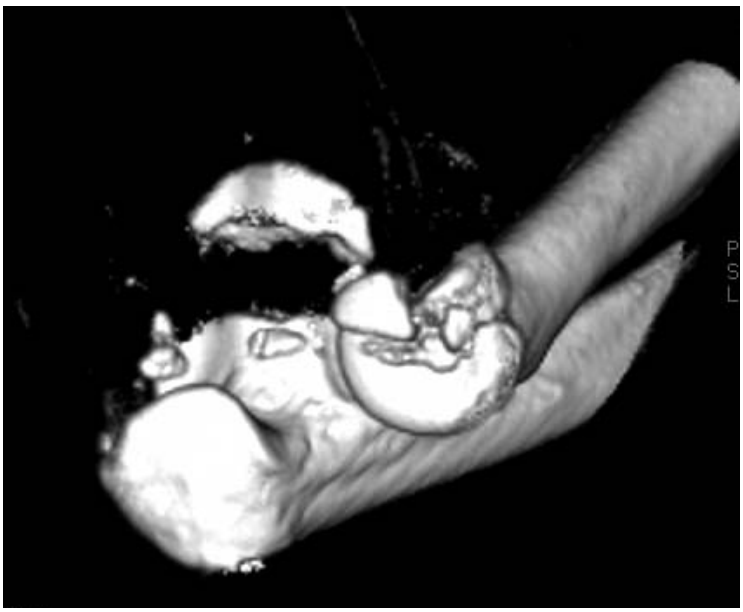

RESULTS

The total height of the coronoid process of the ulna averaged 18.7 mm (range, 12.1 mm to 25.3 mm). The average size of the coronoid fracture fragment was 6.7 mm (range, 2.6 mm to 11.5 mm). This corresponds to an average of 35% of the total height of the coronoid process (range, 19% to 59%).

DISCUSSION

The transverse coronoid fractures associated with terrible triad elbow injuries have a variable size that may not be easy to classify according to the system of Regan and Morrey. Classification of coronoid fractures according to fracture morphology and injury pattern may be preferable.

INTRA-ARTICULAR DISTAL HUMERUS: 12 -30 YEARS FOLLOW-UP

*Doornberg JN, *van Duijn PJ, *Linzel D, *Ring D, **Marti RK, **Kloen P*Orthopaedic Hand and Upper Extremity Service, Massachusetts General Hospital, Harvard Medical School, Boston MA

jdoornberg@partners.org

INTRODUCTION

The majority of studies report excellent or good short-term results of open reduction and internal fixation of intra-articular (AO Type C) distal humerus fractures. Reports on long-term results of operative treatment of complex intra-articular distal humerus fractures are scarce. The objective of our study was to assess the long-term (12-30 years) clinical and radiological outcome of surgically treated intra-articular distal humerus fractures (type C) with standardized outcome measures.

METHODS

A total of 31 patients were evaluated after an average of 19.4 years (range, 12 to 30 years) (60%). There were 19 men and 12 women with an average age of 35 years (range, 13 to 64 years). 11 of 31 (36%) patients had multi-trauma. After a standard posterior approach with (n=20) or without olecranon (n=11) osteotomy, internal fixation was achieved with unilateral or bilateral plates and screws, or isolated screws and/or Kirschner wires. None of the ulnar nerves were transposed during the index procedure. Patients were hospitalized for an average of 19 days (range, 1-99 days).

RESULTS

After a mean follow-up of 19.4 years, flexion-extension averaged 100° (range, 0-140°). The average pronation-supination arc was 165° (range, 140-180°). Mean ASES-score was 91 points (range, 69 to 100 points) with a reported satisfaction of 88% (range, 36-100%) at final follow-up. MEPI-scores averaged 91 points (range, 55 to 100). All elbows were rendered stable at final follow-up. ASES pain scores averaged 22 points out of 50 (range, 8 to 25) (0 equals no pain). The mean DASH–score was 7 points (range, 0 to 57 points). The categorical rating of the Mayo Elbow Performance Index (MEPI) was as follows: 19 patients had an excellent result (63%) and 9 patients achieved a good result (30%). The remaining two patients had a fair and poor result respectively. These last two patients rated their pain 21 and 34 points on the five 10-point Likert scales. Both these patients had Grade 2 arthrosis according to the classification of Broberg and Morrey. DASH-scores were 66 and 22 points (compared to an average of 7 points). 86% of the patients had arthrosis according to Broberg and Morrey. Arthrosis did not correlate with the reported pain. 10 patients had a subsequent procedure including hardware removal in 8 patients, capsular release in 4, ulnar nerve release in 2 and revision of osteosynthesis in 2 patients. In one patient the distal humerus fracture was complicated by a C5-6-7 root avulsion as part of high energy multitrauma and an amputation at shoulder level was necessary.

DISCUSSION

Open reduction and internal fixation of Type C intra-articular distal humerus fractures is safe and effective. After successful operative repair, satisfactory long-term results are to be expected. Arthrosis is present in the majority of cases but does not seem to impair function and does not attribute to subjective pain assessment.

AFFILIATED INSTITUTIONS

**Department of Orthopaedic Traumatology, Academic Medical Center, University of Amsterdam, Amsterdam, The Netherlands

INVESTIGATING WHY NEWER INTRAMEDULLARY NAILS FAIL TO ACHIEVE THE DESIRED CLINICAL RESULT: THE UNTOLD STORY

*Karuppiah SV, Johnstone AJ
*Aberdeen Royal Infirmary, Aberdeen, UK
saravanavail@yahoo.com

INTRODUCTION

For years traditional intramedullary (IM) nails have been used with great success to treat diaphyseal (shaft) fractures of long bones. However, based upon our clinical observations we hypothesise that changes in the design of newer IM femoral nails reduces fracture stability compared with traditional IM femoral nails, resulting is a higher incidence of non-union.
To biomechanically test the factors that may contribute to fracture instability using a composite model.

MATERIALS AND METHODS

The fracture fixation model consisted of custom made stainless steel IM nails of different wall thicknesses and outer diameters. High density polyethylene cylinders of differing inner diameters and wall thicknesses were used, and were chosen to resemble the dimensions commonly observed in the distal femur. The cylinders were bolted to an Instron mechanical testing machine. The test nails and cylinders were connected using a single 5mm diameter rod made from medical grade stainless steel or titanium alloy. Axial loading was undertaken up to 2KN (at a constant rate of 0.5KN/sec) and each test was repeated a minimum of three times. The effect of various factors such as IM nail wall thickness and outer diameter, the alloy from which the bolt was manufactured and the diameter and wall thickness of the polyethylene cylinders, were studied.

RESULTS

As expected, the factors that most affected stability were the diameter and the wall thickness of the cylinders, with the least stable configuration being a diameter of 75mm combined with a wall thickness of 3mm. Greatest stability was achieved using a 50mm diameter cylinder with a wall thickness of 5mm. (Fig 1).

DISCUSSION

In clinical practice, new IM femoral nail systems permit even longer cross screws to be inserted in the distal femur where the diameter is greatest and the cortical bone is thinnest. Since the metaphyseal bone offers little resistance, cross screws effectively span from one cortex to the other gaining limited purchase in the cortical bone. As a result, IM nails that have been secured using extreme distal locking screws are more likely to displace regardless of the direction and force applied. This effect is exaggerated by using a more elastic alloy such as titanium. Overall the combination of screw length, choice of alloy and cortical thickness could easily explain our unsatisfactory clinical observations.

AFFILIATED INSTITUTIONS FOR CO-AUTHORS:

Orthopaedic Trauma Unit, Aberdeen Royal Infirmary, Foresterhill, Aberdeen AB25 2ZN, UK

Fig: Variables contributing to composite model

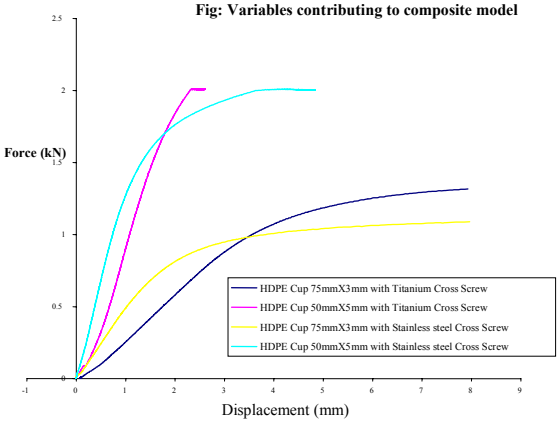

SEVERITY OF INJURIES ASSOCIATED WITH FEMORAL FRACTURES AS A RESULT OF MOTOR VEHICLE COLLISIONS

*Kwong Y, **Chong M, **Hassan A, **Kelly R
*University of Warwick, Warwick, UK
yune8@yahoo.com

INTRODUCTION

Femoral fractures frequently result from automobile accidents where a considerable amount of energy is generated. As such, a high incidence of associated injuries can be expected, and the identification of life-threatening injuries is important to improve outcome. Previous reports looking at injuries associated with femoral fractures have mainly consisted of case series from trauma registries, and there have since been numerous improvements in vehicle safety design and restraint use. In this report, we aim to examine the distribution of skeletal and visceral injuries sustained by motor vehicle occupants who have a femoral fracture, using a real-life prospectively updated crash database.

METHODS

All cases of femoral fractures were extracted from the UK Co-operative Crash Injury Study (CCIS) database, from 1995 to 2002. The CCIS database is maintained by Transport Research Laboratory, UK, and is sponsored by a consortium of motor vehicle manufacturers and the UK Department of Transport. About 1500 crashes are investigated annually. To be included onto the database, accidents must fulfill the following criteria:

- at least one of the vehicles in the accident must be a car or car derivative;
- the vehicle is less than 7 years old at the time of the accident;
- the vehicle was sufficiently damaged for it to have been removed (towed away) from the accident scene by a removal agent;
- the vehicle contained at least one injured occupant according to the Police.

The CCIS database records the injuries sustained by each patient using the Abbreviated Injury Scale (AIS), which ranges from 1 (minor injury) to 6 (maximum severity/fatal). The Injury Severity Score (ISS) is the sum of the squares of the highest AIS codes in each of the three most severe injured body regions, and serves as a marker of overall injury severity.

RESULTS

From 1995 to 2002, a total of 5841 vehicle crashes were investigated. 365 occupants in 282 vehicles sustained a femoral fracture. 2 occupants sustained bilateral femoral fractures, resulting in a total of 367 fractures. Males accounted for 61.1% of cases and the 16-35 age group accounted for about half of all cases (51.5%). Drivers were the car occupants most likely to be found with this injury in our study cohort. The mean ISS of all occupants was 29.2 +/- 22.5, with an ISS of more than 15 being considered to represent severe injuries.

In this analysis, we have excluded AIS 1 injuries (simple lacerations/contusions), as they represent only minor injuries. 313 patients (85.2%) had at least one other concomitant significant injury, of which 84 (23.0%) had a skeletal injury only, 45 (12.3%) had a non-skeletal injury only, and 184 (50.4%) had both.

Skeletal Injury	**n**	**%**
Opposite lower limb	130	35.6
Pelvis	115	31.5
Right upper limb	95	26.0
Left upper limb	83	22.7
Spine	55	15.1
Bilateral upper limb	25	6.8
Non-Skeletal Injury		
Head	138	37.8
Thorax	186	51.0
Abdomen	130	35.6

There were 148 deaths (40.5%) out of the 365 cases. Thoracic injuries accounted for the highest percentage (60.4%) of severe, life-threatening injuries (AIS 5-6).

DISCUSSION

Our study showed that there was a high incidence of associated skeletal and visceral injuries in motor vehicle accident victims who sustained a femoral fracture. Young men were the demographic group most likely to be involved. The mean ISS was high and indicates that a large amount of energy was dissipated during the crash. As such, a femoral fracture serves as a marker of crash severity, and less obvious life-threatening injuries should be expected and actively sought out. In our study, the opposite lower limb was the most common skeletal injury, and thoracic injuries were the most common visceral injuries. Chest injuries also accounted for the most severe injuries. We believe there should be a low threshold for involving the general surgery trauma team early in such cases.

**Birmingham Automotive Safety Centre, Birmingham, UK

ALENDRONATE IMPROVES SCREW FIXATION IN OSTEOPOROTIC BONE: A CLINICAL STUDY OF PERTROCHANTERIC FRACTURES

Moroni A, Faldini C, Hoang-Kim A, Pegreffi F, Giannini S
Department of Orthopaedic Surgery, University of Bologna, Rizzoli Orthopaedic Institute, Bologna, Italy
a.moroni@ior.it

INTRODUCTION

Screw loosening is a common cause of fracture malunion and nonunion, particularly in osteoporotic bone. Because of this, fixation augmentation techniques such as the use of hydroxyapatite(HA)-coated screws have been recommended for treatment of fragility fractures. Another innovative approach to enhance implant fixation is bisphosphonate therapy. Animal studies have shown that alendronate (ALN) inhibits bone resorption at the bone-screw interface thereby enhancing fixation. However, no clinical data is yet available. We wanted to assess whether fixation with HA-coated screws could be further improved by postoperative ALN therapy in osteoporotic pertrochanteric fracture patients.

METHODS

16 consecutive patients with pertrochanteric fractures were selected. Inclusion criteria were: female, age ≥65yrs, BMD T-score <-2.5SD. Exclusion criteria included pin insertion torque ≤1,000N/mm and bisphosphonate treatment during the 2-yr period prior to fracture. Fractures were fixed with a pertrochanteric fixator and 4 HA-coated pins. Two pins were implanted in the femoral head (pin positions 1 and 2) and two in the femoral diaphysis (pin positions 3 and 4). Patients were randomized to therapy with either ALN (Group A) or control (Group B) for a three-month post-op period. Group A patients received an oral dose of 70 mg of ALN/week. Fixators were removed at 3 m post-op.

RESULTS

All the fractures healed. No pin loosening or infection occurred in either group and no differences between femoral neck-shaft angle at 6 months versus post-op were observed. There was no significant difference in pin insertion torque between the two groups. The combined mean extraction torque of the pins implanted at positions 1 and 2 (cancellous bone of the femoral head) was 3181 ± 1385N/mm in Group A and 1890 ± 813N/mm in Group B ($p < 0.001$). The combined mean extraction torque of the pins implanted at positions 3 and 4 (cortical bone of the femoral diaphysis) was 4327 ± 1720 N/mm in Group A and 3785 ± 1181N/mm in Group B (ns).

DISCUSSION/CONCLUSIONS

This is the first clinical study to show improved fixation following post-operative ALN treatment. We observed a two-fold fixation increase in the pins implanted in cancellous bone. With cortical bone, the difference in pin fixation was less marked. We believe that the effect of ALN on implant fixation could be even more pronounced with standard metal screws which have a lower osteointegrative ability than HA-coated screws. These findings also have enormous implications for other implant fixation procedures in weak bone.

REFERENCES

1. Stromse K. Fracture fixation problems in osteoporosis. Injury 2004; 35 (2), 107-113
2. Moroni A, Faldini C, Marchetti S, Manca M, Consoli V, Giannini S: Improvement of the bone-pin interface strength in osteoporotic bone with use of hydroxyapatite-coated tapered external fixation pins. A prospective, randomized clinical study of wrist fractures. J Bone Joint Surg Am 2001; 83-A(5): 717-721
3. Miyaji T, Nakase T, Azuma Y, Shimizu N, Uchiyama Y, Yoshikawa H: Alendronate inhibits bone resorption at the bone-screw interface. Clinical Orthopaedics and Related Research 2005; 430: 195-201
4. Plotkin LI, Weinstein RS, Parfitt AM, Roberson PK, Manolagas SC, Bellido T. Prevention of osteocyte and osteoblast apoptosis by bisphosphonates and calcitonin. J Clin Invest 1999; 104: 1363-74
5. Morris C, Einhorn T. Bisphosphonates in Orthoapedic Surgery. J Bone Joint Surg Am. 87: 1609-1618, 2005.
6. B Peter, Gauthier O, Laib S et al. Local delivery of bisphosphonate from coated orthopaedic implants increases implants mechanical stability in osteoporotic rats. J Biomedical Materials Research Part A. Jan 2006 76 (A); 1; 133-143.
7. Skoglund, B, Holmertz J, Aspenberg P: Systemic and local ibandronate enhance screw fixation. J Orthopaedic Research 2004; 22: 1108-1113
8. Bobyn, J, Hacking S, Krygier, J, Harvey E, Little, D, Tanzer, M. Zolendronic acid causes enhancement of bone growth into porous implants. J Bone Joint Surg (Br) 2005; 87-B: 416-20.
9. Moroni A, Faldini C, Pegreffi F, Hoang-Kim A, Vannini F, Giannini S. Dynamic hip screw compared with external fixation for treatment of osteoporotic pertrochanteric fractures. A prospective, randomized study. J Bone Joint Surg Am. 2005 Apr;87(4):753-9.
10. Tanzer M, Kerabasl, D, Krygier J, Cohen R, Bobyn J. Bone augmentation around and within porous implants by local bisphosphonate elution. The Otto Aufranc award. Hip society meeting. 2004.

FLUOROSCOPIC NAVIGATION OF KYPHOPLASTY WITH A NEW PERCUTANEOUS DRB-CONCEPT

*,***Ohnsorge JAK, **Schkommodau, E; ***Mahnken, AH; ****Prescher, A;*Siebert, CH; *Weisskopf, M; *Niethard FU
*Orthopädische Universitätsklinik, UKA, RWTH, Aachen, Germany

johnsorge@ukaachen.de

INTRODUCTION

Various pathologies at the spine demand high pin-point accuracy of therapeutic or diagnostic interventions with a needle. The percutaneous treatment of vertebral fractures is a highly relevant example. In orthopaedic surgery, the implementation of image guidance and computer-assistance (CAOS) is best realized with fluoroscopic navigation. Costs and radiation exposure can thus be minimized in addition. Yet, the opto-electronic tracking of the anatomy depends on light-emitting or –reflecting markers closely attached to the bone. A so called dynamic reference base (DRB) is rather bulky and sensible to accidental displacement by the surgeons acting within a very small operation field. The fixation of such a standard DRB also requires a mini-incision to place a screw or a clamp onto the bone. This additional trauma defeats the percutaneous character of the needle and hitherto forbids fluoroscopic navigation of these procedures for its dependence on such a DRB.

METHODS

As a means to open minimal-invasive interventions at the spine for navigation a new DRB design and a truly minimal-invasive fixation modus were developed. The "epiDRB" is to be placed epicutaneously, directly onto the skin and can be fixed percutaneously with K-wires. This and a low center of gravity provide enough stability for surgical use. A dog-bone-like shape was chosen to leave more room for instrumentation, allowing fixation and simultaneous registration of several vertebral bodies. Experimental trials were undertaken to compare the new "epiDRB" to conventional models and to assess its advantages. Having proven reliability and benefit experimentally, the clinical application for kyphoplasty was prospectively studied. With kyphoplasty a needle is navigated through the skin and through both pedicles into a crushed vertebral body to place an inflatable balloon and to fill the cavity with polymethamethylacrylate. The adjacent spinal cord, the nerves and vessels need to be circumnavigated. Additional damage to the bony structures is to be avoided. The gained accuracy was investigated as were radiation exposure and applicability.

RESULTS

The development of the "epiDRB" allowed navigating a procedure that was up to then performed under permanent x-ray control. The insufficient accuracy on one side and the high radiation exposure on the other were both overcome by the new CAOS technique. The new design paid off as it left the operation field undisturbed though positioned immediately next to it. The fixation was accurate and stable throughout the course of all experimental testing and so was the tracking. Kyphoplasty as an example of various similar applications was performed easier, faster and more accurate with the help of fluoroscopic navigation than in the previous routine. The clinical outcome shows excellent results and no complications within the first series of cases.

DISCUSSION

Despite the obvious need, computer-assisted navigation has not been applied for percutaneous procedures at the spine such as kyphoplasty. The main reason was the unproportionate trauma due to fixation of the dynamic reference base. With invention of the "epiDRB" this problem is overcome and navigation becomes a reasonable alternative in cases of difficult anatomy. The original procedure suffers from the necessity of permanent x-ray control, accordingly high radiation exposure of the patient and the staff. Even more important, the placement of the needle into the vertebra is often inaccurate implicating an increased risk of complications. Using fluoroscopic navigation the risk of damage to the bone, the vessels and especially to the nerves can be reduced to a high extent as can be radiation exposure.

Subject to the availability of a navigation system fluoroscopic navigation of percutaneous interventions at the spine now is feasible, cheap and highly beneficial using the new "epiDRB".

REFERENCES

1. Ohnsorge JAK, Weisskopf M, Siebert CH. epiDRB-a new minimally invasive concept for registration in Computer Assisted Orthopaedic Surgery. Z Orthop 2005; 143: 316-322.
2. Ohnsorge JAK, Siebert CH, Schkommodau E, Mahnken, Prescher A, Weisskopf M. Minimally invasive computer-assisted fluoroscopic navigation for kyphoplasty. Z Orthop 2005; 143:195-203.

AFFILIATED INSTITUTIONS FOR CO-AUTHORS

** Institute of Biomedical Technologies,
*** Radiologische Klinik, UKA,
**** Institut für Anatomie, UKA,
Rheinisch-Westfälische Technische Hochschule
Aachen, Germany

DIAGNOSIS OF OCCULT WRIST INJURIES USING MRI SCANNING

Khalid M, Kanagaraj K, Jummani Z, Hussain A, Robinson D, Walker R

Nevill Hall Hospital
Abergavenny, South Wales, UK

khalidbones@hotmail.com

INTRODUCTION

Scaphoid fracture is the most common undiagnosed fracture.Occult scaphoid fractures occur in 20-25 percent cases where the initial X-rays are negative. Currently, there is no consensus as to the most appropriate investigation to diagnose these occult frctures. At our institution MRI has been used for this purpose for over 3 years. We report on our experience and discuss the results.

MATERIALS AND METHODS

All patients with occult scaphoid fractures who underwent MRI scans over a 3 year period were included in the study. There were a total of 619 patients. From the original cohort 611 (98.7%) agreed to have a scan, 6 (0.97%) were claustrophobic and did not undergo the investigation and 2 (0.34%) refused an examination. 86 percent of the cases were less than 30 years of age. Imaging was performed on a one Tiesla Siemen's scanner using a dedicated wrist coil. Coronal 3mm T1 and STIR images were obtained using a 12-cm field of view as standard. Average scanning time was 7 minutes.

RESULTS

Majority of the scans were performed within 2 weeks of the request. The breakdown of results is as follows:

Normal.....45%
Scaphoid bruise.....10%
Scaphoid fracture.....9%
Distal radius fracture.....8%
Distal radius bruise.....7%
TFCC tear.....4%
Wrist ganglion.....3%
Basal thumb arthritis.....3%
Miscellaneous.....12%

We did not have any missed scaphoid fractures during this period.

CONCLUSIONS

- Patients with a clinically suspected scaphoid fracture could have a wide range of possible diagnoses.
- Almost half the patients had a negative scan and therefore did not require further immobilisation / activity restriction.
- It is possible to perform MRIs within a reasonable timeframe in a DGH setting.
- Patient acceptance was very high (99%).
- There were no missed diagnoses.
- Scaphoid bruising could be picked up and consequently un-necessary immobilisation avoided.
- In patients with other diagnoses a reliable prognosis could be given.

RELIABILITY AND DIAGNOSTIC ACCURACY OF TWO- VERSUS THREE-DIMENSIONAL COMPUTED TOMOGRAPHY IN THE CLASSIFICATION AND MANAGEMENT OF DISTAL HUMERUS FRACTURES

*Lindenhovius ALC, *Doornberg JN, **Kloen P, *Mudgal C, *Forthman C,
*Jupiter JB, **van Dijk CN, ***Zurakowski D, *Ring D, *Orthopaedic Hand and Upper Extremity Service, Massachusetts General Hospital, Harvard Medical School, Boston MA
alindenhovius@partners.org

INTRODUCTION

Complex fractures of the distal humerus can be difficult to characterize on plain radiographs. We tested the hypothesis that three-dimensional (3D) reconstructions of computed tomography scans improve the reliability and accuracy of fracture characterization as compared to 2D-CT scans.

METHODS

Five independent observers evaluated 30 consecutive intra-articular fractures of the distal humerus for the presence of six fracture characteristics: a fracture line in the coronal plane, the presence of articular comminution, metaphyseal comminution, the presence of separate entirely articular fragments, and impaction of articular surface. Fractures were also classified according to the Comprehensive Classification of Fractures and the Mehne/Matta classification. Two rounds of evaluation were compared: plain radiographs and 2D-CT scans initially versus radiographs, 2D-CT scans and 3D-CT reconstructions two weeks later. These rounds were repeated after an interval of two weeks to evaluate intra-observer reliability.

RESULTS

3D-CT improved both the intra-observer and inter-observer reliability for the AO classification and the Mehne/Matta classification compared to reliability of 2D imaging. 3D-CT reconstructions improved the intra-observer agreement from moderate to substantial for all fracture characteristics compared to 2D-CT (average κ_{2D} = 0.55, range 0.15 to 0.89 vs. average κ_{3D} = 0.79, range 0.58 to 0.94). Addition of 3D-CT improved categorical inter-observer agreement for a coronal fracture line, but not for any of the fracture characteristics (average κ_{2D} = 0.40, range 0.14 to 0.60 vs. average κ_{3D} = 0.44, range 0.13 to 0.57). Addition of 3D-CT images had limited influence on sensitivity, specificity and accuracy for recognition of fracture characteristics. 3D images also improved intra-observer reliability for choice of treatment (κ_{2D} = 0.62 vs. κ_{3D} = 0.75), but there was no statistical significance. Inter-observer agreement for treatment was only fair for both imaging modalities (κ_{2D} = 0.24 versus κ_{3D} = 0.28)

DISCUSSION

Three-dimensional reconstructions of CT scans of distal humerus fractures improve intra-observer agreement, but have a limited influence on inter-observer agreement. This suggests that the 3D reconstructions do help with characterization of the fracture, but that different observers see different things in the scans—most likely a reflection of the training, knowledge, and experience with these relatively uncommon injuries.

AFFILIATED INSTITUTIONS

**Department of Orthopaedic Surgery, Academic Medical Center, University of Amsterdam, Amsterdam, The Netherlands
***Department of Orthopaedic Surgery, Children's Hospital, Harvard Medical School, Boston MA, United States of America

INFLUENCE OF JOINT CONFORMITY ON HYDRODYNAMIC LUBRICATION

†Pascau A, †Guardia B, ‡García-Álvarez F, ‡Puértolas JA, *Gómez Barrena E
*Dept. Orthopaedic Surgery, Fundación Jiménez Díaz, Universidad Autónoma de Madrid, Madrid, Spain

Enrique.gomezbarrena@uam.es

INTRODUCTION

The influence of total joint components elastic deformation on lubrication is generally accepted, but little is known about the influence of joint conformity under hydrodynamic lubrication based on fluid film interposition. This may be a key aspect not only in hard friction pairs in the hip (ceramics-on-ceramics, metal-on-metal), but also in hardened pairs (X-linked PE with metal or ceramic), and in new knee designs with variable conformity based on these hardened materials. Besides, minor changes in conformity due to wear may modify this kind of lubrication. The aim of this study was to evaluate induced pressure and stresses under fluid film lubrication with walking loads in different joint conformities.

METHODS

A theoretical 2D geometric model of joint prosthesis contact, with Dirichlet boundary conditions at both edges, and with conformity index (C.I.) of 0, 0.3, 0.5, 0.6, 0.7, 0.8, 0.9, 0.92, 0.94, 0.96, 0.98, 0.99, 0.995, and 1, was used to calculate the spatiotemporal lubricant flow on a synovial fluid rheological model with a non-newtonian strain-rate-dependent viscosity. Conformity index was calculated from both articular surfaces, with 1 a full conformity (both radius equal) and 0 no conformity (one flat surface). With the instantaneous load as a source term, the Reynolds lubrication equation was subsequently solved following a finite volume approach. A FORTRAN computer program was developed for this study.

RESULTS

The influence of the synovial fluid viscosity was calculated using the non Newtonian synovial behavior from a minimum separation between components of 2 mm. A very high approaching velocity occurred during the walking cycle, and the induced fluid velocities were so high and the gap so narrow that a very high strain rate was present in all points of the domain. The results were thus equivalent to those obtained with constant viscosity at the highest shear rate. For conformity indexes below 0.96, the differences were not significant. The time up to contact was less than 10-3 s. This time was very short for configurations with C.I. values close to zero and increased when increasing the conformity index. Only in the run with full conformity (CI=1), the stance phase time limit (0.6 s) was reached.

When the components were approaching, the simulation provided the gap evolution between them at each time interval, h(x,t), and the spatial distribution of the pressure, p(x,t), with a gaussian-like shape (Fig 1A) that sharpened when the distance between components was reduced. The maximum peak pressure also evolved with the C.I. (Fig 1B): there was a smooth maximum pressure decrease with increasing C.I. In contrast, the maximum pressure fell abruptly with conformity higher than 0.96, a transition C.I. in our model results (Fig. 1B).

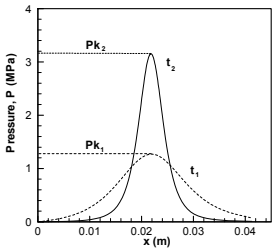

Figure 1A

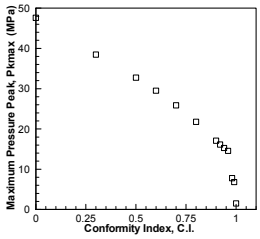

Figure 1B

C.I. increases significantly reduced time to contact. Conformity strongly influenced the peak pressure, from 47 MPa with C.I.=0 to 1.4 MPa with C.I.=1. In most studied cases, the role of hydrodynamic lubrication was restricted to very early steps of the stance phase. Earlier contact and higher peak pressure were associated with with C.I. of 0.96 (Fig. 2A), whereas C.I. of 0.99 showed later contact and lower peak pressure (Fig. 2B).

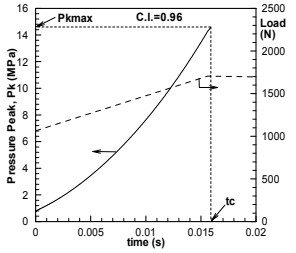

Figure 2A

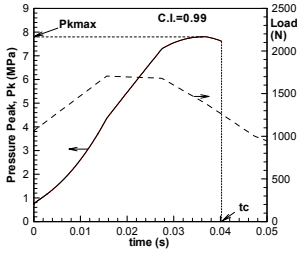

Figure 2B

DISCUSSION

Early contact between joint components decreases the relevance of hydrodynamic lubrication, thus limiting the influence of synovial fluid variables. Induced pressure and stresses relate more to conformity, and conformity changes influence time to contact and maximum peak pressure in non-deforming joint components. Two phases of peak pressure were found under and over CI=0.96. Minor conformity changes around this value may modify the maximum peak pressure in the contact areas of an artificial joint.

ACKNOWLEDGEMENTS

CICYT (Spain), MAT2003-02140.

AFFILIATED INSTITUTIONS FOR COAUTHORS

†Fluid mechanics Group, Universidad de Zaragoza
‡Biomaterials Group, Universidad de Zaragoza

A NEW APPROACH TO MEASURE *IN VIVO* CARRYING ANGLE BY ANATOMICAL LANDMARKS

Zampagni ML, Casino D, Martelli S, Visani A, Marcacci M
Biomechanics Laboratory, Istituti Ortopedici Rizzoli, Bologna, Italy

m.l.zampagni@biomec.ior.it

INTRODUCTION

The elbow joint presents an angular offset, called carrying angle[1,2], formed by the long axis of the ulna and the long axis of the humerus. As reported in the literature, this angle is subject to a linear variation during the flexion-extension movement in *in-vitro* investigations. Little is known about the carrying angle *in-vivo* behaviour. The identification of new non-invasive methods to *in-vivo* estimation of the carrying angle could contribute to the creation of a model of the upper arm useful for clinical issues. Currently, we are validating a new method for *in-vivo* estimation of the carrying angle by 3D digitized coordinates of anatomical landmarks and by fitting numerical algorithms. The aim of this work was to present a new approach and to test the validity and repeatability of the measurements.

METHODS

Forty-four fit subjects (aged 61±11.1) were considered in this study. Two operators acquired each arm two times. An electrogoniometer (Faro Arm) was used to digitalize the 3-D coordinates of each landmark on the arm and forearm. The landmarks were chosen according to ISB recommendation [3]. In order to obtain the carrying angle value we adopted a numeric algorithm based on Cardan decomposition angles.

The validity of the method was tested by calculating Pearson's correlation coefficients between the values returned by our algorithm and the values measured by a goniometer adopted as gold standard.

To estimate the intra-operator and inter-operator reliability, t-student test was adopted and interclass correlation coefficient (ICC) and standard error of measurement (SEM) were calculated. For the interpretation of the ICC, the criteria suggested by Cincchetti and Sparrow was used [4].

RESULTS

The mean carrying angle between all considered subjects was 12.0±3.2°. The validity of the method resulted good (r=0.72). The mean difference between repeated measures on the same subject by the same operator and by different operators was not significant in both cases (P=0.84 and P=0.7) and measured 0.56° and 0.83° respectively. The standard error of measurements was 1.62°. The intra-operator repeatability was excellent (ICC=0.85) and good the inter-operator (ICC=0.66).

DISCUSSION

The obtained carrying angle values were similar to ranges reported in the literature. The method resulted valid compared to a gold standard and reliable. Concluding, this method could be used to measure *in-vivo* carrying angle with a standard error of measurements less than 1.7°. This gaining could contribute at developing an individual model for the upper arm and future perspectives will include measures in subjects affected by upper arm pathologies. Moreover, our approach could also be used for the assessment of carrying angle in elbow reconstruction. This article presents a preliminary study to test the method in full extension position and further investigations are needed to adapt the method to movement analysis of the arm.

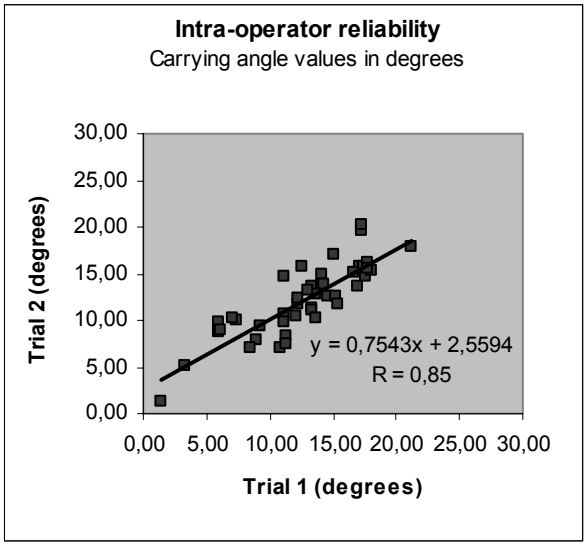

REFERENCES:

[1] An KN et al. "Carrying angle of the human elbow joint". J Orthop Res 1984; (1): 369-378.[2] Morrey B. F. et al. Passive motion of the elbow joint" JBJS 1976; (58a):501-8. [3] Wu G ISB recommendation on definitions of joint coordinate systems of various joints for the reporting of human joint motion--Part II: shoulder, elbow, wrist and hand. J Biomech. 2005; 38: 981-992. [4] Stokdijk M. et al. Determining the optimal flexion-extension axis of the elbow in vivo - a study of interobserver and intraobserver reliability. J Biomech. 2000;33:1139-45.[5] Stokdijk M et al. The glenohumeral joint rotation centre in vivo. J Biomech. 2000;33:1629-36.

CONTRIBUTION OF THE FLEXOR-PRONATOR MASS FOR VALGUS STABILITY OF THE ELBOW AT THROWING POSTURES

*Lim D, *Perlmutter S, **Lin F, ***Kohli N, ***Nuber GW, ****Makhsous M
Depts *Phy. Ther. & Human Movement Sci., **Phy. Med. & Rehab, ***Orth. Surg,
Northwestern University, Chicago, IL ****SMPP, Rehab. Inst of Chicago, Chicago, IL
m-makhsous@northwestern.edu

INTRODUCTION The flexor-pronator mass (FPM) is particularly important for valgus stability in overhead throwing athletes of the elbow, who place tremendous repetitive valgus moment across the elbow [1-2]. The aim of current study was to identify the relative contribution of each flexor-pronator (FP) muscle - flexor carpi radialis (FCR), flexor carpi ulnaris (FCU), pronator teres (PT), and flexor digitorum superficialis (FDS) - to the valgus stability at two representative throwing postures.

MATERIALS AND METHODS

Specimen Preparation: Eight fresh-frozen elbow specimens (73.8±14.1 yrs.) were tested. Specimens included at least 14cm of the humerus, along with the entire forearm and hand. The skin and subcutaneous tissues were removed up to the wrist. All muscles of the forearm were left intact. The specimen was mounted on a customized experimental apparatus (Fig 1).

Experimental Setup (Fig 1): A differential variable reluctance transducer (DVRT) (Microminiature DVRT, MicroStrain Inc., Williston, VT) was mounted on the isometric aspect of the anterior bundle of the medial ulnar collateral ligament (MUCL) to measure the ligament strain corresponding to each FP muscle loading. A load cell (M31, Honeywell Sensotec, Columbus, OH, USA) was used to measure the pulling force during individual muscle loading.

FP Muscle Loading Application and Measure: First, all muscles were loaded by deadweights corresponding to 2% of maximum muscle force representing physiological low level muscle tone contraction. Second, two trials of passive range of motion (ROM) test were conducted by passively moving the forearm from 0º to 90º flexion to confirm that consistent measurement of DVRT was provided. Finally, the FP muscles were individually loaded at consecutive loads of ~13N (loading cycle 1), ~26N (loading cycle 2), and ~39N (loading cycle 3), respectively, for 4 seconds, with 4 second intervals between loading levels. All tests were performed at both fixed 45° and 90° of elbow flexion assumed as representative throwing postures, which can be frequently captured for throwing.

Data Analysis: To characterize the contribution of each FP muscle, the MUCL strains corresponding to the muscle loading for simulated quasi-static loading cycles were analyzed. A least square linear regression was then used to fit the MUCL strain, which was interpreted as strain over every 10N of load for each individual muscle. Here, the strain was obtained by computation of displacement changes relative to the initial length, which was assumed as local length of the MUCL, between the 2 attachments of the DVRT sensor.

Statistical Test: For strain data obtained during each individual muscle loading, a comparison with zeros was made by t-test to determine whether or not the strain change caused by individual FP muscle loading was significant. A one-way ANOVA with Tukey *post hoc test* was then performed to detect the significant difference among all individual muscles at both fixed 45º and 90º. The significant levels were set at 0.05 for t-test and ANOVA.

RESULTS Fig 2 shows the average of the slope of strain changes on the MUCL induced by 10N loading on each FP muscle (%/10N) and the normalized strain relieve (%) of each muscle to the MUCL. At 45° and 90° elbow flexion postures, individual loading of the FCU, FDS, and FCR caused significant MUCL release (p<0.05), while the PT brought no significant change (p>0.05). One-way ANOVA test showed that FCU loading caused the greatest MUCL release compared with FDS, FCR, or PT loading at both postures (p<0.05) while no significant difference was found among the other FP muscles. FDS loading at 90° elbow flexion provided higher release of the MUCL strain compared with that at 45° elbow flexion (p<0.05). The relative contribution of the muscle (Fig 2. right) showed that the FCU, FDS, FCR, and PT released the strain about 70%, 15-25%, 5%, 0% for a given muscle load, respectively. Here, the contribution of FDS was depended on throwing posture.

DISCUSSIONS: Our findings suggest that the FCU may be a primary and the most efficient dynamic stabilizer for valgus stability of the elbow incorporating with the MUCL for all throwing postures and the FDS can be functioned as a second dynamics stabilizer at specific throwing postures.

References: [1] Safran et al., 2005, J. Shoulder. Elbow. Surg., 14(1), s179-s85, [2] Park et. al., 2004, J. Bone Joint Surg., 86A(10), 2268-2274

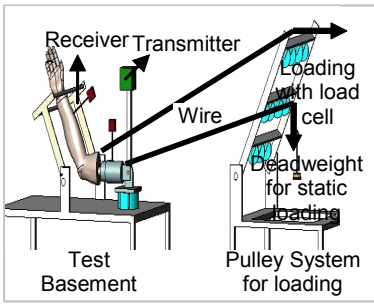

Fig 1. Experimental Setup. Fiberglass meshes were sutured to muscles for application of simulated muscle loading through cotton wires and steel eyelets, which guided the loading direction of muscle.

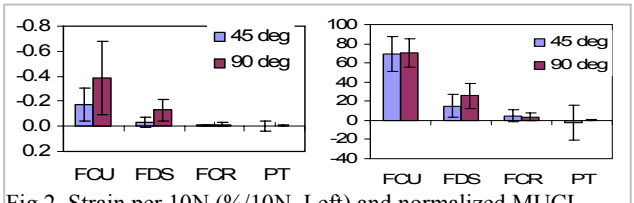

Fig 2. Strain per 10N (%/10N, Left) and normalized MUCL strain relief when loading each FP muscle (Right)

OPTOELECTRONICAL ANALYSIS OF UPPER EXTREMITY FUNCTION – A NEW EVALUATION TOOL FOR SURGICAL TREATMENT

Mickel M, Gradl B, Kranzl A, Weigel G, Schmidt M, Girsch W
Orthopaedic Hospital Speising - Paediatric Department, Vienna, Austria

michael.mickel@gmx.at

INTRODUCTION

A new evaluation method of upper extremity function is presented. It is a video based system providing accurate and reproducible 3D kinematic data by tracking movements. It is to overcome the deficiencies of subjective investigations.

METHODS

A 3-dimentional optoelectronic camera system with passive markers was used to capture the possible active range of motion. 27 markers coated with retro reflective tape were applied over anatomical landmarks on both upper limbs. These markers were recorded simultaneous by 6 cameras. A 3-dimensional reconstruction of the position of the markers was done by special designed software. Joint centres and joint movements were calculated by using the Expert Vision and ORTHOTRAK software (Motion Analysis Corporation). Beside from healthy probands we investigated six patents with obstetrical upper brachial plexus injury before and after humeral-derotation.

RESULTS

Obtained pre- and postoperative kinematic data document the enhancement of the involved limbs` function: The rotational-positioning of the upper arm, which can be measured very accurately, was shifted outwards about 30° average. Active shoulder rotation increased in all patients, the average improvement was 10°. The system measured increased abduction, with a difference ranging from 6° to 20°. Active elbow flexion didn't increase, however postoperative motion curves – containing kinematic information during the whole movement and not only the maximum of joint deflection – run smoother and faster.

DISCUSSION

The method enabled analysis of upper extremity motion, especially in shoulder, upper- and forearm and wrist function. Measured angles were reliable and reproducible. Because of the more complex nature of upper limbkinematics the transfer of the system from lower to upper extremity still involves unsolved problems. Simplifications of the biomechanical model and limitations in accuracy are detailed and discussed.

IMPACT OF SOMATOTYPE AND POSTURE ON PLANTAR PRESSURES AT CHILDREN

*Badurova J, **Pridalova M, *Kostelnikova L, *Hlavacek P
*Tomas Bata University, Faculty of technology, Zlin, The Czech Republic

badurova@ft.utb.cz

INTRODUCTION

The problem of high local plantar pressures is frequently discussed problem among scientists. Different authors present differently significant correlation between BMI or weight and the size of plantar pressure. The body mass can but do not have to increase plantar pressure. It depends much more on the fact that the structure of the foot might be destroyed by overweight especially in area of longitudinal arch. However, the different type of obesity can have an impact of local peak pressures as well. The study is an attempt to evaluate somatotype and posture at children and youth in school age, who suffer from excessive pronation and flat foot, and their plantar pressure.

METHODS

In the eye of the research were 70 children in age from 8 to 11 years. 27 of them suffer from excessive pronation in range from 2° to 15°. Deformities were determined by the use of podoskop and protractor.

The plantar pressures were recorded on the Pedar system. Moreover, their posture and constitution were examined as well.

Pedar system means system, which is able to record dynamic load of feet. It contains from sensorial insoles connected to the PC, where is possible to record few steps and with a help of special software evaluate them from different sides. The Hath Carter method (1967) was used to examine constitution of the subject's body. For the posture evaluation a method of Jaroš and Lomíček (1957) was selected.

RESULTS

As it is clear from the first graph just below no big differences are in basic parameters between group of valgous children and the other children

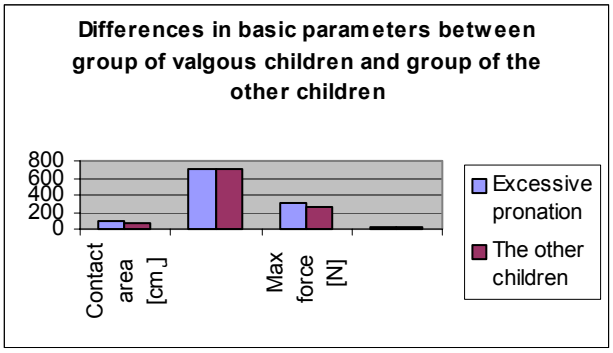

Sensorial insoles were divided into five regions or so called masks. M1 – area of inner heel part, M2 – area if outer heel part, M3 – area of midfoot, M4 – area of big toe, M5 – area of the other toes. . Children who suffer from excessive pronation have in average bigger contact area even in all particular masks, however the difference is significantly bigger in area of midfoot. Values of peak preassure are in average almost equal. However, looking more deep into particular regions valgous children have higher peak pressures in area of big toe and inner heel part. In case of maximal force children with excessive pronation are significantly higher in all masks, but the opposite phenomena is evident in case of contact time.

DISCUSSION

The indexes expressing the constitution of subjects revealed that the group of children with excessive pronation have in average higher index of the fat content and lower index expressing the content of muscle mass. Among this group of children was heightened the frequency of spike disorders in lumbar region. Athough 70 % of all subjects fosters an interest in some sport activity; only 3 % of them had perfect posture. However, many followed parameters and few subjects do not allow formulating any definitive conclusions.

REFERENCES:

MURAT, C. et. al. The evaluation of plantar pressure distribution in obese and non-obese adults. Clin Biomech. 2004, no. 19, p. 1055-1059.

VELA, S. A. et. al. The effect of increased weight on peak pressures: implication for obesity and diabetic foot pathology. J Foot Ankle Surg. 1998, no. 37, p. 416-420, 448-449

AFFILIATED INSTITUTIONS FOR CO-AUTHOR

**Palacký University, Faculty of physical culture, Olomouc, The Czech Republic

DO THE INSOLES PROPERTIES CHANGE DURING WEARING?

*Durisova J, *Michutova M
*Institute of Footwear Engineering and Hygiene, Faculty of Technology, Tomas Bata University, Zlin, Czech Republic

durisova@ft.utb.cz

INTRODUCTION

The average person takes between 8,000 and 10,000 steps each day. The impact of every step exerts force – about 50 % greater than the person´s body weight. About 80 % of population experience foot pain at some point in their lives.

Nearly everyone who wears shoes and moves on hard surfaces has foot problems. The loss of absorbing abilities of hard surfaces is replaced so by the damping ability of footwear bottom parts. For this reason, footwear is being provided with insoles.

There are lots of studies concerning an optimum solution of the insoles. Because of the results of the previous research a new hypothesis was established. The question was if the material pressure reducing ability might decrease during longer wearing time period, it means if the local pressures on feet could increase when walking or not.

METHODS

The aim of the experiment was to confirm or to refute the hypothesis. For this reason, the following types of lining insoles were chosen (size 42):

1. sock lining of latex foam
2. gel insoles
3. silicone insoles
4. water-filled insoles
5. special shaped health promoting sock lining used for prophylactic shoes for diabetics.

The insoles were tested in total by 5 subjects. The only criterion in selecting the probands there was the foot size.

The insoles were tested for 300 hours and each 50 hours were measured. The total time of wearing by subjects was 3 months.

For measuring the treading forces, the Pedar mobil (Novel Munich) was used which consists of a recording unit and of sensoric insoles.

This measuring was carried out in laboratory conditions. The probands have been walked on a flat PVC floor covering on a track about 10m long.

RESULTS

The graphs 1 and 2 give an overview of maximum local pressures for each tested insole during the 300 hours period.

As can be seen, the value of local pressure alternate very often. It might be said that only slight trend could be found in point of view of increasing material disability to reduce pressure after long time wearing.

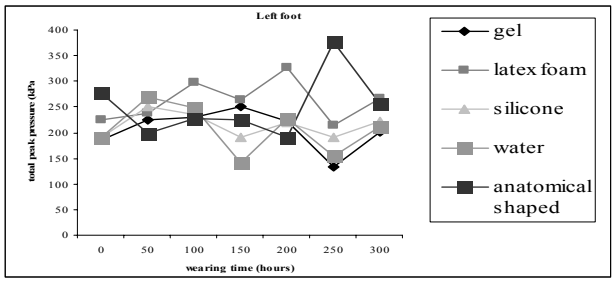

Graph 1: Total value of peak pressure for each insole during 300 hours period – left foot

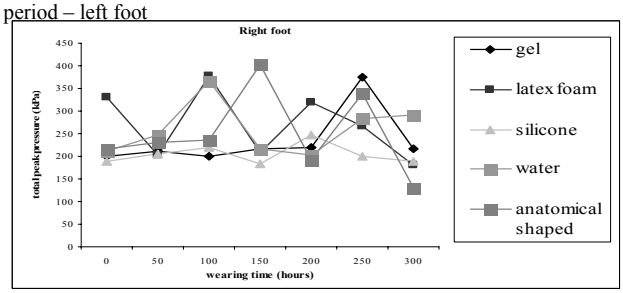

Graph 2: Total value of peak pressure for each insole during 300 hours period – right foot

DISCUSSION

It is obvious from the above results that the hypothesis was not confirmed that the material reducing ability did not decrease after 300 hours wearing period. It is possible to find only slight trend for this. In virtue of the above results, it is possible to say that 300 hours are not enough for the experiment and it would be better to do the measurement for longer time period.

REFERENCES

1. RAZEGHI, M., BATT, M.E. The Effect of Foot Orthoses on Selected Ground Reaction Force Parameters during Ground Walking, *6th Symposium on Footwear Biomechanics,* Queenstown 2003

2. BIRKE, J.A., FOTO, J.G. et al. Effect of Orthosis Material Hardness on Walking Pressure in High-Risk Diabetes Patients, *Journal of Prostetics and Orthotics,* 1999 Vol.11, Num.2, p. 43-46

3. FIOLKOWSKI, P., BAUER, J. The Effects of Viscoelastic Insoles on Gait Kinetics, *3rd Symposium on Footwear Biomechanics,* Tokyo 1997

4. DURISOVA, J., HLAVACEK, P. Stepping forces absorption by different lining insoles: preliminary study. *3rdSalford Conference on Biomechanics of the Lower Limb in Health, Disease and Rehabilitation, Salford, September 5.-7.2005*

CHANGES IN PLANTAR PRESSURE DISTRIBUTION OF OBESE CHILDREN AFTER WEIGHT REDUCTION PROGRAM

*Kostelnikova L, *Hlavacek P
Tomas Bata University, Faculty of technology, Zlin, The Czech Republic

hlavacek@ft.utb.cz

INTRODUCTION

The number of obese people has been steadily rising, while at the same time, the very unsettling fact is that this also affects children. Currently, a series of studies have been commenting on the relationship between children's obesity and future health complications.

To reduce the weight of children, a change in eating habits and the addition of movement exercises are critical. A recommended increase in movement is very important, but there is no unified opinion regarding shoes that would be appropriate for children. In the assortment of sports shoes, footwear models have appeared that were once marked as "straight," where the lengthwise axis of the footwear's insole was identical to the symmetrical axis of the heel. The second tier of questions concerns functional changes in the foot of obese children in connection with weight or changes in weight (possible increases in weight and weight-loss).

METHODS

Over the course of 2004 and 2005, two spa facilities were visited, which focus on treatment for overweight and obese children and where under a physician's supervision, children were involved in movement activities and their meals controlled by a dietician. At the beginning of the diet, a total of 110 obese children (50 boys and 60 girls) underwent printing and measurement of the feet Dynamic pressures were measured between the foot and footwear insoles using a Pedar system. Peak pressures (N/cm^2), were then derived for six regions of child's feet: Total foot (TO), heel (M01), midfoot (M02), medial forefoot (M03), lateral forefoot (M04), medial toes (M05) and lateral toes (M06). This was also repeated at the end of the five-week weight reduction program. Also recorded were age (14.02 ± 2.2y.), weight, height (163.5 ± 10.3 cm) and BMI (under 28.89 ± 4.0 and over 26.8 ± 3.8). The average weight at the beginning of the course was 78.1 kg and at the end 72.2 kg. On average, there was a decrease in weight by 5.3 kg (i.e. 7.6 % of the initial weight).

RESULTS SECTION

From the measured values, a matrix of correlation coefficients was generated, which enabled an extensive step analysis of factors. These confirmed that the average weight-loss 5.3 kg were manifest in changes to foot pressure values on the insole of footwear under dynamic conditions. Because foot prints were also measured and assessed, it was also possible to determine changes in foot functionality. This was primarily the difference in values for the toe girth under load and lightened status (sitting and standing). The second auxiliary parameter was flat footvalue.

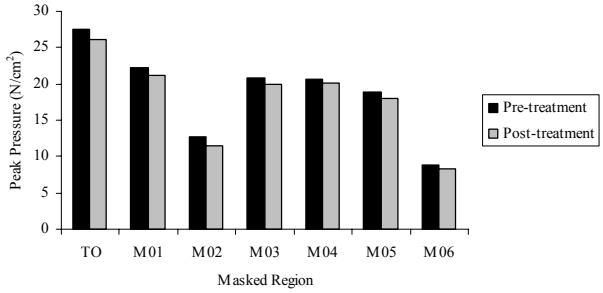

Fig. 1 The average values of peak pressures generated in each masked region of the foot before and after weight reduction program.

DISCUSSION

In all cases, a significant decrease in measured maximum pressure was successfully determined statistically (Fig. 1). This means that the functionality of growing children's feet is not seriously limited and weight loss leads to a return to values comparable to the children's population with average BMI values.

REFERENCES

BOLTE K, et al. Pressure changes under the feet of obese adults after a weight reduction program. XXV^{e} Congres de la Société de Biomécanique – XIth Congress of the Canadien Society for Biomecnanics, p. 70. 2000.

DOWLING AM, et al. How does obesity and gender affect foot structure in children? ISB XXth Congress – ASB 29th Annual Meeting, Cleveland, Ohio, p. 512, 2004.

HILLS AP, et al. Plantar pressure differences between obese and non-obese adults: a biomechanical analysis. *Int J Obes Relat Metab Disord*. 2002. Vol. 25, p. 1674-1676.

MICKLE JK, et al. Do overweight and obesity affect dynamic plantar pressure distribution in preschool children? ISB XXth Congress – ASB 29th Annual Meeting, Cleveland, Ohio, p. 351, 2004.

DOWLING AM, et al., What are the effects of obesity in children on plantar pressure distribution? *Int J Obes Related Metab Disord*. 2004. Vol. 28, p. 1514-1519.

COMPARISON OF THE FUNCTIONAL AND MAXIMUM RANGE OF MOVEMENT OF THE FIRST METATARSOPHALANGEAL JOINT

*Lever C, *Simmons D, *Moorehead J, *Butcher C
University Hospital Aintree, Liverpool, UK

john.moorehead@aintree.nhs.uk

INTRODUCTION

One of the main issues of metatarsophalangeal (MTP) joint replacements is that they do not restore full range of movement (ROM). However, there is little evidence recorded about the normal functional and maximum ROMs. Therefore, clinicians normally use their own subjective judgment to assess these parameters.
The aim of this study was to use a computerised imaging system to objectively measure both the functional ROM in walking, and maximum standing ROM in clinical tests of the first MTP joint.

METHODS

A computerised video imaging system was used to measure MTP joint ROM in walking and maximum standing extension tests (see Fig 1-3).

Fig 1: Neutral

Fig 2: Max Stand

Fig 3: Stand ROM

Thirty two feet in sixteen normal subjects (aged 23-58 years) were tested as they walked past the imaging system and as they performed standing maximum extension tests. Image Pro-Plus (TM) software was used to measure MTP joint angle in neutral and in maximum extension. These angles were then used to calculate the extension ROM.

RESULTS

During functional walking tests the mean ROM was 37.9 degrees (SD 12.2). During maximum standing tests the mean ROM was 64.9 degrees (SD 11.3). Therefore the maximum standing ROM was 71 % more than the functional walking ROM, with a mean difference of 27 degrees. These results are shown graphically in Fig 4.
A paired T-test comparison showed $P<0.0001$.

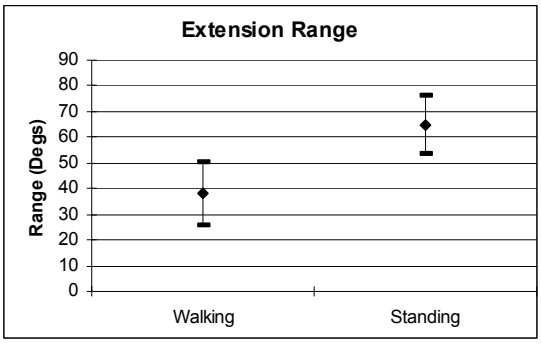

Figure 4:- Comparison of walking with standing (Mean +/- 1 SD)

DISCUSSION

Previously, the first MTP joint ROM has been measured either subjectively or with the use of goniometers. It has therefore been difficult to assess the amount of functional movement required in walking. With the use of computerised imaging, it has been shown that there is a significant difference between the functional and maximum range of movement of the first metatarsophalangeal joint.
Arthritis of the first MTP joint is known as hallux rigidus due to the reduction in movement of the joint. Arthrodesis reduces pain from arthritis but results in permanent stiffness. Arthroplasty has previously been criticised as an alternative because it does not restore full movements of the joint. However the results of this study suggest that functional movements required in normal gait are significantly less than what can be maximally achieved in clinical standing tests. Therefore arthroplasty can be a suitable alternative to arthrodesis if it can provide an adequate functional range of movement.

CONCLUSION

The results of this study show that functional range of movement required for walking (37.9 degrees) is significantly less than the maximum extension ROM (64.9 degrees) of the first MTP joint. Therefore, MTP joint replacements do not need to restore maximum extension, as normal gait can be achieved without this.

THE INFLUENCE OF THE LATERAL PLASTY IN RESTORING KNEE STABILITY DURING ACL RECONSTRUCTION

Bignozzi S, Zaffagnini S, Martelli S, Lopomo N, Marcacci M
Laboratorio di Biomeccanica, Istituti Ortopedici Rizzoli, Bologna, Italy

s.bignozzi@biomec.ior.it

INTRODUCTION

It has been widely accepted that anterior cruciate ligament (ACL) is primary constrain to anterior displacement of tibia and secondary restrain to internal/external (IE) and varus/valgus (VV) rotations. For this reason the ACL reconstruction should control not only the AP translation but also IE and VV rotation.

Recently our institute has developed a surgical technique for ACL replacement consisting in an over the top single-bundle graft with additional lateral plasty, to better control rotatory instabilities.

The aim of this study is to verify if the lateral plasty has an effective contribution in the restoring of knee stability and, in particular, in the control of rotational laxities.

In order to asses the efficacy of the technique we evaluated, intra-operatively, the kinematic of the joint, after each step of the surgical technique. These measurements permit to address if the contribution of the lateral plasty is statistically significant in controlling knee laxities.

METHODS

We studied 16 patients, with a mean age of 30 years. Surgery consisted of an arthroscopic single-bundle over the top ACL reconstruction with lateral plasty.

During the intervention we evaluated the effect of the reconstruction on the kinematic of the knee. The operating surgeon performed standard kinematic tests, during three steps: after ligament harvesting, after single bundle insertion and fixation and after lateral plasty fixation. To evaluate the joint laxity we used a custom navigation system consisting of an optical localizer and software developed at our institute for this purpose. During intervention, reference frames were fixed on bones and a brief registration phase was performed through percutaneous digitization of bone reference points, in order to define reference systems of the femur and tibia.

To evaluate joint laxities the operating surgeon, performed the following manual tests:

- Varus-valgus (VV) stress test at maximum force at 0º and 30º of flexion.
- Internal-external (IE) rotation at maximum force at 30º and 90º of flexion.
- Antero-posterior (AP) stress test at maximum force at 30º and 90º of flexion.

In order to evaluate the effect of each bundle, in restoring knee stability, comparisons between levels of laxity at specific angles of knee flexion were made using values obtained during tests (Tab. 1). Moreover, to evaluate the contribution of each bundle, percent laxity control, for each bundle was evaluated (Tab. 2). For both tests nonparametric Wilcoxon test for dependent samples was used, the level of significance was set at $P = 0.05$.

RESULTS

Mean laxity values during tests are summarized in table 1, Proportional laxity control is summarized in table 2.

test	pre-op	SB	SB+lat.p
VV 0º	5.4(1.3)	3.6(1.1)	2.9(1.0) †
VV 30º	4.6(1.5)	3.5(1.3)	3.0(1.3) †
AP 30º	13(2.6)	7.3(2.6)	6.6(1.8)
AP 90º	8.7(1.7)	5.3(1.9)	4.2(14) †
IE 30º	20.4(6.0)	16.7(6.9)	16.3(6.3)
IE 90º	24.9(6.8)	18.9(6.2)	17.4(5.2)

Table 1. Results of kinematic tests. Legenda : pre-op=pre-operative, SB=single bundle, SB+lat.p= single bundle +lateral plasty. †Significantly different from group SB ($p < 0.05$). The values are given as the mean, with the standard deviation in parentheses, unit is deg for VV and IE rotations and mm for AP translations.

	VV0	VV30	AP30	AP90	IE30	IE90
SB	60(21)	57(48)	82(31)	76(22)	49(127)	43(155)
Lat.p	40(21) †	43(48)	18(31) †	24(22) †	51(127)	57(155)

Table 2. Percent contribution of each bundle. Legenda: SB=single bundle, SB+lat.p= single bundle +lateral plasty. †Significantly different from group SB ($p < 0.05$). The values are given as the mean, with the standard deviation in parentheses, unit is %.

DISCUSSION

Results summarized in table 1 show how the single-bundle techniques restores knee stability for each measured laxity, but it also highlights the importance of the lateral plasty in controlling VV rotation and AP displacement at 90º of flexion. It has been found, in fact, a statistical difference between SB and SB+lateral plasty values. Table 2 confirms the fact that ACL is primary constrain to AP laxity: the single bundle restores about 80% of knee AP stability, while only 20% is due to the lateral plasty. On the contrary, for VV rotation, the contribution of the lateral plasty is important, it is, in fact, about 40% and statistically significant at 0º of flexion. For IE rotation the contribution of each step is about 50% but there was a lot of inter-patient variability, and measurements did not reach statistical significance.

This study is the first that describes *in vivo* the effect of the surgical technique in restoring knee stability. A more extensive study will permit to understand the *in vivo* kinematic of the joint and the contribution of different bundles in controlling knee laxities.

TUNNELS IN ACL PLASTY: "THE QUEST FOR THE ISOMETRIC POINT"

D'Hooghe P, Bellemans J, Vandekerckhove B
University Hospital Leuven, Pellenberg, AZ Sint-Jan ziekenhuis Brugge, Belgium
pieter@medscape.com

INTRODUCTION

Is ACL reconstruction as reliable as many profess? The proper selection of the insertion sites of the graft remain a difficult point and a key objective. A recent literature survey shows that each conventional system creates significantly different tunnel positions and that up to 25 % of the results are considered insufficient. This partially explains why the literature revision rate is up to 25 % according to Peterman et al. If results are to be improved, then it´s necessary to improve tunnel placement and consequently the tools utilized to generate the tunnel position. Some systems use only ´statical´ rules to search for the anatomical positions of the tunnels. More advanced systems combine anatomical data with kinematic measurements to find the favourable isometric point and to constitute the ´anatomometric´ criteria..

The objective of this study is to gain data comparing tunnel placement accuracy and to gain data optimizing the favourable isometry, comparing the standard with the navigation assisted system(Praxim Medivision).

MATERIALS AND METHODS

We performed a cadaveric study in which tunnel placement was compared between 15 conventional arthroscopic ACL reconstructions and 15 navigation-assisted arthroscopic ACL reconstructions. We looked at both femoral and tibial tunnel position and collected the necessary fluoroscopic data.

RESULTS

The results show a significant improvement in tibial tunnel position reaching the isometric point , using the navigation assisted system ($p<0,01$). It shows that the computer acts like a third eye to provide us with valuable information since the (an-)isomety profile and the prediction of notch impingement are very useful data for tunnel placement. This study helps the surgeon in placing and positioning the tibial and femoral tunnel according to the highest available standards during ACL reconstruction nowadays.

DISCUSSION

The system is only a measuring tool and it requires training before it can be used optimally and many technical details and pitfalls have to be very well understood (e.g. not bending the pointer, perform a smooth and complete flexion-extension, calibrate instruments with care,etc.). Recent clinical studies show that notch impingement is avoided in all cases using navigation.

A large numbers of failures and revisions of ACL surgery do exist. Can we conclude that the tunnels are better positioned using navigation than without? On the tibia, this study shows that there exists a significant difference in tunnel positioning. The extension of the anterior border of the tibial tunnel remains at the same level or posterior to the roof of the notch in the navigation group. Therefore , it is possible to place the tibial tunnel as anteriorly as possible while preventing notch impingement. In addition, navigation makes it possible to avoid notch impingement not only in the most anterior part of the notch, but also on the medial and external wall, for any given degree of flexion.

On the femur, using the system makes it very clear that a small variation of the tunnel placement drastically changes the isometric profile. This study could not demonstrate a significant difference in the geometrical placement of the femoral tunnel between the two groups. However, the measurements on lateral X-rays probably hide a true difference. Because the variation of the isometric profile is so closely related to the tunnel placement in the femur, it is very unlikely that a difference does not exist between both groups in 3D. Further investigations on post-operative CT or MRI images should be necessary.

It is also known that a small rotation of the femoral aiming device, that still preserves the hook constraint and that looks correct, can influense significantly the isometric profile.

In the navigated group, the computer could help us to find a correct location of tunnels - that avoid impingement – in all cases. No further notch plasty was performed at the end of surgery to reach this result. Notchplasty is only performed a priori at the beginning of surgery when it is estimated that the shape is too narrow on the preoperative assessment.

In the conventional group, notch plasty was performed at the end of surgery since it is sometimes very difficult to estimate if there is a conflict or not in full extension, but literature suggests that in 2/3 cases this leads to potential impingement.

Correcting the anterior drawer by making the tibial tunnel as anterior as possible, leads to a potential conflict with the notch in 2/3 of the conventional group, while no potential conflict has been detected in the navigated group.

CONCLUSION

The navigation system is only a tool in ACL reconstruction. It provides 3D data that is very rich and detailed on each individual patient's anatomy and function. It makes it possible to optimize the compromises that were made intuitively until now during ACL surgery.

This study helps the surgeon in placing and positioning the tibial and femoral tunnel according to the highest available standards during ACL reconstruction nowadays.

REFERENCES

- Plaweski, Cazal, Merloz. ACL reconstruction using navigation: a comparative study on 60 patients. *ACL logistics Julliard Protocol.*
- Jackson DW, Gasser SI. Tibial tunnel placement in ACL reconstruction. *Arthroscopy*, 1994 ; 10 :124-131.
- Pässler HH , Mansat C. Le test de lachman radiologique. *Sport et médecine*, 1986, 10 : 22-27.
- Stäubi HU, Sati M, Kazermann S, Bourquin Y, Kunz M, Nolte LP. Clinical application of new computer assisted technology of anatomic ACL reconstruction under arthroscopic control. *5th international symposium on CAOS, Davos, Switzeland*, February 2000; 17-19:22.
- Zavras TD, Race A, Bull AMJ, Amis AA. A comparative study of isometric points for ACL graft attachment.*Knee surg, Sports Traumatology, Arthroscopy*, 2001; 9:28-33.
- Petermann J, Schierl M, Pashimeh – Azar A, Gotzen L. Computer and robot assisted ACL reconstruction with CASPAR system.*European society of sports Traumatology, Knee surgery and Arthroscopy*, London U.K., September 2000;16-20:283.

SUBJECT-SPECIFIC MUSCLE-SKELETAL MODELS OF THE LOWER LIMBS FOR THE PREDICTION OF MUSCLE FORCES DURING GAIT

*Montanari L, *Taddei F, *Martelli S, **Leardini A, ***Manfrini M, *Viceconti M
*Istituti Ortopedici Rizzoli, Laboratorio di Tecnologia Medica, Bologna, Italy
montanari@tecno.ior.it

INTRODUCTION

The estimation of the forces exerted by the muscles on the lower-limb skeleton during movement is essential for the understanding of the mechanical function of the body and for the estimation of the stresses and strains induced in the bone segments. At present, however, it is impossible to measure muscle forces non-invasively *in-vivo*, hence it is necessary to generate a muscle-skeletal model and predict those forces numerically. Several works have been published in the literature that reports those forces [1,2], however, the reported results present a high range of variability and are not easily scalable to a different subject.

In order to build a complete subject-specific muscle-skeletal model data coming from different sources need to be merged and registered.

Aim of this work is to present the preliminary results of our current studies to show, on a real clinical case, a possible strategy of data fusion, based on the DataManager© [3] software, for the generation of a complete subject-specific muscle-skeletal model of the lower limb to predict the forces acting on the skeleton during gait.

MATERIALS AND METHODS

The selected patient underwent a complex distal femoral reconstruction for a primary bone sarcoma in 2001 at the age of 10. In 2004 the patient was CT scanned for routinely control exam. An innovative protocol was adopted to allow the registration of the patient's skeleton with the kinematics recorded during the gait session. Prior to CT scanning, the patient was instrumented with 34 markers for the gait analysis (14mm diameter). Since the markers are visible on CT images (Fig. 1), their positions, relative to the patient skeleton, were derived from the CT dataset. With the markers still in place a motion analysis was performed (Vicon Motion Systems, UK).

The skeletal model of the patient was generated segmenting the CT dataset (Amira, Mercury System Inc., USA). Ninety-five skeletal landmarks were identified onto the bone segments using the Virtual Palpation functionality implemented in the Data Manager ©. The muscles' origins and insertions were estimated registering a standardized atlas [4] onto the patient bones morphology using an affine registration algorithm implemented in the DataManager©. Eighty-four muscles were identified (Fig. 1). Muscles were represented with linear segments starting from the muscles' origin to its insertion. Muscles with broad origins or insertions area were represented with more than one segment.

Positions and orientations of the bone segments during gait were obtained by matching marker arrays of the rigid morphological models and collected marker trajectories using a rigid registration algorithm. The moments at the hip, knee and ankle joints were calculated imposing the rotational equilibrium at all joints. The Physiological Cross Sections Area (PCSA) of all muscles were estimated. A static optimisation algorithm based on the minimization muscular stresses [5] was used to estimate the muscles' forces.

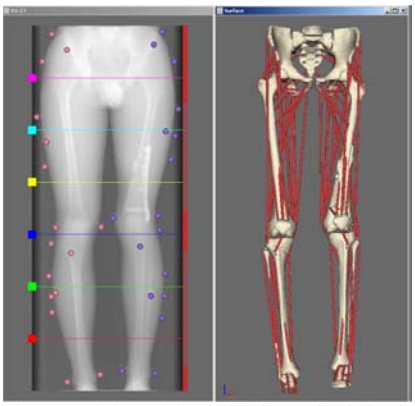

Fig.1 CT (left) and the derived muscle-skeletal model (right)

RESULTS AND CONCLUSIONS

The considerable improved bone pose estimation, achieved with this innovative technique, allowed the development of a truly subject-specific muscle-skeletal model of the patient lower limbs. The forces predicted by the model correlated well with the literature results and were used in the estimation of the risk of fracture of the reconstructed segment. This tool may be of great help in the optimisation of the rehabilitation therapy management or in the post-operative functional assessments of difficult clinical cases, as, for example, patients that undergone a massive skeletal reconstruction due to bone tumours.

REFERENCES

[1] Anderson, et al., Gait Posture, 2003. **17**(2).
[2] Brand, et al. J Biomech, 1986. **19**.
[3] www.tecno.ior.it/multimod/
[4] Kepple, et al., J Biomech, 1998. **31**(1).
[5] Challis, Med Eng Phys, 1997. **19**(3).

ACKNOWLEDGMENTS

This work has been partially funded by the AIRC (Associazione Italiana per la Ricerca sul Cancro)

**Movement Analysis Laboratory
***Skeletal Oncology Department
Istituti Ortopedici Rizzoli,Bologna, Italy

I-ARM: A PASSIVE ROBOTIC ARM FOR ACCURATE ORTHOPAEDIC SURGERY

*De Candido Alba F, **Bertocci F, **Allotta B, *Paggetti C, *Marcacci M
*Biomechanics laboratory Istituti Ortopedici Rizzoli Bologna, Italy
**Dept. of Energetic Engineering S.Stecco University of Firenze, Italy

INTRODUCTION

The guidelines on which the research, development, engineering, and prototyping of the system are based are: versatility; accuracy; easy sterilization; easy assembly; minimally invasive; navigable.
The system is made of two sub-systems which have different tasks:

- The first arm holds the treated leg steadily, it is fixed directly onto the articulation and can be easily unhooked in a rapid and safe way to allow normal movements of the leg.
- The second arm holds the cutting tool, interfaced with navigation system, which identifies the cutting plane. Practically, the surgeon's hands guide the robot to the appropriate position and then, using the information received from the navigation system, puts the cutting tool on the right plane and makes the cuts.

The two arms have 6 degrees of freedom. Besides, there are other subsystem with open interface to complete the architecture of I-arm:

- The moving system: two slides, which allow two translation movements to place the system near the working zone and to approach it to the patient's knee.
- The rapid hooking-release system (Fig.1a): a spring system that fix the leg of patient using percutaneous plates and pins screwed into the bone.
- The fixing system of cutting tool: an eccentric lever permit a very simple lock of pneumatic cutter (Fig.1b).

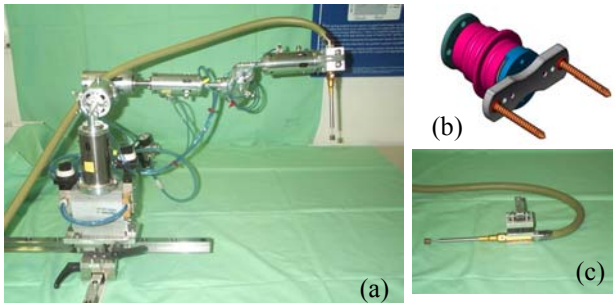

Fig. 1 a) I-arm prototype b) Cad model of rapid hooking-realise; c) The fixing system of cutting tool system

METHODS

- *Work space study* The work space is analyzed using the direct cinematic theory for the study of roto-transfer homogenous matrix and using the Denavit-Hartemberg convention for the identification of reference systems. A Matlab code, which implements any single reference system, is used for computation.
- *Stiffness test* To test the stiffness of I-arm we performed two tests using the NDI Polaris optical system to register displacement, and a dynamometer to apply the force to the end effector of the system. In particular, we performed some cycles of load-unload increasing of 1 kg for each cycle to test whether there was residual displacement after each cycle.
- *I-Arm Usability* Usability of the system was tested collecting the impressions of three surgeon after using I-Arm during a simulated implantation of a knee prosthesis.

RESULTS

The I-Arm resulting work space is 1778,3x1478,3 mm and the skill space is 1619,4x1319,4 mm. Stiffness test's results are summarized in Fig 2. Usability tests results are shown in table 1.

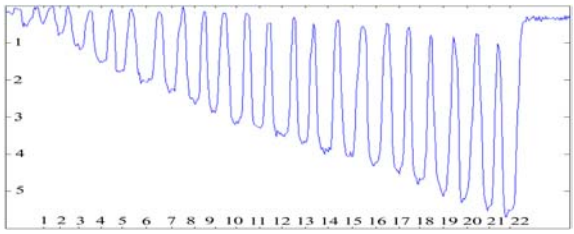

Fig.2 stiffness test's graphic

Possibility of having right orientation of instrument in the desired position	**sufficient**
Easiness of reaching position	**sufficient**
Easiness of locking and unlocking	**Very good**
Easiness of fixing and releasing device	**sufficient**
Displacement from desired position	**little**
Compatibility with surgical procedure	**large**

Table 1 Usability tests results

DISCUSSION

Results show that I-Arm has a very large work space and skill space, and this features are very remarkable especially considering that I-Arm has a rest volume of 26,25 dm^3. Regarding to stiffness we found considerable residual displacement, which was probably due to the ball bearing wear. However, the results were satisfactory considering that for two joints the maximum displacement was 5.5 mm with an applied force of 22 kg. The system, designed for total and partial knee arthroplasty, has shown to be light and not cumbersome. In addition this system has a modular architecture, so it can be use for many type of operation. Moreover this particular structure permits to add or remove some joints in the cinematic chain modifying the degree of freedom and work space of I-arm. The versatility of the end effector allows to insert other instruments as the cutting blades, drill etc…. Finally, I-arm is easy to sterilize and it can be entirely put in autoclave. The next steps are: continue experimentation by using different solutions, for example for ball bearings or different materials for the carter of joint and links between joints and interfacing the system with the navigator and subsequently define surgical procedure based on I-arm.

COBALT ALLOYS WITH TANTALUM SURFACE ENRICHMENT FOR HIP AND KNEE PROSTHESES

*Spriano S, *Vernè E, *Matekovits I, **Faga MG, **Bugliosi S
Politecnico di Torino, Italy

Silvia.spriano@polito.it

INTRODUCTION

The aim of this research is the synthesis and characterization of cobalt alloys after surface modification with tantalum, in order to obtain a biocompatible material presenting at the same time good wear performances, low metal ion release and low toxicity. It is of interest for hip and knee joints with metal-on-metal or metal-on-UHMWPE contacts. In the first case the main aim is to enhance the biocompatibily of the surface and to reduce the amount and the toxicity of the metal debris [1]. In the second case the main aim is to reduce the amount of polymeric debris [2]. Tantalum was selected according to its high corrosion resistance and biocompatibility [3]. The employed process is of interest because it is low-cost and it does not involve the formation of a brittle ceramic coating. The BIODUR alloy was selected as substrate, because it is widely used in hip joints.

METHODS

The surface modification was obtained by a thermal treatment in molten salts containing Ta (1000°C – 1h) without applying any electrical current. The characterization was performed by x-ray diffraction analysis (Cu Kα), nano-hardness indentation (10mN), friction measurements and wear tests (dilute bovine serum as lubricant; 37°C), SEM-EDS observations, scratch tests (Revetest; scratch grids at constant load of 40N), surface profiling analysis (Rank Taylor Hobson instrument), wettability tests (Leitz optical stage microscope; dilute bovine serum).

RESULTS AND DISCUSSION

A surface enrichment with tantalum was obtained through a thickness of several microns (3-6 μm) and SEM observations showed a continuous and crack free interface between the substrate and the modified layer. The maximum tantalum content on the surface is about 90 wt%. The surface is monophasic presenting an intermetallic compound ($CoTa_3$). The modified alloy is slightly rougher than the substrate, with a maximum roughness of 40 nm. This is an acceptable value according to the normative for metal on metal implants (ISO7206-2). Scratch tests showed that the modified layer is well adherent to the substrate through a diffusion layer and its first detachment appeared at 55 N without any brittle or catastrophic event. The damage of the treated material is low also when crossing scratch lines are perfomed as grids. The employed load during this test (40N) is comparable with the maximum scratch load during in-vivo implantation [4]. The modified layer presented a higher wettability than the untreated one, with a contact angle of about 48° respect to 82°. This contact angle is comparable with that of alumina. The elastic modulus of the treated surface layer (nano-indentation tests) is 352 GPa, while it is 241 GPa in the untreated alloy and its hardness is 1.7 GPa while it is 1.5 GPa in the untreated one. So the enrichment with tantalum and the formation of an intermetallic compound involved a stiffer and harder surface. The surface presents also a better wear resistance in pin-on-disc tests with a metal-on-metal contact ($0.7 \cdot 10^{-4}$ respect to 5.7 mm^3/Nm) and lower friction coefficients (0.24 respect to 0.34). This behaviour is in agreement with the presence of a surface with a higher hardness and wettability and the same trend was obtained in the case of metal-on-UHMEPE contact. This is of interest both in the case of metal-on-metal joints, in order to reduce toxic metal debris, and in the case of metal-on-UHMWPE, in order to reduce polymeric debris. Concluding a surface with high tantalum content can be obtained by a low-cost process. It shows good mechanical properties (high elastic modulus, high hardness value, low friction coefficient, high wear resistance) and chemical properties (high wettability, good corrosion resistance [5]). So it is of interest for joints presenting good biocompatibility and long duration.

REFERENCES

[1 L.Savarino, D.Granchi, G.Ciapetti et al., Ion release in stable hip arthroplasties using metal-on-metal articulating surfaces: A comparison between short-and medium-term results, J.Biom.Mat.Res.Part A 66, 450 (2003)

[2] D.Granchi, I.Amato, L.Battistelli et al., Molecular basis of osteoclastogenesis induced by osteoblasts exposed to wear particles, Biomat. 26, 2371(2005)

[3] D.M.Findlay, K.Welldon, G.J.Atkins et al, The proliferation and phenotypic expression of human osteoblasts on tantalum metal, Biomat. 25, 2215 (2004)

[4] K.L. Dahm, P.A. Dearnley, Abrasion response and abrasion–corrosion interactions for a coated biomedical stainless steel" Wear 259, 933 (2005

[5] S.Spriano, E.Vernè, M.G.Faga et al., Surface treatment on an implant cobalt alloy for high biocompatibility and wear resistance, Wear 259, 919 (2005)

AFFILIATED INSTITUTIONS FOR CO-AUTHORS

** Istituto di Scienza e Tecnologia dei Materiali Ceramici – CNR, Torino - Italy

DELTOID MECHANICS IN THE CUFF DEFICIENT SHOULDER

Audenaert E, *De Wilde L, *Audenaert A, *Verdonk R
Department of Orthopedic Surgery, Ghent University Hospital, Ghent, Belgium

emmanuel.audenaert@azbrugge.be

INTRODUCTION

In the progression to cuff tear arthropathy, the shoulder function is often impaired, ranging from weakness to frank pseudoparalysis. The stages can be followed radiographically in terms of progressive ascension and medialization of the humeral centre of rotation.
We investigated theoretically to what extent both parameters mechanically influence the functional performance of the deltoid muscle and so contribute to the clinically observed functional loss in the cuff deficient shoulder.

MATERIALS AND METHODS

Normal glenohumeral relationships in the scapular plane were derived from true anteroposterior X-ray views of the dominant shoulder of fifty three healthy medical students. The Ethics Committee of Ghent University Hospital approved the radiographic study. All subjects gave written informed consent.
A biomechanical model of the shoulder was than used to simulate ascension and medialization of the humeral centre of rotation and mechanically analyze their influence on deltoid muscle performance in absence of the rotator cuff muscles.
The model was build based on the reconstructed osteology derived from a CT-scan of a healthy 28 year old subject. The software package Mimics ® (Materialise NV, Leuven, Belgium) was used to perform the bony reconstructions and data retrieval. In this bony model the humerus was then translated in the scapular plane in order to fit the observed mean normal values for glenohumeral relationships.
The deltoid muscle was reconstructed in two layers using the global optimization method as described by Audenaert et al. for spherical-cylindrical muscle wrapping. (1) Doing so, the inner and outer boundaries of the deltoid muscle were defined in a muscle model containing in total 98 fibres. (Figure 1)
The changes in total deltoid moment caused by ascension and medialization of the humeral centre of rotation, as seen in the cuff deficient shoulder, were calculated for increments of one millimeter in both directions.

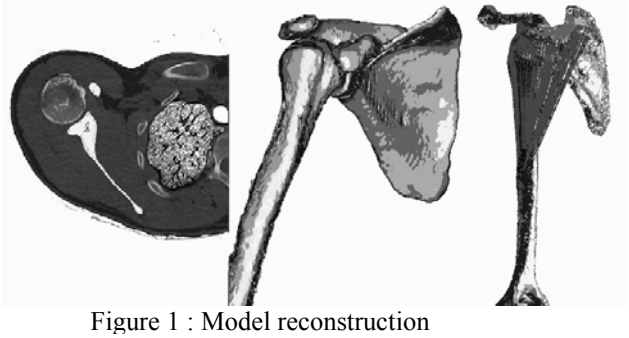

Figure 1 : Model reconstruction

RESULTS

Ascension of the humeral centre of rotation was found to cause an important loss in total deltoid moment, whereas medialization enhanced the deltoid moment but less importantly.
Subacromial bony impingement of the greater tuberosity occurred from an acromiohumeral distance of less than 7 mm. When the acromiohumeral distance became less than 3 mm and rotator cuff function was completely absent, the deltoid muscle alone seemed mechanically unable to allow full functional use of the arm.

DISCUSSION AND CONCLUSION

Ascension of the humeral centre of rotation in the progression to cuff tear arthropathy significantly alters biomechanics of shoulder function. Medialization of the humeral centre of rotation, as seen in severe stages of cuff tear arthropathy, is probably insufficient to completely compensate for the mechanical loss in deltoid moment caused by humeral head ascension.

REFERENCES

1. Defining the shortest path in wrapping algorithms for musculoskeletal modeling. E. Audenaert, A. Audenaert, L. De Wilde, R. Verdonk. Computer Methods in Biomechanics and Biomedical Engineering, 2005:Suppl. 1. 9-11

AFFILIATED INSTITUTIONS FOR CO-AUTHORS:
** Department of Environnement, Technology and Technology Management, University of Antwerp, Prinsstraat 13, B-2000 Antwerp, Belgium

GLOBAL OPTIMIZATION METHOD FOR SPHERICAL AND CYLINDRICAL WRAPPING IN MUSCULOSKELETAL MODELLING

*Audenaert E, **Audenaert A
*Department of Orthopedic Surgery, Ghent University Hospital, Ghent, Belgium
emmanuel.audenaert@azbrugge.be

INTRODUCTION

In musculoskeletal modelling, many muscles cannot be represented as straight lines from origin to insertion as bony and musculotendinous morphology of neighboring structures causes them to wrap. The majority of these passive structures can be adequately described as simple geometric shapes like spheres and cylinders.
Techniques for describing smooth muscles paths over multiple obstacles have been developed for modeling use.
For diarthodial muscles in the available obstacle-set methods, a path is composed that satisfies single object wrapping algorithms by connecting the different shortest paths around the individual obstacles. Nevertheless this does not analytical calculate the shortest smooth muscle path between origin and insertion but finds only a path for which each of the individual wrapping algorithms are satisfied. For example: in cases a sphere is included in a classical multi-obstacle set wrapping algorithm, muscle paths around the sphere are restricted to the sphere radius and a plane containing the sphere center. This assumed restriction can compromise the iteration process to find a workable solution for the true shortest muscle path that obeys to all restrictions of a smooth path, i.e. finding a tangential to both the sphere and the cylinder. This can cause model instability.
In this study a method for spherical and cylindrical wrapping is presented to select the shortest smooth muscular path between origin and insertion from all possible smooth paths between these two points without restricting the spherical muscle path to the sphere radius or a bundle of planes through the sphere center. As an illustration of this global optimization method a model of the deltoid muscle was compared with the obstacle set method for spherical and cylindrical wrapping.

MATERIALS AND METHODS

1) Wrapping algorithm

In the upper limb the humeral head is described by a sphere and the humeral shaft is defined by a cylinder.
The shortest possible path to connect origin (O) and insertion (I) is a straight line OI. This path without wrapping is only possible if the straight line between O and I has no common points with the cylinder or the sphere. Whenever the cylinder and/or sphere intersect this path, the muscle will wrap around one or both obstacles. From the muscle origin on, all possible smooth paths are now calculated and the shortest smooth path will be selected as real connecting path (Fig 1). The minimization algorithm is based on Golden Section search and parabolic interpolation.

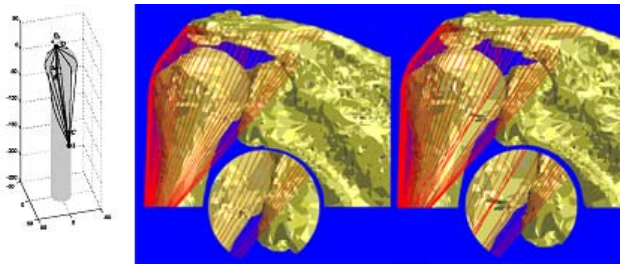

Figure 1

2) Comparison of the global optimization method with the obstacle set method

A model was build from a 1 mm slice thickness CT scanning of a cadaveric specimen. The software package Mimics ® (Materialise NV,Leuven, Belgium) was used to reconstruct the bony surfaces. The deltoid muscle was then reconstructed by both the global optimization method and obstacle set wrapping method. Muscle lengths, moment arms and wrapping radius around the sphere were obtained from both methods.

RESULTS

A total of 61 muscle paths were calculated to wrap either single spherical (n = 37) or spherical -cylindrical (n= 24). As expected, for single spherical wrapping paths both the global optimization method as the obstacle set method calculated the same muscle paths, all wrapping around the sphere with a wrapping radius equal to the radius of the sphere. When the paths combined spherical and cylindrical wrapping, different muscle paths were calculated. None of the obstacle set method paths completely fulfilled all restrictions for a smooth muscle path. Two types of model instabilities were observed in the obstacle set method: convergence of bundles phenomena and wrong path selection.

DISCUSSION AND CONCLUSION

Within the context of musculoskeletal modeling a precise estimation of the musculotendinous path is highly crucial as muscle moments arms and forces depend directly from it. Disregarded some instability errors, when a large number of fibres is used to describe a muscle, the obstacle set method results in a very close approximation of the results obtained by the proposed global optimizing technique. However, errors up to 12 mm were calculated for example for the rotational moment arm in single fibres. This type of errors can become very significant in models that use a limited number of fibres to describe a muscle.

AFFILIATED INSTITUTIONS FOR CO-AUTHORS:
** Department of Environnement, Technology and Technology Management, University of Antwerp, Prinsstraat 13, B-2000 Antwerp, Belgium

KINEMATICAL STUDY IN VITRO OF THE GLENOHUMERAL JOINT

* ** *** Billuart F, *Devun L, *Skalli W, **** *****Gagey O, *Mitton D
Laboratoire de Biomécanique, ENSAM-CNRS, Paris, France
fbilluart@ass-hopital-cheminots.asso.fr

INTRODUCTION

The glenohumeral joint is particularly mobile and allows the displacement of the upper limb in the 3 planes of space. The intrinsic stability of the joint is poor because of the low congruence of articular areas and the releasing ligaments when the shoulder is relaxed.

The aim of the study is to carry out a 3D kinematics analysis in vitro of the glenohumeral joint during the movement of abduction.

MATERIALS AND METHODS

6 frozen anatomic pieces were tested (4 left and 2 right shoulders). The freezing period doesn't last more than 2 months. The average age of death is 79 years old, the younger was 70 and the older was 94.

The first step of the dissection is the disarticulation of the scapulothoracic and the elbow. The clavicle is cut at the junction of its external third and its internal two thirds leaving intact the anterior deltoideus. All the soft tissues are removed except the following muscles: deltoideus and suprasupinatus, and the following tendons: subscapularis, infrasupinatus, teres minor, long head of the biceps and all the capsuloligamentar elements.

The acromion is cut in the coronal plan in its posterior part. The external third of the clavicle and the acromion are raised after having cut the ligaments: coracoglenoïdal, coracoacromial, coracohumeral, trapezoid, conoid and coracoclavicular internal. The acromion and the clavicle are perforated where the muscle fibres converge. A flexible and inextensible bond is fixed between the acromion and the clavicle through two screws. A pulley passes inside this bound. The scapula is perforated in three points and fixed on its rotating support through 3 screws.

The kinematics follow-up of the osseous parts is carried out using an optoelectronic system polaris®. A tripod is fixed on the external edge of the point of the scapula, another is fixed on the cortical external humeral diaphysis in its low part.

Biplane radiographies are obtained using the system of low dose stereo-radiographs EOS ®.

Stereoradiographies are carried out, the tripod being fixed to the bone and allowing the axes of the movement to be defined from corresponding radiographic reference marks.

The medial edge of the scapula is vertically directed then an horizontal traction at constant speed ($8{,}3\times10^{-4}\,ms^{-1}$) of the acromion and the clavicle is carried out using a universal machine test (instron®)

RESULTS

For an horizontal displacement of the acromion and the clavicle of 30 millimeters: the abduction angle is contained between 40° and 20°. The higher displacement of the humeral head is under 5 millimeters.

DISCUSSION

This test leads to a lateral rise of the humerus by tracting on the deltoideus with a very good synchronization of the results. It is the first shoulder's kinematics test, the humerus being nonconstrained. These results suggest that the deltoideus ensures by himself the centering of the head from the beginning of the elevation since the ligaments are not used during this phases. Nevertheless, the articular kinematics can be disturbed during the tests because of the removal of the coracoarcromial ligament. Moreover the reduction of weight of the upper limb can disturb the course of the movement.

These experiments will make it possible to evaluate a three-dimensional model in finite elements of the shoulder.

ACKNOWLEDGEMENTS:

Technique support: Magnier J, Menant.ù C, Le Caloch B

AFFILIATED INSTITUTIONS FOR CO-AUTHORS:

* Laboratoire de biomécanique, ENSAM-CNRS, Paris, France
** Groupe Hospitalier « les Cheminots », Draveil, France
*** Institut de Formation en Physiothérapie « commerce », Paris, France
**** Service de Chirurgie Orthopédique, CHU de Bicêtre, Le Kremlin-Bicêtre, France
***** Institut d'Anatomie de Paris, Université Paris 5, France

ARTHROSCOPIC REPAIR OF THE ROTATOR CUFF: EXPERIMENTAL STUDY OF DIFFERENT REPAIR TECHNIQUES

*Öhman C, *Baleani M, **Marinelli A, ***Giavaresi G, *Toni A
*Laboratorio di Tecnologia Medica, Istituti Ortopedici Rizzoli, Bologna, Italy
ohman@tecno.iot.it

INTRODUCTION

Even though in the last years progress has been made in the surgical technique of rotator cuff repairs, retears occur relatively frequently [1]. Therefore, there is still a need for a high strength repair. The aim of this study was to determine experimentally the mechanical performance of different techniques for arthroscopic rotator cuff repair.

MATERIALS AND METHODS

Humera and infraspinatus tendons of sheep were used in all the in vitro experimental tests.

Firstly, the strengths of four different tendon grasping techniques were compared: Simple stitch (SS), Mattress, modified Mason-Allen, and a simple stitch closed over a horizontal loop (SS+HL). The SS+HL was developed as an alternative to the modified Mason-Allen stitch. The latter can be assumed as the golden standard in open rotator cuff surgery. Unfortunately, since the thread can not slide within the tendon, the modified Mason-Allen is difficult to stitch correctly in arthroscopic surgery [2].

Secondly, the pull-out strength of two different titanium anchors (5.0-mm Super Revo® and 5.0-mm Twinfix™) was tested.

Finally, testing of the mechanical behaviour of the whole repair was performed. Two different tendon grasping techniques were compared: 2SS and 2SS+HL. The latter is a modified SS+HL stitch: as a suture anchor carries two threads, it is possible to make two SS over the horizontal loop. Two different sutures (Ethibond® N°2 and Herculine™ N°2) and two anchors (5.0-mm Super Revo® and 5.0-mm Twinfix™) were used. The strength and stiffness of the whole repair were determined.

Analysis of variance (ANOVA) or a t-test was used to analyse the experimental data.

RESULTS

The strength of the SS+HL was more than twice as high as that of the Mattress and the SS. No significant difference was found between the SS+HL and the modified Mason-Allen (Figure 1).

The pull-out strength of the Super Revo® suture anchor (674N±196) was significantly greater than that of the Twinfix™ anchor (448N±116).

Finally, the results obtained testing the whole repair, stitched using Herculine™, showed that the strength of the 2SS+HL (290N±58) was more than twice as high as that measured for the 2 SS (115N±35), regardless of the anchor type. A strength reduction was found in the 2SS+HL repair shifting from Herculine™ (290N±58) to Ethibond® (169N±19). Also the stiffness of the repair depended on the suture type while no significant effect was due to the anchor or to the stitch (Figure 2).

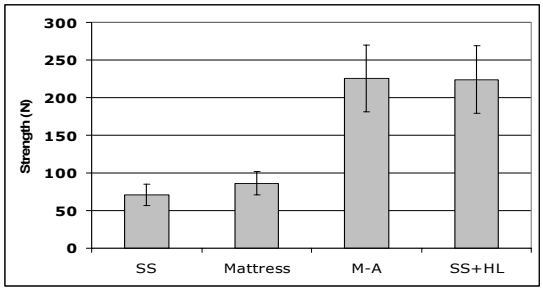

Figure 1 – Holding power of the four stitches.

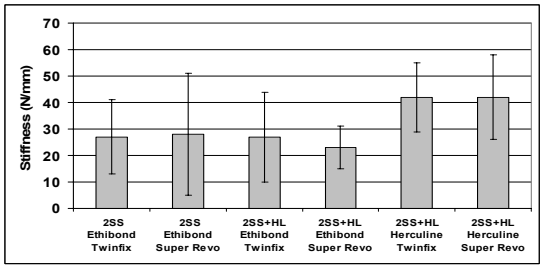

Figure 2 – Stiffness of the whole repairs.

DISCUSSION

The SS+HL could be a potential substitute of the Modified Mason-Allen. In fact, it seems like the horizontal loop enables a protection from the thread cutting through the tendon and thereby increasing the holding power of the stitch.

The Super Revo® shows a higher pull-out strength than Twinfix™ in healthy bone. However, both anchors have a pull-out strength larger than the holding strength of the best grasping technique. This seems to be the weak point of the repair. The use of the 2SS+HL instead of 2SS should increase the strength of this weak link. Additionally, the stiffness of the suture seems important for the stiffness of the repair. This could be of importance: a higher stiffness might prevent the formation of a gap between the tendon and the bone during loading of the repair reducing the risk of delayed healing or failure of the repair.

REFERENCES

[1]Gleyze [et al] (2000), Arthroscopic rotator cuff repair: a multicentric retrospective study of 87 cases with anatomical assessment. *Rev Chir Orthop Reparatrice Appar Mot.* Vol. 86, No 6, 924-30.

[2] Schneeberger [et al] (2002), Mechanical strength of arthroscopic rotator cuff repair techniques: an in vitro study. *J Bone Joint Surg Am.*, Vol. 84-A, No 12, 2152-60.

**Sezione B di Chirurgia Ortopedico Traumatologia, Istituti Ortopedici Rizzoli, Bologna, Italy
*** Laboratorio Chirurgia Sperimentale, Istituti Ortopedici Rizzoli, Bologna, Italy

ESTIMATION AND VISUALIZATION OF LOWER LIMBS ORIENTATION ANGLES USING BODY-FIXED SENSORS: APPLICATION TO TOTAL KNEE ARTHROPLASTY

*Jolles BM, **Aminian K, **Dejnabadi H, **Urtasun R, **Fua P, *Pichonnaz C, *Voracek C, *Leyvraz PF
University Hospital of Lausanne CHUV-HOSR, Lausanne, Switzerland
Brigitte.Jolles@chuv.ch

INTRODUCTION

As an alternative to optical motion analysis systems which are often used in the study of human movement, body-fixed sensors have been recently used as an ambulatory solution. Body-fixed miniature sensors consisting of accelerometers and gyroscopes can be used to obtain joints and segments kinematic values, allowing the realization of low-power, ambulatory recording systems carried by the subject for long-term measurements. This study presents a new method for accurate estimation of lower limb angles in the sagittal plane based on a combination of accelerometers and gyroscopes. It presents also a new tool to visualize motion data with synthetic skeletons performing the same actions as the patients.

METHODS

Lower limbs movements during gait were captured by 4 modules of sensors attached on both shanks and thighs. Each module consisted of a gyroscope and bi-axial accelerometers. The model of knee angle estimation was based on processing the outputs of a pair of virtual sensors placed at the knee center of rotation on the adjacent segments. Since both virtual accelerometers express the acceleration of the same point, they should have the same modulus, while their arguments' difference yields the knee joint angle.

The model of shank orientation angle estimation was based on placing a virtual sensor on ankle aligned with the shank segment orientation. The method fuses the information of the angles obtained by gyroscope and accelerometers to cancel gyroscope drift. Since the acceleration on ankle is low during foot-flat and quiet standing periods, the information of accelerometers can be used as an inclinometer to correct the gyroscope drift. Finally, the thigh angle is obtained by just adding shank angle with knee angle.

After ethical approval from our institutional board and written informed consent of each patient, ten healthy subjects, aged between 44 and 70 years, participated in the first validation part of this experiment. The volunteers performed three 30s flat treadmill walking trials at speeds 2km/h, 3km/h and 4km/h, as well as a freely arbitrary flexion and extension of knee such as sitting, standing and swinging. For comparison and validity appreciation, a motion measurement system (Zebris, D) was used as the reference system.

The gait signatures of 23 patients with mobile-bearing were compared to the gait signatures of 28 patients with fixed-bearing pre-operatively and post-operatively at 6 weeks, 3 months, 6 months and 1 year in an on-going double-blind randomized controlled trial.

Each participant was asked to perform two walking trials of 30m long at his/her preferred speed and to complete an EQ-5D questionnaire, a WOMAC and Knee Society Score (KSS).

RESULTS

The results of all validation tests were very close to those of the reference system and presented very small errors (mean<0.70°, standard deviation<2.0° for knee angle estimation, and mean<0.87°, standard deviation<94.0° for shank angle estimation) and excellent correlation coefficients (>0.994 for knee and >0.997 for shank). Figure 1 shows the calculation of knee flexion-extension angle of a subject during walking at 3 km/h.

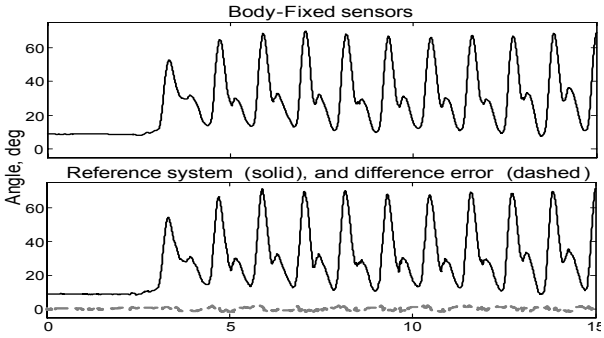

Fig. 1: Knee angles estimated using body-fixed sensors, and compared with reference system. The difference between both signals appeared at the bottom part as a dashed line.

No statistical differences were found between fixed and mobile bearings in terms of EQ-5D, WOMAC or KSS scores at 6 weeks, 3 months, 6 months and 1 year. However, better improvements for fixed-bearing TKA were found with the range of knee angles and peak swing speeds of shank at 3 and 6 months (p=0.03).

DISCUSSION & CONCLUSIONS

The proposed system offers a new accurate tool for lower limbs motion monitoring. The gait visualization tool provides a simple tool to monitor and display motion for long-term monitoring where camera based systems could not be used.

ACKNOWLEDGEMENTS:

This work was supported by a Swiss National Foundation Grant (FNRS 3200-064951).

AFFILIATED INSTITUTIONS FOR CO-AUTHORS:

** Swiss Federal Institute of Technology EPFL, Lausanne, Switzerland

A FLUID PRESSURE OF 5 KPa IS ASSOCIATED WITH A THRESHOLD FOR BONE RESORPTION IN A RAT MODEL

*Fahlgren A, **Johansson L, **Edlund U, *Aspenberg P
*Department of Orthopaedics and Sports Medicine, Faculty of Health Sciences, **Department of Mechanical Engineering, Linköping
Anna Fahlgren@inr.liu.se

INTRODUCTION

Several animal studies have shown that both increased and constant pressure are strong stimuli for bone resorption [1-3]. Elevated intracapsular pressure and increased pressure in lytic lesions has been observed in patients with loose prostheses [4, 5]. An increased fluid pressure can be created through compression of the fibrous membrane surrounding an unstable prosthesis. We have an animal model for fluid pressure induced bone resorption. A fibrous membrane is created and the model compresses this tissue between bone and implant. In this way a hydrostatic pressure is created. This result in a resorptive bone lesion within 5 days, which shares many histological characteristics with the osteolysis observed in cases of loosening. The aim of the current study was to investigate the fluid pressure during different stages of osteolysis in an animal model for prosthesis loosening.

MATERIAL AND METHODS

25 Sprauge-Dawley rats received a titanium plate at the proximal tibia. A central plug was inserted. After 4 weeks of osseointegration, the central plug was changed to a piston. A soft tissue was allowed to form between the piston and the bone for 5 days. Thereafter the pressure piston was subjected to a transcutanous force of 5N. Each episode of pressure comprised 20 pressure cycles, which was done twice a day, with a frequency of 0.17 Hz.

The animals were divided into 3 groups. 10 rats were killed before the first pressure episode (controls), 10 rats day after 5 days of pressurizing and 5 after 14 days. Immediately before the rats were killed, a pressure transducer was connected to the piston and the fluid pressure under the piston was measured. The tissue under the piston was then prepared for histology. Institutional guidelines for care and treatment of experimental animals were followed.

RESULTS

There were 3 exclusions, one in the 5 days group because of instability of the titanium plate and 2 in the 14 days group because of an inflammatory reaction around the piston.

In controls and in the 5 days group the fluid pressure was 377±286 mmHg and 173±76 mmHg respectively The maximum fluid pressure after 14 days of daily pressure episodes was 39±70 mmHg. (Figure 1).
Massive bone resorption was seen in all pressurized specimens. The lytic lesions communicated with the subcutaneous space via wide resorbed canals through the bone. After 14 days newly formed bone layer delineated the lytic lesion from the underlying marrow space. In the controls no resorption pit was found.

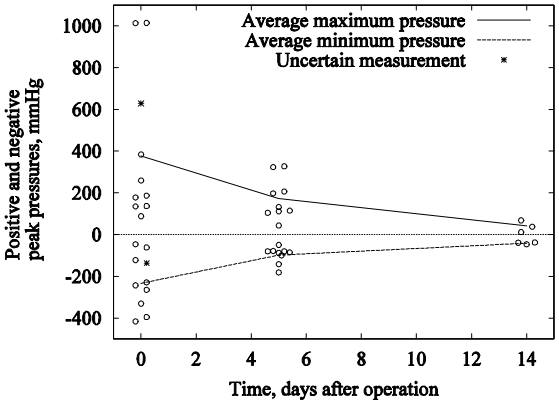

Figure 1. The fluid pressure under the piston.

DISCUSSION

The pressure decrease at 14 days is explained by the communication with the subcutaneous space, effectively draining the lytic lesions. A fluid pressure of 39 mmHg was associated with a steady state, where the lytic lesion appeared to have stopped growing and was becoming walled of by new forming bone. The fluid pressure in these animals has relevant pressure amplitudes compared to clinical examples. In the hip joint capsule prior a revision the pressure has been measure to 31 to 150 mmHg [6], and in osteolytic lesions in the femur prior to revision the amplitude was measured to 12-159 mmHg [4, 5]. The fibrous tissue surrounding loose prostheses has an important role for transforming microinstability to fluid pressure. The current study shows that very low pressures are associated with bone resorption.

REFERENCES

1. Sato, T., et al., J Dent Res, 1998. 77(2): p. 387-92.
2. Skripitz, R. and P. Aspenberg,. J Orthop Res, 2000. 18(3): p. 481-4.
3. Van der Vis, H.M., et al., Clin Orthop Relat Res, 1998(350): p. 201-8.
4. Anthony, P.P., et al., J Bone Joint Surg Br, 1990. 72(6): p. 971-9.
5. Robertsson, O., et al., Acta Orthop Scand, 1997. 68(3): p. 231-4.
6. Walter, W.L., et al., J Arthroplasty, 2004. 19(2): p. 230-4.

ACKNOWLEDGEMENTS

We thank Bibbi Mård for technical assistance. This investigation was supported by the Swedish Research Council (projectx), Materials in Medicine and Tore Nilssons Foundations.

THE ANTEROMEDIAL FACET OF THE CORONOID PROCESS; AN ANATOMICAL STUDY

*Doornberg JN, *Lindenhovius ALC, *de Jong IM, *Ring D
*Orthopaedic Hand and Upper Extremity Service, Massachusetts General Hospital, Harvard Medical School, Boston MA, United States of America.
jdoornberg@partners.org

INTRODUCTION

Fractures of the coronoid process of the ulna are associated with complex traumatic elbow instability. In particular, the anteromedial facet of the coronoid process has been associated with a newly recognized pattern of injury (varus posteromedial rotational instability) and is often a separate fracture fragment in olecranon fracture dislocations. We performed a quantitative three-dimensional analysis of the anatomy of the anteromedial facet of the coronoid process in order to better understand the importance and vulnerability of this structure.

METHODS

Twenty-one computed tomography scans of the intact forearm were analyzed. The anteromedial facet width and total coronoid width were measured from the sagittal axis of the trochlear notch in the anatomical coronal plane through the ulna. The difference between the maximum anteromedial facet width and the anteromedial facet that is supported by the metaphysic of the proximal ulna was defined as the unsupported anteromedial facet—the portion that protrudes as a separate process.

RESULTS

The average distance between the center axis of the trochlear notch and the most medial edge of the anteromedial facet averaged 7.2 millimeters (range, 4.5 to 8.9 mm). The width of the coronoid process in the defined coronal plane averaged 13.4 mm (range, 8.7 to 16.8). The supported and unsupported anteromedial facet width averaged 3.1 mm (range, 1.0 to 5.0 mm) and 4.1 mm (range, 1.4 to 6.8 mm) respectively. This means that on average 57% (range, 26 to 82%) of the anteromedial facet of the coronoid is unsupported.

DISCUSSION

More than half of the anteromedial facet of the coronoid process is unsupported by the proximal ulnar metaphysis and diaphysis. It is not surprising that this relatively vulnerable protrusion from the anteromedial facet of the coronoid is frequently a separate fracture fragment in complex traumatic elbow instability.

Figure 1: Example of the protruding anteromedial facet illustrating the relative vulnerability of the process to varus stress. Our measurements show that the medial articular facet of the coronoid protruded an average of nearly 7 millimeters (over 55% of the entire facet) from the proximal ulnar metaphysis and was unsupported.

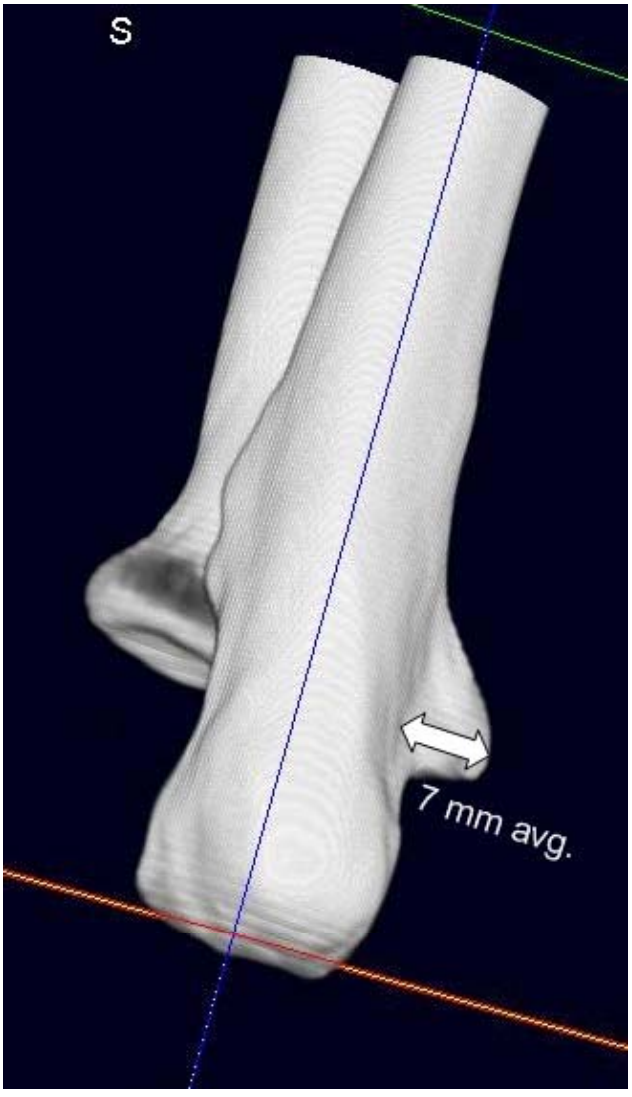

GROWTH OF LONG BONES. A COMPLEX INTERSECTION OF DIFFERENT BIOLOGICAL PROCESSES

*Pazzaglia UE, **Benetti A, ***Bondioni MP, *Bonaspetti G, **Donzelli C
*Clinica Ortopedica e Traumatologica Spedali Civili di Brescia, Università degli Studi di Brescia, 25123 Brescia, Italy

pazzagli@med.unibs.it

INTRODUCTION

Growth plate cartilages of long bones is tradictionally considered the metaepiphyseal structure controlling the length increase of the bone. However the biological mechanisms of bone growth are much more complex, because involve not only that on longitudinal axis but also latitudinal expansion. Epiphyseal ossification center has only a role in length increments in a limited period of infantile growth.

METHODS

Histological samples for the study of the normal morphology and development of human long bones were collected: these included three autoptic cases who died for diseases not involving the physeal structure and twenty-five vertebral columns from 12 to 16 weeks old.

RESULTS

Growth was characterized by specific organization of different tissues in structures with a definite temporal sequence. Biological processes included interstitial growth of the cartilage anlage, endochondral ossification, periosteal apposition and bone remodeling.

DISCUSSION

On the base of the physiological bone development and morphology it is possible to outline the complex variety of cellular mechanisms and their temporal sequence which determine the shape modulation and armonic growth of a bone.

** Cattedra di Anatomia Patologica, Università degli Studi di Brescia, 25123 Brescia, Italy
*** 2^ Radiologia, Spedali Civili di Brescia, 25123 Brescia, Italy

BIOLOGICAL EFFECTS OF EXTRACORPOREAL SHOCK WAVE THERAPY ON HUMAN OSTEOBLASTS IN MODULATION OF INTERLUKIN-10

Moretti B, Corrado M, Notarnicola A, Moretti L, *Iannone F, Patella V
Department of Clinical Methodology and Surgical Technique, Orthopedics Section II, University of Bari, Bari, Italy
DIMIMP- Rheumatology Unit, University of Bari, Bari, Italy

b.moretti@ortop2.uniba.it

INTRODUCTION

Extracorporeal shock wave treatment (ESWT) is successfully used in various musculoskeletal disorders and pathologies.There is growing evidence that ESWT can influence cell metabolism. We have previously shown that ESWT can modify interlukin-10 (IL-10) expression by human articular chondrocytes "in vitro". Beside chondrocytes, osteoblasts play a pivotal role in physiopathology of osteoarthrtitis.
We investigated the effects of ESWT on the expression of IL-10, TNF-a, CD29, CD105 on human subchondral osteoblasts from osteoarthritis (OA) patients and healthy donors (HD).

METHODS

Osteoblasts were isolated by subchondral bone obtained from 13 OA patients undergoing surgical knee or hip replacement and from 7 young HD. After reaching the 2^{nd} -3^{rd} culture passage, osteoblasts were detached and treated with ESWT by an electromagnetic lithotripter (Minilith SL1-Storz Medical) by selecting two different energy levels (0,055-0,17mJ/mm2) and two total impulses (500, 1000) for each level. Control osteoblasts received no ESWT treatment, but were kept with the device off the same time. After ESWT treatment osteoblasts were cultured for 48 hours and IL-10, TNF-a, CD29, CD105 espression was then evaluated by flow-cytometry. To assess intra-cellular levels of IL-10 and TNF-a, osteoblasts were previously permeabilized.

RESULTS

Expressions of IL-10, TNF-a, CD29, CD105 on OA and HD osteoblasts were similar at baseline. Intra-cellular expression of IL-10 significantly increased in osteoblasts treated with ESWT at 0,17 mJ/mm2 with 500 impulse (16,8+/-4) in comparison with control osteoblasts (13,1+/-3) ($p<0,05$). No statistically significant differences were dected among the other groups of ESWT treatment and similar patterns of response were seen in OA and HD osteoblasts.

DISCUSSION

Our preliminary data suggest that ESWT treatment modulates IL-10 expression by human osteoblasts. It has been shown that IL-10 inhibits osteoclastogenesis by inhibiting differentiation of osteoclast progenitors. These experimental data suggest the possibility that treatment with ESWT works modifying the pathological process of ostheoarthritis. Further studies are need to investigate the meaning of these results and possible applications of ESWT in bone human pathology.

REFERENCES

1. Xu, L.X. et al. Interlukin-10 selectively inhibits osteoclastogenesis by inhibiting differentation of osteoblast progenitors into preosteoclast-like cells in rat bone marrow culture system. J. Cell Physiol, 165: 624-629,1995
2. Effetti biologici delle Onde d'Urto su colture cellulari. Atti del 6° Congresso Nazionale SITOD, 3-5 Novembre, Roma 2004; Moretti B, Iannone F, Corrado M, Iasella PA, Amoruso L, De Donno G, Patella V.
3. Effetti delle Onde d'Urto su colture cellulari di condrociti di osteoporosi umana. Atti del 7° Congresso Nazionale IORS, Varese 29-30 Settembre 2005; Moretti B, Iannone F, Corrado M, Iasella PA, Patella V, Simone C.
4. ESWT effects on chondrocytes from OA human subjects , Atti del 8° International Congress of ISMST, Vienna 29 May – 1 June 2005 Moretti B, Iannone F, Corrado M, Iasella PA, PatellaV

PURIFICATION OF PROTEINS INDUCING OSTEOBLAST MIGRATION

*Nakasaski M, *Sotobori T, **Yoshioka K, *Yoshikawa H, **Itoh K
*Department of Orthopaedics, Osaka University Graduate School of Medicine, Suita, Osaka, Japan

man-and@umin.ac.jp

INTRODUCTION

Osteoblast recruitment to the site of future bone formation is essential for skeletal development, bone remodeling and fracture repair, but the mechanism of which remains to be clarified. Several lines of evidence have suggested that various growth factors, including transforming growth factor-β, platelet-derived growth factor and bone morphogenetic protein induced the osteoblast migration. The aim of current study is to identify novel protein factor that induce osteoblast migration and the clinically desired bone regeneration. Here we detected the migration stimulating activity for MC3T3-E1 osteoblastic cells in the serum free culture conditioned medium of MC3T3-E1 themselves, from which we partially purified the high-activity fractions.

METHODS

Serum free conditioned media obtained from MC3T3-E1 osteoblastic cell cultures were sequentially processed with gelatin, blue, heparin affinity column chromatography and separated into several fractions. Migratory activity from the different purification steps was monitored with a modified Boyden chamber assay. In brief, upper wells and lower wells were separated by PET (polyethlene terephthalate) membranes with 8 μm pores. Aliquotes of samples were added to the lower chamber (chemotaxis assay) or the bottom surface of the PET membranes were coated with these samples (haptotaxis assay). $2.5x10^4$ MC3T3-E1 cells were loaded onto the upper chamber and incubated for 4 hours to allow migration, then the migrated cells to the bottom side of the membrane was counted. To identify the proteins that induce osteoblast migration, the high migratory activity fractions were separated by SDS-PAGE (SDS polyacrylamide gel electrophoresis), then analyzed by LC-MS/MS (Liquid Chromatography-Mass Spectrometry/Mass Spectrometry). We focused on several identified proteins and made recombinant proteins of these candidates to examine the migratory activity.

RESULTS

Pools of conditioned media were processed by gelatin affinity chromatography. In the bound fraction of the gelatin column, fibronectin was recognized as major proteins by SDS-PAGE and confirmed by LC-MS. Osteoblast migration was observed when the bottom side of the membrane was coated with the (fibronectin-rich) bound fraction in cell migration assay, but not with the flow through fraction. Interestingly, these flow through fractions showed chemotactic activity for osteoblasts, then by these fractions were further separated by blue and heparin affinity chromatography. The fraction eluted with 50% ethylene glycol from blue affinity column was loaded onto heparin affinity column and eluted with a linear gradient of NaCl(0-1.0 M). These fractions were examined for chemotactic activity and the highest chemoattractive fraction was analyzed by SDS-PAGE and LC-MS/MS. Ultimately we identified several candidate proteins, including periostin and progranulin. Recombinant progranulin did not induce chemotaxis but periostin showed very weak chemotactic activity and increased adhesion of MC3T3-E1 cells.

DISCUSSION

From this study, MC3T3-E1 serum free conditioned medium induced migration of MC3T3-E1 cells themselves. The protein that mainly induce osteoblast haptotaxis was fibronectin and gelatin column flow through fraction enhanced chemotaxis. We then identified several proteins that may induce osteoblast chemotaxis from this fraction. Here we focused on periostin and progranulin, since these proteins have been suggested as candidates of cell migration factor in the literature. Recombinant progranulin did not induce chemotaxis but periostin showed very weak chemotactic activity. It appears that there is another factor that induce MC3T3-E1 migration. It is necessary to apply more powerful methods of chromatography to narrow down the candidate proteins. We are currently undertaking further detection in order to identify the more potent osteoblast migratory factor for the clinical bone regeneration.

** Department of Biology, Osaka Medical Center for Cancer & Cardiovascular Diseases, Osaka, Japan

THE EFFECTS OF HIGH ENERGY SHOCK WAVES ON RABBIT TIBIA. AN IN VIVO HISTOLOGYCAL AND MORPHOMETRIC STUDY

*Pazzaglia UE, **Benetti A, *Bonaspetti G, *Ranchetti F, ***Bodini G, ****Zatti G
*Clinica Ortopedica e Traumatologica Spedali Civili di Brescia, Università degli Studi di Brescia, 25123 Brescia, Italy

pazzagli@med.unibs.it

INTRODUCTION

Shock waves have been applied in the therapy of fractures non-unions on the base of their effects of transition sites between tissues with divergent acoustic impedence like bone and periosteum or endosteum. These are contradictory experimental evidences on the mechanism of action in relation to the models employed in experimental studies, some supporting a pure mechanical effect, while others postulate a not well definited action on osteoblasts mediated trough biochemical factors. There is also uncertainty on the energy level necessary to reach the pursued effects.

METHODS

A single treatment with 2000 pulses of shock waves was applied to the intact tibia of New Zealand white rabbits employing different energy levels: 0.5, 1.0 and 1.5mJ/mm² at the frequency of 4Hz. The bone response was studied at 5 and 20 days and compared with untreated control tibiae employing the following techniques: perfusion of the vascular tree with black China dye, standard bright field histology and morphometry on decalcied sections, tetracycline labelling and fluorescent histology on undecalcified sections.

RESULTS

Five of seven tibias treated with 1.5mJ/mm² showed focal subperiosteal and subendosteal haemorrage with a significant increase at 5 days of osteoblast number, osteoblasts mitoses, neo-apposed bone matrix area. No significant differences with controls were observed in groups which received shock waves energies of 0.5 and 1.0 mJ/mm². At 20 days interval there was no more evidence of enhanced activity at both the endosteal and periosteal surface.

DISCUSSION

Shock waves at 1.5mJ/mm² applicated to the rabbit intact tibia activated matrix synthesis by osteoblasts present in a resting state at both endosteal and periosteal surfaces and stimulated proliferation of the same cells. These effects were focal and closely associated with red cells infiltration, supporting the mechanical theory of shock waves mechanism of action. The stimulatory effect on osteoblasts has a time limit lower than 20 days and three is an energy threshold rather than a continous dose-effect relationship. The latter observations suggest in non-union therapy high energy shock waves application under anaesthesia with intervals between applications of at least 20 days.

**Cattedra di Anatomia Patologica Università degli Studi di Brescia, 25123 Brescia, Italy.
***Casa di Cura S. Camillo, 25123 Brescia, Italy.
****Clinica Ortopedica dell' Università dell'Insubria, Varese, Italy.

TISSUE TRANGLUTAMINASE 2 (TG2) IS NOT ESSENTIAL FOR SKELETAL DEVELOPMENT. Study on TG2 knock-out mice

*Tarantino U, *Oliva F, *Taurisano G, **Ciucci A, **Orlandi A
*Department of Orthopaedics and Traumatology, **Department of Anatomy Pathology
University of Rome "Tor Vergata" School of Medicine, Viale Oxford 81, 00133 Roma, Italy
olivafrancesco@hotmail.com

INTRODUCTION

During chondrogenesis, growth plate chondrocytes proliferate in orderly columns, then they stop proliferating and become prehypertrophic chondrocytes. The latter chondrocytes then undergo hypertrophy, produce a characteristic matrix and die. Hypertrophic chondrocytes play a pivotal role in coordinating chondrogenesis and osteogenesis in the growth plate. In mice endochondral ossification starts since 14,5 day until 19 day, when the ossification is complete.(1)

Transglutaminases are widely distributed enzymes that stabilize protein assembly by catalyzing the Ca^{2+}-dependent formation of covalent [redacted]-(glutamyl)-[redacted]-lysyl bonds (i.e., isopeptide bonds). (2)

Aeschlimann et al. have demonstrated in vitro increasing expression of transglutaminase parallels the maturation of the cartilage in the growth plate of long bones in the epiphyseal cartilage of newborn rats. (3)

Here, we analyze the consequences of Tg 2 deficiency, generated by a gene-targeting approach, for the development of skeletal elements in the mouse.

MATERIALS AND METHODS

Histology: To exclude a possible delay or eventual deformities in skeletal development, we focused our interest on the early development of skeletal structures in embryos since the 13,5 to first day newborn animals by staining cartilaginous and bony structures. Animals were euthanized with an overdose of cloroform. After some skin incisions embryos were processed. All samples were fixed in 10% buffered formalin for 12 hours and decalcified for 48 hours in Decalcifier II (Surgipath Medical Industries, Richmond, IL, USA). After usual processing and paraffin embedding, 5µm section were placed on SuperFrost Plus glass slides (Menzel-Gläser, Braunschweig, Germany) and used for haematoxylin-eosin or immunohistochemical stainings. Femurs were selected for this study.

Immunohistochemistry: Slides were baked overnight at 60°C, deparaffinized in xylene and rehydrated in graded concentrations of ethanol. Endogenous peroxidase activity was blocked by incubation in 0.3 percent hydrogen peroxide and methanol. Slides were rehydrated in phosphate-buffered saline. Non-specific antibody binding was blocked by incubation with normal goat serum (Dako Cytomation, Glostrup, Denmark). Optimal anti-TgII antibody (Covalab, Vinci-Biochem, Firenze, Italy) dilution was found to be 1:75 for 30 minutes. Slides were then incubated with a biotin-labeled goat anti-rabbit secondary antibody (Dako Cytomation, Glostrup, Denmark), followed by a streptavidin-horseradish peroxidase conjugate. Bound antibody was revealed with the use of the substrate 3,3'-diaminobenzidine. Sections were counterstained with haematoxylin, washed, dehydrated with graded concentrations of ethanol, cleared in xylene, mounted and microscopically examined. Human breast carcinoma was included with each batch of sections as a positive control. The location of the Tg 2 was determinated by comparing each immunohistochemical section with the adjacent slice stained with hematoxylin-eosyn.

RESULTS

The size of the skeletal elements and the relative ratio of cartilage to bone in Tg2-deficient mice were indistinguishable from those of wild-type animals.

Histological analysis of the femur from newborn animals displayed no overt changes in the organization of the growth plate in the absence of TG2. Tg 2 deficient animals were indistinguishable in size and behavior from wild-type mice up to an age of 1 year. Adult mice lacking Tg2 displayed no obvious abnormalities in the developing skeleton, and no skeletal elements were missing or deformed. Further, X-ray analysis of the skeleton from 6-month-old animals revealed no apparent differences in size or in the density of the bone.

Immunohistochemical study confirmed the expression of the Tg2 in the hypertrophic chondrocytes of wild type mice and the almost total absence of immunoreactivity in knock-out mice.

CONCLUSION

The deficiency causes no obvious consequences during embryo skeletal development and in adulthood.

REFERENCES

1) Wirtschafter Z.T. Genesis of the mouse skeleton. Springfield: CH. C. Thomas 1966.

2). Folk JE, Cole PW 1966 Transglutaminase: Mechanistic features of the active site as determined by kinetic and inhibitor studies. Biochim Biophys Acta 122:244-264.

3) Aeschlimann D,Wetterwald A, Fleisch H and Paulsson M (1993) Expression of tissue transglutaminase in skeletal tissues correlates with events of terminal differentiation of chondrocytes. J. Cell. Biol. 120: 1461 - 1470.

SPONTANEOUS OSTEOCLASTOGENESIS IN HUMAN CD14-POSITIVE MONOCYTES

*,** Yuasa K, **Ito Y, *Sudo A, *Kusuzaki K, *Uchida A
*Department of Orthopaedic Surgery, Mie University Graduate School of Medicine, Mie, Japan
**Department of Microbiology, Mie University Graduate School of Medicine, Mie, Japan

yuasa911@doc.medic.mie-u.ac.jp

INTRODUCTION

Osteoclasts are multinucleated giant cells responsible for bone resorption and known to be hematopoietic in origin. The detailed mechanisms of their differentiation and activation are not understood sufficiently, however, a cell stage of osteoclast is consisted of three steps regarded as, firstly differentiation, secondary activation and thirdly apoptosis. In other words osteoclasts are finally differentiated and activated cells, and therefore the establishment of cell-line becomes very difficult.

On the other hand, macropharge colony stimulating factor (M-CSF) was concerned with osteoclastic survival and chemotactic behavior by conventional reports. But it is unclear to maintain osteoclasts for a long time.

We have analyzed two kinds of osteoclasts using human peripheral blood CD14-positive monocytes until today, that is, Fusion Regulatory Protein-1 (FRP-1/CD98)-mediated osteoclast and receptor activator of nuclear factor-κB ligand (RANKL) + M-CSF-mediated osteoclast. These cells have osteoclastic properties; tartrate resistant acid phosphatase (TRAP)-positive multinucleated giant cells, calcitonin receptor, cathepsin-k, vitonectin receptor (VNR) and bone resorption ability. These results have suggested that CD14-positive monocytes are probably osteoclast progenitors.

In this study, we used CD14-positive monocytes, probably osteoclast progenitor, and investigated their passage and survival ability.

METHODS

Isolation of monocytes: After enough informed consent, CD14-positive monocytes were isolated from healthy young volunteers' whole blood by Ficoll-Hypaque density gradient centrifugation and using feature of monocyte to attachment to a plastic dish. The purity of CD14-positive monocytes was more than 95%. More than three human monocytes were utilized per experiment.

Passage study: When monocytes were cultured in α-minimum essential medium with 10% fetal calf serum for 14 days at 37℃ in humidified atmosphere containing 5% CO_2, we tore them off with a cell scraper and did passage. Furthermore, we incubated them for 14 days and analyzed by fusion assay using Giemsa staining.

Survival study: In time, we analyzed 3 groups; monocytes without any stimulator, monocytes with M-CSF and monocytes with anti-M-CSF. After 2 weeks incubation, we changed medium and cytokines. Doing this action every 2 weeks, we incubated them for eight weeks and estimated 3 groups using fusion assay (staining with Giemsa and TRAP) and pit formation assay to phosphatase calcium plates (Ca plates).

RESULTS

When monocytes were cultured without passage, spontaneous polykaryocytes began to appear for 28 days incubation. However, when monocytes precultured for 14 days were further subcultured, the living cells decreased and eventually all cells died. After all, passage of monocytes using a cell scraper is impossible in our system.

We got interesting results in Survival study. When monocytes were incubated for 2 weeks spontaneous polykaryocytes were rarely. However incubated for 8 weeks, even in a group of monocytes without any stimulator we found TRAP-positive multinucleated giant cells. In addition, bone resorption ability to Ca plates increased remarkably. In comparison with 2 week incubation, it is about 37-fold in group of survival. On the other hand, anti-M-CSF inhibited spontaneous osteoclastogenesis in dose-dependent manner.

DISCUSSION

A conventional report about osteoclast survival was used mature animal osteoclasts. Therefore, our review is the first report about properties of passage and survival in human model. These experimental results suggested that adherent condition is an important role for survival and spontaneous osteoclastogenesis.

It is known from analyzing op/op mice that monocyte is a cell belonging to macropharge lineage and that M-CSF is a necessary cytokine for osteoclast progenitor. Anti-M-CSF inhibited spontaneous osteoclastogenesis in our vitro study, suggesting that monocyte was osteoclast progenitor.

Then, we thought about a role of VNR, integrin. In our previous research, we confirmed manifestation of VNR in monocytes freshly isolated as well as FRP-1-mediated osteoclasts. And besides, there was not the significant difference between monocytes freshly isolated and monocytes cultured with anti-FRP-1 monoclonal antibody.

In this study, we found that participation of M-CSF and VNR was involved in mechanisms of spontaneous osteoclastogenesis from CD14-positive monocytes, probably osteoclast progenitor, and further analysis is now in progress.

IMMUNOHISTOCHEMICAL LOCALIZATION OF CALCITONINGENE-RELATED PEPTIDE AND SUBSTANCE P IN THE RAT KNEE CARTILAGE AT BIRTH

Oliva F, Tarantino U.
Department of Orthopaedics and Traumatology, Università di Roma Tor Vergata, Roma, Italy.
olivafrancesco@hotmail.com

INTRODUCTION

Autonomic innervation seems to be involved in afferent sensory input for stretch and pain (1). It may also cooperate with the immune system (2), play a local effector role for immune (3) and inflammatory responses (4), and in the modulation of hemodynamics and vascular permeability (5). Previous studies revealed the presence of neuropeptides in regions with high osteogenesis (6), during fracture healing (7) and healing of soft tissues (8), and at the interface membrane of aseptic loose hip prosthesis (9), where they influence cellular proliferation, metabolism and differentiation (10), and growth factor production (11). In the young rat, two areas participate in the formation of the mature epiphyses: the periostal surface or collar center, and the secondary or epiphyseal centers. The primary center of ossification forms the diaphysis and the metaphysis. The cartilage canals are fundamental in the development of the vascular system of the secondary center of the cartilagineous epiphysis. They appear in the rat from the 5th postnatal day before the appearance of secondary or epiphyseal center, crossing the epiphyseal hyaline cartilage (12). The connective tissue of the cartilage canals contains several cell types: chondroclasts, osteoprogenitor cells, fibroblasts and macrophages, polymorphic cells, multivacuolated cells, perivascular cells. The chondrocytes around the canals undergo hypertrophy before the development of the secondary ossification center (13). Cartilage canals are not a complete extension of the perichondrium, and an "invasion" process underlies their formation (13). Previous studies evidenced free nerve endings immunoreactive for the neuropeptides substance P (SP) and calcitonin gene related peptide (CGRP) within the cartilage canals (14). The presence of neuropeptides during the development of the cartilagineous epiphyses of the knee joint has not been widely investigated. SP and CGRP synthesized in dorsal root ganglion are transported peripherally and stored in large electrondense vesicles, the accumulation of which constitutes varicosal enlargements of axon. In addition, these neuropeptides are found in unmyelinated (C type) and small myelinated (A-δ type) primary sensory neurons (nociceptive fibers) (15). This arrangement enables their release upon stimulation very close to their targets (15). Together with the labile chemical nature of neuropeptides, their short half-life clearly depicts the need to confine the effects of these potent mediators and modulators exactly to the right moment (15).

We report the results of a histological and immunohistochemical study aiming to ascertain whether these two neuropeptides were present in the epiphysis of rat knee at birth.

MATERIAL AND METHODS

Tissue preparation

Newborn (four hours of life) Wistar rats (n=14) weighing 40-50 g were euthanized with an overdose of chloroform. After removal of the skin and of the superficial soft tissues, the 28 knees joints were cut out and processed in 7 different fashions (4 knees each). Fixation was performed with two different solutions, namely paraformaldehyde 4 % and Zamboni's fixative (4 % paraformaldehyde in 0.2 M Söresen phosphate buffer pH 7.3, containing 0.2 % picric acid) for six hours. The demineralizing solution used was EDTAcacodylate: 40.0 g ethylene-diamine-tetraacetic acid (EDTA; Titriplex II), 24.2 g. sodium cacodylate, and 15.0 g sodium hydroxide dissolved in 1000 ml of distilled water and pH adjusted to 7.3. Demineralization took place over an average of 12 days (11-13 days) at 4 °C under continuous stirring and with daily changes of the solution. The specimens were washed in a Söresen phosphate buffer 0.1M (pH 7.2-7.4) and subsequently washed in Söresen phoshate buffer 0.1 M containing 15 % sucrose. After immersion in Tissue-Tec, 12 of the specimens were frozen in methylbutan (–70 °C) and 16 were dehydrated and embedded in paraffin (Table 1). The 12 knees frozen in methyl-butan were sectioned at a thickness of 15 µ on a Leitz 1720 cryostat at –20 °C and mounted on SuperFrost/Plus glass slides. These sections were used for immunohistochemistry. The 16 knees embedded in paraffin were sectioned perpendicularly to the transverse axis of the joint at a thickness of 6 µ. These sections were used for histology and for immunohistochemistry. They were then mounted on poly-L-lysine-coated slides at room temperature. The section selected for immunohistochemistry were stained with Alcian blue-PAS-hematoxylin.

Immunohistochemical study

The serial sections were processed according to the indirect immunohistochemical procedure of Coons . The sections were pre-incubated with TRISbuffered saline (TBS-buffer) containing 1 % bovine serum albumin, 10 % normal serum and 0.5 % Triton X- 100. PBS (0.01 mol/l at pH 7.3 phosphate-buffered saline) was used to rinse the sections. Immunostaining consisted of an overnight incubation in a wet chamber at room temperature with the primary antibody (Table 2), and of a second incubation with cyanine (Cy3)- conjugated secondary antiserum at room temperature for 1 hour. Protein gene product (PGP), a neural protein, was used to detect peripheric nervous fibers. As a negative control, two sections of each specimen were treated in the same manner but without the primary antibody. The slides were mounted with glycerine-PBS and examined with a fluorescence microscope (Axioplan 2 Zeiss) by the main author. The location of the neuropeptides studied was determinated by comparing each immunohistochemical section with the adjacent slice stained with Alcian blue- PAS-hematoxylin.

RESULTS

Antibodies against PGP, CGRP and SP gave a positive immunoreaction responses in the rat epiphysis at birth. We obtained a positive immunoreaction in each of the 7 tissue preparations used in this study. The quality of the immunofluorescence was better in the specimens treated with paraformaldehyde 4 %, with or without the demineralizing solution, and frozen. The epiphysis of the rat knee were composed of a massive cap of hyaline cartilage, rich of clonal cells, covered by perichondrium, rich of mesenchymal cells, which show the classical arrangement in three layers. The chondral tissue at this time is stained strongly with Alcian blue. Many nerves fibers immunoreacting to PGP, CGRP and SP were found in the inner aspect of the perichondrium in close contact with the chondrocytes at the interface between the epiphysis and the perichondrium. No nerve fibers were found within the center of the epiphysis.

CONCLUSION

This study shows the presence of CGRP and SP in the rat knee epiphysis at birth. The inner layer of the perichondrium is richly innervated by peripheral nervous fibers. These fibers were often found at the interface with the cartilage, in a close contact with the outer layers of epiphyseal chondrocytes, actively producing cartilagineous matrix and arranged in clonal grouping. Our study shows that, in the rat knee, CGRP and SP nerves fibers precede the development of the cartilage canals.

REFERENCES:

1) *Pain* 55: 5-54, 1993.
2) *Clin Exp Rheumatol* 12: 583-587, 1994.
3) *Clin Rheumatol* 10: 175-183, 1996.
4) *Ann N Y Acad Sci* 966: 384-399, 2002.
5) *Microvascular Res* 50: 45-55, 1995.
6) *Peptides* 9: 165-171, 1988.
7) *Neuroscience* 54: 969-979, 1993.
8) *J Orthop Res* 20: 849-56, 2002.
9) *J Bone Joint Surg* 80: 151-155, 1998.
10) *Peptides* 11: 625-632, 1990.
11) *Bone* 18: 331-335, 1996.
12) *Anat Embryol* 192: 247-255, 1995.
13) *Acta Anat Basel* 141: 31-35, 1991.
14) *Cell Tissue Res* 299: 193-200, 2000.
15) *Ann N Y Acad Sci* 966: 384-399, 2002.

HYPERTROPHY DURING IN VITRO CHONDROGENESIS OF MESENCHYMAL STEM CELLS CORRELATES WITH CALCIFICATION AND VASCULAR INVASION OF ECTOPIC CARTILAGE TRANSPLANTS

*Pelttari K, *Winter A, *Steck E, *Lorenz H, *Hennig T, **Aigner T, *Richter W
Orthopaedic University Hospital Heidelberg, Germany

karoliina.pelttari@ok.uni-heidelberg.de

INTRODUCTION

Functional suitability and phenotypic stability are imperative for the clinical application of mesenchymal stem cells (MSC) in articular cartilage repair and might require a stringent control of chondrogenic differentiation. We here evaluated whether human bone marrow-derived MSC adopt natural differentiation stages during chondrogenic induction in vitro and form ectopic stable cartilage resistant to vascular invasion and calcification in vivo.

METHODS

During in vitro chondrogenesis of MSC the expression of 44 cartilage-, stem cell-, and bone-related genes and deposition of aggrecan, collagen types II and X were determined. Similarly treated expanded articular chondrocytes served as controls. MSC micromasses differentiated for 3-7 weeks and chondrocytes were implanted subcutaneously into SCID mice and evaluated by histology 4 weeks later.

RESULTS

The three-stage chondrogenic differentiation cascade initiated in MSC was hallmarked by sequential up-regulation of common cartilage genes. Premature induction of hypertrophy-related molecules (collagen type X; MMP13) occurred before production of collagen type II and was followed by up-regulation of alkaline phosphatase activity. In contrast, hypertrophy-associated genes were not induced in chondrocytes. While chondrocyte micromasses resisted calcification and vascular invasion in vivo, most MSC pellets mineralized in spite of persisting proteoglycan and collagen type II content.

DISCUSSION

An unnatural differentiation pathway to chondrocyte-like cells was induced in MSC by common in vitro protocols and micromasses underwent alterations related to endochondral ossification rather than adapting a stable chondrogenic phenotype at ectopic sites. Further studies are needed to evaluate whether a more stringent control of MSC-differentiation to chondrocytes can be obtained during cartilage repair in a natural joint environment.

ACKNOWLEDGEMENT: We are very grateful to the physicians of the Department of Orthopaedic Surgery, University of Heidelberg, for providing cartilage and bone marrow samples. We thank S. Schneider for statistical

data analysis, and S. Kadel, K. Götzke, R. Föhr for technical assistance This work was supported by the German Research Association (DFG) and the Orthopaedic University Hospital Heidelberg

AFFILIATED INSTITUTIONS FOR CO-AUTHORS
** Cartilage Research, Department of Pathology, University of Erlangen-Nuernberg, Germany

EXPERIMENTAL INVESTIGATION ON HETEROTOPIC OSSIFICATION AND FRACTURE HEALING AFTER BRAIN INJURY

*Pellacani A, *Pagani S, *Ciapetti G, **Gambale F, *Baldini N, *Giunti A
*Laboratorio di Fisiopatologia Ortopedica & 7^ Divisione, Università di Bologna, Istituti Ortopedici Rizzoli.
** Department of Anestesiology, Ospedale Maggiore, Bologna, Italy
fisiopatologia@ior.it

INTRODUCTION

Heterotopic ossification (HO) is a potential complication of spinal cord and brain injury and has been described in the main joints and may lead to joint ankylosis. It seems that enhanced osteogenesis in patients suffering from traumatic brain injury (TBI) could be caused by some humoral factors, since the sera of these patients strongly promote the growth of osteoblastic cells in vitro. In this study blood from patients with trauma brain injury (TBI) and from patients with diaphyseal fracture was collected before surgery and 1, 2, and 3 weeks post-surgery. The bone-forming activity in such blood samples was assayed using osteoblast-like Saos-2 cells, which were tested for viability and proliferation after culture in serum-added medium. Insulin-like Growth Factor I (IGF-I), Transforming Growth Factor β-1 (TGF-β1), which are known bone promoting cytokines, and IL-6 levels were measured in the patient blood, too.

MATERIALS AND METHOD

Blood was collected from 10 patients who underwent orthopaedic surgery for brain injury (5 patients: TBI group) or diaphyseal fracture (5 patients: fracture group).
The blood collection occurred pre-operatively (T_0) and at 1 week (T_1), 2 weeks (T_2) and 3 weeks (T_3) post-surgery.
In the lab the blood samples were centrifuged and before use the sera were heated at 56°C for 35 min for complement inactivation. Saos-2 cells, a human osteosarcoma cell line, were seeded in complete culture medium (α-MEM) and after twenty-four hours this medium was changed to serum-free α-MEM.
After an additional 24h, the 'basal' viability and cell number prior to any stimulation were assayed, then some culture were fed with 5% autologous human serum (AHS)-added medium ('samples') and others were fed with 5% FCS-added medium ('control').
On the seventh day after seeding the experiment was stopped and the assays performed.
The cell viability was tested using Alamar test, which measures the products of redox reaction occurring in mitochondria of viable cells; while morphology and cell proliferation was measured using crystal violet dye.
To evaluate the amount of TGF-β, IL-6 and IGF-I in serum, it have been immunoenzymatic test (ELISA) employed.
Differences between groups, i.e. TBI vs fracture, and between two time endpoints within a group, e.g. T1 vs T0 in TBI, were analyzed using the Mann-Whitney test calculated with the Monte Carlo method for small samples.

RESULTS

The viability test for Saos-2 cells cultured with autologous serum (AHS) from patients showed a different behaviour of the groups. Cells grown with AHS from TBI patients all scored an increased value when comparing T0 (pre surgery) with T2 (2 weeks after surgery).
Instead, in the group with fracture no appreciable increase was seen when viability at T_2 were compared to T_0.
We have scored a statistically significance in viability T2/T0, in spite of a small number of sample.
Proliferation of Saos-2 cells showed an increase when added with AHS from TBI patients in four cases out of five (comparing T0 vs T2), whereas in the 'fracture' group only two out of five showed an enhanced number of cells at T2, and one patient had an increase at T1.
Circulating IGF-I was found to be within 'normal values' for adults, at the different endpoints in both groups. In TBI group only two subjects scored higher values respectively at T1 and over time, whereas in fracture group a single high value was recorded at T2 for one patient.
Serum TGF-β values were oscillating in both groups: in TBI group three patients showed TGF-β levels higher than 'normal values' in at least one endpoint. In fracture group the same occurs.
IL-6 in patients from both groups was under the detection limit at each endpoint.

DISCUSSION

Our data suggest that a mitogenic factor is present in serum of TBI group, as the viability and, even less evident, the growth of Saos-2 bone-forming cells are enhanced in comparison to the same parameters measured in the "diaphyseal fracture" group. Systemic IGF-I show values within the range for 'healthy subjects'.
TGF-β is increased compared to 'healthy subjects', but such enhancement was expected, as it is known that patients with fracture show high TGF-β levels up to 1 year after trauma.
IL-6 release was very low, so we suggest it is not related to enhanced fracture healing.. More investigations using a large number of subjects are needed to get a better understanding of the mechanism(s) triggering HO and enhanced fracture healing, but our study is confirming the presence of an unrecognized promoting factor in peripheral blood of TBI patients.

THE MECHANICAL EFFECTS ON THE IMPLANT-BONE CONTACT AFTER WITHDRAWAL OF INTERMITTENT PTH TREATMENT

*[a,b]Johansson H R, *[a,b]Skripitz R, **Aspenberg P

*[a] Department of Trauma, Hand, and Reconstructive Surgery,
University Hospital Eppendorf, Hamburg, Germany
*[b] Department of Orthopedics, University Hospital Eppendorf, Hamburg, Germany
** Section for Orthopedics and Sports Medicine, Department of Neuroscience and Locomotion,
Faculty of Health Sciences, Linköping, Sweden
Skripitz@uke.uni-hamburg.de

INTRODUCTION

The primary implant-bone contact co-decides about future implant loosening. It is well known, that administration of intermittent PTH, as well as administration of bisphosphonates enhances the implant-bone stability. However, in osteoporosis therapy there have been a few cases described, where withdrawal of intermittent PTH resulted in a major loss of bone mass.

This study investigated the implant-bone contact after withdrawal of intermittent PTH.

METHODS

48 adult male rats received tibial placement of one steel screw (right) and steel rod (left). They were randomly divided into four groups of twelve rats each.
Group 1: five weeks of daily NaCl-injections.
Group 2: two weeks of daily injections of PTH (60 µg/kg), followed by three weeks of NaCl-injections.
Group 3: two weeks of daily injections of PTH, followed by three weeks of daily bisphosphonate injections (pamidronate 500 µg/kg).
Group 4: two weeks daily NaCl-injections, followed by three weeks of daily bisphosphonate injections (pamidronate 500 µg/kg).

The animals were killed five weeks after implantation. The screws were tested by pull-out in a materials testing machine directly after euthanizing. The rod-implanted tibiae were decalcified and evaluated by light microscopy. Histomorphometric measurements were obtained using a computer-based image analyzer to quantify the rate of implant-bone contact. Analysis of variance (ANOVA) was used for statistics.

The institutional review board, conforming to the laws and regulations of Sweden, approved the study.

RESULTS

Eight animals were excluded due to implant failure (n=4) or death (n=4). The combination of intermittent PTH and bisphosphonates resulted in an increased pull-out force (Table). The other treatments had no effect. Thus, PTH alone, given during the first two weeks or pamidronate alone given weeks 3 to 5 had no effect at 5 weeks, but given in succession the effect on the implant-bone contact is major (ANOVA $p < 0.0001$).

Table: Pull-out force (Newton) and SD

	Week 1,2	Week 3,4,5	n	Mean	SD
1	**NaCl**	**NaCl**	11	78	26
2	**PTH**	**NaCl**	12	77	22
3	**PTH**	**pamidr**	9	152	24
4	**NaCl**	**pamidr**	8	89	23

DISCUSSION

At the end of this study, there was no difference if the rats were treated with PTH or NaCl in the first two weeks. It is well known that intermittent PTH enhances the implant-bone contact, and so do bisphosphonates. It is likely, that the withdrawal of intermittent PTH has led to a so called "rebound effect" which is carried out by the bone resorbing osteoclasts.
The results show that this "rebound effect" can be avoided, if the intermittent PTH administration is followed up by bisphosphonates. It is likely that the treatment with bisphosphonates preserved the results achieved by intermittent PTH, since the therapeutic regimen of group 4 did not lead to an improvement of the implant-bone contact. The conclusion would be that the intermittent administration of PTH in the first two weeks contributes the most to the improvement on the implant-bone contact.

MECHANICAL PROPERTIES AND HISTOMORPHOMETRIC PARAMETERS IN CANCELLOUS BONE: AGE-RELATED CHANGES IN THE HUMAN FEMORAL HEAD IN SEVERE ARTHROSIS

*Perilli E, *Baleani M, *Fognani R, *Visentin M, *Stea S, **Traina F, *Baruffaldi F
*Laboratorio di Tecnologia Medica, Istituti Ortopedici Rizzoli, Bologna, Italy
**1° Divisione, Chirurgia Ortopedico-Traumatologica, Istituti Ortopedici Rizzoli, Bologna, Italy
perilli@tecno.ior.it

AIM

To investigate the relationships between the mechanical compressive properties and histomorphometric parameters of cancellous bone collected from femoral heads of patients having severe arthrosis, together with their dependence on age[1,2].

MATERIALS AND METHODS

29 Femoral heads were collected from patients having severe primary arthrosis of the hip (mean age 64, youngest 42, oldest 87). A cylindrical cancellous bone specimen was milled from the principal compressive region of each femoral head, with the cylinder axis aligned with the inferior-superior orientation of the trabeculae. The bone samples were examined by microCT (fig.1) for the quantification of the histomorphometric parameters, such as bone volume fraction (BV/TV), trabecular thickness (Tb.Th), trabecular separation (Tb.Sp), trabecular number (Tb.N) and structure model index (SMI). Then the specimens were tested mechanically in uniaxial compression[3], to determine elastic modulus (E) and ultimate stress (Su), and finally submitted to ashing procedure.

RESULTS

A strong linear relationship was found between ash density and BV/TV (r^2=0.92). This finding supported the use of BV/TV as a predictor of the density. E and Su correlated significantly with BV/TV (E vs. BV/TV, r^2=0.80; Su vs. BV/TV, r^2=0.88). Significant correlations were also found between mechanical properties and the other histomorphometric parameters Tb.Th, Tb.Sp, Tb.N and SMI. Regression analysis showed that the age-dependencies of E, Su, and BV/TV (fig.2) were not statistically significant. (p=0.83, p=0.36, p=0.54, respectively).

Fig.1: 3D representation of a cylindrical cancellous bone sample examined by microCT

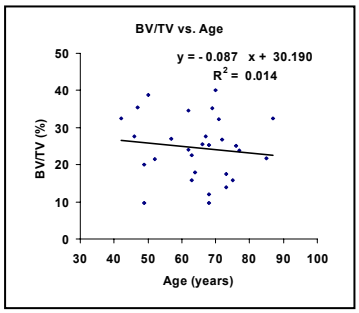

Fig.2: Scatter plot showing the linear regressions BV/TV vs. age (p=0.54).

DISCUSSION

The compressive properties of cancellous bone of the femoral head of patients having severe arthrosis are significantly correlated with the histomorphometric parameters BV/TV, Tb.Th, Tb.Sp, Tb.N, SMI. The best predictor of E and Su is BV/TV. The bone volume fraction does not depend on age. This finding is in agreement with data reported by other authors for the femoral head in severe arthrosis[1,2]. Furthermore, in the present study it is shown that also the mechanical properties do not depend on age. This independence on age of the parameters E, Su and BV/TV seems to be consistent with the strong relationships between mechanical properties and BV/TV found in this study.

REFERENCES:

1. Fazzalari NL, Forwood MR, Smith K, Manthey BA, Herreen P. Assessment of cancellous bone quality in severe osteoarthrosis: bone mineral density, mechanics, and microdamage. *Bone 1998;22-4:381-8.*
2. Crane GJ, Fazzalari NL, Parkinson IH, Vernon-Roberts B. Age-related changes in femoral trabecular bone in arthrosis. *Acta Orthop Scand 1990;61-5:421-6.*
3. Keaveny TM, Pinilla TP, Crawford RP, Kopperdahl DL, Lou A. Systematic and random errors in compression testing of trabecular bone. *J Orthop Res 1997;15-1:101-10.*

NEUROMUSCULAR ABUNDANCE OF RB1CC1 CONTRIBUTES THE ENLARGED CELL PHENOTYPE VIA TOR PATHWAY

*Chano T, *Saji M, **Kobayashi T, **Hino O, *Okabe H

*Department of Clinical Laboratory Medicine, Shiga University of Medical Science, Shiga 520-2192;

**Department of Pathology, Juntendo University, Tokyo 113-8412, Japan

chano@belle.shiga-med.ac.jp

INTRODUCTION

RB1-inducible Coiled-Coil 1 (RB1CC1) is a novel tumor suppressor implicated in the regulation of RB1 expression. It is abundant in post-mitotic neuromuscular cells, which are matured and enlarged, but scarce in smaller leukocytes, indicating an association between RB1CC1 and cell size.

METHODS

To clarify whether RB1CC1 is involved in cell size control, we modified the expressional status using RNAi etc., and investigated the contribution of RB1CC1 to TSC-mTOR pathway, which plays an important role in the control through translational regulation.

RESULTS

RNAi-mediated knockdown of *RB1CC1* reduced the activation of mTOR and S6K as well as the size of HEK293, C2C12 and Neuro2a cells. Such knockdown also suppressed RB1 expression and the population of G1-phase cells. Exogenous expression of *RB1CC1* maintained

S6K activity and cell size, and decreased TSC1/hamartin contents under nutritionally starved conditions, which usually inhibit mTOR-S6K pathway. Furthermore, RB1CC1 combined with and degraded TSC1 through the ubiquitin-proteasomal pathway. A lentiviral RNAi for *RB1CC1* reduced the size of mouse leg muscles.

DISCUSSION

These findings suggest that RB1CC1 is required to maintain both RB1 expression and mTOR activity. The activity of mTOR was supported by RB1CC1 through TSC1 degradation. RB1CC1 preserved cell size without cell cycle progression especially in neuromuscular tissues, and the abundance contributed to the non-proliferating enlarged cell phenotype.

IMMUNOHISTOLOGICAL CHARACTERIZATION OF A NOVEL BIOMECHANICAL *IN VITRO*-MODEL OF OSTEOARTHRITIC-LIKE CARTILAGE - COMPARISON TO HUMAN AND MURINE OA

Jahn N, Raiss RX, Steinmeyer J
Lab. f. Experimental Orthopaedics, Dept. of Orthopaedic Surgery, University Hospital Gießen & Marburg, Gießen, Germany

juergen.steinmeyer@ortho.med.uni-giessen.de

INTRODUCTION

Trauma, obesity or joint overuse are regarded as major contributing factors in the development and progression of osteoarthritis (OA). In response to mechanical stimuli applied, chondrocytes are known to regulate their own metabolic activities. We previously identified and reported a loading protocol able to induce degenerative metabolic changes in articular cartilage explants similar to those seen in OA. Monitoring subtle changes in the expression and localization of several extracellular matrix components by immunohistology might help to identify the onset of pathological events. Among those, e.g. the cartilage oligomeric matrix protein (COMP) seems promising, as various studies support its role as a molecular indicator of events in OA.

The aim of the presented histological study was 1) to characterize histologically and immunohistochemically this novel *in vitro*-model for its ability to mimick an OA-like appearance and tissue reactivity, 2) to compare the cartilage of this new *in vitro*-model with cartilage from human knee OA as well as from an murine *in vivo*-model of OA, and 3) to investigate if therapeutic principles proposed as drugs for OA were able to counteract these degenerative changes.

METHODS

Biomechanical *in vitro*-model: Full-thickness bovine articular cartilage discs were intermittently loaded for a period of 1 to 9 days using a mechanical loading device designed and constructed to load living cartilage explants over extended time periods under sterile conditions in a normal bench top incubator at 37°C, 5% $C0_2$ and 95% humidity. The cyclic loads (0.5 MPa) were applied with a sinusoidal waveform of 0.1-Hz frequency for 10 s followed by a period of unloading lasting 100 s. In separate experiments, explants were loaded for 6 days using the same loading protocol and treated with drug vehicle or with 10^{-5} M of a MMP-inhibitor (A976157). Unloaded cartilage discs of the same condyle served as controls. Each experiment was repeated five times (N=6).

Murine and human OA cartilage: The STR-1N mouse is a strain that consistently develops severe spontaneous OA in a short time, which is most pronounced in the knee joint. For comparison with our mechanical *in vitro*-model, murine knee cartilage with an age of 7 weeks were selected, which displayed moderate OA alterations. Human articular cartilage were obtained from autopsies and knee-joint replacement surgeries. Approval of the institutional review board and informed consent were obtained.

Immunohistology: The OA status of all cartilage samples was staged by staining with Safranin-O / Fast Green using a modified Mankin-score. In addition, formalin-fixed and paraffin-embedded sections of all samples were subjected to immunohistology using antibody against bovine COMP and the alkaline-phosphatase method with Fast Red as substrate.

RESULTS

Mechanical loading of cartilage explants induced time-dependently the expression of COMP. Samples loaded for up to 3 days did not show remarkable differences to their unloaded controls. Loading for 6 days led to distinct changes in the expression of COMP with an OA-like appearance. Intermittent loading of explants for 9 days further enhanced the expression of COMP.

The expression and localization of COMP appears to be similar to those seen in human OA cartilage as well as in osteoarthritic mice. In all cases, the COMP immunolocalization is complementary to the distribution pattern of the Safranin-O staining, thus becoming more pronounced with an increasing OA morphology.

Treatment of loaded bovine explants with an MMP-inhibitor markedly reduced histopathological alterations.

DISCUSSION

COMP expression and localization within articular cartilage appears to be influenced by biomechanical factors *in vitro*. Our histological results presented here are in accordance with our previously reported OA-like metabolism of bovine explants superimposed to the same loading protocol.

In addition, the expression of COMP by loaded bovine explants are in accordance with human as well as murine OA-cartilage which strengthens the value of this novel biomechanical *in vitro*-model of cartilage degeneration.

The drug mediated reduction of histopathological alterations suggest that this novel biomechanical *in vitro*-model is suitable for pharmacological investigations. However, further studies are necessary and already in progress to test this novel biomechanical *in vitro*-model for its applicability to screen different classes of drugs.

ACKNOWLEDGEMENTS

This work was supported by the Federal Ministry of Education and Research (BMBF no. 0311058) and by the foundation S.E.T.

PROLIFERATION AND COLLAGEN TYPE I EXPRESSION IS SIGNIFICANTLY INDUCED BY CHEMOKINES IN OSTEOBLASTS FROM OSTEOARTHRITIS PATIENTS

*Lisignoli G, *Piacentini A, *Cristino S, *Grassi F, *Cavallo C, *Tonnarelli B, *Manferdini C, *Facchini A
*Laboratorio di Immunologia e Genetica, Istituti Ortopedici Rizzoli, Bologna, Italy

ginalisi@alma.unibo.it

Progression of joint cartilage degeneration in osteoarthritis (OA) is associated with subchondral bone modification mainly due to soluble factors. We analysed the effects of CXC chemokines CXCL8 (IL8), CXCL10 (IP-10), CXCL12 (SDF-1) and CXCL13 (BCA-1) on osteoblasts (OBs) obtained from subchondral trabecular bone tissue of OA and post-traumatic (PT) patients. The expression of CXC receptors/ligands was analysed in cultured OBs and confirmed in bone tissue samples. Functional assays were performed to analyse cellular proliferation and the enzymatic response to chemokine activation. Collagen type I and alkaline phosphatase mRNA expression were analysed on CXCL12- and CXCL13-treated OBs by Real-time PCR.

OBs from both OA and PT patients expressed high levels of CXCR3 and CXCR5 and lower amounts of CXCR1 and CXCR4. CXCL12 and CXCL13, only in OBs from OA patients, induced a significant proliferation that was also confirmed by specific blocking experiments. Moreover, OBs from OA patients released a higher amount of CXCL13 than those of PT patients while no differences were found for CXCL12. In the remodeling area of bone tissue samples, immunohistochemical analysis confirmed that OBs expressed CXCL12/CXCR4 and CXCL13/CXCR5 both in OA and PT samples. CXCL12 and CXCL13 upregulated collagen type I mRNA expression in OBs from OA patients.

These data suggest that CXCL12 and CXCL13 may directly modulate cellular proliferation and collagen type I in OA patients, so contributing to the remodeling process that occurs in the evolution of this disease.

STIMULATION OF CELL PROLIFERATION IN NORMAL AND OSTEOARTHRITIC HUMAN ARTICULAR CARTILAGE *IN* SITU VIA RAAV-MEDIATED OVEREXPRESSION OF HUMAN FGF-2

*Madry H, *Thurn T, **Ma C, *Kohn D, **Terwilliger EF, +*Cucchiarini M
+*Laboratory for Experimental Orthopaedics, Department of Orthopaedic Surgery, Saarland University Medical Center, mmcucchiarini@hotmail.com

INTRODUCTION

Stimulation of the reparative activities in human articular cartilage may benefit from the transfer of therapeutic gene candidates. We have demonstrated that vectors based on rAAV can deliver marker genes to human chondrocytes within their native matrix [1,2]. Here, we hypothetized that rAAV-mediated overexpression of FGF-2 promotes cell proliferation in normal and osteoarthritic human articular cartilage *in situ*.

METHODS

rAAV were packaged, purified, and titrated by real-time PCR [1-4]. Titers averaged about 10^{10} functional units/ml. rAAV-*lacZ* carries the *E. coli* beta-galactosidase (β-gal) marker gene (*lacZ*) controlled by the CMV-IE promoter/enhancer [1-4]. A human basic fibroblast growth factor (hFGF-2) cDNA (480 bp) [3] was cloned in rAAV-*lacZ* instead of *lacZ* to produce rAAV-hFGF-2. Normal human articular cartilage was obtained from knee joints removed during tumor surgery. Osteoarthritic human articular cartilage was obtained from joints treated by total knee arthroplasty (Mankin score 7-9). The explants were transduced by rAAV as previously described [1,2], maintained in culture for 12 days, and processed to monitor transgene expression and for histological analyses. Paraffin-embedded sections (5 μm) were stained with safranin O and hematoxylin eosin. Indirect immunostaining was performed to detect β-gal (Sigma), FGF-2 (Oncogene Research Products), and type-II collagen (Acris). Transduction efficiencies were calculated as previously described [1]. Transgene expression was also assayed using an FGF-2 ELISA (R&D Systems). Morphometric measurements were performed at 3 standardized sites along the explant surface by image analysis using SIS AnalySIS, Adobe Photoshop, and Scion Image [2]. Safranin O staining intensity was calculated as the ratio of the surface of positively stained tissue to the total surface of the site examined [2]. Type-II collagen staining intensity is in pixels per standardized area (intensity units) [2]. The DNA contents were monitored by a fluorimetric assay using Hoechst 33258 [3]. The proteoglycan contents were detected by binding to the DMMB dye [3]. The type-II collagen contents were determined by ELISA (Chondrex). All data were obtained by two individuals that were blinded with respect to the treatment groups. Each condition was performed in triplicate in 2 independent experiments. Data are expressed as the mean ± SD. The t-test and the Mann-Whitney Rank Sum Test were employed where appropriate.

RESULTS

lacZ expression was restricted to the rAAV-*lacZ*-transduced (control) explants while FGF-2 was seen only in the rAAV-hFGF-2-transduced explants. Transgene expression occurred in a dose-dependent manner both in the tangential and transitional zones. Transduction efficiencies in the normal explants were of 45 ± 2% with 20 μl vector and 58 ± 3% with 50 μl. In the osteoarthritic explants, the efficiencies increased from 44.0 ± 1.6% to 58 ± 2%. FGF-2 secretion levels in the normal explants were of 768 pg/ml using 20 μl vector and 1,810 pg/ml with 50 μl. Similar results were obtained in the osteoarthritic explants (407 and 995 pg/ml). The levels in the control explants were below the threshold of detection of the assay.

Application of rAAV-hFGF-2 promoted a significant, dose-dependent increase in the cell densities in the explants (Fig. 1). In the normal explants, a mean value of 475 ± 20 cells/mm^2 was noted using 20 μl rAAV-hFGF-2, compared with 255 ± 17 cells/mm^2 using rAAV-*lacZ* ($P < 0.001$). With 50 μl, the values were of 633 ± 12 versus 252 ± 16 cells/mm^2 ($P = 0.029$). Similar results were obtained in the osteoarthritic explants using 20 μl (338 ± 9 versus 238 ± 11 cells/mm^2, $P < 0.001$) or 50 μl vector (419 ± 14 versus 245 ± 11 cells/mm^2, $P < 0.001$). Transduction by rAAV-hFGF-2 induced a significant, dose-dependent increase in the DNA contents in the explants. Values were of 1.47 ± 0.03 μg/mg dry weight with 20 μl rAAV-hFGF-2 and 1.73 ± 0.03 μg/mg dry weight with 50 μl in the normal explants, compared with 1.28 ± 0.01 and 1.32 ± 0.01 μg/mg dry weight in the control explants ($P < 0.001$ and $P < 0.001$). In the osteoarthritic explants, values were of 1.38 ± 0.03 and 1.51 ± 0.04 μg/mg dry weight using 20 and 50 μl rAAV-hFGF-2, compared with 1.24 ± 0.01 and 1.25 ± 0.02 μg/mg dry weight in the control explants ($P < 0.001$ and $P < 0.001$).

Treatment by rAAV-hFGF-2 did not modify the safranin O staining intensity in the explants (Fig. 1). Values were of 47 ± 3% staining with 20 μl rAAV-hFGF-2 and 48 ± 3% with 50 μl in the normal explants, compared with 47 ± 2% and 47 ± 1% in the control explants ($P = 0.488$ and $P = 0.190$). In the osteoarthritic explants, values were of 30 ± 2% and 32 ± 2% using 20 and 50 μl rAAV-hFGF-2, compared with 31 ± 1% and 31 ± 2% in the control explants ($P = 0.228$ and $P = 0.107$). Transduction by rAAV-hFGF-2 did not modify the proteoglycan contents in the explants. Values were of 2.67 ± 0.03 μg/mg dry weight with 20 μl rAAV-hFGF-2 and 2.68 ± 0.04 μg/mg dry weight with 50 μl in the normal explants, compared with 2.68 ± 0.01 and 2.68 ± 0.02 μg/mg dry weight in the control explants ($P = 0.708$ and $P = 0.287$). In the osteoarthritic explants, values were of 2.47 ± 0.04 and 2.45 ± 0.03 μg/mg dry weight using 20 and 50 μl rAAV-hFGF-2, compared with 2.46 ± 0.01 and 2.47 ± 0.03 μg/mg dry weight in the control explants ($P = 0.694$ and $P = 0.290$). Application of rAAV-hFGF-2 did not modify the type-II collagen immunostaining intensity in the explants. Values were of 41 ± 2 units with 20 μl rAAV-hFGF-2 and 40 ± 3 units with 50 μl in the normal explants, compared with 43 ± 2 and 41 ± 1 units in the control explants ($P = 0.315$ and $P = 0.356$). In the osteoarthritic explants, values were of 37 ± 1 and 37 ± 2 units using 20 and 50 μl rAAV-hFGF-2, compared with 38 ± 1 and 36 ± 2 units in the control explants ($P = 0.620$ and $P = 0.200$). Treatment by rAAV-hFGF-2 did not modify the type-II collagen contents in the explants. Values were of 0.021 ± 0.005 ng/mg dry weight with 20 μl rAAV-hFGF-2 and 0.023 ± 0.002 ng/mg dry weight with 50 μl in the normal explants, compared with 0.022 ± 0.001 and 0.021 ± 0.003 ng/mg dry weight in the control explants ($P = 0.278$ and $P = 0.570$). In the osteoarthritic explants, values were of 0.017 ± 0.001 and 0.019 ± 0.001 ng/mg dry weight using 20 and 50 μl rAAV-hFGF-2, compared with 0.017 ± 0.001 and 0.018 ± 0.001 ng/mg dry weight in the control explants ($P = 0.620$ and $P = 0.356$).

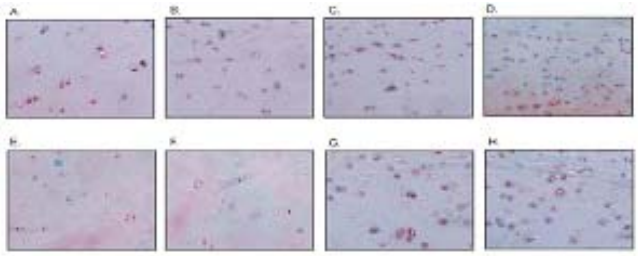

Fig. 1. Safranin O/HE staining of transduced explants. Normal (**A-D**) and osteoarthritic (**E-H**) explants were transduced by rAAV-hFGF-2 (20 μl: **C** and **G**; 50 μl: **D** and **H**) or rAAV-*lacZ* (20 μl: **A** and **E**; 50 μl: **B** and **F**) for 12 days. Magnification x40.

DISCUSSION

We report that overexpression of FGF-2 in normal and osteoarthritic human articular cartilage *in situ* via rAAV promotes cell proliferation in both types of explants, suggesting that the therapeutic rAAV-hFGF-2 vector might have value in enhancing the reparative properties of human articular cartilage.

REFERENCES

[1] Madry *et al. Hum Gene Ther* **2003**; [2] Madry *et al. Trans ORS* **2005;** [3] Cucchiarini *et al. Mol Ther* **2005**; [4] Cucchiarini *et al. Gene Ther* **2003**.

ACKOWLEDGMENTS

Funded by grants from the German Research Society (DFG CU 55/1-1 MC, HM) and the German Osteoarthritis Foundation (DAH MC, HM, DK).

Listing for additional author affiliation

**Division of Experimental Medicine, Harvard Institutes of Medicine and Beth Israel Deaconess Medical Center, Boston, MA

TISSUE TRANGLUTAMINASE 2 (TG2) AND TRANSFORMING GROWTH FACTOR-BETA (TGF-ß) IN MOUSE TG2 KNOCK-OUT KNEE OSTEOARTHRITIS MODEL AND HUMAN HIP OSTEOARTHRITIS

*Oliva F, **Orlandi A, *Taurisano G, **Ciucci A, *Tarantino U
*Department of Orthopaedics and Traumatology, **Department of Anatomy Pathology
University of Rome "Tor Vergata" School of Medicine, Viale Oxford 81, 00133 Roma, Italy

olivafrancesco@hotmail.com

INTRODUCTION

Degradation of articular cartilage is a major feature of osteoarthritis and calcification of the pericellular matrix is a prevalent finding in aging and osteoarthritic articular cartilages and meniscal fibrocartilages. Moreover, crystals of hydroxyapatite and calcium pyrophosphate dihydrate released from the cartilage matrix can activate resident intra-articular mononuclear leukocytes and synovial lining cells. Consequent crystal-induced inflammation and expression of connective-tissue degrading enzymes can contribute to further cartilage degradation in degenerative joint disease. In contrast to the physiological mineralization that occurs in growth plate cartilage, articular cartilage does not normally calcify.

Transglutaminase activity in cartilage and bone is thought to be correlated with matrix mineralization. It has been proposed that tissue transglutaminase 2 (TG2) may induce polymerization of pericellular skeletal matrix calcium-binding proteins stabilizes the matrix and promotes nucleation and/or growth of calcium-containing crystals.

But it also has been demonstrated that TG2 have the capacity to modulate processes that may indirectly affect matrix calcification in chondrocytes, such as signal transduction, cell adhesion, and activation of latent TGases also modulate the apoptotic process, which is pro-mineralizing.(1) Previous studies show that TGF-ß may induce TGase 2 in a variety of cell lines of fibroblasts, hepatoma cells, ocular trabecular meshwork, preosteoblastic cells, and epidermal keratinocytes. but may modulate also matrix production by regulating the conversion of latent into active TGF- ß. (2)

Due to rapid progress of mouse genomics and the availability of transgenic and knockout mice, the mouse is now the most ideal animal model for the study of molecular backgrounds of physiological and pathological conditions.

MATERIALS AND METHODS

Using a microsurgical technique we have produced an experimental model of instability in the mice knee joints wild type and TG 2 knock-out thereby we have reproduced an osteoarthritis reproducible animal model.(3) Besides we have investigated femoral heads of 20 patients (75 +/- one year; 10 were operated for a total hip replacement (THR)while the latter half of them were submitted to endoprosthesis for femoral neck fracture). All samples were used for histology (haematoxylin-eosin and safranin-O) and for immunohistochemistry.

RESULTS

We first performed radiological analyses of the knee joints at 2, 4 and 8 weeks after surgery. This experimental model showed articular cartilage damage at 2 weeks and osteophyte formation at the posterior tibiae 4 weeks after surgery, while at 8 weeks all radiological characteristics of osteoarthritis are present with pluricompartimental joint damage. Histology confirm the radiological analyses. Immunohistochemistry performed with anti-TG2 and anti-TGF-ß shows their involvement in the regulation of extracellular matrix degeneration during osteoarthritis.

CONCLUSION

Our study try to clarify the role of TG2 and is relation with TGF-ß in a stressed tissue as osteoarthritic cartilage, adding knowledge to the physiopathology of osteoarthritis.

REFERENCES

1) Kristen Johnson, Sanshiro Hashimoto, Martin Lotz, Kenneth Pritzker, Robert Terkeltaub: Interleukin-1 Induces Pro-Mineralizing Activity of Cartilage Tissue Transglutaminase and Factor XIIIa Am J Pathol. 2001 Jul;159:149-163.

2) Akimov SS, Belkin AM Cell-surface transglutaminase promotes fibronectin assembly via interaction with the gelatinbinding domain of fibronectin: a role in TGF b dependent matrix deposition. J Cell Sci 2001;114: 2989–3000.

3) Kamekura S, Hoshi K, Shimoaka T, Chung U, Chikuda H, Yamada T, Uchida M, Ogata N, Seichi A, Nakamura K, Kawaguchi H. Osteoarthritis development in novel experimental mouse models induced by knee joint instability. Osteoarthritis Cartilage. 2005; 13: 632-641.

ABERRANT EXPRESSION OF MHC CLASS II MOLECULES IN JOINTS OF MICE PROVIDES A NEW ARTHRITIS MODEL WITH EXTRA-ARTICULAR MANIFESTATIONS SIMILAR TO RHEUMATOID ARTHRITIS

*Ota S, **Kanazawa S, ***Peterlin B M, ****Sekine C, *****Sonderstrup G,
******Tada T, *Kobayashi M, **Okamoto T, *Otsuka T
*Department of Musculoskeletal Medicine, Nagoya City University Graduate School of Medical Sciences,
Kawasumi 1, Mizuho-cho, Mizuho-ku, Nagoya, 467-8601 Japan

shu-ohta@se.starcat.ne.jp

INTRODUCTION

Genetic susceptibility to rheumatoid arthritis (RA) involves certain major histocompatibility complex class II (MHC II) molecules. Class II transactivator (CIITA) is the master transcriptional integrator that leads to the expression of the MHC II related genes (Fontes 1999, Kanazawa 2001). To clarify the role of these determinants in RA, we first generated the transgenic D1CC (DBA/1, CII promoter/enhancer-driven CIITA) mouse that expressed genes involved in antigen processing and presentation by the MHC II pathway in chondrocytes.

METHODS

To create the CIITA transgene (pCII.CIITA), the HA epitope-tagged human full-length CIITA cDNA was placed downsteam of the rat type II collagen (CII) promoter and pCII.CIITA DNA was then injected into F1 blastocysts from FVB/NJ and DBA/1 mice. The resulting transgenic mouse was named the D1CC mouse. For the induction of arthritis, D1CC and DBA/1 mice at 8 weeks of age were housed in a pathogen-free animal care facility of Nagoya City University Medical School in accordance with institutional guidelines. They were immunized with very low dosages of the bovine CII (ldCII, 10 microgram/mouse) two times. We monitored D1CC mice from the onset of disease to the end of active inflammation in twice weekly. And we evaluated serum levels of anti-collagen antibodies (Ota 2005), histochemical staining, radiographs, computed tomography (CT) and bone mineral density. DBA/1 mice were used as controls.

RESULTS

In D1CC mice, congenic for the H-2^q (DBA/1) background, small amounts of bovine CII induced reproducibly an inflammatory arthritis resembling RA. Importantly, these stimuli had no effect in parental DBA/1 mice. 90% of D1CC mice developed chronic disease (ldCII-D1CC: 90% vs control: 0%, $p<0.01$) with swelling, redness, local heat as well as pannus formation and mononuclear infiltration of synovial membranes. Granulomatous lesions resembling rheumatoid nodules as well as interstitial pneumonitis were also observed. Finally, joints in D1CC mice displayed juxta-articular demineralization (ldCII-D1CC: 80% vs control: 100%, $p<0.05$), severe narrowing of joint space and erosions, which led to ankylosis, but without the appearance of osteophytes.

DISCUSSION

In D1CC mice, the entire machinery for antigen processing and presentation by the MHC II pathway was activated aberrantly via CIITA in synovial joints. The aberrant expression of MHC II determinants in D1CC mice led to a chronic inflammatory arthritis that resembled closely RA in humans. We conclude that D1CC mice represent an attractive additional animal model for the study of RA.

REFERENCES

Fontes JD et al. Mol Cell Biol. 1999 Jan; 19(1): 941-7.
Kanazawa S et al. Int Immunol. 2001 Jul; 13(7), 951-8.
Ota S et al. J Immunol Methods. 2005 Apr; 299(1-2): 189-98.

ACKNOWLEDGEMENTS:

This work was sported by grants-in-aid from the Ministry of Health, Labor and Welfare, and Ministry of Education, Culture, Sports, Science and Technology, Japan, from the NIH and the Nora Eccles Treadwell Foundation.
** Department of Molecular and Cellular Biology, Nagoya City University Graduate School of Medical Sciences, Nagoya, Japan.
*** Rosalind Russell Medical Research Center, Department of Medicine, Microbiology and Immunology, University of California, San Francisco, CA, USA.
**** Riken Research Center for Allergy and Immunology, Research Unit for Clinical Immunology, Tokyo, Japan.
***** Department of Microbiology and Immunology, Stanford University School of Medicine, Stanford, CA, USA.
****** Department of Pathology, Nagoya City University Graduate School of Nursing, Nagoya, Japan.

ASSOCIATION BETWEEN INTERLEUKIN-6 GENE POLYMORPHISM AND RISK OF OSTEOARTHRITIS OF THE HIP: A CASE-CONTROL STUDY

*Pola E, *Logroscino G, *Arbucci A, *Tamburelli FC, *Logroscino CA
*Department of Orthopaedics and Traumatology,
Università Cattolica del Sacro Cuore School of Medicine, Rome, Italy

enricopola@hotmail.com

INTRODUCTION

Osteoarthritis (OA) is considered a polygenic disease controlled by the expression of genetic factors. Genes encoding for cytokines have been associated with susceptibility for joint OA and interleukin (IL)-6 gene is also supposed to be involved in the cartilage degradation process. In this case-control study, we evaluated for the first time whether the risk of hip OA might be influenced by the -174 IL-6 gene polymorphism.

METHODS

A single nucleotide polymorphism (SNP) has been described at position _174 of the promoter region of the IL-6 gene, resulting in three possible genotypes, GG, GC, and CC. The distribution of IL-6 genotypes was evaluated in 75 patients affected by hip OA and in 107 age- and sex-matched controls recruited among subjects consecutively admitted to the Department of Orthopaedics at the A. Gemelli University Hospital of Rome, Italy.

RESULTS

The distribution of IL-6 genotypes in (1) patients with hip OA: 33 GG, 30 GC, 12 CC and (2) control subjects: 34 GG, 40 GC, 33 CC. The frequency of the CC genotype was significantly higher in control patients (P=0.02). Logistic regression analysis indicated that the presence of the CC genotype is independently associated with a decreased risk of OA (odds ratio 0.4 [95% confidence interval 0.1-0.9], P=0.04).

DISCUSSION

Inflammatory mechanisms play a crucial role in the pathogenesis and evolution of cartilage degradation. Recent studies have suggested that OA might be considered a chronic in.ammatory disorder, and elevated levels of IL-1, tumor necrosis factor-a, IL-6 and other acute-phase proteins are found in patients with cartilage degradation. Moreover, variations of genes encoding for cytokines such as IL-6, may play an important role in the series of events responsible for the pathophysiology of OA. Our data suggest that IL-6 gene polymorphism could play a role in the process of the cartilage degradation. IL-6 in fact regulates production of many acute-phase proteins, promoting and maintaining the in.ammatory phenotype. Because this interaction and ampli.cation process would change on the basis of IL-6 levels, the clinical relevance of the IL-6 gene polymorphism is based on the fact that its gene variants in.uence levels and functional activity of the protein.

In conclusion, our results show that the CC and the GG genotypes of the _174 G/C polymorphism of IL-6 gene promoter determine respectively a lower and an higher risk profile for osteoarthritic disease.

INFLUENCE OF TNF-α AND IL-1β ON THE MATRIX DEGRADATION BY SYNOVIAL FIBROBLASTS IN AN IN VITRO CARTILAGE/PANNUS MODEL

*Pretzel D, *Pohlers D, **Mollenhauer J, ***Richter W, *Kinne RW
Experimental Rheumatology Unit, Clinic of Orthopedics, Friedrich Schiller University Jena, Germany

david.pretzel@med.uni-jena

INTRODUCTION

Aggressive synovial fibroblasts (SF) at the cartilage/pannus-junction play an important role in joint destruction/inflammation in rheumatoid arthritis (RA) by locally expressing tissue-destructive enzymes (e.g. MMPs, aggrecanase). In vivo, SF and articular chondrocytes are stimulated by soluble cytokines and/or cell-cell contact with infiltrating inflammatory cells.
Thus, the present study aimed at analyzing the influence of stimulation with the pro-inflammatory cytokines TNF-α and IL-1β on SF from RA, osteoarthritis (OA), and joint trauma (JT) in an in vitro co-culture system with bovine articular cartilage (BC) explants.

METHODS

Standardized BC discs were embedded in 48-well plates containing agarose. RA-, OA-, and JT-SF (n = 5 each) were co-cultured with BC for 2 weeks and permanently treated with TNF-α (10 ng/ml), IL-1β (5 ng/ml) or the combination of both cytokines.
Alteration of the BC was monitored by measuring the release of proteoglycan into the supernatant (dimethylene-blue binding assay of sulfated glycosaminoglycans). Overall MMP activity was quantified using a fluorescence assay with a broadly MMP-specific peptide substrate. Distinction of individual MMP family members and discrimination of latent and active forms was achieved by gelatine zymography, secretion of TIMP-1 was determined by reverse gelatine zymography. Morphology of the cartilage surface and SF in co-culture with BC was examined by raster electron microscopy (REM).

RESULTS

The proteoglycan release following non-stimulated co-culture of BC with RA-, OA-, and JT-SF did not differ from the release in the corresponding BC-monoculture. In BC-monoculture, stimulation with IL-1β or IL-1β/TNF-α, but not TNF-α alone, significantly increased the proteoglycan depletion from cartilage as compared to non-stimulated controls. In co-culture with RA-, OA- or JT-SF, however, all stimuli led to significantly higher proteoglycan release than in non-stimulated co-culture. Notably, the values in TNF-α and/or IL-1β/TNF-α-stimulated co-culture with RA- and OA-SF were significantly higher than in the respective BC-monoculture. Interestingly, significantly higher levels of overall MMP activity were observed after stimulation with IL-1β, TNF-α or IL-1β/TNF-α in both BC-monoculture and co-culture with RA-, OA-, and JT-SF. Quantitatively, however, the overall MMP activity in all stimulated co-cultures showed significant higher levels (up to 4-fold) compared with BC-monocultures. In zymography, cytokine stimulation increased latent-MMP-9, but not latent MMP-2 activity in BC-monoculture and co-culture with SF; however, co-culture showed higher values than BC-monoculture for both latent MMP-2 and MMP-9. TIMP-1 secretion was induced by co-culture with SF, without a significant influence of cytokine stimulation. REM revealed that cytokine treatment induced: i) degradation of the cartilage matrix already in BC-monoculture; and ii) an activated phenotype of SF in co-culture.

DISCUSSION

Stimulation with TNF-α, IL-1ß or TNF-α/IL-1ß results in increased cartilage degradation and MMP-activity in both BC-monoculture and co-culture with SF. Significantly or numerically increased overall MMP-, MMP-2-, and MMP-9 activity following co-culture with SF, on the other hand, underlines the central role of SF for cartilage degradation. Comparison of the 2 culture systems may allow to distinguish the relative contribution of BC and SF to cartilage degradation.

***Center for Electron Microscopy; Friedrich Schiller University Jena, Germany
**Waldkrankenhaus "Rudolf Elle" gGmbH, Eisenberg, Germany

EXTRACELLULAR MATRIX REMODELLING IN OSTEOARTHRITIS

Tarantino U, Iundusi R, Lecce D, Tresoldi I, *Cereda V, *Modesti A
Università degli Studi di Roma Tor Vergata, Azienda Ospedaliera Universitaria Policlinico Tor Vergata, Divisione di Ortopedia e Traumatologia, Roma, Italy
umberto.tarantino@uniroma2.it

INTRODUCTION

Osteoarthritis is the result of several complaints and processes that lead to structural and often symptomatic malfunction of one or more synovial joints, including the subchondral bone, capsule, synovial membrane and articular cartilage. In this context osteoarthritis might be considered a dynamic process involving an increased turnover of cartilage matrix components, joint remodelling, bone formation and degeneration of articular tissues. These events involve extracellular matrix remodelling. The objective of this study was to determine by immunohistochemistry the expression of extracellular matrix components (fibronectin, laminin, tenascin and Type I and II collagens) and matrix metalloproteinases (MMP1, MMP2, MMP7 and MMP9) in femoral head articular cartilage from patients with hip osteoarthritis undergoing hip replacement surgery.

METHODS

Femoral head articular cartilage samples were obtained from 30 patients undergoing total hip arthroplasty for severe osteoarthritis. Control tissue samples included femoral head articular cartilage from patients undergoing surgery for femur neck fractures. The severity of hip osteoarthritis was classified according to clinical and radiological parameters. Our study protocol was approved by the Ethics Committee for Research involving human subjects of University of Tor Vergata. Three biopsies from three different articular cartilage areas at the same distance between each other and forming 120° angles were evaluated.

Articular cartilage samples were fixed in 4% buffered formaldheyde in phosphate buffered saline and embedded in paraffin. For light microscopy 3-5 μm thin sections were stained with Hematoxylin-eosin, Mallory-Azan and Alcyan blue staining. For immunohistochemistry monoclonal and polyclonal antibodies specific for fibronectin, laminin, tenascin, Type I and II collagens and matrix metalloproteinases (MMP1, MMP2, MMP7 and MMP9) were used. Antigen-antibody complexes were visualized by 3-amino-9-ethylcarbazole (AEC). Sections were counterstained with hematoxylin. Immunohistochemical stained samples were evaluated dividing the cartilage sections in three different zones: superficial (upper 1/4), deep (1/4 of section above tidemark) and middle (1/2 between). Staining intensity was semiquantitatively classified as negative (-), weak (+) and strong (++).

Two independent observers evaluated the different samples.

RESULTS

Femoral head articular cartilage from patients affected by hip osteoarthritis showed histological defects including fibrillation and fissures into the deep zone. Both superficial and intermediate articular cartilage layers displayed a significant chondrocytes number reduction, while the deep layers were characterized by the presence of chondrocyte clones.

Immunohistochemical analyses showed, in the superficial zone from femoral head articular cartilage, a weak expression of MMP1 in hip osteoarthritis patients compared to controls. On the other hand, a strong expression of MMP9, usually not expressed in normal cartilage, was observed in articular cartilage samples with severe osteoarthritis. MMP2 showed strong expression in the articular cartilage without differences regarding severity of osteoarthritis. Fibronectin distribution was always altered in articular cartilage with all grade of osteoarthritis. A significant reduction of type II collagen as opposite to an increase of type I collagen was observed in articular cartilage with osteoarthritis closed to bone sclerotic areas. Cartilage from femoral heads with severe osteoarthritis showed a very strong expression of tenascin both in the middle and deep zone of the biopsy. In most cases the high expression level of tenascin correlated with high expression level of MMP2.

DISCUSSION

Our findings demonstrated that articular cartilage from femoral head with osteoarthritis displayed a remarkable extracellular matrix remodelling. In particular, articular cartilage samples with severe osteoarthritis showed high tenascin expression level through all zones and this expression was associated with strong expression of MMP2 and MMP9. These results might suggest that tenascin could be the molecule responsible for the activation of MMPs, thus causing collagens and proteoglycans degradation and ultimately determining the remodelling of the extracellular matrix.

*Università degli Studi di Roma Tor Vergata, Cattedra di Patologia Generale, Rome, Italy

THE ROLE OF GEODES IN THE HIP ARTHROSIS SECONDARY TO THE REUMATOID ARTHRITIS

Zirattu G, Zirattu F, Fadda M, Satta G, Mele A, Tranquilli Leali P
Orthopaedic Dpt, University of Sassari, Sassari, Italy

gziratt@tin.it

INTRODUCTION

The different spacial sideway of geodes in the same femural head, their number, dimensions, origin, suggested to us the present document. Bifore now, it has already been analyzed cystic hollows in primary arthrosis. Actuqlly on our study, we relate the outcomes regarding the same phenomenon in reumathoid arthritis.

METHODS

We choose 20 femural head previousl scheduled, considerin the same preoperatory radiographic weightiness diagrams. These were undergone to a parrellel and vertical planes cut among them. On three millimeters thickness slices, thanks to constant radiographic enlargement by semi-automatic images analyzator, we detected the number, site and dimensions of geodes. The datas obtained, formed into a groups for quadrant (limited by two orthogonal planes crossing the centre of rotation), has been tretaed by statistical analysis (Anova and t-test).

RESULTS

92 geodes has been counted, in almost the same measure distributed in all quadrant.
Aggregating the statistics for sector there are, not significative differences between all quadrant.
We can see the prevalence of the bigger geodes between all quadrant.

DISCUSSION

According to preliminary results, it would turn out just one difference between the geodes observed in primari arthrosis and in hip arthrosis secondary to reumathoid arthritis. This difference it consists in the dimensioni of cystic hollows that are bigger in reumathoid arthritis according to the phisiopatology and the anatomo-pathologic particularities.

EXPRESSION OF COMPONENTS OF THE TGFβ SIGNALING PATHWAY IN POSTNATAL MOUSE VERTEBRAL GROWTH PLATE

*Dahia CL, *Mahoney E, **Durrani AA, ***Wylie C
[*]Divisions of Orthopaedics and Developmental Biology, Cincinnati Children's Hospital and Medical Center, Cincinnati, OH-45229

Chitra.Dahia@cchmc.org

INTRODUCTION

Idiopathic scoliosis is the most common type of spinal deformity, and results from unsynchronized growth of the growth plates between the vertebrae. Paracrine and humoral factors play important roles in the regulation of normal bone growth. The goal of the study is to determine how cell signaling pathways control symmetrical growth of vertebrae at their growth plates during postnatal life cycle.

METHODS

FVB mice were selected from 1-9 weeks of age and their longitudinal growth was determined by measuring the lengths of the mice at one-week intervals. The thoracic vertebrae and knee joints were removed from 1-4 weeks old male mice and immediately frozen. 10 μm cryosections in the coronal plane were collected from the thoracic vertebrae and knee joints. Immunolocalization of TGFβ1, TGFβ RII and its downstream signaling intermediate (p)Smad2/3 was carried out on 10 μm thick cryosections. Histological details of the zones of the vertebral growth plates were analyzed by hematoxylin and eosin staining.

RESULTS

Maximum longitudinal growth of the mice was observed between 1-4 weeks of age. Histological analysis of the vertebral and tibial growth plates from 2-week-old mice revealed the spatial organization of the chondrocytes in the different zones of the growth plate. Immunolocalization showed that the active form of TGFβ1 was present in all the zones of the growth plate, however TGFβ RII was localized at the boundaries of proliferative and early hypertrophic chondrocytes. The downstream signaling molecule of TGFβ pathway, (p)Smad2/3 was also observed in the proliferative and early hypertrophic zone of the growth plate. (p)Smad2/3 was found to be nuclear in vertebral as well as tibial growth plates (Fig A & B).

DISCUSSION

Cells responding to TGFβ1 signals were in the proliferative and early hypertrophic zone of the growth plate, suggesting a role of TGFβ signals in the transition from cell proliferation to hypertrophy of chondrocytes. Understanding the molecular biology of postnatal vertebral growth plate development will allow future understanding of the defect(s) in the regulatory pathways that causes scoliosis and will lead to development of novel therapies for management of these growth related disorders.

[**]Division of Orthopaedics, Cincinnati Children's Hospital and Medical Center, Cincinnati, OH-45229, USA.
[***]Division of Developmental Biology, Cincinnati Children's Hospital and Medical Center, Cincinnati, OH-45229, USA.

A

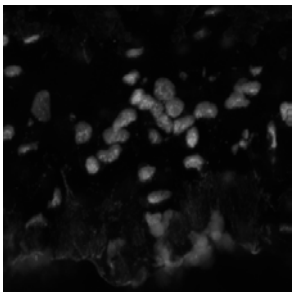

B

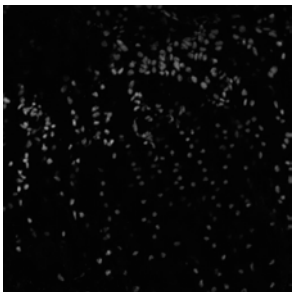

A RAT MODEL FOR BIOMECHANICAL TESTING OF TENDON HEALING IN A BONE TUNNEL

*Fahlgren A, *Aspenberg P
*Department of Orthopedics and Sports Medicine, Faculty of Health Sciences, Linköping University, Linköping

Anna Fahlgren@inr.liu.se

INTRODUCTION

Ligament reconstruction is usually performed by the implantation of a tendon graft in a bone tunnel. The healing occurs via attachment of the bone tissue into the tendon. Maximum values for pull-out strength have been found to be proportional to osseous ingrowth [1]. The cells responsible for healing are derived from the bone compartment, and healing can be stimulated by osteogenic factors such as BMP-2. PTH stimulates bone formation when administered intermittently. PTH has a dose-dependent effect of fixation of implants in bone [2, 3]. We developed a rat model to characterize biomechanical properties of tendon healing in a bone tunnel. We also tested whether intermittent treatment with PTH stimulates healing in this model.

MATERIALS AND METHODS

Forty-one SD male rats were used. The tibialis anterior tendon was detached from its muscle and bone insertion, folded double and transplanted through a bone tunnel at the level of the tibio-fibular bifurcation. A plastic tube was used as a stop for the loop of the doubled tendon graft. The rats were randomized into 4 groups. 20 rats were followed for 2 weeks and 21 rats for 6 weeks. 10 rats in the 2 weeks group and 11 in the 6 weeks group were treated with 60ug/kg PTH three days a week. As a positive control, a screw was inserted in left proximal tibia, to document increased pull-out force due to PTH.
An additional group was done with 10 rats followed for 4 weeks without PTH treatment.
After the rats were killed, the plastic tube was pulled out from the tendon loop and replace by a hook for pull-out testing. Using a material testing machine (100R, DDL Inc., Eden Praire, Mn, USA) a constant speed of 1 mm/sec was applied until failure. We recorded the peak force at failure and stiffness. Statistical analysis was performed using one-way ANOVA.
Institutional guidelines for care and treatment of experimental animals were followed.

RESULTS

There were 3 exclusions because of technical problems during biomechanical testing.
After 4 and 6 weeks there was an increase in force at failure compared to 2 weeks. After 6 weeks there was an increase in stiffness compared to 2 weeks. There was no effect of PTH on tendon to bone healing (Table 1).
PTH improved screw fixation. After 2 weeks the force at failure was increased by 37% (53 versus 71 N) and after 6 weeks by 54% (80N versus 123N).

Table 1 Force at failure and stiffness

Treatment	n	Force (N)		Stiffness (N/mm)	
		mean	sd	mean	sd
Controls					
2 weeks	9	3,3	1,1	4,9	3,4
4 weeks	10	5,7	1,3	7,3	2,8
6 weeks	11	6,5	1,9	9,4	3,5
PTH					
2 weeks	8	3,5	1,1	3,7	1,5
6 weeks	10	6,8	2,7	10,4	3,6

DISCUSSION

This new rat model is a relatively simple method to test biomechanical properties during tendon healing in a bone tunnel. Results showed a progressive increase in strength of the tendon to bone attachment during the first 6 weeks. The time for healing is in line with previous studies on tendon to bone healing. The time is needed for revascularization, fibrous healing and the intraosseous response [1]. PTH improved the bony response to the intraosseous screws, but not tendon to bone healing. One explanation could be that PTH only activates cells of the osteoblastic lineage when they are too differentiated to participate in the early callus formation that precedes bone to ligament healing. Some data indicate that PTH activates bone linings cells rather than progenitor cells [4].

REFERENCES

1.Rodeo, S.A., et al., J Bone Joint Surg Am, 1993. **75**(12): p. 1795-803.
2.Skripitz, R. et al, Acta Orthop Scand, 2004. **75**(6): p. 654-62.
3.Skripitz, R. et al, J Bone Joint Surg Br, 2001. **83**(3): p. 437-40.
4.Dobnig, H. and R.T. Turner, Endocrinology, 1995. **136**(8): p. 3632-8.

ACKNOWLEDGEMENTS

We thank Bibbi Mårdh for technical assistance. This investigation was supported by the Swedish Research Council (project 2031), Materials in Medicine and the Tore Nilsson Foundaion.

DOSE-DEPENDENT GROWTH INHIBITORY EFFECTS OF INDOMETHACIN ON TENDON-DERIVED CELLS

*Mallick E, * Rolf CG, *#Scutt A
*Sheffield Centre for Sports Medicine, Division of Clinical Sciences South, University of Sheffield Medical School; #Tissue Engineering Group, Department of Engineering Materials, University of Sheffield, Sheffield, UK

dremad_smap@yahoo.com

INTRODUCTION

Non-steroidal anti-inflammatory drugs (NSAIDs) are commonly used for the treatment of a number of musculoskeletal sports injuries including the inflammation of tendons and ligaments. A number of studies have however, suggested that NSAIDs may delay ligament healing in animal models although the exact mechanism of action for this is unknown.

Some *in vitro* investigations on the effects of NSAIDs on tenocytes have been performed however; they have used limited dose-ranges of NSAIDs and subcultures of tenocytes.

We have previously argued that subculturing tenocytes selects for rapidly proliferating population of cells not-necessarily representative of the situation found *in vivo*. We have therefore investigated the effects of NSAIDs on primary tenocytes and secondary and tertiary subcultures of the cells.

MATERIALS AND METHODS

Tenocytes were obtained from rat tail tendon by overnight digestion in collagenase.

The cells were then plated out in 24 well plates at a density of 10,000 cells per well in DMEM containing 10% FCS, penicillin/streptomycin and glutamine. The cells were treated with indomethacin (10 mM- 10 nM) for 6 days. The cultures were then stopped and cell number determined by either alamar blue assay, methylene blue assay or by direct counting using a GuavaPCS.

RESULTS

It was found that treating primary cells with indomethacin lead to a dose related inhibition of cell proliferation however, rather unexpectedly the relation ship was negative with the greatest inhibition being seen at 10 nM. In secondary subcultures the cells became relatively refractive to treatment with indomethacin and then by the third subculture a biphasic stimulation of proliferation was seen with a maximum at 1-10 μM.

CONCLUSIONS

These data suggest that primary tenocytes respond to indomethacin quite differently compared to secondary and tertiary subcultures and this may be due to the selection of a specific population of tenocytes that is present in the primary digest only at low levels.

This would suggest that *in vitro* investigations into tenocyte metabolism should preferentially be performed using primary cells and that results obtained using subcultures should be viewed with some caution.

ANATOMICAL BASIS OF THE MEDIAL SURAL ARTERY PERFORATOR FLAP

*Okamoto H, *Sekiya I, *Otsuka T
Department of Orthopaedic Surgery, Nagoya City University Medical School, Nagoya, Japan

yands53okamoto@yahoo.co.jp

INTRODUCTION

There was no paper of a large anatomical study in the perforators of the medial sural artery. We first presented a large number of cadavatic study in the perforators of the medial sural artery in Asian race. The purpose of this investigation was to detect the perforator of medial sural artery, to record their pattern and number, and to make easier the flap sculpturing.

METHODS

Forty-four formolized lower limbs of adult cadavers in Asian race were used for the study. The number and location of perforating vessels were recorded, expressed in centimeters, from the popliteal crease (PC) and from the posterior midline. Only perforating vessels clearly coming from the medial and lateral sural arteries were recorded. The length of each pedicle and diameter of each perforator was then measured.

RESULTS

Perforating branches from the medial sural artery were found in all 44 specimens, numbering one to five, with a mean of 2.4. No perforators were found higher than 5cm or lower than 17.5cm from the PC in this study. All perforators gathered in an area between 0.5cm and 4.5cm from the midline of the gastrocnemius muscles. In terms of external diameter, the vein of the perforating bundle was little larger (mean; 0.9mm, range; 0.2 to 2.0mm) than the artery (mean; 0.8mm, range; 0.2 to 2.0mm).
The average external diameter of the medial sural artery after dividing from popliteal artery was 2.5mm (range; 2.0 to 3.5mm). The average pedicle length from the bifurcation of the medial sural artery to the skin was 14.6cm (range; 7.7 to 20.7cm).

DISCUSSION

In this study, perforators were found in the distal half of the medial gastrocnemius muscle, 5.5 to 17.2cm from PC. Cavadas described that perforators were found at 8.5 to 19cm from PC. This difference of the distances was because of the length of the leg and muscle belly. The mean distance from PC to distal limit of the gastrocnemius medialis muscles was 18.6cm and 22.8cm in our study and Cavadas's, respectively. Because of these differences for the length of the muscle berry, the distribution of perforators might be difference between European and Asian. The average external diameter of the perforator of the medial sural artery was 0.8mm in our study. This is almost the same to previous reports. The number of perforators was 1 to 5 in this study, which look like to literature. The risk of muscle ischemia after the sacrifice of even entire medial sural artery should be remote, because several sources of secondary vascular pedicles; a proximal secondary pedicle, vascular connections with the lateral gastrocnemius muscle, and branches from the posterior tibial and peroneal arteries. The average diameter of the medial sural artery after bifurcation was of such dimensions to allow easy microanastomosis with most of the recipient vessels in the body. The medial sural artery perforator flap is useful for soft tissue coverage of the proximal third of the tibia and anterior and medial aspect of the knee and for free flap because of maintaining the function of medial gastrocnemius muscle, thick and long enough pedicle.

IN VITRO EFFECTS OF INTERFERON-ALPHA ON DIFFERENT CELLULAR ELEMENTS EXISTING IN A BONE METASTASIS OF RENAL CELL CARCINOMA

*Avnet S, *Cenni E, *Gancitano G, *Perut F, *Granchi D, **Brandi ML, *Giunti A, *Baldini N

*Laboratorio di Fisiopatologia Ortopedica, Istituti Ortopedici Rizzoli; Università di Bologna, Bologna; and
**Department of Internal Medicine, University of Florence, Florence, Italy
sofia.avnet@ior.it

INTRODUCTION

Since bone metastases of renal cell carcinoma (RCC) are typically osteolytic and highly vascularized, drugs targeting both angiogenesis and bone resorption could be considered as adjuvants. Interferons (IFN) are able to inhibit both angiogenesis and tumor growth of RCC, however the ability of IFN-alpha (IFN-α) to modulate bone metabolism is largely unknown. To investigate if IFN-α can impair osteoclast differentiation, in addition to inhibit angiogenesis and tumorigenesis, we considered the effects of IFN-α on cells derived from RCC, bone endothelial cells, and human osteoclasts.

METHODS

CRBM-1990 and ACHN cell lines were used as models of RCC, BBE cell line was used as a model of endothelial cells. Osteoclasts were obtained from mononuclear cells of peripheral blood through the addition of RANKL and M-CSF. The formation of osteoclasts was verified by the analysis of tartrate resistant acid phosphatase (TRACP) and multinuclearity. PBMC seeded in differentiating medium in the presence of IFN-alpha (extracted from leukocytes, obtained by Alfa Wassermann, Bologna, Italy), were evaluated for TRACP 5b activity (BoneTRACP Assay, SBA Sciences, Turku, Finland), or for resorption activity (Osteologic Multitest Slide, BD Biosciences, Erembodegem, Belgium). By Western blot, c-Fos protein expression was also tested in osteoclasts, while FGF-2 protein expression was analyzed in RCC cells. The analysis of FGF-2, VEGF-A, VEGF-B, and VEGF-C mRNA expression of CRBM and ACHN cells was performed by semiquantitative RT-PCR. IFN-α inhibition of the migratory ability of BBE induced by RCC cells was analyzed by a chemotaxis assay (Boyden chamber technique). Inhibition of the proliferation rate of BBE incubated with IFN-α was analyzed by the construction of a growth curve, and apoptotic cells were quantified by FACS analysis (annexin-V-FITC test). Inhibiton of anchorage-independent growth of RCC cells was analyzed by seeding cells in 0.33% agarose and counting colonies at 10 days.

RESULTS

To verify if IFN-α inhibits angiogenesis in the bone microenvironment, we treated endothelial cells and verified that IFN-α was able to inhibit both their growth via apoptosis induction and their migratory activity elicited by tumor cells. We also demonstrated that IFN-α is able to inhibit the *in vitro* tumorigenesis of RCC cells (60% inhibition at 1000 U/ml in a semisolid medium) and the synthesis of the angiogenetic factors FGF-2 and VEGF (as shown by RT-PCR and Western blot). Moreover, at a very low dose (250 U/ml), IFN-α significantly reduced the expression of TRAP 5b, a specific marker of osteoclast number (Figure A), and *in vitro* bone resorption by human osteoclasts (Figure B), therefore suggesting that this molecule interferes with the early steps of osteoclast differentiation. This effect is a consequence of the inhibition of expression of c-Fos, a pro-osteoclastogenesis transcription factor involved in RANKL signaling, as shown by Western blot.

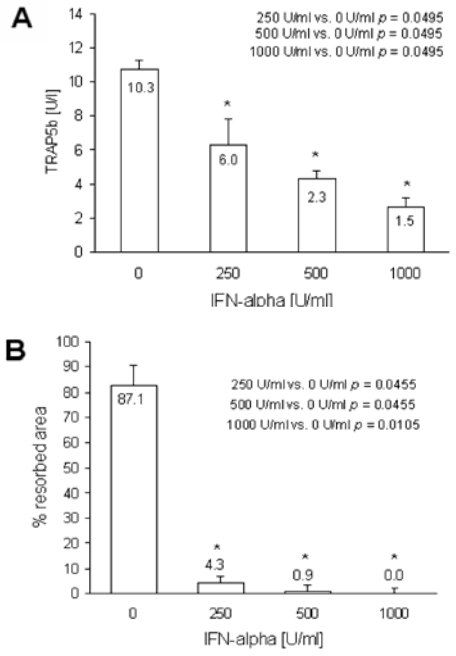

CONCLUSION

This study indicates that, under therapeutic dose limits, IFN-α may significantly inhibit *in vitro* bone resorption and angiogenesis, two features commonly associated with bone metastases of RCC, in addition to a direct inhibitory effect on cancer cells.

AKNOWLEDGMENT

This study was supported by grants from the Italian Association for Cancer Research and from the Ministry of Health of Italy.

ELEVATED SERUM ACTIVITY OF TRACP5B IN OSTEOSARCOMA PATIENTS IS ASSOCIATED WITH AN AGGRESSIVE PHENOTYPE

Cavaciocchi M, Avnet S, Pellacani A, *Longhi A, Perut F, Granchi D, Giunti A, Baldini N
Laboratory di Fisiopatologia Ortopedica, and *Servizio di Chemioterapia, Istituti Ortopedici Rizzoli, Bologna, Italy
Mikecava2000@yahoo.it

INTRODUCTION

Osteosarcoma (OS) is a highly aggressive tumor that rapidly destroys bone and commonly spreads to the lungs. In this study, we tried to dissect the complexity of events occurring in the bone microenvironment in the presence of OS and considered different serum markers reflecting bone invasion and destruction, including the proteases MMP-9 (directly secreted by tumor cells) and pro-MMP-13 (secreted by mononuclear cells associated to osteoclasts), and NTX, an index of collagen degradation. In addition, we considered the isoenzyme 5b of tartrate resistant acid phosphatase (TRACP 5b), a marker of activated osteoclasts. These markers were investigated in a clinical series and correlated with outcome.

METHODS

Forty-six patients with newly diagnosed osteosarcoma, and 19 age-matched individuals without evidence of benign or malignant bone disease were enrolled in this retrospective case-control study. All OS were high-grade tumors, 9 metastatic to the lungs, and 4 with more than one osseous localization. The remaining 33 were localized at a single skeletal site. Serum was separated from venous peripheral blood. All patients and parents, when necessary, had given written informed consent. Serum concentrations of MMP-9 and pro-MMP-13 were measured using human MMP-9 and pro-MMP-13 kit (R&D Systems Inc., Minneapolis, MN). Serum TRACP 5b (BoneTRAP®; SBA-Sciences, Oulu, Finland) and NTX (Osteomark®, Ostex International, Seattle, WA) were determined using a commercial immunoassay. To evaluate differences between groups the Mann-Whitney test was applied. Correlations were assessed by the Spearman Rank test. The diagnostic performance was evaluated by the ROC curves. The Kaplan-Meier product-limit method was employed to estimate the overall survival rate, and the log rank 'Mantel-Cox' test was applied to highlight significant differences between groups with high/low tested parameters.

RESULTS

We found a significant difference in serum levels of MMP-9 between OS and controls (median: 728 in OS vs. 399 in controls; $p < 0.0001$), and this could be considered as a marker with a good diagnostic accuracy (AUC 0.837, 95% CI 0.723-0.918).

No other differences between OS and control subjects were found. To evaluate variance among the tumor population, OS developing lung metastases and multicentric OS were collected and considered as 'aggressive' compared to 'conventional' OS. In 'aggressive' OS, TRACP 5b values were significantly higher (median 12.8 U/L vs. 8.0 U/L in 'classical' OS, $p = 0.0152$). Moreover, TRACP 5b levels were positively associated to the serum levels of NTX and pro-MMP-13, possibly suggesting a higher degree of bone resorption/remodelling in more aggressive lesions. Finally, higher levels of TRACP 5b were significantly associated with a decreased probability of survival (Fig. A). By contrast, the probability of survival in patients did not correlate to the level of MMP-9 (Fig. B).

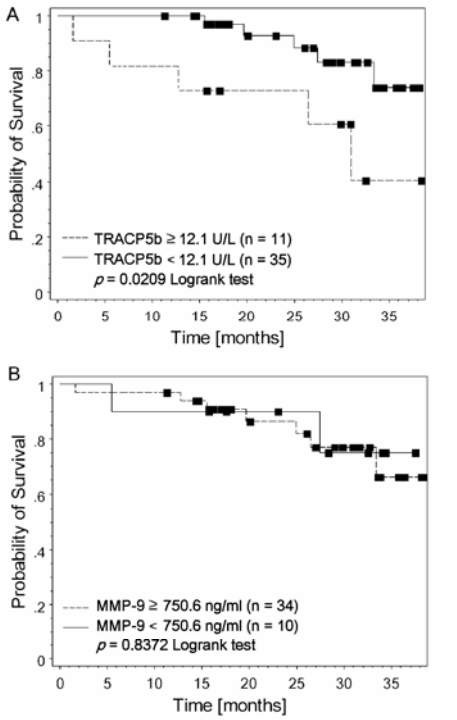

DISCUSSION

MMP-9, but not MMP-13 is secreted by OS and its serum levels, reflecting the presence of the tumor, may be diagnostically relevant. High serum levels of TRACP 5b but not of MMP-9 were correlated with a poor outcome. Since TRACP 5b corresponds to the number of circulating activated osteoclasts, the observed higher levels of this marker in OS that are systemically, but not locally more aggressive (metastatic and multicentric OS) may reflects the ability of this subset of tumors to elicit an immune response mediated by the recruitment and activation of osteoclasts rather that the simple local activation of osteoclasts at the primary site.

ACKNOWLEDGMENTS

This work was supported by AIRC and the Italian Ministry of Health.

EFFICACY OF THE THIRD-GENERATION BISPHOSPHONATE AGAINST MURINE OSTEOSARCOMA CELL LINE

***Horie N, *Murata H, *Sakabe T, *Matsui T, ***Kimura S, ***Maekawa T, **Fushiki S, *Kubo T
*Department of Orthopaedics, and **Department of Pathology and Applied Neurobiology,
Graduate School of Medical Science. Kyoto Prefectural University of Medicine, Kyoto, Japan
***Department of Transfusion Medicine and Cell Therapy, Kyoto University Hospital, Kyoto, Japan
n-horie@koto.kpu-m.ac.jp

INTRODUCTION

The nitrogen-containing BPs (second- or third-generation BPs) inhibit protein prenylation, and exhibit anti-tumor effects in some cancer cells. Although second-generation BPs have been reported to directly block the growth of osteosarcoma cells, the anti-osteosarcoma effects of third-generation BPs have not yet been fully studied. Therefore we examined the effect of third-generation BPs, YM529, on the osteosarcoma cells.

METHODS

We used YM529 and 6 anti-tumor drugs, doxorubicin, cisplatin, methotrexate, imatinib mesylate, paclitaxel, and gemcitabine. We used murine osteosarcoma cell lines, MOS and its multidrug-resistant subclone, MOS/ADR, which overexpresses P-glycoprotein.

(1) *Effects of BPs on cell proliferation:* The cell proliferation was determined by MTT assay. The IC_{50} values were obtained by using CalcuSyn (Biosoft).

(2) *Cell cycle analysis and induction of apoptosis:* The nuclei were stained with propidium iodide. DNA histograms were measured using a flow cytometer. These cells were also evaluated for apoptosis by using TUNEL.

(3) *Western blot analysis:* We used goat polyclonal anti-Rap1A antibody (diluted 1:1,000). Rap1A is substrate of geranylgeranyl transferase (GGTase I).

(4)*Combined effects of BPs and other 6 anti-tumor drugs:* Cells were treated with YM529 alone, an anti-cancer drug alone and the YM529/anti-cancer drug combination in each plate, and was evaluated individually for efficacy. The fraction affected (Fa) (i.e., Fa of 0.25 is equivalent to 75% viable cells) and the combination index (CI) were calculated with CalcuSyn.

RESULTS

(1) *Inhibition of cell growth by YM529:* The growth of MOS cells was inhibited by YM529 in a time and dose dependent manner. The IC_{50} value of the MOS cells for YM529 was 0.52 μM (Figure 1A).

(2) *Effects of YM529 on the cell cycle and induction of apoptosis:* YM529 decreased the MOS cells in the G_2/M phase and increased in the S phase (Figure 1B).

A TUNEL assay revealed that YM529 induced MOS cells into apoptosis in time dependent manner (Figure 1C).

(3) *Effect of YM529 on small GTP binding protein prenylation:* Unprenylated Rap1A was absent in untreated MOS cells but accumulated markedly after treatment with 0.3, 0.6, 1.2 μM YM529 (Figure 2).

(4)*Effect of YM529 on MOS/ADR cells:* The MOS/ADR cells were not as sensitive to YM529 as MOS cells.

(5) *Combined effects of BPs and other six anti-tumor drugs:* The effects of combination are synergistically, when combined with paclitaxel or gemcitabine (Figure3).

Figure 1.

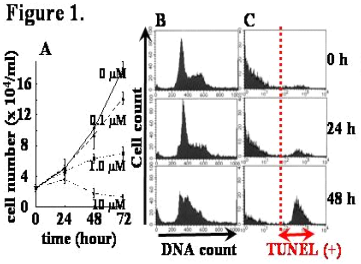

Figure 2.

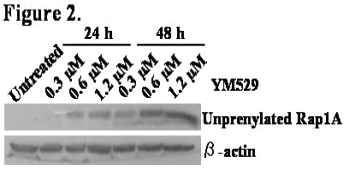

Figure 3.

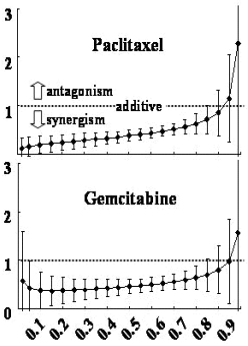

DISCUSSION

The aim of this study was to identify a novel antitumor therapeutic agent to osteosarcoma. The nitrogen-containing BPs are known to block the mevalonate pathway by inhibiting the activation of small GTP-binding protein prenylation. We have also shown in current studies that YM529 blocked the prenylation of Rap1A proteins. Since the Ras/MAPK pathway is crucial for regulating intracellular signaling in proliferation of tumor cells, blockage of prenylation of small GTP-binding protein could result in blockage of the mevalonate pathway which then act as against tumor growth. Therefore, the direct antitumor effects of YM529 on osteosarcoma cells are evaluated in vitro.

Then, we have demonstrated that the P-￥glycoprotein-overexpressing cells were resistant to YM529, which indicates that YM529 may also be subject to multidrug resistant mechanisms. We also examined the combined effects of YM529 with other anti-cancer drugs to determine whether the anti-tumor effect of BPs can be strengthened. We found that the anti-growth activities of paclitaxel and gemcitabine were completely augmented by YM529. Therefore, YM529 may have therapeutic application in enhancing the efficacy of these drugs such that their effective doses against other malignant neoplasms, such as lung cancer and ovarian cancer, can be reduced.

Taken together, YM529 has antitumor effects to oseteosarcoma, and can be strengthened the anti-tumor effect when it was combined with other anti-cancer drugs, such as paclitaxel or gemcitabine, which may be beneficial in treating osteosarcoma patients effectively.

ACRIDINE ORANGE USED FOR PHOTODYNAMIC THERAPY ACCUMULATES IN MUSCULOSKELETAL TUMORS DEPENDING ON pH GRADIENT

*Matsubara T, *Kusuzaki K, *Matsumine A, *Shintani S, *Satonaka H, *Uchida A
*Department of Orthopedic Surgery, Mie University Faculty of Medicine, Tsu City, Japan
Takao-m@clin.medic.mie-u.ac.jp

INTRODUCTION: We found that acridine orange (AO) specifically accumulated in musculoskeletal sarcomas and emitted green fluorescence with a strong cytocidal effect on mouse osteosarcoma cells after illumination. Since 1999, based on *in vitro* and *in vivo* basic research studies, we have been using AO photodynamic therapy (AO-PDT) to treat patients with musculoskeletal sarcomas, and have achieved a local recurrence rate and excellent limb function. However, it remains unclear why AO specifically accumulates in tumor cells, especially malignant tumor cells. AO is a basic dye and densely accumulates in lysosomes, which are strongly acidic organelles, and it is generally assumed that extracellular pH (pHe) is more acidic in tumors than in normal tissues. Based on these findings, we hypothesize that AO accumulates in tumor cells, due to acidic conditions around the tumor. In the present study, we investigated the relationship between AO accumulation and pHe of human musculoskeletal tumors and normal tissues.

MATERIALS AND METHODS: 1. *In vivo* study

62 musculoskeletal tumors with 27 benign tumors and 35 malignant tumors were investigated. Normal muscles and subcutaneous or intramuscular adipose tissues were also investigated.

Measurement of pHe For measurement of pHe in tumors and normal tissues, we used an MP120 Basic pH Meter (Mettler Toledo, France).

Measurement of AO fluorescent intensity The fresh tumor material used to measure pHe was exposed to 1 μg/ml AO (Sigma-Aldrich Chemie Gmbh, Germany) solution. The cut surface of the tumor material was then illuminated with 10,000-lux blue light. We calculated the fluorescence intensity ratio (X) using Scion analysis software.

2. *In vitro* study

Influence of bafilomycin A1 (BA) on uptake of AO BA down-regulates ΔpH between intra- and extra-cellular fluids by inhibiting the V-ATPase. A murine osteosarcoma cell line, LM8 cells (1×10^5) cultured in 5cm plates were exposed to 10 nM BA in DMEM conditioned at pH 7.4 for 24 hours, and were then exposed to 1 μg/ml AO. The cells were subsequently washed with PBS (pH 7.4), and 5ml of 2-propanol with 10 mM HCl was then added to dissolve the AO in the cells. The fluorescence intensity of these extract solutions was measured using a micro plate spectrofluorometer.

Effect of BA on cytocidal activity of AO-PDT LM8 cells (1×10^4) cultured in 96-wells plates with DMEM were exposed to 10 nM BA for 24 hours, followed by exposure to 0.1 μg/ml AO. Cells containing AO were illuminated with unfiltered light from a halogen lamp, but the control group cells were not illuminated. The viable cells in each well were counted. Phototoxicity was assessed using the MTS assay.

RESULTS: 1. *In vivo* study

pHe in the tumor tissues The average pHe was 7.1(±0.25) in the 27 benign tumors, 6.7(±0.26) in the 35 malignant tumors, 7.3 (±0.14) in the normal muscles, and 7.4(±0.11) in the normal adipose tissues. The malignant tumors were significantly more acidic than the benign tumors ($p<0.05$) and normal tissues ($p<0.01$).

AO fluorescent intensity in the tumor tissues The average fluorescence intensity ratio (X) was 3.6(±1.67) in the 27 benign tumors, 5.5(±2.56) in the 35 malignant tumors, 1.5(±0.48) in the normal muscles, and 1.4(±0.78) in the adipose tissues. AO fluorescence intensity, which correlates with AO accumulation in the tumor, was significantly higher in the malignant tumors (Fig.).

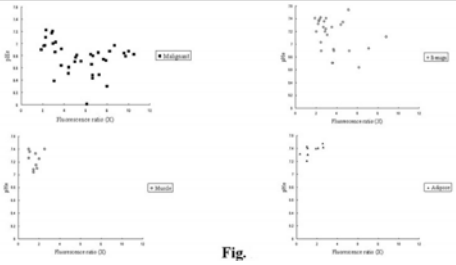

Fig.

2. *In vitro* study

Effect of BA on AO uptake and cytocidal activity of AO-PDT Uptake of AO by LM8 cells exposed to 0.1μg/ml AO decreased by 1/3 after pre-exposure to BA. Viability ratio of LM8 cells exposed to AO also markedly decreased after pre-exposure to BA.

DISCUSSION: Results obtained from this study suggested that AO may accumulate in musculoskeletal tumors, depending on extracellular acidity (pHe). Malignant tumor cells actively produce H+, however, they should maintain intracellular pH within a narrow range (7.2~7.4) to provide a favorable environment. Therefore malignant tumor cells mainly pomp out H+ to extracellular fluid via vacuolar-ATPases. Recent report suggested that malignant tumor cells produce intracellular acidic vacuoles like lysosome under hypoxic condition. We therefore hypothesized that AO accumulates in environments with a large ΔpH. This hypothesis is supported by the results of the present *in vitro* study using BA, which inhibits V-ATPase and decreases the ΔpH of intracellular acidic organelles. These results show that BA inhibited accumulation of AO in acidic organelles such as lysosomes, and that BA also markedly inhibited the cytocidal effect of AO-PDT. Therefore, AO accumulates such malignant tumor. Finally we believe that AO-PDT may be more effective on malignant tumors with highly acidic environment.

SULFORAPHANE ENHANCES TRAIL-INDUCED APOPTOSIS THROUGH THE INDUCTION OF DR5 EXPRESSION IN HUMAN OSTEOSARCOMA CELLS

***Matsui T, * Murata H, * Sakabe T, * Horie N, **Sowa Y, **Yoshida T, ** Sakai T, *Kubo T
*Department of Orthopaedics, Graduate School of Medical Science. Kyoto Prefectural University of Medicine, Kyoto, Japan
** Department of Molecular-Targeting Cancer Prevention, Graduate School of Medical Science, Kyoto Prefectural University of Medicine, Kyoto, Japan
takaakig@koto.kpu-m.ac.jp

INTRODUCTION

Tumor necrosis factor (TNF) -related apoptosis-inducing ligand (TRAIL) selectively induces apoptosis in cancer cells *in vitro* and *in vivo* with little or no toxicity toward normal cells. Therefore, TRAIL is one of the most promising new candidates for antitumor therapeutics. Death receptor 5 (DR5) is a member of the TNF-receptor family, and a receptor for TRAIL. In addition, DR5 is a downstream gene of the p53 tumor-suppressor gene, and up-regulated by conventional anticancer drugs such as doxorubicin and etoposide. DR5 is an attractive molecular target for effective cancer therapy. Sulforaphane (SFN), a naturally occurring member of the isothiocyanate family, is produced from cruciferous vegetables. SFN has attracted particular attention due to its potent anticancer effects. Recent studies have indicated that SFN can suppress proliferation of cancer cells *in vitro* and *in vivo* by inhibiting cell cycle progression and/or causing apoptosis. In this study, we tested an effective usage of the combined treatment of SFN with TRAIL in human osteosarcoma cells.

METHODS

We used human osteosarcoma cell line Saos2, and normal human peripheral blood mononuclear cells (PBMC).

(1) *Reagents.* Sulforafane and soluble recombinant human TRAIL/APO2L were purchased from LKT (St. Paul, MN, USA) and PeproTech (London, UK) respectively.

(2) *Detection of Apoptosis.* DNA fragmentation was quantified as the percentage of cells with hypodiploid DNA (Sub-G1). The nuclei were stained with propidium iodide (SIGMA, St Louis, MO, USA). The DNA content was measured using a FACSCalibur flow cytometer and Cell Quest software (Becton Dickinson, Franklin Lakes, NJ, USA).

(3)*Western Blot Analysis.* We used rabbit polyclonal anti-DR5 antibody (1:250; Cayman Chemical, Ann Arbor, MI, USA). Enhanced chemiluminescence (Amersham Bioscience, Piscataway, NJ, USA) was used for detection.

RESULTS

(1) SFN up-regulates DR5 expression in Saos2 cells. SFN induced DR5 protein expression in dose- and time-dependent manners using Western blotting (Figure 1).

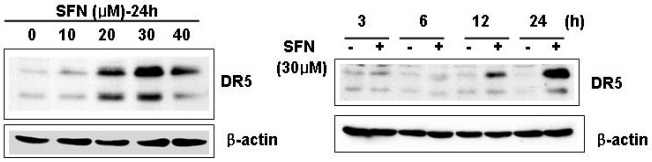

Figure 1 Saos2 cells were treated with SFN at the indicated concentrations for 24h or with SFN (30μM) for indicate periods.

(2) The level of DR5 expression in PBMC was not up-regulated by SFN treatment (Figure 2A). Furthermore, SFN did not enhance TRAIL-induced apoptosis in PBMC like Saos2 cells (Figure 2B). As a single agent, both of SFN and TRAIL very weakly induced apoptosis in Saos2 cells. However, SFN strongly enhanced TRAIL-induced apoptosis (Figure 2B).

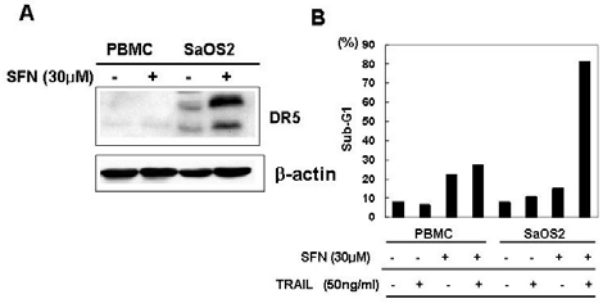

Figure 2 (A) Saos2 cells and PBMC were treated with or without SFN (30μM) for 24h. (B) Saos2 cells and PBMC were treated with SFN (30μM) and/or TRAIL (50ng/ml) for 24h.

DISCUSSION

To improve the prognosis of osteosarcoma, new strategies are necessary. In the search for new strategies and antitumor agents, we found that SFN is a potent enhancer of TRAIL-induced apoptosis in osteosarcoma cells. Furthermore, SFN up-regulates DR5 expression and sensitize TRAIL-induced apoptosis in a p53-independent manner because functionally-inactivated mutations of p53 gene exist in Saos2 cells. Several studies have shown the relationship of the inactivation of p53 with resistance to conventional antitumor agents. Therefore, the combined treatment with SFN and TRAIL may be effective for osteosarcoma with resistance to conventional agents caused by inactivated p53. On the other hand, SFN did not enhance TRAIL-induced apoptosis in normal human PBMC, suggesting that this regimen is expected to be safe in clinic. In conclusion, we show for the first time that SFN synergistically enhances TRAIL-induced apoptosis through the induction of DR5 expression in human osteosarcoma cells but not in primary non-malignant human cells. These results raise a possibility that the combination of SFN and TRAIL might be a promising molecular-targeting chemotherapy for malignant osteosarcoma.

THE PLANT ALKALOIDS CRYPTOLEPINE INDUCED P21 AND CELL CYCLE ARREST IN HUMAN OSTEOSARCOMA CELL LINE

*Sakabe T, *Murata H, *Matsui T, *Horie N, ** Sowa Y, ** Sakai T, *Kubo T
*Department of Orthopaedics, Graduate School of Medical Science. Kyoto Prefectural University of Medicine, Kyoto, Japan
** Department of Molecular-Targeting Cancer Prevention, Graduate School of Medical Science, Kyoto Prefectural University of Medicine, Kyoto, Japan
tsakabe@koto.kpu-m.ac.jp

INTRODUCTION

p21 is a member of cyclin-dependent kinase inhibitors and induces G1- and G2/M-phase cell cycle arrest. p21 is an attractive molecular target to suppress the growth of malignant tumor cells. In osteosarcoma cells, p53 is inactivated frequently. The transcription of p21 is directly activated by wild-type p53 protein, and the p21-inducing agents of p53-independent pathway might be effective for chemotherapy for osteosarcoma. As an activator of p21 in a p53-independent manner, we isolated cryptolepine (CLP: 5-methyl indolo(2,3b)-quiniine), an indoloquinoline alkaloid, from the traditional Ayurvedic medicinal plant *Sida cordifolia*, using p53-negative human osteosarcoma MG63 cells. In this study, we show for the first time that CLP is a potent inducer of p21 in human osteosarcoma cells.

METHODS

(1) *Isolation of cryptolepine*

CLP was isolated from the traditional Ayurvedic medicinal plant *Sida cordifolia*. (purchased from local market in Colombo, Sri Lanka in 2001).

(2) *Cell growth study*

MG63 cells were inoculated at a density of 1 x 10^4 cells in 12-well plate. Next day, CLP was added at various concentrations. From the second day to forth day from the inoculation, the number of viable cells was counted by a trypan blue dye exclution test.

(3) *Analysis of cell cycle progression*

The nuclei were stained with propidium iodide (PI). DNA content was measured using a FACSCalibur flow cytometer and Cell Quest software (Becton Dickinson, Franklin Lakes, NJ, USA).

(4) *Western blot analysis*

We used rabbit polyclonal anti-p21 antibody (1:500; Santa Cruz, CA, USA). Enhanced chemiluminescence (Amersham Bioscience, Piscataway, NJ, USA) was used for detection.

(5) *DNA transient transfection and luciferase assay*

MG63 cells (3 x 10^4 cells) were seeded in 12-well plate, and 1.0 μg per well of reporter plasmid DNA was transfected using a CellPhect transfection kit (Amersham Biosciences, Piscataway, NJ, USA). After 24 h incubation, the cells were treated with CLP. Lucifearse assay was performed, and the activity was determined as luminescence units normalized for the amount of protein in the cell lysates.

RESULTS

(1) CLP inhibits the growth of MG63 human osteosarcoma cells in a dose-dependent manner (A).

(2) CLP arrests MG63 cells at the G2/M phase in cell cycle progression (B). CLP up-regulates p21 expression in MG63 cells in a dose-dependent manner (C).

(3) The activation by CLP in p21/mt-SP1 decreased from the activation in p21. These results indicate that the Sp1 site is the main CLP-responsible element (D). ✓

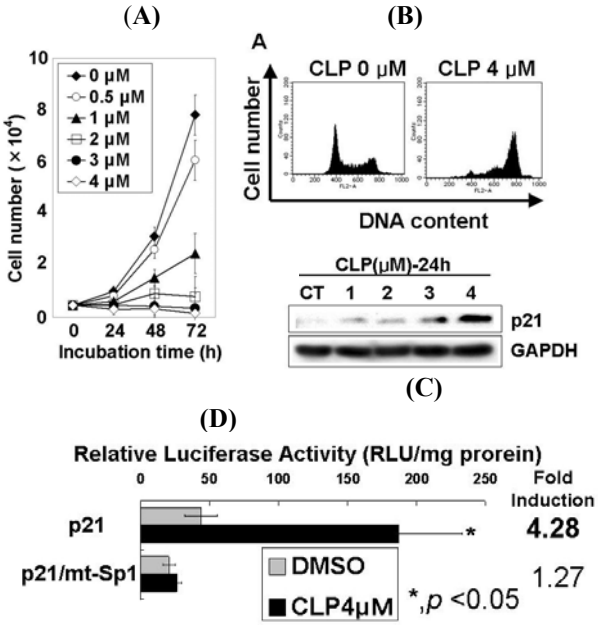

Figure(A)(B)(C)(D) MG63 cells were treated with CLP at the indicate concentrations for 24h.

DISCUSSION

To improve the prognosis of osteosarcoma, new strategies are necessary. To screening new agents for chemotherapy against osteosarcoma, we used the promoter screening of p21 and we searched the activator of p21 promoter in a p53-dependent manner, inducing cell growth arrest in human osteosarcoma cells that have inactivated p53. In the present study, we have shown that treatment of MG63 cells with CLP induces p21, resulting in G2/M-phase cell cycle arrest in a p53-independent manner. In addition, using a series of mutant p21 promoter constructs, we also found that Sp1 sites at -87 and -69 relative to the transcription start site are involved in the activation of the p21 promoter in MG63 cells by CLP. In conclusion, CLP induced growth arrest in MG63 cells through the activation of p21, and p21 promotor mediated through specific Sp1 sites in the promoter region. These results indicate that p53 is not required for the transcriptional activation of p21 by CLP, and raise a possibility that the treatment of CLP might be promising for the molecular-targeting chemotherapy of malignant osteosarcoma.

STROMAL CELLS DERIVED FROM GIANT CELL TUMOR OF BONE SHOW OSTEOBLAST-LIKE FEATURES

Salerno M, Avnet S, Pellacani A, Giunti A, Baldini N
Laboratorio di Fisiopatologia Ortopedica, University of Bologna and Istituti Ortopedici Rizzoli, Bologna, Italy
manu1510@hotmail.com

INTRODUCTION

Giant cell tumor of bone (GCT) is a benign neoplasm of bone with a local aggressive behaviour. GCT consists of three major cell types: 1. multinucleated giant cells, that have been well characterized as the osteoclast-like cells, that are responsible for tumor osteolysis; 2. stromal cells, that can be propagated *in vitro* and express pre-osteoblast markers;[1] 3. CD68-positive monocytes or macrophages.
Although the histogenesis of the stromal component is not well defined, recent studies have shown that these cells are able to induce the fusion and differentiation of monocyte/macrophage precursor cells to active osteoclasts by secreting cytokines, such as IL6 and RANKL, and they are therefore considered as the true neoplastic component of GCT.[2]
In this study, we characterized the stromal component of GCT by a morphological and molecular analysis, in order to elucidate the *in vitro* neoplastic features of these cells.

METHODS

Human mesenchimal stem cells (hMSCs) were isolated from two different bone marrow samples by density gradient, maintained in α-Modified Minimum Essential Medium (α-MEM, Sigma, St. Louis, MO) plus 10% FCS and considered as a control. Six primary cultures of stromal cells (TCG) were obtained from different samples of GCT by mechanical mincing, and maintained in Iscove's Modified Dulbecco Medium (IMDM, Invitrogen, Carlsbad, CA), plus 10% FCS. Cells were maintained in humidified atmosphere at 37°C and 5% CO_2. Nuclear morphology at early passages was evaluated by Hoechst 33342 staining (Sigma, St. Louis, MO). Cell growth rates were assessed by 3-(4,5-dimethylthiazol-2-yl-2,5-diphenyltetrazolium (MTT) bromide colorimetric assay (Sigma). The tumorigenesis of the stromal cell lines was evaluated by the analysis of the growth in a semi-solid medium (soft agar assay). The Saos-2 osteosarcoma cell line was considered as a positive control. Intracellular alkaline phosphatase (ALP) activity was revealed by a cytoenzymatic assay (Sigma). mRNA of Runx2/Cbfa1, and Osterix was analyzed by RT-PCR in both TCG and hMSC cultures.

RESULTS

The morphology of stromal cells *in vitro* was fibroblast-like, and these cells were very adherent to the plastic substrate and grew in monolayer. Only one cell line, derived from a recurrence of GCT, did not rich the confluence and proliferated in an anchorage-independent way. After nuclear staining, in addition to mononuclear cells, a binuclear cell population was also observed as reported previuosly by other group. Late passages (around 30th passage), induced a replicative senescence in almost all the cell lines examined (as well as in hMSC cell line).
In MTT assay (Fig. 1) the proliferation rate was similar among different cultures and to hMSC cells, although one (TCG2594) showed a lower rate. Compared to Saos-2 cell lines, all stromal cell lines were unable to form colonies in soft agar. Four cultures showed an intense ALP activity. RT-PCR analysis revealed the transcription of mRNA for the pre-osteoblast marker Runx2 in all GCT cultures while Osterix was present only in two of them (TCG1931 and TCG2594), although in hMSC cultures mRNA expression for Runx2 and osterix were both positive.

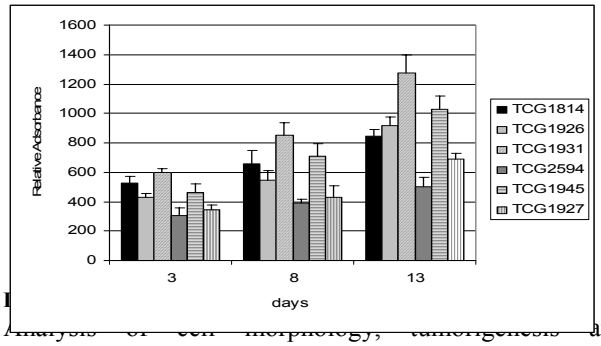

Analysis of cell morphology, tumorigenesis and proliferation indicate that stromal cells obtained from GCT tumor specimens and maintained *in vitro* do not show a transformed phenotype. In fact, these cells did not grow in soft agar, were not immortalized, and showed a proliferation rate similar to that of normal human osteoblasts isolated from bone marrow. Moreover, ALP activity, and analysis of gene expression suggested that stromal cells have an osteoblast-like phenotype. According to our observations, the stromal cells of GCT do not represent the neoplastic component, and the real nature of this lesion remains elusive.

AKNOWLEDGMENT
This work was supported by grants from the Italian Association for Cancer Research and the Ministry of Health of Italy.

REFERENCES

1. Huang L, Teng XY, Cheng YY, Lee KM, Kumta SM. Bone. 2004 34:393-401.
2. Nishimura M, Yuasa K, Mori K, Miyamoto N, Ito M, Tsurudome M, Nishio M, Kawano M, Komada H, Uchida A, Ito Y. Orthop Res. 2005 23:979-87.

PROGNOSTIC SIGNIFICANCE OF WT1 (WILMS' TUMOR GENE) MESSENGER RNA EXPRESSION IN SOFT-TISSUE SARCOMA

*Sotobori T, *Ueda T, **Oji Y, ***Naka N, ***Araki N, *Myoui A, **Sugiyama H, *Yoshikawa H
*Department of Orthopaedics, Osaka University Graduate School of Medicine, Suita, Osaka, Japan

soto@yo.rim.or.jp

INTRODUCTION

The Wilms' tumor gene (*WT1*) was first identified by positional cloning strategies from the tumors of children who developed Wilms' tumor in the context of WAGR syndrome. The gene is inactivated in the germline of children with genetic predisposition to Wilms' tumor and in a subset of sporadic Wilms' tumors. The *WT1* gene was originally categorized as a tumor suppressor gene, however, several recent studies reported that *WT1* mRNA was overexpressed in many types of neoplasms and suggested that WT1 have an oncogenic property. The objective of current study was to evaluate the prognostic significance of *WT1* mRNA expression in patients with soft-tissue sarcoma.

METHODS

52 soft-tissue sarcoma and 13 normal soft-tissue samples were obtained at the Departments of Orthopaedic Surgery, Osaka University Medical Hospital and Osaka Medical Center for Cancer and Cardiovascular Diseases, Japan. Approval of the institutional review boards and written informed consent were obtained. Levels of *WT1* mRNA expression were examined by quantitative reverse transcription PCR. The correlation between *WT1* mRNA expression levels of soft-tissue sarcomas and those of normal tissues was estimated using the Mann-Whitney U test. The relationship between *WT1* mRNA expression level and various clinicopathological variables was assessed by Fisher's exact test. Cumulative disease-specific survival curves were calculated by the Kaplan-Meier method, and the differences were estimated using the log-rank test in univariate survival analysis. Cox's proportional hazards model was used for multivariate survival analysis to assess the independent prognostic significance of clinicopathological variables, including *WT1* mRNA expression level.

RESULTS

The levels of *WT1* mRNA expression in a variety of soft-tissue sarcomas were significantly higher than those in normal soft-tissue samples (median, 2.2×10^{-3} vs 8.7×10^{-5}; P=0.0212: The expression level of human leukemia cell line K562 was defined as 1.0). No significant correlation was observed between *WT1* mRNA expression level and clinicopathological factors including sex, age, primary tumor site, tumor depth, tumor size, histological grade, and distant metastasis at initial presentation. The disease-specific survival rate of patients with high *WT1* mRNA expression levels was found to be significantly poorer than in those with low *WT1* levels (P=0.0182, see Figure). Univariate analysis for disease-specific survival according to various clinicopathological factors, other than *WT1* mRNA expression level, revealed age less than 60 years, low histological grade, and no distant metastasis at presentation were significantly favorable prognostic factors. Furthermore, multivariate survival analysis indicated that *WT1* mRNA expression level is a significant prognostic factor (hazard ratio, 2.6; P=0.0488), independent of other prognostic factors including age, histological grade, and distant metastasis at presentation.

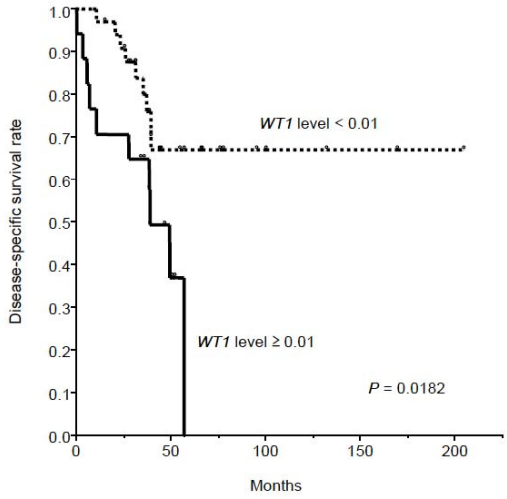

DISCUSSION

We demonstrated that *WT1* mRNA is frequently overexpressed in various types of soft-tissue sarcomas, and that *WT1* mRNA expression level is a significant prognostic indicator for soft-tissue sarcoma patients. These results strongly suggest that WT1 can be a candidate for a potent molecular marker to predict patient prognosis, and a promising target as a tumor antigen for tumor specific immunotherapy against soft-tissue sarcomas.

** Department of Functional Diagnostic Science, Osaka University Graduate School of Medicine, Suita, Japan
***Department of Orthopaedic Surgery, Osaka Medical Center for Cancer & Cardiovascular Diseases, Osaka, Japan

CYTOKERATIN EXPRESSION AND PROGNOSIS OF SKELETAL METASTASES

*Boriani L, *Pellacani A, *Antonioli D, *Bertoni F, *Bacchini P, *Baldini N, *Giunti A
Università degli Studi di Bologna, Istituti Ortopedici Rizzoli, Bologna, Italy
fisiopatologia@ior.it

INTRODUCTION

Immunohistochemical evaluation of organ-specific cytokeratin expression in bone metastases of carcinomas may be helpful for the identification of the primary. In this paper, we investigated the prognostic significance of cytokeratins as differentiative markers of advanced cancer.

PATIENTS AND METHODS

We collected a continuous series of 194 patients with metastatic carcinoma to the skeleton that were treated at our Institution from January 1, 1999 to June 30, 2001. Of these, 35 cases were excluded because the primary was different from carcinoma. Thirty-four additional patients were lost to follow-up. At the time of diagnosis of metastatic bone disease, the primary was known in 58 patients (46.4%). Of the 125 patients, 75 (60%) were males, and 50 (40%) females. The mean age at onset of bone metastases was 63 years (range, 39-87). Bone metastases were synchronous in 74 patients (59.5%), and metachronous in 51 (40.5%). In the latter group, the time of appearance of bone lesions after the initial diagnosis averaged 40 months. Bone metastases were found in the femur (40) humerus (32), spine (22), pelvis (17), tibia (10), radius (5), scapula (7), and clavicle (4). Multiple lesions were observed in 5 patients. Follow-up was evaluated in August, 2002. At a minimum one-year interval since the diagnosis of bone metastases, only 36 patients (29%) were alive. Tissue samples from all 125 patients were obtained on surgery, and processed for cytokeratin marker immunohistochemistry in addition to routine HE staining. The following markers were considered: cytokeratin 7, cytockeratin 20, CEA, CDX2, APS, FAP, ER, PGR, GCDFP, TTF1, WT1, HEP, and TIR. Statistical analysis: analysis between groups was performed by Pearson's Chi Square Test; Cohen's K Test and ROC analysis were used to compare estimated and effective values between the groups; the Kaplan Meier survival analysis was used to assess differences between the groups.

RESULTS

Of the 58 patients with a known primary, immunohistochemical analysis of marker expression confirmed the histotype in 51 cases (88%). There was no significant difference in survival between patients with synchronous versus metachronous metastatic lesions (Figure 1) or between patients with a known primary versus an unknown primary (Figure 2). Independently of the knowledge of primary at the time of diagnosis of metastatic bone disease, the lack of expression of organ-specific phenotype as detected by immunohistochemistry was associated with a worse prognosis (Figure 3).

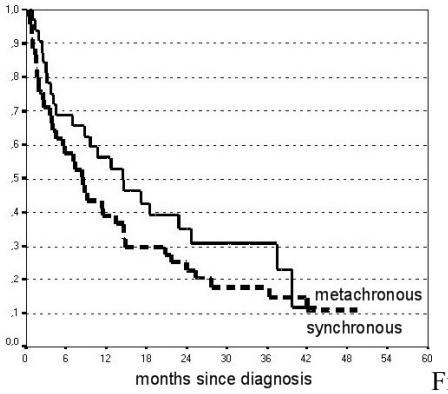

Figure 1

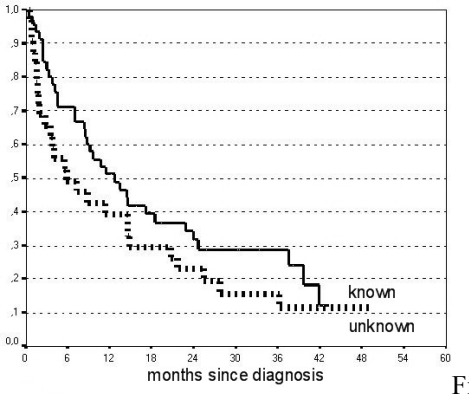

Figure 2

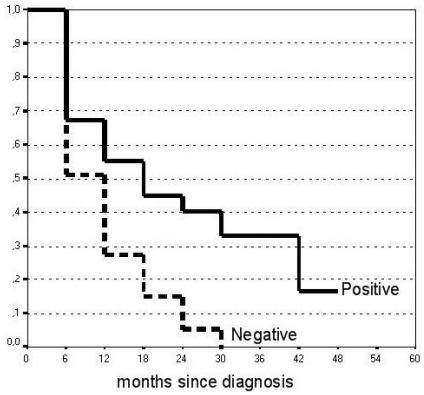

Figure 3

DISCUSSION

The lack of expression of differentiative markers may reflect cancer progression. Evaluating the expression of those markers by immunohistochemistry is prognostically relevant for patients with bone metastases of carcinomas.

METHOTREXATE LOADED BONE CEMENT FOR THE TREATMENT OF BONE METASTASES: IN VITRO BIOLOGICAL AND MECHANICAL PROPERTIES

*Maccauro G, **Spadoni A, *Muratori F, **Casarci M, *Sgambato A, *Piconi C, ***Caminiti R, ***Alesci M, ***Rosa MA
Department of Orthopaedic Sciences, Catholic University, Rome, Italy

giuliomac@tiscali.it

INTRODUCTION

PMMA is currently used as grouting agent of arthroprostheses and for filling of bone cavities after bone curettage. It is moreover used as a carrier of antibiotics in the local treatment of bone infections and it has been proposed as a carrier of antiblastic drugs in the local treatment of bone metastases. The aim of this study is to analyse the biological properties and compressive strength of PMMA-Methotrexate mixture to be used for the local treatment of bone metastases.

METHODS

Cylinders of PMMA containing Methotrexate in different concentrations were manufactured according to ASTM F-451. Cylinders of PMMA were used as control. The porosity of the cylinders was characterised by SEM. Drug elution rate in saline solution was measured by HPLC. The biological activity of Methotrexate was analysed on human breast cancer cells using MTT test at different time (from 5 minutes to 30 days). Compressive tests was performed in conformity to ASTM F-451 on PMMA- Methotrexate samples and control as-made and after 30 days of aging in saline .

RESULTS

SEM analysis showed the presence of granules of Methotrexate on the surface of as-made cylinders that can be readily released from PMMA cylinders. The release occurred in large amount within 24 hours after immersion. We observed that a relative release rate is more sustained in samples containing the drug in lower concentration. Also the biological activity was time dependent: cell death decreased progressively from 60% at 24 hours to 10% at 30 days.
Compressive tests showed no statistical differences between PMMA cylinders containing Methotrexate and controls before and after aging in saline.

DISCUSSION AND CONCLUSIONS

The results show that PMMA-Methotrexate may be considered an interesting option in the treatment of bone metastases because cement allows mechanical resistance after bone curettage or resection and Methotrexate improves locally anticancer activity.

AFFILIATED ISTITUTIONS:
** ENEA Casaccia - Rome - Italy
*** Surgical Specialties Department-Orthopaedic Section-University of Messina - Italy

FGF-2 INHIBITION IN A BONE METASTATIC RENAL CARCINOMA CELL LINE BY ANTISENSE OLIGONUCLEOTIDE AND MONOCLONAL ANTIBODY STRATEGIES

*Perut F, *Cenni E, *Granchi D, **Brandi ML, *Giunti A, *Baldini N
Laboratorio di Fisiopatologia Ortopedica, Istituti Ortopedici Rizzoli, Bologna, Italy
francesca.perut@ior.it

INTRODUCTION

Renal cell carcinoma (RCC) results in a high proportion of patients with metastasis at the time of diagnosis. Renal cell carcinoma is well vascularized, for both the primary tumor and metastasis. Bone metastasis from RCC are highly vascularized and predominantly osteolytic. Fibroblast growth factor-2 (FGF-2) has been implicated in angiogenesis; FGF-2 plasma levels were correlated with the presence of metastasis in patients with RCC. Therefore, the inhibition of FGF-2 in renal carcinoma could decrease angiogenesis and tumor spread.

METHODS

Treatment of the cells with antisense oligonucleotide

The effect of blocking FGF-2 expression by an antisense phosphorothioate oligonucleotide (ODN) was evaluated on a cell line isolated from a bone metastasis of renal cell carcinoma (CRBM) and on the established lines Caki-1 and ACHN. Cell lines were transfected with ODN (400 nM), vehiculated by lipofectamine. After 6 hours the efficiency of the ODN uptake was evaluated by confocal microscopy, then the medium was refreshed with 0.1% FCS medium. After 48 hours, a new treatment with ODN (200 nM) was performed. FGF-2 mRNA and protein (intracellular and released) expression were evaluated after 72 hours since the first transfection.

Treatment of the cells with anti-FGF-2 mAb

The cell lines were incubated with a mouse neutralizing anti-human FGF-2 monoclonal antibody (anti-FGF-2-mAb) at the concentration of 1 μg/ml. As controls, FGF-2 (5 ng/ml) or anti-FGF-2-mAb + FGF-2 were added to the cultures. FGF-2 mRNA, protein expression in the cell lysates and in the supernatants were determined after 24 hours.

Effect of FGF-2 inhibition on endothelial cells proliferation

To measure the effect of ODN or anti-FGF-2-mAb on endothelial cell proliferation, co-cultures of endothelial cells and ODN- or mAb-treated Caki-1, CRBM, and ACHN were performed.

Statistical analysis

The effect of FGF-2 inhibition on renal carcinoma cells was evaluated by the Wilcoxon test. The effect on the endothelial cells proliferation was evaluated by the Student's t test for paired samples.

RESULTS

Neither ODN nor anti-FGF-2-mAb significantly decreased specific mRNA or intracellular protein expression. mAb treatment induced a 32.7±7.5% reduction of FGF-2 released by ACHN, a 31.0±30.3% reduction by Caki-1 and a 69.7±18.1% reduction by CRBM (figure 1).

Figure 1. Mean and standard error of FGF-2 in the supernatants. The results are reported as the % of the untreated cells.

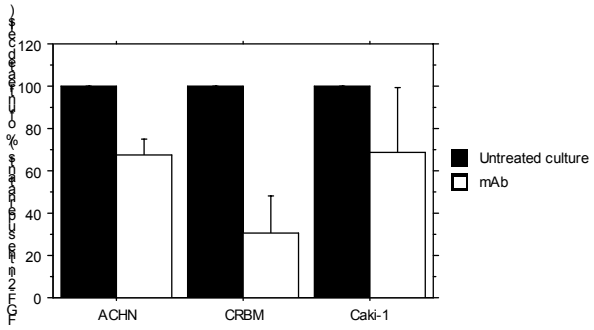

ODN treatment of renal carcinoma cells did not inhibit endothelial cell proliferation. Instead, anti-FGF-2-mAb significantly decreased endothelial cells proliferation induced by ACHN (p=0.0317) and by CRBM (p=0.0042) (figure 2). The inhibition of endothelial cells growth was reverted by the addition of rhFGF-2. mAb treatment of Caki-1 did not induce any significant decrease of endothelial cells proliferation. However, the reduction induced by mAb was significant compared to the cells treated with rhFGF-2 and mAb (p=0.0231).

Figure 2. Mean and standard error of the proliferation of endothelial cells co-cultured with ACHN and with CRBM. The results are reported as the % of the untreated cells.

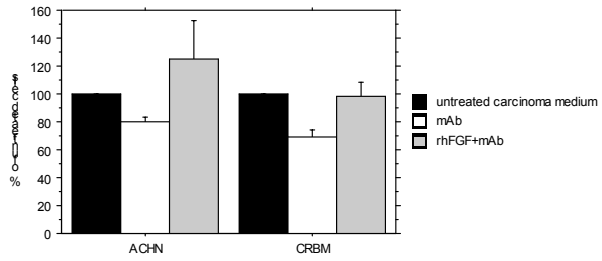

CONCLUSIONS

The results confirmed the proangiogenic role of FGF-2 in RCC. FGF-2 inhibition with mAb determined better results than ODN strategy, above all in the reduction of endothelial cells proliferation. The cell line derived by the bone metastasis was the most sensitive to the mAb treatment.

ACKNOWLEDGEMENTS

This research was supported by a grant from A.I.R.C.

**Dipartimento di Medicina Interna, Università di Firenze, Firenze, Italy

EXTRACELLULAR MATRIX REMODELLING IN DUPUYTREN'S DISEASE: HISTOPATHOLOGICAL ASPECTS

Tresoldi I, *Modesti A, *Trono P, Tarantino U
Università degli Studi di Roma Tor Vergata, Azienda Ospedaliera Universitaria Policlinico Tor Vergata, Divisione di Ortopedia e Traumatologia, Rome, Italy

umberto.tarantino@uniroma2.it

INTRODUCTION

Dupuytren's disease is a fibroproliferative disorder that is responsible for progressive and permanent contracture of the palmar fascia with subsequent irreducible flexion deformities of the fingers and loss of hand function. Although the etiology and pathogenesis of the disease is unclear, it has been established that palmer fascia in Dupuytren's contracture is characterized by an abnormal fibroblast proliferation, the appearance of myofibroblasts and by a progressive deposition and remodelling of the extracellular matrix. However little is known about the main events implicated in the palmar fascia extracellular matrix remodelling. Our hypothesis is that type V collagen produced by myofibroblasts leads to type I collagen alteration during extracellular matrix remodelling in Dupuytren's disease.

METHODS

Palmar fascia samples were obtained from 14 patients undergoing surgical fasciectomy for Dupuytren's disease. Patients were between 49 and 78 years old. Control tissue samples included palmar fascia from 30 patients undergoing hand surgery for carpal tunnel syndrome.
Our study protocol was approved by the Ethics Committee for Research involving human subjects of University of Tor Vergata.
Tissue samples were fixed in 2.5% glutaraldheyde in phosphate buffered saline, post-fixed in 1.33% osmium tetroxide, embedded in Epon 812 and processed for transmission electron microscopy. For light microscopy 1-2 μm semithin sections were stained with tolouidine blue. For electron microscopy 900 Å ultrathin sections were stained with uranyl acetate-lead hydroxide. Two independent observers evaluated the different samples.

RESULTS

The histological features of palmar fascia in Dupuytren's disease patients showed areas of cellular proliferation or transitional and involutional areas, the latter being characterized by an expansion of extracellular matrix with cellular elements reduction.
Ultrastructural analysis of the transitional areas showed the presence of a large number of proliferating myofibroblasts with increased synthesis activity euchromatic nuclei with peripheral heterochromatin, large nucleoli, markedly dilated RER cisternae containing electrondense materials, bundles of peripheral thin filaments and few mitosis).
A marked extracellular matrix remodelling was observed in all areas of palmar aponeurosis analyzed. Banded type I collagen fibrils showed diameter alterations in the palmar fascia from Dupuytren's disease patients compared to carpal tunnel's disease patients. Such fibrils were strictly closed to type V collagen fibrils as demonstrated by immunoelectron microscopy. Palmar fascia in Dupuytren's contracture, showed areas with interrupted banded collagen fibrils closely to stromal cells, thus indicating extracellular matrix degradation. In few areas fusiform long spacing collagen fibers (Luse bodies) with a highly periodicity of 100-150 nm, along with a deposition of glycosaminoglycans, were observed. To note that diseased tissue displayed a large number of inflammatory cells, mainly mast cells that were often degranulated.

DISCUSSION

Our findings demonstrated that in palmar fascia from Dupuytren's disease patients occurred an increased deposition of extracellular matrix components, mainly Type I and Type V collagens along with glycosaminoglycans. This extracellular matrix remodelling might be sustained by the increase of activated myofibroblasts that through an enhanced synthesis of type V collagen might contribute to the disarrangement of the Type I collagen organization.
The histological features of palmar aponeurosis in Dupuytren's contracture showed pictures common with chronic inflammatory or tissue repair processes and with fibroproliferative disorders, both characterized by an extracellular matrix remodelling similar to that observed in the desmoplasia occurring in breast carcinoma. Such extracellular matrix remodelling is characterized by an increase of Type V collagen sustained by the production of platelet derived growth factor-b. Furthermore, the involvement of mast cells might support the modification of the microenvironment distinguishing the inflammatory process.

*Università degli Studi di Roma Tor Vergata, Cattedra di Patologia Generale,Rome, Italy

EFFECTS OF HYPERTHERMIA ON HUMAN OSTEOSARCOMA CELLS

*,**Trieb K, *Blahovec H, *Kubista B
*Department of Orthopaedics, University of Vienna, Austria

k.trieb.co@klinikumffo.de

INTRODUCTION

Temperature is a physical factor with strong influence on growth processes in general, only second to oxygen supply. Hyperthermia is used as adjuvant therapy in treatment of cancer patients. The cellular response to stress is represented at the molecular level by the induced synthesis of heat shock proteins (HSPs). HSP70 is the central component of a multi-chaperone machine involved in many essential cellular processes and in the response of cells to proteotoxic stresses (e.g.) heat shock. Furthermore, HSP70 is a potent anti-apoptotic protein that can enhance transformation and the tumorigenic potential of cells. In this study, the direct effect of temperature to the osteosarcoma derived cell lines HOS85, MG-63 and SaOS-2 is investigated.

METHODS

Human osteosarcoma cells HOS 85 (DRL 1543, ATCC, Rockville, MD, USA), SaoS2 (HTB85, ATCC) and MG-63 (CRL 1427, ATCC) were grown in RPMI 1640 containing 10% fetal calf serum and Penicillin/Streptomycin in 75 cm^2 tissue culture flasks (Falcon, Franklin Lakes, NY) at 37°C in a 5% CO_2 humidified atmosphere. Once grown to confluency, cells were split from the bottom of the flask through incubation with 1x Trypsin and used for further experiments.

Heat shock was applied by incubation of one group of cells for 1 hour at 42°C, whereas a second group of cells was incubated at 37°C, serving as a control.

10^4 cells were seeded in 96-multiwell microplates (Falcon) and grown to a confluency of 80% to be subjected to hyperthermia treatment. After the heat shock the medium was removed in the hyperthermia group as well as in the control group and the cells were washed with phosphate buffered saline. Then the medium was decanted, and after 3 cycles of subsequent freeze-thaw, 50 µl 0.5% Triton X-100 (MERCK, Darmstadt, Germany) in distilled water was added. Thereafter, the cells were incubated for 1-30 min with 50 µl 20 mmol/l *p*-nitrophenyl-phosphate in 100 mmol/l $MgCl_2$ at pH 9.5) at 24°C. The reaction was stopped with 50 µl 0.1 mol/l EDTA in 1 mol/l NaOH. The absorption was measured at 405/490 nm in a microplate reader.

10^4 cells were seeded in black 96-multiwell microplates and grown to a confluency of 80% to be subjected to hyperthermia treatment. Thereafter cells were washed twice with PBS and incubated for at least 16 h in culture medium containing 1 µCi of tritium labelled thymidine per well. The plates were then frozen at –80°C and thawn three times. Liquid scintillator was added and scintillation was measured in a betaplate reader.

RESULTS

Exposure to 42°C for 1 hour inhibits proliferation in all three cell lines.

A sublethal heat shock at 42°C inhibits proliferation, asessed by ^{3}H-thymidine-uptake, most notably in MG-63 to less than 60% compared to cells grown continuously at 37°C. Inhibition of proliferation to 63% occurs in HOS85 cells, while in SaOS-2 cells proliferation only falls to 92% of the control at physiological temperature. Furthermore a sublethal heat shock decreases alkaline phosphatase activity, the very marker for osteoblast like cells, in all of the three cell lines.

When compared to cells grown continuously at 37°C, in cells, which have undergone hyperthermia treatment, a significant decrease of alkaline phosphatase activity to less than 15% and one third in HOS85 and SaOS-2, respectively, was found. In MG-63 cells alkaline phosphatase is decreased to about 75%.

The response of the expression of the anti-apoptotic heat shock protein HSP70 to heat shock was investigated by western blot analysis. HSP70 was expressed constitutively and was found to be up-regulated in cells exposed to 42°C for 1 hour. During recovery of heat shock the expression of HSP70 was decreased to about 50% after 6 hours. However, after 36 hours the level of expression had been increased to 154% compared to cells lacking history of hyperthermia.

DISCUSSION

Hyperthermia reduces the rate of proliferation. In addition the expression of alkaline phosphatase, a key protein in osteoblast-like cells, is also decreased, but increases the level of HSP70 expression. The results of this study indicates that heat shock has an inhibitory effect on osteosarcoma cells. These data suggest that hyperthermia has an anti-tumor effect and might be a possible adjuvant treatment for patients with osteosarcoma.

AFFILIATIONS

**Department of Orthopedics, Klinikum Frankfurt/Oder, Germany

RADIOHYPERTHERMOCHEMOTHERAPY ON MALIGNANT FIBROUS HISTIOCYTOMA IN VITRO

*Otsuka Y , *Otsuka T , *Matsushita T , *Yamada S, *Tsuji H, *Fukuoka M, *Kobayashi M
*Department of Musculoskeletal Medicine, Nagoya City University, Graguate School of Medical Science, Japan

yoshihisa4913@yahoo.co.jp

INTRODUCTION

Soft tissue sarcoma is the malignant tumor, which occurs everywhere of mesenchymal tissue.
Most of them are resistant to radiotherapy and chemotherapy and recurrence rate are high.
However, we may expect good result by using hyperthermia treatment together with these therapies.
We made malignant fibrous histiocytoma (MFH) invaded rat model. And experienced about the effectiveness of radiation, combined with hyperthermo-chemotherapy, by measuring tumor growth speed.

METHODS

"Rat4-HAQO induced MFH", was transplanted in left femoral region subcutaneous layer of a F344 rat of five or six week of age male. A volume of tumor cell was measured to evaluate of each therapy.
We measured tumor major and minor diameters. Then, measured the relative tumor volume sequentially. We made a tumor growth curve and count the days to need though a tumor volume doubled as "tumor growth time". Rats were divided groups and treated about chemotherapy, radiotherapy, hyperthermia, or this combination therapy.
For hyperthermia, we used "Thermothoron RF I.V." That made 8 mega Hertz RF waves same as "Thermothoron RF8" that was really used for thermotherapy in clinic.To radiotherapy group, totally, 500R was irradiated. To chemotherapy group, Pirarubicine 10mg/kg and/or Cisplatin 3mg/kg, were injected intraperitoneally.

RESULTS

The tumor growth effect was restrained in hyperthermia treatment, but the contraction of tumor was not present. Both Pirarubicine and Cisplatin were effective. And the effectiveness was increased by conbination with hyperthermia. Especially, the antitumor effect was strong in Cisplatin.
Contraction of a tumor was present in hyperthermia and combination with radiotherapy.
It revealed augmentation of antitumor effect by these combinations, too.
Stronger antitumor effect was present in a group of “radio-hyperthermo-chemotherapy”.
A tumor showed contraction and reduced to 2.7% after the day 24th, and the size growing was not shown.

DISCUSSION

Hyperthermia can expect effectiveness to soft tissue tumor alone, and that cellular breeding is inhibited at 43 degrees Celsius is proved by an experiment of in vitro. However, clinically, hyperthermia monotherapy is thought to be difficult to reach to complete cure.A problem of heating technology is difficult. Therefore combined therapy with radiotherapy and chemotherapy is taken.
From our results, it became clear that “radio-hyperthermo-chemotherapy” gave high effectiveness to MFH. We have started to develop this method into clinic and apply these methods. This enables a minimal invasive operation. And it seems that it is connected for degradation of recurrence rate and improvement of prognosis.

FGF-2 EFFECTS ON THE OSTEOGENIC COMMITMENT OF BONE MARROW STROMAL CELLS

*Cenni E, *Perut F, **Cenacchi A, **Fornasari PM, ***Dallari D, *,***Giunti A, ***Baldini N
Laboratorio di Fisiopatologia Ortopedica, Istituti Ortopedici Rizzoli, Bologna, Italy
elisabetta.cenni@ior.it

INTRODUCTION

Recombinant FGF-2 could be added to bone marrow stromal cells (BMSC) cultures in order to increase proliferation and osteogenic committment. However, FGF-2 is synthesized by osteoblasts too. The aim of this research is to evaluate if the addition of autologous growth factors contained in platelet α-granules affects the FGF-2 production by BMSC *in vitro*.

MATERIALS AND METHODS

The study protocol was approved by the Institutional Ethical Committee on human research and the patients signed an informed consent. Bone marrow from the iliac crest of 10 patients undergoing high tibial osteotomy for genu varum was anticoagulated with heparin. Platelet rich plasma (PRP) was activated by addition of autologous thrombin and calcium. On surgery, BMSC were added to activated PRP in order to improve bone repair.

For the *in vitro* study, BMSC added with activated PRP (PRP +) and BMSC alone (PRP -) were cultured for a comparative analysis on osteogenic differentiation. The mixture of BMSC with activated PRP was seeded directly on the culture plate. BMSC without additives were purified by Ficoll in order to isolate the mononuclear cells. BMSC were cultured in α-MEM, supplemented with 10% FCS, 100 μg/ml ascorbic acid and 10 nM dexamethasone (Dex).

After 8, 11, 15 and 25 days, FGF-2 was determined on the superrnatants by ELISA. At 15 days the mRNA of core binding trascription factor (Cbfa1/ Runx2), osterix (Osx), alkaline phosphatase (ALP) and osteocalcin (OC) were tested by RT-PCR. BMSC proliferation and ALP activity on the cell lysates were evaluated at 25 days. Mineral nodule formation, induced by α-MEM supplemented with 10 mM β-glycerophosphate, was evaluated at 38 days.

RESULTS

FGF-2 levels in the supernatants of PRP + samples were higher than PRP - after 8, 11, 15 and 25 days (fig. 1). Besides, at 15 days Runx2, Osx and ALP mRNA expressions were higher in PRP+ cultures, even though non significantly (fig. 2). After 25 days, the growth of BMSC treated with activated PRP was lower than that of untreated cells, possibly reflecting a higher degree of differentiation. Intracellular ALP activity was higher in PRP-treated BMSC than untreated BMSC (Table 1).

Table 1. Mean ± SE of proliferation and ALP activity of BMSC after 25 days of culture.

Treatment	Growth Cell No. (x 10^3)	Intracellular ALP activity /cell
PRP -	62.0 ± 21.7	0.22 ± 0.10
PRP +	16.8 ± 3.6	1.66 ± 0.51

After 38 days an evident mineralization was shown by PRP-treated BMSC compared to untreated BMSC.

Figure 1. Mean ± SE of FGF-2 concentration in the BMSC cultures.

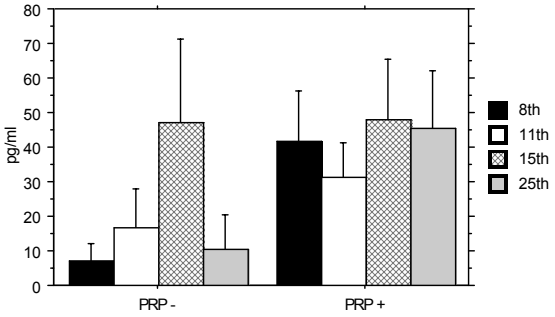

Figure 2. Mean ± SE of differentiation gene expression in BMSC after 15 days of culture.

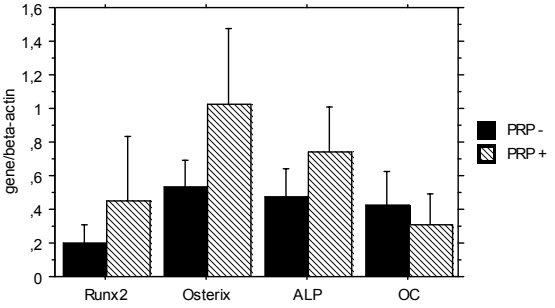

DISCUSSION AND CONCLUSIONS

It was demonstrated by other authors[1] that FGF/dex expansion of BMSC increased mRNA levels of BMP-2, bone sialo protein II and osteopontin, while FGF had little effect on proliferation[2]. We have observed that the incubation with PRP increased FGF-2 production by BMSC themselves. These results could explain Runx2 and Osx increase after 15 days in PRP+ samples, as these genes are activated by FGF-2. In conclusion, the treatment with PRP induced BMSC to produce FGF-2, so favouring osteogenic committment.

[1] Frank O et al, J Cell Biochem 2002;85:737-46.
[2] Satomura K et al, J Cell Physiol 1998;177:426-38.

ACKNOWLEDGEMENT

This research was supported by a FIRB grant (project No. RBAU01N79B).

**Musculoskeletal Tissue Bank, Istituti Ortopedici Rizzoli, Bologna, Italy
***Department of Orthopedic Surgery, University of Bologna, Istituti Ortopedici Rizzoli, Bologna, Italy

BONE HEALING ENHANCEMENT BY LYOPHILIZED BONE GRAFTS SUPPLEMENTED WITH PLATELET GEL OR PLATELET GEL–BONE MARROW STROMAL CELLS IN PATIENTS WITH HIGH TIBIAL OSTEOTOMY: A RANDOMIZED STUDY

*Stagni C, *Dallari D, *Savarino L, *Tarabusi C, *Del Piccolo N, **Cenacchi A, **Dal Vento A , **Fornasari PM, *Baldini N, *,***Giunti A

*Laboratorio di Fisiopatologia Ortopedica & 7^ Divisione, Istituti Ortopedici Rizzoli, Bologna, Italy

dante.dallari@ior.it

INTRODUCTION

Orthopedic practice may be adversely affected by an inadequate repair reaction, which might compromise the success of surgery. In recent years new approaches have been sought to promote the formation of bone tissue. Bone remodeling is controlled by different substances, including growth factors such as FGFs, PDGFs, TGFs, IGFs, and BMPs, contained in the alpha-granules of platelets. Activated autologous platelets have therefore been used to accelerate repair process. Moreover, the use of autologous bone marrow stromal cells (BMSCs) provides an increased population of cells stimulated by PDGF and TGFbeta released from platelets. An adequate number and activity of pre-osteoblasts, especially in large defects where these cells are lacking in the defect core, is necessary to growth factors in order to develop their stimulatory action. In orthopedic surgery, the growth factors released by platelets should favour the proliferation of bone marrow mesenchimal cells and their differentiation into osteoblasts. The treatment of bone grafts with activated autologous platelets and BMSCs should accelerate the repair process. The aim of this study was to evaluate the effect of lyophilized bone chips with/without autologous platelet gel and BMSCs on the bone repair process after tibial osteotomy for genu varum.

METHODS

Thirty patients, divided into 3 groups by the generation of random sampling numbers, were treated by valgus osteotomy for genu varum with a minimum correction of 8 mm and fixation using a titanium plate. The groups were thus divided: Group 1: lyophilized bone chips; Group 2: lyophilized bone chips + gel, obtained from venous blood (450 g) the day before surgery and activated with calcium and thrombin; Group 3: lyophilized bone chips + gel + autologous BMSCs (Buffy coat).

Forty-five days after surgery a biopsy in the site of graft insertion was performed, in order to define the presence of osteogenesis, angiogenesis, and presence of fibrous tissue. Other X-rays were carried out at 12, 24 and 48 weeks after surgery.

RESULTS

The results confirmed that the use of platelet gel and autologous BMSCs as adjuvants for the lyophilized bone aids bone repair and graft integration. Activated gel significantly enhanced stromal cell differentiation toward an osteoblastic phenotype. Morphological and morphometric tests showed that at six weeks the newly formed bone of group 3 had better mechanical properties. Radiographic evaluation (Fig.1) suggested a faster integration of bone graft in Group 2 and Group 3 with differences statistically significant at 6 and 12 weeks after surgery.

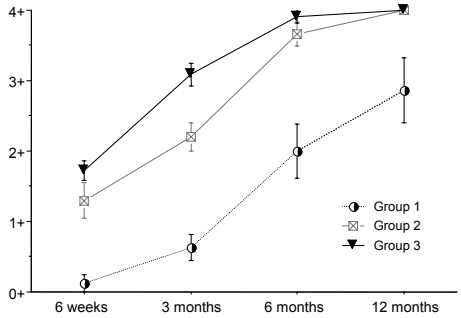

Figure 1.
Osteointegration rate evaluated on anteroposterior X-rays

DISCUSSION

This study shows that concentrated stromal cells and platelet gel are efficacious as adjuvants in bone graft integration. Bone chips alone undergo a resorption process and a fibrous and histiocytic/giant-cell reaction is always present. On the contrary, the lyophilized bone added with platelet gel and BMCs seems to enhance the bone formation process.

Stromal cells combined with gel produce faster osteointegration and have greater angiogenetic activity compared to gel alone, as shown by new vessel formation and deposition of new bone.

Although these phenomena may not determine substantial differences in minor defects, they might be crucial in major ones.

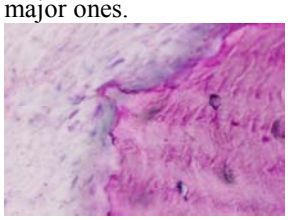

Figure 2.
Fibrous tissue surrounding lyophilized bone chips (H.E. stain, x40)

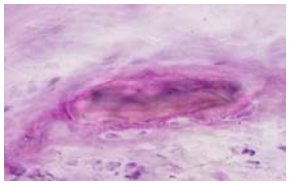

Figure 3.
New bone formation in contact with lyophilized bone with platelet gel. (Paragon stain, x60)

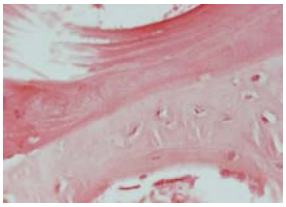

Figure 4.
New bone formation in contact with lyophilized bone with platelet gel and BMSCs. (Paragon stain, x20

** Servizio di Immunoematologia e Medicina Trasfusionale, Istituti Ortopedici Rizzoli, Bologna, Italy
*** University of Bologna, Bologna, Italy

PLATELET RICH PLASMA IMPROVES BONE FORMATION IN A CRITICAL SIZE BONE DEFECT ON A NEW HIGH SURFACE SCAFFOLD CALLED CALCIUM DEFICIENT HYDROXYPATITE

*Kasten P, *Szalay K, *Vogel J, *Geiger F, **Luginbühl R, *Ewerbeck V, *Richter W
*Division of Experimental Orthopaedics, Orthopaedic Clinic, University of Heidelberg, Heidelberg, Germany

philip.kasten@ok.uni-heidelberg.de

INTRODUCTION

Today, autogenous bone grafting is considered as the golden standard for filling bone defects, despite significant problems arising from high complication rate, i.e. donor-site morbidity, and limited amount of donor bone. The concept of tissue engineering is based on three pillars including scaffolds, cells and growth factors. There is a new high surface mineral scaffold called calcium deficient hydroxyapatite (CDHA) that proved to be superior to known low surface scaffolds regarding bone formation. Well established potent cells are mesenchymal stem cells (MSC) that can be obtained autogenously from bone marrow and can be rapidly expanded. Platelet rich plasma (PRP) contains high concentrations of growth factors, which play an important role in the early phase of bone healing.

The aim of this study was to assess the effect of PRP on new bone formation in a critical sized diaphyseal bone defect with combination of MSC and an absorbable CDHA scaffold in a rabbit model.

METHODS

Animals were treated in compliance with the guiding principles in the Care and Use of Animals. The Committee on Animal Experimentation of Baden-Wuerttemberg approved the experiment.

Critical sized bone defects (1.5 cm) were created in the radius of New Zealand White rabbits (n=6/group). The defect was filled with CDHA ceramic cylinders alone, MSC/CDHA composites, PRP/CDHA composites or PRP/MSC/CDHA composites. Empty defects and defects filled with autogenous spongiosa served as controls. The observation period was 16 weeks. Bone marrow was aspirated of the tibia, MSC were isolated and expanded to cell numbers of $5x10^6$. PRP was produced allogeneously by centrifugation of whole blood from 5 rabbits.

X-rays were taken every 4 weeks to determine the actual position of the ceramic implant and time course of bone formation. Mechanical stiffness was evaluated by a four-point non-destructive bending test. µ-CT scans were used to assess the amount of newly formed bone and the resorption of the implanted ceramic, and verified by analysis of histological slides. The effects of the independent variables, i.e., “stiffness”, “bone formation” and the “resorption of CDHA” were examined by multifactorial analysis of variance (ANOVA). Differences between the subgroups of the independent variables were checked in post-hoc tests. The alpha error was adjusted; $p < 0.05$ was considered significant.

RESULTS

We did not observe displacement of the implant. µ-CT scan showed significantly higher amounts of new bone formation ($p<0.001$) and ceramic resorption ($p<0.0005$) in the MSC/CDHA, PRP/CDHA and PRP/MSC/CDHA groups compared to the empty CDHA, but there were no differences among these groups. Biomechanical testing showed a higher flexural rigidity of the groups with MSC and PRP ($p<0.05$) compared to the empty CDHA group. Histologic analysis supported our findings.

DISCUSSION

Bone healing is significantly better in constructs using either mesenchymal stem cells or PRP together with the new high surface mineral CDHA in critical size bone defects. However, an additive effect was not observed using combination of the two components.

AFFILIATED INSTITUTIONS FOR CO-AUTHORS

*Division of Experimental Orthopaedics, Orthopaedic Clinic, University of Heidelberg, Heidelberg, Germany
**Skeletal Substitutes, Dr. hc. Robert Mathys Foundation, Bettlach, Switzerland

TREATMENT OF LARGE BONE DEFECTS WITH AUTOLOGOUS CULTURED BONE MARROW STROMAL CELL LOADED ON BIOCERAMIC SCAFFOLD

*Marcacci M, *Kon E, *Neri MP, *Iacono F, *Zaffagnini S, *Filardo G, *Delcogliano M, **Cancedda R

*Istituti Ortopedici Rizzoli, Bologna, Italy

INTRODUCTION

Large bone defect repair has always been a problem of difficult solution. We investigated the used of a cell-based therapeutic approach to treat 4 patients with large segmental bone defects. The efficacy of this innovative technique was previously demonstrated in an experimental large-size animal model.

METHODS

The patients were 41, 31, 22 and 16 years old and had large tibial, ulnar or humeral diaphiseal gaps that ranged in size from 3,0 to 28,3 cm3. Marrow samples were harvested from the iliac crest and osteogenic progenitors isolated and expanded “ex vivo”. The expanded cells were then loaded on highly porous bioceramic scaffolds based on hydroxyapatite (Fin-Ceramica, Faenza, Italy) whose size and shape reflected each single bony defect. The cell/bioceramic composites were implanted at the lesion sites. External fixation was used to stabilize the grafts.

RESULTS AND DISCUSSION

At present all patients have been followed up for 4 to 6 years. Initial integration at the bone/implant interface was evident already a month after implantation. Three patients achieved full functional recovery at 6 months after surgery, one patient at 12 months after surgery. New bone formation within the implants and osteointegration progressed steadily in the follow up period as assessed by x-ray analysis and CT scanning.

CONCLUSIONS

The present report shows that the use of osteoprogenitor cells loaded on porous bioceramic scaffolds allows for large segmental bone reconstruction in humans.
Work is in progress to achieve better osteointegration and faster bone formation by using a new generation of biodegradable and biomimetic hydroxiapatite scaffolds.

AFFILIATED INSTITUTIONS FOR CO-AUTORS:
**Laboratorio di Differenziamento Cellulare, Centro di Biotecnologie Avanzate, Istituto Nazionale per la Ricerca sul Cancro, Genova.

IMPACT OF A RESORBABLE CaP COATING IN A GAP MODEL IN GÖTTINGEN MINIPIG

*Schwarz M, *Feuerstack M, **Herbig J, ***Brade J, ****Becker K, **Scheller G
* Laboratory for Biomechanics and Experimental Orthopaedics,
e-mail: markus.schwarz@ortho.ma.uni-heidelberg.de

INTRODUCTION: Gap healing in cementless joint replacement is enhanced by the use of hydroxyapatite (HA) coatings. We were able to show, that a resorbable CaP layer, deposited on a porous TPS coating, increased the percentage of bone-implant contact on press- fit implanted titanium cylindrical test-bodies in the transcortical Göttingen Minipig (GM) model. The **aim** of the present study was: 1st: to investigate whether the resorbable CaP layer has a gap healing capacity too 2nd: to validate the transcortical (GM) gap model.

MATERIALS AND METHODS: The main criteria were the tissue-implant contact (mineralized and osteoid) and the tissue density measured in the gap after 4 and 8 weeks of implantation. The study was authorized by the local committee (Ref.No.:35-9185.81/86/00). 40 dumbbell shaped 30mm long titanium implants were implanted. The outer diameter was 8mm; in the middle region a gap of ~1.05mm x 15mm was processed around the implant. The gap areas of the implants were coated with TPS (~250µm), with a porosity of ~28% and an average pore size of ~41µm (DOT, Rostock, D). 20 implants received an additional resorbable CaP layer, which was ~20µm thick and consisted of mainly brushite ($CaHPO_4.2H_2O$) and a phase of HA. The layer was electro-chemically deposited on the TPS surface (BONIT®, DOT, Rostock, D). The test-bodies were implanted transcortically in both femora of 10 adult male GM. 20 implants were placed proximally in the intertrochanteric area and 20 were placed distally in the intercondylar region under general anesthesia. 5 animals were sacrificed after 4 weeks, the other 5 animals after 8 weeks. After preparation for undecalcified sections the specimens were cut along implant axis. The middle section of the serial cuts were dyed according to Masson-Goldner staining. The percentage of tissue-implant contact was measured with a calibrated image assessment software, using a ZEISS Axioscop, with a Sony CCD camera (AVT Horn, Aalen, D). Tissue density within the gap was measured with a Leica DMRE system (Leica Q Win software, Leica Microsystems Digital Imaging, Cambridge, UK) and expressed in percentage.

Statistics: The statistical computation has been performed with the SAS software (8.2). Differences were analyzed using a repeated measurement anova model (GLM procedure). The variables were: implant, animal, localization, and the interactions: implant * time and implant * localization. A subsequent multiple testing (LS means) was completed (level of significance α=0.05).

RESULTS: All implants were assessed, however 6 proximal gaps had to be excluded because the gap formation was uncompleted as the implant was not completely covered by bone. Remnants of the resorbable CaP coating were found after 4 and 8 weeks. After 4 and 8 weeks, bone-implant contact in the gap for the test group with the CaP layer was 12.49% ±7.67 and 32.25% ±12.58 respectively; for the control group (only TPS) it was 0.01% ±0.03 and 0.7% ±0.73 respectively. Bone density in the gap was 13.63% ±5.5 (CaP) and 12.93% ±3.57 (co) after 4 weeks and 10.79% ±3.76 (CaP) and 9.55% ±5.24 (co) after 8 weeks. An increase of the bone-implant contact was found between 4 and 8 weeks for the resorbable CaP-coating group ($p<0.0001$), not for the TPS-coating group ($p=0.9318$). The additional CaP layer led to significantly higher values of bone-implant contact in comparison to the control surface at 4 ($p=0.0016$) and 8 ($p<0.0001$) weeks. For osteoid tissue-implant contact, the difference between the groups according to implant surface was not significant ($p=0.653$). For bone density in the gap, no difference was found between the two assessed surfaces ($p=0.3708$). For formation of osteoid tissue in the gap, no difference was found between the two assessed surfaces ($p=0.7874$). (Data not shown for osteoid implant contact and tissue density). No significance was found for localization and the interaction between localization* implant, regarding the criteria tissue contact and density. In one case the animal showed an influence over the results (Table 1).

variable	bone impl. cont.	osteoid impl.cont.	bone density	osteoid density
animal	0.7073	0.0158	0.0781	0.4638
loc	0.4633	0.0964	0.3521	0.3410
impl*loc	0.6794	0.8395	0.6309	0.8479

Table1: p-values for the variables, which assess the transcortical GM gap model.

DISCUSSION: In the presented gap model, the resorbable CaP layer showed a gap healing capacity after 4 and 8 weeks. Dissolution of the CaP layer at the implant surface might lead to high local concentrations of Ca and P ions, which may effect a chemotaxis [Overgaard S. 2000] on osteoblasts with subsequent increased bone formation at the surface. Nevertheless, the CaP coating did not affect bone density in the gap. These first results indicate that a resorbable bioactive layer may accelerate the gap healing process. The transcortical model in the GM proved to be relevant and robust. The implantation of several test-bodies in one animal makes the model more economical, but the biological variability may not be equalized as less animals are used. Therefore herds of GM should be assembled homogenously.

ACKNOWLEDGMENTS This study was supported by the Faculty of Clinical Medicine Mannheim, University of Heidelberg (Juniorf. #932072) and Fa.DOT, Rostock, D.

AFFILIATED INSTITUTIONS FOR CO-AUTHORS
Department of Orthopedic Surgery, University Hospital Mannheim, Germany, * Department of Medical Statistics, Faculty of Clinical Medicine Mannheim, **** Interfakultäre Biomedizinische Forschungseinrichtung (IBF) University of Heidelberg, Germany.

OPTIMIZATION OF CULTURE CONDITIONS FOR DIFFERENTIATION OF ADULT BONE MARROW DERIVED HUMAN MESENCHYMAL STEM CELLS INTO FUNCTIONAL OSTEOBLASTS

*Yrjans JJ, **Hentunen TA, **Väänänen KH, *Aro HT
Orthopaedic Research Unit, Department of Orthopaedic Surgery and Traumatology,
University of Turku, Turku, Finland

jessica.yrjans@utu.fi

INTRODUCTION

In vitro expansion and differentiation of human mesenchymal stem cells (hMSCs) into osteoblasts (OBs) provides a promising tool for skeletal reconstruction. Also, bone formation assays with hMSCs are useful *in vitro* model systems for studying the effects of different parameters on osteoblastic differentiation and bone turnover. The basic method for in vitro osteogenesis of hMSCs, i.e., in presence of organic phosphatase and ascorbic acid, is well known. Dexamethasone (Dex) is also widely used as an osteogenic agent but the effects are complex and not yet fully understood. Dex stimulates differentiation and is required for mineralization, but inhibits cell proliferation.

To optimize the *in vitro* bone formation assay and to find methods by which to control and adjust the culturing conditions according to the source of cells and the application, we investigated the effect of plating density and timing and concentration of Dex supplementation. Further, we studied how stabilization of the pH during the osteoblastic induction with 20 mM HEPES affected differentiation and bone formation.

Our hypothesis was that by transient Dex supplementation the inhibitory effect of Dex on cell proliferation could be overcome but still achieve good mineralization. And that buffering with HEPES inhibits bone formation by hMSCs in vitro.

METHODS

hMSCs were isolated from iliac crest bone marrow aspirates of a strictly homogenous population of female middle-aged patients (n=40) with hip osteoarthritis but no co-morbidities. The study was approved by the local ethical committee and all patients signed an informed written consent. To study the effect of Dex on osteogenic differentiation and mineralization of the extracellular matrix (ECM), hMSCs were cultured in osteoblastic induction medium (OB) (alpha-MEM with 10% FCS, glycerophosphate and ascorbic acid), or in OB supplemented with 10 or 100 nM Dex for the first week only or constantly. We also investigated Dex supplementation during four different time periods (days 1-7, 15-28, 22-28 and 1-28), and the effect of plating density (1000, 2500 and 5000 cells/cm^2).

The effect of pH was investigated by culturing with or without 20 mM HEPES. Differentiation and calcification were detected by staining for alkaline phosphatase (ALP) and von Kossa with subsequent histomorphometry and by measuring the accumulation of extra cellular calcium. Also, the proliferation rate in different Dex treatments was analyzed. The pH for the cultures in the HEPES study was followed every week for 28 days.

Normally distributed data with equal variances was statistically analyzed with One-way ANOVA with Sidak *post hoc* test. Data not meeting the requirements was analyzed using Mann-Whitney U test. A significance level of 0.05 (p=0.05) was applied.

RESULTS

ALP expression and calcification was significantly higher in cultures supplemented with 100 nM Dex for the first week only compared to constant supplementation with 10 or 100 nM. Interestingly, there were no differences between 100 nM Dex 1 week and cultures without Dex (Dex$^-$). Constant supplementation with 10 or 100 nM Dex inhibited while transient supplementation stimulated cell proliferation compared to Dex$^-$. When comparing transient Dex supplementation for different time periods, we found significantly higher ALP expression and calcification at day 28 when Dex was present during days 1-7 and 1-28, compared to other time periods, suggesting that the first week of induction culturing is critical. Using 2500 cells/cm^2 yielded significantly higher ALP expression and calcification compared to 1000 and 5000 cells/cm^2.

We also found that buffering of osteogenic media with 20 mM Hepes alters osteoblastic differentiation and inhibits mineralization. ALP expression and calcification was significantly higher in control cultures. At 28 days, the pH in HEPES buffered cultures was 7.7, while 8.3 in control cultures.

DISCUSSION

Our study suggests that osteoblastic differentiation of hMSCs can be optimized by controlling cell density, pH and timing of dexamethasone supplementation.

**Department of Anatomy, University of Turku, Turku, Finland

CARBON FIBRE REINFORCED POLYMER (CFRP) CAGE INDUCES BETTER CELLS ADHESION, SPREADING AND PROLIFERATION THAN POLI-ETERE-ETRE-KETONE(PEEK) CAGE. ANALYSIS BY A NEW CELLULAR MODEL FOR IN VITRO STUDY OF ORTHOPAEDIC BIOMATERIALS

+*Barbanti-Brodano G, **Morelli C, **Ciannilli A, **Campioni K, *Boriani S, **Tognon M
+C.A. Pizzardi Hospital, Bologna, Italy **University of Ferrara, Italy

INTRODUCTION

In the orthopaedic perspective, tissue engineering is focused on the development of innovative materials whose action consists in recruiting bone progenitor cells and in stimulating their proliferation. Doing so, they favourite the development of the tissue which should be replaced. In this context, it is clear that these materials should not only allow cells adhesion and proliferation, but also ensure that the attached cells will maintain the histological features of the original tissue. Employing an innovative human cellular model (patent FI2005A000038), we present the *in vitro* determination of the above parameters for different biomaterials.

MATERIALS AND METHODS

Cell culture: Engineered osteoblast cells or were seeded on PEEK and carbon (CFRP) vertebral cages. Culture of the cells on glass cylinder was the negative control. Cell quantification: Samples containing an increasing number of cells, were centrifuged, washed in PBS, and resuspended in 1 ml of reading buffer (NaH_2PO_4 50 mM, Tris-HCl 10 mM, NaCl 200 mM, pH 8.0). The fluorescence of each sample was measured spectrophotometrically at λ=490 nm and used to obtain the calibration curve. The number of cells on vertebral cages and glass cylinders was determined on the calibration curve based on the fluorescence intensity. Immunofluorescence assay: Cells grown on the cages and glass cylinders were fixed with ice cold ethanol for 5'. Primary antibody diluted in PBS containing 0,2% of Triton 100 was applied on the cells for 1 hour at 37°C. After two washes at room temperature in PBS, appropriate secondary antibody was applied, and the washes repeated. Cells were then visualized by fluorescence microscopy.

RESULTS

Engineered human osteoblast cells (patent N. FI2005A000038) which constitutively expresses high level of enhanced green fluorescent protein (EGFP), were tested by immunofluorescence analysis for expression and cellular localization of bone specific markers, such as osteopontin and osteocalcin. Cellular localization and distribution of the marker proteins were indistinguishable between parental and engineered cells. We also investigated the cytoskeletal organization, by visualizing actin fibers using TRITC-conjugated phalloydin. We observed the same architecture of cytoskeletal fibers in parental and engineerd cells.

In our essay, we considered that parental Saos-2 cells need approximately 36 hours to complete a single cell cycle, while the glass was the material used as comparative internal control (100%) of the CFRP and PEEK cages. Cultures analyzed at 36 hours indicated that the percentage of cells grown on PEEK (121%) was slightly higher than that on CFRP (116%).

Cell adhesion and proliferation on the two different materials were re-evaluated at 84 h. The percentage of cells grown on PEEK increased in a fashion similar to that observed on the glass (13%), while cells on CFRP increased more than five times (53%).

The observation of the living cells directly on the cages showed a different distribution of the cells on the two different biomaterials. On the CFRP cage the cells were homogeneously distributed as a continuous monolayer, while on the PEEK cage the cells were layered in a discontinuous mode, distributed in non-homogeneous way, and associated in clusters.

Table 1. Adhesion of osteoblast cells on different artificial surfaces (number of cells/ cm^2)

	GLASS (control)	CFRP	PEEK
36 H	65392,75 (100%)	75731,52 (116%)	79350,09 (121%)
84 H	74180,71 (13%)	115794,3 (53%)	89430,4 (13%)

DISCUSSION

Comparative analysis carried out on parental and engineered cells demonstrated a perfect matching in expression, cellular localization and distribution of molecular markers specific for bone tissue, such as osteocalcin and osteonectin, indicating that their functional properties were not altered. Also the cytoskeletal architecture between the two cell populations was undistinguishable. This feature is essential for cell attachment and stabilization, since actin bundles coupled with adhesion plaques can transmit forces to the substrate and help to maintain cell shape and facilitate cell adhesion.

Orthopedic surgeons need to have more information about the biological characteristics of different biomaterials they use during surgery. In particular spine surgeons have fusion of the functional spinal unit as most important goal during most procedures; the possibility to know which cages enhance osteobalsts adhesion and proliferation could be an important step in trying to obtain a solid spine fusion. This knowledge is important in particular treating osteoporotic traumatic pathology that will be the most frequent pathology of the next 50 years. Adhesion, spreading and proliferation of osteoblast cells can dramatically differ depending on the material. Here we demonstrated that CFRP surfaces enhanced these characteristics of osteoblast cells in comparison with PEEK.

Similar assays on biomaterials are in progress using mesenchymal stem cells (MSC) to evaluate the osteoinduction, osteoconduction, and osteogenesis that are specific characteristics of MSC, when they are induced in the osteogenic lineage.

IRRADIATION DOES NOT INFLUENCE INCORPORATION OF IMPACTED MORSELIZED BONE

*Hannink G, *Schreurs BW, *Buma P
*Orthopaedic Research Laboratory, Radboud University Nijmegen Medical Center, The Netherlands
g.hannink@orthop.umcn.nl

INTRODUCTION

In revision surgery bone defects can be filled with impacted bone grafts. The use of graft material carries a potential but well established risk of disease transmission. Gamma irradiation of the graft material is getting more popular for prevention of disease transmission. Due to changes in mechanical properties of bone by gamma irradiation, it has been used with some cautiousness in clinical practice. Irradiated bone is known to be less strong, less stiff and significantly more brittle than fresh frozen controls when tested in compression models. Recently, it was shown that irradiated freeze-dried impacted grafts provide a more stable femoral reconstruction than fresh-frozen grafts, when tested in a hip simulator [1]. However, the higher compactness caused by impaction of irradiated bone, may reduce the speed of remodeling.
Of major concern is the biological performance of irradiated bone used in impaction grafting. Formation of free radicals during sterilization of bone grafts using gamma irradiation might have a detrimental effect on the osteoinductive activity of BMPs. Therefore, we performed a bone chamber study with impacted morselized processed and non-processed allografts. We studied the effects of irradiation on the incorporation of impacted morselized allografts.

METHODS

Cancellous allografts were obtained from the sternum of six donor goats. One third of the grafts were not processed. From the remaining two thirds, blood and marrow were removed macroscopically, by rinsing the grafts with saline for approximately one minute, leaving only a white bone structure. Rinsing was done using a high-pressure pulsatile lavage system (SurgiLav® Plus, Stryker). Grafts were in a sieve during rinsing. Half of the rinsed cancellous allografts were irradiated (gamma irradiation) with a minimal dose of 25kGy (2.5MRad). Irradiation was carried out at a temperature of 4°C by a commercial facility (Isotron B.V., Ede, The Netherlands NL) using a ^{60}Co gamma-ray source.
We used a modified model of the bone conduction chamber (BCC) which is a model for membranous ossification [3] [Fig.1]. This model consists of a titanium screw with a cylindrical interior space. It is made up of two threaded half cylinders held together by a closed screw cap. The chamber has four openings allowing bone and tissue ingrowth.
Impaction was performed by gradually filling the chamber followed by impaction of the material by a constant force of 40N for 2 minutes. The applied pressure was calculated to be 12.5MPa.
We tested four groups, empty (EMP), allograft (ALL), rinsed allograft (RIN) and both rinsed and irradiated allograft (IRR).
Twelve goats were operated under general anesthesia. Each goat received four implants. The chambers were placed in the tibia of the goat, two chambers per tibia [Fig. 2].

Fig. 1. Modified model of the BCC, with four ingrowth openings.

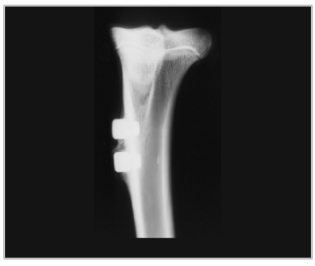

Fig. 2. Bone conduction chamber and implanted chambers in the proximal medial tibia of the goat.

The implantation position of the four chambers was randomized. After 12 weeks the goats were killed and the content was carefully removed from the chambers. Each specimen was embedded in PMMA and 5µm sections were made. In order to get a tissue and bone penetration distance, the area of the total tissue and the ingrown bone were divided by the width of the specimen, to yield the mean ingrowth distance [4]. The mean of the three sections at 0, 300 and 600 µm from the center yields a value for each specimen.
Furthermore, µCT-scans were made from chamber content in order to compare BV/TV of the remnants. Statistical analysis was performed using One Way Repeated Measurements ANOVA and Tukey post hoc tests.

RESULTS

Histologic examination of the specimens revealed cancellous bone in all chambers. Distally, a zone containing vascularized fibrous tissue was observed, followed by a zone with woven-fibered bone more proximally. No difference in osteoclastic resorption between the tested group could be found. New bone was formed by intramembranous ossification, growing upwards to the top of the chamber. If the resorption of the graft remnant was not complete, new bone was apposited on these remnants. No difference in amount of fibrous tissue ingrowth between the ALL, RIN and IRR groups were found. Bone ingrowth was lowest in the non-processed group (ALL), but only significantly lower compared with the empty chambers (EMP) [Fig. 3]. In the non-processed group significantly more graft remnant was found. No difference in amount of remnant between rinsed (RIN) and both rinsed and irradiated. From our µCT-data a higher, but not significantly higher, compactness of the remnant was found in the both rinsed and irradiated group compared with the other groups.

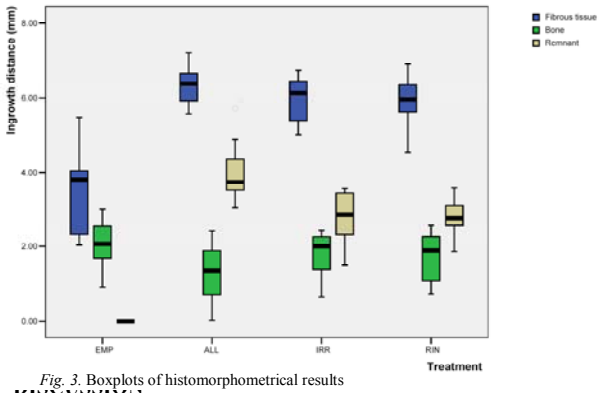

Fig. 3. Boxplots of histomorphometrical results

DISCUSSION

In the present paper, we studied whether there is a difference in incorporation and remodelling between non-processed, rinsed and both rinsed and irradiated bone. Possible harmful effects of irradiation procedure on the osteoinductive/conductive properties of the graft could not be found. Non-processed bone showed, although not significantly, less bone ingrowth, whereas, significantly more graft remnants were found in this group. No difference between rinsed and both rinsed and irradiated bone ingrowth was found. Similarly, comparing fresh-frozen bone and irradiated bone in bone impaction grafting of the acetabulum, no difference in clinical performance after 6 and 13 months was found, using radiologic criteria to determine allograft incorporation and remodeling [5]. The increase in compactness, as measured with µCT, of the irradiated bone did not seem to influence the incorporation of the grafts. We conclude that sterilization with gamma irradiation does not influence the incorporation of impacted rinsed bone allografts, and that gamma irradiation can be used for sterilization of bone grafts for clinical purposes.

REFERENCES:

[1] Cornu et al., Acta Orthop Scand, 72:78-82, 2001
[2] Aspenberg et al., Eur J Exp Musculoskel Res, 2:69-74, 1993
[3] Van der Donk et al., Clin Orthop, 408:302-310, 2003
[4] Robinson et al., J Arthroplasty, 17:834-840, 2002

BIOCART™ II, A NOVEL APPROACH FOR 3D RECONSTRUCTION OF ARTICULAR CARTILAGE

*Nehrer S, *Chiari-Grisar C, *Dorotka R, **Buchta Ch, ***Trattnig S, ****Neria E, ****Stern B, ****Barkai H, ****Zak R, ****Yaniv Y, ****Blumenstein S, ****Yayon A
*Medical University of Vienna, Department of Orthopaedics; **Medical University of Vienna, Department of Blood Group Serology and Transfusion Medicine; ***Medical University of Vienna, Department of Radiology
****ProChon Biotech, Rehovot, Israel
yayon@prochon.co.il

INTRODUCTION

Autologous chondrocyte transplantation (ACI) is a well established treatment method for articular cartilage injuries. However, the use of the periosteal flap is associated with a second surgery site and the problems of hypertrophy.[1,2] Delivery of the cells within a matrix eliminates the need for a periosteal flap and enables implantation by a minimally invasive procedure thus significantly simplifying the surgical procedure. The combination of high quality autologous chondrocytes embedded within a three dimensional scaffold made of only natural components - human fibrin and hyaluronic acid - provides a novel safe and effective therapeutic approach for articular cartilage repair.

METHODS

Biomaterial: Fibrin hyaluronic acid scaffolds were prepared by mixing human fibrinogen solution with hyaluronic acid and thrombin to produce a clot. The clot is freeze dried to produce an open channel porous scaffold into which cells can be seeded. Human chondrocytes were expanded in culture using human serum supplemented with a fibroblast growth factor (FGF) variant. Chondrogenic potential of the cultured chondrocytes was determined by in vitro high density pellet culture. The pellet cultures were analyzed for expression of cartilage specific markers by PCR and histology. Distribution of the cells within the scaffold was studied by histology using H&E staining, presence of proteoglycans and collagen type II was determined by specific stains and immunohistochemistry (IHC).

Clinical study: According to the inclusion/exclusion criteria of the study protocol 8 patients (7 male, 1 female) with osteochondrosis of their knee (4 left, 4 right) were enrolled from August 2004 to September 2005. The mean age at surgery was 30 years. Except for 1 lesion all were treated with more than one layer of the scaffold. There were no complications postoperatively.

RESULTS

Biomaterial: Cells cultured in the presence of the FGF variant exhibit an increased proliferation rate compared with untreated cells. Cells cultured for 7 and 10 days formed pellets with a hyaline like structure expressing proteoglycans and collagen type II. Real time PCR showed a significantly increased Col-II expression compared with Col-I in pellet culture. Chondrocytes cultured in-vitro were seeded into the fibrin-hyaluronic acid scaffold to create tissue-like implants.

Clinical Study: A 6 months clinical result is available for 6 patients. 2 patients finished the study (Table 1). In the MRI two patients showed a favourable development after 6 months (Fig. 1, 2). A partial delamination was observed in one patient after six months, which was completely resolved in the 12 months follow-up. So far, no severe adverse events occurred during the study, laboratory tests and vital signs were normal at all visits. 1 patient had a rearthroscopy after 12 months due to a suspected meniscal tear and effusion. It showed a completely filled cartilage defect with white shiny tissue (Fig. 3).The surface was resilient during physical probing similar to adjacent normal cartilage with very mild fibrillation on the surface. The effusion was due to an unrelated residual plica mediopatellaris which was resected, the meniscus surface was intact.

DISCUSSION

Fibrin is used as the scaffolding material for BioCart™ II thereby mimicing the natural healing process. The open channel and porous structure of the scaffold allows for an immediate three-dimensional distribution of the cells so to guarantee full thickness repair. The in vitro experiments demonstrated that the cells maintained the cartilaginous phenotype. The properties of the scaffold allowed excellent surgical application and revealed good results in the in the first clinical study.

Table 1

Patient	001	002	003	004	005	006
IKDC						
Preop	D	C	B	C	D	D
6 Mo	A	C	A	B	B	B
12 Mo	A	B				
Lysholm						
Preop	44	68	71	67	51	51
6 Mo	100	81	95	96	100	85
12 Mo	100	82				

Figure 1 **Figure 2** **Figure 3**



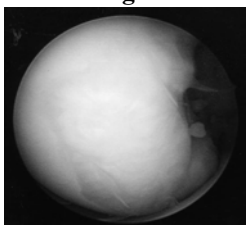

Fig. 1: Preop. MRI, Osteochondrosis dissecans medial femoral condyle. Fig.2: 6 months result showing consolidation of the cartilage and and partial restoration of the subchondral bone. Fig. 3: Filled cartilage defect after 12 months.

REFERENCES: 1. Micheli LJ et al. Clin J Sport Med. (2001). 2. Nehrer S et al. Clin Orthop. (1999).

A NOVEL ENGINEERED OSTEOCHONDRAL COMPOSITE

*Peretti G, *Buragas M, *Sosio C, *Mangiavini L, *Scotti C, **Di Giancamillo A, **Domeneghini C, *Fraschini GF
Divisione di Ortopedia e Traumatologia, Università Vita-Salute San Raffaele, Milano, Italy

peretti.giuseppe@hsr.it

INTRODUCTION

One of the principal limitations for successful cartilage repair using transplanted chondrocytes is the integration of the newly formed cartilage to the native tissue [1]. Both cartilage to cartilage [1,2] and cartilage to bone [3] bonding represent crucial aspects of this issue. We believe that an osteochondral composite, engineered in vitro, could represent a potential model for cartilage repair.
The purpose of this work is to create an in vitro model of engineered osteochondral composite by combining a cylinder of calcium phosphate and cartilage tissue produced by isolated swine articular chondrocytes seeded onto fibrin glue.

METHODS

Swine articular chondrocytes were enzimatically isolated and expanded in monolayer culture. When confluence was reached, cells were re-suspended in fibrinogen (80 millions cells/cc). Thrombin was added to the cell solution in order to form fibrin glue, embedding chondrocytes. Immediately before gel polymerization, the fibrin glue was placed in contact with the cylinders of calcium phosphate (fig. 1).

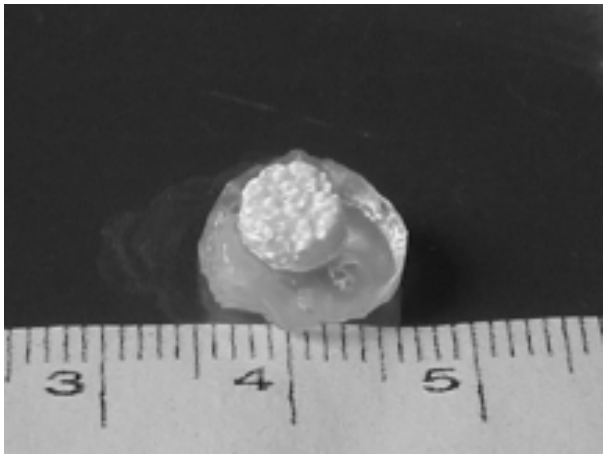

Figure 1: Osteochondral composite pre-implantation

The osteochondral composites were left in standard culture conditions for 1, 3, and 5 weeks. At the end of experimental times the samples were macroscopically analyzed and processed for histological evaluation.

RESULTS

Results showed a macroscopically integrity of the osteochondral samples with gross adherence of the chondral part to the calcium phosphate scaffold (fig. 2).

Histological evaluation showed cartilage like tissue maturing within the fibrin glue scaffold and between the phosphate trabeculae (fig. 3). Throughout the time points, a degradation of the fibrin glue was noted, while the cells duplicate and produce new matrix, replacing the existing fibrin gel.

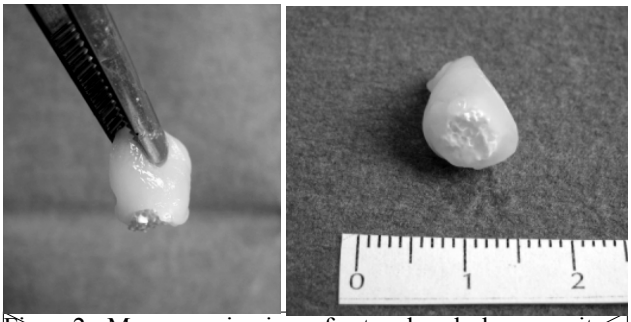

Figure2 : Macroscopic view of osteochondral composites

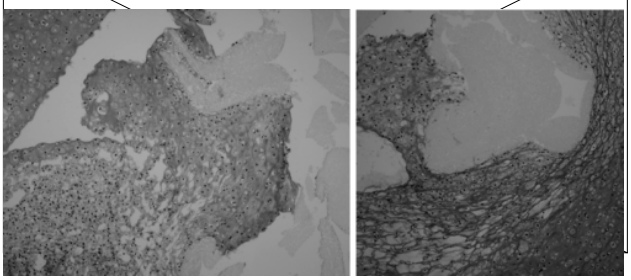
Figure 3: Histological view of integration area between newly formed cartilage and calcium phosphate

DISCUSSION

The results demostrate that isolated chondrocytes, seeded onto fibrin glue, produce a cartilage-like matrix that integrates with a cylinder of calcium phosphate.
This tissue engineered osteochondral composite could represent a valuable model for further in vivo studies on the repair of osteochondral lesions.

REFERENCES

1. Peretti et al. Tissue Engineering 1999, 5:317-26
2. Peretti et al. J Biomed Mater Res, 2003 1;64A:517-24
3. Randolph et al. Newsletter ICRS 2000, Gothenburg Issue: 11-13

ACKNOWLEDGEMENT

Supported by the Orthopaedic Department, Hospital San Raffaele, Milan, Italy

AFFILIATED INSTITUTIONS FOR CO-AUTHORS

** Department of Veterinary Sciences and Technologies for Food Safety, Università degli Studi di Milano, Italy

EFFECT OF BLOOD ON ENGINEERED CARTILAGE

*Sosio C, *Peretti GM, **Boschetti F, ***Gigante A, ***Bevilacqua C, *Mangiavini L, *Scotti C, **Gervaso F, ****Biressi S, *Fraschini G
*Orthopaedic Department – Hospital San Raffaele – Università Vita-Salute, Milan, Italy

sosio.corrado@hsr.it

INTRODUCTION

In the past years the use of enzimatically isolated autologous chondrocytes, first expanded in vitro and then seeded onto a biological scaffold, has become a clinical reality for the repair of cartilage lesions [1]. However, the effect of the contact of blood on engineered cartilage is still unknown. Some studies have demonstrated the negative effect of blood contact on cartilage explants. The nature of the engineered cartilage, however, is different compared to articular cartilage: the "pre-cartilaginous" membrane is made of a cell-compatible material and cells seeded within its structure, producing extracellular matrix. The aim of this study was to investigate the effect of blood contact on the morphological, biochemical and biomechanical properties of engineered cartilage.

METHODS

Chondrocytes were obtained from swine joints and then expanded in vitro. When confluence was reached, chondrocytes were re-suspended and seeded onto biological collagen type I and III scaffolds in vitro for two weeks. Then, peripheral blood was obtained from pigs of the same spices. The cell-seeded collagen membranes were divided into four groups: the "B" group (from "Blood") samples were placed in contact with a 50% blood-medium solution for 3 days; the B+ group with a 80% blood, 20% medium solution; as controls, the "C" group samples were left in the standard culture conditions and the "P" group in a phosphate buffered solution (PBS) for 3 days. After this period, some samples from all groups were retrieved from cultures; others were left in standard culture conditions for 3 more weeks. Samples were analyzed grossly by simple probing, histologically (safranin-O), by immunostaining for type II collagen, biochemically (MTT) and by biomechanical tests under unconfined geometry for compression and shear.

RESULTS

Upon retrieval, samples left in standard culture conditions (group "C") showed overtime an increase in the gross mechanical integrity, dimensions and weight, in the mitochondrial condrocytes activity and in shear and compression modulus. Histological evaluation demonstrated survival of the seeded chondrocytes, abundant sulfurated glycosaminoglycan production and intensive uptake of cartilage matrix-specific stains.
Biochemical evaluation of groups B, B+ and P act showed a transient reduction of the mitochondrial activity after blood or PBS contact. This phenomenon tends to recover in the three following weeks. Histological evaluation demonstrated in all groups a sulfurated glycosaminoglycan production for all groups (fig. 1) and intensive uptake of matrix-specific stains.
Biomechanical evaluation showed a transient loss of the shear and compression modulus of samples after blood contact, followed by an increase of these biomechanical properties in the subsequent 3 weeks of standard culture conditions. This phenomenon was more evident for samples belonging to group "C".

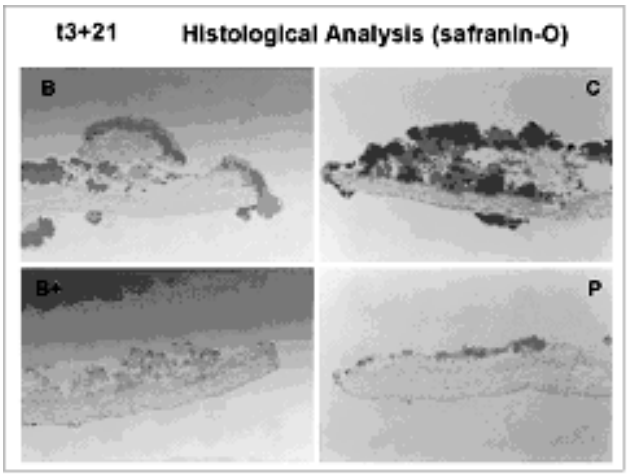

Figure 1. Histological evaluation showing presence of glycosaminoglycan by Safranin-O staining.

DISCUSSION

Although the blood contact seems to produce a reduction in physical, biochemical and biomechanical properties of the samples, chondrocytes seemed to tend to recover in the following standard culture period and produce matrix-specific elements approximating the characteristics of the control group. Further longer time studies are needed to confirm this tendency of the seeded cells to completely recover from the contact with blood.

REFERENCES

[1] Marcacci et al. Knee Surg Sports Traumatol Arthrosc 2002;10(3):154-9

ACKNOWLEDGMENTS

Supported by the "Società Italiana di Chirurgia del Ginocchio" (SICG) Scholarship 2003

AFFILIATED INSTITUTIONS FOR CO-AUTHORS

** Laboratory of Biological Structure Mechanics, Politecnico di Milano, Milan
*** Department of Orthopaedics, University of Ancona, Italy
****Stem Cell Research Institute, directed by Prof. Giulio Cossu

BMPs PROMOTE THE CHONDROGENIC DIFFERENTIATION OF ADIPOSE TISSUE DERIVED MESENCHYMAL STEM CELLS, BUT INDUCE HYPERTROPHIC MARKERS

*Lorenz H,_ *Hennig T, *Thiel A, *Dickhut A, *Richter W
*Department of Orthopaedic Surgery, University of Heidelberg, Germany

Helga.Lorenz@ok.uni-heidelberg.de

INTRODUCTION

Mesenchymal stem cells represent an attractive cell source for tissue engineering and regenerative therapy due to their remarkable potential in proliferation and differentiation. A highly interesting cell population are stem cells originating from adipose tissue (ATSC) because of their easy availability and abundance. With common TGF-ß-driven protocols their chondrogenic differentiation potential, however, is inferior to that of bone marrow derived mesenchymal stem cells (BMSC) (Winter et al. 2003). The aim of this study was to improve the chondrogenic differentiation of ATSC by applying different growth factors and growth factor combinations and to characterize the gene expression of the final differentiation stages.

METHODS

ATSC were derived by liposuction surgery after informed consent. The cells were expanded for up to 8 passages and differentiation was induced by incubating ATSCs in high density pellet culture in serum-free medium containing ascorbate and 10ng/ml of TGF-ß, BMP2, 4, 6, 7, FGFa, FGFb, IGF-1 or PtHrP or the same factors in combination with TGF-ß (10ng/ml). Differentiation was assessed by immunohistological staining and gene expression profiles were determined by cDNA-array analysis and real-time RT-PCR.

RESULTS

The combination of TGF-ß and BMP6 was most effective for chondrogenic induction of ATSC. Both factors had to be applied simultaneously for successful chondrogenic differentiation. The combination of TGF-ß and BMP4 also induced chondrogenesis of ATSC, but did not lead to a complete differentiation. ATSC induced with TGF-ß and BMP6 expressed cartilage relevant molecules like col2, aggrecan, CRTL-1, COMP, PRELP and fibromodulin. Their expression profile was similar to the expression profile of BMSC induced with TGF-ß. Surprisingly, like BMSC ATSC showed an early upregulation of hypertrophic markers like col10 and ALP. In vivo ectopic implantation of the chondrogenically induced ATSC into SCID mice led to formation of calcified cartilage with vascular invasion, calcification and microossicle formation.

DISCUSSION

ATSC like BMSC can be differentiated into chondrocyte like cells under appropriate culture conditions. Their easy availability makes them a promising cell source for cell therapy and tissue engineering of cartilage. To improve the quality of chondrogenic induction the inhibition of hypertrophic differentiation should be aimed at in further studies.

REFERENCES:

Winter et al. (2003) Arthritis & Rheumatism 48:418-429

A TISSUE ENGINEERING APPROACH TO MENISCUS REGENERATION IN A SHEEP MODEL

*Chiari-Grisar C, *Koller U, *Dorotka R, *Plasenzotti R, *Lang S,
**Ambrosio L, ***Tognana E, ****Kon E, *****Salter D, *Nehrer S
*Medical University of Vienna, Vienna, Austria. **IMCB-CNR, Naples, Italy. ***Fidia Advanced Biopolymers srl, Abano Terme, Italy. **** Istituto Ortopedico Rizzoli, Bologna, Italy. *****Edinburgh University Medical School, Edinburgh, UK
catharina.chiari@meduniwien.ac.at

INTRODUCTION

Meniscus injuries are the most common knee injury. Loss of the meniscal tissue leads to cartilage degeneration and osteoarthritis. A new resorbable biomaterial constisting of hyaluronic acid ester and poly-ε caprolactone, developed to serve either as a partial or a total meniscus substitute, was tested in an *in vivo* study in sheep.

METHODS

Study design: All procedures were approved by the local ethics committee for animal studies (GZ 66.009/114-BrGT/2004). 8 skeletally mature Austrian stone sheep (50-64 kg) were divided into 2 groups, the animals underwent arthrotomy of their right stifle joints. Group TM (total meniscus replacement, n=3) received a total medial meniscectomy and a total meniscus implant with transosseous fixation and reconstruction of the medial collateral ligament (MCL) (Fig. 1a), Group PM (partial meniscus replacement, n=3) received a resection of the anterior part of the medial meniscus and a partial implant sutured to the original meniscus (Fig. 1b). The left non-operated stifle joints served as controls. For each group an empty control (without implant) was performed.

Biomaterial: The scaffold is a porous composite of polyc-ε caprolactone and HYAFF® (Fidia Advanced Biopolymers, Abano Terme, Italy, Europe) with a pore size between 200 and 300µm.

Gross inspection: The sheep were euthanized 6 weeks after surgery. The joints were evaluated macroscopically, focusing on tissue ingrowth and integration to the capsule and the original meniscus, the implant´s fixation and location,.

Histology: A routine histological processing with paraffin embedding and 3µm cuts was performed. The specimen were subjected to staining of Hematoxilin/Eosin for general morphology, Safranin O/Fast Green for glycoseaminoglycans (GAG) and Azan for collagen. A mapping system for the implant was created, dividing the implant into a peripheral (zone1), intermediate (zone 2) and central (zone 3) zone, moreover a superficial (zone s) and a core (zone c) zone were determined. The cartilage underneath the implant was assessed in the periphery (cart – p) and the center (cart – c) (Fig. 2). The bonding of the implant to the capsule was noted and integration to the original meniscus were noted.

RESULTS

Gross inspection: I all cases there was excellent tissue ingrowth from the capsule to the implant. In group PM tissue had formed in the contact area between the biomaterial and the original meniscus. The surface of the biomaterial was completely covered with a synovial-like tissue, which showed signs of blood vessel formation.

Histology: The main histological findings were an excellent bonding between implant and the capsule in all specimen. In Group PM, tissue formation between the biomaterial and the residual part of the original meniscus could be demonstrated. Moreover, there was notable tissue formation throughout the implant and at the surface. Bloodvessel formation was present in the zone s in all and in zone c in about two thirds of the sections. All specimen showed accumulation of giant-cells in contact with the biomaterial, however, fibroblast-like cells were detected in-between.

DISCUSSION

Experimental studies of synthetic devices as possible alternatives to meniscus allografts showed unsatisfying results in terms of biocompatibility and material properties[1]. The results of a dog model study of a collagen meniscus implant were similar to ours, showing immature vascular connective tissue with fibroblasts, numerous capillaries and a fine fibrillar matrix after 3 months[2]. The presence of giant cells at this early point is interpreted as a part of the physiological resorption process of the biomaterial. Long-term studies on the adaptive remodelling of the tissue to a meniscus-like structure and cartilage protection will follow.

Fig.1a

Fig.1b

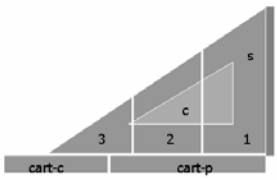

Fig.2

Surgical technique of the total (Fig. 1a) and the partial (Fig. 1b) meniscus replacement. Histological mapping system of the implant (Fig. 2).

Acknowledgments: Funding support was from European Framework V Program (Project No GRD1-2001-40401, Contract No G5RD-CT-2002-00703).

1. Klompmaker J et al. Meniscal replacement using a porous polymerprosthesis: a preliminary study in the dog. Biomaterials 17, 1996. 2. Stone KR et al. Meniscal regeneration with copolymeric collagen scaffolds. In vitro and in vivo studies evaluated clinically, histologically, and biochemically. Am J Sports Med 20, 1992.

ATTACHMENT OF MENISCAL FIBROCHONDROCYTES TO A COLLAGEN TYPE I SCAFFOLD INDUCES MMP AND IL-6 EXPRESSION

+*Hoberg M, *Aicher WK, *Rudert M
*University Hospital of Tuebingen, Department of Orthopaedics, Tuebingen, Germany

Maik.Hoberg@med.uni-tuebingen.de

INTRODUCTION

After a meniscus trauma, preservation of the meniscus is the most important surgical goal. However, depending on the type of damage, partial or complete removal of menisci is the only therapeutical option. This frequently results in cartilage degeneration and consecutive osteoarthrosis of the affected knee joint. The use of scaffolds colonized with meniscus cells (fibrochondrocytes) to reconstruct the defect seems to be a promising way for treatment of a meniscus trauma. Such a transplant could be integrated in the tear and promote the healing of the meniscus. The goal of our investigations was the analysis of expression of different anabolic and catabolic factors in human fibrochondrocytes after seeding these cells onto a collagen I scaffold to investigate the regenerative potential of such a construct for treatments of meniscus tears.

MATERIAL AND METHODS

To isolate fibrochondrocytes, menisci were minced with scalpell and scissors. The tissue was digested in collagenase and Dispase (Roche, Mannheim, FRG). Cells were washed in PBS and expanded in DMEM medium enriched with 10% FCS and antibiotics. Cells were characterized by immunohistochemistry. To test scaffolds, we used a commercially available bovine collagen I matrix approved for surgical purposes (Martricard®, Jotec, Hechingen, FRG) . The scaffold was colonized with human fibrochondrocytes in a density of 10^6 cells per cm^2. Cells expanded at the same ínoculation density w/o scaffold served as mock-controls. After 14 days in culture, the cells were extracted from the scaffold by aid of collagenase (Sigma, Deisenhofen, FGR) and analyzed for the expression of different factors, including IL-1ß, IL-6, TGF-ß, TIMP-1, TIMP3, MMP1, and MMP3 using a quantitative RT-PCR-technology (LightCycler®, Roche, Mannheim, FRG) and commercially available PCR primers (SearchLC, Heidelberg, FRG). GAPDH-RT-PCR served as external standard in each PCR. Data represent mean induction indices of mRNA amounts over mock-treated controls. For statistical evaluation a 2-sides T-test was performed and p-values ? 0.05 were considered to be statistically significant.

RESULTS

Bovine collagen I matrices could be colonized with human fibrochondrocytes. After 14 days of incubation on the scaffolds, the cells show the same mRNA expression levels of IL-1ß, TIMP1, TIMP3 and TGF-ß when compared to controls. In contrast, IL-6 (6.6-fold, not significant), MMP-1 (12.3-fold, not significant) and MMP3 (13.7 ± 6.8, $p<0.032$) were upregulated on transcription levels in the scaffold when compared to controls after the same period of culture.

DISCUSSION/CONCLUSION

We were able to cultivate and characterize human fibrochondrocytes from menisci of the knee joint colonized onto a bovine collagen I matrix. We could show that meniscus cells revealed a significantly increased expression of MMP3, and also an elevation of MMP1 and IL-6 mRNA. No changes were found in the expression levels of IL-1ß TGF-ß and the TIMP's. This suggests that the meniscus cells colonized onto a collagen I scaffold produce a considerable amount of catabolic or inflammatory factors. This may lead to a destruction of the scaffold-matrix itself and the extracellular matrix of the meniscus. Secondly, IL-6 could induce a global inflammation around the scaffold by activating the IL-6 inflammation cascade. Alternatively, MMP activation may be necessary for remodelling processes during replacement of the scaffold matrix with autologous extracellular matrix. However, to prove these hypotheses, long-term scaffold cultures and animal studies are a prerequisite.

ACKNOWLEDGEMENT

This project has been funded in part by grants from the *Deutsche Arthrose Hilfe* and the "fortüne"- programm for young researchers of the University of Tuebingen Medical faculty..

IN VITRO STUDY OF SHEEP MENISCUS CELLS SEEDED ON TWO SLIGHTLY DIFFERENT BIOMATERIALS MADE FROM HYALURONIC ACID AND POLYCAPROLACTONE

*Koller U, *Chiari-Grisar C, **Kapeller B, *Vavken P, *Kotz R, ***Ambrosio L, ****Tognana E, *Nehrer S
*Medical University of Vienna, Department of Orthopaedics

Ulrich.Koller@ebox.at

INTRODUCTION

Meniscus lesions are among the most frequent injuries. The menisci are fibrocartilaginous structures that play a critical role in load bearing, stability and energy distribution, nutrition and lubrication in the knee joint. Loss or removal of the meniscus alters the magnitude and distribution of stresses on the tibial and femoral articular cartilage. 1948 Fairbanks[1] described changes in the knee after menisectomy over years like joint degeneration and osteoarthritis. The regeneration of meniscus or treatment of meniscus lesions with tissue engineered scaffolds has become the focus of Tissue Engineering. This in vitro study investigated the behaviour of sheep meniscus cells seeded on 2 slightly different biomaterials made from hyaluoronic acid and polycaprolactone with the aim to assess the biomaterials´ feasability as a possible tissue-egineered meniscus substitute.

METHODS

Both biodegradable and semi-biodegradable composites, the BF-1 and the BF-1 CO-PET are made from PCL/HYAFF-11 p75 HE 70/30 w/w with a pore size of 150µm to 200µm. The BF-1 CO-PET scaffolds were augmented by polyethyleneterephtalate fibers. Both scaffolds are "autoloaded", this means that they are coated with Sodium Hyaluronan to ease scaffold hydration. 47 matrix cylinders (6mm diameter, 5mm height) were punched out of each biomaterial and seeded with $2x10^6$ sheep meniscus cells each. The specimens were harvested in triplets after 12 hours, 7, 14, 21 and 28 days. Histological (Hematoxilin/Eosin staining for general morphology) and immunohistochemical analysis (collagen I and II) were performed. The glycosaminoglycan GAG content was measured biochemically and RT (reverse transcriptase)-PCR was performed for collagen I and II. 2 cylinders were evaluated by electronic microscopy at 28days.

RESULTS

On the BF-1 the cell morphology distribution continuously changed from a spherical (67,4% ±3,7) at the time point 12 hours to a more not assignable (77,3% ±11,6) phenotype up to the time point 28d, whereas the cells on the BF-1 CO-PET showed the same behaviour till the 14days time point, but then changed their morphology to the spherical phenotype again. Collagen I mRNA expression was present on both materials at all time points. Collagen II mRNA expression on BF-1 decreased over time, whereas on the BF-1 CO-PET an increase of collagen II m RNA was seen between 14 and 28 days. In the BF-1 the immunohistochemical staining was slightly positive for type-II collagen, but negative for type-I collagen. In the BF-1 CO-PET the type-II collagen staining was clearly positive at 12 hours, but decreased until 28 days. The type-I collagen staining was negative. The GAG-content significantly increased in both materials over time. The increase was about the eightfold in the BF-1 CO-PET compared to the BF-1. (Figure 1)

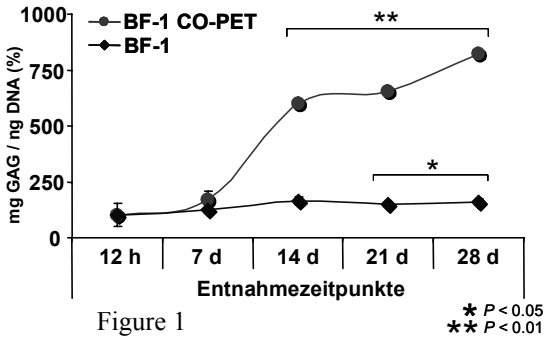

Figure 1

CONCLUSION

This in vitro experiment showed that sheep meniscus cells could be cultivated on both materials. The cells seeded on the BF-1 CO-PET showed a more cartilagineous phenotype, as spherical morphology, increased Collagen II mRNA expression and a higher GAG content were detected.

REFERENCES

[1]Fairbanks T: Knee joint changes after menisectomy. J Bone Joint Surg Br 30:664-670, 1948.

ACKNOWLEDGMENTS

Funding support was from the 5th European Framework Program (Project No GRD1-2001-40401, Contract No G5RD-CT-2002-00703)

AFFILIATION

*Medical University of Vienna, Department of Orthopaedics, Vienna, Austria
**Medical University of Vienna, Core Unit of Biomedical Research, Vienna, Austria
***University of Naples & IMCB-CNR, Naples, Italy
****Fidia Advanced Biopolymers s.r.l., Abano Terme, Italy

EXPRESSION OF GROWTH FACTORS, CYTOKINES, ANGIOGENIC FACTORS AND OTHER PROTEINS IN HUMAN FIBROCHONDROCYTE/ENDOTHELIAL CELL COCULTURES

+*Rudert M, *Aicher WK, *Hoberg M
*University Hospital of Tuebingen, Department of Orthopaedics, Tuebingen, Germany

Maximilian.Rudert@med.uni-tuebingen.de

INTRODUCTION

The meniscus of the human knee joint has an outstanding function for articular stability, shock absorption and power transmission. After a meniscus trauma, up to now partial or complete removal of the meniscus was the only therapeutical option in many cases eventually, this often results in cartilage degeneration and consecutive osteoarthrosis of the knee joint. The highest goal after meniscus damage is the preservation of the meniscus, which is often not possible due to the bad healing of meniscus lesions in the avascular zone. Progress of cell culture techniques raised hope to treat damaged menisci by tissue engineering. Therefore, the goal of our investigations was the analysis of expression of different angiogenic factors, growth hormones and cytokines in human fibrochondrocytes (meniscus cells). The mutual influence of the meniscus cells by endothelial cell cocultures was analyzed, in order to examine the molecular bases of the healing of meniscus tears in vascularized zones more exactly. For this purpose, commercially available HUVEC [human umbilical vein endothelial cells] were used as well established and stable endothelial cell model.

MATERIALS AND METHODS

Meniscal fibrochondrocytes were isolated from menisci of patients of the University Hospital after written consent. To this end, menisci were minced with scalpel and scissors and the tissue was degraded by incubation in collagenase/PBS solution. Cells were collected by centrifugation, washed in expanded in DMEM medium enriched with antibiotics and 10% FCS.
Cocultures of mensical cells and HUVEC were incubated in transwells over four and twelve days, separated by a semipermeable membrane. The expression of Angiopoietin-1, Angiopoietin-2, Endostatin, VEGF, SMAD-4, Thrombospondin-1, Aggrecan, Biglycan, Fibronectin, Vimentin, Connexin-43, IL-1ß, iNOS, MMP-1, MMP-3, MMP-13, collagen-I, -II, -III, -VI and -X were examined by RT-PCR and immunhistochemistry in fibrochondrocytes in the comparison to cultures without endothelial coculture. A proliferation assay was used to investigate the mitotic activity in the coculture compared to the control culture after 7 and 14 days.

RESULTS

In presence of HUVEC, meniscal fibrochondrocytes expressed the following factors at rates comparable to cells w/o HUVECS: Angiopoietin-1, Angiopoietin-2, VEGF, SMAD-4, Aggrecan, Biglycan, Fibronectin, Vimentin, Connexin-43, iNOS, MMP-1, MMP-3, MMP-13, Thrombostatin-1, collagen-I, -II, -III, -VI and -X. In contrast, expression of endostatin (3-fold, $p< 0,001$) and IL-1ß (9-fold, $p<0,001$) were expressed significantly higher in the coculture when compared to the individual cell cultures. The proliferation rate of fibrochondrocytes was significantly decreased in coculture when compared to controls: 32 % after 7 days and 55 % after 14 days ($p<0,001$).

DISCUSSION/CONCLUSION

We were able to cultivate and characterize human fibrochondrocytes from menisci of the knee joint. We could show that coculture of meniscus cells with endothelial cells revealed an increased expression of an anti-angiogenetic factor and the pro-inflammatory IL-1ß. This suggests that the meniscal fibrochondrocytes are able to slow down the proliferation of endothelial cells in their neighbourhood, which may contribute to the poor healing capacity in rather avascular zones of menisci. Further, the elevated IL-1ß contributes to inflammation after meniscus injury.

ACKNOWLEDGEMENT

This research has been partly funded by the Deutsche Arthrose Hilfe and the “fortuen”- programm for young researchers of the university of Tuebingen.

OSTEOBLAST-INDUCED BIODEGRADATION OF POLY(ε-CAPROLACTONE)-CARBONATED APATITE COMPOSITES FOR BONE TISSUE ENGINEERING

*Di Foggia M., *Taddei P, **Ciapetti G, **Baldini N, ***Guarino V, ***Causa F, ***Ambrosio L, *Fagnano C
*Dipartimento di Biochimica "G. Moruzzi", Sezione di Chimica e Propedeutica Biochimica, University of Bologna, Italy
micheled@chem.unibo.it

INTRODUCTION

Poly(ε-caprolactone)-apatite (PCL-AP) composites are promising devices as long-term biodegradable scaffolds for bone repair. To evaluate the influence of the PCL/AP ratio on *in vitro* degradation and bioactivity, the PCL-AP scaffolds were immersed in different aqueous media and analysed at different degradation times by vibrational spectroscopy and thermal analysis. The same techniques were used to comparatively characterise the composites incubated with human osteoblasts (HOB), in order to evaluate the cell role in degradation.

METHODS

The samples were synthesised using phase-inversion and a salt-leaching technique. The composites had different PCL/AP ratios: 50/50, 60/40 and 75/25. Pure PCL samples were analysed as control. The *in vitro* biodegradation was investigated under sterile conditions at 37°C in different media: saline phosphate buffer at pH 7.4 (SPB), 0.01 M NaOH solution, simulated body fluid at pH 7.4 (SBF). The samples were analysed before and after biodegradation for different degradation times (up to 2 months) by Raman spectroscopy, thermogravimetry (TG) and differential scanning calorimetry (DSC).
HOB were isolated from bone fragments obtained during surgery for total hip replacement and cultivated in α-MEM with 10% FBS on the PCL-AP samples for 4 weeks.

RESULTS

Thermal analysis of the undegraded samples showed that in the 50/50 sample the PCL component was the most crystalline. Raman analysis confirmed this result as well as the relative composition of the scaffolds.
The NaOH degradation medium was found to be the most aggressive towards both pure PCL and composites, confirming the catalytic effect of the OH^- ion on degradation. Accordingly, the pure PCL samples degraded in NaOH solution underwent the most pronounced morphology changes: crystallinity increased as well as the intensity of the Raman bands due to crystalline PCL (Fig.1A) and the crystallisable fraction. These findings indicate that degradation preferentially involved the amorphous domains of the polymer with a consequent chain fragmentation and enrichment in crystalline PCL. Among the PCL-AP composites, the PCL component of the 50/50 sample showed the least degradation extent upon degradation in NaOH solution, as expected on the basis of its initially highest crystallinity. In the SPB medium, a certain degree of chain fragmentation was revealed. Upon immersion in SBF solution all the composites showed deposition of an apatitic phase; gravimetric measurements coupled to Raman and TG analyses indicated that the 50/50 sample was the most bioactive (Fig.1B).
The thermal analysis of the cell-incubated samples indicated a significant degradation of the polymeric component present in the composites, especially in the 75/25 sample, while the pure PCL samples appeared the least degraded.

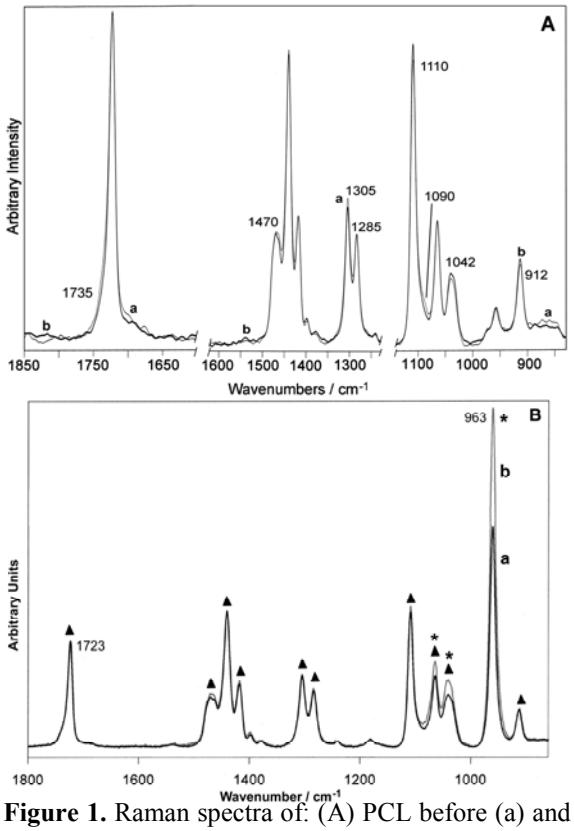

Figure 1. Raman spectra of: (A) PCL before (a) and after degradation in NaOH solution for 2 months; (B) 50/50 sample before (a) and after (b) immersion in SBF for 2 months (*: bands of the AP phase increase in intensity).

DISCUSSION

Raman spectroscopy coupled to thermal analysis proved a valid method to characterise the samples under study and their behavior in different media and after osteoblast-incubation.

**Laboratorio di Fisiopatologia Ortopedica, Istituti Ortopedici Rizzoli, Bologna, Italy
***Istituto per la Tecnologia dei Materiali Compositi-CNR, Centro Interdisciplinare di Ricerca sui Biomateriali, Università di Napoli Federico II, Italy

EXPRESSION OF COMPONENTS OF THE FGF SIGNALING PATHWAY IN POSTNATAL MOUSE VERTEBRAL GROWTH PLATE

*Dahia CL, *Mahoney E, **Durrani AA, ***Wylie C
[*]Divisions of Orthopaedics and Developmental Biology, Cincinnati Children's Hospital and Medical Center, Cincinnati, OH-45229
Chitra.Dahia@cchmc.org

INTRODUCTION

Idiopathic scoliosis is the most common type of spinal deformity. It is thought to occur from unsynchronized growth of the vertebral growth plates. The goal of this study is to find out how cell signaling pathways control symmetrical growth of vertebrae during postnatal life.

METHODS

FVB mice were selected from 1-9 weeks of age and their longitudinal growth was determined by measuring the lengths of the mice at one-week intervals. Vertebra and knee joints were removed from 1-4 weeks old male mice and immediately frozen. 10 μm cryosections in the coronal plane were collected from the thoracic vertebrae and knee joints, and histological analysis was carried out by staining with hematoxylin and eosin. Immunolocalization of FGF-2, the activated form of FGFR, and its downstream signaling molecule, the di-phosphorylated form of ERK1/2 [Di(p)-ERK1/2] was carried out on 10 μm thick cryosections.

RESULTS

Maximum longitudinal growth of the mice was observed between 1-4 weeks of age and these ages were selected for further study. Histological analysis of the vertebrae and tibia revealed the spatial organization of the chondrocytes in the different zones of the growth plate. Immunolocalization revealed that FGF-2, the active form of FGF, was found in the late proliferating and hypertrophic chondrocytes layer. The activated receptor for FGF was observed only in the hypertrophic and apoptotic chondrocytes in both vertebral and tibial growth plates (Fig. A & B). Di(p)-ERK1/2 was also observed only in the hypertrophic and apoptotic chondrocytes in the vertebral and tibial growth plates.

DISCUSSION

Active signaling of FGF in the hypertrophic and apoptotic zone of the vertebral growth plate suggests its involvement in the hypertrophy and apoptosis of chondrocytes which then leads to the ossification of the matrix laid down by the growth plate chondrocytes. Understanding the molecular biology of postnatal vertebral growth plate development will allow future understanding of the defect(s) that cause scoliosis and will lead to development of novel therapies for management of these growth related disorders.

[**]Division of Orthopaedics, Cincinnati Children's Hospital and Medical Center, Cincinnati, OH-45229, USA.
[***]Division of Developmental Biology, Cincinnati Children's Hospital and Medical Center, Cincinnati, OH-45229, USA.

A

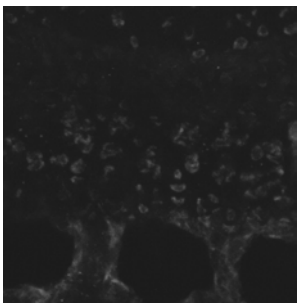

B

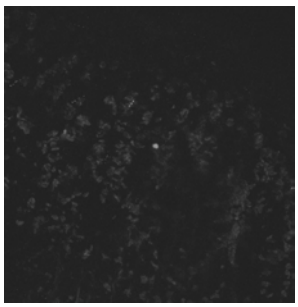

POST-NATAL NOTOCHORDAL CELLS EXPRESS ORGANIZER SIGNALS SUCH AS SONIC HEDGEHOG AND DO NOT UNDERGO IN VITRO DIFFERENTIATION

*Vadalà G, ? Michienzi S, ? Funari A, **? Riminucci M, ***? Bianco P, *Denaro V
*Department of Orthopaedic Surgery, Università Campus Bio-Medico, Rome, Italy
g.vadala@unicampus.it

INTRODUCTION

After the embryonic period, notochordal remnants persist inside the intervertebral disc, where they give rise to the nucleus pulposus. Notochordal cells (NTCs) gradually disappear during maturation and are replaced by chondrocyte-like cells. This phenomenon is correlated with onset of disc degeneration in different species[1]. The biological function of the post-natal NTCs remains unclear.

The objectives of this study were to evaluate either (1) if post-natal NTCs are stem cells capable of giving rise to other cell types under specific culture conditions, or (2) if they still express embryonic organizer signals such as Sonic Hedgehog (Shh), Indian Hedgehog (Ihh) and their receptor Patched (Ptch).

METHODS

Lumbar Intervertebral discs from 3 week-old SD rats were analyzed. Cells were isolated by enzymatic dissociation of the IVD, and NTCs were separated from the intervertebral disc cells (IVDCs) on a Percoll step gradient described by Oegema[2]. Both NTCs and IVDCs were cultured under conducive conditions for either osteogenic or adipogenic differentiation of mesenchymal progenitors[3]. Differentiation was assessed by Oil red O, Alkaline Phosphatase (ALP), Von Kossa, and Alizarin red staining.

Gene expression analysis was performed both on the notochordal tissue selectively aspirated from the nucleus pulposus and on the remaining IVD. Shh, Ihh, Ptch, and the house keeping gene GAPDH expression was assessed by RT-PCR.

RESULTS

Notochordal cells were readily detectable in histological cells as vimentin positive, PAS-negative, vacuolated, "physalipherous" cells.

A homogeneous population of large, vacuolated, physalipherous cells (NTCs), was obtained in culture after density gradient centrifugation

No evidence of adipogenic differentiation was obtained in cultures of NTCs. In contrast, IVDCs did accumulate intracellular lipids under adipogenic conditions, although they failed to generate mineralization nodules under osteogenic culture conditions (Fig. 1).

The gene expression analysis of the notochordal tissue and mesenchymal disc tissue showed that NTCs expressed Shh and not Ihh, while the surrounding mesenchymal disc tissue expressed Ihh and not Shh expression. Ptch was expressed by both notochordal and mesenchymal tissue (Fig. 2).

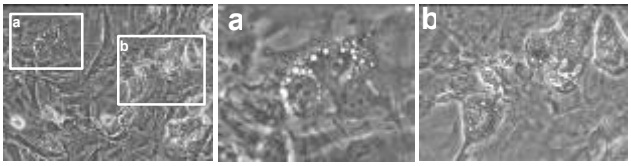

Figure 4. *Oil Red-O staining of IVDCs and NTCs after culture under adipogenic condition;* ***a****: no evidence of adipogenic differentiation of the vaculated cells (NTCs);* ***b****: adipogenic differentaition of IVDCs.*

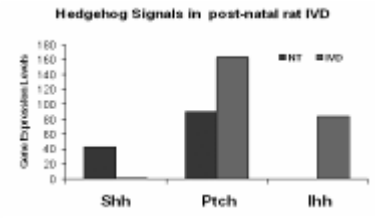

Figure 4: *Gene expression level of Shh, Ihh, and Ptch in the notochordal tissue (NT) obtained by mechanical aspiration and in the remaining intervertebral disc tissue (IVD)*

DISCUSSION

Our data highlights remarkable diversity in differentiation potential of NTCs vs IVDCs, and suggests that NTCs are unable to enter differentiation pathways typical of mesenchymal progenitors in culture. In contrast, chondrocytes of the intervertebral discs, although differentiated, may be able to convert to adipocytes, like other classes of skeletal cells and progenitors.

During the development of the vertebral column, chondrogenic differentiation of the mesenchymal cells requires signals from the notochord such as Shh and Ihh.[4].

In this study we demonstarted that post-natal notochordal cells still produce Shh, therefore, they could act as organizer cells on the surrounding IVD, influencing IVD cells to express Ihh, enhancing the proliferation and the activity of IVD cells.

Therefore we believe that the loss of notochordal cells and their signals from the IVD are the *primum movens* in the pathogenesis of intervertebral disc degeneration.

REFERENCES

1. Hunter C.J. et al Tissue Eng. 2003(4):667-77
2. Aguiar D.J. et al. Exp Cell Res. 1999 Jan 10;246(1): 129-37.
3. Pittenger MF et al. Science. 1999;284(5411):143-7.
4. Christ B. et al. Anat Embryol (Berl). 2002(3): 179-94.

AFFILIATED INSTITUTIONS FOR CO-AUTHORS:

? Biomedical Science Park San Raffaele of Rome, Rome, Italy;
**Department of Experimental Medicine, Università del L'Aquila, L'Aquila, Italy;

REGULATION OF TRANSGENE EXPRESSION USING AN INDUCIBLE SYSTEM FOR IMPROVED SAFETY OF INTRADISCAL GENE THERAPY

*? Vadalà G, *Hubert MG, *Gilbertson LG, *Kang, JD
*Ferguson Laboratory for Orthopaedic Research, Department of Orthopaedic Surgery, University of Pittsburgh, Pittsburgh, PA, USA

kangjd@upmc.edu

INTRODUCTION

The concept of intradiscal gene therapy for the treatment of intervertebral disc degeneration has been extant since the late 1990s. The viral transfer of growth factor genes (TGF-ß, BMP-2) to the cells of the intervertebral has revealed promising initial results with increased proteoglycan production in-vitro and in-vivo [1,2]. However, we have observed that expression of transgenic growth factors outside the IVD in the event of a misdirected injection has potentially detrimental consequences (e.g., toxicity) [3]. To date, a sefety system that allows the transgenes to be turned "off" or "on" has not been produced for intradiscal gene therapy.

The aim of the study is to describe the application of a tet-off inducible system for intervertebral disc gene therapy, testing an adenoviral vector that expresses FasL and GFP under the control of a tetracycline-regulated gene expression system.

METHODS

Human nucleus pulposus cells (NPC) were plated in 6 well-plates and transduced with Ad/FasL-GFP$_{tet}$, at 0, 50, 100, and 200 multiplicity of infection (MOI). After one day cells were cultured in the presence (1, 10, 100mg/l) or absence of tetracycline for two days and then cultured again without tetracycline. Cells were imaged at day 1, 3, and 6 after transduction. The FasL expression was also checked. Apoptosis was assessed and quantified by FACS 24 hours after transduction and again after tetracycline administration.

RESULTS

The hNPC expressed GFP one day after transduction, proportional to the MOI used for transduction. GFP positivity was not observed three days after administration of tetracycline at each concentration used, either at the fluoro-microscope or at the FACS. The cells expressed GFP again six days after removal of tetracycline (Figure 1). The apoptosis rates decreased after stopping FasL transgene expression.

DISCUSSION:

The transgene expression of FasL-GFP was efficiently regulated by administration of tetracycline in cell culture media of the hNPC. The presence of tetracycline turns off the protein expression and subsequent absence turns it on again.

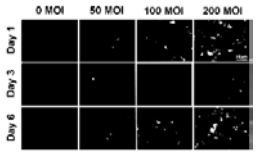

Figure 1. *Nucleus Pulposus Cells transduced with Ad/FasL-GFPTET at different multiplicity of infection (MOI). Cells were imaged at day 1, 3, and 6 after transduction. 1mg/l of Tetracycline was added at 1 day and stopped after 3 days.*

Intradiscal gene therapy is safe procedure when appropriately dosed and delivered into the disc, but could cause toxic effects in the event of excessively dosed or misdirected gene therapy [3]. Therefore, we propose a tet-off inducible system as an efficient tool for modulating the transgene expression either for optimizing the therapeutic efficacy of the exogenous growth factors or for avoiding the toxicity that could derive from a missed injection.

REFERENCES

1. Nishida K. et al. Spine 1999, 24:2419-25
2. Shimer A.L. et al. Orthop Res Soc Trans 2005; 0183
3. Kim J.S. et al. Orthop Res Soc Trans 2005; 0042

ACKNOWLEDGMENTS:

This study was supported by a NIH Grant and The Pittsburgh Foundation.

AFFILIATED INSTITUTIONS FOR CO-AUTHORS:

? Department of Orthopaedic Surgery, Università Campus Bio-Medico, Rome, Italy;

GENE EXPRESSION PROFILING OF MULTIPOTENT ADULT RAT MESENCHYMAL STEM CELLS

*, **Ahmed N, ***Lundgren-Akerlund E, **Grifka J, *, **Grässel S
*Experimentelle Orthopädie, Zentrum für Medizinische Biotechnologie, BioPark, Regensburg, Germany

nazish.ahmed@stud.uni-r.de

INTRODUCTION

Adult multipotent mesenchymal stem cells (MSCs) are adherent stromal cells of non-haematopoietic origin. MSCs are easily isolated from bone marrow and expanded *in vitro*. Upon expansion they retain their self renewal capacity as well as their differentiation competence. In a variety of species MSCs have shown potential to differentiate into tissues of mesenchymal lineage including bone, cartilage, muscle, tendon and connective tissue. This makes them a good candidate for therapeutic regenerative medicine or tissue engineering. It is known that MSCs exert influence on haematopoietic stem cells via secretory cytokines; it is also known that they play a role in bone physiology and pathophysiology.
Identification and better understanding of the molecular events characterizing differentiation of MSCs is needed to allow manipulation of MSCs for tissue regeneration. Prior to clinical trials studies must be carried out in experimental animal models, rat is an appropriate mammalian model for such purposes however; basic expression profiling of rat MSCs is not complete. This study concentrates on a comprehensive profiling of basal gene expression level of osteo-chondro specific genes in undifferentiated rat adult MSCs. Furthermore, secretory cytokine profile of the MSCs is also being examined.

MATERIALS AND METHODS

MSCs are isolated from rat bone marrow (BM) and are allowed to adhere to tissue culture flasks for 3 days before removal of non-adherent cells. Cells are expanded until they reach 70% confluence. Selected surface markers are evaluated by immunohistochemistry. Cells are placed in osteogenic and chondrogenic favorable environment and osteo/ chondro differentiation potential is determined by immunofluorescence and histology. mRNA expression of the selected genes is analyzed by quantitative RT-PCR after normalizing cycle threshold (Ct) values against the endogenous control ß-actin. SDS-PAGE and immunoblotting are done for protein expression analysis. Cytokine secretion profile will be determined by antibody array from RayBiotech™. For statistical analysis one-way ANOVA is used on triplicate experiments.

RESULTS

BM isolated MSCs exhibit $CD45^{-/low}$, $D7fib^{+}$ and $CD49a^{+}$ cell surface marker profile. Immunofluorescent staining of MSCs cultured for 21 days in chondrogenesis favorable 3-D milieu showed increased intensity of COMP and collagen II. In undifferentiated MSCs we have observed high gene expression of transcription factors sox9 and Cbfa1 and comparatively low expression of indian hedgehog (Ihh). Growth factor TGFß-3 exhibited a very high basal gene expression level in undifferentiated MSCs while BMP-7 showed lowest expression. Chondrogenesis specific COMP, aggrecan, collagen II and collagen X revealed low expressions. Highest expression was observed for osteogenic marker collagen I followed by that of alpha11 integrin. Qualitative selected protein analysis reciprocated gene expression results. Gene expression of tissue inhibitor of metalloproteinase-1 and 2 appeared at a very high level compared with much lower expression of MMP-2. Collagen IX, sox-5 and tbox-2 mRNA expression was not detected in multipotent MSCs.

DISCUSSION AND CONCLUSION

Observed cell surface marker profile demonstrates that the method of isolation procures relatively pure MSCs. The chondrogenic differentiation potential of these cells was confirmed by accumulation of COMP and collagen II in the extracellular matrix when kept under chondrogenesis favorable conditions. Alzarin red positive staining on day 21 of osteogenic differentiation was used as an indicator for osteogenic potential of MSCs. Gene and protein expression shows that collagen I, TIMP-1 and TIMP-2 are among the highest expressed genes in undifferentiated MSCs while BMP-7 and collagen X are the least expressed. Cytokine secretion profile and gene expression relative to that of chondrocytes is to be determined. With this study we have acquired an osteo-chondro specific base-line gene expression profile of undifferentiated rat MSCs. Knowledge of this profile has significant implications for differentiation studies utilizing rat MSCs.

REFERENCES

Jones E. A., *etal*. (2002) Arthritis and rheumatism, 46; 12. 3349-3360.
Maniatopolous C., *etal*. (1988) Cell tissue Res. 254; 2. 317-330

AFFILIATED INSTITIONS FOR CO-AUTHORS:

**Orthopädische Universitätsklinik Regensburg, Bad Abbach, Germany
*** Cartela AB, Biomedical Center B12, SE-221 84 Lund, Sweden

ADULT MESENCHYMAL STEM CELLS GROWN ON DIFFERENT SCAFFOLDS FOR BONE AND CARTILAGE ENGINEERING

Bevilacqua C, Gigante A, Greco F
Department of Orthopaedics, Polytechnic University of Marche, Ancona, Italy

claudiadw@libero.it

INTRODUCTION

It has been demonstrated that marrow mesenchymal stem cells (MSCs) may differentiate into fibroblast, chondrocytes or osteoblasts (1-5). The present study evaluated the behaviour of human MSCs cultured on different scaffold matrices in order to establish if cell-matrix interaction can modulate their differentiation.

METHODS

Bone marrow was obtained from acetabulum during hip arthroplasties. MSCs were isolated by cell sorting, expanded and characterised by FACSCalibur flow cytometry system. Cells were grown on different scaffolds: type I collagen, type I+II collagen and type I collagen + hydroxyapatite matrices. After 15 and 30 days histochemical, immunohistochemical and spectrophotometric (cell proliferation, ALP activity) analyses were performed.

RESULTS

Among the scaffold matrices tested we observed a great variability in terms of MSCs adhesion and proliferation. MSCs grown on type I+II collagen matrice differentiated into cells expressing chondrocytes markers. MSCs grown on type I collagen + hydroxyapatite matrice differentiated into osteoblast-like cells.

DISCUSSION

These data evidenced that the characteristics of the scaffold can influence phenotype expression, cell adhesion and growth rate of human adult MSCs. Hence, cell-matrix interaction would be utilized for MSCs differentiation in skeletal tissue engineering.

ACKNOWLEDGEMENTS

The authors thanks Opocrin SpA (Corlo di Formigine, Italy) for providing the scaffold matrices.

REFERENCES

1) Kipnes J, Carlberg AL, Loredo GA, et al. Osteoarthritis Cart 2003;11(6):442-454.
2) Mastrogiacomo M, Cancedda R, Quarto R. Osteoarthritis Cart 2001;9(SupplA): S36-40.
3) Pittinger MF, Mackay AM, Beck SC, et al. Science 1999;284:143-147.
4) Reyes M, Lund T, Lenvik T, et al. Blood 2001;98:2615-2625.
5) Yoo JU, Barthel TS, Nishimura K, et al. J Bone Joint Surg Am 1998;80:1745-1757.

IN VITRO CHARACTERIZATION OF HUMAN STROMAL CELLS FROM FEMORAL MARROW FOR BONE ENGINEERING

Ciapetti G, Perut F, Pagani S, Devescovi V, Amato I, Granchi D, Giunti A, Baldini N
Laboratorio di Fisiopatologia Ortopedica, Istituti Ortopedici Rizzoli, Università di Bologna, Italy

gabriela.ciapetti@ior.it

INTRODUCTION

Stromal cells from marrow hold a great promise for bone regeneration. Even if they have already being exploited in many clinical settings, the maintenance of their proliferation/differentiation potential after *in vitro* isolation and expansion needs further investigation. Best results have been obtained when MSC are loaded onto 3D carriers, natural or synthetic, which provide a substrate for cells and mechanical strength to the defect, although these add variability to the outcome of the construct. In our study, human MSC are derived from bone marrow of the femur during hip replacement procedures. After *in vitro* isolation, these cells are grown in osteogenic medium. Their proliferation and differentiation characteristics, in the absence of any added growth factor, are verified at different time endpoints by means of morphological, biochemical and molecular techniques. Moreover, the release of factors regulating the proliferation and differentiation of MSC in culture, is also studied.

MATERIALS AND METHODS

Human stromal cells were isolated from bone marrow collected from patients undergoing total hip replacement. After gradient centrifugation, and 4 days of culture, cells adherent to culture plastic were considered as BMSC and grown in α-MEM plus 15% FCS, glutamine, antibiotic and 100 μmol/L ascorbic acid-2 phosphate. The cultures were run with/without 10 nmol/L dexamethasone, and fed at 3-4 day intervals. Osteoblast phenotype development was verified using CFU-assay and 10 mM β-GP was added for 2 wks for mineralization. At the different time endpoints along culture, viability, ALP, and proliferation of cells were measured, and RNA, as well supernatants, stored for further analysis.

RESULTS

BMSC from bone marrow of adult patients maintained a proliferative potential which, in our experimental conditions, was not directly related to the age of the patient, with a time to confluence ranging from 10 to 48 days. Differentiation too, in terms of ALP production and mineral deposition, showed large variability among individuals. In this respect, the addition of 10 nM dexamethasone was not found to significantly change the pattern of ALP production. Colony Forming Units were obtained, and the presence of cells at various stages of differentiation was mirrored by the different positivity to ALP cytochemical staining within the same colony (Fig. 1, left). At 2-3 weeks after mineralization induction, either well-organized nodules or a diffuse CaP deposition were observed (Fig. 1, right), both considered as a proof of osteogenic differentiation. The regulation of the Wnt/βcatenin signaling, which is crucial for the differentiation establishment of MSC to osteoblasts, was investigated by measuring dickkopf-1 (Dkk-1) in the culture medium at different endpoints. The release of Dkk1 reflects the proliferative potential of human MSC as it increases progressively in the log-phase of the culture.

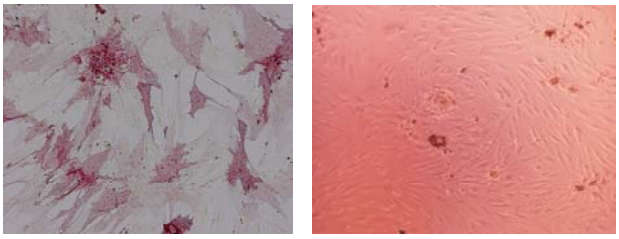

Fig. 1. BMSC at 2 wks from seeding (ALP, 20X, left) and at 2 wks after mineralization induction (10X, right)

DISCUSSION

Several reports have shown that BMSC cultures have a high therapeutic potential, but the *in vivo* regeneration of bone tissue depends on the presence of precursors than can proliferate and differentiate to bone forming cells. Switch from proliferation to differentiation of BMSC expanded *in vitro* is being attempted by means of biochemical inducers, including dexamethasone, ascorbate, and β-glycerophosphate, in order to measure the osteogenic potential of such precursors.
In our study, BMSC were derived from the marrow of the femur of patients undergoing total hip replacement: this tissue is often used by surgeons to fill in the gaps around implants, therefore our cell model is significant. Using a standard protocol of culture, we found a large variability in the response of BMSC, not related to the age/gender of the donor. As a matter of fact, we observed that BMSC populations retain their proliferative potential, but display a variable proportion of ALP-positive cells, even when stimulated with dexamethasone. The recurrent finding of a diffuse CaP deposition at the final endpoint of *in vitro* cultures, that is mineralization, confirms the presence of cells at different stages of maturation. In conclusion, femur marrow may be used clinically as an autologous bone regenerating agent, as it shows a consistent proportion of BMSC responding to osteogenic signals.

ACKNOWLEDGEMENTS

Partially funded by FIRB2001 project.

OSTEOGENIC POTENTIAL OF BONE MARROW MESENCHYMAL STEM CELLS IN CONGENITAL TIBIAL PSEUDARTHROSIS ASSOCIATED WITH TYPE I NEUROFIBROMATOSIS

*Devescovi V, *Pagani S, *Amato I, *Magnani M, *Donzelli O, *Ciapetti G, *Giunti A, *Baldini N, *Granchi D
Laboratorio di Fisiopatologia Ortopedica & 8^ Divisione, Istituti Ortopedici Rizzoli, Bologna, Italy

donatella.granchi@ior.it

INTRODUCTION

Congenital pseudarthrosis of the tibia is an uncommon entity with a reported incidence of 1:140,000-1:250,000 neonates. Usually the disease becomes evident within a child's first year of life but may be undetected up to the age of 12 years. The most common cause of congenital bowing and pseudarthrosis of tibia (50% cases) is the neurofibromatosis type 1 (NF1). Treatment options depend on the type of disease and include different bone-grafting techniques: the Ilizarow method, electric stimulation, or amputation. New strategies based on the use of autologous mesenchymal stem cells (MSC) could be employed in order to increase the success rate in restoring the tibial union. The MSC pool contains precursors which are able to differentiateinto bone-forming cells, which could favor the formation of physiologic 'bony callus' and ultimately the ossification of the tibial defect. Preliminary studies on neurofibromatosis observed that levels of osteoblastic markers in cells derived from tibial pseudarthrosis were lower than those observed in MSCs obtained from iliac crest [1]. In this study, we compared the osteogenic potential of MSCs derived from both tibial pseudoarthrosis and iliac crest of children affected by NF1. Our goal was to establish whether the autologous MSC transplantation may be an effective strategy for the therapy of tibial pseudarthrosis in neurofibromatosis or not.

MATERIALS AND METHODS

The observational pilot study was approved by the institutional Ethical Committee on human research. From June 2005, six patients, who underwent surgery for tibial congenital pseudarthrosis associated to NF1, have been enrolled in the study. In each patient bone marrow samples were collected from iliac crest (IC) and from pseudarthrosis lesion (P). Both IC-MSC and P-MSC were cultured in α-MEM medium added with 10% fetal bovine serum (FBS) or with 10% autologus serum (AUT), 10^{-8}M dexamethasone (DEX), and 50 μg/mL acsorbic acid. Furthermore, all cultures were performed without dexamethasone.

The osteogenic potential of MSCs was evaluated at different endpoints. The Alamar Blue test was performed at the 15th and 25th day in order to evaluate the viability and metabolic activity of the cells; the expression of osteoblast related genes, i.e. osterix, Alkaline phosphatase (ALP) and osteocalcin, were analyzed at the time of seeding (time 0) and after 14 days of culture. The confluent MSCs were subcultured in order to quantify the 'Colony-Forming-Units' (CFUs). The CFUs were counted after 14 days (crystal violet staining) and the osteoblast phenotype was confirmed by the presence of ALP activity. Finally, the osteogenic potential was verified by the qualitative analysis of the mineral nodule deposition (Alizarina Red). The release of factors involved in the regulation of osteogenesis, i.e. Dickkopf 1 (Dkk1) and secreted 'frizzled related protein' (sFRP), was measured in culture supernatant by immunoenzymatic method (ELISA).

RESULTS

The differentiation of MSC into osteoblasts varied largely among patients. In most cases, the cell growth and the osteoblast phenotype were favoured by the addition of FBS in culture medium, although the presence of dexamethasone concealed the differences. The cell number and viability were increased in IC-MSC cultures compared to P-MSC ones. At the early culture time, pseudarthrosis derived cells did not show the typical osteoblastic-like morphology. A higher capability to form ALP positive colonies was found in IC-MSCs than in P-MSCs. Osterix was detectable in all cultures either at time 0 or after 14 days, even if the quantification of transcript was reliable only in IC-MSC cultures at time 0. The amount of ALP transcripts reflected the ALP activity in CFU. The osteocalcin was never detectable at time 0, and after 14 days the amplification product was detectable, but not measurable. Soluble Dkk1 levels were higher in P-MSC than in IC-MSC cultures, while no differences were found in sFRP release.

DISCUSSION

Taken together our results show that in patients affected by congenital tibial pseudoarthrosis the IC-MSC generates more osteoblast than P-MSC. Nevertheless, this statement does not seem to be the rule because the differentiation varied largely among patients. These findings suggest that autologous MSC derived from iliac crest may be a promising strategy for the therapy of tibial pseudarthrosis in neurofibromatosis, but the potential effectiveness of this approach should be considered on a case by case basis.

ACKNOWLEDGEMENTS:
Granted by 'Io ci sono' Association.
REFERENCE: Leskelä HV, et al. Bone 2005;36S:SO-03.

REINDEER BMP EXTRACT IN THE HEALING OF CRITICAL SIZE LONG BONE DEFECT

*Pekkarinen T, **Jämsä T, **Määttä M, *Hietala O, *Jalovaara P
*Department of Surgery, University of Oulu, Oulu, Finland

pekka.jalovaara@oulu.fi

INTRODUCTION

Bone morphogenetic proteins (BMP) are shown to stimulate bone and cartilage regeneration. The reindeer native BMP extracts induce effectively ectopic new bone formation *in vivo* (Pekkarinen et al. 2003, 2005). However, its bone healing capacity has not yet been evaluated. The aim of this study was to investigate the effect of the reindeer BMP extract on the healing of rabbit radius critical size bone defect. The bone inducing capacity of reindeer BMP extracts was compared to rhBMP-2, because its bone healing capacity is well documented.

METHODS

Tested implants contained 5mg and 10mg of non-sterilized reindeer BMP extract and 10mg of gamma sterilized reindeer BMP extract administered with collagen carrier (Lyostypt®). 70µg of rhBMP-2 with collagen carrier (InductOs™) served as positive control, and collagen (Lyostypt®) implants and untreated defects as negative controls. NZW-rabbit with 1.5 cm of critical size radius bone defect and eight weeks follow-up was used. Bone healing was evaluated by radiographs, peripheral quantitative computed tomography (pQCT) and mechanical torsion testing. The non-parametric Kruskall-Wallis test was used to evaluate the statistical differences between the groups and the Mann-Whitney test for pairwise comparison. Values of $p<0.05$ were considered statistically significant. The experimental setup was approved by the institutional review board for animal experiments.

RESULTS

Radiographical analysis showed bone formation (BF) to be significantly higher in all groups containing BMPs than in the untreated controls. BF was also significantly higher in the rhBMP-2 group and nearly significantly higher in the group treated with 10 mg of non-sterilized reindeer BMP extract ($p=0.061$) when compared to the collagen controls. Bone union (BU) was significantly better in the non-sterilized BMP extract groups and rhBMP-2 group than in the untreated controls. BU was also better in the 10mg of non-sterilized reindeer BMP extract and rhBMP-2 implants when compared to the collagen implants. The mean new bone area at defect site proved to be higher in the all implants containing BMP than in the untreated defects. It was also higher in the 10mg of non-sterilized reindeer BMP extract group and rhBMP-2 group when compared to the collagen controls. Mechanical tests showed torsional stiffness of the bones to be higher in the 10 mg of non-sterilized BMP extract group than in the collagen group. The mean cross-sectional bone area measured by pQCT densitometry was higher in the rhBMP-2 group than in the collagen group. The mean bone density at the defect area was higher in the 10mg of non-sterilized BMP extract group than in the rhBMP-2 group.

DISCUSSION

Previously it has been shown that reindeer BMP extract induce effectively new bone in muscle pouch model of mouse. Here we investigated its effect on the healing of a critical size long bone defect. The study showed that reindeer BMP extract induced effectively the healing of rabbit radius bone defect and was comparable with rhBMP-2. Only slight differences were found between the study groups in the mechanical properties of the bones. This was mainly due to the small sample number and the limited ability of mechanical testing to discriminate bones with non-union. Gamma sterilization of reindeer BMP extract reduced osteoinductivity slightly but not significantly.

REFERENCES

Pekkarinen et al. (2003) Scand J Surg 92: 227-230
Pekkarinen et al. (2005) Arch Orthop Trauma Surg 125: 10-15

ACKNOWLEDGEMENTS

The authors would like to present many thanks to Mrs. Marja Juustila for her kind assistance with the preparations of the implants and surgical assistance.

AFFILIATED INSTITUTIONS FOR CO-AUTHORS

**Department of Medical Technology, University of Oulu, Oulu, Finland

OMENTAL PROPERTIES OF HOFFA'S FAT PAD: A PRELIMINARY INVESTIGATION

*Nash A, Smitham P, Yu Y, Hale D, Walsh WR
*The Surgical & Orthopaedic Research Lab, Prince of Wales Hospital, University of New South Wales, Randwick, Australia
a.nash@unsw.edu.au

INTRODUCTION: The infrapatellar (Hoffa's) fat pad is a vascularised body of adipose and stromal tissue. It is commonly excised to enhance the surgical exposure of the joint space. Based on clinical observation during such procedures it was hypothesized that the fat pad had the ability to sequester loose bodies in the knee. The objective of this study was to explore whether (as the omentum does in the abdomen) the fat pad readily adheres to and isolates areas of inflammation. Specifically to the knee, it was hypothesized that this applies to loose bodies such as cartilaginous or osseous debris, sources of joint pain. Furthermore, the study sought to investigate the pathway of this resorption.

METHODS: After gaining approval from the Animal Ethics Committee of the University of New South Wales, six sheep had a 10 mm^3 osteochondral body resected from the trochlear groove and placed between the patella tendon and anterior aspect of the fat pad. The sheep were sacrificed 6 weeks post-operatively. Two infrapatellar fat pads from non-operated knees were processed as controls. Similarly, two omental samples were taken for histological comparison. Sample were fixed in formalin and decalcified in formic-acid/ formalin. After histological processing sections were stained for H&E. Immuno-histochemistry was performed for matrix-metalloproteinase-1. Histological observations were then recorded. These results were also compared to a clinical case.

RESULTS: Histology showed these osteochondral fragments to be sequestered and surrounded by moderately vascularised fibrous tissue with a presence of osteoclast-like cells and signs of bone resorption. Immunohistochemical staining revealed over-expression of matrix-metalloproteinase-1 particularly in fibroblast populations adjacent to the bone sequestrum. (Figure 1) After comparison to the control fat pads, reactive fat pads were noted to have increased vascularity, hyperplasia of the stromal components, adipose cellular activation (increased nucleus: cytoplasm ratio, increased variation in cell size) and presence of mild chronic inflammatory infiltrate around the sequestered osteochondral body.

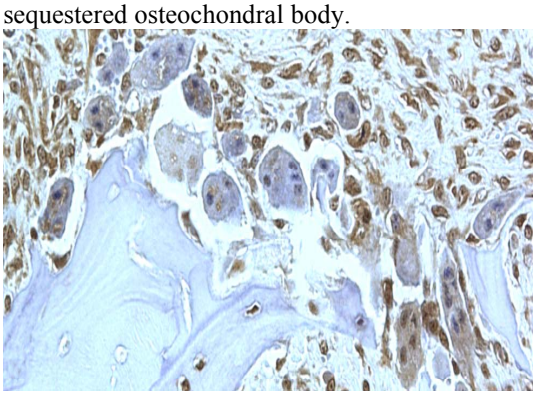

Figure 1: 20x Light micrograph. Ovine infrapatellar fat pad stained for MMP-1. Over expression of MMP-1. Many osteoclasts are evident adjacent to bone fragment.

A case study involving a 64 year old female also demonstrated loose body sequestration by the fat pad.

DISCUSSION: The results of this study were encouraging in supporting that, like omentum, the infrapatellar fat pad may readily adhere to inflamed tissues in the knee. In doing so, it may "mop up" loose bodies that can be a source of joint pain. This preliminary study sought to elucidate this hypothesized role of the fat pad in the knee. The novel surgical method in this study, ie placing the osteochondral body on the anterior surface of the fat pad, posterior to the patella tendon does not represent a likely site for adhesion in clinical practice. However, the histological results mimicked those seen in the clinical case included in this study. A preliminary investigation of the pathway of bone and cartilage resorption by the fat pad included osteoclastic activity and presence of MMP-1 however further investigation is necessary.

AFFILIATED INSTITUTIONS
- Sydney Adventist Hospital Limited.
- San Pathology, Sydney Adventist Hospital.

A TGFß3 AND bFGF COATED CHITOSAN MATRIX STIMULATES TENDON HEALING IN RATS

*Wang H, *Lorenz H, *Eschlbeck A, *Heitkemper S, *Richter W, *Rickert M
*Orthopaedic University Hospital of Heidelberg, Germany

haili.wang@ok.uni-heidelberg.de

INTRODUCTION

Tendon healing demonstrates a relatively slow process because of different steps in collagen synthesis and remodelling and because of low vascularity of tendon tissue 1-2. It is known that different growth factors have stimulatory effects on tendon healing 3. Matrices can be used as a slow-release-carrier for growth factors. The hypothesis of our project was that a combined release of TGFß3 and bFGF on an absorbable Chitosan matrix can enhance tendon healing.

METHODS

Thirty-six male Sprague Dawley rats were used. The right Achilles tendon was sharply transected and repaired with Kirchmeyer Kessler suture technique. A tube like Chitosan matrix as tendon sheath was wrapped around the repair. 10ng TGFß3 and 100ng bFGF were applicated inside the matrix with 50µl fibrin glue. This dosage was chosen according to in vitro results. The same surgical procedures were performed in the control group, with the same volume of fibrin injected into the repair sites.
At 10 and 30 days after repair the Achilles tendons were harvested and were evaluated for gene expression, histological and biomechanical effects.

RESULTS

At 10 days postoperatively, the tendon scars in the experimental group were significantly thicker (p=0.003) and stronger (p=0.022) compared to controls. They also exhibited significantly more stiffness (p=0.046) (Fig 1). At 30 days the cross section area was still significantly higher in the experimental group (p=0.01). The gene expressional showed that mRNA expression of collagen type III but not type I was up-regulated in the late stage of tendon healing (p=0.028) (Fig 2).

DISCUSSION

In conclusion, exogenous administration of combined TGFß3 and bFGF on a Chitosan matrix significantly improved tensile strength, stiffness and thickness in the early stages of Achilles tendon healing. This study provides important information about stimulation of tendon healing by the use of TGF-beta3 and bFGF and may help to develop a more functional rehabilitation of the

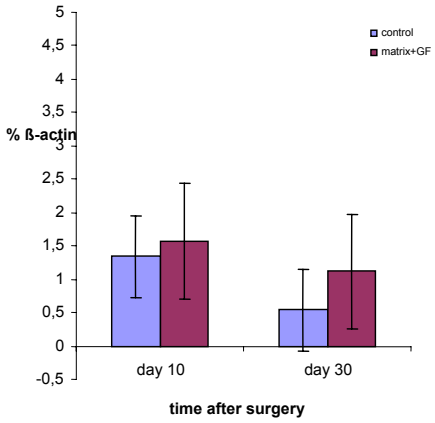

Fig 2: Gene expression (quantitative rt-PCR) of collagen type 3 in the healing Achilles tendon at 10 and 30 days after growth factor administration.

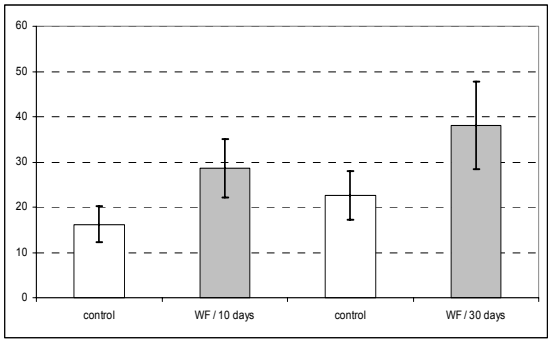

Fig 1: Stiffness of Achilles tendons was improved both at 10 days and 30 days postoperatively.

REFERENCES

1. Liu S et al. 1995, Clin Orthop 318:265.
2. Chang J et al., 1997, Plast Reconstr Surg 100: 937.
3. Thomopoulos S et al., 2005, J Hand Surg, 30A, 441-7.

COVALENT BONDING OF LAMININ-5 TO Ti6Al4V – AN *IN VITRO* STABILITY STUDY

Gordon D, Pendegrass C, Blunn G
The Centre for Biomedical Engineering & The Institute of Orthopaedics and Musculoskeletal Science,
Royal National Orthopaedic Hospital, University College London, UK
mrdjgordon@hotmail.com

INTRODUCTION

The Intraosseous Transcutaneous Amputation Prosthesis (ITAP) is an alternative for transfemoral amputees to conventional stump-socket prostheses which have many problems. These include: poor fit, stump pressure sores, pain, infections and unnatural gait. ITAP aims to overcome these by being osseointegrated into the femoral medulla with a pin protruding through the skin to which the external prosthesis attaches. Thus, the forces normally encountered by the stump soft tissues are now transferred directly to the skeleton. The transcutaneous pin produces a route for infection from the external to internal environment. Therefore, a key feature to the success of the ITAP is to produce a biological seal at the transcutaneous interface.

The protein Laminin-5 (L-5) is a 'biological glue', which is integral to epitheial cell adhesion. It is fundamental in the formation of adhesion complexes such as hemidesmosomes, vital for epithelial integrity. If L-5 can be bonded to the transcutaneous titanium alloy (Ti_6Al_4V) portion of the ITAP, it may enhance the strength of the skin-ITAP interface.

Silanisation is a chemical technique that covalently bonds proteins to metals. This method was investigated to determine if L-5 could be immobilized on Ti_6Al_4V. We have assessed the characteristics L-5 silanised Ti_6Al_4V as a potential substrate for ITAP and it's bond stability *in vitro*.

METHOD

To determine the maximum quantity of L-5 that could be silanised to Ti_6Al_4V and its relative stability when soaked in foetal calf serum (FCS) over time; 6 polished Ti_6Al_4V discs were silanised by immersing in aminopropyltriethoxysilane followed by glutaraldehyde. Radiolabelled rat laminin-5-I^{125} was then added. Discs were immersed in FCS for 4 days (37 °C) and analysed at 24 hour intervals in a liquid scintillation counter. Un-silanised discs were used as controls. Kruskal Wallis and Mann-Whitney U tests were used to determine significance.

RESULTS

L-5 was successfully covalently bound to Ti_6Al_4V (fig.1). 10ng, 100ng, 250ng and 500ng droplets yielded significantly more silanised L-5 ($p<0.05$), but no difference was observed between 750ng and 1000ng. The actual L-5 amount covalently bound ranged from 33% and 65%. After 24 hours of FCS soaking a small decrease in bound L-5 occurred ($p<0.05$), but subsequent to this no significant reduction was observed over 4 days ($p<0.05$) (fig 1). Controls showed a significantly larger reduction after 24 hours ($p<0.05$) (fig 2).

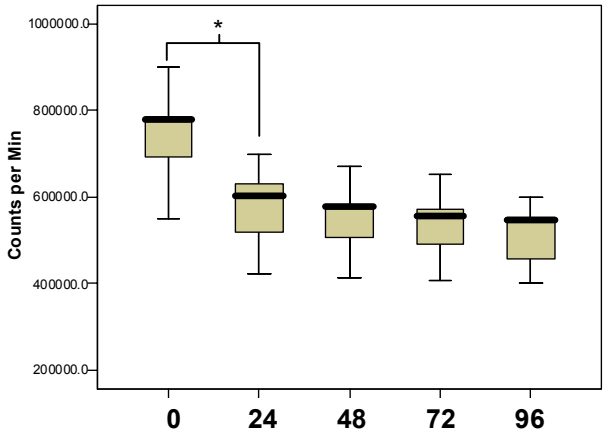

Figure 1. Silanised L-5 detected on disc surface over tir (hrs) while soaked in FCS. * ($p<0.05$)

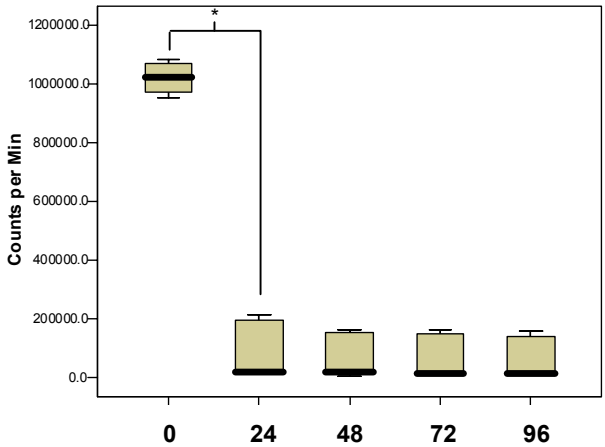

Figure 2. Controls - Un-silanised L-5 detected on disc surface over time while soaked in FCS. * ($p<0.05$)

CONCLUSION

Covalently bonding L-5 to Ti6Al4V by silanisation can be achieved with predictable results. Large enough quantities can
be immobilised to influence cellular function. L-5 silanised to Ti6Al4V remains stable *in vitro* over time and is not removed. Following the study of cellular interactions with silanised L-5,
a stable skin seal may be achieved at the transcutaneous portion of the ITAP.

THE DEVELOPMENT OF A SMALL ANIMAL MODEL OF WEAR-DEBRIS INDUCED OSTEOLYSIS

*Ibrahim T, **Ong SM, ***Taylor GJS
University of Leicester, Leicester, UK
ti11@le.ac.uk

INTRODUCTION

The commonest cause of long term failure of total joint arthroplasty is aseptic loosening. The aim of this study was to develop a small animal model of wear-debris induced osteolysis. This model can then be utilised for screening potential pharmaceutical agents to inhibit aseptic loosening.

MATERIALS AND METHODS

Two sets of animals were utilised in this study. First set of animals consisted of 52 offspring from 7 time mated female mice that were injected with radioactive calcium 45 on day 14 of gestation. The 52 offspring were divided into 2 equal groups and subjected to either the implantation of clinically relevant ceramic particles or sham surgery into their femora. The non-operated femora were used as control. Animals were killed 4 weeks following surgery. Second set of animals consisted of 46 offspring from 6 time mated female mice that were injected with radioactive calcium 45 on day 14 of gestation. The 46 offspring were divided into 2 equal groups and subjected to either the implantation of clinically relevant ceramic particles or sham surgery into their femora. The non-operated femora were used as control. Animals were killed 10 weeks following surgery. Femora were retrieved, weighed, dissolved and radioactivity measured as outcome (CPM/mg = Counts per Minute per milligram). A Linear mixed effects model was utilised to examine the difference in outcome between the 2 groups. All animal procedures undertaken were approved by the Home Office conforming to the laws and regulations of the United Kingdom.

RESULTS

From the analysis it was estimated that the mean effect on outcome of implantation of ceramic particles relative to sham surgery at 4 weeks was estimated at 29.11 CPM/mg (95% CI: 4.66 to 53.55 CPM/mg) and this was statistically significant but no clinically relevant The other covariate significant at the 5% level in this model was whether the femur that underwent surgery had been fractured which tended to decrease the effect of surgery by 74.58 CPM/mg. There was evidence that sham surgery affected the scintillation count of the femur relative to the non operated femur of the same animal at 4 weeks. The mean size of this effect was estimated to be by 61.01 CPM/mg (95%CI: 36.77 to 85.24; $p < 0.001$).

From the analysis it was estimated that the mean effect on outcome of implantation of ceramic particles relative to sham surgery at 10 weeks was estimated at 11.85 CPM/mg (95% CI: -14.04 to 37.75 CPM/mg) and this was not statistically significant.

The other covariates (leak and fracture) were not significant at the 5% level in this model.

There was evidence that sham surgery affected the scintillation count of the femur relative to the non operated femur of the same animal at 10 weeks. The mean size of this effect was estimated to be by 67.27 CPM/mg (95%CI: 42.97 to 90.94; $p < 0.001$).

DISCUSSION

The implantation of ceramic particles decreased the uptake of radioactive calcium compared to sham surgery at 4 weeks. This difference was statistically significant; however, the difference between the scintillation counts between the animals that had ceramic particles implanted and sham surgery was not clinically significant. We were expecting a minimum difference of 50 CPM/mg between the groups. Therefore, we decided that several factors could have been responsible for this small difference. We then decided to extend the postoperative time to 10 weeks. We thought that this time period will allow the inflammatory process and bone resorption to develop and will allow us to detect a difference between the mice that underwent implantation of ceramic particles and sham surgery. Unfortunately, we were not able to detect a difference between the animals at 10 weeks and our simple model failed to work. This model does show that the implantation of ceramic particles did cause bone resorption due to the fact that the scintillation counts in the femora that underwent implantation of ceramic particles was less than those in femora that underwent sham surgery or control femora. However, the model did not work could be due to the lack of sensitivity of the model or other potential problems with this model. Factors that are known to be important in the development of osteolysis and aseptic loosening could be limiting factors in the development of this model.

AFFILIATED INSTITUTIONS FOR CO-AUTHORS:
** Queen's Medical Centre, Nottingham, United Kingdom
***University Hospitals of Leicester, Leicester, United Kingdom

THE UTILISATION OF URINARY BONE MARKERS IN A SMALL ANIMAL OF WEAR-DEBRIS INDUCED OSTEOLYSIS

*Ibrahim T, **Ong SM, ***Taylor GJS
University of Leicester, Leicester, United Kingdom
ti11@le.ac.uk

INTRODUCTION

Aseptic loosening of total joint arthroplasty is characterised by osteolysis caused by osteoclasts and macrophages. Osteolysis occurs by acidification and dissolution of hydroxyapatite crystals then proteolysis of the bone collagen matrix. N-Telopeptide (NTx) and deoxypyridonolone (DPD) represent highly specific markers for bone resorption. The aim of this study was to investigate whether urinary NTx and DPD generated *in-vivo* can be used as bone markers in a small animal model of wear debris induced osteolysis.

MATERIALS AND METHODS

Urinary samples were collected from two sets of mice at necropsy at four and ten weeks following either the implantation of clinically relevant ceramic particles or sham surgery into their femora and assayed for N-Telopeptide (NTx) and deoxypyridonolone (DPD). Bone markers were corrected for urinary creatinine. The urine samples of 24 controls animals were also collected. The first and second sets of animals consisted of 52 and 46 mice respectively.

All animal procedures undertaken were approved by the Home Office conforming to the laws and regulations of the United Kingdom.

RESULTS

The urinary NTx concentrations between animals at 4 weeks that underwent the implantation of ceramic particles into their femora compared to those who underwent sham surgery was not statistically significant ($p=0.864$). The comparison of urinary NTx of all three groups at 4 weeks (ceramic particles, sham surgery and control) was also not statistically significant ($p=0.834$).

The urinary DPD concentrations between animals at 4 weeks that underwent the implantation of ceramic particles into their femora compared to those who underwent sham surgery was not statistically significant ($p=0.837$). The comparison of urinary DPD of all three groups at 4 weeks (ceramic particles, sham surgery and control) was also not statistically significant ($p=0.188$).

The urinary NTx concentrations between animals at 10 weeks that underwent the implantation of ceramic particles into their femora compared to those who underwent sham surgery was not statistically significant ($p=0.613$).

The comparison of urinary NTx of all three groups at 10 weeks (ceramic particles, sham surgery and control) was also not statistically significant ($p=0.309$).

The urinary DPD concentrations between animals at 10 weeks that underwent the implantation of ceramic particles into their femora compared to those who underwent sham surgery was statistically significant ($p=0.045$). The comparison of urinary DPD of all three groups at 10 weeks (ceramic particles, sham surgery and control) was also statistically significant ($p<0.001$).

The concentration of urinary NTx in animals that were culled at 4 weeks compared to those that were culled at 10 weeks was not statistically significant ($p=0.732$). However, the urinary DPD concentrations differed between the 2 sets of animals and this was statistically significant ($p=0.002$).

DISCUSSION

The model was unable to detect a difference in the urinary NTx concentration between animals that underwent the implantation of ceramic particles into their medullary canal compared to sham surgery. The urinary NTx concentration was not statistically different between the 2 groups even when keeping the ceramic particles in the medullary canal from 4 to 10 weeks. This can be attributed that our model is not sensitive enough to detect changes in urinary NTx concentrations between the ceramic particle and sham surgery groups. Our results also showed no difference between the 2 treatment groups and control urinary NTx concentrations at 4 and 10 weeks.

We were able to show a difference between the urinary DPD concentrations between animals that had ceramic particles implantation into their femora compared to those who underwent sham surgery. This difference was only significant at 10 weeks after injection of ceramic particles. The urinary DPD concentrations were higher in the animals that had the ceramic particles compared to sham surgery but the concentrations were higher in the control animals. Our results show that the urinary DPD concentration may be a more sensitive marker in this model as concentrations were higher and statistically significant when compared to urinary NTx concentrations.

In this *in vivo* model of wear debris induced osteolysis, most of the tested urinary markers of bone resorption were negative. This could be explained by the lack of bone resorption activity in the model or the urinary bone markers simply did not reach a detectable level of significance if bone resorption was present.

AFFILIATED INSTITUTIONS FOR CO-AUTHORS:
** Queen's Medical Centre, Nottingham, United Kingdom
***University Hospitals of Leicester, Leicester, United Kingdom

VANCOMYCIN AND MEROPENEM IN BONE CEMENT

*Persson C, *Baleani M, **Zolezzi C, **Bertoni G, ***Tigani D, ***Trentani F, ****Borrelli A, *Toni A, ***Giunti A
*Laboratorio di Tecnologia Medica, Istituti Ortopedici Rizzoli, Bologna, Italy
persson@tecno.ior.it

INTRODUCTION

Antibiotic-loaded bone cement is extensively used to fix joint prostheses. Unfortunately, bacteria resistance is increasing and new, alternative antibiotics are being considerated. Bone cement containing new additives must be characterized in an antibacterial way, but also mechanically since the material's strength is important for the long-term functionality of a cemented implant. In this study elution kinetics, antibacterial activity, static and dynamic mechanical properties were evaluated for bone cement loaded with vancomycin and/or meropenem.

MATERIALS AND METHODS

The bone cement used in this study was Cemex® XL. Vancomycin and meropenem were added to the cement powder (total powder weight 40g) before mixing the cement following ISO5833 recommendations. 4 different formulations of bone cement were investigated: A) without antibiotics (control), B) with 0.5g of vancomycin and 0.5g of meropenem, C) with 1g of vancomycin and D) with 1g of vancomycin and 1g of meropenem (all amounts/40g of PMMA powder).

Elution kinetic studies of the vancomycin were performed immersing small disks (15mm diameter, 10mm thick) of bone cement in 15 ml of saline solution at 37°C, sampling 1 ml of the solution at fixed times to obtain its concentration. 4 disks were tested for each formulation. The results were analysed statistically by a nonparametric test and a post-hoc test at each time of immersion.

Antibacterial activity tests were made against Staphylococcus aureus, Enterococcus, Pseudomonas aeruginosa, Escherichia coli and methicillin-resistant Staphylococcus epidermis. 2 disks of each type of cement were tested for each type of organism, except for Pseudomonas aeruginosa and Escherichia coli, that were tested against B and D only since vancomycin alone is ineffective against these bacteria.

Static and dynamic mechanical tests were performed on A, B and C only, on the basis of the experimental results. Compressive and bending strength were determined according to ISO5833 recommendations. For both tests, 24 specimens of each formulation were tested. Fatigue tests were performed according to a previously validated internal procedure [1]. The test results were analysed statistically by analysis of variance and post-hoc tests.

RESULTS

The results of the **elution kinetic studies** are shown in figure 1. No significant difference was generally found comparing the elution of vancomycin from formulations B and C. Conversely, the formulation D showed a statistically higher elution rate than the other two.

The **antibacterial activity tests** showed that all formulations containing antibiotics eliminated all tested bacteria, except for one case: a few colonies of

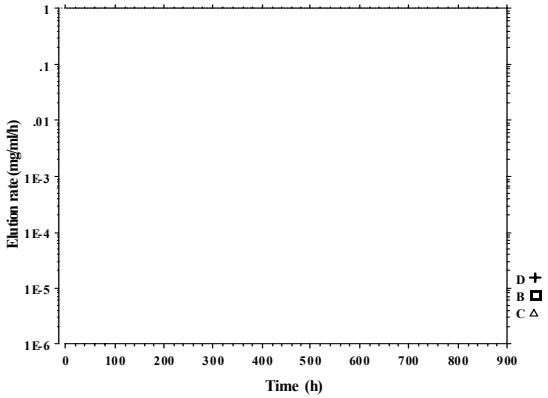

Fig.1. The elution rate over time for the tested formulations.

Pseudomonas aeruginosa were still observed at six days when tested against formulation B. The results of the **static mechanical tests** are shown in figure 2.

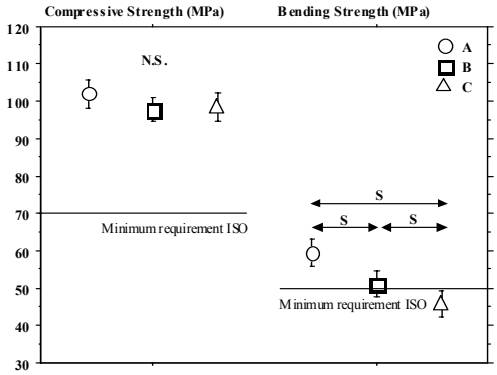

Fig. 2. Compressive and bending strength tests results.

From the **fatigue test** results the endurance limit was estimated and was found to be 9.4MPa for the control, 9.0MPa for formulation B and 8.3MPa for formulation C. A significant difference was found only between formulations A and C.

DISCUSSION

The presence of meropenem broadened the antibacterial spectrum and enhanced the elution of vancomycin. The mechanical properties seemed to be negatively affected by vancomycin but not by meropenem. The best compromise would probably be a formulation with 0.5g of vancomycin and 1.0g of meropenem, but further investigation is necessary to confirm this hypothesis.

REFERENCES

1. Cristofolini L et al. FatigueFractureEngMaterStructs 23, 2000.

ACKNOWLEDGEMENTS

Thanks to Tecres SpA (Verona, Italy) for the bone cement

AFFILIATED INSTITUTIONS FOR CO-AUTHORS:

**Banca del Tessuto Muscolo-Scheletrico, IOR, Bologna
***Clinica Ortopedica dell'Università di Bologna
****Comitato Infezioni Ospedaliere, IOR, Bologna

ANALYSIS OF LIVING CELLS GROWN ON TITANIUM BY REAL TIME CLSM

Uggeri J, Gatti R, Orlandini G, Belletti S, Galli C, Scandroglio R, Guizzardi S
Department of Experimental Medicine – Section of Histology, University of Parma, Parma – Italy
jacopo.uggeri@unipr.it

INTRODUCTION

A crucial issue in the study of new biomaterials is to assess what actually happens at the cell/implant interface. Scanning electron microscopy and atomic force microscopy allow the simultaneous visualization of cells and surrounding biomaterial, although on fixed samples.
Recently, confocal laser scanning microscopy (CLSM) has provided high resolution images of the structures involved in cell adhesion to the substrate. This type of approach has been developed mostly on fixed samples although confocal microscope allows also the real time visualization of living cells. In this paper we introduce a newly designed flow chamber for time lapse observation of living cells grown on a given substrate in a controlled microenvironment. To test the system, we have employed osteoblasts seeded onto two differently finished titanium surfaces and loaded alternatively with the vital fluorescent probes Calcein-AM and Tetramethylrhodamine methyl ester (TMRM).

MATERIALS AND METHODS

Titanium disks (cpTi-OR-Vit Castelmaggiore - Bologna) with two different types of surface were employed: Smooth surface (SS) and Sand blasted surface (SLA) treated with 60 µm Ø ZrO2 particles.
Human jaw osteoblasts were seeded at $5x10^4$ cells/cm^2 onto titanium disks in standard culture medium.
Confocal system employed in this study was the LSM 510 Meta scan head integrated with the Axiovert 200 M inverted microscope (Carl Zeiss, Jena, Germany).
A flow chamber, which is an adaptation of a previous one (Orlandini *et al.*, 1999), was designed specifically to carry out real time images acquisition of living osteoblasts grown on biomaterials. The whole device was lodged on the microscope stage inside a microincubator, where culture conditions were kept constant during experiments (pH 7,4, temp. 37°C, 5% CO_2).
To assess cell adhesion, shape and viability, living cells were loaded with 2 µM Calcein-acetoxymethylester (Calcein-AM) (Gatti *et al.*, 1998). For mitochondria visualization, they were loaded in complete medium with 100 nm Tetramethylrhodamine methyl ester (TMRM).
Image acquisition was carried out in multitrack mode namely through consecutive and independent optical pathways. Vertical sections were obtained by scanning repeatedly a single line of the frame in sequential steps along the z axis.

RESULTS

Titanium surface was obtained by reflection of the 633 nm laser line. The SS actually showed the presence of shallow and parallel grooves.
Calcein loading allowed a clear visualization of living cells grown on titanium disks. The dye provides a whole view of the cell shape: cells grown on SS were spindled and orderly arranged in parallel rows, otherwise those grown on SLA were unevenly clustered, with irregular morphology, polygonal shapes and higher cell density.
The simultaneous visualization of the signals from material and cells showed that cells grown on SS followed the direction of the grooves on the titanium while cells grown on SLA fitted their shape to the underlying topography of the support.
Three-dimensional reconstructions clearly visualize the cell/titanium relationship. Cells grew on SS were flat and scattered while those on SLA were taller and globular. Cytoplasmic processes of the latter branched from the bodies anchoring over the peaks and often bridging over the hollows of the material. In vertical section the microgrooves of the SS appeared as multiple little spikes between the fluorescent cell profiles.
Mitochondrial staining by the vital, potentiometric dye TMRM showed the typical filamentous network of polarized mitochondria surrounding a central negative nucleus. Density, shape and polarization of the mitochondria was very similar both in cells grown on SS and on SLA.

DISCUSSION

In this study we have combined reflection-CLSM and fluorescence–CLSM for the real time, simultaneous visualization of the material surface and living cells. The system provides more detailed information about cell shape and titanium morphology as compared to scanning electron microscopy, a technique that requires fixation and metallization with inherent incidental potential artifacts. Moreover confocal microscopy provides vertical scans of the sample, allows to visualize planes within the cell and shows the surface beneath them. CLSM implemented with the specifically designed flow chamber proved reliable and effective in the morphological analysis of living osteoblasts grown on opaque, thick supports, thus representing a promising tool for real time long term observation. Finally the use of specific functional fluorophores allows to monitor, also quantitatively, a series of cell parameters under basal or stimulated conditions.

REFERENCES

Orlandini G, *et al.* (1999). *Methods Enzymol* 307:340-50.
Gatti R, *et al.* (1998). *J Histochem Cytoch* 46(8):895-900.

CHARACTERIZATION OF WEAR DEBRIS OF POLYETHYLENE HYLAMER INSERT GAMMA IRRADIATED IN AIR

*Visentin M, *Stea S, *Bordini B, *De Clerico M, °Squarzoni S, ^Reggiani M, ^Fagnano C^, *§Toni A
*Laboratorio di Tecnologia Medica, Istituti Ortopedici Rizzoli, Via di Barbiano 1/10, 40136 Bologna, Italy

visentin@tecno.ior.it

INTRODUCTION

Hylamer polyethylene insert was used in the early 1990's to make hip joint components and, compared with traditional UHMWPE, claimed to have doubled elastic modulus, increased compressive and tensile strengths and greater resistance to crack propagation and creep. Based on favorable pre-clinical evaluations, Hylamer was preferentially selected by surgeons.
Clinical experience has shown that Hylamer insert if sterilized by gamma rays in the presence of oxygen, are easily affected by wear, which leads to osteolysis.
The aim of this study was to analyze the morphology of Hylamer polyethylene wear debris with wear debris from traditional polyethylene inserts sterilized by the same method.

METHODS

-Periprosthetic tissue was obtained from :
7 patients with Hylamer inserts gamma sterilized in air (Duraloc cup, Depuy Orthopedics, Indiana, USA)
6 patients with traditional UHMWPE (PCA cup, Stryker Howmedica, New Jersey, USA) sterilized by the same method .
-Joint capsule biopsy was paraffin embedded.
-20 micron thick slices were placed onto the polycarbonate (size pore 0.2 micron) filter placed onto a polypropylene holder.
-Slice were de-waxed and digested with hypochlorite.
-Double distilled water was flushed through the filter.
-Filters were observed by SEM at 10.000X.
-Particles were counted and measured.
-Comparisons between the means of the number of particles and their shape descriptions were made by Student's t test, or the Kolmogorov–Smirnov test according to the variance of data.

RESULTS

Sections of the newly formed joint capsule were characterized by the presence of a fibrous layer of variable thickness, many mononuclear phagocytes and sometimes a few giant cells. The frequency distribution of globular and fibrillar particles was similar in both groups. The globular particles in the Hylamer samples had a mean area of 0.12 micron^2, which was significantly less than that of controls (0.30 micron^2) (Tab.1). The width of fibrillar particles in the Hylamer samples was significantly lower than that of controls. (Tab.2)

Tab.1 Size of globular particles

	measured particles	Area (μm^2)	Length (μm)	Width (μm)
Hylamer	318	0.12±0.23	0.35±0.31	0.22±0.17
Traditional UHMWPE	123	0.30±0.54	0.63±0.39	0.37±0.22
P value		S	S	S

Tab.2 Size of fibrillar particles

	measured particles	Area (μm^2)	Length (μm)	Width (μm)
Hylamer	509	0.70±0.91	2.05±1.93	0.28±0.16
Traditional UHMWPE	149	1.14±2.21	1.98±2.07	0.39±0.29
p value		NS	NS	S

DISCUSSION

The two materials, despite undergoing the same type of sterilization, produced different types of wear, connected to their different properties. The difference in morphology of Hylamer polyethylene wear particles in comparison with traditional UHMWPE might have caused a more intensive biological response, early and massive osteolysis, and therefore, early loosening.

AFFILIATED INSTITUTIONS FOR CO-AUTHORS:
° ITOI – CNR, Unità di Bologna c/o Istituti Ortopedici Rizzoli, Bologna, Italy
§ I Divisione di Ortopedia e Traumatologia, Istituti Ortopedici Rizzoli, Bologna, Italy
^ Dipartimento di Biochimica G. Moruzzi – Sez di Chimica e Propedeutica Biochimica,Bologna, Italy

INFLUENCE OF SURFACE PROPERTIES OF CALCIUM PHOSPHATE COATINGS ON REPARATIVE REGENERATION OF BONE

Karlov AV, Khlusov IA, Druzhinina TV, Makienko IA, Popov VP

The Center of Orthopaedy and Medical Material Sciences of
the Tomsk Scientific Center of Siberian Branch of the Russian Academy of Medical Sciences
The Tomsk branch of the G. A. Ilizarov RSC "RTO"
Tomsk, Russia
orthop@rambler.ru

INTRODUCTION

Various materials (polymers, ceramics, composites) find the wide use in medicine. The specially attention is paid in traumatology to calcium phosphates, natural metabolites and regulators of bone tissue having the maximal biocompatibility and ability to integrate with bone tissue. However, up to now significance of structural and chemical properties of biomaterials for their interaction with organism tissue is not determined.

METHODS

Influence of osteosynthesis implants with different surfaces (metallic – ceramic, calcium phosphate ceramics) on reparative osteogenesis have been studied in *in vivo* experiments. ^{99m}Tc-pyrophospat in fractured femurs of 26 rats was determined in 45 lays after intramedullary introducing of implants.

RESULTS

Results show that different structure of implant surface determined coating degradation degree and, in turn, level of bone tissue reactions on intramedullary osteosynthesis. Distribution of ^{99m}Tc pyrophosphat is evidence, in certain degree, of bone tissue reparation vector. Bionert implants do not influence on regeneration in the fracture area. Bioactive implants with dense calcium phosphate coating on the contrary promote local regeneration of fractured extremity. At this X-ray amorphous layers intensify reparative processes in distance from the site of introducing of pins.

Crystallization of a coating promotes to direct regeneration vector in the fracture area (one of introducing of implant). Presence of calcium phosphate ceramic coating on implants defines triggering both local and system reparation leading to considerable deposition of ^{99m}Tc pyrophosphate both in fractured and healthy femur.

DISCUSSION

Obtained data can form basis for:

- firstly – to search coatings which combine by optimal way biological, physical - chemical and mechanical characteristics;
- secondly: to reveal the scope of clinical application of each type of implant (traumatology, orthopaedy on background of local or system osteoporosis, lowered consolidation, non-knitting fractures, false joints etc.);
- thirdly: to form the set of implants for actual clinical situations on the basis of individual characteristics of their surface.

FEMORAL CEMENTING TECHNIQUES FOR HIP RESURFACING ARTHROPLASTY

*Bitsch RG, **Loidolt T, *Heisel C, **Schmalzried TP
*University of Heidelberg, Germany

rbitsch@ix.urz.uni-heidelberg.de

INTRODUCTION

There are numerous reports on cementing techniques for conventional total hip prostheses, acetabular cup fixation and for knee prostheses. A 2-5 mm-depth of cement penetration into cancellous bone is believed to be optimal. Depths of 5 mm and more would likely lead to thermal necrosis of bone.

There is a paucity of information regarding cement fixation of femoral resurfacing prostheses. We developed a laboratory model to analyze differences in cement penetration, cement pressures and interface temperatures for resurfacing arthroplasty.

MATERIALS AND METHODS

We used 25 open-cell, reticulated carbon foam specimens with the same geometry as the prepared femoral head for resurfacing (ASR™ system, Size 49, DePuy; Leeds, England) to approximate bone. Custom aluminum shells were made with the same inner geometry as the femoral resurfacing components.

Analyses of five different cementing techniques were performed using high viscosity (HVC) (Smart Set GHV, DePuy, Blackpool, England) and low viscosity cement (LVC) (Endurance, DePuy, Blackpool, England): 1) use of an applicator prototype with HVC, 2) manual application and filling of one quarter of the component with LVC, 3) manual application and filling of one quarter of the component with HVC, 4) filling of half of the component with LVC, 5) filling of half of the component with HVC.

A force of 150 N was used to press five shells in each cement technique group on foam specimens. During seating, cement pressures at the top, the chamfer and at the outer wall of the femoral components were measured. Temperatures were measured 5 and 15 mm under the foam surface.

Specimens were cut into quarters, surfaces were digitalized and cement penetration areas and depths were quantified using a pixel-analysis-software. Pixel analysis was run twice for each specimen. First, area of cement penetration 3 mm deep from the foam surface was analyzed. Then the overall area of cement penetration was measured. Group comparisons were done with an ANOVA using SPSS for Windows 12.0 (SPSS Inc., Chicago, Illinois).

RESULTS

None of the components was completely seated for half component HVC (technique 5). These components had a mean cement cap thickness of 6.3 mm. Average pressures at the top and chamfer area were higher for the use of HVC than for LVC. The highest pressure at the top was 1.1 ± 0.08 and at the chamfer was 0.9 ± 0.05 bar for technique 5. Cement pressures at the outer wall showed no significant difference for the cementing techniques.

The duration of temperatures over 50 °C five mm below the foam surface were 253 ± 28, 123 ± 13, 321 ± 16, 237 ± 18 sec for technique 2, 3, 4 and 5. The shortest time, 120 ± 25 sec was observed using technique 1.

The highest cement penetration in the 3 mm thick outer fixation area was 76 ± 6 mm^2 for technique 1, followed by 60 ± 10 mm^2 for technique 3. Cement penetrations for techniques 2, 4 and 5 were 41 ± 14, 45 ± 12, 46 ± 9 mm^2 respectively. Techniques 4 and 5 did not allow the cement to reach the lower-outer edges of the foam. The highest cement penetration in the interior area deeper then 3 mm was 123 ± 20 mm^2 for half component LVC (technique 4). The interior penetrations areas were 70 ± 6, 54 ± 23, 59 ± 10 and 61 ± 18 mm^2 for techniques 1, 2, 3, and 5.

DISCUSSION

Component filling cementing technique 4 resulted in variable degrees of over-penetration of the interior area and a lack of cement at the lower-outer edges of the foam under the resurfacing components. This caused exposure to high temperatures which can cause bone necrosis. Technique 5 showed incomplete seating, which has been associated with early fracture. Manual technique 3 and technique 1, both with high viscosity cement, showed advantages in our model. It was possible to reach high cement contents in the outer fixation area without the negative effects of interior area penetration.

ACKNOWLEDGEMENTS

This study was supported by DePuy (Leeds, GB) with cementation materials.

AFFILIATED INSTITUTIONS FOR CO-AUTHORS:

**Joint Replacement Institute, Los Angeles, USA

A STRUCTURAL ENGINEERING APPROACH TO BONE MATERIAL BEHAVIOUR AND FAILURE

*Donohoo SM, *Hogg M, ***Kohan L, ***Gillies RM
*WorleyParsons Advanced Analysis, L1, 95 Nicholson Street, St Leonards, Sydney, NSW 2065, Australia
Mark.Gillies@WorleyParsons.com

INTRODUCTION

Reinforced concrete is a commonly used building material. The overall dimensions of structural beams and columns, the concrete material properties, and the distribution of reinforcing material result in different section capacities. These sections need to be able to withstand different combinations of axial and bending loads. To evaluate the suitability of different design options, the non-linear capacity of the section is expressed in terms of an "interaction diagram" or design envelope. Bone is a composite material comprising a mineral phase (compressive loading) and an organic phase (tensile loading). Bone is also subjected to load combinations through normal daily activity (working loads), and in some cases extreme or ultimate load conditions such as stumbling where the loads may be up to nine times body weight [1, 2]. This study has investigated the applicability of this approach in developing load envelopes for the evaluation and performance comparison of different joint replacements using the finite element method and an interaction diagram.

METHODS

CT scans were used to reconstruct the femur geometry. A 3D finite element mesh was created using PATRAN (MSC Software, Santa Ana, CA). The femur was reconstructed with a Birmingham hip replacement (BHR) (Smith & Nephew Inc, Memphis, TN) (Fig 1.) The femur was then loaded and an analysis was carried out using the finite element method. The following process is then taken:

Figure 1

- A critical section of bone is selected and is discretised into many points.
- The bone density at each point is assigned.
- A non-linear stress strain relationship is assigned to each bone density
- Strain levels are assigned to the periosteal surface of the cortex and at other points these are calculated using interpolation.
- Stress and corresponding forces and moments are calculated based on the assigned strains.
- A working stress envelope providing axial and bending action is developed for any chosen bending axes
- An ultimate stress level is then determined for the chosen bending axes.

RESULTS

Figure 2 presents the cut section point location planes.

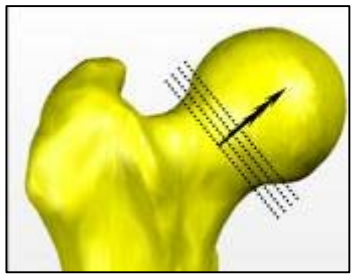

Figure 2

Figure 3 presents an example plot of the interaction diagram. This illustrates an envelope for bending occurring in the coronal plane.

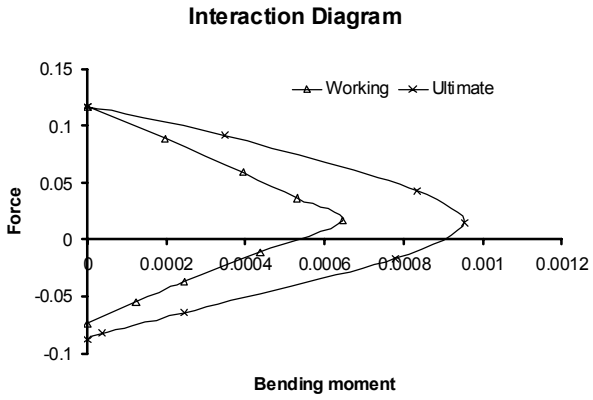

Figure 3

DISCUSSION

Applied loadings with different regular daily activities, such as walking, standing up, jogging, can be mapped against the working stress envelope

Extreme loadings, such as stumbling, can be mapped against the ultimate limit state curve.

Factors of safety or "unity checks" will be calculated for the different events.

REFERENCES:

1. Bergmann, G., *et al.*, J Biomech, 1993. **26**(8): p. 969-90.
2. Bergmann, G., *et al.*, Langenbecks Arch Surg, 2004. **389**(1): p. 53-9.

** Orthopaedic & Traumatic Surgery, University of Sydney, Royal North Shore Hospital, Sydney, Australia
*** Joint Orthopaedic Centre, Sydney, Australia

CRACK SURFACE INVESTIGATION OF COMMERCIAL TYPES OF BONE CEMENT

*Erani P, **Cotifava M, *,***Cristofolini L, **Bignozzi MC, *Baleani M

*Istituti Ortopedici Rizzoli, Laboratorio di Tecnologia Medica
Via di Barbiano, 1/10 – 40136 Bologna, Italy
cristofolini@tecno.ior.it

INTRODUCTION

Clinical *ex-vivo* assessment is very important to evaluate the quality of an orthopaedic implant. In retrieved implants, several types of cracks are observed, some of them possibly generated by the surgeon during stem extraction. In this work, the effect of different types of propagation on the aspect of the crack surface was investigated. The aim was to define a procedure that could discriminate between surgeon artifact and fatigue crack in acrylic cements.

METHODS

Six cement types were investigated: Simplex P, Cemex RX, Cemex Isoplastic, Cemex System, Cemex Genta, Fluoride Bone Cement.

Thirty specimens (five per cement type) were prepared following ASTM-E647. Fatigue crack propagation tests were performed (sinusoidal zero-tensile load, ramping up to 60N, frequency 4Hz). During cyclic tests, crack gages accurately measured crack length and propagation rate (mm/cycle) [1].

Based on crack-surface appearance, three consistent regions were identified, depending on propagation rate: 1) slow-cyclic propagation (from crack initiation to 10^{-5} mm/cycle); 2) fast-cyclic propagation ($10^{-3} \div 10^{-2}$ mm/cycle); 3) final sudden fracture (until the end of the specimen).

Crack surfaces were observed using reflected light microscope, cracked beads were counted per area unit in each region. Specimens were gold-sputter coated and inspected using SEM. Moreover the roughness of the crack surface was measured.

The same analysis were applied to two retrieved cement mantles (Cemex System cement – unknown cement). Data were compared with *in-vitro* results.

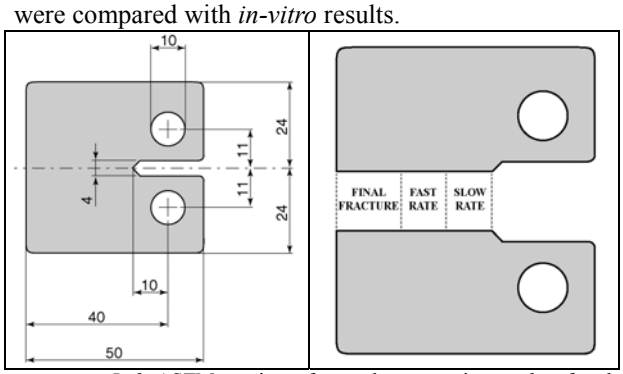

Fig. 1 – *Left:* ASTM specimen for crack propagation*; right:* after the mechanical test, different regions of crack propagation

RESULTS

In-vitro results: optical observations and roughness measures (Ra) showed consistent differences between "slow" and "fast" propagation regions for all cement types. Final sudden fractures had an inconsistent appearance between cement types (ANOVA, $p<<0.05$).

Ex-vivo results: cracks of a Cemex System mantle were compared with *in-vitro* results of the same cement. Most of the cracks were classified as sudden fracture. Conversely, classification was impossible for retrieved cement mantles made of unknown cement.

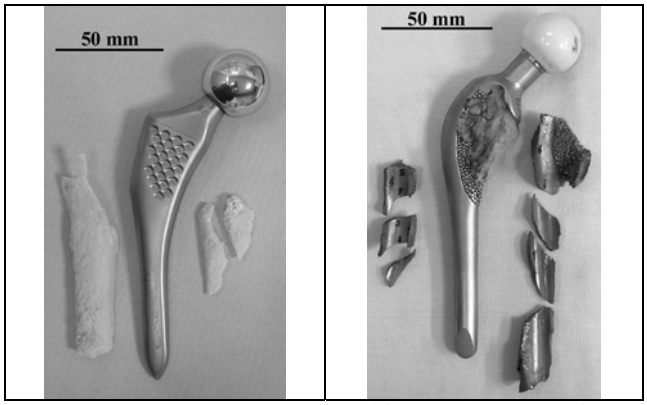

Fig. 2 – Retrievals: two stem types with parts of cement mantle

DISCUSSION

The difference between fast-cyclic crack and final fracture for Simplex-P is in agreement with Topolesky [2]. Conversely the fast-final fracture change is different in other cement types. Additionally, we observed a consistent (statistically significant, ANOVA, $p<<0.05$) transition from slow to fast growth for all cement types.

The comparison between *in-vivo* and *ex-vivo* results was fruitful for known-cement mantle: a large number of cracks was classified as surgical artifacts. It will be necessary to extend this study to more well-known retrievals to validate this procedure. Classification remains impossible for retrievals made of unknown cement types.

REFERENCES:

[1] Baleani M. *et al.*, Bone cement and cemented fixation of implants, edited by Pipino F., 2001.

[2] Topolesky L.D.T. *et al.*, Biomat., 1993.

OTHER AFFILIATED INSTITUTIONS:

**University of Bologna, Engineering Faculty. V. Risorgimento 2, 40136 Bologna, Italy. Fax +39 051 2093412. E-mail: luca.cristofolini@unibo.it

ACCELERATED CORROSION TESTING OF A MODULAR ACETABULAR CUP: AN INVESTIGATION OF LOADING FREQUENCY

*Gillies RM, **Bush A, **Payten W, ***Sekel R, *Appleyard RC
*WorleyParsons Advanced Analysis, L1, 95 Nicholson Street, St Leonards, Sydney, NSW 2065, Australia
Mark.Gillies@WorleyParsons.com

INTRODUCTION

Modularity of total hip replacement (THR) designs has become a primary concept used in total hip arthroplasty. Corrosion at the modular interfaces is, however, evident at these interfaces as seen in retrieval analyses [1]. It has been shown in retrieval analyses that both mixed (CoCrMo-Ti6Al4V) and similar (CoCrMo-CoCrMo & Ti6Al4V-Ti6Al4V) material couples have corrosive attack occurring at the interfaces [1] illustrating that the corrosive attack is not just solely due to mixing of the dissimilar materials. Mechanical fretting occurring at the modular interface is playing a role by breaking down the oxide film and setting into place the mechanical-electrochemical interaction. This project investigated the mechanical fretting and chemical corrosion in an artificial environment.

METHODS

Twelve modular acetabular components were assembled with a ceramic and polyethylene (PE) bearing (CeramTec AG, Polchingen, Germany & Poly Hi Solidur, Fort Wayne, IN), cobalt chrome adapter ring and dome and titanium alloy acetabular shell (Equator plus, Portland Orthopaedics, Sydney, Australia) (Fig 1). The modular

Figure 1. Schematic of ceramic (L) and PE (R) liner modular combinations

components were then mounted in a jig specially designed to hold the acetabular cups at the correct orientation (stem oriented in accordance with ISO 7206-4 and the cup at 45º of inclination) and to load without causing buckling of the femoral component. Mechanical testing was carried out in Ringers solution at 50ºC at a pH of 3.5 The solution covered the entire construct allowing fluid ingress into the rear of the acetabular cup system. The servo-hydraulic testing machine (MTS 858 Bionix, MTS Systems, MN) was run in load control mode to apply 10 million cycles at a frequency of 5Hz for the ceramic liner combination and 10Hz for the PE liner combination. The range of loading was between 400N and 4000N (R = 0.1) [2]. At the completion of the testing, the components were immersed in distilled water and then ultrasonically cleaned for 30 minutes. The modular interfaces were examined visually, optically and also by scanning electron microscopy. The condition of the modular interfaces was classified on a scale from 1-6, where (1 = No Fretting, Corrosion, or Discoloration of Contact Surfaces) (2 = Fretting < 10% of the Contact Surface, Debris on the Contact Surface) (3 = Fretting > 10% of the Contact Surface, Debris on the Contact Surface) (4 = Chemical Etching of Structure, Fretting, Debris on the Contact Surface) (5 = Corrosion Pits and Fretting, Debris on the Contact Surface) (6 = Severe Corrosion (>50% surface area eroded), Fretting, Debris on the Contact Surface)

RESULTS

Each of the samples were classified according to the scale 1-6 following cleaning and sectioning, and are presented in table 2.

Table 2

5Hz	Cup	Adapter	10Hz	Cup	Dome
#1	2	2	**#7**	3	3
#2	2	2	**#8**	2	3
#3	3	2	**#9**	1	2
#4	1	1	**#10**	2	2
#5	2	2	**#11**	1	1
#6	3	2	**#12**	1	1

DISCUSSION:

Generally, all the modular interfaces show mechanical fretting to a range of 2 for both loading frequencies. There were no large quantities of particulates generated. There was no indication of the modular interfaces being at risk of failure due the harsh environment and loading regime. The accelerated corrosion ratings show that the in-vivo environment will have no effect on the taper interfaces and will not be of clinical concern for either of the designs. Cook et al [3] found no correlation between time *in-vivo* and the corrosion of an implant. The protocol used for this testing produces surface morphological changes representative of observations reported.

REFERENCES

[1] Gilbert, J.L. and J.J. Jacobs, ASTM STP1173. 45-59.
[2] Bhambri, S. and L. Gilbertson, ASTM STP 1173. 146-156.
[3] Cook, S.D., R.L. Barrack, and A.J. Clemow, JBJS Br, 1994. **76**(1): p. 68-72

**Australian Nuclear Science & Technology Organisation (ANSTO), Lucas Heights, NSW 2234, Australia
***Portland Orthopaedics P/L, Sydney, Australia

FRACTOGRAPHY OF FAILED SILICONE METACARPOPHALANGEAL PROSTHESES

Joyce T J
Centre for Rehabilitation and Engineering Studies, School of Mechanical and Systems Engineering,
University of Newcastle upon Tyne, Newcastle upon Tyne, UK
t.j.joyce@ncl.ac.uk

INTRODUCTION

The replacement of finger joints lacks the long-term clinical success associated with hip and knee prostheses. The most commonly implanted type of finger prosthesis consists of single-piece silicone designs such as the Swanson and the Sutter [1]. Such designs act as flexible spacers around which a process of encapsulation can occur. A recent long-term study stated that, at an average of 14 years after surgery, Swanson metacarpophalangeal (MCP) prostheses showed a fracture rate of 67% compared with 52% for Sutter MCP prostheses [2]. A 2005 paper reported that, at 2 years follow-up, the fracture rates were 13% and 20% respectively for these two designs [3]. If a better understanding of the nature of fracture of these implants was obtained, perhaps such high fracture rates could be reduced.

MATERIALS AND METHODS

Twelve Sutter MCP prostheses were obtained from three hands (two dominant) of two women and one man who were aged 56-66 years at time of surgery [4]. They were retrieved at a mean of 42 (range 32-53) months following implantation. All patients had rheumatoid arthritis. Of the twelve explanted prostheses, eleven had fractured, ten completely. These fractured prostheses were visually examined and were then sliced so that, after washing and gold-coating, the two fracture faces of each prosthesis could be examined using a Hitachi S-4700 scanning electron microscope (SEM).

RESULTS

Figure 1 shows the four prostheses retrieved from the hand of one patient. The uppermost prosthesis has not fractured and therefore indicates what an undamaged Sutter prosthesis looks like.

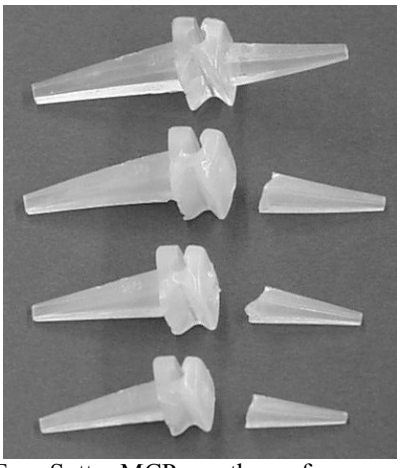

Fig 1: Four Sutter MCP prostheses from one patient

All of the ten total fractures occurred at the junction of the distal stem and the hinge. Visual inspection showed that the initial point of fracture was on the dorsal aspect of the prosthesis, indicating that fracture was due to the subluxing forces seen in rheumatoid MCP joints. Also, as revealed in figure 1, it appears that the crack began distally and traveled gradually in a proximal direction. Some faces showed classic features of fatigue fractures, as exposed in figure 2, including radial marks (A) indicating the origin of fracture on the dorsal aspect towards the radial side, beach marks (B) signifying that fatigue crack propagation advanced in an arc, and a shear lip (C) on the palmar aspect indicative of the point of final fracture. Therefore, it appeared that the crack direction was from radial to ulnar, and from dorsal to palmar. However, when all of the fracture faces were examined by SEM, a great deal of variation was seen.

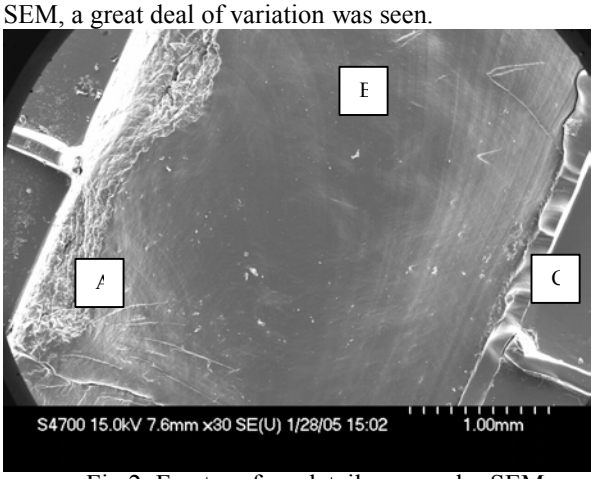

Fig 2: Fracture face detail seen under SEM

DISCUSSION

Despite 158 SEM images being analyzed, further explants would be desirable before definitive conclusions could be made. The author is not aware of any similar topographical analysis having been undertaken elsewhere on fractured, ex-vivo silicone MCP prostheses. While the time span between fracture and removal of the implant can never be known precisely, so that the 'virgin' fracture face could have been damaged post-fracture, it is still hoped that such ex-vivo analysis can contribute to improve finger prostheses, with the long-term aim of helping patients suffering from crippling hand diseases.

ACKNOWLEDGEMENTS

Mr Rick Milner, Consultant Plastic Surgeon, at the Royal Victoria Infirmary, Newcastle upon Tyne, UK kindly supplied the explanted Sutter prostheses.

REFERENCES

[1] Joyce TJ. Expert Rev Med Devs, 2004; 1(2): 193-204. [2] Goldfarb CA & PJ Stern. J Bone Joint Surg, 2003; 85A(10): 1869-1878. [3] Moller K et al J Hand Surg:, 2005; 30(1): 8-13. [4] Joyce TJ et al. J Hand Surg , 2003; 28B(1): 86-91.

DETERMINATION OF THEORETICAL LUBRICATION REGIMES IN TWO-PIECE FINGER PROSTHESES

Joyce TJ

Centre for Rehabilitation and Engineering Studies, School of Mechanical and Systems Engineering,
University of Newcastle upon Tyne, Newcastle upon Tyne, UK
t.j.joyce@ncl.ac.uk

INTRODUCTION

A range of concepts for metacarpophalangeal (MCP) arthroplasty have been proposed over the years, with single-piece silicone prostheses dominating this market [1]. However, various two-piece designs which tend to aim for a more anatomical solution by having spherical bearing surfaces in a ball and socket arrangement have also been put forward. These have used a range of biomaterial couples including ceramic-on-ceramic (CoC), metal-on-metal (MoM), pyrocarbon-on-pyrocarbon (PyoPy) and metal-on-polymer (MoP) [1]. The aim of this paper was to compare the predicted lubrication regimes for these various biomaterial couples.

MATERIALS AND METHODS

Modeling the ball and socket implant as an equivalent ball-on-plane model and employing elastohydrodynamic theory [2] allowed the minimum effective film thickness to be calculated. In turn the lambda ratios were calculated which allowed the lubrication regime to be identified, as $\lambda < 1$ indicates boundary lubrication, $\lambda > 3$ indicates fluid film lubrication, and between these values mixed lubrication is indicated [3]. The calculations were undertaken for a 2 to 50N range of loading values, a 0 to 30mm/s range of entraining velocities, and a 3 to 10mm radius range of sizes of prosthesis. Other relevant values were taken for the literature [4] [5].

RESULTS

For a typical application of a 7.5mm nominal radius prosthesis, under a 15N load and an entraining velocity of 11.8mm/s, it was found that the CoC and MoM combinations offered the potential of fluid film lubrication with λ ratios of 7.1 and 4.4 respectively, while the PyoPy combination offered mixed lubrication with a λ ratio of 1.9, and the MoP combination fell within the boundary lubrication regime with a λ ratio of 0.2. As can be seen by varying first the entraining velocity (fig 1), then the load (fig 2), then the prosthesis radius (fig 3), the results from greatest to least λ were always CoC, MoM, PyoPy, and MoP.

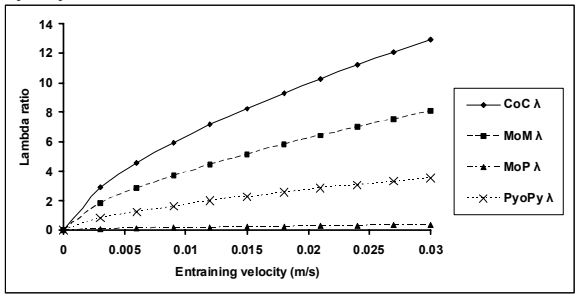

Fig 1: Variation of lambda ratio with entraining velocity

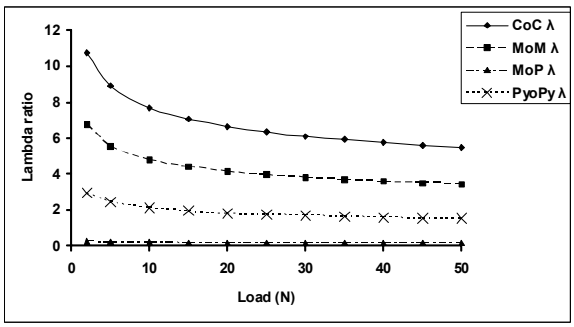

Fig 2: Variation of lambda ratio with prosthesis load

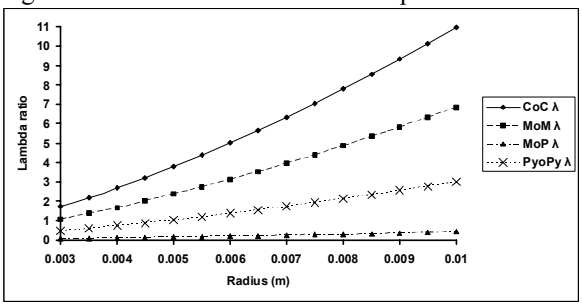

Fig 3: Variation of lambda ratio with prosthesis radius

DISCUSSION

The positive results for CoC, MoM and, to a lesser extent, PyoPy need to be set against recognition that when the finger is not moving the entraining velocity is zero and so surface contact will occur at the articulating surfaces of such two-piece prostheses, with a related potential for wear. Therefore appropriate in vitro testing is required and a recent paper has shown acceptably low wear for a MoP finger prosthesis [6] despite the fact that it likely operates in the boundary lubrication regime. While lubrication theory indicates that, for the prostheses considered, CoC and MoM designs could operate with fluid film lubrication, PyoPy with mixed lubrication, and MoP likely to operate in the boundary lubrication regime, other factors may come into play when choosing a material combination for a finger prosthesis.

REFERENCES

[1] Joyce TJ. Expert Rev Med Devs, 2004; 1(2): 193-204. [2] Hamrock, BJ & D Dowson. Trans ASME. J Lubn Tech, 1978; 100: 236-245. [3] Johnson KL, JA Greenwood & SY Poon, Wear, 1972; 19: 91-108. [4] Scholes SC, A Unsworth & A Goldsmith, Phys Med Biol, 2000; 45: 3721-3735. [5] Smith SL, D Dowson & A Goldsmith, J Engng Tribology, 2001; 215(5): 483-493. [6] Joyce TJ, Rieker C & A Unsworth, Bio-med Matls Engng, 2006; 16(1): 1-10.

DEVELOPMENT OF A BIOMECHANICALLY OPTIMIZED MULTI-COMPONENT FIBER-REINFORCED COMPOSITE IMPLANT FOR LOAD-BEARING CONDITIONS

*Moritz N, *Zhao D, **Mattila R, ***Pasila P, **Lassila L, ***Mäntylä T, **Vallittu P, *Aro HT
*Orthopaedic Research Unit, University of Turku, Finland

niko.moritz@utu.fi

INTRODUCTION

The metallic materials commonly used in orthopaedic surgery for load-bearing applications have mechanical properties different from those of bone. The mismatch of the mechanical properties could lead to high interfacial stresses that may result in failure of the metal implants.

The fiber-reinforced composite (FRC) materials have good biocompatibility and their strength is equal or higher than that of the metallic alloys. The elastic modulus of the FRC materials (14 – 22 GPa) is similar to that of cortical bone. Thus, these materials have the potential to be used as load-bearing implants in orthopaedic surgery.

The goal of this study was to test FRC implants in vivo and by using FEA to develop a mechanobiological model to predict in vivo implant performance. The specific aims of the study were to mimic the treatment of a long-bone fracture or bone metastasis by means of intramedullary implant.

METHODS

As a first step, three-point bending of cadaver rabbit femora, with and without implants, was performed. Prior to the biomechanical tests, cadaver bones were imaged with pQCT to create three-dimensional surface geometries that were further used in ABAQUS CAE to simulate the actual experiments. The elastic material properties, both isotropic and transversely isotropic, were obtained from the literature and semi-empirically. Torsion tests of cadaver rabbit femora were performed to obtain the value of the shear modulus for the semi-empirical transversely isotropic material. Verification of the model was made against load-displacement data and strain gauge data of the bending tests without implants.

Cylindrical Ø 3 mm, 90 mm long intramedullary stem implants were manufactured for the animal study. The implants were slightly curved: the deflection of the middle of the implant was 4 mm. Control implants (n=6) were made of surface-roughened titanium implants. The FRC implants (n=6) were made of EverStick (StickTech Ltd, Turku, Finland) with the surface covered with BAG granules (AbMinCranio™, Vivoxid Ltd, Turku, Finland). Similar implants were used for the in vitro studies with cadaver bones.

Twelve New Zealand White rabbits were used. The animal study protocol was approved by the Provincial State Office of Western Finland.

An oblong defect (width of 20% cortex diameter, length three times the width) with rounded ends was created in the anterior aspect of the femur shaft. The medullary canal was hand-reamed. The intramedullary stem implant was then introduced into the medullary canal. After 12 weeks the bones were harvested and analysed using CT-imaging (pQCT, MicroCT), biomechanical testing in torsion, and histomorphometry.

RESULTS

FEA modelling of the in vitro tests of long bones was challenging, still reasonable correlation to experimental data was obtained.

In the in vivo study, none of the control femurs (n=6) with titanium implants fractured. In the FRC group one third of the femurs fractured. Implants were intact and complete defect healing occurred in all cases. In biomechanical test, under torsional loading, no significant differences were observed between the groups and also compared with intact bones. New cancellous bone formation was observed at the interface of the implants in both groups. MicroCT imaging after torsional loading indicated the failure of bone-implant interface in titanium implant group. In the FRC group failure occurred in the newly formed periimplant cancellous bone.

DISCUSSION

The failures of the femurs with the FRC implants seemed to result from excessive load at the initial stage after the implantation. Thus, further development of the FRC implants is needed. Comparison of failure modes with results of FEA modelling could give further insight into the problem. The BAG coating of the FRC implants was efficient in providing new bone attachment. When bioactive component that provides bone attachment, is resorbed, bone can further grow into the voids left by glass granules providing morphological fixation and thus the long-term stability of the implant.

ACKNOWLEDGEMENTS

This study was supported by the National Technology Agency, Finland

AFFILIATED INSTITUTIONS FOR CO-AUTHORS:

**Biomaterials research, Institute of Dentistry, University of Turku, Finland
**Institute of Materials Science, Tampere University of Technology

PREPARATION AND CHARACTERIZATION FO NOVEL BIOABSORBABLE PHOSPHATE GLASS FIBRE—POLY(ε-CAPROLACTONE) COMPOSITES

Yang J, Jones IA, Walker G, Rudd CD
Composites Research Group, School of M3,University of Nottingham, Nottingham, UK
mailto:itxjy4@nottingham.ac.uk

INTRODUCTION

Phosphate glasses and poly(ε-caprolactone) have been proven degradable and biocompatible in literatures. Composites of these two materials have been emerging as a possible way of creating degradation-controlled materials with potentials for use as hard tissue replacements such as cranio-maxillofacial implants. In this study, new bioabsorbable phosphate glass fibre reinforced poly(ε-caprolactone) composites have been prepared and characterized.

MATERIALS AND METHODS

Phosphate glass fibres based on $(Na_2O)_{0.2}(MgO)_{0.24}(CaO)_{0.16}(P_2O_5)_{0.4}$ system were produced using a laboratory scale fibre drawing rig and chopped into short fibres to make random phosphate glass fibre veils by using a paper making process. Phosphate glass fibre veils were stacked with poly(ε-caprolactone)(PCL) films to make composites using a hot press process. 3-point bending tests were carried out to measure the flexural properties of composites. A degradation study was carried out to investigate the water uptake and flexural properties change of these composites and PCL in distilled water at 37°C. The effect of annealing and surface treatment on these fibres was studied by comparing the flexural properties and observing the facture surface using SEM.

RESULTS

Phosphate glass fibres were dispersed and evenly distributed to form a web structure (see figure 1).

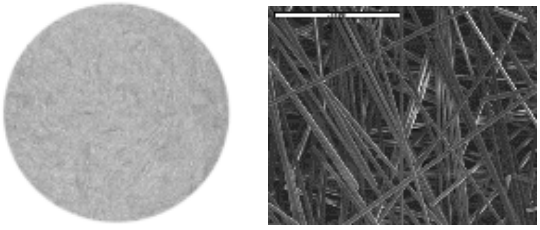

Fig. 1. Formation of phosphate glass fibre veil: whole view(left image) and microstructure(right image).

The composite modulus increased with increasing fibre content, although the composite strengths decreased with the increasing fibre content (see figure 2).

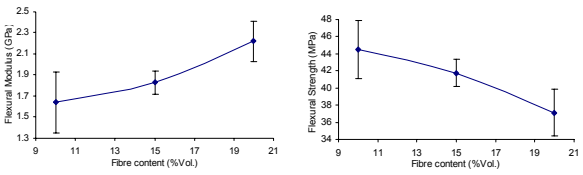

Fig. 2. Fibre content versus flexural properties.

All composites experienced weight increase and then gradually decreased during the degradation period (see figure 3).

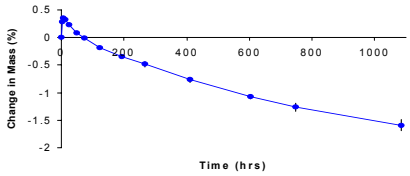

Fig. 3. Change in mass of composites over time.

Composites experienced significant loss in modulus values whereas PCL maintained its original modulus (see figure 4).

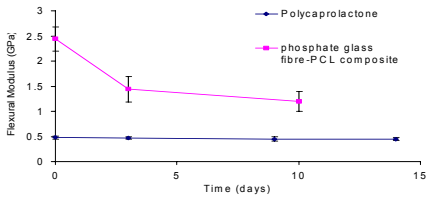

Fig. 4. Modulus behaviour of composites over time.

Fracture morphology showed that the annealed fibres degraded much slower than the non-annealed fibres. SEM pictures showed strong evidence of fibre solubilization for the non-annealed fibres, however the annealed fibres still kept their shapes and did not show any visible sign of fibre degradation (see figure 5).

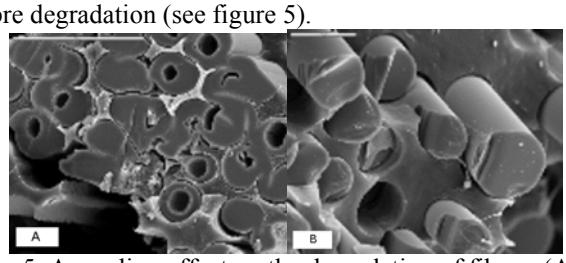

Fig. 5. Annealing effect on the degradation of fibres: (A) non-annealed fibres after degradation, (B) annealed fibres after degradation.

Composite with sized fibres were found to have a better adhesion between the fibre and matrix and more resistant to moisture, but after one week immersion in water, the bonding was deteriorated.

CONCLUSIONS

The results have showed that by varying the fibre content and treatments it is possible to produce a biomaterial whose properties may be tailored. More comprehensive work needs to be done to investigate ways to manipulate the degradation behaviour.

A SIMPLE DEVICE TO PRE-CONDITION THE SOFFIX ACL CONSTRUCT. CAN IT IMPROVE THE BIOMECHANICAL PROPERTIES?

*Sharif K, *Mowbray MASM, **Shelton, J
Mayday University Hospital, Croydon, UK

Khalidsharif2005@yahoo.co.uk

INTRODUCTION

The effects of preconditioning on ACL grafts is controversial. The aim of this research work was to test the effectiveness of a simple instrument which is theatre compatible to precondition the soffix tendon constructs used for ACL reconstructions and its ability to improve the biomechanical properties.

MATERIALS AND METHODS

Cadaveric specimens of equine extensor tendon models were used. approved by the institutional review board at Queen Mary's college. Five constructs of tailored equine extensor tendon and soffix animal models were cyclically loaded 3000 times without preconditioning and were then tested to failure using a sensitive hydraulic testing machine. Another five were preconditioned using a devise consisting of an Omega pneumatic cylinder and a through the hole force transducer and then cyclically loaded using the same testing machine. The preconditioning force used was 500N for a period of one minute The creep and ultimate tensile force were measured and compared.

RESULTS

The mean creep after 3000 cycles was reduced from 14mm without preconditioning to 4.2mm after using the device. The mean ultimate tensile strength was increased from 1250 to 1400N P> 0.05

DISCUSSION & CONCLUSION

Although human tendon was not used the double stranded tailored equine tendon graft has been found to correspond to the quadruple hamstring graft in a previous study. Preconditioning hamstring tendons with this novel theatre compatible devise improves the biomechanical properties by reducing creep without adverse effects on the ultimate tensile strength.

AFFILIATED INSTITUTIONS FOR CO-AUTHORS
**University of London, Queen Mary's College

THE EFFECTS OF IRRADIATION AND ARTIFICIAL AGING ON THE WEAR BEHAVIOUR OF UHMWPE

*Zavalloni M, *Affatato S, *Leardini W, **Taddei P, **Fagnano C, ***Toni A
*Laboratorio di Tecnologia Medica, Istituti Ortopedici Rizzoli, Bologna, Italy

affatato@tecno.ior.it

INTRODUCTION

Ultra-high-molecular-weight-polyethylene (UHMWPE) for hip implants can present serious clinical problems: the cyclic nature of the contact stresses at the articular surface can lead to pitting, delamination and crystallinity changes of the polymer with formation of PE debris, which may lead to extensive bone loss around the implant and consequently osteolysis and implant loosening.
The effects of different sterilization methods have been studied by various authors, but no one produced a full conclusive verdict (1,2). To assess long term stability of polymers, various accelerated aging methods have been developed. In this study, an internal protocol was developed to evaluate the effects of the accelerated aging on wear.

METHODS

Three EtO-sterilised and six gamma-irradiated (standard 3 Mrads dose in air) UHMWPE acetabular cups (Chirulen GUR 1050, POLY HI SOLIDUR, France) were aged in air at 80°C for 4 weeks and thereafter tested in conjunction with nine 28-mm CoCrMo femoral heads.
Wear tests were carried out using a 12-station hip joint simulator (Shore Western, USA) run for 3 million cycles, with bovine calf serum as lubricant. A frequency of 1 Hz, according to the rotation test frequency, was applied with a sinusoidal load having a peak magnitude of about 2 kN.
Wear behaviour was evaluated by gravimetric measurements and Raman analysis. Since Raman spectra reflect PE morphology, Raman spectroscopy was used to investigate the crystallinity changes induced by aging and wear testing. Micro-Raman spectra were obtained in a non-destructive way using a Jasco NRS-2000C instrument (λ_{exc}=488 nm, 20× magnification). For each cup, 12 spectra were recorded in the inner surface within 1.5 mm from the centre, the most worn area. Crystallinity (C%) was determined from Raman spectra using the partial least-squares (PLS) regression.

RESULTS

Figure 1 shows the volumetric wear behaviour of the all UHMWPE acetabular cups after 3 million cycles. Significant differences were observed between the wear behaviours of the two sets of acetabular cups (α = 0.0001).
The mean C% values obtained for untreated gamma and EtO-sterilised UHMWPE unworn cups were significantly different (62 and 60%, respectively).
Upon ageing significant changes in C% were observed for all the cups and were more pronounced for gamma-sterilised cups (meanly from about 62% to 65%) than for EtO-sterilised cups (meanly from 60% to 61%). Upon wear testing of the gamma-sterilised cups, only three samples showed significant increases in C%. Conversely, all the EtO-sterilized cups showed significant C% changes: one cup showed a C% increase (from (60.9±0.2)% to (61.9±0.4)%), while the other two underwent a C% decrease (from (60.3±0.3)% to (56.4±0.7)% and from (60.9±0.3)% to (59.4±0.4)%).

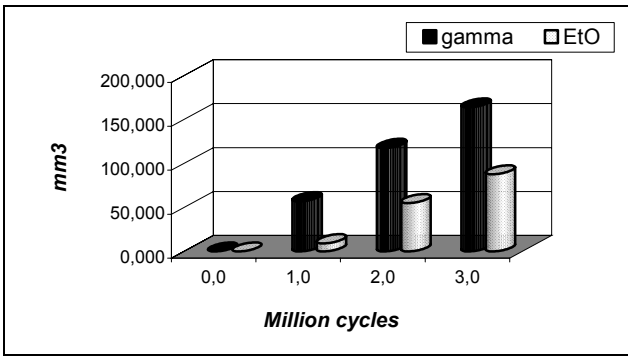

Fig. 1 – Volumetric wear trend of the UHMWPE cups.

DISCUSSION

The higher crystallinity found for the gamma-sterilised cups can be explained by considering that the energy of the gamma rays is sufficiently high to break the UHMWPE polymeric chains, resulting in a reduction of molecular weight and in a corresponding increase in crystallinity.
Raman spectroscopy proved a valid tool to non-destructively monitor the C% changes the samples underwent upon aging and wear tests. By Raman-PLS analysis it was confirmed that aging affected more significantly the morphology and wear behaviour of the gamma-sterilised cups; also the EtO-sterilised cups underwent detectable C% changes, which, however, did not affect so dramatically wear behaviour.

REFERENCES

1. Affatato S. et al. Biomaterials 2003; 24:4045-4055
2. Kurtz S.M. et al. Biomaterials 1999; 20:1659-1688

**Centro di Studio sulla Spettroscopia Raman, Dipartimento di Biochimica "G. Moruzzi", Sezione di Chimica e Propedeutica Biochimica, University of Bologna, Italy
***I° Divisione di Ortopedia e Traumatologia

EFFICACY AND BIOLOGICAL COMPATIBILITY OF A NEW PROCESSING TECHNIQUE FOR FRESH FROZEN FEMORAL HEADS AND COMPARISON WITH CURRENT WASHING PROCEDURES

*Board TN, *Mann J, *Eagle M, *Hogg P, * Rooney P, *Kearney JN, **Kay PR
*National Blood Service, Liverpool, UK
** Wrightington Hospital, Wigan, UK

boardtim@hotmail.com

INTRODUCTION

The major tissue supplied by Tissue Banks to surgeons is whole fresh-frozen femoral heads (FFH) which currently are not processed. Some FFH users wash the bone in theatre whilst others do not. Concern regarding disease transmission combined with evidence of improved stability and enhanced incorporation of washed bone has led the National Blood Service (NBS) to develop a processing technique for whole femoral heads. The aim of this study was to compare marrow-component content of NBS-processed FFHs with current theatre-washing techniques, namely sequential washing and pulsed lavage.

METHODS

A four-hour, 13 stage process utilising irrigation, sonication and centrifugation has been developed by NBS and amounts of soluble protein, haemoglobin, DNA and lipid, removed at each stage and in residual, morsellised bone were determined using biochemical assays. These same assays were used to compare the efficacy of sequential washing or pulsed lavage over a sieve. Biocompatibility of the end product was determined by contact and extract cytotoxicity assays using human osteoblastic (MG63) and fibroblastic (HSF) cell lines.

RESULTS

In duplicate samples from 24 femoral heads, the processing technique removed a minimum of 95% of protein, haemoglobin and DNA. In comparison sequential washing removed a minimum of 41% and pulsed lavage 28%. Unwashed bone demonstrated distinct contact cytotoxicity with both MG63 and HSF cell lines whereas NBS-processed and theatre-washed bone showed none. Quantitative extract cytotoxicity assays showed similar results.

DISCUSSION

This new NBS processing technique has been shown to be more efficacious at removing bone-marrow components from femoral heads than currently utilised techniques of washing after milling. The data indicate that unwashed morsellised bone can be cytotoxic to osteoblastic and fibroblastic cell lines and the processed bone appears to be more biocompatible than unwashed bone. This technique will allow for safer, quicker more biocompatible allograft usage in the future.

.

EVALUATION OF A BIPHASIC CALCIUM PHOSPHATE CERAMIC IMPLANTED DURING OPEN WEDGE MEDIAL TIBIAL OSTEOTOMY

*Rouvillain JL, **Pascal-Moussellard H, *Lavallé F, **Catonné Y, *Delattre O, ***Daculsi G
CHU de Fort de France – Service de Chirurgie Orthopédique et Traumatologique – B.P. 632 – 97200 Fort de France

jlrouvillain@sasi.fr

INTRODUCTION

This radiologic and histologic study was done to evaluate micro and macroporous biphasic calcium phosphate ceramic (MBCP™) blocs associated with a special plate and adjustable screw for valgisation tibial osteotomy by medial augmentation.

Methods

Between December 1999 and March 2002, 27 open wedge medial tibial osteotomies were performed on 26 patients for medial tibial plateau arthritis. There was 6 women and 20 men. Average age was 50 years. There was 16 right knees and 11 left knees.

Three patients were lost on follow up. 23 patients had a complete radiologic protocol with X-Ray at J+1,J+90 and J+360 days. Height patients had a biopsy of the biomaterial during removal plate procedure.

Bone fusion was evaluated radiologicaly by the construction of bone bridge in the tibial lateral metaphysis and osteo-integration on the fusion between bone and substitute. Histological analysis pointed out the biomaterial resorbtion but also the osseous recolonisation of the biomaterial .Three D Imaging using micro CT Scan were used on the biopsies. Quantitative measurements were reported on bone ingrowth and MBCP resorption in suuportt of the 2D image analysis performed in section observed in SEM (Sacnning Electron Microsocpy)

Post operative control of the HKA angle was also correlate with the angle between the tibial plateau and the medio-diaphysal axis of the tibia (β angle).

RESULTS

Consolidation occur in every cases. Osteointegration occur on all cases at J+360 days except one. That was also confirm by histologic analysis .

No difference between radiologic angles measurements on post operative J+1 and J+360 was found in 98,5% of the cases.

Three peri-operative fracture of the MBCP, and three proximal screw ruptures were observed with no consequences on the final result. All the histological analysis of the biopsies confirm the construction of organised bone apposition in place of the biomaterial.

Discussion-Conclusion

The osteotomy with open wedge procedure with a bony gap filled with micro macroporous biphasic calcium phosphate bioceramic substitute (MBCP™) and a well stable plate with orientable screw is a very safe method.

** Hôpital Pitié Salpetrière – Pavillon Gaston CORDIER - 83 Bld de l'Hôpital – 75651 PARIS Cedex 13

*** UMR S INSERM Osteoarticular and dental Tissue engineering Research Center – 1 place Alexis Ricordeau – B.P 8421 – 44042 Nantes Cedex1

CELL-INDUCED BIODEGRADATION OF POLY(L-LACTIC ACID) FIBER-REINFORCED POLY(ε-CAPROLACTONE) SCAFFOLDS FOR BONE REGENERATION

*Taddei P, *Di Foggia M, **Pagani S, **Ciapetti G, ***Guarino V, ***Causa F, ***Ambrosio L, *Fagnano C
*Dipartimento di Biochimica "G. Moruzzi", Sezione di Chimica e Propedeutica Biochimica, Università di Bologna, Italy
micheled@chem.unibo.it

INTRODUCTION

Polymer blending can be used in alternative to copolymerisation for tailoring the biodegradation rate of aliphatic polyesters. To evaluate *in vitro* degradation mechanism and kinetics, poly(ε-caprolactone)-poly(L-lactic acid) (PCL-PLLA) scaffolds were immersed in different aqueous media and characterized at different degradation times by vibrational spectroscopy and thermal analysis. To evaluate the role of cells in degradation, the same techniques were used to comparatively characterize the scaffolds incubated with both stromal cells from bone marrow (MSC) and osteoblasts (HOB) from orthopaedic patients.

METHODS

The PCL-PLLA composites were hollow cylindrical samples consisting of PLLA fibers embedded in a PCL matrix. PLLA fibers (75dtex) impregnated in the PCL (65000Da)/DMAc (Dimethylacetamide)/NaCl system were wound with an angle of 45° on Teflon coated steel mandrel by a winding machine (mod. AS LAB 101). DMAc was then removed by ethanol, and NaCl crystals by water. The *in vitro* biodegradation was investigated under sterile conditions at 37°C in different media: saline phosphate buffer at pH 7.4 (SPB), esterase in SPB, 0.01 M NaOH solution and simulated body fluid at pH 7.4 (SBF). The samples were analyzed before and after biodegradation for 4 weeks by polarized micro-Raman spectroscopy, thermogravimetry (TG) and differential scanning calorimetry (DSC).
MSC and HOB were isolated from marrow/bone fragments obtained during surgery for total hip replacement and cultivated in α-MEM with 10% FBS on the PCL-PLLA samples for 4 weeks.

RESULTS SECTION

Among the *in vitro* degradation media, the NaOH solution induced the highest weight loss in the PCL-PLLA scaffolds, confirming the catalytic effect of the OH^- ion on degradation. Accordingly, the samples degraded in NaOH solution showed the most pronounced composition and morphology changes: thermal analysis showed an enrichment in the PCL component, suggesting a preferential involvement of the more hydrophilic PLLA component in degradation. At the same time, the crystallinity of both polymeric components increased. The Raman results confirmed these findings. In particular, as regards the PLLA component, the observed spectral changes (Fig.1A) were explained in terms of structural rearrangements and decrease of the polymeric chain length.
The I_{875}/I_{923} and I_{1050}/I_{1103} intensity ratios were identified as marker of the degradation extent (Fig.1B).

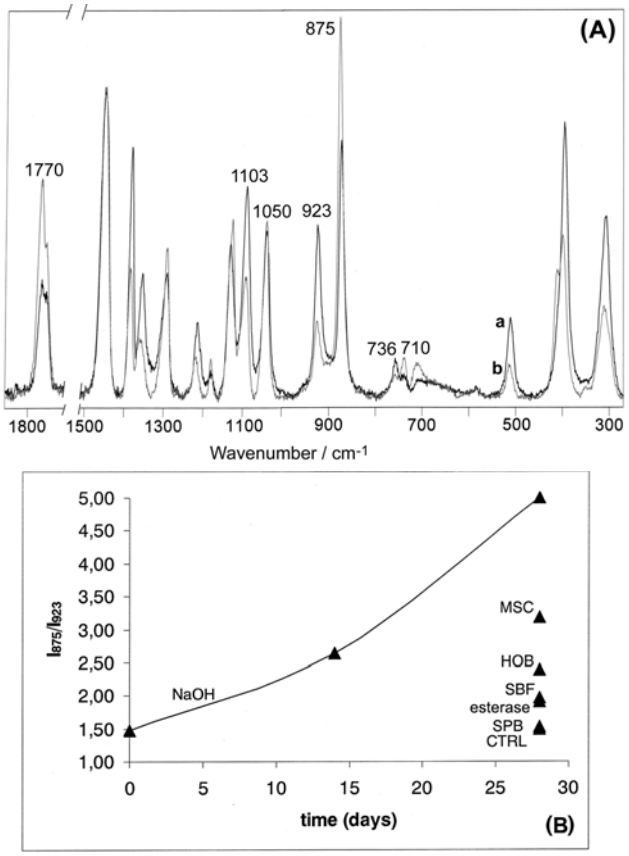

Figure 1. (**A**) Micro-Raman spectra of a PLLA fiber before (a) and after (b) degradation in NaOH solution for 4 weeks. (**B**) Trend of the I_{875}/I_{923} intensity ratio obtained from the Raman spectra of PLLA. CTRL = control samples for cell cultures.

DISCUSSION

The NaOH solution was found to induce the highest degradation rate. Raman analysis showed that also the PLLA fibres in the samples incubated with HOB and MSC underwent significant structural rearrangements, although to a lower extent than in NaOH solution; MSC were more aggressive than HOB (Fig.1B).

**Laboratorio di Fisiopatologia degli Impianti Ortopedici, Istituti Ortopedici Rizzoli, Bologna, Italy
***Istituto per la Tecnologia dei Materiali Compositi-CNR, Centro Interdisciplinare di Ricerca sui Biomateriali, Università di Napoli Federico II, Italy

AUTHOR INDEX

T